PO Box 2345, Beijing 100023, China
www.wjgnet.com
wjg@wjgnet.com

ELSEVIER

World J Gastroenterol 2005;11(25):3811-3816
World Journal of Gastroenterology ISSN 1007-9327

• *REVIEW* •

Role of *Helicobacter pylori* eradication in aspirin or non-steroidal anti-inflammatory drug users

George V. Papatheodoridis, Athanasios J. Archimandritis

George V. Papatheodoridis, Athanasios J. Archimandritis, Second Academic Department of Internal Medicine, Medical School of Athens University, Hippokration General Hospital, Athens, Greece
Correspondence to: George V. Papatheodoridis, MD, Assistant Professor in Medicine and Gastroenterology, Second Academic Department of Internal Medicine, Medical School of Athens University, Hippokration General Hospital of Athens, 114 Vas. Sophias Ave., Athens 115 27, Greece. gpapath@cc.uoa.gr
Telephone: +30-210-7774742 Fax: +30-210-7706871
Received: 2004-07-09 Accepted: 2004-11-04

Abstract

Helicobacter pylori (*H pylori*) infection and the use of non-steroidal anti-inflammatory drugs (NSAIDs) including aspirin at any dosage and formulation represent well-established risk factors for the development of uncomplicated and complicated peptic ulcer disease accounting for the majority of such cases. Although the interaction between *H pylori* and NSAID/aspirin use in the same individuals was questioned in some epidemiological studies, it has now become widely accepted that they are at least independent risk factors for peptic ulcer disease. According to data from randomized intervention trials, naive NSAID users certainly benefit from testing for *H pylori* infection and, if positive, *H pylori* eradication therapy prior to the initiation of NSAID. A similar strategy is also suggested for naive aspirin users, although the efficacy of such an approach has not been evaluated yet. Strong data also support that chronic aspirin users with a recent ulcer complication should be tested for *H pylori* infection and, if positive, receive *H pylori* eradication therapy after ulcer healing, while they appear to benefit from additional long-term therapy with a proton pump inhibitor (PPI). A similar approach is often recommended to chronic aspirin users at a high risk of ulcer complication. *H pylori* eradication alone does not efficiently protect chronic NSAID users with a recent ulcer complication or those at a high-risk, who certainly should be treated with long-term PPI therapy, but *H pylori* eradication may be additionally offered even in this setting. In contrast, testing for *H pylori* or PPI therapy is not recommended for chronic NSAID/aspirin users with no ulcer complications or those at a low risk of complications.

Key words: *Helicobacter pylori*; Aspirin

Papatheodoridis GV, Archimandritis AJ. Role of *Helicobacter pylori* eradication in aspirin or non-steroidal anti-inflammatory drug users. *World J Gastroenterol* 2005; 11(25): 3811-3816
http://www.wjgnet.com/1007-9327/11/3811.asp

INTRODUCTION

Salicylates have been used in therapeutic medicine since the Hippocrates' era and their use is still growing. During the last 50 years, there is a continuously increasing consumption of aspirin for cardioprotection and for secondary prophylaxis of recurrent stroke or other vascular occlusion, while the drug seems to have a possible role in chemoprevention of cancer and Alzheimer's disease[1-4]. Non-steroidal anti-inflammatory drugs (NSAIDs) are also widely used agents[5]. In the USA, it is estimated that more than 50% of the population over 65 years take aspirin or NSAIDs frequently[6].

The increasing widespread consumption of aspirin/NSAIDs, however, is associated with an increasing incidence of their well-known gastrointestinal complications, which include dyspepsia, gastric and/or duodenal erosions and ulcers and peptic ulcer complications. Peptic ulcer complications, usually bleeding, represent the most frequent serious adverse events of the use of aspirin/NSAIDs[1,7]. Peptic ulcer(s) may be found at endoscopy in up to 20-25% and ulcer complications requiring hospital admission develop in 2-5% of chronic users of NSAIDs[7-12]. Use of NSAIDs has also been shown to increase the risk of lower gastrointestinal bleeding[13]. The damaging effect of aspirin on the gastric mucosa may be less potent than the effect of NSAIDs[14]. Thus, it is estimated that the chronic use of aspirin increases the absolute annual risk of gastrointestinal bleeding by 0.04% (absolute annual risk of bleeding with and without aspirin: 0.09% and 0.05% respectively)[15]. Nevertheless, despite the relatively low absolute risk of bleeding in aspirin users, the numbers of aspirin related acute gastrointestinal bleeding episodes are rather high probably due to the huge numbers of individuals who take the drug regularly for long periods often having additional factors with increased risk for bleeding, such as old age and history of peptic ulcer disease. The use of selective NSAIDs, such as selective cyclo-oxygenase 2 (COX-2) inhibitors, significantly reduces but does not completely eliminate the risk of gastrointestinal complications[11,12,16], while their gastrointestinal benefit appears to be significantly restricted in cases of concomitant use of aspirin, even at low doses[11,17].

Helicobacter pylori (*H pylori*) is undoubtedly associated with the development of gastritis and uncomplicated and complicated peptic ulcer diseases[18]. Although the presence of two factors that can damage the gastric mucosa, such as *H pylori* and aspirin/NSAIDs, would be reasonably considered

to increase the risk for development of uncomplicated and complicated peptic ulcer, data from several, mainly epidemiological, studies appear to be controversial and do not always confirm such an assumption[19]. This review focuses on the role of *H pylori* infection and the need for its eradication for prevention of gastrointestinal complications among aspirin/NSAIDs users by evaluating the relevant pathophysiological and epidemiological data as well as the results of the randomized, controlled clinical trials of therapeutic intervention.

PATHOPHYSIOLOGY

Aspirin or NSAIDs use is associated with the development of peptic erosions or ulcers through several mechanisms. First, aspirin acts locally through the release of salicylic acid in the stomach, which is not ionized by the gastric acid. Salicylic acid enters and accumulates within the gastric epithelial cells, is ionized intracellularly and disrupts cell metabolic functions increasing mucosal permeability and permitting the back diffusion of H^+ ions[20]. Moreover, aspirin promotes topical inflammation by inducing recruitment of leukocytes, which eventually results in capillary constriction and topical ischemia. The topical gastrotoxic effect of aspirin, however, does not seem to be particularly important, since it is associated only with superficial ulcerations that often resolve spontaneously despite the continued aspirin use[20]. The systemic gastrotoxic effect of aspirin is related to the inhibition of cyclo-oxygenase-1 (COX-1) and the subsequent disruption of prostaglandin synthesis and to the antiplatelet function that promotes bleeding complications[20]. The key role of the systemic effects of aspirin in the development of gastrointestinal complications is strongly supported by the data showing that the risk of such complications is independent of the drug formulation[17,21,22]. Even low doses of aspirin, such as 75 mg/d, have been shown to increase the risk of gastroduodenal ulcerations[21,22]. Inhibition of COX-1 with disruption of prostaglandin production is also the main mechanism of NSAIDs induced gastroduodenal complications[11-13].

H pylori infection induces a substantial inflammatory reaction in the gastric mucosa with recruitment of leukocytes and production of several inflammatory cytokines, which eventually result in attenuation of mucosal defense mechanisms[18]. Thus, *H pylori* infection and aspirin/NSAID use impaired gastric mucosal defense by different mechanisms and therefore an interaction between these two factors is biologically plausible.

EPIDEMIOLOGICAL STUDIES

The interaction between *H pylori* infection and aspirin/NSAIDs use in the development of ulcer and ulcer complications has been initially evaluated in several cohort or case-control studies. The findings of these studies, however, have been controversial, since some studies suggested an independent or additive role of *H pylori* infection and aspirin/NSAIDs use in gastrointestinal complications[21-30] and others proposed no association or even a protective role of *H pylori* infection in users of aspirin/NSAIDs[31-33]. Moreover, in one study, *H pylori* infection was found to increase the risk of gastric but not of duodenal ulceration in this setting[34]. The heterogeneity in study design and methodology, definitions, power, outcome, and selection of controls have been suggested to be responsible for such conflicting results[19].

In a systemic review published in 2002, the combined analysis of the data available up to October 2000 showed that there is synergism for the development of peptic ulcer and ulcer bleeding between *H pylori* infection and aspirin/NSAID use[35]. In particular, the presence of *H pylori* infection was found to increase 3-5-fold the risk of peptic ulcer in aspirin/NSAID users (prevalence of peptic ulcer in *H pylori* positive: 53% and *H pylori* negative: 21%, OR: 3.5) and 18-fold in subjects not taking aspirin/NSAID (prevalence of peptic ulcer in *H pylori* positive: 18% and *H pylori* negative: 0%, OR: 18.1)[35]. Thus, the risk of peptic ulcer is approximately 60-fold higher in *H pylori* positive aspirin/NSAID users compared with *H pylori* negative subjects not taking aspirin/NSAID[35]. Moreover, *H pylori* infection was shown to increase the risk of ulcer bleeding 1.8-fold, aspirin/NSAID use 4.85-fold, and the presence of both factors 6.1-fold compared with the risk of bleeding among *H pylori* negative subjects not taking aspirin/NSAID[35]. *H pylori* infection has also been found to increase the risk of upper gastrointestinal bleeding even in chronic users of low dose aspirin[27]. In a more recent case-control study from our group, *H pylori* infection was again found to increase the risk for upper gastrointestinal bleeding in aspirin/NSAID users 2.9-fold, or 1.7-fold when adjustment for other risk factors for bleeding was performed[28]. Taking all together, it seems that aspirin/NSAID use and presence of *H pylori* infection are at least independent risk factors for peptic ulcer and bleeding from peptic ulcer.

RANDOMIZED CLINICAL TRIALS

H pylori eradication in naive aspirin/NSAID users

If *H pylori* gastritis does enhance the risk for ulcer bleeding in aspirin/NSAID users, then *H pylori* eradication should substantially reduce such a risk in this setting. Since the risk of bleeding in aspirin/NSAID users is strongly related to the duration of drug use, being higher in subjects with new or recent drug onset (<1-3 mo) than in chronic drug users (>1-3 mo)[36-38], the possible beneficial effect of *H pylori* eradication on naive aspirin/NSAID users was initially evaluated. In fact, only naive users of non-aspirin NSAIDs have been included in the relevant clinical trials to date, while the possible benefit of *H pylori* eradication in naive users of aspirin has not been evaluated yet.

H pylori eradication before NSAID use was found to significantly reduce the occurrence of peptic ulcers in 92 *H pylori* positive, NSAID naive patients with musculoskeletal pain treated with an 8-wk course of naproxen at a daily dose of 750 mg (peptic ulcers: 3/45 or 7% of patients in the *H pylori* eradication group *vs* 12/47 or 26% of patients in the placebo group, $P = 0.01$)[39]. In a longer trial with a similar design, *H pylori* eradication before NSAID use was again found to significantly reduce the risk of peptic ulcers in 100 *H pylori* positive, NSAID naive, patients with arthritis and a history of peptic ulcer or dyspepsia treated with a 6-mo course of diclofenac slow release at a daily dose of 100 mg (peptic ulcers: 5/51 or 12% *vs* 15/49 or 34%, $P = 0.0085$)[40]. In the latter trial, *H pylori* eradication

was also found to significantly reduce the risk of ulcer complications as well [6-mo probability: 4.2% (1.3-9.7) *vs* 27.1% (14.7-39.5), $P = 0.0026$][40].

H pylori eradication in chronic aspirin/NSAID users without a history of peptic ulcer complications

The results of the first large clinical trial of *H pylori* eradication in chronic NSAID users raised several questions for the benefit of such an intervention. In this trial[41], 285 *H pylori* positive chronic NSAID users with past or current peptic ulcers or NSAID-associated dyspepsia who continued a minimum dosage of NSAID for at least 6 mo were randomized to receive *H pylori* eradication therapy with omeprazole, amoxycillin and clarithromycin ($n = 142$) or omeprazole plus placebo antibiotics ($n = 143$) for 1 wk. Subsequently, all patients received omeprazole 20 mg daily for 3 wk followed by an additional 4-wk omeprazole course in cases with endoscopically detected peptic ulcers at 4th wk. The probability of being peptic ulcer free at 6th mo was similar in the *H pylori* eradication [0.56 (95%CI: 0.47-0.65)] and the omeprazole-control group [0.53 (95%CI: 0.44-0.62)], while healing of gastric ulcers was significantly impaired in the *H pylori* eradication group (gastric ulcers healed at 8th wk: 72% in the *H pylori* eradication group *vs* 100% in the omeprazole-control group, $P = 0.006$)[41].

The design of the latter trial, however, was different from the design of the trials in naive NSAID users, since *H pylori* eradication therapy was given to subjects with ulcers or at high-risk of ulcers, who had already been on long-term NSAID consumption. Moreover, both the *H pylori* eradication and control groups were treated with 4-8 wk of omeprazole for ulcer healing. The lower probability of gastric ulcer healing at 8th wk in the *H pylori* eradication group should be associated with the more potent antisecretory activity of the PPIs including omeprazole in the presence than absence of *H pylori* infection[42]. Similar findings have also been observed in another large study including 692 chronic NSAID users, in which gastric ulcer healing with ranitidine or lansoprazole was shown to be significantly enhanced in the presence of *H pylori* infection (healing of gastric ulcers at 8th wk: 70% in *H pylori* positive *vs* 61% in *H pylori* negative, $P<0.05$)[43]. According to these data, it has been reasonably suggested that any attempt to eradicate *H pylori* infection should follow ulcer healing in the management of chronic NSAID users, although the efficacy of such an approach remains to be tested. The efficacy of *H pylori* eradication in chronic aspirin users has not been evaluated yet.

H pylori eradication in chronic aspirin/NSAID users with a recent peptic ulcer complication

Subjects with a history of upper gastrointestinal bleeding or other peptic ulcer complications represent a particular subgroup of aspirin/NSAID users who are at a high risk for recurrent bleeding during continued aspirin/NSAID use[44,45]. Strategies that may prevent bleeding in this setting include concurrent therapy with a PPI or eradication of *H pylori* infection in *H pylori* positive subjects. The efficacy of these two strategies was evaluated in a large clinical trial including 400 *H pylori* positive aspirin/NSAID users with a history of upper gastrointestinal bleeding[46]. All patients initially discontinued aspirin or NSAID therapy and were treated with omeprazole 20 mg daily for at least 8 wk to promote ulcer healing. Once the healing of ulcer was confirmed, 250 patients who were given 80 mg of aspirin daily for heart disease or stroke and 150 patients who were given 500 mg of naproxen twice daily for arthritis, both for at least 6 mo, were separately randomized to receive 20 mg of omeprazole daily for 6 mo or a 7-d course of *H pylori* eradication therapy followed by placebo once daily for 6 mo. In patients taking aspirin, no significant difference in the probability of recurrent bleeding during the 6-mo follow-up period was observed between those who received *H pylori* eradication therapy (1.9%) and those who received omeprazole (0.9%) (absolute difference: 1%, 95%CI: -1.9-3.9%). In contrast, in patients taking naproxen, the 6-mo probability of recurrent bleeding was significantly lower in the omeprazole (4.4%) than in the *H pylori* eradication group (18.8%) (absolute difference: 14.4%, 95%CI: 4.4-24.4%, $P = 0.005$)[46]. According to these data, it seems that, after ulcer healing, *H pylori* eradication may be effective in preventing recurrence of upper gastrointestinal bleeding in chronic aspirin users, but not in chronic NSAID users, who require long-term potent antisecretory therapy with a PPI.

Whether the combination of *H pylori* eradication and long-term use of PPIs may further decrease the risk of recurrence of peptic ulcer complications in chronic aspirin users was evaluated in a recent clinical trial[47]. Thus, 123 *H pylori* positive patients with a history of an aspirin-related peptic ulcer complication and current peptic ulcer were initially treated with a 7-d *H pylori* eradication therapy followed by 40 mg of famotidine daily for 5 or 13 additional weeks until ulcer healing. Then, they all restarted taking 100 mg of aspirin daily and randomized to receive 30 mg of lansoprazole daily or placebo. During a median follow-up of 12 mo, recurrence of ulcer complications was observed in 9 (14.8%) of 61 patients in the placebo group and in only 1 (1.6%) of 62 patients in the lansoprazole group (adjusted hazard ratio: 9.6, 95%CI: 1.2-76.1, $P = 0.008$)[47]. It should be noted, however, that four of the nine placebo treated patients with a recurrence of ulcer complications were reinfected with *H pylori* and an additional two patients of this group took other NSAIDs. Despite these problems in the latter trial, it is becoming widely accepted that long-term therapy with a PPI after *H pylori* eradication offers additional benefit in preventing peptic ulcer complications in high risk *H pylori* positive chronic aspirin users[19].

DISCUSSION

All existing data suggest that the presence of *H pylori* infection represents an additional risk factor for peptic ulcer complications in aspirin/NSAID users[19,48]. However, in current clinical practice which should be guided by the evidence-based medicine and should take into account the cost/benefit analysis of any major intervention, the management of *H pylori* infection and generally the gastrointestinal prevention in aspirin/NSAID users should probably be individualized (Table 1). Thus, the optimal management of such subjects appears to depend on the main factors affecting the risk of ulcer complications, which are: (1) whether the subject is a

Table 1 Recommendations[19,48] and evidence for the *H pylori* test-and-treat approach and/or the long-term therapy with a proton pump inhibitor (PPI) in users of aspirin or non-steroidal anti-inflammatory drugs (NSAIDs)

	H pylori test-and-treat approach	Long-term PPI therapy
Naive aspirin users	Recommendation	No
Naive NSAIDs users	Recommendation-evidence[39,40]	No
Chronic aspirin users		
With a recent ulcer complication	Recommendation[1]-evidence[46,47]	Recommendation-evidence[47]
At high risk for ulcer complication	Recommendation[1]	Recommendation
At low risk for ulcer complication	No	No
Chronic NSAIDs users		
With a recent ulcer complication	Potential benefit[1,2]	Recommendation-evidence[46]
At high risk for ulcer complication	Potential benefit[1,2]	Recommendation
At low risk for ulcer complication	No	No

[1]*H pylori* eradication therapy in chronic users of aspirin or NSAIDs with a recent ulcer complication or those at a high-risk should be administered after confirmation of ulcer healing. [2]*H pylori* eradication therapy in chronic NSAIDs users with a recent ulcer complication or those at a high-risk may be given as a potentially beneficial intervention in addition to the long-term PPI therapy.

naive aspirin/NSAID user or already on long-term (>1-3 mo) or chronic drug use[36-38]; (2) whether the subject is at high risk for bleeding or other complication of peptic ulcer (history of complicated or uncomplicated peptic ulcer, age older than 60-65 years, recent dyspepsia, treatment with anticoagulants)[6,36-38,49]; and (3) perhaps whether they take aspirin or non-aspirin NSAID[19,48].

In naive NSAID users, it is well accepted and supported by strong data[39,40] that they should be tested for the presence of *H pylori* infection and, if positive, receive *H pylori* eradication therapy before NSAID use[19-48]. A similar strategy is also suggested for naive aspirin users[19], although the efficacy of such an approach has not been evaluated yet.

In chronic aspirin/NSAIDs users, the recommendations may depend on the risk for peptic ulcer complications[6] and the type of drug. The indication for use of aspirin or NSAIDs should be first evaluated in all such users at high risk for peptic ulcer complications. Moreover, the probability and the cost/benefit of replacement of aspirin or NSAID with a less gastrotoxic antiplatelet agent or a selective COX-2 inhibitor respectively may be considered[6,11,12].

All individuals, who should continue taking aspirin after development of a peptic ulcer complication, should be tested for the presence of *H pylori* infection and, if positive, receive *H pylori* eradication therapy after peptic ulcer healing. In addition, they should subsequently receive long-term therapy with a PPI[19,47]. A similar approach may be recommended in chronic aspirin users without a recent ulcer complication but at high risk for ulcer complication, such as those with a history of peptic ulcer[19]. It should be noted, however, that there are no strong data to support the combined prophylactic approach with both *H pylori* eradication and long-term PPI therapy in this setting.

All individuals, who should continue taking NSAIDs being at high-risk for peptic ulcer complication, certainly benefit from long-term therapy with a PPI[19,46,48]. The risk of relapse of ulcer complication in chronic NSAIDs users taking PPI, however, is higher than the risk of such a relapse in aspirin users irrespective of the type of gastroprotection[46]. Thus, given that *H pylori* infection represents an independent risk factor for gastrointestinal bleeding in chronic NSAIDs users[35], it is often recommended that testing for *H pylori* infection and, if positive, *H pylori* eradication therapy should be offered to high-risk chronic NSAIDs users in addition to the long-term PPI therapy[19], despite that there are no strong data to support such an approach.

Finally, testing for *H pylori* infection or PPI therapy is not recommended for chronic users of aspirin or NSAIDs with no peptic ulcer or complication or those at a low risk of the same[19].

REFERENCES

1 **Lauer MS.** Aspirin for primary prevention of coronary events. *N Engl J Med* 2002; **346**: 1468-1474

2 Antiplatelet Trialists' Collaboration. Collaborative overview of randomised trials of antiplatelet therapy prevention of death, myocardial infarction, and stroke by prolonged antiplatelet therapy in various categories. *Br Med J* 1994; **308**: 81-106

3 **Giovannucci E,** Egan KM, Hunter DJ, Stampfer MJ, Colditz GA, Willett WC, Speizer FE. Aspirin and the risk of colorectal cancer in women. *N Engl J Med* 1995; **333**: 609-614

4 **Arber N,** DuBois RN. Nonsteroidal anti-inflammatory drugs and prevention of colorectal cancer. *Curr Gastroenterol Rep* 1999; **1**: 441-448

5 **Baum C,** Kennedy DL, Forbes MB. Utilization of nonsteroidal antiinflammatory drugs. *Arthritis Rheum* 1985; **28**: 686-692

6 **Laine L.** Approaches to nonsteroidal anti-inflammatory drugs use in the high-risk patient. *Gastroenterology* 2001; **120**: 594-606

7 **Singh G,** Ramey DR, Morfeld D, Shi H, Hatoum HT, Fries JF. Gastrointestinal tract complications of nonsteroidal anti-inflammatory drug treatment in rheumatoid arthritis. A prospective observational cohort study. *Arch Intern Med* 1996; **156**: 1530-1536

8 **Hawkey CJ,** Laine L, Simon T, Quan H, Shingo S, Evans J. Incidence of gastroduodenal ulcers in patients with rheumatoid arthritis after 12 wk of rofecoxib, naproxen, or placebo: a multicentre, randomised, double blind study. *Gut* 2003; **52**: 820-826

9 **Geis GS.** Update on clinical developments with celecoxib, a new specific COX-2 inhibitor: what can we expect? *J Rheumatol* 1999; **26** (Suppl 56): 31-36

10 **Silverstein FE,** Graham DY, Senior JR, Davies HW, Struthers BJ, Bittman RM, Geis GS. Misoprostol reduces serious gastrointestinal complications in patients with rheumatoid ar-

thritis receiving nonsteroidal anti-inflammatory drugs. A randomized, double-blind, placebo-controlled trial. *Ann Intern Med* 1995; **123**: 241-249

11 **Silverstein FE,** Faich G, Goldstein JL, Simon LS, Pincus T, Whelton A, Makuch R, Eisen G, Agrawal NM, Stenson WF, Burr AM, Zhao WW, Kent JD, Lefkowith JB, Verburg KM, Geis GS. Gastrointestinal toxicity with celecoxib *vs* nonsteroidal anti-inflammatory drugs for osteoarthritis and rheumatoid arthritis: the CLASS study: A randomized controlled trial. Celecoxib Long-term Arthritis Safety Study. *JAMA* 2000; **284**: 1247-1255

12 **Bombardier C,** Laine L, Reicin A, Shapiro D, Burgos-Vargas R, Davis B, Day R, Ferraz MB, Hawkey CJ, Hochberg MC, Kvien TK, Schnitzer TJ. Comparison of upper gastrointestinal toxicity of rofecoxib and naproxen in patients with rheumatoid arthritis. VIGOR Study Group. *N Engl J Med* 2000; **343**: 1520-1528

13 **Laine L,** Connors LG, Reicin A, Hawkey CJ, Burgos-Vargas R, Schnitzer TJ, Yu Q, Bombardier C. Serious lower gastrointestinal clinical events with nonselective NSAID or coxib use. *Gastroenterology* 2003; **124**: 288-292

14 **Singh G,** Ramey DR, Morfeld D, Fries JF. Comparative toxicity of non-steroidal anti-inflammatory agents. *Pharmacol Ther* 1994; **62**: 175-191

15 **Sanmuganathan PS,** Ghahramani P, Jackson PR, Wallis EJ, Ramsay LE. Aspirin for primary prevention of coronary heart disease: safety and absolute benefit related to coronary risk derived from meta-analysis of randomised trials. *Heart* 2001; **85**: 265-271

16 **Hawkey CJ,** Laine L, Harper SE, Quan HU, Bolognese JA, Mortensen E. Influence of risk factors on endoscopic and clinical ulcers in patients taking rofecoxib or ibuprofen in two randomized controlled trials. *Aliment Pharmacol Ther* 2001; **15**: 1593-1601

17 **Sorensen HT,** Mellemkjaer L, Blot WJ, Nielsen GL, Steffensen FH, McLaughlin JK, Olsen JH. Risk of upper gastrointestinal bleeding associated with use of low-dose aspirin. *Am J Gastroenterol* 2000; **95**: 2218-2224

18 **Suerbaum S,** Michetti P. *Helicobacter pylori* infection. *N Engl J Med* 2002; **347**: 1175-1186

19 **Hunt RH,** Bazzoli F. Should NSAID/low-dose aspirin takers be tested routinely for *H pylori* infection and treated if positive? Implications for primary risk of ulcer and ulcer relapse after initial healing. *Aliment Pharmacol Ther* 2004; **19** (Suppl 1): 9-16

20 **Kaufman G.** Aspirin-induced gastric mucosal injury: lessons learned from animal models. *Gastroenterology* 1989; **96**: 606-614

21 **Derry S,** Loke YK. Risk of gastrointestinal haemorrhage with long term use of aspirin: meta-analysis. *Br Med J* 2000; **321**: 1183-1187

22 **Kelly JP,** Kaufman DW, Jurgelon JM, Sheehan J, Koff RS, Shapiro S. Risk of aspirin-associated major upper-gastrointestinal bleeding with enteric-coated or buffered product. *Lancet* 1996; **348**: 1413-1416

23 **Lichtenstein DR,** Syngal S, Wolfe MM. Nonsteroidal antiinflammatory drugs and the gastrointestinal tract. *Arthritis Rheum* 1995; **38**: 5-18

24 **Labenz J,** Peitz U, Kohl H, Kaiser J, Malfertheiner P, Hackelsberger A, Borsch G. *Helicobacter pylori* increases the risk of peptic ulcer bleeding: a case-control study. *Ital J Gastroenterol Hepatol* 1999; **31**: 110-115

25 **Aalykke C,** Lauritsen JM, Hallas J, Reinholdt S, Krogfelt K, Lauritsen K. *Helicobacter pylori* and risk of ulcer bleeding among users of nonsteroidal anti-inflammatory drugs: a case-control study. *Gastroenterology* 1999; **116**: 1305-1309

26 **Ng TM,** Fock KM, Khor JL, Teo EK, Sim CS, Tan AL, Machin D. Non-steroidal anti-inflammatory drugs, *Helicobacter pylori* and bleeding gastric ulcer. *Aliment Pharmacol Ther* 2000; **14**: 203-209

27 **Lanas A,** Fuentes J, Benito R, Serrano P, Bajador E, Sainz R. *Helicobacter pylori* increases the risk of upper gastrointestinal bleeding in patients taking low-dose aspirin. *Aliment Pharmacol Ther* 2002; **16**: 779-786

28 **Papatheodoridis GV,** Papadelli D, Cholongitas E, Vassilopoulos D, Mentis A, Hadziyannis SJ. Effect of *Helicobacter pylori* infection on the risk of upper gastrointestinal bleeding in users of non-steroidal anti-inflammatory drugs: a prospective, case-control study. *Am J Med* 2004; **116**: 601-605

29 **Laine L,** Marin-Sorensen M, Weinstein WM. Nonsteroidal anti-inflammatory drug associated gastric ulcers do not require *Hepicobacter pylori* for their development. *Am J Gastroenterol* 1992; **87**: 1398-1402

30 **Cullen DJ,** Hawkey GM, Greenwood DC, Humphreys H, Shepherd V, Logan RF, Hawkey CJ. Peptic ulcer bleeding in the elderly: relative roles of *Helicobacter pylori* and non-steroidal anti-inflammatory drugs. *Gut* 1997; **41**: 459-462

31 **Loeb DS,** Talley NJ, Ahlquist DA, Carpenter HA, Zinsmeister AR. Long-term nonsteroidal anti-inflammatory drug use and gastroduodenal injury: the role of *Helicobacter pylori* infection. *Gastroenterology* 1992; **102**: 1899-1905

32 **Pilotto A,** Leandro G, Di Mario F, Franceschi M, Bozzola L, Valerio G. Role of *Helicobacter pylori* infection on upper gastrointestinal bleeding in the elderly: a case-control study. *Dig Dis Sci* 1997; **42**: 586-591

33 **Stack WA,** Atherton JC, Hawkey GM, Logan RF, Hawkey CJ. Interactions between *Helicobacter pylori* and other risk factors for peptic ulcer bleeding. *Aliment Pharmacol Ther* 2002; **16**: 497-506

34 **Santolaria S,** Lanas A, Benito R, Perez-Aisa M, Montoro M, Sainz R. *Helicobacter pylori* infection is a protective factor for bleeding gastric ulcers but not for bleeding duodenal ulcers in NSAID users. *Aliment Pharmacol Ther* 1999; **13**: 1511-1518

35 **Huang JQ,** Sridhar S, Hunt RH. Role of *Helicobacter pylori* infection and non-steroidal anti-inflammatory drugs in peptic-ulcer disease: a meta-analysis. *Lancet* 2002; **359**: 14-22

36 **Gabriel SE,** Jaakkimainen L, Bombardier C. Risk for serious gastrointestinal complications related to use of nonsteroidal anti-inflammatory drugs. A meta-analysis. *Ann Intern Med* 1991; **115**: 787-796

37 **Griffin MR,** Piper JM, Daugherty JR, Snowden M, Ray WA. Nonsteroidal anti-inflammatory drug use and increased risk for peptic ulcer disease in elderly persons. *Ann Intern Med* 1991; **114**: 257-263

38 **Langman MJ,** Weil J, Wainwright P, Lawson DH, Rawlins MD, Logan RF, Murphy M, Vessey MP, Colin-Jones DG. Risks of bleeding peptic ulcer associated with individual non-steroidal anti-inflammatory drugs. *Lancet* 1994; **343**: 1075-1078

39 **Chan FK,** Sung JJ, Chung SC, To KF, Yung MY, Leung VK, Lee YT, Chan CS, Li EK, Woo J. Randomised trial of eradication of *Helicobacter pylori* before non-steroidal anti-inflammatory drug therapy to prevent peptic ulcers. *Lancet* 1997; **350**: 975-979

40 **Chan FK,** To KF, Wu JC, Yung MY, Leung WK, Kwok T, Hui Y, Chan HL, Chan CS, Hui E, Woo J, Sung JJ. Eradication of *Helicobacter pylori* and risk of peptic ulcers in patients starting long-term treatment with non-steroidal anti-inflammatory drugs: a randomised trial. *Lancet* 2002; **359**: 9-13

41 **Hawkey CJ,** Tulassay Z, Szczepanski L, van Rensburg CJ, Filipowicz-Sosnowska A, Lanas A, Wason CM, Peacock RA, Gillon KR. Randomised controlled trial of *Helicobacter pylori* eradication in patients on non-steroidal anti-inflammatory drugs: HELP NSAIDs study. Helicobacter Eradication for Lesion Prevention. *Lancet* 1998; **352**: 1016-1021

42 **van Herwaarden MA,** Samsom M, van Nispen CH, Mulder PG, Smout AJ. The effect of *Helicobacter pylori* eradication on intragastric pH during dosing with lansoprazole or ranitidine. *Aliment Pharmacol Ther* 1999; **13**: 731-740

43 **Campbell DR,** Haber MM, Sheldon E, Collis C, Lukasik N, Huang B, Goldstein JL. Effect of *H pylori* status on

gastric ulcer healing in patients continuing nonsteroidal anti-inflammatory therapy and receiving treatment with lansoprazole or ranitidine. *Am J Gastroenterol* 2002; **97**: 2208-2214

44 **Lanas A,** Bajador E, Serrano P, Fuentes J, Carreno S, Guardia J, Sanz M, Montoro M, Sainz R. Nitrovasodilators, low-dose aspirin, other nonsteroidal antiinflammatory drugs, and the risk of upper gastrointestinal bleeding. *N Engl J Med* 2000; **343**: 834-839

45 **Garcia Rodriguez LA,** Jick H. Risk of upper gastrointestinal bleeding and perforation associated with individual non-steroidal anti-inflammatory drugs. *Lancet* 1994; **343**: 769-772

46 **Chan FK,** Chung SC, Suen BY, Lee YT, Leung WK, Leung VK, Wu JC, Lau JY, Hui Y, Lai MS, Chan HL, Sung JJ. Preventing recurrent upper gastrointestinal bleeding in patients with *Helicobacter pylori* infection who are taking low-dose aspirin or naproxen. *N Engl J Med* 2001; **344**: 967-973

47 **Lai KC,** Lam SK, Chu KM, Wong BC, Hui WM, Hu WH, Lau GK, Wong WM, Yuen MF, Chan AO, Lai CL, Wong J. Lansoprazole for the prevention of recurrences of ulcer complications from long-term low-dose aspirin use. *N Engl J Med* 2002; **346**: 2033-2038

48 **Malfertheiner P,** Megraud F, O'Morain C, Hungin AP, Jones R, Axon A, Graham DY, Tytgat G. Current concepts in the management of *Helicobacter pylori* infection-the Maastricht 2-2000 Consensus Report. *Aliment Pharmacol Ther* 2002; **16**: 167-180

49 **Laine L,** Bombardier C, Hawkey CJ, Davis B, Shapiro D, Brett C, Reicin A. Stratifying the risk of NSAID-related upper gastrointestinal clinical events: results of a double-blind outcomes study in patients with rheumatoid arthritis. *Gastroenterology* 2002; **123**: 1006-1012

Science Editor Zhu LH and Guo SY **Language Editor** Elsevier HK

PO Box 2345, Beijing 100023, China
www.wjgnet.com
wjg@wjgnet.com

ELSEVIER

World J Gastroenterol 2005;11(25):3817-3822
World Journal of Gastroenterology ISSN 1007-9327

• *REVIEW* •

Current preventive treatment for recurrence after curative hepatectomy for liver metastases of colorectal carcinoma: A literature review of randomized control trials

Peng Wang, Zhen Chen, Wen-Xia Huang, Lu-Ming Liu

Peng Wang, Zhen Chen, Wen-Xia Huang, Lu-Ming Liu, Department of Oncology, Shanghai Medical College of Fudan University and Department of Liver Neoplasms, Cancer Hospital of Fudan University, Shanghai 200032, China
Correspondence to: Peng Wang, Department of Liver Neoplasms, Cancer Hospital of Fudan University, 270 Dong An Road, Shanghai 200032, China. wangp413@yahoo.com.cn
Telephone: +86-21-64175590-1304 Fax: +86-21-64434191
Received: 2004-09-18 Accepted: 2004-12-21

Abstract

To review the preventive approaches for recurrence after curative resection of hepatic metastases from colorectal carcinoma, we have summarized all available publications reporting randomized control trials (RCTs) covered in PubMed. The treatment approaches presented above include adjuvant intrahepatic arterial infusion chemotherapy, systemic chemotherapy, neoadjuvant chemotherapy, and immunotherapy. Although no standard treatment has been established, several approaches present promising results, which are both effective and tolerable in post-hepatectomy patients. Intrahepatic arterial infusion chemotherapy should be regarded as effective and tolerable and it increases overall survival (OS) and disease-free survival (DFS) of patients, while 5-fluorouracil-based systemic chemotherapy has not shown any significant survival benefit. Fortunately chemotherapy combined with hepatic arterial infusion and intravenous infusion has shown OS and DFS benefit in many researches. Few neoadjuvant RCT studies have been conducted to evaluate its effect on prolonging survivals although many retrospective studies and case reports are published in which unresectable colorectal liver metastases are downstaged and made resectable with neoadjuvant chemotherapy. Liver resection supplemented with immunotherapy is associated with optimal results; however, it is also questioned by others. In conclusion, several adjuvant approaches have been studied for their efficacy on recurrence after hepatectomy for liver metastases from colorectal cancer (CRC), but multi-centric RCT is still needed for further evaluation on their efficacy and systemic or local toxicities. In addition, new adjuvant treatment should be investigated to provide more effective and tolerable methods for the patients with resectable hepatic metastases from CRC.

Key words: Preventive treatment; Recurrence; Hepatectomy; Metastatic colorectal cancer; Randomized control trials

Wang P, Chen Z, Huang WX, Liu LM. Current preventive treatment for recurrence after curative hepatectomy for liver metastases of colorectal carcinoma: A literature review of randomized control trials. *World J Gastroenterol* 2005; 11(25): 3817-3822
http://www.wjgnet.com/1007-9327/11/3817.asp

INTRODUCTION

Although many approaches have been invented for the treatment of liver metastases from colorectal cancer (CRC)[1], resection continues to be the only curative therapeutic option. Liver resection is today a safe procedure, with a low mortality rate of 0.8%[2] and a morbidity of 7.2%[3]. Though the 5- and 10-year overall survival (OS) rates are 37% and 22% respectively[4], recurrence is already evidenced, either in the liver or with extrahepatic disease in about half of all resected patients within 18 mo after resection[5]. Intrahepatic recurrence, alone or with other localization, is common. However, about 60% recurrences are seen in the remnant liver[6]. In the last two decades people have tried a number of approaches to prevent recurrence, but only a few of them were designed as randomized control trials (RCTs), which provide evidence-based results for those treatment modalities. In this paper, we summarized the results from RCTs, attempting to find a more suitable treatment modality for prevention of recurrence.

LITERATURE REVIEWS OF RANDOMIZED CONTROL TRIALS TO PREVENT RECURRENCE AFTER CURATIVE HEPATECTOMY FOR LIVER METASTASES OF COLORECTAL CARCINOMA

Hepatic arterial infusion

Rationale for regional therapy after resection of liver metastases is that hepatic metastases are perfused almost exclusively by the hepatic artery, while normal hepatocytes derive their blood supply from the portal vein, which provides the basis for the use of regional hepatic arterial infusion (HAI) therapy after resection of hepatic metastases. Though favorable long-term results can be achieved after surgery for colorectal metastases to the liver, recurrences both intrahepatic and extrahepatic commonly occur[5,6]. Tumor cells from colorectal carcinoma spread hematogenously

via the pertal circulation, making liver the first site of metastases. The most common site of failure after resection is within the remnant liver. Hence, additional therapy, either regional or systemic or both, has potential as an adjunct treatment after surgery. Extraction of drugs from the hepatic arterial circulation ensures high drug concentrations to residual cancer cells while minimizing systemic toxicity, provided the agent used has a high first-pass extraction. Of the various chemotherapy agents, 5-fluoro-2-deoxyuridine (FUDR) is the most commonly used drug for this purpose, which demonstrates 95% hepatic extraction when given via HAI. FUDR via HAI markedly increases its estimated exposure up to 400-fold. 5-FU is the other agent used in this setting of regional therapy and its response rate can be expected higher when used in combination with concomitant leukovorin[7]. Combining 5-FU with other agents by hepatic artery infusion has been proven to be an effective treatment for liver metastases from CRC.

Table 1 summarizes the randomized series of adjuvant intrahepatic therapy (with or without systemic therapy) after potentially curative hepatic resection of metastatic CRC.

A small study by Lygidakis *et al*.[8], prospectively randomized 40 patients to hepatic surgery alone or surgery combined with post-operative regional chemoimmunotherapy via implanted splenic and gastroduodenal arterial catheters, and found that liver resection supplemented with postoperative targeted transarterial locoregional immunotherapy-chemotherapy is associated with optimal results.

Asahara *et al*.[9], conducted a study to evaluate the efficacy of postoperative transarterial infusion chemotherapy for the prevention of recurrence after hepatectomy following curative surgery for colorectal carcinoma. The result showed that the 3- and 4-year survival rates are 100% in the experimental group, and 60% and 47% respectively in the control group.

Kemeny *et al*.[12], tried to improve the outcomes by treating patients with HAI of floxuridine plus systemic fluorouracil after liver resection, and found that a 2-year OS and DFS benefit in HAI group is 86% *vs* 72%, 57% *vs* 42%. After 2 years, the rate of survival free of hepatic recurrence is 90% in the HAI group and 60% in the monotherapy group, suggesting that for patients who undergo resection of liver metastases from CRC, postoperative treatment with a combination of HAI of floxuridine and intravenous fluorouracil improves the outcome.

Tono *et al*.[13], divided 19 patients who underwent curative hepatectomy for metastatic colorectal carcinoma into HAI group and control group. Patients in HAI group received continuous intra-arterial infusion of 5-FU (500 mg/d), 4 d a week for 6 wk. The study showed a significant 1-, 2-, 3-year prolongation of DFS in the HAI group (77.8% *vs* 50.0%, 77.8% *vs* 30.0%, 66.7% *vs* 20.0%, $P = 0.045$). The 1-, 3-, and 5-year cumulative survival rates for the HAI group were 88.9%, 77.8%, and 77.8%, respectively, whereas those of the control group were 100.0%, 50.0%, and 50.0%, respectively. This randomized study reveals that short-term HAI of 5-FU after curative resection of colorectal hepatic metastases is effective in preventing the recurrence of disease and has no serious complications.

Kemeny *et al*.[14], studied the effect of postoperative hepatic arterial floxuridine combined with intravenous continuous infusion of fluorouracil on the OS and DFS of patients, and found that the 4-year recurrence-free rate is 25% in the control group and 46% in the chemotherapy group, the median survival time of the 75 assessable patients is 49 mo in the control group and 63.7 mo in the chemotherapy group, demonstrating that adjuvant intra-arterial and intravenous chemotherapy is beneficial to the prevention of hepatic recurrence after hepatic resection of CRC.

However, in a German co-operative multicenter study[11], patients were randomized to resection only or resection plus 6 mo of HAI of 5-FU/LV given as a 5-d continuous

Table 1 Randomized series of adjuvant intrahepatic arterial chemotherapy after surgical resection of hepatic metastases

Authors	Treatment protocol	Sample size (Tx / Ctl)	Observation time	DFS Tx *vs* Ctl	OS Tx *vs* Ctl	Conclusions
Lygidakis *et al*.[8]	Surgery+HAI chemoimmunotherapy *vs* surgery alone	40 (20 / 20)	3 yr	NA	Median 20 *vs* 11 (mo) ($P<0.05$)	Beneficial
Asahara *et al*.[9]	Surgery+HAI chemotherapy *vs* surgery alone	38 (10 / 28)	NA	NA	3-yr 100% *vs* 60% 4-yr 100% *vs* 47%, respectively ($P<0.05$)	Beneficial
Rudroff *et al*.[10]	Surgery+HAI 5-FU / MMC *vs* surgery alone	30 (14 / 16)	5 yr	5-yr 15% *vs* 23% ($P>0.05$)	5-yr 25% *vs* 31% ($P>0.05$)	Not beneficial
Lorenz *et al*.[11]	Surgery+HAI 5-FU / LV *vs* surgery alone	226 (113 / 113)	NA	Median 14.2 *vs* 13.7 (mo) ($P>0.05$)	Median 34.5 *vs* 40.8 (mo) ($P>0.05$)	Not beneficial
Kemeny *et al*.[12]	Surgery+HAI FUDR / DEXA+IV 5-FU / LV *vs* surgery+IV 5-FU / LV	156 (74 / 82)	2 yr	2-yr 57% *vs* 42% ($P = 0.07$)	2-yr 86% *vs* 72% ($P = 0.03$)	Beneficial
Tono *et al*.[13]	Surgery+HAI 5-FU+oral 5-FU *vs* surgery+oral 5-FU	19 (9 / 10)	62.2 (mo) (mean)	1-, 2-, 3-yr 77.8%, 77.8%, 66.7% *vs* 50.0%, 30.0%, 20.0% respectively ($P = 0.045$)	1-, 2-, 3-yr 88.9%, 77.8%, 77.8% *vs* 100.0%, 50.0%, and 50.0% respectively ($P = 0.2686$)	Beneficial
Kemeny *et al*.[14]	Surgery+HAI FUDR+IV 5-FU vs surgery	109 (53 / 56)	NA	4-yr 46% *vs* 25% ($P = 0.04$)	Median 63.7 *vs* 49 (mo) ($P = 0.60$)	Beneficial

Tx: treatment; Ctl: control; DFS: disease-free survival; OS: overall survival; NA: not available.

infusion every 28 d. No differences in time-to-progression, time-to-hepatic progression, or median OS are noted in this study.

Rudroff *et al*.[10], evaluated the preventive effect of adjuvant intra-arterial chemotherapy after R0 liver resection and found that there is no significant difference in either 5-year survival or long-term disease-free status between the two groups. They concluded that routine application of adjuvant regional chemotherapy after R0 liver resection is not warranted.

A recent meta-analysis[15] also showed that hepatic artery chemotherapy after curative hepatectomy metastases cannot improve the OS.

The above data suggest that adjuvant intrahepatic arterial chemotherapy combined with or without intravenous chemotherapy can inhibit the recurrence, and that the toxicity and side effects are tolerable.

At present, the superior rates of response and survival reported with irinotecan- and oxaliplatin-based regimens[16-19] provide a new standard first-line treatment of metastatic CRC, which have led to more clinical trials to re-evaluate the efficiency of HAI combining irinotecan or oxaliplatin on recurrence after curative hepatectomy for CRC. At the Memorial Sloan-Kettering Cancer Center (MSKCC), a phase I/II study used HAI with floxuridine and dexamethasone in combination with systemic irinotecan as adjuvant therapy following curative hepatectomy in 90 CRC patients. The maximum tolerable dose of combined HAI+systemic irinotecan is 0.12 mg/kg FUDR with systemic CPT-11 at 200 mg/m^2 every other week, the 2-year survival rate is 87%[20-22]. Oxaliplatin, a new cytotoxic agent, when used in combination with 5-FU/LV (FOLFOX), can achieve more than 50% clinical response and a median survival time of 16.2 mo in untreated patients with metastatic CRC[18,19], suggesting that oxaliplatin-based regimens combined with HAI of FUDR have a promising result.

HAI of FUDR plus systemic 5-FU/LV following resection of hepatic metastases decreases local recurrence and improves OS. It is necessary to further study the effect of HAI combing newer systemic agents, such as irinotecan and oxaliplatin and to make it clear which combination of regimens are the most effective and well-tolerated.

Systemic chemotherapy

While patients who undergo resection of liver metastases from CRC can prolong their survival time, the majority will have relapse not only intrahepatically but also extrahepatically. Therefore, the investigation of adjuvant therapies designed to decrease relapse is warranted. Adjuvant chemotherapy via HAI after resection of liver metastases has shown its efficacy in terms of both disease-free survival (DFS) and OS. On the contrary, the role of "adjuvant" chemotherapy following liver resection for hepatic colorectal metastases remains unclear. Some retrospective trials about adjuvant 5-FU-based systemic chemotherapy have not shown any significant survival benefit[18,19]. Few prospective randomized studies have been performed to answer the question whether postoperative chemotherapy improves survival in comparison to liver resection alone. However, the effects on survival of postoperative systemic chemotherapy are currently under evaluation. The following are recent RCT studies on systemic chemotherapy (Table 2).

Lopez-Ladron *et al*.[24], studied the outcome of 38 patients with resection of liver metastases from CRC, and found that the median OS time of patients who did not receive CT is 15 mo, while patients who received CT after hepatic surgery have a median survival time of 30 mo. The actual OS of patients who received adjuvant CT seems to be higher, suggesting that these results should be confirmed in phase III studies.

An intergroup multicentric randomized study[23] was performed to evaluate the value of FU/FA after complete resection of liver metastases compared to surgery alone. The result is in favor of patients who received systemic chemotherapy after resection of liver metastases.

At present, more studies are focused on the effect of HAI combined with systemic chemotherapy on the OS and DFS[12,14] (Table 1).

In general, systemic chemotherapy alone cannot inhibit recurrence in patients after resection of hepatic colorectal metastases, although systemic 5-FU/LV and HAI of FUDR following resection of hepatic metastases decrease local recurrence and improve 2-year survival. Both hepatic and extrahepatic relapses remain a problem. Studies on newer systemic agents such as irinotecan and oxaliplatin are under way.

Neoadjuvant therapy

The application of neoadjuvant chemotherapy has a number of potential advantages in patients with resectable liver metastases. Firstly, it helps the selection of chemotherapeutic agents after resection. The degree of response gives information on the *in vivo* chemosensitivity of the tumor. In patients with fewer responses or severe toxicity, the same agents should be avoided and alternative agents should

Table 2 RCT studies on efficacy of systemic chemotherapy on prevention of recurrence

Authors	Treatment protocol	Sample size (Tx/Ctl)	Observation time	DFS Tx *vs* Ctl	OS Tx *vs* Ctl	Conclusions
Lopez-Ladron *et al*.[24]	Surgery+post-operative chemotherapy vs surgery alone	38 (28/10)	Median 15 (mo)	Median 15 *vs* 9 (mo) (P = 0.352)	Median 30*vs*15 (mo) (P = 0.066)	Not beneficial, needing further study
Portier *et al*.[23]	Surgery+post-operative chemotherapy (FU/FA) vs surgery alone	162 (81/81)	5 yr	5-yr 33% *vs* 24% (P>0.05)	5-yr 51% *vs* 44% (P>0.05)	Not beneficial

Tx: treatment; Ctl: control; DFS: disease-free survival; OS: overall survival; NA: not available.

Table 3 RCTs on efficacy of neoadjuvant chemotherapy

Authors	Treatment protocol	Sample size (Tx / Ctl)	Observation time	DFS Tx *vs* Ctl	OS Tx *vs* Ctl	Conclusions
Lorenz *et al*.[29]	Biweekly FOLFOX regimen×6 cycles *vs* biweekly FOLFOX regimen×3 cycles	40 (20 / 20)	NA	NA	NA	Induced significant remissions without increasing morbidity
Bathe *et al*.[30]	5-FU+leukovorin+CPT-11					Ongoing

Tx: treatment; Ctl: control; DFS: disease-free survival; OS: overall survival; NA: not available.

be considered after resection. Secondly, neoadjuvant chemotherapy may also help the selection of candidates for resection, which means patients who develop extrahepatic disease during a short course of chemotherapy are unsuitable for resection in the first place. Finally, neoadjuvant chemotherapy enhances resectability in some instances[25-27]. Reduction of tumor volume may limit the amount of liver that needs to be removed to accomplish eradication of the tumor and preserve more normal hepatic tissues.

Most reports on neoadjuvant chemotherapy for liver metastasis focus on the strategies for unresectable tumors[25,28]. The reported resectability rate ranges from 10% to 40% for unresectable colorectal liver metastases after preoperative chemotherapy.

Recently, Lorenz *et al*.[29], conducted a prospective pilot study of neoadjuvant chemotherapy with 5-fluorouracil, folinic acid and oxaliplatin for resectable liver metastases of CRC, and found that neoadjuvant chemotherapy for resectable liver metastases induces significant remissions without increasing morbidity (Table 3).

Due to the potential advantage in patients with resectable liver metastases and new regimens using either oxaliplatin or irinotecan in combination with 5-FU, one phase II study[30] of neoadjuvant 5-FU+leukovorin+CPT-11 in patients with resectable liver metastases from colorectal adenocarcinoma is under investigation. The general aim of this study is to determine the efficacy of neoadjuvant chemotherapy for patients with ablatable liver metastases from CRC in reducing recurrence rate. Response to the chemotherapy regimen will constitute an *in vivo* chemosensitivity test, and this will guide adjuvant chemotherapy following resection of liver metastases from CRC.

Immunotherapy

Since early 1990s, immunotherapy has become a very attractive cancer treatment modality. However, it is not so effective as expected in a number of clinical trials[31,32]. Recently a series of clinical trials have begun to investigate the effect immunotherapy on recurrence of cancer after surgery. The summary of these RCTs are as follows (Table 4).

Lygidakis *et al*.[8], compared the effect of liver resection combined with post-operative locoregional immunotherapy +chemotherapy on recurrence after curative hepatectomy of hepatic colorectal metastases, and found that the survival time of control group ranges from 4 to 25 mo (mean 11 mo), suggesting that liver resection in combination with postoperative targeted transarterial locoregional immunotherapy -chemotherapy is associated with good results. It is highly recommended as the procedure of choice for patients with liver metastasis of colorectal carcinoma.

Lygidakis *et al*.[33], showed the same results, which support post-operatively locoregional chemotherapy for hepatic metastases of CRC. Lygidakis *et al*.[34], reported that regional immunochemotherapy combined with systemic chemotherapy leads to a lower incidence of disease recurrence and a significant prolongation of the OS and DFS time.

Table 4 RCTs of immunotherapy

Authors	Treatment protocol	Sample size (Tx / Ctl)	Observation time	DFS Tx *vs* Ctl	OS Tx *vs* Ctl	Conclusions
Lygidakis *et al*.[8]	Surgery+post-operative HAI immunochemotherapy *vs* surgery alone	40 (20 / 20)	3 yr	NA	Median 20 *vs* 11 (mo) (P<0.05)	Beneficial
Lygidakis *et al*.[33]	Post-operatively locoregional immunochemotherapy *vs* post-operatively locoregional chemotherapy	45 (33 / 15)	NA	NA	Median 20.3 *vs* 9.9 (mo)	Beneficial
Lygidakis *et al*.[34]	Locoregional chemoimmunotherapy with systemic chemotherapy *vs* systemic immunochemotherapy	122 (62 / 60)	NA	2-yr 66% *vs* 48%	2-yr 92% *vs* 75% 5-yr 73% *vs* 60%	Beneficial
Elias *et al*.[35]	Preoperative rIL-2 continuous intravenous infusion	19 (12 / 7)	NA	NA	NA	Beneficial (well tolerated and reverse postoperative immunodepression)
Gardini *et al*.[36]	Post-operative TIL+IL-2 *vs* post-operative+chemotherapy	45 (25 / 22)	NA	1-, 3-, and 5- yr No difference	1-, 3-, and 5-yr No difference	Not beneficial

Tx: treatment; Ctl: control; DFS: disease-free survival; OS: overall survival; NA: not available.

Elias *et al*.[35], investigated prehepatectomy immunostimulation with recombinant interleukin-2 (rIL-2) and evaluated the tolerance of rIL-2 in association with major hepatectomy to verify the effect of preoperative immunostimulation (neoadjuvant immunotherapy), and found that toxicity during rIL-2 infusion is acceptable, suggesting that infusion of rIL-2 before major hepatectomy for liver metastases of CRC is well tolerated and reverses postoperative immunodepression.

Gardini *et al*.[36], also studied immunotherapy with tumor infiltrating lymphocytes (TIL) plus interleukin-2 (IL-2) as adjuvant treatment, and found that there are no significant differences in the actual and DFS rates after 1, 3, and 5 years, suggesting that whether TIL+IL-2 treatment is an effective adjuvant therapy needs to be further studied.

SUMMARY

Number of preventive treatment protocols for inhibiting recurrence after curative resection of liver metastases from colorectal origin have been evaluated by RCT. Although no standard treatment has been proven to be effective in all patients, several approaches present promising results, which are both effective and tolerable in post-operative patients. Generally intrahepatic arterial infusion chemotherapy is effective in preventing the recurrence of disease without serious complications, while systemic chemotherapy is not in favor of patients who receive systemic chemotherapy after liver metastases resection. Neoadjuvant chemotherapy has shown an advantage in patients with resectable liver metastases. Immunotherapy approaches can achieve a better outcome, but need more evidence before wide acceptance.

REFERENCES

1 **Liu LX,** Zhang WH, Jiang HC. Current treatment for liver metastases from colorectal cancer. *World J Gastroenterol* 2003; **9**: 193-200
2 **Cavallari A,** Vivarelli M, Bellusci R, Montalti R, De Ruvo N, Cucchetti A, De Vivo A, De Raffele E, Salone M, La Barba G. Liver metastases from colorectal cancer: present surgical approach. *Hepatogastroenterology* 2003; **50**: 2067-2071
3 **Teh CS,** Ooi LL. Hepatic resection for colorectal metastases to the liver: the national cancer centre/singapore general hospital experience. *Ann Acad Med Singapore* 2003; **32**: 196-204
4 **Fong Y,** Fortner J, Sun RL, Brennan MF, Blumgart LH. Clinical score for predicting recurrence after hepatic resection for metastatic colorectal cancer: analysis of 1001 consecutive cases. *Ann Surg* 1999; **230**: 309-318
5 **Topal B,** Kaufman L, Aerts R, Penninckx F. Patterns of failure following curative resection of colorectal liver metastases. *Eur J Surg Oncol* 2003; **29**: 248-253
6 **Nakajima Y,** Nagao M, Ko S, Kanehiro H, Hisanaga M, Aomatsu Y, Ikeda N, Shibaji T, Ogawa S, Nakano H. Clinical predictors of recurrence site after hepatectomy for metastatic colorectal cancer. *Hepatogastroenterology* 2001; **48**: 1680-1684
7 **Rustum YM,** Harstrick A, Cao S, Vanhoefer U, Yin MB, Wilke H, Seeber S. Thymidylate synthase inhibitors in cancer therapy: direct and indirect inhibitors. *J Clin Oncol* 1997; **15**: 389-400
8 **Lygidakis NJ,** Ziras N, Parissis J. Resection versus resection combined with adjuvant pre- and post-operative chemotherapy-immunotherapy for metastatic colorectal liver cancer. A new look at an old problem. *Hepatogastroenterology* 1995; **42**: 155-161
9 **Asahara T,** Kikkawa M, Okajima M, Ojima Y, Toyota K, Nakahara H, Katayama K, Itamoto T, Marubayashi S, One E, Yahata H, Dohi K, Azuma K, Ito K. Studies of postoperative transarterial infusion chemotherapy for liver metastasis of colorectal carcinoma after hepatectomy. *Hepatogastroenterology* 1998; **45**: 805-811
10 **Rudroff C,** Altendorf-Hoffmann A, Stangl R, Scheele J. Prospective randomised trial on adjuvant hepatic-artery infusion chemotherapy after R0 resection of colorectal liver metastases. *Langenbecks Arch Surg* 1999; **384**: 243-249
11 **Lorenz M,** Muller HH, Schramm H, Gassel HJ, Rau HG, Ridwelski K, Hauss J, Stieger R, Jauch KW, Bechstein WO, Encke A. Randomized trial of surgery versus surgery followed by adjuvant hepatic arterial infusion with 5-fluorouracil and folinic acid for liver metastases of colorectal cancer. German Cooperative on Liver Metastases (Arbeitsgruppe Lebermetastasen). *Ann Surg* 1998; **228**: 756-762
12 **Kemeny N,** Huang Y, Cohen AM, Shi W, Conti JA, Brennan MF, Bertino JR, Turnbull AD, Sullivan D, Stockman J, Blumgart LH, Fong Y. Hepatic arterial infusion of chemotherapy after resection of hepatic metastases from colorectal cancer. *N Engl J Med* 1999; **341**: 2039-2048
13 **Tono T,** Hasuike Y, Ohzato H, Takatsuka Y, Kikkawa N. Limited but definite efficacy of prophylactic hepatic arterial infusion chemotherapy after curative resection of colorectal liver metastases: A randomized study. *Cancer* 2000; **88**: 1549-1556
14 **Kemeny MM,** Adak S, Gray B, Macdonald JS, Smith T, Lipsitz S, Sigurdson ER, O'Dwyer PJ, Benson AB 3rd. Combined-modality treatment for resectable metastatic colorectal carcinoma to the liver: surgical resection of hepatic metastases in combination with continuous infusion of chemotherapy-an intergroup study. *J Clin Oncol* 2002; **20**: 1499-1505
15 **Nelson RL,** Freels S. A systematic review of hepatic artery chemotherapy after hepatic resection of colorectal cancer metastatic to the liver. *Dis Colon Rectum* 2004; **47**: 739-745
16 **Douillard JY,** Cunningham D, Roth AD, Navarro M, James RD, Karasek P, Jandik P, Iveson T, Carmichael J, Alakl M, Gruia G, Awad L, Rougier P. Irinotecan combined with fluorouracil compared with fluorouracil alone as first-line treatment for metastatic colorectal cancer: a multicentre randomised trial. *Lancet* 2000; **355**: 1041-1047
17 **Saltz LB,** Cox JV, Blanke C, Rosen LS, Fehrenbacher L, Moore MJ, Maroun JA, Ackland SP, Locker PK, Pirotta N, Elfring GL, Miller LL. Irinotecan plus fluorouracil and leucovorin for metastatic colorectal cancer. Irinotecan Study Group. *N Engl J Med* 2000; **343**: 905-914
18 **de Gramont A,** Figer A, Seymour M, Homerin M, Hmissi A, Cassidy J, Boni C, Cortes-Funes H, Cervantes A, Freyer G, Papamichael D, Le Bail N, Louvet C, Hendler D, de Braud F, Wilson C, Morvan F, Bonetti A. Leucovorin and fluorouracil with or without oxaliplatin as first-line treatment in advanced colorectal cancer. *J Clin Oncol* 2000; **18**: 2938-2947
19 **Tournigand C,** Louvet C, Quinaux E, Andre T, Lledo G, Flesch M, Ganem G, Landi B, Colin P, Denet C, Mery-Mignard D, Risse ML, Buyse M, de Gramont A. FOLFIRI Followed by FOLFOX Versus FOLFOX Followed by FOLFIRI in Metastatic Colorectal Cancer (MCRC): Final Results of a Phase III Study. *Proc Am Soc Clin Oncol* 2001; abstr494. Available from: URL: http://www.asco.org/ac/1,1003,_12-002643-00_18-0010-00_19-00494,00.asp
20 **Jarnagin WR,** Gonen M, Blumgart L, Sperber D, Koenigsberg A, Fong Y, Kemeny N. Completed phase I trial of hepatic arterial infusion with floxuridine and dexamethasone in combination with systemic irinotecan after resection of hepatic metastases from colorectal cancer. *Proc Am Soc Clin Oncol* 2003; abstr 1073. Available from: URL: http://www.asco.org/ac/1,1003,_12-002643-00_18-0023-00_19-00100969,00.asp
21 **Ruers T,** Bleichrodt RP. Treatment of liver metastases, an update on the possibilities and results. *Eur J Cancer* 2002; **38**: 1023-1033
22 **Yap B,** Sheen A, Eaton D, Swindell R, James R, Levine E, Valle J, Hawkins R, Sherlock D, Saunders M. A large single centre cohort of adjuvant chemotherapy following curative resec-

tion of hepatic colorectal metastases. *Proc Am Soc Clin Oncol* 2002; abstr 2367. Available from: URL: http://www.asco.org/ac/1,1003,_12-002643-00_18-0016-00_19-002367,00.asp

23 **Portier G,** Rougier P, Milan C, Bouché O, Gillet M, Bosset JF, Ducreux M, Saric J, Bugat R, Stremsdoerfer N, Nordlinger B, Bedenne L, Lazorthes F. Adjuvant systemic chemotherapy (CT) using 5-fluorouracil (FU) and folinic acid (FA) after resection of liver metastases (LM) from colorectal (CRC) origin. Results of an intergroup phase III study (trial FFCD - ACHBTH - AURC 9002). *Proc Am Soc Clin Oncol* 2002; abstr 528. Available from: URL:http://www.asco.org/ac/1,1003,_12-002643-00_18-0016-00_19-00528,00.asp

24 **Lopez-Ladron A,** Salvador J, Bernabe R, Bernardos A, Arriola E, Serrano J, Reina JJ, Gomez MA, Barneto I, Moreno-Nogueira JA. Observation versus postoperative chemotherapy after resection of liver metastases in patients with advanced colorectal cancer. *Proc Am Soc Clin Oncol* 2003 abstr 1497. Available from: URL:http://www.asco.org/ac/1,1003,_12-002643-00_18-0023-00_19-00104357,00.asp

25 **Bismuth H,** Adam R, Levi F, Farabos C, Waechter F, Castaing D, Majno P, Engerran L. Resection of nonresectable liver metastases from colorectal cancer after neoadjuvant chemotherapy. *Ann Surg* 1996; **224**: 509-520

26 **Meric F,** Patt YZ, Curley SA, Chase J, Roh MS, Vauthey JN, Ellis LM. Surgery after downstaging of unresectable hepatic tumors with intra-arterial chemotherapy. *Ann Surg Oncol* 2000; **7**: 490-495

27 **Adam R,** Huguet E, Azoulay D, Castaing D, Kunstlinger F, Levi F, Bismuth H. Hepatic resection after down-staging of unresectable hepatic colorectal metastases. *Surg Oncol Clin N Am* 2003; **12**: 211-220

28 **Clavien PA,** Selzner N, Morse M, Selzner M, Paulson E. Downstaging of hepatocellular carcinoma and liver metastases from colorectal cancer by selective intra-arterial chemotherapy. *Surgery* 2002; **131**: 433-442

29 **Lorenz M,** Staib-Sebler E, Gog C, Proschek D, Jauch KW, Ridwelski K, Hohenberger W, Gassel HJ, Lehmann U, Vestweber KH, Padberg W, Zamzow K, Muller HH. Prospective pilot study of neoadjuvant chemotherapy with 5-fluorouracil, folinic acid and oxaliplatin in resectable liver metastases of colorectal cancer. Analysis of 42 neoadjuvant chemotherapies. *Zentralbl Chir* 2003; **128**: 87-94

30 **Bathe OF,** Dowden S, Sutherland F, Dixon E, Butts C, Bigam D, Walley B, Ruether D, Ernst S. Phase II study of neoadjuvant 5-FU + leucovorin + CPT-11 in patients with resectable liver metastases from colorectal adenocarcinoma. *BMC Cancer* 2004; **4**: 32

31 **Hanna MG Jr,** Hoover HC Jr, Vermorken JB, Harris JE, Pinedo HM. Adjuvant active specific immunotherapy of stage II and stage III colon cancer with an autologous tumor cell vaccine: first randomized phase III trials show promise. *Vaccine* 2001; **19**: 2576-2582

32 **Huncharek M,** Caubet JF, McGarry R. Single-agent DTIC versus combination chemotherapy with or without immunotherapy in metastatic melanoma: a meta-analysis of 3273 patients from 20 randomized trials. *Melanoma Res* 2001; **11**: 75-81

33 **Lygidakis NJ,** Stringaris K, Kokinis K, Lyberopoulos K, Raptis S. Locoregional chemotherapy versus locoregional combined immuno-chemotherapy for patients with advanced metastatic liver disease of colorectal origin: a prospective randomized study. *Hepatogastroenterology* 1996; **43**: 212-220

34 **Lygidakis NJ,** Sgourakis G, Vlachos L, Raptis S, Safioleas M, Boura P, Kountouras J, Alamani M. Metastatic liver disease of colorectal origin: the value of locoregional immunochemotherapy combined with systemic chemotherapy following liver resection. Results of a prospective randomized study. *Hepatogastroenterology* 2001; **48**: 1685-1691

35 **Elias D,** Farace F, Triebel F, Hattchouel JM, Pignon JP, Lecesne A, Rougier P, Lasser P, Duvillard P, Escudier B. Phase I-II randomized study on prehepatectomy recombinant interleukin-2 immunotherapy in patients with metastatic carcinoma of the colon and rectum. *J Am Coll Surg* 1995; **181**: 303-310

36 **Gardini A,** Ercolani G, Riccobon A, Ravaioli M, Ridolfi L, Flamini E, Ridolfi R, Grazi GL, Cavallari A, Amadori D. Adjuvant, adoptive immunotherapy with tumor infiltrating lymphocytes plus interleukin-2 after radical hepatic resection for colorectal liver metastases: 5-year analysis. *J Surg Oncol* 2004; **87**: 46-52

Science Editor Wang XL and Guo SY **Language Editor** Elsevier HK

PO Box 2345, Beijing 100023, China
www.wjgnet.com
wjg@wjgnet.com

ELSEVIER

World J Gastroenterol 2005;11(25):3823-3829
World Journal of Gastroenterology ISSN 1007-9327

• *ESOPHAGEAL CANCER* •

Impact of simultaneous assay, the PCNA, cyclinD1, and DNA content with specimens before and after preoperative radiotherapy on prognosis of esophageal cancer-possible incorporation into clinical TNM staging system

Shu-Chai Zhu, Ren Li, Yu-Xiang Wang, Wei Feng, Juan Li, Rong Qiu

Shu-Chai Zhu, Ren Li, Yu-Xiang Wang, Wei Feng, Juan Li, Rong Qiu, Department of Radiation Oncology, Fourth Hospital, Hebei Medical University, Shijiazhuang 050011, Hebei Province, China
Supported by the Distinguished Young Teacher Programs Foundation of Ministry of Education of China, No. 2001125
Co-first-author: Ren Li
Correspondence to: Professor Shu-Chai Zhu, Department of Radiation Oncology, Fourth Hospital, Hebei Medical University, Jiankanglu 12, Shijiazhuang 050011, Hebei Province, China. sczhu@heinfo.net
Telephone: +86-311-6033941-317 Fax: +86-311-6992121
Received: 2004-10-26 Accepted: 2004-12-26

Abstract

AIM: The aim of the present study is to use immunohistochemical methods to investigate the clinical implications of tumor markers in esophageal squamous cell carcinoma and evaluate their impact on prognosis.

METHODS: From November 1990 to December 1996, 47 patients were treated with preoperative radiation followed by radical esophagectomy. All patients were confirmed pathologically as suffering from squamous cell carcinoma. Immunohistochemical stain was done for PCNA, cyclinD1 protein expression and DNA content analyzed by image cytometry. Kaplan-Meier method for single prognostic factor and log-rank test was used to test the significant difference. Cox stepwise regression model and prognosis index model were used for survival analysis with multiple prognostic factors.

RESULTS: Radio-pathological change, T stage and N stage, as the traditional prognostic factors had statistical difference in 3-, 5- and 10-year survival rates. While, tumor cell proliferating marked PCNA, cyclinD1 and DNA content served as independent prognostic factors of esophageal carcinoma. There was definitely an identity between the single and multiple factor analyses. PI was more accurate to evaluate the prognosis of esophageal carcinoma.

CONCLUSION: It is possible that tumor cell proliferating marked PCNA, cyclinD1 and DNA content would become the endpoints for evaluating the prognosis of esophageal carcinoma.

Key words: Esophageal carcinoma; Radiotherapy; Cell proliferating marker

Zhu SC, Li R, Wang YX, Feng W, Li J, Qiu R. Impact of simultaneous assay, the PCNA, cyclinD1, and DNA content with specimens before and after preoperative radiotherapy on prognosis of esophageal cancer-possible incorporation into clinical TNM staging system. *World J Gastroenterol* 2005; 11(25): 3823-3829
http://www.wjgnet.com/1007-9327/11/3823.asp

INTRODUCTION

Esophageal cancer, the sixth most common cancer worldwide, is one of the most interesting cancers in terms of its geographic distribution, variety of environmental factors including tobacco, alcohol, nutritional deficiencies and nitrosamines[1,2]. The ratio of the incidence rates between high-risk and low-risk areas can be as great as 500:1, e.g., Cixian, in Hebei Province of northern China, has received worldwide attention over the past decades because of its high esophageal cancer incidence. Results from earlier studies show that malignant transformation of human esophageal mucosa is a multistage process. An early indicator of abnormality in persons predisposed to squamous cell carcinoma (SCC) is the proliferation of esophageal epithelial cells, morphologically manifested as basal-cell hyperplasia (BCH) and dysphasia (DYS). However, key molecular changes in the esophageal carcinogenesis still remain to be characterized[3].

Furthermore, genetic factors, such as the activation of oncogene and the inactivation of tumor suppressor genes, are believed to play important roles. Earlier studies have shown the PCNA (proliferating cell nuclear antigen) is a 36-ku, 261-amino acid non-histone polypeptide that is localized in the nucleus and is associated with cell proliferation with function as an auxiliary protein to DNA polymerase-delta. PCNA appears to be necessary for DNA replication and elevated level of this protein at the G_1/S phase transition are present in cells undergoing division[4,5].

Recent evidence has suggested that cyclinD1 gene (also referred to as prad1) amplification might also be involved in the development of esophageal carcinoma. The cyclinD1 gene has been mapped to the chromosome 11q13 locus close to the int2 and hst1 genes. The complex of cyclinD1 protein and cyclin-dependent protein kinases (cdks) may

govern key transitions in the cell cycle. Zhang[6] found that cyclinD1 gene was amplified and its protein expression increased in only one-third of the esophageal SCC. However, the knowledge of the role of cyclinD1 in esophageal carcinogenesis is not yet definite in detail, since the level of cyclinD1 protein in different stages of carcinogenesis of esophageal carcinoma has not been determined[6].

In the current study, it is possible to use only cancer cells for analyzing the DNA patterns and ploidy in cytophotometry. Most investigators have shown in clinical esophageal SCC, high-ploidy tumors grow more rapidly than low-ploidy ones, and the duration from curative esophagectomy to recurrence decreases in proportion to the degree of DNA aneuploidy[7].

Thus, despite aggressive therapy for esophageal cancer, the outcome is generally poor with a large number of patients developing rapid recurrence even after curative operation[8,9]. If the prospect of prognosis and metastasis could be predicted preoperatively, it would be appropriate to select the most adequate treatment for individual cancer patient. Thus multi-disciplinary treatment including chemotherapy and irradiation would be reserved for patients predicted to have a poor prognosis while a less aggressive approach could be undertaken for those with better prognosis. Though most of the previous lectures showing DNA ploidy, AgNoRs and amplification of some oncogenes had been investigated to determine their prognostic value in esophageal cancer, the indication by PCNA, cyclinD1 protein expression combined with DNA ploidy have not been reported. It is expected to be of interest to evaluate them together as predictors of the malignant potential. In this report, we examined the cyclinD1, PCNA protein and DNA ploidy of esophageal carcinoma in 47 paired specimens from endoscopic biopsy and surgical resection tissue, with biologic features and prognostic value was also discussed.

MATERIALS AND METHODS

Patients

There are 47 patients (median age 62 years, range 33-74 years, 28 males and 19 females) with SCC of esophagus treated from November 1990 to December 1993 by preoperative radiotherapy followed by curative esophagectomy at the Fourth Hospital, Hebei Medical University, in northern China. All patients had been examined by gastrointestinal endoscopy, barium swallow, chest X-ray and liver ultrasound scans. Patients with stage IV disease shown by computed tomography were excluded. Pathological evaluation done according to the criteria established by the Chinese Society for Esophageal Disease (Henan,1987), showed all patients were suffering from SCC. We had obtained two sets of specimens from each patient: endoscopic biopsy before preoperative radiotherapy and the surgical specimens of the same patient after esophagectomy of which the tumor markers in all 47 paired specimens were investigated. The maximum follow-up was 144 mo with a median of 56 mo.

Radiotherapy

All the 47 patients received preoperative radiotherapy, the external beam radiation was given by a 10-MV X-ray (Linear Accelerator, SIEMENS, PRIMUS) using the conventional fractionated irradiation. The irradiated volume included the gross tumor with a safety margin of 5.0 cm both proximally and distally. Treatment was given through two opposing fields (anterior and posterior); 2.0 Gy was delivered daily for 5 d a wk to a total dose of 30-40 Gy in 15-20 fractions over 3-4 wk.

Esophagectomy

Transthoracic esophagectomy, the most common approach through a right or left thoracotomy incision depending on the preference of the surgeon and the location of the tumor was performed. Tumor located in the lower third of the esophagus usually was approached through a left thoracotomy. A left sixth interspace incision provides excellent exposure of the lower mediastinum. Gastrointestinal reconstruction was subsequently achieved by prepared esophageal substitute (usually the stomach), by passing of a prepared esophageal substitute, usually the stomach underneath the aortic arch and suture to the esophageal stump. Definite esophagectomy was undertaken 3 wk after radiotherapy.

Immunohistochemical stain

Biopsy and surgical specimens were fixed in 40 g/L formaldehyde and embedded in paraffin wax. Five-micron sections cut from each specimen, dewaxed in xylene, rehydrated through grading concentrations of ethanol were immersed in 3% hydrogen peroxide to block the endogenous peroxidase and washed in phosphate buffered saline. For cyclinD1 and PCNA immunohistochemical stain, tissue sections were heated in 10 mmol/L sodium citrate (pH 6.0) in a microwave oven for 10 min to expose the antigens, and, then, treated with normal goat serum (10%) before staining to reduce nonspecific antibody binding. Tissue sections were incubated at 4 ℃ overnight for cyclinD1. CyclinD1 and PCNA stain with the following antibodies: mouse monoclonal anti-cyclinD1 antibody (Novocastra Laboratories Ltd., UK) at 1:20 dilution and mouse monoclonal anti-PCNA antibody (PC-10, Dakopath,Glostrup, Denmark) at 1:100 dilution. The sections were then washed and incubated with biotinylated goat anti-rabbit IgG (Vector Laboratories, Burlingame, CA) at room temperature for 30 min. After washing, the sections were incubated with avidin-biotin-peroxidase complex at room temperature for 30 min with the vectastain Elite ABC kit (Vector Laboratories Burlingame, CA). Color developed with 3,3-diaminobenzidine as the substrate. Sections were counter-stained with Harris acid hematoxylin to demonstrate the specificity of the immunostain and the primary antibodies were replaced with similar protein concentrations of normal rabbit IgG.

The PCNA, cyclinD1 protein expression of the endoscopic biopsy and surgical specimens were compared by two histopathologists by the double-blind arrangement in assessing the tumor response to radiotherapy. For cyclinD1 and PCNA, 1 000 tumor cells in five high-power fields were counted respectively. PCNA index was the percentage of nuclei stained positive. PCNA index greater than 25% was taken as PCNA positive. PCNA index lower than 25% was taken as PCNA-negative. For cyclinD1, positive cell nucleus not found was taken as negative. When the percentage of positive cell nucleus was greater than 30%, it was taken

as strongly positive. Between the two levels, it was positive. Therefore three grades were ascertained for cyclinD1 expression[5,9,10].

Analysis of DNA content

Cellular DNA analysis was performed on paraffin sections cut 100 μm thick. The sections were stained with Feulgen stain and examined using a microspectrophotometer by two-wavelength method. Data processing was carried out with a personal computer (HP-85, Hewlett-Packard, Palo Alto, CA, USA). In each section, the mean DNA value of 20 stromal lymphocytes was used as a control of the normal diploid complement (2C). The relative DNA content as compared with the 2C value was determined in 100 tumor cells in each lesion as previously described[11,12]. The DNA distribution patterns were then classified into four types, according to the degree of the peak and dispersion on the DNA histogram, as follows: Type I, a prominent peak in the 2C region with a dispersion to the 4C region, Type II, a relative high peak in the 2C-3C regions with a dispersion limited to the 6C region, Type III, a low peak beyond the 3C region with less than 20% of the cells beyond the 6C region and Type IV, multiple peaks with a broad dispersion and more than 20% of cells beyond the 6C region.

Statistical analysis

PCNA, cyclinD1 protein expression index and DNA distribution pattern were analyzed and regarded in the clinico-pathological features as determined by the χ^2 test. Difference between the cumulative survival rates of patient groups were calculated by log-rank test for comparison of Kaplan–Meier survival curves. The significance of various parameters on survival were analyzed by multivariate Cox regression model. A P value of 0.05 or less was considered statistically significant (statistical software SPSS 10.0 for Windows).

RESULTS

Response to preoperative radiotherapy and the overall survival of patients

All the patients had received preoperative radiotherapy followed by definite surgical resection. The complete response rate as shown by pathology was 29.8% (14/47) for the entire group treated by preoperative radiotherapy and 5-year survival rate was 71.4% (10/14) for 14 patients with complete response by pathology. The overall survival rates of all these patients in the 3, 5 and 10-years were 54.3%, 46.2% and 38.8%, respectively.

Expression of PCNA, cyclinD1 immunoreactivity and DNA content in the tumor cells by histopathology

PCNA stain was almost entirely confined to the cell nuclei and showed diffuse and granular pattern or a mixture of both. While cyclinD1 stain was present in the cytoplasm around the cell nuclei in most parts, and a few parts in the tumor cell nuclei. At the same time, PCNA stain was observed in the basal layer of stratified squamous epithelium in normal tissue. In this study, all cyclinD1 present both in the stained nuclei and the cytoplasm around them were considered as protein expression positive carcinoma cells. We took both Types I and II DNA content as the low ploidy pattern and Types III and IV as the high ploidy pattern.

Analysis of cyclinD1, PCNA expression and DNA distribution pattern with regard to clinicopathological features and prognosis

Kaplan-Meier method was used to analyze the single factors, including age, sex, irradiation dose, location of disease, length, and radiation response observed by pathology, T stage, N stage, PCNA index, cyclinD1 protein expression and DNA content pattern, e.g. Types I and II or Types III and IV influenced the prognosis of esophageal carcinoma obviously. The P value as checked by the log-rank test $\geqslant 0.05$ was taken as significant. Only the four preoperative radiotherapy factors: radiation changes observed by pathology, T stage, N stage and cyclinD1 protein expression before radiation in the endoscopic biopsies; those observed in the surgery rescected specimens showing, PCNA index, cyclinD1expression level, DNA content pattern, revealed significant difference ($P<0.05$, Table 1), whereas age, sex, total tumor dose, location and length of disease possessed no value in prognosis.

Multiple varieties combined by Cox hazard risk model analysis

T stage, N stage, pathological changes after radiotherapy, pre-radiotherapy cyclinD1 protein expression and post-radiotherapy PCNA index, cyclinD1 protein expression and DNA content pattern with Cox hazard risk regression model were analyzed. The most significant factors were the post-radiotherapy PCNA index and DNA content pattern (specimens from surgical specimens). Furthermore, each factor by single parameter analysis gave the most marked prognostic difference, while multivariation considered by Cox model, clearly affected the prognosis of esophageal cancer patients (Table 2).

Analysis of esophageal squamous cell carcinoma by prognosis index model

According to the formulation of prognosis index (PI) model from statistic software, it was defined as 0 which had the least influence on prognosis. Number 2 had the greatest effect on prognosis .When the number was 1, the prognosis was between 0 and 2. For example, T stage divided by T_1, T_2, T_3 would show difference on patients survival and we gave them the number 0, 1, 2 respectively as shown in Table 2. The group's weight (0, 1, 2 or 0, 1) times the coefficient of Cox regression model (β value). Then by adding each group's data results would give each patient's PI value, e.g., different factors (T stage, N stage, PCNA, cyclinD1 expression, etc.) at the same weight number. For example, all number 0 patients, or number 1 patients, or number 2 patients would give the PI (prognosis index) value for each patient (Table 3).

Different PI values give different prognosis

According to the distribution of PI values in all patients, the four subgroups were divided according to different PI values. PI values lower than 2.0, between 2.0 and 5.0, between 5.0 and 7.0 or higher than 7.0 may go stepwise further with the median survival terms and 3-, 5-, 10-year survival rates of the four subgroup patients would reveal significant

Table 1 Relation between accumulated survival rates and clinicopathological and tumor cell protein expression pre- or post-radiotherapy

Factors	Patient number	Median (mo)	Mean (mo)	3 yr (%)	5 yr (%)	10 yr (%)	Log-rank	*P*
Sex								
Male	28	48	76	60.7	49.7	38.2		
Female	19	27	62	44.9	45.1	38.1	0.6705	0.2513
Age (yr)								
≤50	26	31	66.6	50.4	49.7	36.8		
>50	21	50	74.2	57.7	45.2	39.6	0.2317	0.4084
Total dose								
≤35 Gy	23	53	78.4	56.5	56.5	46.3		
>35 Gy	24	35.5	63.5	52.6	39.6	30.3	0.6470	0.2588
Site of lesion								
Upper-thoracic	10	69.5	81.5	70.0	70.0	46.7		
Middle-thoracic	37	31.0	67.9	50.2	41.7	35.4	0.8864	0.1877
Tumor length								
≤7.0 cm	39	48	77.1	58.1	50.1	41.4		
>7.0 cm	8	22.5	40.0	37.5	37.5	18.8	0.9653	0.1672
Pathological change after radiation								
Grade III	24	93	95.0	70.8	62.3	57.6		
Grade II	15	26	49.3	40.0	40.0	16.0		
Grade I	8	13	38.6	31.1	15.6	15.6	5.1450	0.0764
T stage								
T_1	11	135	112.9	90.9	81.8	61.9		
T_2	19	48	77.5	57.9	46.9	41.0		
T_3	17	19	36.1	26.0	26.0	17.3	8.9800	0.0113
N stage								
N_0	39	60	81.7	61.5	53.7	42.6		
N_1	8	12	17.6	16.7	16.7	0	2.4170	0.0078
Pre-radiotherapy PCNA								
Low expression	21	35.5	67.4	50.0	42.0	32.9		
High expression	26	48	75.1	60.4	55.2	44.2	0.8880	0.1873
Pre-radiotherapy cyclinD1								
Negative	21	135	106.3	80.9	71.4	61.6		
Positive	20	19	46.2	32.5	32.5	24.4		
Strong positive	6	24	28.7	33.3	16.7	0	10.3990	0.0055
Pre-radiotherapy DNA content								
I+II Type	10	98.5	88.9	60.0	60.0	50.0		
III+IV Type	37	40.0	65.9	53.0	44.3	34.3	0.5158	0.3032
Post-radiotherapy PCNA								
Low expression	17	135	107.4	81.5	73.9	61.8		
High expression	30	18	21.4	16.1	9.8	0	4.1124	0.00002
Post-radiotherapy cyclinD1								
Negative	17	77	94.1	76.5	70.4	49.8		
Positive	22	30	64.4	53.1	43.1	37.8		
Strongly positive	8	21	39.0	12.5	12.5	12.5	7.9215	0.0191
Pre-radiotherapy DNA content								
I+II Type	23	135	110.7	87.0	78.3	60.2		
III+IV III+IV Type	24	20	32.5	22.0	16.6	16.6	3.7074	0.0001

Prognostic parameters in 47 patients with SCC of esophagus.

Table 2 Independent predictors of survival in 47 esophageal SCC patients according to multivariate Cox regression analysis

Factors	Group	Group value	β value	SD	*P*	Risk
Pathological radiation change's	III / II / I Grades	0 / 1 / 2	0.6405	0.2451	0.0090	0.1582
Surgical specimens T stage	T_1 / T_2 / T_3	0 / 1 / 2	0.7678	0.2737	0.0050	0.1744
Surgical specimens N stage	N_0 / N_1	0 / 1	1.2957	0.4845	0.0075	0.1634
Pre-radiotherapy cyclinD	N / P / SP	0 / 1 / 2	0.8434	0.2564	0.0010	0.2139
Post-radiotherapy cyclinD1	N / P / SP	0 / 1 / 2	0.6538	0.2643	0.0134	0.1462
Post-radiotherapy PCNA	Low / high expression	0 / 1	2.0965	0.4720	0.0000	0.3032
Post-radiotherapy DNA	I+II Type / III+IV Type	0 / 1	1.5593	0.4287	0.0003	0.2413

Table 3 Formula for calculation of prognosis index with different indicator factors

Factors	Group	Group value (1)	β (2)	prognosis index (PI)1
Pathological radiation change's	III / II / I Grades	0 / 1 / 2	0.6405	(1)x(2)
Surgical specimens T stage	T_1 / T_2 / T_3	0 / 1 / 2	0.7678	(1)x(2)
Surgical specimens N stage	N_0 / N_1	0 / 1	1.2957	(1)x(2)
Pre-radiotherapy cyclinD	N / P / SP	0 / 1 / 2	0.8434	(1)x(2)
Post-radiotherapy cyclinD1	N / P / SP	0 / 1 / 2	0.6538	(1)x(2)
Post-radiotherapy PCNA	low / high expression	0 / 1	2.0965	(1)x(2)
Post-radiotherapy DNA	I+II Type / III+IV Type	0 / 1	1.5593	(1)x(2)

Each prognosis indexes were added together.

differences (Table 4, Figure 1). It was multiple variety combined analysis, which showed a clear difference in survival among the four subgroups.

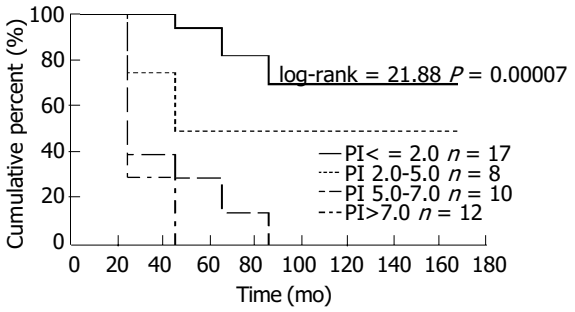

Figure 1 The survival curves with different PI value.

DISCUSSION

Cancer of the esophagus is the most common cancer in northern China, for which current consensus of treatment varies from surgery, radiotherapy, chemotherapy, and endoscopic laser surgery or their combination. The outcome, however, remains dismal because most patients are seen with advanced disease on diagnosis[13-15]. Thus, what the majority of patients need is a multimodality program. Yet how to know which patients really need which modality is still an open focus. Nevertheless, traditional prognostic factors: T stage, N stage are basically the most important. Yet up to now, their application has merely been used by the surgically treated patients. For conservative treatment, besides the TNM classification system, additional variables such as biological staging for the intrinsic malignant potential of the tumor, are to be useful to determine the treatment and long-term survival[16].

Recently, with rapid advance in biological and genetic studies, more and more tumor markers are being correlated with tumor characteristics[8]. The ability to predict, on the basis of immunocytochemical assessment of pretreatment biopsy, which patients are likely to respond to chemoradiotherapy would be a major advance in the management of cancer patients. Thus, it is possible to provide the most adequate protocol for different patients by combining traditional factors and the markers of tumor cells[16].

Several studies[8,9,15] have shown that high PCNA expression in esophageal tumor is associated with a worse prognosis in surgical patients and greater likelihood of recurrence. However, such a report on PCNA, and cyclinD1 protein expression examined simultaneously in biopsy and resected specimens of esophageal carcinoma has never been seen. Nor possible correlation between PCNA, cyclinD1 protein expression and the traditional prognostic factors (T stage, N stage) to chemoradiotherapy has never been investigated. Immunohistochemical detection of PCNA being simple and useful for the study of cell kinetics, allows the retrospective evaluation of the proliferating state of the tumor as it can be used in conventionally fixed materials. Many authors[17,18] showed the higher PCNA index patients usually gave the worse prognosis with local recurrence. In the past years, it has been proved that the combination of PCNA index with the AgNOR count appears to be an effective means of identifying patients with poor prognosis. For patients with a PCNA index of $\geqslant$ 44 and AgNOR count of $\geqslant$ 6, multidisciplinary treatment should be recommended in an attempt to prolong survival. However, in this study, PCNA index as checked by endoscopic biopsies have not shown such influence on survival[9].

Furthermore, we have found PCNA protein expression to be significantly high in surgically resected specimens with PCNA index 63.8% (30/47) compared to the endoscopic biopsy before radiation 55.3% (26/47). At the same time, patients with high PCNA index in the surgically resected specimens had the worse prognosis. PCNA protein expression examined after radiotherapy made a significant difference to esophageal cancer prognosis. The repopulation of tumor cells after radiation may exist which results in local recurrence of esophageal carcinoma after radiotherapy.

Table 4 Median survivals and survival rates with subgroups divided by prognosis index (%)

Prognosis indexes	Number patients	Median month	3 yr	5 yr	10 yr
<2.0	17	146	100	88.2	69.7
2.0-5.0	8	93.5	50	50	50
5.0-7.0	10	20	30	30	0
>7.0	12	13	9.6	0	0

The most important advantage of PCNA, cyclinD1 immunohistochemical assay is that the analysis changes are restricted to the tumor cells. In contrast, flow cytometry assay, all cells in the tissue block are measured and in DNA diploid cases, this means that SPF reflects the sum of cell proliferation that estimates the malignant and benign (stromal and inflammatory cells) components[9].

Most studies[6,19] reported patients with cyclinD1 amplification and protein expressions had a poor outcome and a higher incidence of distant metastasis than those in amplification-negative or protein expression-negative groups. The surgical survival rates and disease-free survival in the high cyclinD1 expression group were significantly shorter than in the cyclinD1 low or non-expression group. CyclinD1 amplification and protein expression in patients with SCC of the esophagus would mean a grave biological malignancy. Naiton *et al*.[20], reported 55 esophageal cancer patients with a ratio of cyclinD1 protein-positive expression of 38% gave a 5-year survival rate of 7%, as compared with the 5-year survival rate of 59% in patients who showed cyclinD1 protein negative expression ($P<0.01$). In 1998, Ishikawa[21] studied cyclinD1 protein expression in esophageal SCC and observed similar results. Our checked results showing higher cyclinD1 protein expression both in endoscopic biopsy and surgical resected specimens also gave bad prognostic results (Table 1).

In our previous study, the clinical characteristics of patients with SCC of the esophagus, such as outcome and distant organ metastases, were found to be closely correlated with cyclinD1 amplication and protein expression in the tumor tissue. It was observed that parameters were independent from clinicopathological factors for the outcome and metastasis. It was the second highest partial regression coefficient after the pN factor in the life table with Cox proportional hazard model, and the probability rate was significant[19,21]. In this study, the same results were obtained. From Table 2, it is apparent that both the cyclinD1 protein expression in biopsy and surgical specimens had a significant effect on the prognosis of SCC of the esophagus. Specially, cyclinD1 protein-positive expression in endoscopic biopsy was the third highest partial regression coefficient after the PCNA index and DNA content in the resected specimens in multivariate analysis using the Cox proportional hazard model. We speculate that the cyclinD1 protein prognostic value maybe relatively high as the most useful factor for predicting the outcome in SCC of the esophagus in the previous study, e.g., pN factor and pT. According to the results of both univariate and multivariate analyses, the fact that patients with cyclinD1 protein-positive had a poor outcome in every group implies this agent is a useful prognostic indicator in esophageal carcinoma. Hence, it may very well supplement the TNM classification for predicting clinical characteristics and outcome, especially for patients who are destined to undergo non-operative treatment. For these patients, TNM classification could hardly be of any assistance to offer an endpoint and select more appropriate protocol for patients with SCC of the esophagus. By checking cyclinD1 protein expression level, the ultimate combined TNM classification could thus be perfected.

The essence of cell division really is the DNA replication and changes of DNA distribution pattern which predict tumor cell proliferation kinetics. Here cytophotometric technique is to analyze the DNA content pattern both in endoscopic biopsy and resected specimens. The most important advantage of DNA content checked by cytophotometric method is that the analysis is restricted to the tumor cells, as compared to flow cytometry, by which all cells in the tumor tissue are measured .It reflects the sum of cell proliferation which estimates both malignant and benign (stromal cell and inflammatory cell) components[9]. In clinical esophageal carcinoma, high-ploidy tumors grow more rapidly than low-ploidy ones and the duration from curative esophagectomy to recurrence decreases in proportion to the degree of DNA aneuploidy, a view believed by many authors.

During early years, some authors[9,11,22] reported the relationship between DNA content of a variety of human cancer cells and their malignant potential as measured by cytophotometric analysis, most of who reported that such measurement are useful in elucidating the pattern of tumor progression or the prognosis with most of the results being negative between DNA content and long-term survival. For example, Miun *et al*.[22], reported 78 esophageal cancer patients who gave 5-year survival rate of 14% and 57% in high DNA content and low DNA content groups with statistical significance in the difference ($P = 0.03$). Matsuura[11] found that not one patient survived over 5 years in DNA triploids or tetraploidy, but the 5-year survival rate was 70% in DNA diploidy patients. Our study shows no influence on survival or prognosis by biopsy DNA content measurement. The measured results may have been inaccurate due to the very small size of biopsy specimens. From Tables 1 and 2, the surgically resected specimens gave DNA content measurement showing significant correlation between the results and the prognosis of SCC of esophagus as assessed by univariate and multivariate analyses. This result conforms well to most of the studies reported so far[9,11].

Through combination of the traditional prognostic factors and tumor cell markers, the radiation pathological changes, T stage, N stage, cyclinD1, PCNA protein expression and DNA content as analyzed by Cox proportional hazard model, it is found that patients with grade III pathological changes, T_1 stage, N_0 stage, cyclinD1 protein-negative, lower PCNA index and DNA content pattern Types I and II, give higher long-term survival than the control groups.

With the total patients divided into four subgroups according to the formulation of prognosis index model, prognosis is observed to be worse with higher prognosis index, giving significant difference in spite of the few patients allotted. This result clearly demonstrates the evaluation of SCC of esophagus by prognosis index model with multivariate factors is dependable and accurate.

ACKNOWLEDGMENTS

The authors wish to thank Ms Laura Kresty for her expert technical assistance and N Sugimoto (Sanwa Kagakau Co., Ltd, Nagoya, Japan) for his support in the statistical analysis.

REFERENCES

1 **Castellsague X,** Munoz N, De Stefani E, Victora CG, Castelletto R, Rolon PA, Quintana MJ. Independent and

joint effects of tobacco smoking and alcohol drinking on the risk of esophageal cancer in men and women. *Int J Cancer* 1999; **82**: 657-664

2 **Zhao WX,** Shi TX, Gao XP, Zhang HX, Li SL. Association of p53, PCNA expression and trace element content in esophageal mucosa. *Aizheng* 2002; **21**: 757-760

3 **Dong WL,** Bin Yue W, Zhou Y, Wei Feng C, Liu B, Zhou Q, Ying Jia Y, Zheng S, Gao SS, Ji Xie X, Min Fan Z, Min Niou H, Hao Zhuang Z, Yang CS, Min Bai Y, Jun Qi Y. Endoscopic screening and determination of p53 and proliferating cell nuclear antigen in esophageal multistage carcinogenesis: a comparative study between high- and low-risk populations in Henan, northern China. *Dis Esophagus* 2002; **15**: 80-84

4 **Gelb AB,** Kamel OW, Le-Brun DP, Wamke RA. Estimation of tumor growth fractions in archival formalin-fixed, paraffin-embedded tissues using two anti-PCNA/Cyclin monoclonal antibodies. Factors affecting reactivity. *Am J Pathol* 1992; **141**: 1453-1458

5 **Siitonen SM,** Kallioniemi OP, Isola JJ. Proliferating cell nuclear antigen immunohistochemistry using monoclonal antibody 19A2 and a new antigen retrieval technique has prognostic impact in archival paraffin-embedded node-negative breast cancer. *Amer J Pathol* 1993; **142**: 1081-1089

6 **Zhang JH,** Li Y, Wang R, Wen D, Sarbia M, Kuang G, Wu M, Wei L, He M, Zhang L, Wang S. Association of cyclinD1 (G870A) polymorphism with susceptibility to esophageal and gastric cardiac carcinoma in a northern Chinese population. *Int J Cancer* 2003; **105**: 281-284

7 **Morita M,** Kuwano H, Tsutsui S, Ohno S, Matsuda H, Sugimachi K. Cytophotometric DNA content and argyrophilic nucleolar organiser regions of oesophageal carcinoma. *Br J Cancer* 1993; **67**: 480-485

8 **Ueno H,** Hirai T, Nishimoto N, Hihara J, Inoue H, Yoshida K, Yamashita Y, Toge T, Tsubota N. Prediction of lymph node metastasis by p53, p21(Waf1), and PCNA expression in esophageal cancer patients. *J Exp Clin Cancer Res* 2003; **22**: 239-245

9 **Kuwano H,** Sumiyoshi K, Nozoe T, Yasuda M, Watanabe M, Sugimachi K. The prognostic significance of the cytophotometric DNA content and its relationship with the argyrophilic nucleolar organizer regions (AgNOR) and proliferating cell nuclear antigen (PCNA) in oesophageal cancer. *Eur J Surg Oncol* 1995; **21**: 368-373

10 **Hagiwara N,** Tajiri T, Tajiri T, Miyashita M, Sasajima K, Makino H, Matsutani T, Tsuchiya Y, Takubo K, Yamashita K. Biological behavior of mucoepidermoid carcinoma of the esophagus. *J Nippon Med Sch* 2003; **70**: 401-407

11 **Ma J,** Nicholas Terry HA, Lin SX, Patel N, Mai HG, Hong MH, Lu TX, Cui NJ, Min HQ. Prognostic significance of DNA ploidy and proliferative indices in patients with nasopharyngeal carcinoma. *Aizheng* 2002; **22**: 644-650

12 **Korenaga D,** Okamura T, Saito A, Baba H, Sugimachi K. DNA ploidy is closely linked to tumor invasion, lymph node metastasis, and prognosis in clinical gastric cancer. *Cancer* 1988; **62**: 309-313

13 **Michel P,** Magois K, Robert V, Chiron A, Lepessot F, Bodenant C, Roque I, Seng SK, Frebourg T, Paillot B. Prognostic value of TP53 transcriptional activity on p21 and bax in patients with esophageal squamous cell carcinomas treated by definitive chemoradiotherapy. *Int J Radiat Oncol Biol Phys* 2002; **54**: 379-385

14 **Wang LS,** Chow KC, Chi KH, Liu CC, Li WY, Chiu JH, Huang MH. Prognosis of esophageal squamous cell carcinoma: analysis of clinicopathological and biological factors. *Am J Gastroenterol* 1999; **94**: 1933-1940

15 **Yasunaga M,** Tabira Y, Nakano K, Iida S, Ichimaru N, Nagamoto N, Sakaguchi T. Accelerated growth signals and low tumor-infiltrating lymphocyte levels predict poor outcome in T4 esophageal squamous cell carcinoma. *Ann Thorac Surg* 2000; **70**: 1634-1640

16 **Horii N,** Nishimura Y, Okuno Y, Kanamori S, Hiraoka M, Shimada Y, Imamura M. Impact of neoadjuvant chemotherapy on Ki-67 and PCNA labeling indices for esophageal squamous cell carcinomas. *Int J Radiat Oncol Biol Phys* 2001; **49**: 527-532

17 **Dabrowski A,** Szumilo J, Brajerski G, Wallner G. Proliferating nuclear antigen (PCNA) as a prognostic factor of squamous cell carcinoma of the oesophagus. *Ann Univ Mariae Curie Sklodowska* 2001; **56**: 59-67

18 **Shiozaki H,** Doki Y, Kawanishi K, Shamma A, Yano M, Inoue M, Monden M. Clinical application of malignancy potential grading as a prognostic factor of human esophageal cancers. *Surgery* 2000; **127**: 552-561

19 **Shamma A,** Doki Y, Shiozaki H, Tsujinaka T, Yamamoto M, Inoue M, Yano M, Monden M. Cyclin D1 overexpression in esophageal dysplasia: a possible biomarker for carcinogenesis of esophageal squamous cell carcinoma. *Int J Oncol* 2000; **16**: 261-266

20 **Naitoh H,** Shibata J, Kawaguchi A, Kodama M, Hattori T. Overexpression and localization of cyclin D1 mRNA and antigen in esophageal cancer. *Am J Pathol* 1995; **146**: 1161-1169

21 **Ishikawa T,** Furihata M, Ohtsuki Y, Murakami H, Inoue A, Ogoshi S. Cyclin D1 overexpression related to retinoblastoma protein expression as a prognostic marker in human oesophageal squamous cell carcinoma. *Br J Cancer* 1998; **77**: 92-97

22 **Minu AR,** Endo M, Sunagawa M. Role of DNA ploidy patterns in esophageal squamous cell carcinoma. An ultraviolet microspectrophotometric study. *Cancer* 1994; **74**: 578-585

Science Editor Li WZ **Language Editor** Elsevier HK

PO Box 2345, Beijing 100023, China
www.wjgnet.com
wjg@wjgnet.com

ELSEVIER

World J Gastroenterol 2005;11(25):3830-3833
World Journal of Gastroenterology ISSN 1007-9327

Anti-cancer effect of iNOS inhibitor and its correlation with angiogenesis in gastric cancer

Guang-Yi Wang, Bai Ji, Xu Wang, Jian-Hua Gu

Guang-Yi Wang, Bai Ji, Xu Wang, Jian-Hua Gu, Department of General Surgery, the First Hospital, Jilin University, Changchun 130021, Jilin Province, China
Supported by the Natural Science Foundation of Jilin Province, No. 20010536
Correspondence to: Dr. Guang-Yi Wang, Department of General Surgery, the First Hospital, Jilin University, Changchun 130021, Jilin Province, China. wgymd@sina.com
Telephone: +86-431-5613331
Received: 2004-12-07 Accepted: 2005-01-05

Abstract

AIM: To observe the anti-cancer effect of iNOS selective inhibitor (aminoguanidine, AG) and investigate the relationship between iNOS inhibitor and angiogenesis, infiltration or metastasis in MFC gastric cancer xenografts.

METHODS: Fifty athymic mice xenograft models were established by inoculating gastric cancer cell MFC subcutaneously. Twenty-four hours later, 0.9% sodium chloride solution, mitomycin, low dosage AG, high dosage AG, mitomycin and AG were administered by intraperitoneal injection respectively. Thus these mice were divided into five groups of 10 each randomly: control group, MMC group, AG_L group, AG_H group, MMC+AG_H group. Two weeks later the mice were killed, and the tumor weight, inhibitory rate were evaluated. Greiss assay was used to detect the nitric oxide levels in plasma. HE and immunohistochemistry staining were used to examine microvessel density (MVD) and the expression of iNOS, VEGF, and PCNA. Apoptosis was detected by using TUNEL assay.

RESULTS: The inhibitory rates in MMC+AG_H group and AG_H group were 52.9% and 47.1% respectively, which is significant statistically compared with that of control group (0). In treatment groups, the cell proliferation index (PI) was lower and apoptosis index was higher than those of control group. Microvessel density, iNOS, and VEGF in MMC+ AG_H group were 8.8±2.6, 2.4±1.1, and 2.1±1.4 respectively, which is significant statistically compared with those of control group (68.3±10.6, 11.3±1.3, and 10.3±1.6). The NO level in plasma of MMC+ AG_H and AG_H group were 12.7±2.1 and 12.9±2.0 μmol/L. Compared with that of control group (46.6±2.3 μmol/L), the difference is statistically significant.

CONCLUSION: AG has anticancer effect on gastric cancer, and it has positive synergistic effect with chemotherapeutic drugs. It may play important inhibitory roles in angiogenesis of gastric cancer. The anticancer effect of iNOS inhibitors may include inducing cell apoptosis, suppressing cell proliferation and reducing angiogenesis.

Key words: Stomach neoplasms; Inducible nitric oxide synthase; Angiogenesis inhibitors; Vascular endothelial growth factor; Microvessel density

Wang GY, Ji B, Wang X, Gu JH. Anti-cancer effect of iNOS inhibitor and its correlation with angiogenesis in gastric cancer. *World J Gastroenterol* 2005; 11(25): 3830-3833
http://www.wjgnet.com/1007-9327/11/3830.asp

INTRODUCTION

The incidence of gastric cancer is high in China, and more than 170 000 people die of it each year[1]. It is significant if certain drugs are found to lower its incidence, even prevent it.

To date, we know that carcinogenesis has intimate correlation with angiogenesis[2-4]. So to reduce angiogenesis probably may inhibit the growth and development of tumors[5]. It is well known that vascular endothelial growth factor (VEGF) is an important angiogenesis factor[6,7]. We have proved that inducible nitric oxide synthase (iNOS) can induce the expression of VEGF in gastric cancer, and microvessel density (MVD) can increase with the enhancement of iNOS and VEGF[8-10]. So VEGF and iNOS both can induce angiogenesis. So if the activity of iNOS is inhibited, tumor angiogenesis may be reduced. As a result the growth and development of tumors will be inhibited. Although the roles that iNOS inhibitors play in various tumors and their mechanisms are being widely studied recently, few people have gone deep into *in vivo* experiment. Based on *in vitro* cytologic experiments, this study went further into *in vivo* experiment to confirm the anticancer effect of iNOS inhibitor (aminoguanidine, AG).

MATERIALS AND METHODS

Animals and cell line

Fifty Kunming mice (25 females, 25 males) weighing 20-25 g were purchased from Experimental Animal Center of Jilin University. Mice were maintained under specific pathogen-free conditions and fed with sterilized food and autoclaved water. Human gastric cancer cell line MFC was purchased from Shanghai Tumor Cell Research Institute.

Agents

Greiss reagent and AG were purchased from Sigma (St.

Louis, USA). Immunohistochemical S-P kit and polyclonal antibodies to iNOS, VEGF, PCNA, and FVIIIRag were all from Fuzhou Maxim Biotechnical Company (Fuzhou, China).

Animal experiment procedure

Each mouse was inoculated with a subcutaneous injection of MFC cells (2×10^6 in 0.2 mL PBS) into the left hind legs. Then these mice were divided into 5 groups of 10 each according to different agents which were administered to mice by intraperitoneal injection for 14 d. These agents included 0.9% sodium chloride solution (control group), mitomycin (MMC group, twice a week 0.7 mg/kg), low dosage of AG (AG_L group, 50 mg/(kg • d)), high dosage of AG (AG_H group, 150 mg/(kg • d)) and MMC+AG_H group (MMC twice a week 0.7 mg/kg, AG 150 mg/(kg • d)). On the 15th d the mice were killed. The blood was taken from abdominal aorta, then centrifuged for plasma to detect NO level by Greiss assay. All tumors were resected from the body and weighed. The inhibitory rate was deduced according to the formula: inhibitory rate (%) = (1-tumor weight of treatment group/tumor weight of control group) ×100%. Then the tumors were fixed in 40 g/L phosphate-buffered formaldehyde.

HE and immunohistochemical staining

Streptavidin-peroxidase (SP) method was used to detect MVD and the expression of iNOS, VEGF and PCNA. The formalin-fixed tissues were embedded in paraffin, and sectioned at a thickness of 4 μm. The sections were deparaffinized and hydrated gradually and examined by histology of HE staining, immunohistochemistry, and TUNEL technique respectively. Sections were heated in a microwave oven for 15 min to retrieve antigens. Endogenous peroxidase was blocked with 3 mL/L hydrogen peroxide methanol for 10 min at room temperature. After washing with phosphate-buffered saline (0.01 g/L, pH 7.4) for 3 min×5 min, the tumor sections were incubated with normal non-immune serum from bull for 15 min at room temperature to eliminate non-specific staining. The sections were then incubated with the primary antibody against iNOS, VEGF, PCNA, and FVIIIRag (dilution 1/100) for 60 min at room temperature, washed with PBS for 3 min×5 min, and incubated with the secondary antibody for 15 min followed by avidin-biotin-peroxidase for 15 min at room temperature. Finally, the slides were washed for 3-15min with PBS, visualized with DAB reagent and counterstained with hematoxylin. Negative and positive controls were used simultaneously to ensure specificity and reliability of the staining process. The negative controls were performed by substituting the primary antibody with PBS, and a positive section supplied by the manufacturer of the staining kit was taken as positive control. Sections were observed under microscope after being mounted. High vessel density was found in 100×sights. Microvessels in 10 hot regions were counted in 400×sights, and the average of microvessels with FVIIIRag staining in 10 hot regions was calculated as MVD. Positive staining with iNOS, VEGF and PCNA were defined by brown staining of cytoplasm. The staining degree was calculated quantitatively with CIMA-400 Colorful Image Assay System which can calculate the percentages of positive staining region of the whole region. The percentage of positive cells with PCNA staining in five 400×sights was counted as proliferation index (PI).

Apoptosis detection by TUNEL method

The reagent kit for apoptosis detection, TdT-FragEL DNA fragmentation detection kit was bought from ONCOGENE. Test procedures consisting of the following sections were provided in the brochure of the kit. The specimens were deparaffinized and hydrated gradually, and rinsed with 1×TBS, then incubated with proteinase K (20 μg/mL in 10 mmol/L Tris-HCl) for 20 min. After immersed in 30 mL/L H_2O_2 at room temperature for 5 min and in TdT labeling reaction mixture at 37 ℃ for 1.5 h, specimens were covered with 1×conjugate for 30 min, visualized by DAB and counter-stained by hematoxylin afterwards. TBS took the place of primary antibodies as a negative control. After being mounted, sections were observed under microscope. The results of staining were analyzed and evaluated with American Image-Pro Plus software. The percentage of positive cells with TUNEL staining in five 400×sights served as apoptosis index (AI).

Statistical analysis

All data were presented as mean±SD. The results were compared by one-way analysis of variance (ANOVA). All statistical calculations were performed with the SPSS11.0 software package. A P value less than 0.05 was regarded as statistically significant.

RESULTS

Effect of AG on tumor growth

The tumor volume of MMC group on the 7th d was (383.4±179.3) mm^3, and on the 10th d those of AG_H and MMC+AG_H groups were (382.8±132.8) mm^3 and (50.0 ±16.6) mm^3 respectively. The tumor cell proliferation was almost completely suppressed. On the 14th d the tumor weight of control group was (1.7±0.5) g, and those of MMC, AG_H and MMC+AG_H groups were (1.0±0.2), (0.9±0.3) and (0.8±0.2) g, respectively. Compared with control group, the difference was significant statistically (P<0.01). The NO level of plasma in AG_L, AG_H and MMC+AG_H groups were lower than that of the control group, and there was dose-effect relationship. The difference was significant statistically (P<0.05, Table 1).

Table 1 Inhibitory effects of AG on transplanted stomach cancer in mice (n = 10, mean±SD)

Group	Concentration of NO in plasma (μmol/L)	Weight of tumor (g)	Inhibition rate (%)
Control	46.6±2.3	1.7±0.5	-
MMC	42.1±2.3	1.0±0.2[b]	41.2
AG_L	17.3±2.0[b]	1.1±0.3[a]	35.3
AG_H	12.9±2.0[b]	0.9±0.3[b]	47.1
MMC+AG_H	12.7±2.1[b]	0.8±0.2[b]	52.9

[a]P<0.05, [b]P<0.01 *vs* control group.

Expression of iNOS and VEGF and their correlation with MVD

MVD has positive correlation with iNOS and VEGF

respectively. The coefficient of product-moment correlation $r_{VEGF} = 0.80$, $r_{iNOS} = 0.85$, $P<0.05$. The linear regression equation is $Y_{VEGF} = 2.3565+0.1087X$, $n = 46$, $Y_{iNOS} = 1.8485 \pm 0.1227X$, $n = 46$. Student's t test, $P<0.05$ (Table 2).

Table 2 Effects of AG on the microvessel density, the expression of iNOS and VEGF in tumor (n = 10, mean±SD)

Group	iNOS	VEGF	MVD
Control	11.3±1.3	10.3±1.6	68.3±10.6
MMC	9.3±1.8[a]	8.9±2.1	56.9±10.3
AG_L	7.1±1.7[a]	7.6±1.2[a]	44.4±16.5[a]
AG_H	3.8±0.9[b]	4.8±1.6[b]	21.2±12.4[b]
MMC+AG_H	2.4±1.1[b]	2.1±1.4[b]	8.8±2.6[b]

[a]$P<0.05$, [b]$P<0.01$ *vs* control group.

HE staining

In AG and MMC+AG_H groups many necrotic cells were seen and many inflammatory cells were invasive. The tumor tissues were separated by necrosis regions. In MMC group diffusely necrotic tissues could be seen. However, in control group there were a few nuclear mitotic phases in tumor cells and in tumor tissues few muscle fibers could be seen (Figures 1A and B).

Immunohistochemical staining

MVD and the expression of iNOS and VEGF in AG groups were apparently lower than those in the control ($P<0.01$). The difference was significant statistically. This revealed that AG could suppress angiogenesis of MFC xenografts. (Table 2, Figures 1C-H).

Cell proliferation and apoptosis

PI of control group was significantly higher than that of AG group and MMC+AG_H group ($P<0.05$), but the difference was not notable between treatment groups. AI in treatment groups was higher than that in the control group ($P<0.05$), while there was also no difference between the treatment groups. The AI/PI value was calculated and compared among all groups. Consequently, it was apparently larger in treatment groups ($P<0.01$), however no difference was shown between them (data not shown).

DISCUSSION

NO which has many bilological functions is a cytokine in mammifer[11]. It is synthesized from L-Arginine by iNOS which is the only rate-limiting enzyme[12]. It involves a serial physiological and pathological process, such as carcinogenesis. NO can induce angiogenesis, but the mechanisms are not clear[13-16]. However, several researches have revealed that NO can regulate the roles of VEGF in inducing angiogenesis by stimulating vascular endothelial cell proliferation and migration and improving vascular penetration[17-20]. VEGF can increase the activity of iNOS[6,7]. So iNOS and VEGF have positive correlation[8-10]. It has been observed that iNOS is highly expressed in many human tumors, such as colon cancer, gastric cancer, ovarian cancer, breast cancer, *etc.*[21]. In our previous study we have observed that the expression of VEGF and iNOS in gastric cancer presents positive correlation[8-10]. This indicates that iNOS plays an important role in the expression and activity of VEGF. We also found that iNOS and VEGF have positive correlation with the clinicopathological characteristics of gastric cancer, such as infiltration, lymphatic or hematogenous metastasis, *etc.* At the same time MVD was higher with the enhancement of VEGF and iNOS. This revealed that iNOS and VEGF can induce angiogenesis in gastric cancer[8-10,21].

To explore the anticancer mechanisms of iNOS inhibitor (aminoguanidine), in this study we evaluated the effect of

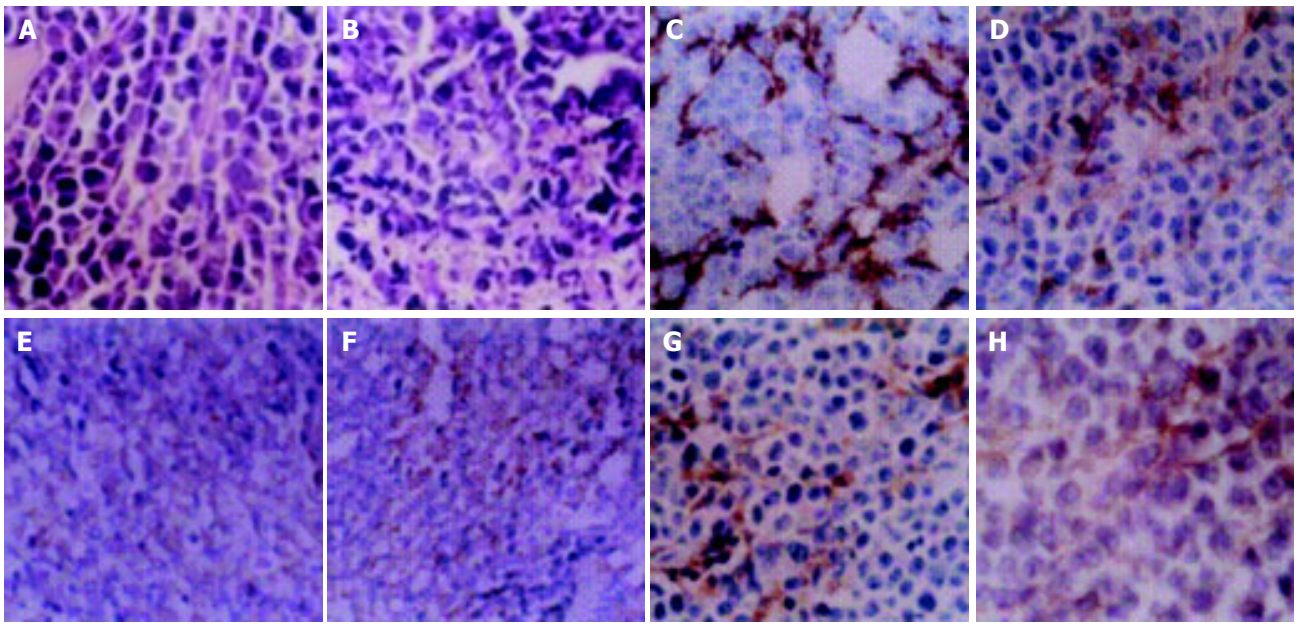

Figure 1 HE staining: morphology of tumor cells in AG group (**A**, original magnification x100) and control group (**B**, original magnification x200); immunohistochemical staining of tumor cells: the expression of FVIIIRag (**C**), iNOS (**E**) and VEGF (**G**) in control group, and the expression of FVIIIRag (**D**), iNOS (**F**) and VEGF (**H**) in AG group. (original magnification, x400).

AG on tumor cell proliferation and apoptosis in xenografts. The AI/PI, a value reflecting cytokinetics, showed a more significant difference. Finally it is shown that compared with control group, the inhibitory rate of treatment groups are apparently higher. We also observed that AG obviously decreases the expression of iNOS and VEGF, and reduces MVD compared to that of control group. By immunohistochemistry (SP method) and Greiss assay we detected the NO level in plasma. The results indicate that the anticancer mechanisms of AG are mainly to inhibit the expression of iNOS and reduce the NO level in plasma. Therefore, the growth of tumor and angiogenesis are inhibited directly, and MVD and the expression of VEGF are suppressed indirectly. In this way the nutrition supply of the tumor is impaired, and further cell proliferation is inhibited and cell apoptosis is improved. These results are consistent with those of Koh *et al*., They observed that AG could inhibit the activity of iNOS in gastric cancer, and suppressed carcinogenesis. At the same time AG and COX-2 selective inhibitors could obviously inhibit the activity of iNOS and COX-2. So, the primitive pathology of colon cancer (aberrant crypt foci, ACF) is prevented.

Compared with traditional anticancer therapy, antiangiogenesis therapy has many superiorities. In this study the effect of MMC group is similar to that of AG group. However, the target of chemotherapeutic drugs is tumor cells which have genetic instability and are apt to mutation and drug-resistance, so the drug-resistance incidence of chemotherapeutic drugs is 30%. And these drugs have many toxic effects. In MMC+AG_H group the anticancer effect is the best which indicates that the effect of AG depends on proper treatment opportunity and scheme. MMC and AG have positive synergy. So certain drugs which can reduce the NO level by inhibiting the expression and activity of iNOS at cellular or genetic level probably may regulate the NO level of tumor microvessel to inhibit carcinogenesis and angiogenesis. And if combined with radiotherapy or bioreactive modulators, it will play a more important role in anticancer effect. This is the first part of a serial study, and we will carry out the further study afterwards with molecular biological technology, such as Southern blotting, Northern blotting, RT-PCR, *etc*.

REFERENCES

1 **Sun XD,** Mu R, Zhou YS, Dai XD, Zhang SW, Huangfu XM, Sun J, Li LD, Lu FZ, Qiao YL. Analysis of mortality rate of stomach cancer and its trend in twenty years in China. *Zhonghua Zhongliu Zazhi* 2004; **26**: 4-9

2 **Feng CW,** Wang LD, Jiao LH, Liu B, Zhang S, Xie XJ. Expression of p53, inducible nitric oxide synthase and vascular endothelial growth factor in gastric precancerous and cancerous lesions: correlation with clinical features. *BMC Cancer* 2002; **2**: 8

3 **Koh E,** Noh SH, Lee YD, Lee HY, Han JW, Lee HW, Hong S. Differential expression of nitric oxide synthase in human stomach cancer. *Cancer Lett* 1999; **146**: 173-180

4 **Doi C,** Noguchi Y, Marat D, Saito A, Fukuzawa K, Yoshikawa T, Tsuburaya A, Ito T. Expression of nitric oxide synthase in gastric cancer. *Cancer Lett* 1999; **144**: 161-167

5 **Eroglu A,** Demirci S, Ayyildiz A, Kocaoglu H, Akbulut H, Akgul H, Elhan HA. Serum concentrations of vascular endothelial growth factor and nitrite as an estimate of *in vivo* nitric oxide in patients with gastric cancer. *Br J Cancer* 1999; **80**: 1630-1634

6 **Lee JC,** Chow NH, Wang ST, Huang SM. Prognostic value of vascular endothelial growth factor expression in colorectal cancer patients. *Eur J Cancer* 2000; **36**: 748-753

7 **Mattern J,** Koomagi R, Volm M. Coexpression of VEGF and bFGF in human epidermoid lung carcinoma is associated with increased vessel density. *Anticancer Res* 1997; **17**: 2249-2252

8 **Wang GY,** Gu JH, Lu GY, Meng XY. Effets of aminoguanidine on transplantation stomach cancer in mice. *J Jilin University* 2004; **30**: 409-412

9 **Wang GY,** Wang X. Relationship between tumor angiogenesis and expression of vascular endothelial growth factor and nitric oxide synthase in human gastric cancer. *Zhongguo Puwai Jichu Yu Linchuang Zazhi* 2004; **11**: 55-57

10 **Wang X,** Wang GY. Expression of vascular endothelial growth factor and nitric oxide synthase in human gastric cancer and its relation to angiogenesis and clinical pathology. *Zhonghua Weichang Waike Zazhi* 2002; **5**: 145-148

11 **Farsky SH,** Borelli P, Fock RA, Proto SZ, Ferreira JM Jr, Mello SB. Chronic blockade of nitric oxide biosynthesis in rats: effect on leukocyte endothelial interaction and on leukocyte recruitment. *Inflamm Res* 2004; **53**: 442-452

12 **Tong BC,** Barbul A. Cellular and physiological effects of arginine. *Mini Rev Med Chem* 2004; **4**: 823-832

13 **Lala PK,** Orucevic A. Role of nitric oxide in tumor progression: lessons from human tumors. *Cancer Metastasis Rev* 1998; **17**: 91-106

14 **Jenkins DC,** Charles IG, Thomsen LL, Moss DW, Holmes LS, Baylis SA, Rhodes P, Westmore K, Emson PC, Moncadas S. Roles of nitric oxide in tumor growth. *Proc Natl Acad Sci USA* 1995; **92**: 4392-4396

15 **Kitadai Y,** Haruma K, Tokutomi T, Tanaka S, Sumii K, Carvalho M, Kuwabara M, Yoshida K, Hirai T, Kajiyama G, Tahara E. Significance of vessel count and vascular endothelial growth factor in human esophageal carcinoma. *Clin Cancer Res* 1998; **4**: 2195-2200

16 **Salvucci O,** Carsana M, Bersani I, Tragni G, Anichini A. Antiapoptotic role of endogenous nitric oxide in human melanoma cells. *Cancer Res* 2001; **61**: 318-326

17 **Gallo O,** Masini E, Morbidelli L, Franchi A, Fini-storchi I, Vergari WA, Ziche M. Role of nitric oxide in angiogenesis and tumor progression in head and neck cancer. *J Natl Cancer Inst* 1998; **90**: 587-596

18 **Rieder G,** Hofmann JA, Hatz RA, Stolte M, Enders GA. Up-regulation of inducible nitric oxide synthase in *Helicobacter pylori*-associated gastritis may represent an increased risk factor to develop gastric carcinoma of the intestinal type. *Int J Med Microbiol* 2003; **293**: 403-412

19 **Rao CV,** Indranie C, Simi B, Manning PT, Connor JR, Reddy BS. Chemopreventive properties of a selective inducible nitric oxide synthase inhibitor in colon carcinogenesis,administered along or in combination with Celecoxib, a selective Cyclooxygenase-2 inhibitor. *Cancer Res* 2002; **62**: 165-170

20 **Jung ID,** Yang SY, Park CG, Lee KB, Kim JS, Lee SY, Han JW, Lee HW, Lee HY. 5-Fluorouracil inhibits nitric oxide production through the inactivation of IkappaB kinase in stomach cancer cells. *Biochem Pharmacol* 2002; **64**: 1439-1445

21 **Chen T,** Nines RG, Peschke SM, Kresty LA, Stoner GD. Chemopreventive effects of a selective nitric oxide synthase inhibitor on carcinogen-induced rat esophageal tumorigenesis. *Cancer Res* 2004; **64**: 3714-3717

Science Editor Guo SY **Language Editor** Elsevier HK

PO Box 2345, Beijing 100023, China
www.wjgnet.com
wjg@wjgnet.com

ELSEVIER

World J Gastroenterol 2005;11(25):3834-3841
World Journal of Gastroenterology ISSN 1007-9327

• *GASTRIC CANCER* •

Effects of dietary intake and genetic factors on hypermethylation of the *hMLH1* gene promoter in gastric cancer

Hong-Mei Nan, Young-Jin Song, Hyo-Yung Yun, Joo-Seung Park, Heon Kim

Hong-Mei Nan, Heon Kim, Department of Preventive Medicine, College of Medicine, Chungbuk National University, Cheongju, Republic of Korea
Young-Jin Song, Hyo-Yung Yun, Departments of Surgery, College of Medicine, Chungbuk National University, Cheongju, Republic of Korea
Joo-Seung Park, Department of Surgery, Eulji University, School of Medicine, Daejon, Republic of Korea
Supported by the Korea Health 21 R and D Project, Ministry of Health and Welfare, Republic of Korea. No. 00-PJ1-PG3-21900-0008
Correspondence to: Heon Kim, MD, PhD, Professor, Department of Preventive Medicine, College of Medicine, Chungbuk National University, 12 Kaeshin-dong, Hungdok-gu, Cheongju-si, Chungbuk 361-763, Republic of Korea. kimheon@cbu.ac.kr
Telephone: +82-43-261-2864 Fax: +82-43-274-2965
Received: 2004-10-9 Accepted: 2004-12-23

Abstract

AIM: Hypermethylation of the promoter of the *hMLH1* gene, which plays an important role in mismatch repair during DNA replication, occurs in more than 30% of human gastric cancer tissues. The purpose of this study was to investigate the effects of environmental factors, genetic polymorphisms of major metabolic enzymes, and microsatellite instability on hypermethylation of the promoter of the *hMLH1* gene in gastric cancer.

METHODS: Data were obtained from a hospital-based, case-control study of gastric cancer. One hundred and ten gastric cancer patients and 220 age- and sex-matched control patients completed a structured questionnaire regarding their exposure to environmental risk factors. Hypermethylation of the *hMLH1* gene promoter, polymorphisms of the *GSTM1*, *GSTT1*, *CYP1A1*, *CYP2E1*, *ALDH2* and *L-myc* genes, microsatellite instability and mutations of *p53* and *Ki-ras* genes were investigated.

RESULTS: Both smoking and alcohol consumption were associated with a higher risk of gastric cancer with hypermethylation of the *hMLH1* gene promoter. High intake of vegetables and low intake of potato were associated with increased likelihood of gastric cancer with hypermethylation of the *hMLH1* gene promoter. Genetic polymorphisms of the *GSTM1*, *GSTT1*, *CYP1A1*, *CYP2E1*, *ALDH2*, and *L-myc* genes were not significantly associated with the risk of gastric cancer either with or without hypermethylation in the promoter of the *hMLH1* gene. Hypermethylation of the *hMLH1* promoter was significantly associated with microsatellite instability (MSI): 10 of the 14 (71.4%) MSI-positive tumors showed hypermethylation, whereas 28 of 94 (29.8%) the MSI-negative tumors were hypermethylated at the *hMLH1* promoter region. Hypermethylation of the *hMLH1* gene promoter was significantly inversely correlated with mutation of the *p53* gene.

CONCLUSION: These results suggest that cigarette smoking and alcohol consumption may influence the development of *hMLH1*-positive gastric cancer. Most dietary factors and polymorphisms of *GSTM1*, *GSTT1*, *CYP1A1*, *CYP2E1*, *ALDH2*, and *L-myc* genes are not independent risk factors for gastric cancer with hypermethylation of the *hMLH1* promoter. These data also suggest that there could be two or more different molecular pathways in the development of gastric cancer, perhaps involving tumor suppression mechanisms or DNA mismatch repair.

Key words: Gastric cancer; Environmental carcinogens; Genetic polymorphisms; *hMTLH1*; Microsatellite instability; p53; Ki-ras

Nan HM, Song YJ, Yun HY, Park JS, Kim H. Effects of dietary intake and genetic factors on hypermethylation of the *hMLH1* gene promoter in gastric cancer. *World J Gastroenterol* 2005; 11(25): 3834-3841
http://www.wjgnet.com/1007-9327/11/3834.asp

INTRODUCTION

Gastric cancer is the most common cancer among Koreans. Environmental factors including cigarette smoking and dietary intake have been implicated in the etiology of gastric cancer[1-4]. Genetic polymorphisms of xenobiotic-metabolizing enzymes can also affect susceptibility to cancer. Several studies have reported that the genetic polymorphisms of metabolic enzymes, such as cytochrome p450 2E1 (*CYP2E1*)[5], glutathione S-transferase mu 1 (*GSTM1*)[6], glutathione *S*-transferase theta 1 (*GSTT1*)[7], aldehyde dehydrogenase 2 (*ALDH2*)[8], and L-myc proto-oncogene[9], and mutations of p53[10] and Ki-ras[11] genes are associated with the development of gastric cancer.

Promoter hypermethylation is an alternative mechanism of gene inactivation in carcinogenesis[12]. Several studies have suggested that aberrant methylation of the promoter causes transcriptional silencing of some important suppressor genes, such as *p16*[13], *E-cadherin*[14], and von Hippel Lindau (*VHL*) gene[15], and this has been implicated in the carcinogenic process in many cancers[12]. In addition, it was recently shown that hypermethylation of gene promoters increases along

the pathway of development from chronic gastritis, intestinal metaplasia, and adenomas to carcinomas of the stomach[16,17].

The *hMLH1* protein, a mismatch repair enzyme, maintains the fidelity of the genome during cellular proliferation. It has no known enzymatic activity and probably acts as a 'molecular matchmaker', recruiting other DNA-repair proteins to the mismatch repair complex[18]. Dysfunction of a mismatch repair system such as *hMLH1* and *hMSH2* could alter microsatellites, short tandem repetitive sequences[19]. Several reports have suggested that hypermethylation of the *hMLH1* promoter correlates with a loss of expression of the gene, resulting in microsatellite instability in gastric cancer[20,21].

There is evidence that diet may be associated with hypermethylation of the *hMLH1* gene promoter in gastric cancer. Aberrant hypermethylation of the *hMLH1* gene promoter is frequently observed in cancers of digestive organs such as the colon, rectum, and stomach[21,22], and decreased levels of folate, vitamin C, and niacin can induce hypermethylation of gene promoters[23]. These facts led us to hypothesize that genetic polymorphisms and environmental factors, such as cigarette smoking, alcohol consumption, and diet, may interact during the hypermethylation of the *hMLH1* gene promoter and in the carcinogenesis of gastric cancer. We studied the association between hypermethylation of the *hMLH1* gene promoter and environmental factors, genetic polymorphisms of major metabolic enzymes, genetic mutation of p53 and Ki-ras genes, and microsatellite instability in gastric cancer.

MATERIALS AND METHODS

Subjects

One hundred and ten individuals with gastric cancer and 220 age-matched (within 3 years) and sex-matched controls were enrolled in this study. Cases of cancer were all histologically confirmed from February 1997 to June 2002 at Chungbuk National University Hospital and Eulji University Hospital, Korea. Control subjects were selected from patients newly diagnosed with diseases other than cancer at the same hospitals or from individuals receiving routine medical examinations in Chungbuk National University Hospital. Table 1 shows the age and gender distribution of the subjects according to hypermethylation of the *hMLH1* gene promoter. The mean±SD ages were 59.81±11.23 years for cases and 59.60±11.03 years for controls. This study was conducted in accordance with the recommendations outlined in the Declaration of Helsinki and all subjects provided written informed consent.

Table 1 Gender and age distribution of cases and controls

	Cases	Controls
Gender		
Male	70	140
Female	40	80
Age (yr)		
–39	6	12
40–49	11	22
50–59	34	68
60–69	40	80
70–	19	38

Exposure to environmental factors

Trained interviewers interviewed subjects using a structured questionnaire within a month after the diagnosis of gastric cancer or benign diseases or at the time of the hospital visit for control subjects undergoing routine medical examination. The questionnaire included questions on demographic factors, smoking habits, alcohol consumption, and diet. Dietary data were collected using a semiquantitative food frequency table previously evaluated for validity and reliability[24]. All subjects were asked about their average frequency of consumption and portion size of 89 common food items during the year preceding the interview. These items were classified into 21 food groups having similar ingredients. The 21 food groups were as follows: cereals; potato; nuts; noodles; breads and cakes; vegetables; mushrooms; fruits; meats; eggs; fishes and shellfishes; stews; chicken; kimchi; soybean foods; soybean pastes; milk and dairy products; butter, cheeses, and margarine; jams, honey, candies, and chocolates; coffee and tea; seaweeds; and alliums.

The amount of calories, nutrients, vitamins, and minerals consumed for each food item was estimated by multiplying the intake amount of the food item and its nutrient value. The total intake of calories, nutrients, vitamins, and minerals was calculated for each subject by summing the respective calories, nutrients, vitamins, and minerals for each food item[25]. The intake amounts of these factors were adjusted for caloric intake using the method of Willett *et al*.[26].

Analysis of genetic polymorphisms

Genomic DNA was isolated from peripheral leukocytes by proteinase K digestion and phenol-chloroform extraction. A multiplex polymerase chain reaction (PCR) method[27] was used simultaneously to detect the presence or absence of the *GSTM1* and *GSTT1* genes with slight modification. The primers used were 5'-GAA GGT GGC CTC CTC CTT GG-3' and 5'-AAT TCT GGA TTG TAG CAG AT-3' for *GSTM1*, 5'-TTC CTT ACT GGT CCT CAC ATC TC-3' and 5'-TCA CCG GAT CAT GGC CAG CA-3' for *GSTT1*, and 5'-CAA CTT CAT CCA CGT TCA CC-3' and 5'-GAA GAG CCA AGG ACA GTT AC-3' for *β-globin*, the internal reference gene. The PCR reactions were performed in 25 μL of a solution containing 50 ng of genomic DNA, 1× PCR buffer [50 mmol/L KCl, 10 mmol/L Tris-HCl (pH 9.0), 1.5 mmol/L $MgCl_2$, and 0.1% Triton X-100], 5 pmoL of each primer, 80 μmol/L each dNTP, and 2.0 units *Taq* polymerase (Promega, Madison, WI). Amplifications were carried out in a thermocycler (MJ Research, Watertown, MA) as follows: 5 min of denaturation at 94 ℃, followed by 35 cycles consisting of denaturation at 94 ℃ for 1 min, annealing at 58 ℃ for 1 min, and extension at 74 ℃ for 1 min. PCR products were separated on 2% agarose gels with ethidium bromide. *GSTM1* and *GSTT1* genotypes were not scored unless the PCR product of the *β-globin* gene was evident.

The A4889G polymorphism in exon 7 of the *CYP1A1* gene was analyzed for each subject as described previously[28]. Briefly, PCR was performed using the primers 5'-GAA CTG CCA CTT CAG CTG TC-3' and 5'-GAA AGA CCT CCC AGC GGT CA-3'. The temperature program for the PCR

reaction was slightly modified. After initial denaturation for 5 min at 94 ℃, a thermal cycle consisting of denaturation for 90 s at 94 ℃, annealing for 90 s at 53 ℃, and extension for 30 s at 74 ℃, was repeated 35 times. The PCR products (187-bp fragments) were digested with *Hin*cII restriction enzyme at 37 ℃ overnight and subjected to electrophoresis on 12% polyacrylamide gels. PCR analysis resulted in the following genotype classification: a predominant homozygote (Ile/Ile), a heterozygote (Ile/Val), and a rare homozygote (Val/Val).

The 5'-flanking region polymorphism of the *CYP2E1* gene was analyzed using procedures described previously[29]. Briefly, PCR was performed using the primers 5'-CCA GTC GAG TCT ACA TTG TCA-3' and 5'-TTC ATT CTG TCT TCT AAC TGG-3'. Initial denaturation was performed at 94 ℃ for 5 min, followed by 35 thermal cycles consisting of denaturation for 1 min at 94 ℃, annealing for 1 min at 53 ℃, and extension for 30 s at 74 ℃. The 410-bp PCR product was digested with *Rsa*I at 37 ℃ overnight and subjected to electrophoresis on 2% agarose gels. The genotypes of *CYP2E1* were classified as follows: a predominant homozygote (c1/c1), a heterozygote (c1/c2), and a rare homozygote (c2/c2).

The *Mbo*II polymorphism of *ALDH2* was identified using a PCR-RFLP method[30] with slight modification. Briefly, PCR was performed using the primers 5'-CCA CAC TCA CAG TTT TCT CTT-3' and 5'-AAA TTA CAG GGT CAA CTG CT-3'. We used the same PCR conditions as in the *CYP1A1* gene analysis. The 134-bp amplicon was digested with *Mbo*II restriction enzyme at 37 ℃ overnight and subjected to electrophoresis on 15% polyacrylamide gels. The genotypes of *ALDH2* were identified as the predominant homozygote (NN), the heterozygote (ND), and the rare homozygote (DD).

The polymorphism of the *L-myc* gene was analyzed using procedures described previously[31]. Briefly, PCR was performed using the primers 5'-ACG GCT GGT GGA GTG GTA GA-3' and 5'-AAG CTT GAG CCC CTT TGT CA-3'. Initial denaturation was performed at 94 ℃ for 5 min, followed by 35 thermal cycles consisting of denaturation for 45 s at 95 ℃, annealing for 40 s at 60 ℃, and extension for 40 s at 74 ℃. The amplified 613-bp PCR product was directly digested with the restriction enzyme *Eco*RI at 37 ℃ overnight and separated by electrophoresis on 2% agarose gels. The genotypes of *L-myc* were classified as follows: a predominant homozygote (LL), a heterozygote (LS), and a rare homozygote (SS).

Methylation-specific PCR for hMLH1 promoter

Tissue samples from gastric cancer patients were immediately frozen and stored in liquid nitrogen until analysis. DNA was extracted using a DNA extraction kit (Promega) according to the manufacturer's instructions.

The promoter methylation status of the *hMLH1* gene was determined by methylation-specific PCR (MSP), as described previously[32]. MSP distinguishes unmethylated from hypermethylated alleles in a given gene based on sequence changes produced after bisulfite treatment of DNA, which converts unmethylated, but not methylated, cytosines to uracils. Briefly, 2 μg of genomic DNA was denatured by treatment with NaOH and modified by sodium bisulfite. DNA samples were then purified using a Wizard DNA Purification Resin (Promega), treated again with NaOH, precipitated with ethanol, and resuspended in water. Modified DNA was amplified using the primer pairs as follows: 5'-TTT TGA TGT AGA TGT TTT ATT AGG GTT GT-3' and 5'-ACC ACC TCA TCA TAA CTA CCC ACA-3' for the unmethylated reaction (124-bp), and 5'-ACG TAG ACG TTT TAT TAG GGT CGC-3' and 5'-CCT CAT CGT AAC TAC CCG CG-3' for the methylated reaction (115-bp)[32]. PCR was performed in a thermocycler (MJ Research) as follows: 5 min of denaturation at 95 ℃, then 35 cycles consisting of denaturation at 95 ℃ for 30 s, annealing at 55 ℃ for 30 s, and extension at 72 ℃ for 30 s. PCR products were separated on 6% polyacrylamide gels with ethidium bromide. DNA from blood samples was used as a negative control for hypermethylated *hMLH1*.

Microsatellite instability

Microsatellite instability (MSI) was examined using BAT25 and BAT26 mononucleotide microsatellite markers. PCR was performed in a 25 μL reaction volume containing 50 ng of genomic DNA, 1× PCR buffer, 5 pmoL of each primer, 80 μmol/L each dNTP, 2.0 units *Taq* polymerase (Takara, Shiga, Japan), and 0.2 μCi of α-^{32}P-labeled dCTP. Amplifications were carried out as follows: 5 min of denaturation at 95 ℃, then 35 cycles consisting of denaturation at 95 ℃ for 50 s, annealing at 58 ℃ for 90 s, and extension at 72 ℃ for 90 s. Two microliters of PCR product was electrophoresed on 6% denaturing polyacrylamide gels containing 6 mol/L urea at room temperature. The gels were dried and autoradiographed on X-ray film. MSI-positive results were identified when the mobility of the microsatellite fragment amplified from tumor DNA differed from the corresponding blood DNA. Tumors were considered microsatellite instability-positive (MSI+) if they manifested instability at one or two loci or microsatellite instability-negative (MSI-) if no unstable microsatellite was found.

Sequencing of p53 *and* Ki-ras *genes*

Reverse transcription (RT)-PCR and direct sequencing methods were used to detect mutations in *p53* and *Ki-ras* genes. Briefly, tissues from gastric cancer patients were homogenized and RNA was isolated using TRIzol solution (Invitrogen Life Technologies, Grand Island, NY). RT-PCR to amplify *p53* and *Ki-ras* cDNA were performed using reagents purchased from Promega. Specific primers synthesized by Bioneer Company (Cheongju, South Korea), *Ex Taq* polymerase (Takara), dNTPs, $MgCl_2$, PCR buffer, and cDNA template were mixed and then amplified for 40 cycles at 95 ℃ for 30 s and at 72 ℃ for 1 min. The cDNA regions were amplified using primers 5'-TCT AGA GCC ACC GTC CAG GGA G-3' and 5'-AAC CTC AGG CGG CTC ATA GGG CA-3' for the +2-+810 region of *p53*, and 5'-ACC AGG GCA GCT ACG GTT TCC GT-3' and 5'-TCA GTC TGA ATC AGG CCC TTC TGT-3' for the +443-+1 317 region of *p53*. Exons 1 and 2 of the *Ki-ras* gene were amplified using primers 5'-GAC TGA ATA TAA ACG TGT GGT AG-3' and 5'-ACT GGT CCC TCA TTG

CAC TG-3'. Before the RT-PCR products were sequenced by cycle sequencing, a PCR purification kit (Boehringer Mannheim, Indianapolis, IN) was used to remove unwanted reagents from the PCR reaction. The purified PCR products were then directly cycle-sequenced using an ABI PRISM 3100 Avant Genetic Analyzer (Applied Biosystems, Foster City, CA) according to the manufacturer's instructions.

Data analysis

Calorie-adjusted intakes of foods, nutrients, vitamins, and minerals were categorized into low- and high-intake groups based on the median values of the control population. Alcohol consumption per week was calculated from questions about the types, frequency, and average amount of alcohol consumed. Alcohol consumption was categorized into three groups: none, ⩽280 g of alcohol/week, and >280 g of alcohol/week. Subjects who had smoked 20 cigarettes or more during their life were classified as smokers and those who had not were considered nonsmokers. Pack-year was used as an index of cumulative smoking.

The purpose of the study was to determine if dietary factors, genetic polymorphisms, MSI, and mutations of *p53* and *Ki-ras* genes were associated with hypermethylation of the *hMLH1* gene promoter. We used unconditional logistic analysis to compare the risk of exhibiting or not exhibiting hypermethylation of the *hMLH1* promoter in tumors and controls using the SAS System for Windows (Release 8.1). *P*-values less than 0.05 were considered significant.

RESULTS

There were significant differences according to the smoking history, pack-years, and higher weekly alcohol intake between patients with gastric cancers with hypermethylation of the *hMLH1* promoter and controls (Table 2). As the amount of cigarette smoking or alcohol drinking increased, the risk of gastric cancer with the *hMLH1* promoter hypermethylation (Table 3).

High consumption of potatoes and butter, cheese and margarine was associated with lower risk of gastric cancer with hypermethylation of the *hMLH1* promoter. In contrast, consumption of vegetables was associated with higher risk of gastric cancer with hypermethylation of the *hMLH1* promoter. High intake of mushrooms and fruits and low intake of cereals and butter, cheese and margarine were associated with higher risk of gastric cancer without hypermethylation of the *hMLH1* promoter (Table 4). Among the nutrients, vitamins, and minerals evaluated, high intake of protein, phosphorus, potassium, vitamin C, zinc, and calcium was associated with higher risk of gastric cancer without hypermethylation of the *hMLH1* gene promoter. However, the intake of nutrients, vitamins, and minerals

Table 2 Interaction between cigarette smoking and alcohol intake, and *hMLH1* gene promoter hypermethylation in gastric cancer

	Controls (*n*)	Cases without hMLH1 promoter hypermethylation (*n*)	Cases with hMLH1 promoter hypermethylation (*n*)	χ^2_{trend}
Smoking history				
Non-smoker	102	27	13	3.827
Smoker	117	42	24	
Odds ratio	Referent (1.00)	1.16 (0.62–2.17)	3.04[a] (1.29–7.19)	
Alcohol drinking				
Never	95	26	15	1.327
Ever	124	43	22	
Odds ratio	Referent (1.00)	1.07 (0.57–2.01)	2.11 (0.90–4.98)	

Odds ratio was adjusted for age and sex. [a]*P*<0.05 *vs* others.

Table 3 Interaction between amount of cigarette smoking and alcohol intake, and *hMLH1* gene promoter hypermethylation in gastric cancer

	OR[1] (95%CI[2])	
	Cases without hMLH1 promoter hypermethylation *vs* controls	Cases with hMLH1 promoter hypermethylation *vs* controls
Cumulative smoking		
0	1.00	1.00
1–15	0.96 (0.38–2.41)	0.86 (0.22–3.41)
16–34	0.92 (0.44–1.93)	0.75 (0.24–2.38)
35–	0.39[a] (0.16–0.93)	3.17[a] (1.20–8.42)
χ^2_{trend}	1.202	6.344[a]
Ethanol uptake per week (g / wk)		
0	1.00	1.00
⩽280	0.58 (0.29–1.14)	1.35 (0.51–3.55)
⩾281	0.68 (0.30–1.53)	3.94[a] (1.21–12.80)
χ^2_{trend}	0.830	5.419[a]

[1]Odds ratio estimated using a conditional logistic analysis. [2]Confidence interval. [a]*P*<0.05 *vs* others.

Table 4 Distribution of controls and cases with or without promoter hypermethylation of the hMLH1 gene according to their intake of food groups which were statistically significant

	Controls (*n*)	Cases without hMLH1 promoter hypermethylation (*n*)	Cases with hMLH1 promoter hypermethylation (*n*)
Cereal			
Low	110	45	17
High	109	24	20
Odds ratio	Referent (1.00)	0.56[a] (0.32–0.99)	0.94 (0.45–1.96)
Potato			
Low	109	36	27
High	110	33	10
Odds ratio	Referent (1.00)	1.00 (0.57–1.74)	0.30[b] (0.14–0.67)
Vegetable			
Low	110	29	12
High	109	40	25
Odds ratio	Referent (1.00)	1.42 (0.82–2.46)	2.17[a] (1.03–4.58)
Mushroom			
Low	110	26	18
High	109	43	19
Odds ratio	Referent (1.00)	1.85[a] (1.05–3.27)	0.89 (0.43–1.83)
Fruit			
Low	110	25	13
High	109	44	24
Odds ratio	Referent (1.00)	1.86[a] (1.06–3.27)	1.69 (0.81–3.54)
Butter, cheese, and margarine			
Low	110	49	24
High	109	20	13
Odds ratio	Referent (1.00)	0.45[b] (0.24–0.81)	0.44[a] (0.20–0.93)

Odds ratio was adjusted for age and sex. [a]*P*<0.05. [b]*P*<0.01 *vs* others.

did not differ significantly between patients with gastric cancers with the *hMLH1* promoter hypermethylation, those with gastric cancers without it, or controls (Table 5).

Genetic polymorphism of *GSTM1*, *GSTT1*, *CYP1A1*, *CYP2E1*, *ALDH2* and *L-myc* was not associated with development of gastric cancers with the *hMLH1* promoter hypermethylation or those without it (Table 6).

Hypermethylation of the *hMLH1* gene promoter was detected in 35.2% of patients with gastric cancer, in 13.6% of those with MSI, in 28.2% of those with mutations of *p53*, and in 4.9% of those with the *Ki-ras* gene (data not shown). Hypermethylation of the *hMLH1* promoter occurred in 10 of 14 MSI+ cases (71.4%) and in 28 of 94 MSI- cases (29.8%). We found a striking association between hypermethylation of the *hMLH1* promoter and MSI (Table 7). Hypermethylation of the *hMLH1* gene promoter was significantly inversely correlated with mutation of the *p53* gene (Table 7).

DISCUSSION

Cigarette smoking and alcohol consumption have been identified as risk factors for gastric cancer in some studies[33-36], although others have not found a causal relationship between these factors[37,38]. Data from our unconditional logistic models showed that both cigarette smoking and alcohol consumption play dominant roles in the development of gastric cancer with hypermethylation of the *hMLH1* promoter, but not in the development of cancer without hypermethylation of the promoter. This finding suggests that smoking- or alcohol-related biological pathways leading to the development of gastric cancer involve hypermethylation of the *hMLH1* promoter. Although it is unclear whether smoking induces hypermethylation of the *hMLH1* gene promoter in humans, recent reports indicate an association between DNA methylation and tobacco carcinogens in animal models[39,40]. Previous studies have also shown that smoking and alcohol consumption increase the risk of developing microsatellite-unstable tumors[41,42].

The exact mechanism of DNA hypermethylation by alcohol is unknown. However, it has been hypothesized that

Table 5 Distribution of controls and cases with or without promoter hypermethylation of the hMLH1 gene according to their intake of nutrients, vitamins, and minerals which were statistically significant

	Controls (*n*)	Cases without hMLH1 promoter hypermethylation (*n*)	Cases with hMLH1 promoter hypermethylation (*n*)
Protein			
Low	109	25	18
High	110	44	19
Odds ratio	Referent (1.00)	1.81[a] (1.03–3.17)	1.00 (0.49–2.02)
Phosphorus			
Low	109	25	20
High	110	44	17
Odds ratio	Referent (1.00)	1.82[a] (1.03–3.19)	0.77 (0.38–1.57)
Potassium			
Low	109	22	15
High	110	47	22
Odds ratio	Referent (1.00)	2.38[b] (1.32–4.26)	1.24 (0.60–2.56)
Vitamin C			
Low	110	19	13
High	109	50	24
Odds ratio	Referent (1.00)	2.78[b] (1.53–5.05)	1.74 (0.84–3.63)
Zinc			
Low	110	23	15
High	109	46	22
Odds ratio	Referent (1.00)	2.20[b] (1.23–3.91)	1.31 (0.64–2.70)
Calcium			
Low	110	22	15
High	109	47	22
Odds ratio	Referent (1.00)	2.32[b] (1.30–4.14)	1.34 (0.65–2.76)

Odds ratio was adjusted for age and sex. [a]$P<0.05$, [b]$P<0.01$ *vs* others.

Table 6 Distribution of controls and cases with or without promoter hypermethylation of the hMLH1 gene according to the genetic polymorphisms of *GSTM1*, *GSTT1*, *CYP1A1*, *CYP2E1*, *NAT2*, *ALDH2*, and *L-myc*

	Controls (*n*)	Cases without hMLH1 promoter hypermethylation (*n*)	Cases with hMLH1 promoter hypermethylation (*n*)
GSTM1			
Undeleted	90	21	13
Deleted	130	48	25
Odds ratio	Referent (1.00)	1.67 (0.93–3.00)	1.18 (0.56–2.47)
GSTT1			
Undeleted	117	32	17
Deleted	103	37	21
Odds ratio	Referent (1.00)	1.32 (0.76–2.29)	1.47 (0.72–2.98)
CYP1A1			
Ile / Ile	115	36	22
Ile / Val+Val / Val	104	33	15
Odds ratio	Referent (1.00)	1.02 (0.59–1.77)	0.74 (0.36–1.52)
CYP2E1			
c1 / c1	129	44	25
c1 / c2+c2 / c2	88	26	13
Odds ratio	Referent (1.00)	0.89 (0.51–1.56)	0.76 (0.37–1.59)
ALDH2			
NN	139	38	26
ND+DD	79	31	11
Odds ratio	Referent (1.00)	1.45 (0.83–2.52)	0.73 (0.34–1.56)
L-myc			
Low	52	20	9
High	164	48	29
Odds ratio	Referent (1.00)	1.59 (0.86–2.92)	1.56 (0.61–3.99)

Odds ratio was adjusted for age and sex.

Table 7 Frequencies of mutations of the *p53* and *Ki-ras* genes, and microsatellite instability according to *hMLH1* promoter hypermethylation

Gene	*hMLH1* promoter hypermethylation		OR[1] (95%CI[2])	χ^2	*P*
	Yes (%)	No (%)			
P53					
No	31 (81.58)	46 (65.71)	1.00	4.199	0.041
Yes	7 (18.42)	24 (34.29)	0.34 (0.12–0.95)		
Ki-ras					
No	37 (97.37)	58 (93.55)	1.00	0.407	0.524
Yes	1 (2.63)	4 (6.45)	0.47 (0.05–4.72)		
[3]MSI					
No	28 (73.68)	66 (92.86)	1.00	7.458	0.006
Yes	10 (26.32)	4 (7.14)	6.19 (1.67–22.88)		

[1]Odds ratio was adjusted for age and sex. [2]Confidence interval. [3]Microsatellite instability.

alcohol could influence carcinogenesis by influencing mucosal cell proliferation and related histological changes[43]. These changes have been associated with mucosal hyperregeneration, which may make the mucosa more susceptible to the action of other carcinogens such as cigarette smoke[43]. Therefore, alcohol consumption might increase the bioavailability of DNA-binding smoke components in the mucosa of the upper digestive tract, increasing the plasma levels of these compounds, or might modify the metabolism of pro-carcinogenic compounds by inducing specific metabolic pathways involving an aberrant mismatch repair system[44].

Folate deficiency is associated with hypermethylation of the H-cadherin promoter[45]. However, we found no significant association between folate intake and hypermethylation of the *hMLH1* promoter. Su and Arab reported that low folate intake is aggravated by high alcohol intake[46], probably because folate is degraded by acetaldehyde, an intermediate metabolite of alcohol[47]. van Engeland *et al*., suggested that intake of folate and alcohol is associated with changes in promoter hypermethylation in colorectal cancer[48]. Our data showing that alcohol intake increased the risk of gastric cancer with hypermethylation of the *hMLH1* promoter are consistent with these previous reports.

Most dietary factors, nutrients, vitamins, and minerals are not associated with gastric cancer with hypermethylation of the *hMLH1* promoter, although we found that a high intake of vegetables and low intake of potato and butter, cheese, and margarine were associated with increased likelihood of gastric cancer without hypermethylation of the *hMLH1* promoter, and high intake of mushrooms and fruits and low intake of cereals and butter, cheese and margarine were associated with higher risk of gastric cancer without hypermethylation of the *hMLH1* promoter. We cannot be certain that these results did not occur by chance, given the low number of comparisons. However, we observed that different dietary factors selectively affected the pathways to gastric cancer with or without hypermethylation of the *hMLH1* promoter. For example, a high intake of butter, cheese, and margarine was associated with a lower risk of gastric cancers either with or without hypermethylation of the *hMLH1* promoter. These findings agree with epidemiological data showing a relatively low incidence of gastric cancer in countries with consumption of high butter, cheese, and margarine[49]. Based on these facts, it could be suggested that butter, cheese and margarine decrease the risk of gastric cancer regardless of the hMLH1 promoter hypermethylation.

It has been reported that vitamin C can induce hypermethylation of gene promoters[23]. However, a higher intake of vitamin C is associated with an increased risk of gastric cancer in this present study. One of the main vitamin C sources for Koreans is kimchi, which has been reported as a potent risk factor for gastric cancer in some Korean epidemiologic studies[3]. Therefore, kimchi intake increases vitamin C intake amount, and, at the same time, the risk of gastric cancer.

Few epidemiological studies on gastric cancer have included genetic polymorphisms in the analysis or evaluated the association between genetic polymorphisms and hypermethylation of the *hMLH1* gene promoter. Several studies have reported an independent, increased risk of gastric cancer for the *GSTM1* null[7], *GSTT1* null[6], *CYP2E1* c1/c2 or c2/c2[50], *2-allele containing *ALDH2* genotypes[9], and shorter (s) allele-containing *L-myc*[10] genotypes. However, other studies have not found any association between gastric cancer and these genotypes[51-53]. We found no significant association between polymorphisms of *GSTM1*, *GSTT1*, *CYP1A1*, *CYP2E1*, *ALDH2*, and *L-myc* and the risk of gastric cancer with or without hypermethylation of the *hMLH1* promoter. These findings suggest that the genetic polymorphisms of the *GSTM1*, *GSTT1*, *CYP1A1*, *CYP2E1*, *ALDH2*, and *L-myc* genes might not be independent risk factors, but could act as effect modifiers of the risk of gastric cancer through environmental factors, such as dietary intake.

We examined the mononucleotide repeats BAT25 and BAT26 to detect genuine MSI because these repeats are considered as ideal diagnostic markers. Mononucleotide repeats are sufficient for the diagnosis of true MSI[54]. A consensus mononucleotide locus, BAT26 is altered in all tumors with genuine MSI[55,56]. We found that 10 of the 14 MSI+ gastric cancer cases (71%) in our patients were hypermethylated in the promoter region of *hMLH1*. We found a significant association between hypermethylation of the *hMLH1* promoter and MSI+ gastric carcinoma ($P = 0.006$), which is consistent with previous reports[21,57].

Point mutations in the *p53* tumor suppressor gene[58,59] and *ras* oncogenes[60,61] are frequently found in human and rodent tumors. Mutations of the *p53* and *Ki-ras* genes were detected in 28.2% and 4.9% of our patients with gastric cancer, respectively. We also found a significant inverse association between hypermethylation of the *hMLH1* gene promoter and *p53* mutations. Previous studies have reported a significantly lower incidence of *p53* gene alterations in MSI+ gastric cancer, in MSI+ colorectal cancers, and in colorectal cancer cell lines[62,63] than in MSI- gastric cancer[64,65]. Together, these data confirm the existence of alternative genetic pathways for gastric cancer, such as the classical 'tumor suppressor' pathway and the 'mismatch repair' pathway.

In conclusion, despite its limited size, this study suggests that cigarette smoking and alcohol consumption are significantly associated with higher risk of gastric cancer having hypermethylation of the *hMLH1* promoter. Polymorphisms of *GSTM1*, *GSTT1*, *CYP1A1*, *CYP2E1*, *ALDH2*, and *L-myc* genes were not associated with gastric cancers either with or without hypermethylation of the *hMLH1* promoter, suggesting that these polymorphisms operate along disease pathways other than those involving the mismatch repair system in gastric cancer. Our data also highlight the importance of aberrant methylation of the *hMLH1* promoter in causing MSI in gastric cancer. The negative association between hypermethylation of the *hMLH1* gene promoter and *p53* mutations suggests that there could be two or more different molecular pathways in the development of gastric cancer, such as tumor suppression mechanisms and DNA mismatch repair.

REFERENCES

1 **Kim JP,** Park JG, Lee MD, Han MD, Park ST, Lee BH, Jung

SE. Co-carcinogenic effects of several Korean foods on gastric cancer induced by N-methyl-N'-nitro-N-nitrosoguanidine in rats. *Jpn J Surg* 1985; **15**: 427-437

2 **Yun TK,** Choi SY. Preventive effect of ginseng intake against various human cancers: a case-control study on 1987 pairs. *Cancer Epidemiol Biomarkers Prev* 1995; **4**: 401-408

3 **Lee JK,** Park BJ, Yoo KY, Ahn YO. Dietary factors and stomach cancer: a case-control study in Korea. *Int J Epidemiol* 1995; **24**: 33-41

4 **Ahn YO.** Diet and stomach cancer in Korea. *Int J Cancer* 1997; **10**: 7-9

5 **Nishimoto IN,** Hanaoka T, Sugimura H, Nagura K, Ihara M, Li XJ, Arai T, Hamada GS, Kowalski LP, Tsugane S. Cytochrome P450 2E1 polymorphism in gastric cancer in Brazil: case-control studies of Japanese Brazilians and non-Japanese Brazilians. *Cancer Epidemiol Biomarkers Prev* 2000; **9**: 675-680

6 **Setiawan VW,** Zhang ZF, Yu GP, Li YL, Lu ML, Tsai CJ, Cordova D, Wang MR, Guo CH, Yu SZ, Kurtz RC. GSTT1 and GSTM1 null genotypes and the risk of gastric cancer: a case-control study in a Chinese population. *Cancer Epidemiol Biomarkers Prev* 2000; **9**: 73-80

7 **Harada S,** Misawa S, Nakamura T, Tanaka N, Ueno E, Nozoe M. Detection of GST1 gene deletion by the polymerase chain reaction and its possible correlation with stomach cancer in Japanese. *Hum Genet* 1992; **90**: 62-64

8 **Yokoyama A,** Muramatsu T, Ohmori T, Yokoyama T, Okuyama K, Takahashi H, Hasegawa Y, Higuchi S, Maruyama K, Shirakura K, Ishii H. Alcohol-related cancers and aldehyde dehydrogenase-2 in Japanese alcoholics. *Carcinogenesis* 1998; **19**: 1383-1387

9 **Shibuta K,** Mori M, Haraguchi M, Yoshikawa K, Ueo H, Akiyoshi T. Association between restriction fragment length polymorphism of the L-myc gene and susceptibility to gastric cancer. *Br J Surg* 1998; **85**: 681-684

10 **Shiao YH,** Rugge M, Correa P, Lehmann HP, Scheer WD. p53 alteration in gastric precancerous lesions. *Am J Pathol* 1994; **144**: 511-517

11 **Craanen ME,** Blok P, Top B, Boerrigter L, Dekker W, Offerhaus GJ, Tytgat GN, Rodenhuis S. Absence of ras gene mutations in early gastric carcinomas. *Gut* 1995; **37**: 758-762

12 **Baylin SB,** Herman JG, Graff JR, Vertino PM, Issa JP. Alterations in DNA methylation: a fundamental aspect of neoplasia. *Adv Cancer Res* 1998; **72**: 141-196

13 **Merlo A,** Herman JG, Mao L, Lee DJ, Gabrielson E, Burger PC, Baylin SB, Sidransky D. 5' CpG island methylation is associated with transcriptional silencing of the tumour suppressor p16/CDKN2/MTS1 in human cancers. *Nat Med* 1995; **1**: 686-692

14 **Graff JR,** Herman JG, Lapidus RG, Chopra H, Xu R, Jarrard DF, Isaacs WB, Pitha PM, Davidson NE, Baylin SB. E-cadherin expression is silenced by DNA hypermethylation in human breast and prostate carcinomas. *Cancer Res* 1995; **55**: 5195-5199

15 **Herman JG,** Latif F, Weng Y, Lerman MI, Zbar B, Liu S, Samid D, Duan DS, Gnarra JR, Linehan WM, Baylin SB. Silencing of the VHL tumor-suppressor gene by DNA methylation in renal carcinoma. *Proc Natl Acad Sci USA* 1994; **91**: 9700-9704

16 **Kang GH,** Shim YH, Jung HY, Kim WH, Ro JY, Rhyu MG. CpG island methylation in premalignant stages of gastric carcinoma. *Cancer Res* 2001; **61**: 2847-2851

17 **Fleisher AS,** Esteller M, Tamura G, Rashid A, Stine OC, Yin J, Zou TT, Abraham JM, Kong D, Nishizuka S, James SP, Wilson KT, Herman JG, Meltzer SJ. Hypermethylation of the hMLH1 gene promoter is associated with microsatellite instability in early human gastric neoplasia. *Oncogene* 2001; **20**: 329-335

18 **Modrich P.** Mechanisms and biological effects of mismatch repair. *Annu Rev Genet* 1991; **25**: 229-253

19 **Thibodeau SN,** Bren G, Schaid D. Microsatellite instability in cancer of the proximal colon. *Science* 1993; **260**: 816-819

20 **Kang GH,** Shim YH, Ro JY. Correlation of methylation of the hMLH1 promoter with lack of expression of hMLH1 in sporadic gastric carcinomas with replication error. *Lab Invest* 1999; **79**: 903-909

21 **Fleisher AS,** Esteller M, Wang S, Tamura G, Suzuki H, Yin J, Zou TT, Abraham JM, Kong D, Smolinski KN, Shi YQ, Rhyu MG, Powell SM, James SP, Wilson KT, Herman JG, Meltzer SJ. Hypermethylation of the hMLH1 gene promoter in human gastric cancers with microsatellite instability. *Cancer Res* 1999; **59**: 1090-1095

22 **Cunningham JM,** Christensen ER, Tester DJ, Kim CY, Roche PC, Burgart LJ, Thibodeau SN. Hypermethylation of the hMLH1 promoter in colon cancer with microsatellite instability. *Cancer Res* 1998; **58**: 3455-3460

23 **Singh SM,** Murphy B, O'Reilly RL. Involvement of gene-diet/drug interaction in DNA methylation and its contribution to complex diseases: from cancer to schizophrenia. *Clin Genet* 2003; **64**: 451-460

24 **Kim MK,** Lee SS, Ahn YO. Reproducibility and validity of a self-administered semiquantitative food frequency questionnaire among middle-aged men in Seoul. *Korean J Commun Nutrit* 1996; **1**: 376-394

25 The Korean Nutrition Society. Recommended dietary allowance for Koreans, 7th Revision. The Korean Nutrition Society, Seoul, 2000

26 **Willett W,** Stampfer MJ. Total energy intake: implications for epidemiologic analyses. *Am J Epidemiol* 1986; **124**: 17-27

27 **Chen H,** Sandler DP, Taylor JA, Shore DL, Liu E, Bloomfield CD, Bell DA. Increased risk for myelodysplastic syndromes in individuals with glutathione transferase theta 1 (GSTT1) gene defect. *Lancet* 1996; **347**: 295-297

28 **Oyama T,** Mitsudomi T, Kawamoto T, Ogami A, Osaki T, Kodama Y, Yasumoto K. Detection of CYP1A1 gene polymorphism using designed RFLP and distributions of CYP1A1 genotypes in Japanese. *Int Arch Occup Environ Health* 1995; **67**: 253-256

29 **Kawamoto T,** Koga M, Murata K, Matsuda S, Kodama Y. Effects of ALDH2, CYP1A1, and CYP2E1 genetic polymorphisms and smoking and drinking habits on toluene metabolism in humans. *Toxicol Appl Pharmacol* 1995; **133**: 295-304

30 **Harada S,** Zhang S. New strategy for detection of ALDH2 mutant. *Alcohol Alcohol Suppl* 1993; **1**A: 11-13

31 **Yaylim I,** Isbir T, Ozturk O, Turna A, Isitmangil T, Zonuzi F, Camlica H. Is there any correlation between restriction fragment length polymorphism of the L-MYC gene and metastasis of human nonsmall cell lung cancer? *Cancer Genet Cytogenet* 2002; **134**: 118-122

32 **Herman JG,** Graff JR, Myohanen S, Nelkin BD, Baylin SB. Methylation-specific PCR: a novel PCR assay for methylation status of CpG islands. *Proc Natl Acad Sci USA* 1996; **93**: 9821-9826

33 **BJain M**, Choi NW, Fodor JG, Pfeiffer CJ, Howe GR, Harrison LW, Craib KJ, Miller AB. Dietary factors and the incidence of cancer of the stomach. *Am J Epidemiol* 1985; **122**: 947-959

34 **You WC,** Blot WJ, Chang YS, Ershow AG, Yang ZT, An Q, Henderson B, Xu GW, Fraumeni JF Jr, Wang TG. Diet and high risk of stomach cancer in Shandong, China. *Cancer Res* 1988; **48**: 3518-3523

35 **McLaughlin JK,** Hrubec Z, Blot WJ, Fraumeni JF Jr. Stomach cancer and cigarette smoking among U.S. veterans, 1954-1980. *Cancer Res* 1990; **50**: 3804

36 **Kabat GC,** Ng SK, Wynder EL. Tobacco, alcohol intake, and diet in relation to adenocarcinoma of the esophagus and gastric cardia. *Cancer Causes Control* 1993; **4**: 123-132

37 **Pollack ES,** Nomura AM, Heilbrun LK, Stemmermann GN, Green SB. Prospective study of alcohol consumption and cancer. *N Engl J Med* 1984; **310**: 617-621

38 **Nomura A,** Grove JS, Stemmermann GN, Severson RK. A prospective study of stomach cancer and its relation to diet, cigarettes, and alcohol consumption. *Cancer Res* 1990; **50**: 627-631

39 **Swafford DS,** Middleton SK, Palmisano WA, Nikula KJ, Tesfaigzi J, Baylin SB, Herman JG, Belinsky SA. Frequent

aberrant methylation of p16INK4a in primary rat lung tumors. *Mol Cell Biol* 1997; **17**: 1366-1374

40 **Lee YW,** Klein CB, Kargacin B, Salnikow K, Kitahara J, Dowjat K, Zhitkovich A, Christie NT, Costa M. Carcinogenic nickel silences gene expression by chromatin condensation and DNA methylation: a new model for epigenetic carcinogens. *Mol Cell Biol* 1995; **15**: 2547-2557

41 **Slattery ML,** Curtin K, Anderson K, Ma KN, Ballard L, Edwards S, Schaffer D, Potter J, Leppert M, Samowitz WS. Associations between cigarette smoking, lifestyle factors, and microsatellite instability in colon tumors. *J Natl Cancer Inst* 2000; **92**: 1831-1836

42 **Slattery ML,** Anderson K, Curtin K, Ma KN, Schaffer D, Samowitz W. Dietary intake and microsatellite instability in colon tumors. *Int J Cancer* 2001; **93**: 601-607

43 **Kune GA,** Vitetta L. Alcohol consumption and the etiology of colorectal cancer: a review of the scientific evidence from 1957 to 1991. *Nutr Cancer* 1992; **18**: 97-111

44 **Izzotti A,** Balansky RM, Blagoeva PM, Mircheva ZI, Tulimiero L, Cartiglia C, De Flora S. DNA alterations in rat organs after chronic exposure to cigarette smoke and / or ethanol ingestion. *FASEB J* 1998; **12**: 753-758

45 **Jhaveri MS,** Wagner C, Trepel JB. Impact Impact of extracellular folate levels on global gene expression. *Mol Pharmacol* 2001; **60**: 1288-1295

46 **Su LJ,** Arab L. ArabNutritional status of folate and colon cancer risk: evidence from NHANES I epidemiologic follow-up study. *Ann Epidemiol* 2001; **11**: 65-72

47 **Homann N,** Tillonen J, Salaspuro M. Microbially produced acetaldehyde from ethanol may increase the risk of colon cancer via folate deficiency. *Int J Cancer* 2000; **86**: 169-173

48 **van Engeland M,** Weijenberg MP, Roemen GM, Brink M, de Bruine AP, Goldbohm RA, van den Brandt PA, Baylin SB, de Goeij AF, Herman JG. Effects of dietary folate and alcohol intake on promoter methylation in sporadic colorectal cancer: the Netherlands cohort study on diet and cancer. *Cancer Res* 2003; **63**: 3133-3137

49 **Stadtlander CT,** Waterbor JW. Molecular epidemiology, pathogenesis and prevention of gastric cancer. *Carcinogenesis* 1999; **20**: 2195-2208

50 **Gao C,** Takezaki T, Wu J, Li Z, Wang J, Ding J, Liu Y, Hu X, Xu T, Tajima K, Sugimura H. Interaction between cytochrome P-450 2E1 polymorphisms and environmental factors with risk of esophageal and stomach cancers in Chinese. *Cancer Epidemiol Biomarkers Prev* 2002; **11**: 29-34

51 **Kato S,** Onda M, Matsukura N, Tokunaga A, Matsuda N, Yamashita K, Shields PG. Genetic polymorphisms of the cancer related gene and Helicobacter pylori infection in Japanese gastric cancer patients. An age and gender matched case-control study. *Cancer* 1996; **77**: 1654-1661

52 **Deakin M,** Elder J, Hendrickse C, Peckham D, Baldwin D, Pantin C, Wild N, Leopard P, Bell DA, Jones P, Duncan H, Brannigan K, Alldersea J, Fryer AA, Strange RC. Glutathione S-transferase GSTT1 genotypes and susceptibility to cancer: studies of interactions with GSTM1 in lung, oral, gastric and colorectal cancers. *Carcinogenesis* 1996; **17**: 881-884

53 **Dlugosz A,** Adler G, Ciechanowicz A, Jaroszewicz-Heigelmann H, Starzynska T. *Eco*RI polymorphism of the L-myc gene in gastric cancer patients. *Eur J Gastroenterol Hepatol* 2002; **14**: 1231-1235

54 **Boland CR,** Thibodeau SN, Hamilton SR, Sidransky D, Eshleman JR, Burt RW, Meltzer SJ, Rodriguez-Bigas MA, Fodde R, Ranzani GN, Srivastava S. National Cancer Institute Workshop on Microsatellite Instability for cancer detection and familial predisposition: development of international criteria for the determination of microsatellite instability in colorectal cancer. *Cancer Res* 1998; **58**: 5248-5257

55 **Yamamoto H,** Itoh F, Fukushima H, Adachi Y, Itoh H, Hinoda Y, Imai K. Frequent Bax frameshift mutations in gastric cancer with high but not low microsatellite instability. *J Exp Clin Cancer Res* 1999; **18**: 103-106

56 **Yamamoto H,** Perez-Piteira J, Yoshida T, Terada M, Itoh F, Imai K, Perucho M. Gastric cancers of the microsatellite mutator phenotype display characteristic genetic and clinical features. *Gastroenterology* 1999; **116**: 1348-1357

57 **Leung SY,** Yuen ST, Chung LP, Chu KM, Chan AS, Ho JC. hMLH1 promoter methylation and lack of hMLH1 expression in sporadic gastric carcinomas with high-frequency microsatellite instability. *Cancer Res* 1999; **59**: 159-164

58 **Hollstein M,** Sidransky D, Vogelstein B, Harris CC. p53 mutations in human cancers. *Science* 1991; **253**: 49-53

59 **Levine AJ,** Momand J, Finlay CA. The p53 tumor suppressor gene. *Nature* 1991; **351**: 453-456

60 **Sukumar S,** Notario V, Martin-Zanca D, Barbacid M. Induction of mammary carcinomas in rats by nitroso-methylurea involves malignant activation of H-ras-1 locus by single point mutations. *Nature* 1983; **306**: 658-661

61 **Zarbl H,** Sukumar S, Arthur AV, Martin-Zanca D, Barbacid M. Direct mutagenesis of Ha-ras-1 oncogenes by N-nitroso-N-methylurea during initiation of mammary carcinogenesis in rats. *Nature* 1985; **315**: 382-385

62 **Olschwang S,** Hamelin R, Laurent-Puig P, Thuille B, De Rycke Y, Li YJ, Muzeau F, Girodet J, Salmon RJ, Thomas G. Alternative genetic pathways in colorectal carcinogenesis. *Proc Natl Acad Sci USA* 1997; **94**: 12122-12127

63 **Cottu PH,** Muzeau F, Estreicher A, Flejou JF, Iggo R, Thomas G, Hamelin R. Inverse correlation between RER+ status and p53 mutation in colorectal cancer cell lines. *Oncogene* 1996; **13**: 2727-2730

64 **Strickler JG,** Zheng J, Shu Q, Burgart LJ, Alberts SR, Shibata D. p53 mutations and microsatellite instability in sporadic gastric cancer: when guardians fail. *Cancer Res* 1994; **54**: 4750-4755

65 **Yamamoto H,** Perez-Piteira J, Yoshida T, Terada M, Itoh F, Imai K, Perucho M. Gastric cancers of the microsatellite mutator phenotype display characteristic genetic and clinical features. *Gastroenterology* 1999; **116**: 1348-1357

Science Editor Guo SY **Language Editor** Elsevier HK

PO Box 2345, Beijing 100023, China
www.wjgnet.com
wjg@wjgnet.com

ELSEVIER

World J Gastroenterol 2005;11(25):3842-3845
World Journal of Gastroenterology ISSN 1007-9327

Use of Fourier-transform infrared spectroscopy to rapidly diagnose gastric endoscopic biopsies

Qing-Bo Li, Xue-Jun Sun, Yi-Zhuang Xu, Li-Min Yang, Yuan-Fu Zhang, Shi-Fu Weng, Jing-Sen Shi, Jin-Guang Wu

Qing-Bo Li, Yi-Zhuang Xu, Li-Min Yang, Yuan-Fu Zhang, Shi-Fu Weng, Jin-Guang Wu, The State Key Laboratory of Rare Earth Materials Chemistry and Applications, College of Chemistry and Molecular Engineering, Peking University, Beijing 100871, China
Xue-Jun Sun, Jing-Sen Shi, Department of General Surgery, First Hospital of Xi'an Jiaotong University, Xi'an 710061, Shaanxi Province, China
Supported by the National Natural Science Foundation of China, No. 30371604 and State Key Project of China, No. 2002CCA01900
Correspondence to: Jin-Guang Wu, the State Key Laboratory of Rare Earth Materials Chemistry and Applications, College of Chemistry and Molecular Engineering, Peking University, Beijing 100871, China. wujg@pku.edu.cn
Telephone: +86-10-62757951 Fax: +86-10-62751708
Received: 2004-07-09 Accepted: 2004-09-09

Abstract

AIM: To determine if Fourier-transform infrared (FT-IR) spectroscopy of endoscopic biopsies could accurately diagnose gastritis and malignancy.

METHODS: A total of 123 gastroscopic samples, including 11 cases of cancerous tissues, 63 cases of chronic atrophic gastritis tissues, 47 cases of chronic superficial gastritis tissues and 2 cases of normal tissues, were obtained from the First Hospital of Xi'an Jiaotong University, China. A modified attenuated total reflectance (ATR) accessory was linked to a WQD-500 FT-IR spectrometer for spectral measurement followed by submission of the samples for pathologic analysis. The spectral characteristics for different types of gastroscopic tissues were summarized and correlated with the corresponding pathologic results.

RESULTS: Distinct differences were observed in the FT-IR spectra of normal, atrophic gastritis, superficial gastritis and malignant gastric tissues. The sensitivity of FT-IR for detection of gastric cancer, chronic atrophic gastritis and superficial gastritis was 90.9%, 82.5%, 91.5%, and specificity was 97.3%, 91.7%, 89.5% respectively.

CONCLUSION: FT-IR spectroscopy can distinguish gastric inflammation from malignancy.

Key words: Fourier-transform infrared spectroscopy; Gastric endoscope; Gastric cancer; Chronic gastritis; Spectral analysis; Infrared detection

Li QB, Sun XJ, Xu YZ, Yang LM, Zhang YF, Weng SF, Shi JS, Wu JG. Use of Fourier-transform infrared spectroscopy to rapidly diagnose gastric endoscopic biopsies. *World J Gastroenterol* 2005; 11(25): 3842-3845
http://www.wjgnet.com/1007-9327/11/3842.asp

INTRODUCTION

Fourier-transform infrared (FT-IR) spectroscopy can effectively provide chemical variation information of the structure and composition of biologic materials at molecular level[1]. Therefore, vibrational spectroscopy is becoming an increasingly powerful tool for the research on biochemistry of cancer[2-5]. Our research group has successfully used FT-IR spectroscopy to diagnose carcinomas, such as carcinoma of stomach, colon, esophagus, lung, salivary gland since 1995[6-9]. There are significant differences between the spectra of malignant and corresponding normal tissues[10-12]. In addition, FT-IR spectroscopy could detect molecular abnormalities which occur before the change in morphology seen under light microscope[13]. Therefore, FT-IR technology makes it possible to detect inflammatory and precancerous changes. Rapid, accurate and convenient detection of gastroscopic tissues can be performed using FT-IR spectroscopy if mid-infrared fiber optics technology and stomach endoscopy technology are combined, however the flexible mid-infrared optical fiber and mini probe are not yet available[14].

MATERIALS AND METHODS

Patients and materials

Informed consent was obtained from each patient prior to the study. A total of 123 fresh surgically resected gastric tissue specimens were obtained from the First Hospital of Xi'an Jiaotong University, China. There were 47 women and 76 men, aged between 18 and 80 years (mean 50.3 years). One endoscopic pinch biopsy, 1-3 mm in diameter, was obtained from each patient. The detected samples consisted of 11 cases of cancerous tissues, 63 cases of chronic atrophic gastritis tissues, 47 cases of chronic superficial gastritis tissues and 2 cases of normal tissues.

Spectral measurement

As the size of samples was too small to obtain an FT-IR spectrum with high quality, the modified ATR accessory linked to a WQD-500 FT-IR spectrometer was used. The FT-IR spectrometer was equipped with a liquid nitrogen cooled mercury cadmium telluride (MCT) detector.

The fresh tissue specimens were obtained in gastroscopy detection, and then immediately and non-invasively measured using the mobile FT-IR spectrometer near the operation

room. The sample was put on ATR accessory to measure the spectrum. The background spectrum was collected. For the collection of each spectrum, 32 scans at a resolution of 4/cm, with a normal range from 4 000/cm to 800/cm were applied. It took about 1-2 min to non-invasively measure the spectrum. After measurement, the samples were stored in liquid nitrogen and sent for the pathologic examination of H&E staining as the reference in the spectral analysis.

RESULTS

The spectral differences among chronic superficial gastritis, atrophic gastritis and malignant gastric endoscopy samples were studied. For the sharper difference in the ratio of peak intensity, baseline corrections of the spectra were performed at first. Several typical spectra of malignant gastric tissues obtained by endoscopy are illustrated in Figure 1A. The spectral characteristics were similar to those of spectra of gastric tissues, which were obtained during surgical operation in our previous research[15]. The spectral features of malignant gastric tissues were in good agreement with the criteria established in our previous work[15]. For example, the broad -3 300/cm absorption band, assigned to N-H stretching vibration of protein and OH stretching vibration of water, was more intense in the malignant stomach samples because of the higher content of water in malignant tissues. C = O band near 1 741/cm was assigned to the fat in tissues, and C-H stretching vibration bands near 2 961, 2 927, and 2 853/cm were related to lipid and fat content and these bands usually disappeared in the spectra of malignant gastric tissues. -1 641/cm absorption peak belonged to amide I band of protein and H-O-H variable-angle vibration of water. In addition, amide II band of protein was located near 1 550/cm. The intensity of amide II band decreased in the spectra of malignant gastric tissues. Thus, the ratio of intensity of -1 641/cm band to -1 550/cm band was higher in the malignant gastric samples. The intensity of -1 400/cm peak was stronger than that of -1 460/cm peak in the spectra of cancerous samples. According to the statistical results, the relative intensity of $I_{1\,460}/I_{1\,400}$ was less than 1 for about 90% of malignant gastric samples. The intensity of absorption peak at about 1 308/cm increased. The peak position shifted to a low wave number. The peak position was lower than 1 310/cm for 72% of the malignant tissues. The intensity of -1 160/cm was often less than that of -1 120/cm in the spectra of stomach cancer samples.

The spectra of chronic atrophic gastritis were close to those of malignant gastric tissues (Figure 1B), and exhibited partial characteristic bands as those of malignant tissues. CH stretching vibrational band near 3 000-2 800/cm and C = O vibrational band about 1 740/cm were still weak in the spectra of atrophic gastritis samples. Compared with the spectra of malignant gastric tissues, the amide II band in the spectra of atrophic gastritis tissues was broader, and the relative intensity of amide II band to amide I band became higher. The decrease in the extent of the intensity of absorption peak near 1 460/cm was not significant, i.e., the intensity of band at about 1 460/cm became a little less than that at 1 400/cm in the spectra of atrophic gastritis samples. In the spectra of about 81% of atrophic gastritis samples, the relative intensity of $I_{1\,460}/I_{1\,400}$ was less than or equal to 1. Compared with the spectra of malignant tissues, the absorption peak near 1 310/cm was weaker in the spectra of atrophic gastritis samples. Similar to gastric cancerous tissues, the peak position of this band at about 1 310/cm often shifted to a low wave number, which was different from the situation of chronic superficial gastritis, indicating that

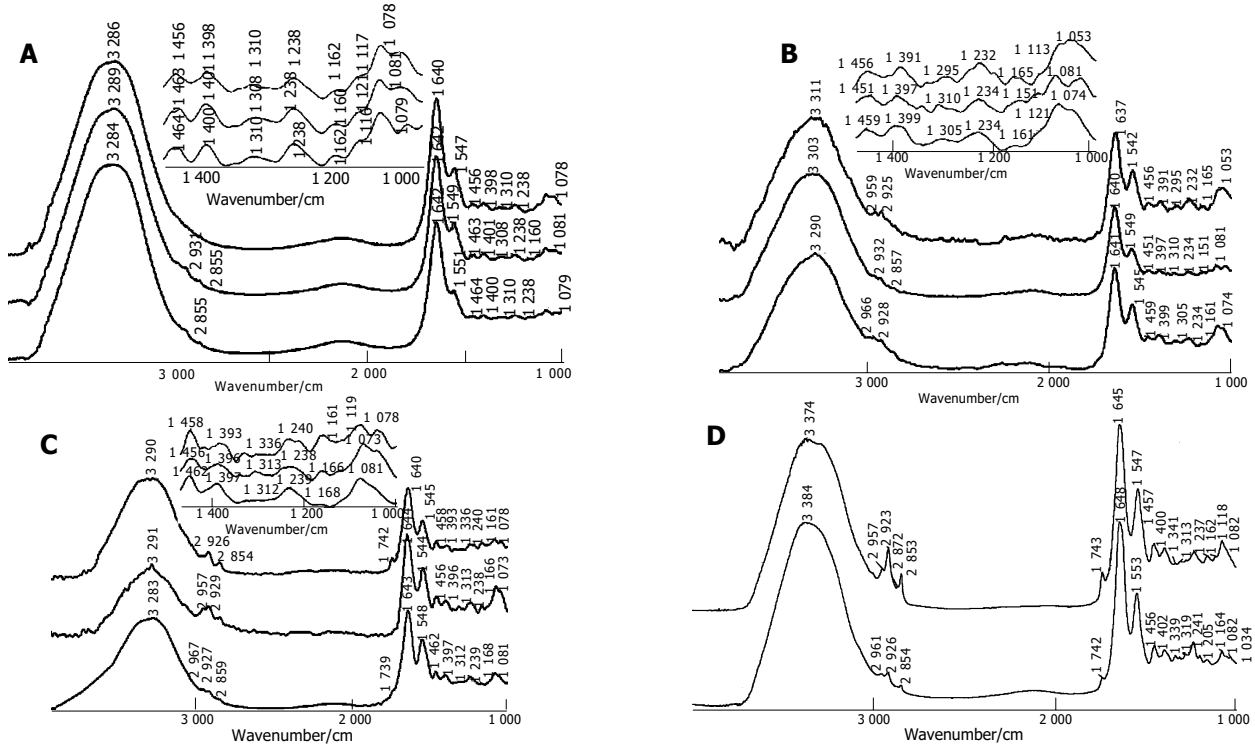

Figure 1 Typical FT-IR spectra of gastric endoscopy samples. **A:** Spectrum of malignant gastric tissue sample; **B:** spectrum of chronic atrophic gastritis tissue sample; **C:** spectrum of chronic superficial gastritis tissue sample; **D:** spectrum of normal gastric tissue sample.

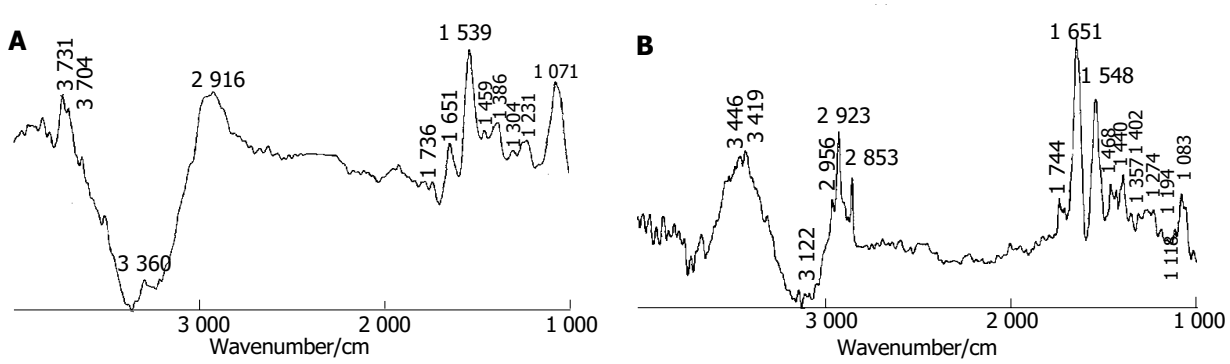

Figure 2 Subtraction spectra of gastric endoscopy samples. **A:** Spectrum of chronic atrophic gastritis tissue minus that of malignant gastric tissue; **B:** spectrum of normal gastric tissue minus that of chronic superficial gastritis tissue.

the peak position was lower than 1 310/cm for 73% of atrophic gastritis tissues.

The spectra of chronic superficial gastritis tissues (Figure 1C) were similar to those of normal stomach tissues[15] (Figure 1D). The spectral features were as follows. CH stretching vibrational band near 3 000-2 800/cm and C = O vibrational band at about 1 740/cm were strong in the spectra of superficial gastritis samples. In general, there existed strong and broad amide II bands in the spectra of superficial gastritis samples. The peak at 1 460/cm was stronger than that at 1 400/cm. The relative intensity of $I_{1\,460}/I_{1\,400}$ was higher than 1 in about 78% of superficial gastritis samples. The peak at about 1 250/cm was stronger, and the band near 1 308/cm disappeared or became weak and the position of this band often shifted to a high wave number, indicating that the peak position was higher than 1 310/cm in 80% of superficial gastritis tissues. Similar to normal gastric tissues, the intensity of peak near 1 160/cm increased and often became stronger than that at about 1 120/cm.

DISCUSSION

To enhance our understanding, the subtraction technique was performed in the spectral analysis[16]. The subtraction spectra (Figures 2A and B) could highlight spectral differences between chronic atrophic gastritis tissue and malignant gastric tissue, and between normal gastric tissue and chronic superficial gastritis tissue. From the two subtraction spectra, some new information could be observed.

Figure 2A illustrates the subtraction result of the spectrum of chronic atrophic gastritis tissue minus that of malignant gastric tissue. It verified that chronic atrophic gastritis tissues exhibited relatively stronger C-H stretching vibration, C = O stretching band, amide I, amide II than gastric cancer tissue. In addition, there was more water in gastric cancer tissue due to the strong negative band located near 3 360/cm in the spectrum of subtraction malignant tissue from chronic atrophic gastritis tissue.

Figure 2B shows the spectral differences between normal gastric tissue and chronic superficial gastritis tissue. The positive peaks in the region of 2 800-3 000/cm and near 1 740/cm were observed in the subtraction spectrum, suggesting that normal gastric tissue contains more components of long-chain C-H and C = O bonds. However, these peaks often decrease and even disappear in the spectra of gastritis and malignant tissues. Because triglyceride contains a large proportion of methyl, methylene and carbonyl, and fat in the region of malignant tissue is consumed because of the necessary nutritional and energy requirement in the development of carcinoma. At the same time, amide I and amide II bands are stronger in the spectrum of normal gastric tissue than in that of chronic superficial gastritis tissue, indicating that normal gastric tissue has more regular protein secondary structures, such as α helical structure.

In conclusion, the results in our study demonstrate that the sensitivity of FT-IR detection to gastric cancer, chronic atrophic gastritis and superficial gastritis is 90.9%, 82.5%, 91.5%, and specificity is 97.3%, 91.7%, 89.5% respectively. FT-IR spectroscopy is effective in distinguishing gastric inflammation from malignancy.

REFERENCES

1 **Wong PT,** Wong RK, Caputo TA, Godwin TA, Rigas B. Infrared spectroscopy of exfoliated human cervical cells: evidence of extensive structural changes during carcinogenesis. *Proc Natl Acad Sci USA* 1991; **88**: 10988-10992

2 **Fujioka N,** Morimoto Y, Arai T, Kikuchi M. Discrimination between normal and malignant human gastric tissues by Fourier transform infrared spectroscopy. *Cancer Detect Prev* 2004; **28**: 32-36

3 **Wong PT,** Lacelle S, Fung Kee Fung M, Senterman M, Mikhael NZ. Characterization of exfoliated cells and tissues from human endocervix and ectocervix by FTIR and ATR/FTIR spectroscopy. *Biospectroscopy* 1995; **1**: 357-364

4 **Sindhuphak R,** Issaravanich S, Udomprasertgul V, Srisookho P, Warakamin S, Sindhuphak S, Boonbundarlchai R, Dusitsin N. A new approach for the detection of cervical cancer in Thai women. *Gynecol Oncol* 2003; **90**: 10-14

5 **Argov S,** Ramesh J, Salman A, Sinelnikov I, Goldstein J, Guterman H, Mordechai S. Diagnostic potential of Fourier-transform infrared microspectroscopy and advanced computational methods in colon cancer patients. *J Biomed Opt* 2002; **7**: 248-254

6 **Ling XF,** Xu YZ, Soloway RD, Xu Z, Zhang TI, Zhou XS, Li WH, Yang ZL, Weng SF, Xu DF, Wu JG. Identification of colorectal and gastric cancer by Fourier transform Infrared (FT-IR) spectroscopy and separation from normal tissue. *Gastroenterology* 2002; **122**: T1584

7 **Li QB,** Yang LM, Ling XF, Wang JS, Zhou XS, Shi JS, Wu JG. Application of the SIMCA method to cancer diagnosis with Fourier-transform infrared spectroscopy. *Guangpuxue Yu*

Guangpu Fenxi 2004; **24**: 414-417
8 **Ren Y,** Xu YZ, Wang J, Zhang YF, Wang F, Shi JS, Wu JG. FTIR spectroscopic and statistical studies on the lung tissues. *Guangpuxue Yu Guangpu Fenxi* 2003; **23**: 681-684
9 **Sun CW,** Xu YZ, Sun KH, Wu QG, Li WH, Xu ZH, Wu JG. A study of the diagnosis of salivary gland tumors by means of mid infrared optical fiber technique. *Guangpuxue Yu Guangpu Fenxi* 1996; **16**: 22-25
10 **Wu JG,** Xu YZ, Sun CW, Soloway RD, Xu DF, Wu QG, Sun KH, Weng SF, Xu GX. Distinguishing malignant from normal oral tissues using FTIR fiber-optic techniques. *Biopolymers* 2001; **62**: 185-192
11 **Xu YZ,** Soloway RD, Lin XF, Zhi X, Weng SF, Wu QG, Shi JS, Sun WX, Zhang TX, Wu JG, Xu DF, Xu GX. Fourier transform infrared (FT-IR) mid-IR spectroscopy separates normal and malignant tissue from the colon and stomach. *Gastroenterology* 2000; **118**: A6438
12 **Wang JS,** Xu YZ, Shi JS, Zhang L, Duan XY, Yang LM, Su YL, Weng SF, Xu DF, Wu JG. FTIR spectroscopic study on normal and cancerous tissues of esophagus. *Guangpuxue Yu Guangpu Fenxi* 2003; **23**: 863-865
13 **Zhang L,** Sun KH, Soloway RD, Ling XF, Xu YZ, Wu QG, Weng SF, Yang ZL, Zhang TL, Yao GQ, Chen HH, Zhou XS, Xu DF, Wu JG. Intraoperative Fourier transform infrared spectroscopy can guide individual resections in patients with gastric cancer. *Gastroenterology* 2004; **126**: A626
14 **Van Dam J.** Novel methods of enhanced endoscopic imaging. *Gut* 2003; **52**(Suppl 4): 12-16
15 **Peng Q,** Xu YZ, Li WH, Zhou XS, Wu JG. FTIR study on the normal and tumor gastrointestinal tissues. *Guangpuxue Yu Guangpu Fenxi* 1998; **18**: 528-531
16 **Ling XF,** Xu YZ, Weng SF, Li WH, Xu Z, Hammaker RM, Fateley WG, Wang F, Zhou XS, Soloway RD, Ferraro JR, Wu JG. Investigation of normal and malignant tissue samples from the human stomach using Fourier transform Raman spectroscopy. *Appl Spectrosc* 2002; **56**: 570-573

Science Editor Wang XL and Guo SY **Language Editor** Elsevier HK

PO Box 2345, Beijing 100023, China
www.wjgnet.com
wjg@wjgnet.com

ELSEVIER

World J Gastroenterol 2005;11(25):3846-3849
World Journal of Gastroenterology ISSN 1007-9327

• *GASTRIC CANCER* •

Clinical significance of expression of apoptotic signal proteins in gastric carcinoma tissue

Xin-Han Zhao, Shan-Zhi Gu, Hong-Gang Tian, Ping Quan, Bo-Rong Pan

Xin-Han Zhao, Shan-Zhi Gu, Hong-Gang Tian, Ping Quan, Key Laboratory of Environment and Genes Related to Diseases of Ministry of Education, Department of Medical Oncology, First Hospital of Xi'an Jiaotong University, Xi'an 710061, Shaanxi Province, China
Bo-Rong Pan, Department of Oncology, Xijing Hospital, Fourth Military Medical University, Xi'an 710032, Shaanxi Province, China
Co-first-authors: Shan-Zhi Gu
Correspondence to: Dr. Xin-Han Zhao, Key Laboratory of Environment and Genes Related to Diseases of Ministry of Education, Department of Forensic Medicine, Medical College of Xi'an Jiaotong University, Xi'an 710061, Shaanxi Province, China. xashanshan@sohu.com
Telephone: +86-29-82655475 Fax: +86-29-82655472
Received: 2004-10-09 Accepted: 2004-11-26

Abstract

AIM: To evaluate the expressions of apoptotic signal proteins FADD, TRADD, FasL, Fas, and NFκB in gastric carcinoma tissues and their clinical significance.

METHODS: Western blot immune trace method was adopted to detect the expressions of apoptotic signal proteins FADD, TRADD, FasL, Fas, and NFκB in 55 tissue specimens of gastric carcinoma.

RESULTS: Five apoptotic signal proteins had different expressions in the gastric carcinoma samples and their expressions were not correlated to age (P = 0.085). Expressions of the FADD, FasL, Fas, and NFκB proteins reduced with increase of the volume of tumor with the exception of increased expression the TRADD protein (64.7-71.1%, P = 0.031). With gradual increase of the malignancy of gastric carcinoma tissues, expressions of the FADD, FasL, and Fas proteins decreased (78.6-28.0%, P = 0.008; 78.6-65.9%, P = 0.071; 100.0-46.3%, P = 0.014), while expressions of the TRADD and NFκB proteins increased (42.9-78.1%, P = 0.063; 78.6-79.1%, P = 0.134). With gradual increase of serum CEA, expression of the FADD protein decreased (62.5-34.0%, P = 0.073), but expressions of the TRADD, FasL, Fas, and NFκB proteins increased (0.0-80.8%, P = 0.005; 62.5-70.2%, P = 0.093; 0.0-70.2%, P = 0.003; 62.5-80.9%, P = 0.075). When compared to the tissues of gastric carcinoma without metastasis, the positive rate of expressions of the FADD and FasL proteins increased, whereas expressions of the TRADD, FADD, and NFκB proteins decreased. There was no significant difference between them (P = 0.095).

CONCLUSION: Gastric carcinoma is endurable to Fas-related apoptosis and apoptotic signal proteins are differently expressed in gastric carcinoma.

Key words: Gastric cancer; Apoptosis; Signal protein; Western blot

Zhao XH, Gu SZ, Tian HG, Quan P, Pan BR. Clinical significance of expression of apoptotic signal proteins in gastric carcinoma tissue. *World J Gastroenterol* 2005; 11(25): 3846-3849
http://www.wjgnet.com/1007-9327/11/3846.asp

INTRODUCTION

Gastric carcinoma is one of the most common causes of malignancy-related death in China[1-4]. Its therapy in clinics is a big challenge. Better remedial method possibly depends on advances in basic research[5-7]. Recent evidence suggests that apoptosis of cells is closely related to occurrence, progress and metastasis of the tumor[8-10]. At present, studies on the apoptosis of tumor cells are an important field of tumor therapy and tumor molecular biology[11-14]. The abnormalities in expressions of apoptotic signal proteins always influence the gastrocellular apoptosis, thus leading to the incidence and development of gastric carcinoma[15-17]. We adopted the Western blot immune trace method to detect the expressions of apoptotic signal proteins FADD, TRADD, FasL, Fas, and NFκB in gastric carcinoma tissues and their significance in gastric carcinoma was assessed.

MATERIALS AND METHODS

Samples

A total of 55 cases were selected from patients with primary gastric carcinoma excision in our hospital from January 2000 to April 2001, who were pathologically diagnosed as adenocarcinoma. There were 35 male and 20 female cases aged 34-78 years with an average age of 54 years. According to Edmondson grading III, the samples were graded as I-II grade in 14 cases and III-IV grade in 41 cases. All samples were submerged in liquid nitrogen within half an hour after the excision and placed in a -80 ℃ refrigerator.

Protein extraction

Fifty-five tumor tissue specimens were homogenized, sonicated for 15 s twice in 500 μL of lysis buffer containing 1× phosphate-buffered saline (PBS), 1% Nonidet-P40, 0.5% sodium deoxycholate, 0.1% SDS and 0.1 mg/mL phenylmethylsulfonyl fluoride, and placed on ice for 30 min. The lysate was centrifuged at 13 000 *g* for 15 min at 4 ℃, the supernatant was collected (450 μL) and the

Table 1 Expressions of FADD, TRADD, FasL, Fas and NFκB proteins in gastric carcinoma tissue specimens, *n* (%)

Sex	*n*	FADD	TRADD	FasL	Fas	NFκB
Male	35	12 (34.3)	26 (74.3)	25 (71.4)	21 (60.0)	28 (80.0)
Female	20	8 (40.0)	12 (60.0)	13 (65.0)	12 (60.0)	15 (75.0)
	55	20 (36.4)	38 (69.1)	38 (69.1)	33 (60.0)	43 (78.2)

protein concentration for each sample was determined by spectroph-otometry (Pharmacia) and using a DC protein assay kit (Bio-Rad).

Reagents and methods

Sheep antihuman FADD, TRADD, FasL, and Fas polyclonal antibodies, rabbit antihuman NFκB polyclonal antibodies, alkaline phophatase marking anti-sheep, anti-rabbit and protein molecular mass marker were also purchased from Santa Cruz Company. Western blot immune trace method was employed to determine the expression of apoptotic signal proteins. Twenty microliters of extracted protein for 120 g/L polyacrylamide gel electrophoresis. When it was semidry, electrical metastasis to the nitrocellulose film was made and enclosed with 100 mL/L bovine serum for 1 h. The first antibody (1∶1 000) was put into PBST (1 g/L Tween20 in PBS) and stored overnight at 4 ℃. After being washed, the sample was enclosed again with 100 mL/L bovine serum for 30 min, and then the second antibody was put in at room temperature for 1 h. After being washed with PBS for 1 h, NBTBCIP development method was performed for coloration.

Assessment standards

The protein molecular mass marker was taken as the standard. In the respective different molecular mass scope, the sample with black stripes was considered positive and vice versa negative. The molecular mass of FADD, TRADD, FasL, Fas, and NFκB proteins was 23, 34, 31, 48, and 65 ku respectively.

Statistical analysis

Chi squared test, accurate 4-chess table method and correlation analysis were used to analyze the correlation of protein expressions with sex, age, tumor size, pathological grading and tumor metastasis. $P<0.05$ was considered statistically significant.

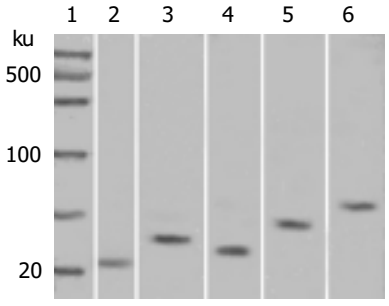

Figure 1 Western blot analysis of the accurate expression of apoptotic signal proteins. Lane 1: marker; lane 2: FADD; lane 3: TRADD; lane 4: FasL; lane 5: Fas; lane 6: NFκB.

RESULTS

Expression of apoptotic signal proteins in gastric carcinoma

The expression of FADD, TRADD, FasL, Fas, and NFκB proteins in gastric carcinoma tissue specimens was 36.4% (20/55), 69.1% (38/55), 69.1% (38/55), 60.0% (33/55) and 78.2% (43/55) respectively (Table 1). We carried out Western blot analysis to determine the accuracy of protein expression (Figure 1).

Relation between apoptotic signal proteins and clinical characteristics

Different expressions of the five apoptotic signal proteins were not correlated to age ($P = 0.085$, Figure 2A). Expressions of the FADD, TRADD, FasL, Fas, and NFκB proteins reduced with increase of the tumor volume, with the exception of increased expression of the TRADD protein (64.7-71.1%, $P = 0.031$). Among them, the positive rate of the expression of the Fas protein in the tissue of gastric carcinoma with a lump ≤5 cm was higher than that of gastric carcinoma >5 cm and the difference was significant ($P = 0.037$, Table 2, Figure 2B).

With the increased of malignancy grade in adenocarcinoma tissues, expressions of the FADD, FasL, and Fas proteins decreased, while expressions of the TRADD and NFκB proteins increased. Expressions of the FADD and Fas

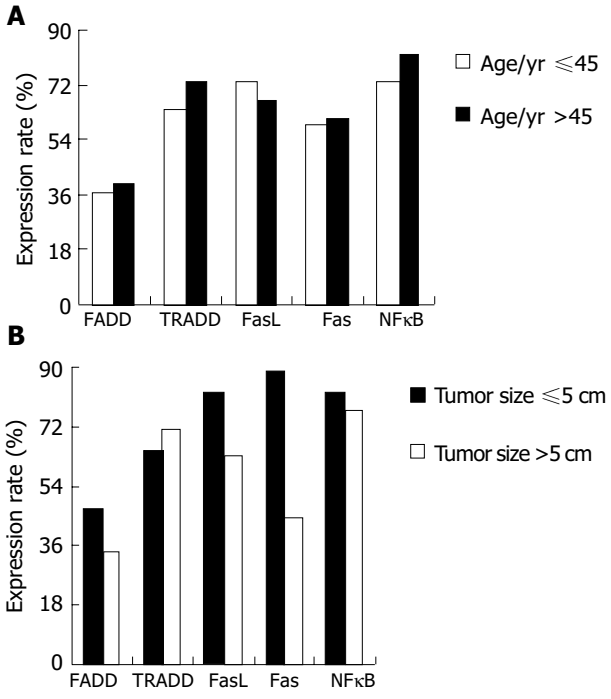

Figure 2 Different expressions of five proteins before and after 45 years (**A**) and different tumor size (**B**).

Table 2 Relationship between expressions of the FADD, TRADD, FasL, Fas, NFκB proteins and clinical characteristics, *n* (%)

Clinical characteristics	*n*	FADD	TRADD	FasL	Fas	NFκB
Male	35	12 (34.3)	26 (74.3)	25 (71.4)	21 (60.0)	28 (80.0)
Female	20	8 (40.0)	12 (60.0)	13 (65.0)	12 (60.0)	15 (75.0)
Age/yr ≤45	22	8 (36.4)	14 (63.6)	16 (72.7)	13 (59.1)	16 (72.7)
>45	33	13 (39.4)	24 (72.7)	22 (66.7)	20 (60.6)	27 (81.8)
Tumor						
Size ≤5 cm	17	8 (47.1)	11 (64.7)	14 (82.4)	15 (88.2)[a]	14 (82.4)
>5 cm	38	13 (34.2)	27 (71.1)	24 (63.2)	17 (44.7)	29 (76.3)
Grading I–II	14	11 (78.6)[b]	6 (42.9)	11 (78.6)	14 (100.0)[c]	11 (78.6)
III–IV	41	9 (22.0)	32 (78.1)	27 (65.9)	19 (46.3)	32 (78.1)
CEA ≤30 (μg/L)	8	5 (62.5)	0 (0.0)	5 (62.5)	0 (0.0)	5 (62.5)
>30 (μg/L)	47	16 (34.0)	38 (80.9)[d]	33 (70.2)	33 (70.2)[d]	38 (80.9)
Tumor						
transformation Yes	6	3 (50.0)	3 (50.0)	5 (83.3)	3 (50.0)	3 (50.0)
No	49	17 (34.2)	35 (71.4)	33 (67.4)	30 (61.2)	39 (79.6)

[a]$P<0.05$ *vs* size >5 cm; [b]$P<0.01$, [c]$P<0.05$ *vs* grading III–IV; [d]$P<0.01$ *vs* CEA ≤30 (μg/L).

proteins were significantly different between the pathological grades ($P = 0.008$ and $P = 0.014$, Figure 3A). With the increase of serum CEA, expression of the FADD protein in gastric carcinoma tissues decreased, while expressions of the TRADD, FasL, Fas and NFκB proteins increased. Expression of the TRADD and Fas proteins were positively correlated with the serum CEA level ($r = 0.700$, $P = 0.005$) and the difference was very significant ($P = 0.003$, Figure 3B). When compared to the tissues of gastric carcinoma with metastasis, the positive expression rate of the FADD and FasL proteins increased, whereas expressions of the TRADD, FAS and NFκB proteins decreased. There was no significant difference between them ($P = 0.095$).

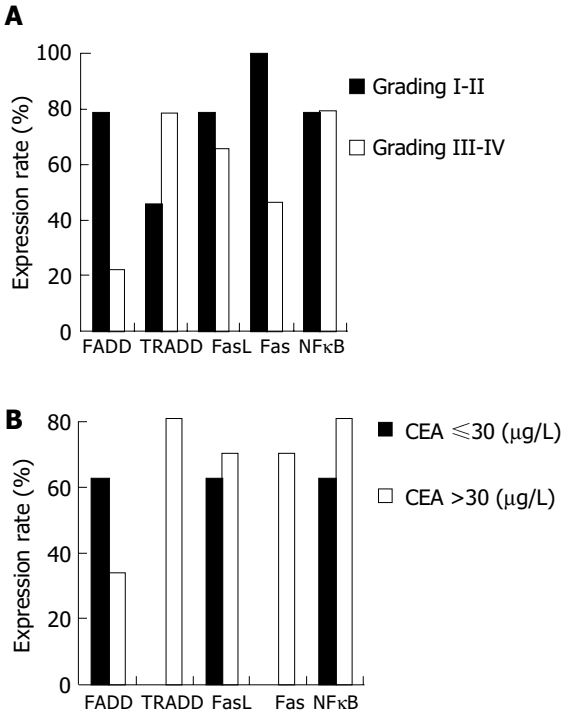

Figure 3 Different expressions of the five proteins with different pathological grading (**A**) and different serum CEA (**B**).

DISCUSSION

Apoptotic abnormality is considered as an important mechanism underlying the development of gastric carcinoma[18,19] and even more crucial than the reproduction of cells of out control[20,21]. The expression of apoptotic signal proteins play different roles in the death of gastric cancer cells. The current studies[22,23] have denoted the main mechanism of the interaction of the apoptotic signal proteins to conduct down the apoptotic signal. FasL is polymerized with its corresponding Fas receptors[24,25]. By activating the FADD and caspase family, the apoptosis of cancer cells ensues; and by activating TRADD, RIP is motivated, causing NFκB to be activated, thereby participating in gene transcription of the survival of cells. The balance between counter signals and paths eventually determines the survival or apoptosis of cells.

In this study, the expression of Fas protein was downregulated with increase of the gastric carcinoma volume and the malignancy degree and positively correlated with the expression of CEA. It was reported[26] that gastric cancer cells inhibit expression of the downregulated FasL, thus escaping Fas-related apoptosis and immune monitoring of the host to enable cancer cells to reproduce continuously and increase their malignancy degree. Expression of the FADD protein is downregulated with increase of the malignancy degree of gastric carcinoma[27]. Gastric cancer cells might through the expression of the downregulated FADD enable caspases 3 and 8 necessary for apoptosis of Fas-related cells to be devitalized, resulting in inhibition of the apoptosis of gastric cancer cells. If FADD is injected, such cells can become sensitive to Fas and induce Fas-related apoptosis, suggesting that the function of FADD is extremely crucial.

The TRADD protein is able to vitalize the NFκB transcription factor and prolong the survival of cells. In the present study, the TRADD protein expression was positively correlated with CEA only when CEA possessed the value of 30 μg/L, suggesting that both of them can be used as indexes to detect gastric carcinoma. However, this can be determined only after investigating a large size of samples[28-30]. As the change of expressions of apoptotic

signal proteins is not much related to metastasis of gastric carcinoma, the abnormalities of the function of these proteins only contribute to the reproduction and rise of malignancy degree of gastric cancer cells, whereas metastasis of gastric carcinoma might correlate to other factors.

In summary, gastric carcinoma is a tumor endurable to Fas-related apoptosis. Apoptotic signal proteins are differently expressed in gastric carcinoma.

REFERENCES

1 **Duan LX,** Zhong DW, Hu FZ, Zhao H, Yang ZL, Yi WJ, Shu GS, Hua SW. Relationship between expression ofVEGF, Flt1, bFGF and P53and outcomein patients with gastric carcinoma. *Shijie Huaren Xiaohua Zazhi* 2004; **12**: 546-549

2 **Xia JG,** Ding YB, Chen GY. Expression of tyrosine kinase Syk and its clinical significance in gastriccarcinoma. *Shijie Huaren Xiaohua Zazhi* 2004; **12**: 767-769

3 **Fukui T,** Matsui K, Kato H, Takao H, Sugiyama Y, Kunieda K, Saji S. Significance of apoptosis induced by tumor necrosis factor-alpha and/or interferon-gamma against human gastric cancer cell lines and the role of the p53 gene. *Surg Today* 2003; **33**: 847-853

4 **Kojima N,** Kunieda K, Matsui K, Kato H, Saji S. Evaluation of carcinoembryonic antigen mRNA in living, necrotic, and apoptotic gastric cancer cells by reverse transcriptase-polymerase chain reaction. *Surg Today* 2003; **33**: 839-846

5 **Igarashi A,** Konno H, Tanaka T, Nakamura S, Sadzuka Y, Hirano T, Fujise Y. Liposomal photofrin enhances therapeutic efficacy of photodynamic therapy against the human gastric cancer. *Toxicol Lett* 2003; **145**: 133-141

6 **Kokura S,** Yoshida N, Ueda M, Imamoto E, Ishikawa T, Takagi T, Naito Y, Okanoue T, Yoshikawa T. Hyperthermia enhances tumor necrosis factor alpha-induced apoptosis of a human gastric cancer cell line. *Cancer Lett* 2003; **201**: 89-96

7 **Huang HL,** Wu BY, You WD, Shen MS, Wang WJ. Influence of dendritic cell infiltration on prognosis and biologic characteristics of progressing gastric cancer. *Zhonghua Zhongliu Zazhi* 2003; **25**: 468-471

8 **Wu YQ,** Wang MW, Wu BY, You WD, Zhu QF. Expression of apoptosis-related proteins and proliferating cell nuclearantigen during stomach canceration. *Shijie Huaren Xiaohua Zazhi* 2004; **12**: 770-773

9 **Nakashima S,** Hiraku Y, Tada-Oikawa S, Hishita T, Gabazza EC, Tamaki S, Imoto I, Adachi Y, Kawanishi S. Vacuolar H+-ATPase inhibitor induces apoptosis via lysosomal dysfunction in the human gastric cancer cell line MKN-1. *J Biochem* 2003; **134**: 359-364

10 **Zhan N,** Xiong YY, Lan J, Wang BC, Tian SF, Yu SP. Relationship between Helicobacter pylori infection and expression of c-myc, Bcl-2, and Bax protein in different gastric mucosa lesions. *Aizheng* 2003; **22**: 1034-1037

11 **Jiang XH,** Wong BC. Cyclooxygenase-2 inhibition and gastric cancer. *Curr Pharm Des* 2003; **9**: 2281-2288

12 **Suzuki H,** Masaoka T, Nomura S, Hoshino Y, Kurabayashi K, Minegishi Y, Suzuki M, Ishii H. Current consensus on the diagnosis and treatment of *H pylori*-associated gastroduodenal disease. *Keio J Med* 2003; **52**: 163-173

13 **Naidu KA.** Vitamin C in human health and disease is still a mystery ? An overview. *Nutr J* 2003; **2**: 7

14 **Fukumoto H,** Tennis M, Locascio JJ, Hyman BT, Growdon JH, Irizarry MC. Age but not diagnosis is the main predictor of plasma amyloid beta-protein levels. *Arch Neurol* 2003; **60**: 958-964

15 **Valbonesi P,** Sartor G, Fabbri E. Characterization of cholinesterase activity in three bivalves inhabiting the North Adriatic sea and their possible use as sentinel organisms for biosurveillance programmes. *Sci Total Environ* 2003; **312**: 79-88

16 **Bjorling-Poulsen M,** Seitz G, Guerra B, Issinger OG. The pro-apoptotic FAS-associated factor 1 is specifically reduced in human gastric carcinomas. *Int J Oncol* 2003; **23**: 1015-1023

17 **Ishii H,** Zanesi N, Vecchione A, Trapasso F, Yendamuri S, Sarti M, Baffa R, During MJ, Huebner K, Fong LY, Croce CM. Regression of upper gastric cancer in mice by FHIT gene delivery. *FASEB J* 2003; **17**: 1768-1770

18 **Hahm KB,** Kim DH, Lee KM, Lee JS, Surh YJ, Kim YB, Yoo BM, Kim JH, Joo HJ, Cho YK, Nam KT, Cho SW. Effect of long-term administration of rebamipide on *Helicobacter pylori* infection in mice. *Aliment Pharmacol Ther* 2003; **18**(Suppl 1): 24-38

19 **Kim DH,** Kim SW, Song YJ, Oh TY, Han SU, Kim YB, Joo HJ, Cho YK, Kim DY, Cho SW, Kim MW, Kim JH, Hahm KB. Long-term evaluation of mice model infected with *Helicobacter pylori*: focus on gastric pathology including gastric cancer. *Aliment Pharmacol Ther* 2003; **18**(Suppl 1): 14-23

20 **Jeong JH,** Park JS, Moon B, Kim MC, Kim JK, Lee S, Suh H, Kim ND, Kim JM, Park YC, Yoo YH. Orphan nuclear receptor Nur77 translocates to mitochondria in the early phase of apoptosis induced by synthetic chenodeoxycholic acid derivatives in human stomach cancer cell line SNU-1. *Ann N Y Acad Sci* 2003; **1010**: 171-177

21 **Ohno S,** Inagawa H, Dhar DK, Fujii T, Ueda S, Tachibana M, Suzuki N, Inoue M, Soma G, Nagasue N. The degree of macrophage infiltration into the cancer cell nest is a significant predictor of survival in gastric cancer patients. *Anticancer Res* 2003; **23**: 5015-5022

22 **Zhao Y,** Wu K, Yu Y, Li G. Roles of ERK1/2 MAPK in vitamin E succinate-induced apoptosis in human gastric cancer SGC-7901 cells. *Weisheng Yanjiu* 2003; **32**: 573-575

23 **Miyachi K,** Sasaki K, Onodera S, Taguchi T, Nagamachi M, Kaneko H, Sunagawa M. Correlation between survivin mRNA expression and lymph node metastasis in gastric cancer. *Gastric Cancer* 2003; **6**: 217-224

24 **Yamaguchi H,** Tanaka F, Sadanaga N, Ohta M, Inoue H, Mori M. Stimulation of CD40 inhibits Fas- or chemotherapy-mediated apoptosis and increases cell motility in human gastric carcinoma cells. *Int J Oncol* 2003; **23**: 1697-1702

25 **Li Z,** Wang Z, Zhao Z, Zhang Y, Ke Y. Expression of Fas, FasL and IFN-gamma in gastric cancer. *Beijing Daxue Xuebao* 2003; **35**: 386-389

26 **Lim SC.** Fas-related apoptosis in gastric adenocarcinoma. *Oncol Rep* 2003; **10**: 57-63

27 **Katoh M,** Katoh M. FLJ10261 gene, located within the CCND1-EMS1 locus on human chromosome 11q13, encodes the eight-transmembrane protein homologous to C12orf3, C11orf25 and FLJ34272 gene products. *Int J Oncol* 2003; **22**: 1375-1381

28 **Dechant MJ,** Fellenberg J, Scheuerpflug CG, Ewerbeck V, Debatin KM. Mutation analysis of the apoptotic "death-receptors" and the adaptors TRADD and FADD/MORT-1 in osteosarcoma tumor samples and osteosarcoma cell lines. *Int J Cancer* 2004; **109**: 661-667

29 **Jamieson NB,** McMillan DC, Brown DJ, Wallace AM. Comparison of simple acid-ethanol precipitation with gel exclusion chromatography for measuring leptin binding in serum of normal subjects and cancer patients. *Ann Clin Biochem* 2003; **40**(Pt 2): 185-187

30 **El Yazidi-Belkoura I,** Adriaenssens E, Dolle L, Descamps S, Hondermarck H. Tumor necrosis factor receptor-associated death domain protein is involved in the neurotrophin receptor-mediated antiapoptotic activity of nerve growth factor in breast cancer cells. *J Biol Chem* 2003; **278**: 16952-16956

Science Editor Wang XL and Guo SY **Language Editor** Elsevier HK

PO Box 2345, Beijing 100023, China
www.wjgnet.com
wjg@wjgnet.com

ELSEVIER

World J Gastroenterol 2005;11(25):3850-3854
World Journal of Gastroenterology ISSN 1007-9327

Expression and significance of tumor-related genes in HCC

Zi-Li Lü, Dian-Zhong Luo, Jian-Ming Wen

Zi-Li Lü, Dian-Zhong Luo, Department of Pathology, Guangxi Medical University, Nanning 530021, Guangxi Zhuang Autonomous Region, China
Jian-Ming Wen, Department of Pathology, Zhongshan Medical College, Sun Yat-Sen University, Guangzhou 510080, Guangdong Province, China
Supported by the National Natural Science Foundation of China, No. 39860079
Correspondence to: Dr. Dian-Zhong Luo, Department of Pathology, Guangxi Medical University, Nanning 530021, Guangxi Zhuang Autonomous Region, China. luodianzhong@yahoo.com.cn
Telephone: +86-771-5356534
Received: 2004-08-18 Accepted: 2004-11-24

Abstract

AIM: To investigate the expression and clinical significance of *DEK, cyclin D1,* insulin-like growth factor II (*IGF-II*), glypican 3 (*GPC3*), ribosomal phosphoprotein 0 (*rpP0*) mRNA in hepatocellular carcinoma (HCC) and its paraneoplastic tissues.

METHODS: The expression of mRNAs of *DEK, cyclin D1, IGF-II, GPC3* and *rpP0* mRNA was detected in HCC and its paraneoplastic tissues by multiplex RT-PCR.

RESULTS: By the simplex RT-PCR, the overexpression of mRNAs of *DEK, cyclin D1, IGF-II, GPC3, rpP0* mRNA in HCC and its paraneoplastic tissues was 78.1%, 87.5%, 87.5%, 75.0%, 81.3% and 15.6%, 40.6%, 37.5%, 21.9%, 31.3% respectively ($P<0.05$). By the multiplex RT-PCR, at least one of the mRNAs was detected in all HCC samples and in 75.0% of paraneoplastic samples ($P>0.05$). However, all these five mRNAs were found in 68.8% of HCC samples, but only in 9.4% of paraneoplastic tissues ($P<0.05$). The positive expression of mRNAs of *DEK, cyclin D1, IGF-II, GPC3, rpP0* in well- and poorly-differentiated HCC was 89.0%, 66.7%, 66.7%, 66.7%, 77.8% and 73.9%, 95.7%, 95.7%, 95.7%, 82.6%, respectively ($P>0.05$). The expression of these genes in HCCs with α-feto protein (AFP) negative and positive was 90.0%, 80.0%, 90.0%, 90.0%, 90.0% and 72.7%, 86.3%, 77.3%, 90.9%, 68.2% respectively ($P>0.05$).

CONCLUSION: The expression of *DEK, cyclin D1, IGF-II, GPC3, rpP0* mRNA in HCC is much higher in HCC than in its paraneoplastic tissues. Multiplex RT-PCR assay is an effective, sensitive, accurate, and cost-effective diagnostic method of HCC.

Key words: HCC; DEK; *Cyclin D1*; *IGF-II*; *GPC3*; *rpP0*

Lü ZL, Luo DZ, Wen JM. Expression and significance of tumor-related genes in HCC. *World J Gastroenterol* 2005; 11(25): 3850-3854
http://www.wjgnet.com/1007-9327/11/3850.asp

INTRODUCTION

Hepatocellular carcinoma (HCC) is an aggressive malignancy with poor prognosis and one of the most common tumors in humans. The development of HCC is a chronic process and involves many factors, including infection of hepatitis virus and contamination with aflatoxin B1[1]. Recent advances in molecular genetics indicate that some tumor suppressor genes, oncogenes, and growth factors may play an important role in hepatocarcinogenesis[2].

Several methods such as DDRT-PCR, cDNA screening[3] are used to identify differential expression of mRNA in tumor and non-tumor tissues. It is reported that some genes, such as *DEK*, *rpP0*[4], *cyclin D1*[5], *IGF-II*[6] , and *GPC3*[7], are overexpressed in HCC tissue. The expression of *DEK, IGF-II* and *rpP0* is higher in HCC than non-tumor tissues in our previous study.

RT-PCR is widely used to analyze gene expression in HCC and paraneoplastic liver tissue. However, the overexpressed genes are only relatively higher in HCC than in paraneoplastic liver tissue and the positive detection rate is relatively low. Moreover, RT-PCR can detect only a single gene once in the past, and the results obtained are fluctuant and less useful in clinics. In order to find a method to enhance the specificity and positive rate, multiplex PCR was used to detect several genes, such as *DEK, cyclin D1, IGF-II, GPC3, rpP0.*

MATERIALS AND METHODS

Tissue samples and patients

HCC and corresponding paraneoplastic tissues were obtained with informed consent from 32 patients who underwent hepatectomy at the First Affiliated Hospital of Guangxi Medical University and Guangxi Tumor Hospital. The profiles were obtained from medical records of 20 male and 12 female patients with an average age of 42.5 years. Twenty-two patients were positive for α-feto protein (AFP). HCC and paraneoplastic tissues were enucleated separately and immediately frozen in liquid nitrogen. Histological classification was performed according to the Edmondson's grading criteria.

Multiplex RT-PCR

Total RNA was isolated from 100 mg of frozen tissue according to the manufacturer's instructions using TRIzol

kit (Sagon Company, Shanghai, China), and then dissolved in water that was treated by DEPC. Four micrograms of total RNA was used to produce cDNA using oligo(dT) primer and MuLV reverse transcription (MBI Company) in a final volume of 20 μL at 42 ℃ for 1 h. The reaction was terminated by incubation at 75 ℃ for 10 min. One microgram of products was PCR amplified with multiple primer sets (0.5 μmol/L, Sagon Company, Shanghai, China), 0.75 units of Taq DNA polymerase (MBI), 0.5 μL 10 mmol/L dNTPs, 2.5 μL 10× buffer. The primers were as follows: *DEK*: 5'-AGG CAC TGT GTC CTC ATT AA and 5'-TCT GAC AGA ATT TCA GGA CA (332 bp); *cyclin D1*: 5'-TAT TTG CAT AAC CCT GAG CG and 5'-GTG ACT ACA TGC ATA TGA GC (350 bp); *IGF*: 5'-AGG AGC TCC TGG ATA ATT TC and 5'-AAT ATT TCA CGT GAC AGA AC (421 bp); *GPC3*: 5'-TGG ACA TCA ATG AGT GCC TC and 5'-CAC ATT CTG GTG AGC ATT CG (204 bp); *rpP0*: 5'-ATG TGA AGT CAC TGT GCC AG and 5'-CTT GGC TTC AAC CTT AGC TG (549 bp). GAPDH was used as control, the primers were 5'-TGA GTA CGT CGT GGA GTC CA and 5'-CAA AGT TGT CAT GGA TGA CC (230 bp). The conditions were initial denaturation at 94 ℃ for 5 min, 30 cycles of amplification, each cycle consisting of denaturation at 94 ℃ for 45 s, annealing at 58 ℃ for 30 s, extension at 72 ℃ for 30 s, final extension at 72 ℃ for 7 min. Because of the limitation by the length of PCR products, the primers of *cyclin D1* and *GPC3* were used together in a single reaction and the primers of *DEK*, *IGF-II*, and *rpP0* were used together in a single reaction.

Analysis by electrophoresis

The amplified products were electrophoresed on 1.2% agarose gel to detect the expression of the genes in HCC and paraneoplastic tissues. The images were analyzed by Quantity One software.

Statistical analysis

Results were analyzed by χ^2 test to compare the differences between the groups. $P<0.05$ was considered statistically significant.

RESULTS

Expression of GAPDH mRNA

The expression of *GAPDH* mRNA was detected in all HCC and non-HCC tissues. There was no difference between the two groups (Figure 1A).

Expression of DEK, cyclin D1, IGF-II, GPC3, rpP0 mRNAs in HCC and adjacent noncancerous liver tissues

The expression of *DEK, cyclin D1, IGF-II, GPC3, rpP0* mRNAs in HCC and adjacent noncancerous liver tissues was 78.1%, 87.5%, 87.5%, 75.0%, 81.3%, and 15.6%, 40.6%, 37.5%, 21.9%, 31.3%, respectively ($P<0.05$, Table 1), which were significantly higher in HCC tissues than in adjacent nontumorous tissue (Figures 1B and C). The density of the bands was also higher in HCC than in adjacent noncancerous liver tissues.

The expression of *DEK, cyclin D1, IGF-II, GPC3, rpP0* mRNAs in well- and poorly-differentiated HCC was 89.0%,

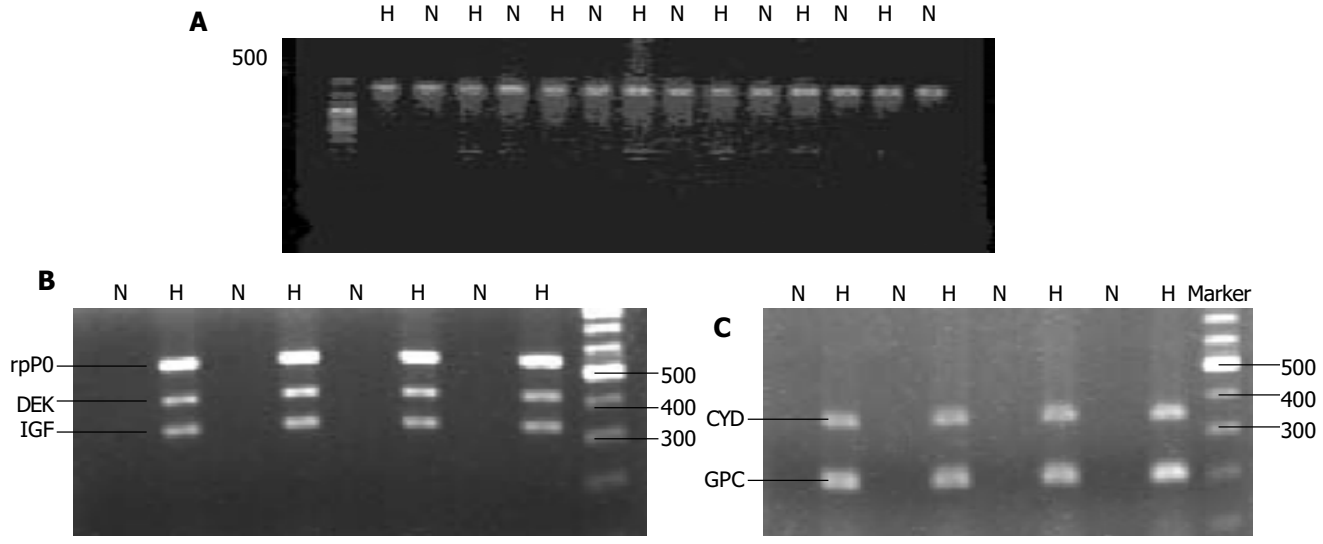

Figure 1 Expression of GAPDH (**A**), mRNA of rpP0, DEK, and IGF-II (**B**), mRNA of cyclin D1 and GPC3 (**C**) in HCC tissue (H) and adjacent nontumorous tissue (N).

Table 1 Expression of *DEK, cyclin D1, IGF-II, GPC3, rpP0* mRNAs in HCC and adjacent noncancerous liver tissues

	Cyclin D1[a]		GPC3[c]		DEK[e]		IGF[g]		rpP0[i]	
	T	N	T	N	T	N	T	N	T	N
Positive	28	13	24	7	25	5	28	12	26	10
Negative	4	19	8	25	7	27	4	20	6	22

T, HCC tumor tissue; N, adjacent nontumorous tissue. χ^2-test: [a]$P<0.05$, [c]$P<0.05$, [e]$P<0.05$, [g]$P<0.05$, [i]$P<0.05$ vs others.

66.7%, 66.7%, 66.7%, 77.8% and 73.9%, 95.7%, 95.7%, 95.7%, 82.6%, respectively (P>0.05, Table 2).

The expression of *DEK, cyclin D1, IGF-II, GPC3, rpP0* mRNAs in HCC with AFP negative and positive was 90.0%, 80.0%, 90.0%, 90.0%, 90.0% and 72.7%, 86.3%, 77.3%, 90.9%, 68.2%, respectively (P>0.05, Table 3).

Expression of DEK, cyclin D1, IGF-II, GPC3, rpP0 mRNAs in HCC and adjacent noncancerous liver tissues shown by multiplex RT-PCR

By multiplex RT-PCR, at least one of the mRNAs could be detected in all HCC tissues and in 75.0% of paraneoplastic tissues (P>0.05) (Table 4). However, all these five mRNAs were found in 68.8% of HCC tissue, but only in 9.4% of paraneoplastic tissues (P<0.05, Table 4).

DISCUSSION

The growth of cells depends on the regulation by many factors, including oncogenes, tumor suppressor genes, growth factors, signal transduction factors, and apoptosis factors, *etc*. The origin of tumor is related to the modification of these genes. Genes such as *DEK, cyclin D1, IGF-II, GPC3, rpP0,* are involved in the initiation and development of HCC, and the possible markers for the diagnosis of HCC in clinic. To identify whether these genes were generally involved in hepatocarcinogenesis, multiplex PCR was used in the present study. We found that these genes had an upregulated expression in HCC and multiplex PCR could enhance the detective positive rate.

Cyclin D1

Cyclin, cyclin-dependent kinases, and tumor suppressor gene products interact and regulate the normal cell cycle. *Cyclin D1* and cyclin-dependent kinases are required for completion of the G_1/S transition in normal mammalian cells[8]. *Cyclin D1* is located on chromosome 11q13 and exhibits many characteristics of cellular oncogenes. Overexpression of *cyclin D1* may be associated with actual gene amplification or transcriptional dysregulation in cancer. *Cyclin D1* is overexpressed in hyperplastic lesions, such as endometrioid adenocarcinoma[9], mantle cell lymphoma[10], and ovarian carcinoma[11]. The results in our study showed that the expression of *cyclin D1* was significantly higher in HCC than in adjacent nontumorous tissue. The mechanism of *cyclin D1* dysregulation in HCC is not clear, but it is likely that the dysregulation contributes to increasing the proportion of cells in transition from G_1 to S phase. The overexpression of *cyclin D1* may be one of the several mechanisms involved in hyperplasia of liver cells.

DEK

DEK is a 43-ku phosphoprotein that was first isolated as part of a fusion protein expressed in a subtype of acute myeloid leukemias with t(6;9) chromosomal translocations[12]. *DEK* was lately identified as an autoimmune antigen in patients with pauciarticular onset juvenile rheumatoid arthritis, systemic lupus erythematosus[13], and other autoimmune diseases. In recent study, it was demonstrated that *DEK* was a site-specific DNA binding protein that was involved likely in transcriptional regulation and signal transduction and it had implications not only for HIV-2 transcription[14] but also for multiple cellular processes involving with *DEK*. Recent data demonstrated that the major portion of *DEK* is associated with chromatin

Table 2 Expression of *DEK, cyclin D1, IGF-II, GPC3, rpP0* mRNAs in well- and poorly-differentiated HCC

	Cyclin D1		GPC3		DEK		IGF-II		rpP0	
	+	-	+	-	+	-	+	-	+	-
Well-differentiated HCC	6	3	6	3	8	1	6	3	7	2
Poor-differentiated HCC	22	1	18	5	17	6	22	1	19	4
Total	28	4	24	8	25	7	28	4	26	6

Table 3 Expression of *DEK, cyclin D1, IGF-II, GPC3*, *rpP0* mRNAs in HCC with AFP negative and positive HCC tissue

	n	Cyclin D1+	GPC3+	DEK+	IGF-II+	rpP0+
AFP(-)	10	8	9	9	9	9
AFP(+)	22	20	15	16	19	17
Total	32	28	24	25	28	26

χ^2 test, P>0.05, the group of APF(+) *vs* the group of AFP(-).

Table 4 Expression of *DEK, cyclin D1, IGF-II, GPC3, rpP0* mRNAs in HCC and adjacent noncancerous liver tissues by multiplex RT-PCR Groups

	n	Positive reaction		Negative reaction	
		Anyone of the five mRNAs (%)	All of the five mRNAs (%)	Anyone of the five mRNAs (%)	All of the five mRNAs (%)
T	32	32 (100)	22 (68.8)	10 (31.3)	0 (0)
N	32	24 (75.0)	3 (9.4)	29 (90.6)	8 (25.0)
		P>0.05	P>0.05	P>0.05	P>0.05

in vivo and suggested that it might play a role in chromatin architecture[15]. Our present experiment shows that the percentage of overexpression of mRNA of *DEK* (78.1%) in HCC was higher than in adjacent nontumorous tissues (15.6%). It indicates the overexpression of DEK may be involved in the transformation from normal liver tissue to HCC, perhaps by activating the oncogenes.

GPC3

GPC3 gene is located at Xq26, and mutated in the Simpson-Golabi-Behmel syndrome[16]. It may be regulated by methylation of the inactive X in expressing tissues, and encodes a developmentally regulated heparin sulfate proteoglycan that is bound to the cell surface through a glycosylphosphatidylinositol anchor. Based on their localization on the cell surface, such glypicans are thought to regulate interactions between growth factor and their receptors. It is associated with apoptosis and cell signal transduction. It is reported that *GPC3* is a tissue-specific gene in breast tumor[17], ovarian tumor[18], and malignant mesothelioma[19] in which it is downregulated by aberrant methylation of the GPC3 promoter region, and upregulated in HCC. In the present study, GPC3 was overexpressed in HCC tissue and the positive expression rate was 75.0%, which was higher than that in adjacent nontumorous tissue (21.9%). Although the role of overexpression of GPC3 in the development of HCC is not known, it may break the balance between cell growth and death.

IGF-II

It was reported that IGF-II is positive in some benign neoplastic nodules and HCC[20]. In the present study, the levels of IGF-II was higher in HCC than in adjacent nontumorous tissue, suggesting that the growth factor may act as an autocrine regulation of cell proliferation, GPC3 may act as a positive regulator of IGF-II, although we have not detected a direct interaction between GPC3 and IGF-II. It is possible that GPC3 positively regulates IGF-II activity by interacting with the components of its signaling system.

rpP0

Ribosome acts as a place for protein synthesis. It is composed of rRNA and ribosomal phosphoproteins. In the family of ribosomal phosphoprotein, there are five members: P0, P1α, P1β, P2α, and P2β. Three functional domains can be defined in the rpP0: one involved in binding to rRNA, one connected to P1/P2 protein interaction, and one associated with elongation factors[21]. It was reported that rpP0 expression increases in colon carcinoma cells[22]. In the present study, rpP0 was overexpressed in HCC tumor tissue, suggesting that upregulation of rpP0 is associated with HCC, which may be a signal for increasing protein synthesis.

Multiplex RT-PCR and HCC

In this study, we used multiplex RT-PCR to detect the expression of mRNAs of *DEK, cyclin D1, IGF-II, GPC3, rpP0* in HCC and adjacent nontumorous liver tissue. We found that at least one of the mRNAs could be detected in all HCC tissues and 68.8% of HCC tissues expressed all these five mRNAs, while only 9.4% of paraneoplastic tissues expressed all of them ($P<0.05$), suggesting that multiplex RT-PCR enhances the detective sensitivity and specificity when combining several specific primers. The expression of anyone of these mRNAs in liver tissue could be regarded as a risk factor for HCC. The higher the expression of these mRNAs the greater the risk. When all these mRNAs are negative in tissues, the possibility of HCC is lower. Multiplex RT-PCR provides an easy and quick method to detect the expression of these genes in liver tissues.

ACKNOWLEDGMENTS

The authors thank Dr. Dang-Rong Li for practical and productive technical advice regarding the RT-PCR technique and Dr. Le-Qun Li for providing useful tissues.

REFERENCES

1 **Park US,** Su JJ, Ban KC, Qin L, Lee EH, Lee YI. Mutations in the p53 tumor suppressor gene in tree shrew hepatocellular carcinoma associated with hepatitis B virus infection and intake of aflatoxin B1. *Gene* 2000; **251**: 73-80
2 **Park DY,** Sol MY, Suh KS, Shin EC, Kim CH. Expressions of transforming growth factor (TGF)-beta1 and TGF-beta type II receptor and their relationship with apoptosis during chemical hepatocarcinogenesis in rats. *Hepatol Res* 2003; **27**: 205-213
3 **Sell S.** Mouse models to study the interaction of risk factors for human liver cancer. *Cancer Res* 2003; **63**: 7553-7562
4 **Kondoh N,** Wakatsuki T, Ryo A, Hada A, Aihara T, Horiuchi S, Goseki N, Matsubara O, Takenaka K, Shichita M, Tanaka K, Shuda M, Yamamoto M. Identification and characterization of genes associated with human hepatocellular carcinoma. *Cancer Res* 1999; **59**: 4990-4996
5 **Azechi H,** Nishida N, Fukuda Y, Nishimura T, Minata M, Katsuma H, Kuno M, Ito T, Komeda T, Kita R, Takahashi R, Nakao K. Disruption of the p16/cyclin D1/retinoblastoma protein pathway in the majority of human hepatocellular carcinoma. *Oncology* 2001; **60**: 346-354
6 **Tsai JF,** Jeng JE, Chuang LY, You HL, Ho MS, Lai CS, Wang LY, Hsieh MY, Chen SC, Chuang WL, Lin ZY, Yu ML, Dai CY. Serum insulin-like growth factor-II and alpha-fetoprotein as tumor markers of heptocellular carcinoma. *Tumour Biol* 2003; **24**: 291-298
7 **Sung YK,** Hwang SY, Park MK, Farooq M, Han IS, Bae HI, Kim JC, Kim M. Glypican-3 is overexpressed in human hepatocellular carcinoma. *Cancer Sci* 2003; **94**: 259-262
8 **Jirstrom K,** Ringberg A, Ferno M, Anagnostaki L, Landberg G. Tissue microarray analyses of G1/S-regulatory proteins in ductal carcinoma *in situ* of the breast indicate that low cyclin D1 is associated with local recurrence. *Br J Cancer* 2003; **89**: 1920-1926
9 **Ruhul Quddus M,** Latkovich P, Castellani WJ, James Sung C, Steinhoff MM, Briggs RC, Miranda RN. Expression of cyclin D1 in normal, metaplastic, hyperplastic endometrium and endometrioid carcinoma suggests a role in endometrial carcinogenesis. *Arch Pathol Lab Med* 2002; **126**: 459-463
10 **Howe JG,** Crouch J, Cooper D, Smith BR. Real-time quantitative reverse transcription-PCR for cyclin D1 mRNA in blood, marrow, and tissue specimens for diagnosis of mantle cell lymphoma. *Clin Chem* 2004; **50**: 80-87
11 **Raju U,** Nakata E, Mason KA, Ang KK, Milas L. Flavopiridol, a cyclin-dependent kinase inhibitor, enhances radiosensitivity of ovarian carcinoma cells. *Cancer Res* 2003; **63**: 3263-3267
12 **Maeda T,** Kosugi S, Ujiie H, Osumi K, Fukui T, Yoshida H, Kashiwagi H, Ishikawa J, Tomiyama Y, Matsuzawa Y. Localized relapse in bone marrow in a posttransplantation patient with t(6;9) acute myeloid leukemia. *Int J Hematol* 2003; **77**: 522-525
13 **Wichmann I,** Respaldiza N, Garcia-Lozano JR, Montes M,

Sanchez-Roman J, Nunez-Roldan A. Autoantibodies to DEK oncoprotein in systemic lupus erythematosus (SLE). *Clin Exp Immunol* 2000; **119**: 530-532

14 **Faulkner NE,** Hilfinger JM, Markovitz DM. Protein phosphatase 2A activates the HIV-2 promoter through enhancer elements that include the pets site. *J Biol Chem* 2001; **276**: 25804-25812

15 **Kappes F,** Burger K, Baack M, Fackelmayer FO, Gruss C. Subcellular localization of the human proto-oncogene protein DEK. *J Biol Chem* 2001; **276**: 26317-26323

16 **Veugelers M,** Cat BD, Muyldermans SY, Reekmans G, Delande N, Frints S, Legius E, Fryns JP, Schrander-Stumpel C, Weidle B, Magdalena N, David G. Mutational analysis of the GPC3/GPC4 glypican gene cluster on Xq26 in patients with Simpson-Golabi-Behmel syndrome: identification of loss-of-function mutations in the GPC3 gene. *Hum Mol Genet* 2000; **9**: 1321-1328

17 **Xiang YY,** Ladeda V, Filmus J. Glypican-3 expression is silenced in human breast cancer. *Oncogene* 2001; **20**: 7408-7412

18 **Lin H**, Huber R, Schlessinger D, Morin PJ. Frequent silencing of the GPC3 gene in ovarian cancer cell lines. *Cancer Res* 1999; **59**: 807-810

19 **Murthy SS,** Shen T, De Rienzo A, Lee WC, Ferriola PC, Jhanwar SC, Mossman BT, Filmus J, Testa JR. Expression of GPC3, an X-linked recessive overgrowth gene, is silenced in malignant mesothelioma. *Oncogene* 2000; **19**: 410-416

20 **Tsai JF,** Jeng JE, Chuang LY, You HL, Ho MS, Lai CS, Wang LY, Hsieh MY, Chen SC, Chuang WL, Lin ZY, Yu ML, Dai CY. Serum insulin-like growth factor-II and alpha-Fetoprotein as tumor markers of hepatocellular carcinoma. *Tumour Biol* 2003; **24**: 291-298

21 **Rodriguez-Gabriel MA,** Remacha M, Ballesta JP. The RNA interacting domain but not the protein interacting domain is highly conserved in ribosomal protein P0. *J Biol Chem* 2000; **275**: 2130-2136

22 **Barnard GF,** Staniunas RJ, Bao S, Mafune K, Steele GD Jr, Gollan JL, Chen LB. Increased expression of human ribosomal phosphoprotein P0 messenger RNA in hepatocellular carcinoma and colon carcinoma. *Cancer Res* 1992; **52**: 3067-3072

Science Editor Wang XL and Guo SY **Language Editor** Elsevier HK

PO Box 2345, Beijing 100023, China
www.wjgnet.com
wjg@wjgnet.com

ELSEVIER

World J Gastroenterol 2005;11(25):3855-3859
World Journal of Gastroenterology ISSN 1007-9327

• *LIVER CANCER* •

Expression and significance of new inhibitor of apoptosis protein survivin in hepatocellular carcinoma

Hong Zhu, Xiao-Ping Chen, Wan-Guang Zhang, Shun-Feng Luo, Bi-Xiang Zhang

Hong Zhu, Xiao-Ping Chen, Wan-Guang Zhang, Shun-Feng Luo, Bi-Xiang Zhang, Hepatic Surgery Center, Tongji Hospital Affiliated to Tongji Medical College, Huazhong University of Science and Technology, Wuhan 430030, Hubei Province, China
Supported by the Grants From Key Subsidy Project of Clinical Speciality of Chinese Ministry of Public Health from 2001 to 2003, No. 321[2001]
Correspondence to: Dr. Hong Zhu, Hepatic Surgery Center, Tongji Hospital Affiliated to Tongji Medical College, Huazhong University of Science and Technology, 1095 Jiefang Dadao, Wuhan 430030, Hubei Province, China. hong_jasmine@hotmail.com
Telephone: +86-27-83662599 Fax: +86-27-83662851
Received: 2003-07-04 Accepted: 2003-11-06

Key words: Survivin; Vascular endothelial growth factor; Hepatocellular carcinoma

Zhu H, Chen XP, Zhang WG, Luo SF, Zhang BX. Expression and significance of new inhibitor of apoptosis protein survivin in hepatocellular carcinoma. *World J Gastroenterol* 2005; 11(25): 3855-3859
http://www.wjgnet.com/1007-9327/11/3855.asp

Abstract

AIM: To investigate expression and significance of inhibitor of apoptosis protein survivin in hepatocellular carcinoma (HCC).

METHODS: The expression of survivin and vascular endothelial growth factor (VEGF) was investigated in 38 cases of HCC tissues and 38 liver cirrhosis tissues by immunohistochemistry and Western blot. The relationship between the expression of survivin and clinicopathological factors of HCC was analyzed.

RESULTS: Survivin protein was detected in 23 (60.5%) of 38 HCCs and 3 (7.9%) of 38 liver cirrhosis tissues. In 23 cases of HCC which expressed survivin, the expression of VEGF was positive in 18 cases and slight positive or negative in 5 cases. While in 15 cases of HCC which did not express survivin, 12 cases did not express or slightly expressed, and 3 cases expressed VEGF. In liver cirrhosis tissues, the expression of VEGF was as follows: 24 cases were negative, 10 cases were weak positive and 4 cases were strong positive. The expression of survivin was coincident with the expression of VEGF in HCC (P<0.01). The expression of survivin in HCC had no relationship with the patients' age, gender, tumor size and differentiation level of HCC, while it was related to the metastasis of HCC. The protein quantitative analysis by Western blot also showed that overexpression of survivin in HCC was closely correlated to the expression of VEGF (P<0.01). Furthermore, stronger expression of survivin and VEGF was also found in patients with metastasis rather than in those with no metastasis (P<0.01).

CONCLUSION: Survivin plays a pivotal role in the metastasis of HCC, and it has some correlation with tumorigenesis. The expression of survivin in the primary lesion is very useful as an indicator for metastasis and prognosis of HCC. It could become a new target of gene therapy of HCC.

INTRODUCTION

In organisms, cell death and cell cycle progression are two sides of the same coin, and these two different phenomena are regulated moderately to maintain the cellular homeostasis[1]. On the other hand, gene mutation could be accumulated and cell growth cycle could be prolonged, thus finally facilitating the formation of tumor. At present, it has been confirmed that P53 and bcl-2 family are critical to the regulation of cell apoptosis. Survivin protein (M_r 16 500) is a recently described member of inhibitor of apoptosis protein (IAP) family of antiapoptotic proteins, which may act simultaneously with the bcl-2 family proteins, but has a different apoptosis inhibitory mechanism[2]. Survivin is conserved across evolution with homologs found in both vertebrate and invertebrate animal species[3]. The tissue distribution of survivin has obvious cell selectivity. Some research has found that survivin is undetectable in terminally differentiated adult tissues, yet it is abundantly expressed in fetal tissues and in a variety of human tumors including lung, colo-rectal, breast, prostate, melanoma, pancreatic, and gastric carcinoma as well as in high-grade lymphomas and neuroblastomas[4-11]. However, the expression and implication of survivin in hepatocellular carcinoma are still unknown.

Vascular endothelial growth factor (VEGF) is considered to be the most primary factor prompting the angiogenesis in tumor tissue, which also holds the central position in the course of formation and metastasis of tumor. However, it is unclear how VEGF accelerates the metastasis of neoplasms.

To explore the role and mechanism of survivin in the progression of HCC and the relationship with VEGF, we adopted immunohistochemistry and Western-blot techniques to investigate the expression of survivin and VEGF in HCC.

MATERIALS AND METHODS

Patients and samples

A total of 38 cases of HCC was involved in this study. The

patients with HCC, who underwent potentially curative tumor resection at Hepatic Surgery Center of Tongji Hospital from 2001 to 2002, had received neither chemotherapy nor radiation therapy before surgery. Among them, there were 33 males and 5 females, and the mean age of the patients was 47.3 years (SD, 11.2 years; range, 18-76 years).

All the specimens were confirmed to be hepatocellular carcinoma by pathological diagnosis. Cell differentiation was graded by Edmondson-Steiner's criteria. Tumors with Edmondson-Steiner's grade I were regarded as moderate to well differentiation and those with grade II-IV were poorly differentiated. The criteria of metastasis included extrahepatic tissue or organ involvement; hilum or remote lymphoid nodule metastasis; tumor thrombus formation in the main portal trunk or hepatic vein or bile duct. Multifocal HCC was excluded from this study because it was a controversial issue[12].

Routinely processed formalin-fixed, paraffin-embedded blocks containing principal tumor were selected. Serial sections of 2-4 μm were prepared from the cut surface of blocks at the maximum cross-section of the tumor.

Immunohistochemical staining for survivin and VEGF

Immunohistochemical staining for survivin and VEGF antigen was carried out by the standard streptavidin-peroxidase-biotin technique (SP technique) using SP kit (Zhongshan Company, Beijing, China). Rabbit-anti-human survivin monoclonal antibody and rat-anti-human VEGF monoclonal antibody were obtained from Neomarkers Company. Experimental procedure was conducted according to the SP kit specification. Primary antibody was diluted at 1∶200. Antigen retrieval was done by microwave citrate salt method. 3,3-diaminobenzidine and hematoxylin were used for color development and counterstaining respectively. Cells whose cytoplasm was dyed brown were regarded as positive ones. One case of stage III gastric cancer was stained intensively and reproducibly for survivin expression in >30% of tumor cells, and was used as a positive control throughout the study. Negative control slides processed without primary antibody were included for each staining. In brief, deparaffinized and rehydrated sections were bathed in a 10^{-3} mol/L sodium citrate buffer (pH 6.0) then the solution was put to a pressure cooker and boiled for 20 min while maintaining the pressure. After endogenous peroxidase was quenched in 3% hydrogen peroxide and blocked for 5 min, the sections were incubated overnight at 4 ℃ with primary polyclonal antibody at a 1∶200 dilution. Biotinylated immunoglobulin and streptavidin conjugated to peroxidase were then added. Finally, 3,3'-diaminobenzidine was used for color development, and hematoxylin was used for counterstaining. The mean percentage of positive tumor cells was determined in at least five areas at 200-fold magnification for survivin and 100-fold magnification for VEGF and scaled as the following: (0) <5%; (1) 5-25%; (2) 25-50%; (3) 50-75%; and (4) >75%. The intensity of survivin immunostaining was scored as follows: 1+, weak; 2+, moderate; and 3+, intense. Because tumors showed heterogeneous staining, the dominant pattern was used for scoring. The scores indicating percentage of positive tumor cells and staining intensity were multiplied to produce a weighed score for each case. Cases with weighed scores <1 were defined as negative; cases with weighed scores >2 were defined as strongly positive and those in between were defined as positive.

Western blot

Proteins were extracted from tissues and cells by detergent lysis using NP-40 lysis buffer (0.2% NP-40, 100 mmol/L Tris-HCl, pH 8.0, 200 mmol/L NaCl, 0.01% SDS). Proteins were fixed quantitatively by ultraviolet spectrophotometer analysis. A total of 20 μg of the proteins of HCC tissue was fractionated on a 75 g/L polyacrylamide slab gel containing 1 g/L SDS and then transferred onto a nitrocellulose filter by electroblotting. The filter was incubated for at least 1 h in 10 mmol/L Tris-HCl buffer (pH 8.0) containing 150 mmol/L NaCl, 0.05% Tween-20 and 50 g/L bovine serum albumin for survivin and in 10 mmol/L Tris-HCl buffer (pH 8.0) containing 150 mmol/L NaCl, 0.05% Tween-20 and 50 g/L milk powder for VEGF to prevent nonspecific binding of antibodies. Then it was incubated with primary antibody (survivin, 1∶1 000; VEGF 1∶2 000) for 12 h, and with second antibodies for 1 h at room temperature in the same buffer. Respectively, the second antibodies of survivin were goat-anti-rabbit polyclonal antibody labeled by alkaline phosphatase and those of VEGF were goat-anti-rat polyclonal antibody labeled by horseradish peroxidase. VEGF was dyed by 0.01% DAB/H_2O_2 form 5 to 15 min and brown straps were viewed as positive results. Survivin was dyed by NBT/BCIP for 10 min or so and blue-black straps were positive. At the same time protein molecular weight marker (M_r 14 000-70 000) was used to identify destined straps. The expressed protein quantity was automatically analyzed by GIS gel image processing system (version 3.10, Tanon Technological Limited Company, Shanghai, China). The net area of strap represented the expressed protein quantity.

Statistical analysis

All statistical analyses were performed using the SPSS 10.0 J software package for Macintosh (SPSS, Inc., Chicago, IL). Variables associated with survivin expression were analyzed by the χ^2 test. The coincident expression of survivin and VEGF protein in HCC or liver cirrhosis tissues was analyzed by the paired *t*-test. The correlation between HCC metastasis and expression of survivin and VEGF protein was tested by bivariate correlation analysis. $P<0.05$ was considered significant and $P<0.01$ was considered remarkably significant.

RESULTS

Immunohistochemical staining

Twenty-three cases (60.5%) of 38 HCCs expressed survivin protein, among them, 8 cases strongly expressed, 12 cases positively expressed, and 3 cases slightly expressed. Survivin protein was detected in only 3 (7.9%) of 38 liver cirrhosis. The relationship between the expression of survivin and clinicopathological factors of HCC is shown in Table 1. In 23 cases of HCC which expressed survivin, the expression of VEGF was positive in 18 cases and slightly positive or negative in 5 cases. In 15 cases which did not express survivin

Table 1 Relationship of the expression of survivin and clinicopathological factors of HCC

	n	Survivin		*P*
		Positive (*n*)	Percent (%)	
Tissue				<0.01
Cirrhosis	38	3	7.9	
HCC	38	23	60.5	
Age (yr)				>0.05
<60	31	19	61.3	
⩾60	7	4	57.1	
Sex				>0.05
Male	33	21	63.6	
Female	5	2	40.0	
Size (cm)				>0.05
⩾5	17	12	70.6	
<5	21	11	52.4	
Differentiation				>0.05
Moderate to well	16	9	56.3	
Poor	22	14	63.6	
Metastasis				<0.05
Positive	14	12	85.7	
Negative	24	11	45.8	

protein, 12 cases of HCC did not express or slightly expressed VEGF and 3 cases expressed VEGF. In liver cirrhosis tissue, the expression of VEGF was negative in 24 cases, weak positive in 10 cases and strong positive in 4 cases. The staining of both survivin and VEGF was mainly localized in cytoplasm.

By statistical analysis, there was a remarkable difference in survivin expression between the tumor tissue and liver cirrhosis tissues ($P<0.01$). The expression of survivin in HCC had no significant relation with the patients' age, gender, tumor size and differentiation level of HCC, while it was related to the metastasis of HCC ($P<0.05$). Furthermore, a high expression of survivin was coincident with the expression of VEGF in HCC ($P<0.01$) (Table 2 and Figures 1 and 2).

Western blot

By analysis with GIS gel image processing system, the values of net area indicating the expressed protein quantity are as shown in Tables 3 and 4, Figures 3 and 4.

DISCUSSION

It has been identified that bcl-2 family and IAPs family have close relations with cell apoptosis. So far six members of IAPs family (NIAP, c-IAP1, c-IAP2, XIAP, Survivin and Bruce) have been cloned[13]. IAPs family expresses extensively among many species, which are of homology in their

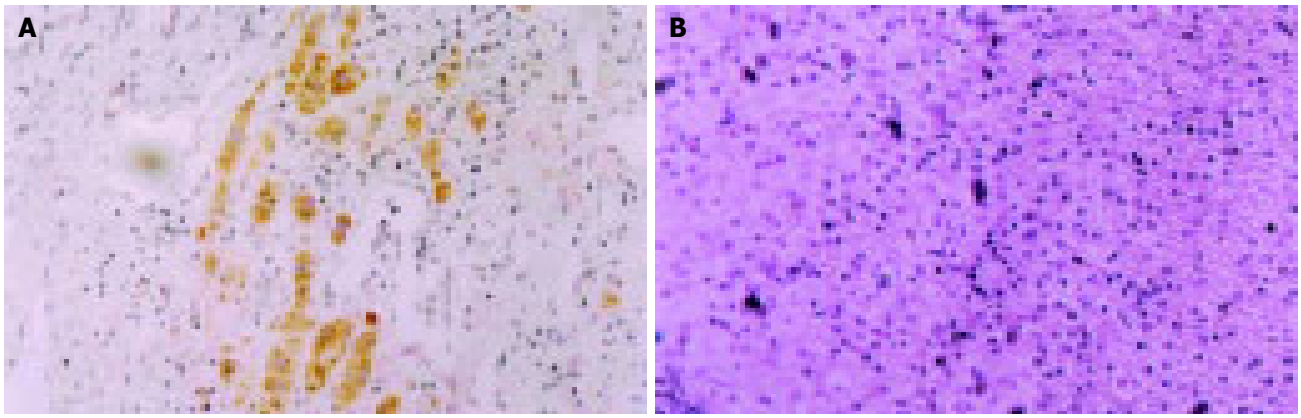

Figure 1 Expression of survivin in HCC and liver cirrhosis tissues (SP method, ×200). **A:** The brown granules in the cytoplasm indicate survivin protein in liver cancer cells; **B:** Survivin protein is not detected in liver cirrhosis tissues.

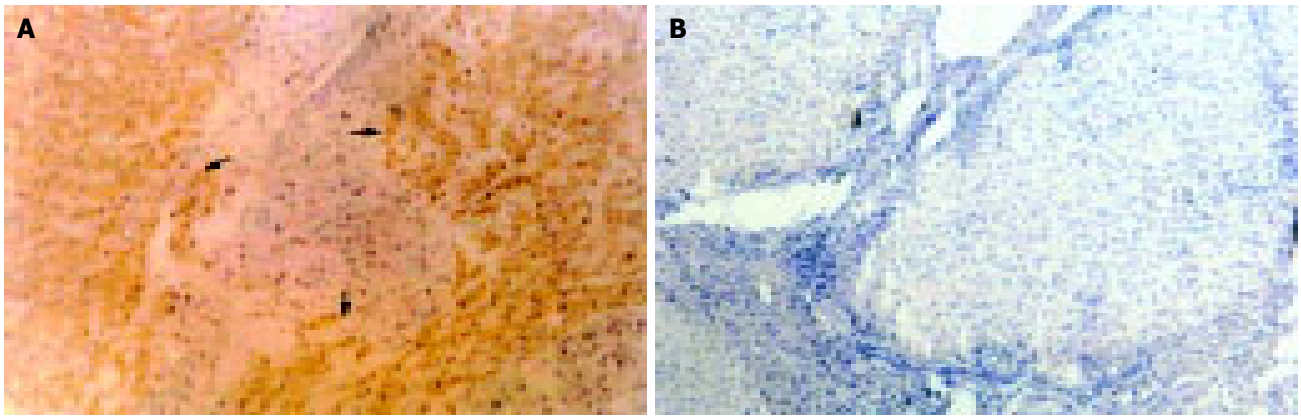

Figure 2 Expression of VEGF in HCC and liver cirrhosis tissues (SP method, ×100). **A:** The brown granules in the cytoplasm indicate VEGF expression in HCC; **B:** Expression of VEGF was weak positive in some liver cirrhosis tissues.

Table 2 Expression of survivin and VEGF protein in HCC tissues

	VEGF		
	Positive	Negative	*P*
Survivin			<0.01
Positive	18	5	
Negative	3	12	

Table 3 Coincident expression of survivin and VEGF protein in HCC or liver cirrhosis tissues

	HCC group (n = 38)	Cirrhosis group (n = 38)	*P*
Survivin	3229.3±1383.2	562.6±226.5	<0.01
VEGF	1134.8±862.2	445.4±322.6	

Table 4 Correlation between HCC metastasis and expression of survivin and VEGF protein

	Metastasis group (n = 14)	Non-metastasis group (n = 24)	*P*
Survivin	3841.4±1061.2	1253.8±725.3	<0.01
VEGF	1388.6±652.4	1081.3±773.5	<0.01

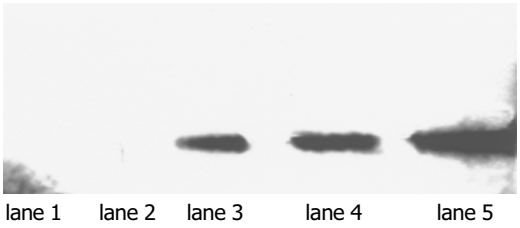

Figure 3 Expression of survivin in HCC and liver cirrhosis tissues. Lanes 1 and 2: liver cirrhosis tissues; lanes 3-5: HCC tissues. M_r of survivin: 16 500.

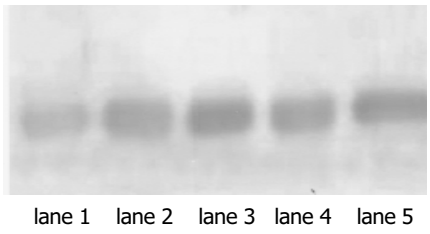

Figure 4 Expression of VEGF in HCC and liver cirrhosis tissues. Lanes 1 and 2: liver cirrhosis tissues; lanes 3-5: HCC tissues. M_r of VEGF: 21 000.

structures and the abilities of inhibiting apoptosis[14]. Survivin is the smallest member among the IAPs family. Altieri of Yale University utilized EPR-1 (effector cell protease receptor-1) cDNA to screen and clone survivin from human GenBank in 1997[3]. It has been suggested (but not proven) that EPR-1 may act as a natural anti-sense to survivin in cells[15].

The expression of survivin depends on cell cycle. Hela blocked tumor cells in G1, S, G2/M phase separately to detect survivin mRNA amount. Survivin mRNA was not detectable in G1 phase, increased 6.2 times in S phase and elevated 40 times in G2/M phase. Therefore, the expression of survivin was closely related to cell proliferation. Survivin can suppress apoptosis of NIH3T3 cell induced by Taxol and 293 cell induced by Fas and Bax[16]. Survivin inhibits apoptosis mainly through targeting the terminal effectors caspase-3 and -7 activity in apoptotic protease cascade reaction[17,18]. These caspases operate in the distal portions of apoptotic protease cascades, functioning as effectors rather than initiators of apoptosis. Survivin is characterized by a unique structure with a single BIR and no zinc-binding domain known as the RING finger, thus survivin cannot bind caspase-3 directly. Survivin is expressed in the G2-M phase of the cell cycle in a cell cycle-regulated manner and associates with microtubules of the mitotic spindle by the coiled spirals zone[19-21]. Survivins are also called chromosomal passenger proteins: they associate with inner centromere regions during prophase, but subsequently relocalize to the midzone of the central spindle and concentrate at the midbody[22]. Survivin has the double function of controlling spindle checkpoint and apoptotic checkpoint. The over-expression of survivin in neoplasms may obliterate this apoptotic checkpoint and allow aberrant progression of transformed cells through mitosis. The disruption of survivin-microtubule interaction results in loss of antiapoptosis function of survivin and increases caspase-3 activity during mitosis[21].

The results revealed that survivin was highly expressed in HCC and seldom detected in liver cirrhosis tissues. The expression of survivin had no association with the patients' age, gender, tumor size and differentiation level of HCC. It suggests that survivin may play some role in tumorigenesis of HCC. Simultaneously, in our series, we found that high expression of survivin was significantly correlated to VEGF in HCC. More importantly, stronger expression of survivin and VEGF was found in patients with metastasis than in those without metastasis. Consequently the expression of survivin seems to be involved in metastatic capacity of HCC.

As we know, VEGF is considered to be the most cardinal vascular growth factor prompting angiogenesis in tumor tissue. The mechanism of liver cancer cell shift induced by VEGF is closely related to increased proliferation ability of liver cells. Emerging studies have implicated a marked induction of survivin by VEGF in vascular endothelial cells, which can facilitate tumor metastasis by controlling apoptosis during angiogenesis. VEGF binding to VEGF-R2 activates the phosphatidylinositol 3-kinase (PI3K) survival pathway, resulting in phosphorylation and activation of the serine/threonine kinase protein kinase B (PKB/Akt). VEGF induces the expression of several anti-apoptotic effector molecules in Ecs by PKB/Akt pathway, including bcl-2, A1, and two members of the IAP family, X-linked IAP (XIAP), and survivin[23-26]. VEGF-dependent upregulation of survivin could be prevented by cell cycle arrest in the G1 and S phases and allows for the maintenance of the microtubule network to inhibit apoptosis of endothelial cells[27-30]. Our results demonstrate that the expression of survivin is consistent with that of VEGF in HCC and both are closely correlated to infiltration and metastasis of HCC. This is similar to findings in endothelial cells. As such, we assume that VEGF probably promotes the expression of survivin in HCC tissues, then the latter inhibits apoptosis of hepatocarcinoma cells and enhances tumor cell ability of infiltration and invasion,

thus accelerating tumor metastasis. To clarify the interaction mechanism between survivin and VEGF in HCC, further studies are needed.

The cancer-specific expression of survivin, coupled with its importance in inhibiting cell death and in regulating cell division, makes it a useful diagnostic marker of cancer and a potential target for cancer treatment[31]. Recently some studies have set about to evaluate the possibility of targeting survivin function *in vivo* as an anticancer strategy in which it is shown that inhibition of survivin could effectively inhibit *de novo* tumor formation and progression[32,33]. In the light of the effect of survivin on the progression of HCC, it is possible that inhibiting the function of survivin can be a new treatment of HCC.

In conclusion, inhibitor of apoptosis protein survivin plays a pivotal role in the metastasis of HCC, and it has some correlation with tumorigenesis. It is associated with the progression of HCC as a late event in tumorigenesis. The expression of survivin in the primary lesion can be an indicator for metastasis and prognosis of HCC. It could become a new target of gene therapy of HCC.

REFERENCES

1 **Suzuki A,** Shiraki K. Tumor cell "dead or alive": caspase and survivin regulate cell death, cell cycle and cell survival. *Histol Histopathol* 2001; **16**: 583-593
2 **Sela B.** Survivin: anti-apoptosis protein and a prognostic marker for tumor progression and recurrence. *Harefuah* 2002; **141**: 103-107
3 **Ambrosini G,** Adida C, Altieri DC. A novel anti-apoptosis gene, survivin, expressed in cancer and lymphoma. *Nat Med* 1997; **3**: 917-921
4 **Falleni M,** Pellegrini C, Marchetti A, Oprandi B, Buttitta F, Barassi F, Santambrogio L, Coggi G, Bosari S. Survivin gene expression in early-stage non-small cell lung cancer. *J Pathol* 2003; **200**: 620-626
5 **Tanaka K,** Iwamoto S, Gon G. Expression of survivin and its relationship to loss of apoptosis in breast carcinomas. *Clin Cancer Res* 2000; **6**: 127-134
6 **McEleny KR,** Watson RW, Coffey RN, O'Neill AJ, Fitzpatrick JM. Inhibitors of apoptosis proteins in prostate cancer cell lines. *Prostate* 2002; **51**: 133-140
7 **Sarela AI,** Macadam RC, Farmery SM. Expression of the antiapoptosis gene, survivin, predicts death from recurrent colorectal carcinoma. *Gut* 2000; **46**: 645-650
8 **Satoh K,** Kaneko K, Hirota M. Expression of survivin is correlated with cancer cell apoptosis and is involved in the development of human pancreatic duct cell tumors. *Cancer* 2001; **92**: 271-278
9 **Hussein MR,** Haemel AK, Wood GS. Apoptosis and melanoma: molecular mechanisms. *J Pathol* 2003; **199**: 275-288
10 **Garcia JF,** Camacho FI, Morente M, Fraga M, Montalban C, Alvaro T, Bellas C, Castano A, Diez A, Flores T, Martin C, Martinez MA, Mazorra F, Menarguez J, Mestre MJ, Mollejo M, Saez AI, Sanchez L, Piris MA. Spanish Hodgkin Lymphoma Study Group. Hodgkin and Reed-Sternberg cells harbor alterations in the major tumor suppressor pathways and cell-cycle checkpoints: analyses using tissue microarrays. *Blood* 2003; **101**: 681-689
11 **Borriello A,** Roberto R, Della Ragione F, Iolascon A. Proliferate and survive: cell division cycle and apoptosis in human neuroblastoma. *Haematologica* 2002; **87**: 196-214
12 **Nakano S,** Haratake J, Okamoto K, Takeda S. Investigation of resected multinodular hepatocellular carcinoma: assessment of unicentric or multicentric genesis from histological and prognosis viewpoint. *Am J Gastroenterol* 1994; **9**: 189-193
13 **Liston P,** Roy N, Tamai K. Suppression of apoptosis in mammalian cells by NAIP and a related family of IAP genes. *Nature* 1996; **379**: 349-353
14 **Hay BA.** Understanding IAP function and regulation: a view from Drosophila. *Cell Death Differ* 2000; **7**: 1045-1056
15 **O'Driscoll L,** Linehan R, Clynes M. Survivin: role in normal cells and in pathological conditions. *Curr Cancer Drug Targets* 2003; **3**: 131-152
16 **Tamm I,** Wang Y, Sausville E. IAP-family protein survivin inhibits caspase activity and apoptosis induced by Fas (CD95), Bax, caspases, and anticancer drugs. *Cancer Res* 1998; **58**: 5315-5320
17 **Sambrook J,** Fritsch EF, Maniatis T. Molecular Cloning: A Laboratory Manual. 2nd ed. USA: *Cold Spring Harbor Laboratory Press* 1989: 870-877
18 **Johnson AL,** Langer JS, Bridgham JT. Survivin as a cell cycle-related and antiapoptotic protein in granulosa cells. *Endocrinology* 2002; **143**: 3405-3413
19 **Kobayashi K,** Hatano M, Otaki M, Ogasawara T, Tokuhisa T. Expression of a murine homologue of the inhibitor of apoptosis protein is related to cell proliferation. *Proc Natl Acad Sci USA* 1999; **96**: 1457-1462
20 **Verdecia MA,** Huang H, Dutil E, Kaiser A, Hunter T, Noel JP. Structure of the human anti-apoptotic protein survivin reveals a dimeric arrangement. *Nat Struct Biol* 2000; **7**: 620-623
21 **Li F,** Ambrosini G, Chu EY, Plescia J, Tognin S, Marchisio PC, Altieri DC. Control of apoptosis and mitotic spindle checkpoint by survivin. *Nature* 1998; **396**: 580-584
22 **Adams RR,** Carmena M, Earnshaw WC. Chromosomal passengers and the (aurora) ABCs of mitosis. *Trends Cell Biol* 2001; **11**: 49–54
23 **Gerber HP,** McMurtrey A, Kowalski J, Yan M, Keyt BA, Dixit V, Ferrara N. Vascular endothelial growth factor regulates endothelial cell survival through the phosphatidylinositol 3'-kinase/Akt signal transduction pathway. Requirement for Flk-1/KDR activation. *J Biol Chem* 1998; **273**: 30336-30343
24 **Gerber HP,** Dixit V, Ferrara N. Vascular endothelial growth factor induces expression of the antiapoptotic proteins Bcl-2 and A1 in vascular endothelial cells. *J Biol Chem* 1998; **273**: 13313-13316
25 **Nor JE,** Christensen J, Liu J, Peters M, Mooney DJ, Strieter RM, Polverini PJ. Up-Regulation of Bcl-2 in microvascular endothelial cells enhances intratumoral angiogenesis and accelerates tumor growth. *Cancer Res* 2001; **61**: 2183-2188
26 **Tran J,** Rak J, Sheehan C, Saibil SD, LaCasse E, Korneluk RG, Kerbel RS. Marked induction of the IAP family antiapoptotic proteins survivin and XIAP by VEGF in vascular endothelial cells. *Biochem Biophys Res Commun* 1999; **264**: 781-788
27 **O'Connor DS,** Schechner JS, Adida C, Mesri M, Rothermel AL, Li F, Nath AK, Pober JS, Altieri DC. Control of apoptosis during angiogenesis by survivin expression in endothelial cells. *Am J Pathol* 2000; **156**: 393-398
28 **Conway EM,** Zwerts F, VanEygen V, DeVriese A, Nagai N, Luo W, Collen D. Survivin-dependent angiogenesis in ischemic brain: molecular mechanisms of hypoxia-induced up-regulation. *Am J Pathol* 2003; **163**: 935-946
29 **Mesri M,** Morales-Ruiz M, Ackermann EJ, Bennett CF, Pober JS, Sessa WC, Altieri DC. Suppression of vascular endothelial growth factor-mediated endothelial cell protection by survivin targeting. *Am J Pathol* 2001; **158**: 1757-1765
30 **Tran J,** Master Z, Yu JL, Rak J, Dumont DJ, Kerbel RS. A role for survivin in chemoresistance of endothelial cells mediated by VEGF. *Proc Natl Acad Sci USA* 2002; **99**: 4349-4354
31 **Chiou SK,** Jones MK, Tarnawski AS. Survivin-an anti-apoptosis protein: its biological roles and implications for cancer and beyond. *Med Sci Moni* 2003; **9**: PI25-29
32 **Kanwar JR,** Shen WP, Kanwar RK, Berg RW, Krissansen GW. Effects of survivin antagonists on growth of established tumors and B7-1 immunogene therapy. *J Nat Cancer Inst* 2001; **93**: 1541-1552
33 **Mesri M,** Wall NR, Li J, Kim RW, Altieri DC. Cancer gene therapy using a survivin mutant adenovirus. *J Clin Invest* 2001; **108**: 981-990

Science Editor Zhu LH **Language Editor** Elsevier HK

PO Box 2345, Beijing 100023, China
www.wjgnet.com
wjg@wjgnet.com

ELSEVIER

World J Gastroenterol 2005;11(25):3860-3865
World Journal of Gastroenterology ISSN 1007-9327

• *LIVER CANCER* •

Activation of transcription factors NF-kappaB and AP-1 and their relations with apoptosis-associated proteins in hepatocellular carcinoma

Lin-Lang Guo, Sha Xiao, Ying Guo

Lin-Lang Guo, Sha Xiao, Ying Guo, Department of Pathology, Zhujiang Hospital, Guangzhou 210282, Guangdong Province, China
Lin-Lang Guo, University of California, Davis Cancer Center, CA 95817, the United States
Correspondence to: Lin-Lang Guo, MD, University of California, Davis Cancer Center, Suite 2300, Research Building III, 4645 Second Avenue, Sacramento, CA 95817, United States. linlangg@yahoo.com
Telephone: +916-734-1479 Fax: +916-734-2361
Received: 2004-08-18 Accepted: 2004-11-29

Abstract

AIM: To study the distribution pattern of transcription factors NF-κB and AP-1 and their relations with the expression of apoptosis associated-proteins Fas/FasL and ICH-1L/S in human hepatocellular carcinoma (HCC).

METHODS: We performed *in situ* hybridization and immunohistochemical techniques for NF-κB, AP-1, Fas/FasL and ICH-1 in 40 cases of human HCC along with corresponding nontumoral tissues and 7 cases of normal liver tissues.

RESULTS: Twenty-two (55%) and 25 (62.5%) of 40 cases for NF-κB and AP-1 were presented for nuclear or both nuclear and cytoplastic staining respectively, while less cases were presented for only cytoplastic staining for NF-κB (18%) and AP-1 (10%) in adjacent nontumoral tissues and negative staining in normal liver tissues. There was no statistically significant difference of NF-κB or AP-1 activation between well differentiated tumors and poorly differentiated tumors ($P>0.05$). NF-κB activity is positively corresponded to AP-1 activation. The expression of ICH-1L/S was associated with the activation of NF-κB and AP-1 ($P<0.05$), but no significant relationship was found between Fas/FasL and NF-κB or AP-1($P>0.05$).

CONCLUSION: Activation of both NF-κB and AP-1 may be required for ICH-1L/S-induced apoptosis in HCC, but not for Fas/FasL-mediated apoptosis. NF-κB and AP-1 may play important roles in the pathogenesis of human HCC.

Key words: Hepatocellular carcinoma (HCC); Transcription factors; Apoptosis; Protein

Guo LL, Xiao S, Guo Y. Activation of transcription factors NF-kappaB and AP-1 and their relations with apoptosis-associated proteins in hepatocellular carcinoma. *World J Gastroenterol* 2005; 11(25): 3860-3865
http://www.wjgnet.com/1007-9327/11/3860.asp

INTRODUCTION

Hepatocellular carcinoma (HCC) is one of the most common cancers and cause of mortality in China. Much advanced progresses in the mechanism of hepatocarcinogenesis have been achieved for these years. Many genes such as proto-oncogenes, tumor suppressor genes, apoptosis genes and growth factors genes have been implicated and apoptosis genes may play an important effect in the process of hepatocarcinogenesis[1-6]. Apoptosis-related genes such as bcl-2/bax, Fas/FasL and caspase are involved in the pathogenesis of HCC[3-6]. However, more steps of apoptosis genes in this process remain unknown yet.

Activated protein-1 (AP-1) and nuclear factor κB (NF-κB), two of important transcription factors, play important roles in signal transduction pathways of cell differentiation, proliferation and apoptosis in response to a variety of physiological and pathological stimuli[7-13]. AP-1 consists of homodimers and heterodimers of the Jun family (c-Jun, JunB, JunD), and the Fos family (c-Fos, FosB, Fra1, Fra2). NF-κB is a heterodimeric complex composed of two subunits of the Rel/NF-κB family, factors including NF-κB1 (p50), NF-κB2 (p52), c-Rel, RelA/p65, and RelB[14]. Some investigators have presented aberrant DNA binding activity of AP-1 and NF-κB in various types of human tumor such as HCC, gastric carcinoma, breast carcinoma and so on[15-22]. These findings suggested that AP-1 and NF-κB may be important in the control of cell proliferation and oncogenesis of these tumors.

The molecular mechanisms of NF-κB and AP-1 in the regulation of Fas/FasL mediated apoptosis may be different in T cells, Jurkat cells, hepatocyte-derived cell lines and colon carcinoma cell[23-27]. However, whether NF-κB and AP-1 play important roles in regulation of Fas/FasL and ICH-1L/S expression in human HCC is still not known. In the present study, we undertook to investigate whether AP-1 and NF-κB are constitutively activated in human HCC tissues and to evaluate the relationship between AP-1 or NF-κB activity and the expression of apoptosis associated proteins (Fas/FasL and ICH-1L/S) by *in situ* hybridization and immunohistochemical techniques.

MATERIALS AND METHODS

Tissue preparation

Forty samples were obtained by surgical resection in our department. All samples were independently reviewed by two pathologists. The cases of HCC were classified according to the criteria described by Edmondson-Steiner and grouped as well differentiated (grade I-II; n = 25) or poorly differentiated (grade III-IV; n = 15). Seven undamaged liver tissues from surgical resection specimens of young adults with minor liver injury who underwent partial hepatectomy were used as normal control. All tissues were fixed in 40 g/L formaldehyde (pH 7.0) for 12-24 h and embedded in paraffin wax and then 4 μm serial sections were cut and mounted on poly-l-lysine coated slides.

Immunohistochemistry staining

Sections were deparaffinized and rehydrated routinely. Antigen was retrieved by heating sections in a microwave oven at 700 W in 10 mmol/L citrate buffer (pH 6.0) for 10 min. After blocking with 0.3% H_2O_2 and swine serum, specimens were then incubated with the primary antibodies, directed against Fas, FasL, and ICH-1L/S (Santa Cruz product, dilution 1:100) at 4 ℃ overnight. Secondary antibodies were applied according to the manufacturer's recommendations (Amersham). The staining was performed by streptavidin-peroxidase enzyme conjugate method using a S-P kit (Zymed product). Reaction products were visualized by DAB (diaminobenzidine). The slides were counterstained with hematoxylin before mounting in paramount. Brown-yellow granules in cytoplasm were recognized as positive staining.

In situ hybridization

Sections were deparaffinized and rehydrated routinely. Oligonucleotides containing the consensus sequence of AP-1 (5'-CGCTTGATGAGTCAGCCGGAA-3') and NF-κB (5'-AGTTGAGGGGACTTTCCCAGGC-3') were respectively used as probes and 3'-labeled with biotin. Preparations were incubated with the labeled probes (37 ℃, overnight). Non-specific antigen was blocked with 2% bovine serum and 0.3% Triton X-100, followed by incubation with anti-biotin antibody alkaline phosphates mixture for 1 h. Slides were then visualized with BCIP/NBT. Purple-blue granules were regarded as positive staining. In general, inactivated NF-κB and AP-1 were located in cytoplasm and nuclei staining scored as activated NF-κB and AP-1.

Negative controls

We used the following negative controls: (a) absence of probes, (b) mutant AP-1 or NF-κB probes 5'-CGCTTGAT-AAATCAGCCGGAA-3', and 5'-AGTTGAGGCTC-CTTTCCCAGGC-3', respectively, labeled with biotin, (c) competition assays with a 100-fold excess of unlabeled AP-1 or NF-κB probes, followed by incubation with its respective labeled probe.

Statistical analysis

Statistical significance was calculated by χ^2 test. The χ^2 test was used to analyze the association between NF-κB/AP-1 and histopathological grades and Fas/FasL and ICH-1L/S. P<0.05 was regarded as significant difference.

RESULTS

Detection of NF-κB and AP-1 in HCC

In situ hybridization was performed to detect the activity status of NF-κB and AP-1 in all 40 HCCs. NF-κB and AP-1 distribution in nuclear or both nuclear and cytoplasm of cancer cells are illustrated in Figures 1 and 2. Of 40

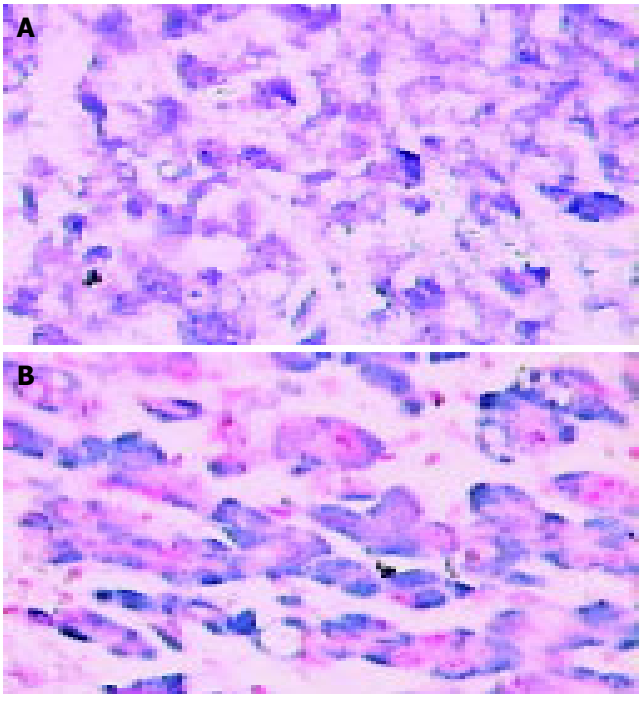

Figure 1 Hepatocellular carcinoma showing nuclear and cytoplasmic positivity for NF-κB (**A**) and AP-1(**B**). *In situ* hybridization (magnification ×200).

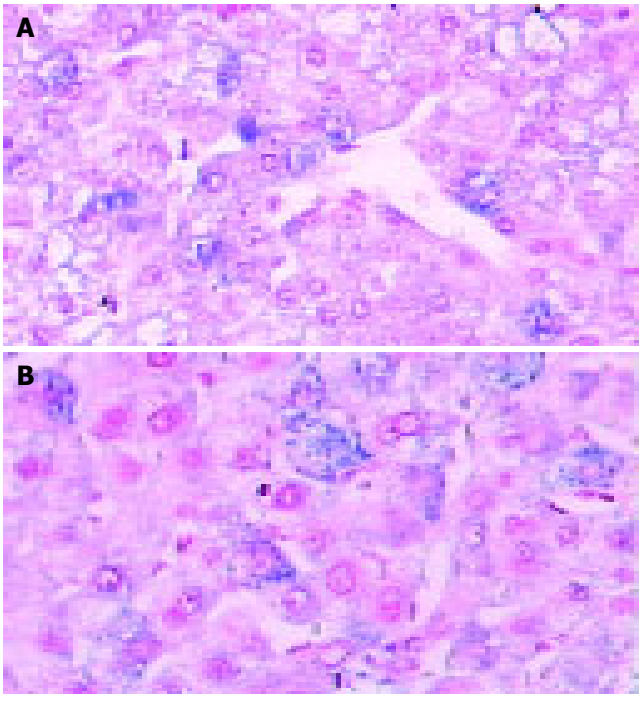

Figure 2 Nontumor liver tissue showing focal and weak cytoplasmic positivity for NF-κB (**A**) and AP-1 (**B**). *In situ* hybridization (magnification ×200).

HCCs, 22 (55%) presented nuclear or both nuclear and cytoplasmic staining of NF-κB by *in situ* hybridization in which 13/25 (52%) were well differentiated tumors and 9/15 (60%) were poorly differentiated tumors. While 25 (62.5%) of 40 cases for AP-1 positive staining were shown in which 14/25 (56%) were well differentiated tumors and 10/15 (66.7%) were poorly differentiated tumors. There was no statistically significant difference of NF-κB or AP-1 activation between well differentiated tumors and poorly differentiated tumors ($P>0.05$). In adjacent non-tumor tissues, cytoplasmic staining of NF-κB or AP-1 was noted in 27(68%) and 23(58%) respectively. But lower nuclear staining for NF-κB (17.5%) and AP-1 (10%) was found in non-tumor tissues than those in HCC with a statistical significance ($P<0.05$). Only few hepatocytes showed cytoplasmic staining for NF-κB (1/7) and AP-1 (2/7) in normal liver tissues, but no staining in the nucleus. NF-κB activity positively corresponded to AP-1 activation (Table 1).

Table 1 Detection of NF-κB and AP-1 in HCC

Group	Cases	NF-κB nucleus/cytoplasm + nucleus (+) (%)	AP-1 nucleus/cytoplasm + nucleus (+) (%)
Tumor tissue	40	22 (55)[a]	24 (60)
Well differentiated	25	13 (52)	14 (56)
Poorly differentiated	15	9 (60)	10 (66.7)
Nontumor tissue	40	7 (17.5)	4 (10)
Normal tissue	7	0	0

[a]$P<0.05$ *vs* tumor tissue.

Expression of apoptosis proteins in HCC

Table 2 summarizes the results of immunohistochemical studies on apoptosis proteins including Fas, FasL, ICH-1L and ICH-1S. Fas, FasL, ICH-1L, and ICH-1S presented cytoplasmic reactivity in 7 (17.5%), 6 (15%), 15 (37.5%) and 21 (52.5%) of tumors, while in 21 (52.5%), 18 (45%), 29 (72.5%) and 31 (77.5%) of nontumor tissues, in 0%, 0%, 2/7 and 1/7 of normal liver tissues, respectively. There were statistically significant differences of the expression of Fas, FasL, ICH-1L, and ICH-1S between non-tumor tissues and tumor tissues ($P<0.05$). The differences of Fas and ICH-1S expression except FasL and ICH-1L were also statistically significant between nontumor tissues and normal liver tissues ($P<0.05$, Figure 3).

Table 2 Expression of Fas, FasL, ICH-1L, and ICH-1S in HCC

Group	Cases	Fas (%)	FasL (%)	ICH-1L (%)	ICH-1S (%)
Tumor tissue	40	7 (17.5)[a]	6 (15)	15 (37.5)	21 (52.5)
Nontumor tissue	40	21 (52.5)[1]	18 (45)[2]	29 (72.5)[3]	31 (77.5)[4]
Normal tissue	7	0[5]	0[b]	2	1[6]

[a]$P<0.05$ *vs* tumor tissue. [1]$\chi^2 = 10.2692$, [2]$\chi^2 = 8.5714$, [3]$\chi^2 = 9.8990$, [4]$\chi^2 = 5.4945$, [5]$\chi^2 = 4.6890$, [6]$\chi^2 = 8.2398$.

Relationship between activated NF-κB and apoptosis proteins in HCC

The expression of Fas and FasL was more frequent in 22 cases of HCC with activated NF-κB compared with 18 cases of HCC with inactivated NF-κB, but the differences were not significant statistically between cases with activated NF-κB group and with inactivated NF-κB group ($P>0.05$). However, there was positive relationship between the expression of ICH-1L and ICH-1S in the cases with activated NF-κB and those with inactivated NF-κB ($P<0.05$, Table 3).

Relationship between activated AP-1 and apoptosis proteins in HCC

The expression of ICH-1L and ICH-1S in HCC with activated AP-1 was also more common with a statistical significance as compared with those with inactivated AP-1 respectively ($P<0.05$). But there was no significant difference between the expression of Fas and FasL in the cases with activated AP-1 and those with inactivated AP-1 ($P>0.05$, Table 4).

Table 3 Relationship between activated NF-κB and apoptosis proteins in HCC

NF-κB	Cases	Apoptosis protein							
		Fas		FasL		ICH-1L		ICH-1S	
		+	–	+	–	+	–	+	–
Activated	22	6	16	5	17	13	12	17	8
Inactivated	18	1	17	1	17	2	13	4	11
χ^2		1.9048		1.4495		4.4444		4.8722	
P		>0.05		>0.05		<0.05		<0.05	

Table 4 Relationship between activated AP-1 and apoptosis proteins in HCC

AP-1	Cases	Apoptosis protein							
		Fas		Fas L		ICH-1L		ICH-1S	
		+	–	+	–	+	–	+	–
Activated	25	7	18	6	19	13	12	16	9
Inactivated	15	0	15	0	15	2	13	3	12
χ^2		3.3362		2.5621		4.4444		5.6207	
P		>0.05		>0.05		<0.05		<0.025	

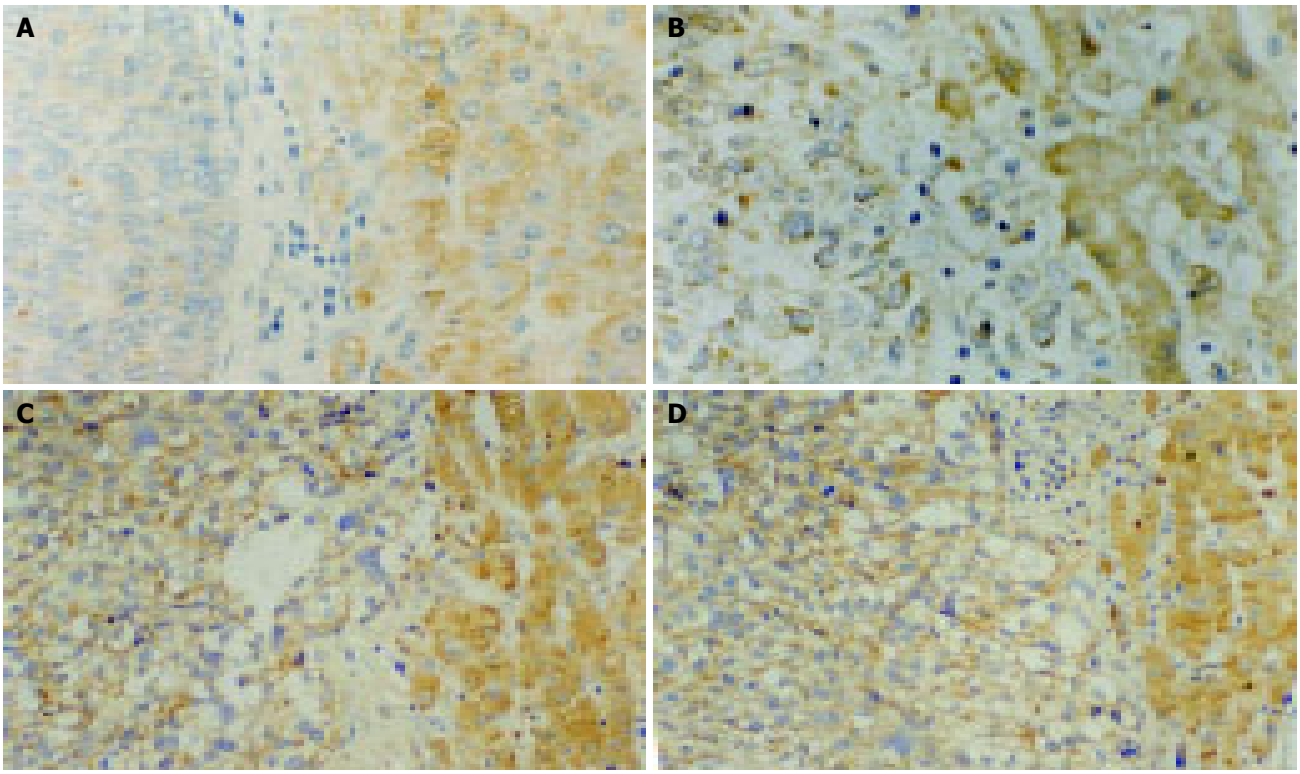

Figure 3 Immunohistochemistry staining showing strong cytoplasmic positivity in adjacent hepatocytes and weak positivity in HCC for Fas (**A**), FasL (**B**), ICH-lL (**C**) and ICH-lS (**D**) (magnification ×200).

DISCUSSION

Electrophoretic mobility shift assays is a common and useful technique for studying transcription factors. However, the distribution of transcription factors either in nucleus or cytoplasm cannot be shown using this technique. *In situ* detection using nonradioactive oligonucleotides in paraffin wax-embedded tissues was successfully used for studying NF-κB and AP-1 activation in kidney and injured vessels[28]. In this study, we performed this technique to detect NF-κB and AP-1 in HCC and obtained ideal results. The distribution of NF-κB and AP-1 was presented in nuclear and cytoplasmic types. Positive signals in HCC were mainly located both in nuclei and cytoplasm while cytoplasmic staining mainly in nontumor. We concluded that *in situ* hybridization is a convenient and efficient tool for studying transcription factors (Table 5).

Some studies have shown that DNA binding activity of NF-κB and AP-1 was aberrant in HCC[15,16]. Liu *et al*., measured the DNA binding activity of AP-1 and NF-κB in the peritumoral and the tumoral parts of 15 primary liver cancers. AP-1 and NF-κB binding activities were in 73% and 87% of the cases in the peritumoral tissue respectively. A further activation of AP-1 and NF-κB binding in the tumoral parts was detected in 40% and 80% of the cases respectively. Early activation of AP-1 and NF-κB contributes probably to the acquisition of a transformed phenotype during hepatocarcinogenesis, whatever the etiology[15]. Tai *et al*., studied the NF-κB-DNA binding activity and its dimmer, active nuclear RelA and nuclear IkappaB-alpha proteins expression in HCC using electrophoretic mobility shift assay and Western blot analysis. The results showed that nuclear NF-κB DNA binding activity and nuclear RelA protein expression were greater in tumor tissue compared with nontumor tissue[16]. Constitutive activation of NF-κB was found more frequently in tumor tissue compared with nontumor tissue. In our study, the results are similar to that by electrophoretic mobility shift assay. Furthermore, our findings presented positive staining for NF-κB and AP-1 distribution in cytoplasm (inactive from) at 68% and 58% in adjacent liver tissues, 1/7 and 2/7 in normal liver, and in nuclei (active form) at 55% and 62.5% in tumor tissues. The possible activation of NF-κB has been shown in some

Table 5 Relationship between activated NF-κB and apoptosis proteins in nontumor tissues

NF-κB	Cases	Adjacent nontumor tissues								Cases	Normal liver tissues							
		Fas		FasL		ICH-1L		ICH-1S			Fas		FasL		ICH-1L		ICH-1S	
		+	–	+	–	+	–	+	–		+	–	+	–	+	–	+	–
Activated	7	15	7	13	9	19	3	21	1	0	0	0	0	0	0	0	0	0
Inactivated	33	6	12	5	13	10	8	10	8	7	0	7	0	7	2	5	1	6
χ^2		4.8211		3.9221		4.7130		6.8946			0		0		0		0	
P		<0.05		<0.05		<0.05		<0.05			>0.05		>0.05		>0.05		>0.05	

carcinoma tissues such as human pancreatic carcinoma, gastric carcinoma and breast carcinoma. NF-κB activation was evaluated on the basis of nuclear translocation from inactive form with NF-κB-IκBs complex in cytoplasm[18,20-22]. However, the mechanism concerning AP-1 activation in carcinoma is not available. We further found that NF-κB activity positively corresponded to AP-1 activation. Taken together, these results demonstrated that NF-κB and AP-1 translocated from cytoplasm (inactive form) to nucleus (active form) during hepatocarcinogenesis and suggested that activation of both NF-κB and AP-1 may be required to produce potential biological function and play important roles in the oncogenesis of human HCC.

Fas/FasL system is involved in apoptosis in human HCC[5,6]. In this study, we further investigated whether there is a relationship between NF-κB or AP-1 activity and Fas/FasL expression in HCC. The results showed that more expression of Fas and FasL was found in cases with activated NF-κB or AP-1 than those with inactivated NF-κB or AP-1 in HCC but the differences were not significant statistically ($P>0.05$). These data indicated that NF-κB and AP-1 activation may not be required for Fas/FasL-induced apoptosis in HCC. Similar results have been reported in other different cells. Nagaki *et al*., found NF-κB blocks hepatocyte apoptosis mediated by the TNF receptor, but not by Fas[23]. In T cells, NF-κB signaling pathway is not required for activation-induced FasL expression[24]. Lack of a requirement for AP-1 induction in Fas-mediated death was substantiated with Jurkat cell[25]. However, the results contrary to those stated above have been implicated in some studies. Marusawae *et al*., demonstrated that NF-κB activity is related to Fas signaling in hepatocyte-derived cell lines, HepG2 and Huh-7 cells. Overexpression of kinase-inactive NF-κB-inducing kinase (NIK) and IkappaB kinase (IKK) inhibited the activation of NF-κB introduced by anti-Fas treatment in these cells. Inactivation of NF-κB by the production of IkappaB-alpha protein made these cells more susceptible to apoptosis induced by Fas stimulation[26]. NF-κB and AP-1 are also found involving in the transcriptional regulation of FasL in Fas-mediated thymineless death of colon carcinoma cell[27]. These results suggested NF-κB and AP-1 may play different roles in the regulation of Fas/FasL-mediated apoptosis in different cells.

ICH-1, a gene related to the *C. elegans* cell death gene ced-3 and the mammalian homolog of ced-3, interleukin-1 beta-converting enzyme (ICE). Alternative splicing results in two distinct ICH-1 mRNA species. One mRNA species encodes a protein product of 435 amino acids (ICH-1L) that is homologous to both the P20 and P10 subunits of ICE (27% identity) and the entire CED-3 protein (28% identity). The other mRNA encodes a 312 amino acid truncated version of ICH-1L protein (ICH-1S). Overexpression of ICH-1L induces programmed cell death, while ICH-1S suppresses Rat-1 cell death induced by serum deprivation. ICH-1 plays an important role in both positive and negative regulation of programmed cell death in vertebrate animals[29]. In this study, we found that aberrant expression of ICH-1 in HCC and adjacent tissues compared to normal liver. The results also showed that there are statistical differences between expression of ICH-1L or ICH-1S and NF-κB or AP-1 activation. These findings suggested that NF-κB and AP-1 may play a role in mediating ICH-1L/S expression during pathogenesis of HCC.

REFERENCES

1 **Shao J,** Li Y, Li H, Wu Q, Hou J, Liew C. Deletion of chromosomes 9p and 17 associated with abnormal expression of p53, p16/MTS1 and p15/MTS2 gene protein in hepatocellular carcinomas. *Chin Med J* 2000; **113**: 817-822

2 **Staib F,** Hussain SP, Hofseth LJ, Wang XW, Harris CC. TP53 and liver carcinogenesis. *Hum Mutat* 2003; **21**: 201-216

3 **Yuen MF,** Wu PC, Lai VC, Lau JY, Lai CL. Expression of c-Myc, c-Fos, and c-jun in hepatocellular carcinoma. *Cancer* 2001; **91**: 106-112

4 **Ikeguchi M,** Hirooka Y, Kaibara N. Quantitative analysis of apoptosis-related gene expression in hepatocellular carcinoma. *Cancer* 2002; **95**: 1938-1945

5 **Lee SH,** Shin MS, Lee HS, Bae JH, Lee HK, Kim HS, Kim SY, Jang JJ, Joo M, Kang YK, Park WS, Park JY, Oh RR, Han SY, Lee JH, Kim SH, Lee JY, Yoo NJ. Expression of Fas and Fas-related molecules in human hepatocellular carcinoma. *Hum Pathol* 2001; **32**: 250-256

6 **Roskams T,** Libbrecht L, Van Damme B, Desmet V. Fas and Fas ligand: strong co-expression in human hepatocytes surrounding hepatocellular carcinoma; can cancer induce suicide in peritumoural cells? *J Pathol* 2000; **191**: 150-153

7 **Angel P,** Karin M. The role of Jun, Fos, and the AP-1 complex in cell-proliferation and transformation. *Biochim Biophys Acta* 1991; **1072**: 129–157

8 **Karin M,** Liu ZG, Zandi E. AP-1 function and regulation. *Curr Opin Cell Biol* 1997; **9**: 240–246

9 **Shaulian E,** Karin M. AP-1 in cell proliferation and survival. *Oncogene* 2001; **20**: 2390–2400

10 **Beg AA,** Sha WC, Bronson RT, Ghosh S, Baltimore D. Embryonic lethality and liver degeneration in mice lacking the RelA component of NF-κB. *Nature* 1995; **376**: 167–170

11 **Van Antwerp DJ,** Martin SJ, Kafri T, Green DR, Verma IM. Suppression of TNF-alpha-induced apoptosis by NF-kappaB. *Science* 1996; **274**: 787–789

12 **Bellas RE,** FitzGerald MJ, Fausto N, Sonenshein GE. Inhibition of NF-κB activity induces apoptosis in murine hepatocytes. *Am J Pathol* 1997; **151**: 891–896

13 **Beg AA,** Baltimore D. An essential role for NF-kappaB in preventing TNF-alpha-induced cell death. *Science* 1996; **274**: 782–784

14 **Siebenlist U,** Franzoso G, Brown K. Structure, regulation and function of NF-kappa B. *Annu Rev Cell Biol* 1994; **10**: 405–455

15 **Liu P,** Kimmoun E, Legrand A, Sauvanet A, Degott C, Lardeux B, Bernuau D. Activation of NF-kappaB, AP-1 and STAT transcription factors is a frequent and early event in human hepatocellular carcinomas. *J Hepatol* 2002; **37**: 63-71

16 **Tai DI,** Tsai SL, Chang YH, Huang SN, Chen TC, Chang KS, Liaw YF. Constitutive activation of nuclear factor kappaB in hepatocellular carcinoma. *Cancer* 2000; **89**: 2274-2281

17 **Fujikawa K,** Shiraki K, Sugimoto K, Ito T, Yamanaka T, Takase K, Nakano T. Reduced expression of ICE/caspase1 and CPP32/caspase3 in human hepatocellular carcinoma. *Anticancer Res* 2000; **20**: 1927-1932

18 **Sasaki N,** Morisaki T, Hashizume K, Yao T, Tsuneyoshi M, Noshiro H, Nakamura K, Yamanaka T, Uchiyama A, Tanaka M, Katano M. Nuclear factor-kappaB p65 (RelA) transcription factor is constitutively activated in human gastric carcinoma tissue. *Clin Cancer Res* 2001; **7**: 4136-4142

19 **Luque I,** Gelinas C. Rel/NF-κB and IκB factors in oncogenesis. *Semin Cancer Biol* 1997; **8**: 103-111

20 **Wang W,** Abbruzzese JL, Evans DB, Larry L, Cleary KR, Chiao PJ. The nuclear factor- κB RelA transcription factor is constitutively activated in human pancreatic adenocarcinoma cells. *Clin Cancer Res* 1999; **5**: 119-127

21 **Sovak MA,** Bellas RE, Kim DW, Zanieski GJ, Rogers AE, Traish AM, Sonenshein GE. Aberrant nuclear factor- κB/Rel expression and the pathogenesis of breast cancer. *J Clin Invest* 1997; **100**: 2952-2960

22 **Kim DW,** Sovak MA, Zanieski G, Nonet G, Romieu-Mourez R, Lau AW, Hafer LJ, Yaswen P, Stampfer M, Rogers AE, Russo J, Sonenshein GE. Activation of NF-κB/Rel occurs early during neoplastic transformation of mammary cells. *Carcinogenesis* 2000; **21**: 871-879

23 **Nagaki M,** Naiki T, Brenner DA, Osawa Y, Imose M, Hayashi H, Banno Y, Nakashima S, Moriwaki H. Tumor necrosis factor alpha prevents tumor necrosis factor receptor-mediated mouse hepatocyte apoptosis, but not fas-mediated apoptosis: role of nuclear factor-kappaB. *Hepatology* 2000; **32**: 1272-1279

24 **Rivera-Walsh I,** Cvijic ME, Xiao G, Sun SC. The NF-kappa B signaling pathway is not required for Fas ligand gene induction but mediates protection from activation-induced cell death. *J Biol Chem* 2000; **275**: 25222-25230

25 **Lenczowski JM,** Dominguez L, Eder AM, King LB, Zacharchuk CM, Ashwell JD. Lack of a role for Jun kinase and AP-1 in Fas-induced apoptosis. *Mol Cell Biol* 1997; **17**: 170-181

26 **Marusawa H,** Hijikata M, Watashi K, Chiba T, Shimotohno K. Regulation of Fas-mediated apoptosis by NF-kappaB activity in human hepatocyte derived cell lines. *Microbiol Immunol* 2001; **45**: 483-489

27 **Harwood FG,** Kasibhatla S, Petak I, Vernes R, Green DR, Houghton JA. Regulation of FasL by NF-kappaB and AP-1 in Fas-dependent thymineless death of human colon carcinoma cells. *J Biol Chem* 2000; **275**: 10023-10029

28 **Hernandez-Presa MA,** Gomez-Guerrero C, Egido J. *In situ*-nonradioactive detection of nuclear factors in paraffin sections by Southwestern histochemistry. *Kidney Int* 1999; **55**: 209-214

29 **Wang L,** Miura M, Bergeron L, Zhu H, Yuan J. Ich-1, an Ice/ced-3-related gene, encodes both positive and negative regulators of programmed cell death. *Cell* 1994; **78**: 739-750

Science Editor Li WZ **Language Editor** Elsevier HK

PO Box 2345, Beijing 100023, China
www.wjgnet.com
wjg@wjgnet.com

ELSEVIER

World J Gastroenterol 2005;11(25):3866-3870
World Journal of Gastroenterology ISSN 1007-9327

Assessment of spiral CT pneumocolon in preoperative colorectal carcinoma

Can-Hui Sun, Zi-Ping Li, Quan-Fei Meng, Shen-Ping Yu, Da-Sheng Xu

Can-Hui Sun, Zi-Ping Li, Quan-Fei Meng, Shen-Ping Yu, Da-Sheng Xu, Department of Radiology, First Affiliated Hospital, Sun Yat-Sen University, Guangzhou 510080, Guangdong Province, China
Supported by the Medical Science Foundation of Guangdong Province, No. A2002185
Correspondence to: Dr. Zi-Ping Li, Department of Radiology, First Affiliated Hospital, Sun Yat-Sen University, Guangzhou 510080, Guangdong Province, China. liziping163@163.net
Telephone: +86-20-87335415 Fax: +86-20-87750632
Received: 2004-10-09 Accepted: 2004-11-26

Abstract

AIM: To investigate the value of spiral CT pneumocolon in preoperative colorectal carcinoma.

METHODS: Spiral CT pneumocolon was performed prior to surgery in 64 patients with colorectal carcinoma. Spiral CT images were compared to specimens from the resected tumor.

RESULTS: Spiral CT depicted the tumor in all patients. Comparison of spiral CT and histologic results showed that the sensitivity and specificity were 95.2%, 40.9% in detection of local invasion, and 75.0%, 90.9% in detection of lymph node metastasis. Compared to the Dukes classification, the disease was correctly staged as A in 6 of 18 patients, as B in 18 of 23, as C in 10 of 15, and as D in 7 of 8. Overall, spiral CT correctly staged 64.1% of patients.

CONCLUSION: Spiral CT pneumocolon may be useful in the preoperative assessment of patients with colorectal carcinoma as a means for assisting surgical planning.

Key words: Tomography; X-ray compute; Pneumocolon; Preoperative staging; Colorectal cancer

Sun CH, Li ZP, Meng QF, Yu SP, Xu DS. Assessment of spiral CT pneumocolon in preoperative colorectal carcinoma. *World J Gastroenterol* 2005; 11(25): 3866-3870
http://www.wjgnet.com/1007-9327/11/3866.asp

INTRODUCTION

With the development of high-resolution scanners, technical refinements in obtaining better quality studies, and the accumulated clinical experience leading to better interpretation, the role, indications, and accuracy of CT of the colon have dramatically enlarged and improved[1-3]. Reliable preoperative determination of the extent of spread of a colorectal carcinoma not only indicates the expected prognosis but also assists management. For obtaining reliable results from CT scan, preparation of the patients, especially complete distention of the colon using water or air as contrast agent, is the most important precondition. Otherwise, collapse of the colon and feces can easily be misinterpreted as tumor. Many studies have shown that water enema spiral CT is a useful modality for preoperative staging of patients with colorectal carcinoma[4-7]. However, water enema can be difficult and distressing in frail elderly patients and has risk of water incontinence. Air insufflation for the colon can be achieved easily and rapidly and is well tolerated by the patients, and air provides an excellent CT contrast medium[8]. There have been few reports concerning the preoperative staging of colorectal carcinoma with spiral CT pneumocolon. Therefore, this study aimed to assess the value of spiral CT pneumocolon in preoperative colorectal carcinoma.

MATERIALS AND METHODS

Patients

From August 1998 to December 2002, 64 patients with colorectal carcinoma, who were operated on at our institution, underwent spiral CT pneumocolon. There were 40 men and 24 women, ranging in age from 32 to 88 years (mean 59 years). Among the 64 patients who had a prior colonoscopy, 4 of 15 patients had an incomplete barium enema due to barium incontinence, and 19 of 64 patients had incomplete colonoscopy due to inability to cross a distal stricture.

Technique

All patients were fasted for at least 12 h before the study and given an oral colon cleansing preparation the night before CT scan. Nine-hundred milliliters of 3% diluted gastrografin solution was given orally 45 min before, so that small bowel loops were opacified. Anisodamine hydrochloride (10 mg, IM) was used to control peristaltic artifact and relax the colon. The patient was previously instructed not to void. As the study progressed, interpretation was more straightforward when the bladder was full.

The patients were positioned on the CT table in supine position. A Foley catheter was inserted into the rectum and 1 500-2 000 mL room air was administered per rectum to distend the colon. The enema was stopped if the patient experienced abdominal discomfort. Adequate distention of the whole colon was confirmed on the scanogram.

Studies were performed on a Toshiba Xpress/SX spiral

CT scanner with a 10-mm collimation and pitch of 1-2, at 120 kV and 200 mA. After plain scanning, 1.5 mL/kg of non-ionic iodinated contrast medium (iopromide, Ultravist 300; Schering, Berlin, Germany) was administered via the antecubital vein at a rate of 3 mL/s using an autoinjector, and scanning commenced 60 s after start of the injection from the dome of the liver to the anal verge. The time between CT scan and surgery ranged 1-8 d (mean 4.7 d).

Evaluating criteria

Based on previous reports[5,7,8] and our own experience, the following three parameters were established and evaluated: (1) local extramural invasion (irregularly serrated or speculated outer contour, tumor mass or strands of soft tissue extending out, and/or indistinctly increased density of the pericolonic fat), (2) lymph node involvement (lymph node short axis 1 cm or larger, or node less than 1 cm in diameter with obvious enhancement), and (3) distal and/or extensive disease (liver or lung metastases, direct extension into adjacent solid or hollow organs).

All patients with colorectal carcinoma were staged on CT according to the modified Dukes' classification[7]: stage A, tumor limited to the colonic wall; stage B, tumor affecting the serosa or the pericolonic fat; stage C, lymph node involvement; and stage D, tumor infiltrating adjacent organs and/or with metastases. The modified Dukes' classification was used because this system was currently used by surgeons at our institution.

Image interpretation

Two experienced radiologists, who were blind to the surgical and pathologic findings of each patient, interpreted the images as compared to above parameters, and any discrepant readings were solved by consensus. After a minimum of 4 wk, the same two radiologists reviewed the images for the second time. Intraobserver variability was evaluated by means of a weighed k-statistic[9].

RESULTS

The overall results showed good agreement between the two reviews by the two radiologists. The k-statistic for the data was 0.77, representing good intraobserver agreement.

Normal findings and primary tumor

All patients tolerated the spiral CT pneumocolon well with no significant discomfort, and had good bowel preparation and no fluid levels or residual fecal material. The distended colon lumen and normal colonic wall were well seen on spiral CT (Figure 1). Using this technique the normal colonic wall represented a single layer which was 1-2-mm thick.

Spiral CT detected the tumor in all patients and the smallest mass was 0.7 cm×1.0 cm. The lesion was shown as an eccentric focal mass with irregular segmental or circumferential wall ranging 0.7-4.5 cm in thickness, and their extension ranged 1.0-10.0 cm (Figures 2A-C). Most lesions had an uneven, lobulated configuration and large masses had patchy areas of necrosis. Different degrees of distal colonic stricture were presented. The majority of the mass showed moderate to obvious enhancement.

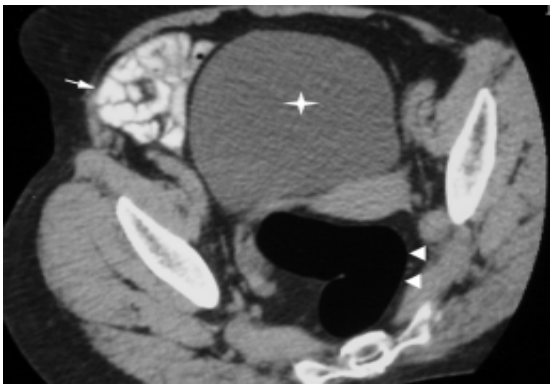

Figure 1 Optimal visualization of normal rectal wall (arrowheads), small intestine (arrow), and urinary bladder (star).

Local invasion

Tumor invasion of serosa and/or pericolonic fat was correctly staged by spiral CT in 49 (76.6%) of 64 patients (Figures 2A and B). In the incorrectly staged group, spiral CT overstaged 12 patients (Figure 3A) and understaged 2 patients (Figure 3B). Spiral CT evaluation had a sensitivity of 95.2% and a specificity of 40.9%.

Lymph node involvement

Involvement of lymph nodes less than 5 mm in diameter was seen in 7 (35.0%) of 20 patients. Spiral CT correctly diagnosed lymph node metastasis in 15 of 20 patients (Figure 2C). In the correctly diagnosed group, seven patients showed nodal enhancement, and eight patients showed no enhancement of lymph nodes larger than 1 cm in diameter. Clusters of three or more smaller nodes (each less than 1 cm in diameter) were seen by CT in five patients, histology revealed no evidence of nodal involvement.

Nodal involvement was correctly staged by spiral CT in 55 (85.9%) of 64 patients. In the incorrectly staged group, spiral CT overstaged 3 (Figure 3C) and understaged 5 of 20 patients. Spiral CT evaluation had a sensitivity of 75.0% and a specificity of 90.9%.

Distal metastasis

Liver metastasis was presented in four patients (Figure 2D), lung metastasis in two patients, and abdominal wall metastasis in one patient. They were all correctly diagnosed by CT. Only one patient with peritoneal seeding was missed due to the small lesion.

Preoperative staging

Staging results are presented in Table 1. CT stage A was correct in 6 of 18, stage B in 18 of 23, stage C in 10 of 15, and stage D in 7 of 8 patients. Overall, the diagnostic accuracy was 64.1% (41/64).

DISCUSSION

Colonoscopy and barium enema are the main methods for diagnosis of colorectal tumors. However, both modalities do not permit a precise preoperative prediction as to whether a tumor is limited to the colonic wall or has spread into surrounding tissues. Patients with severe colonic stricture

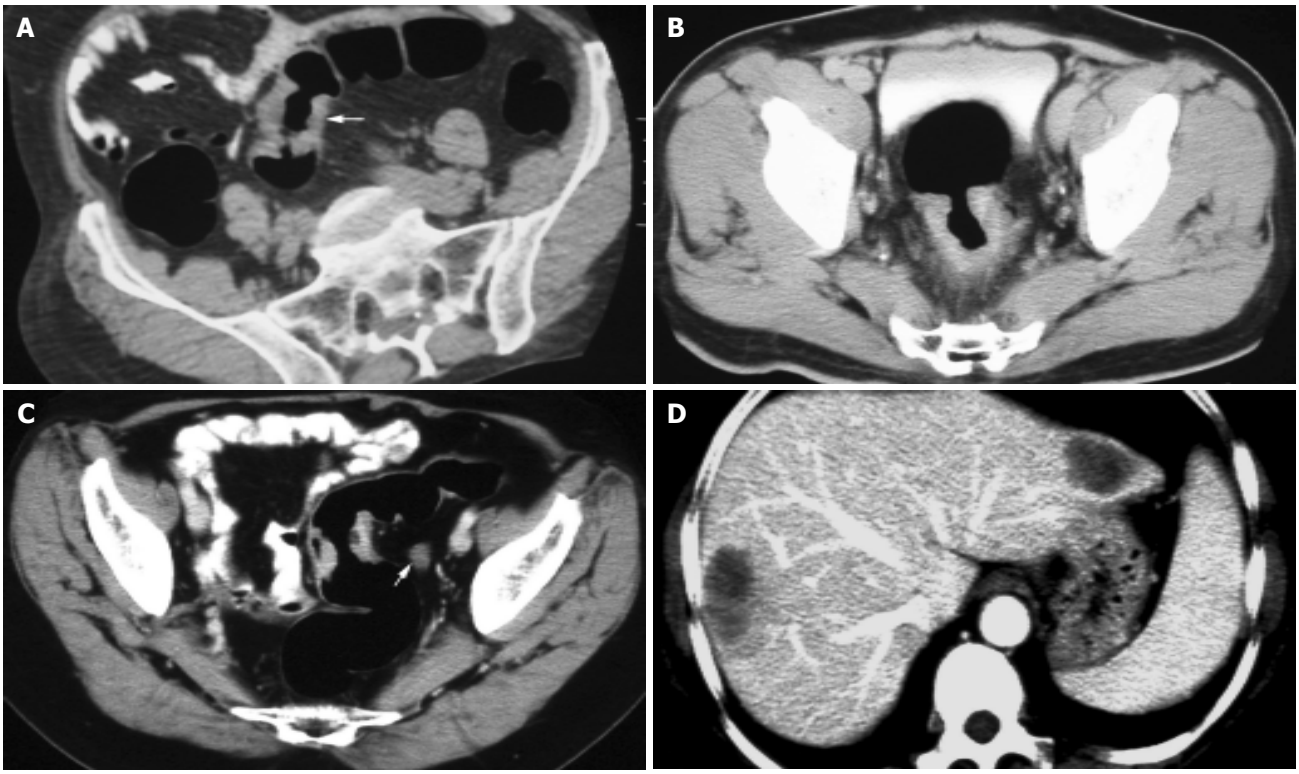

Figure 2 Correctly staged lesions. **A:** Dukes stage A carcinoma (arrow); **B:** Dukes stage B carcinoma; **C:** Dukes stage C carcinoma; **D:** Dukes stage D carcinoma.

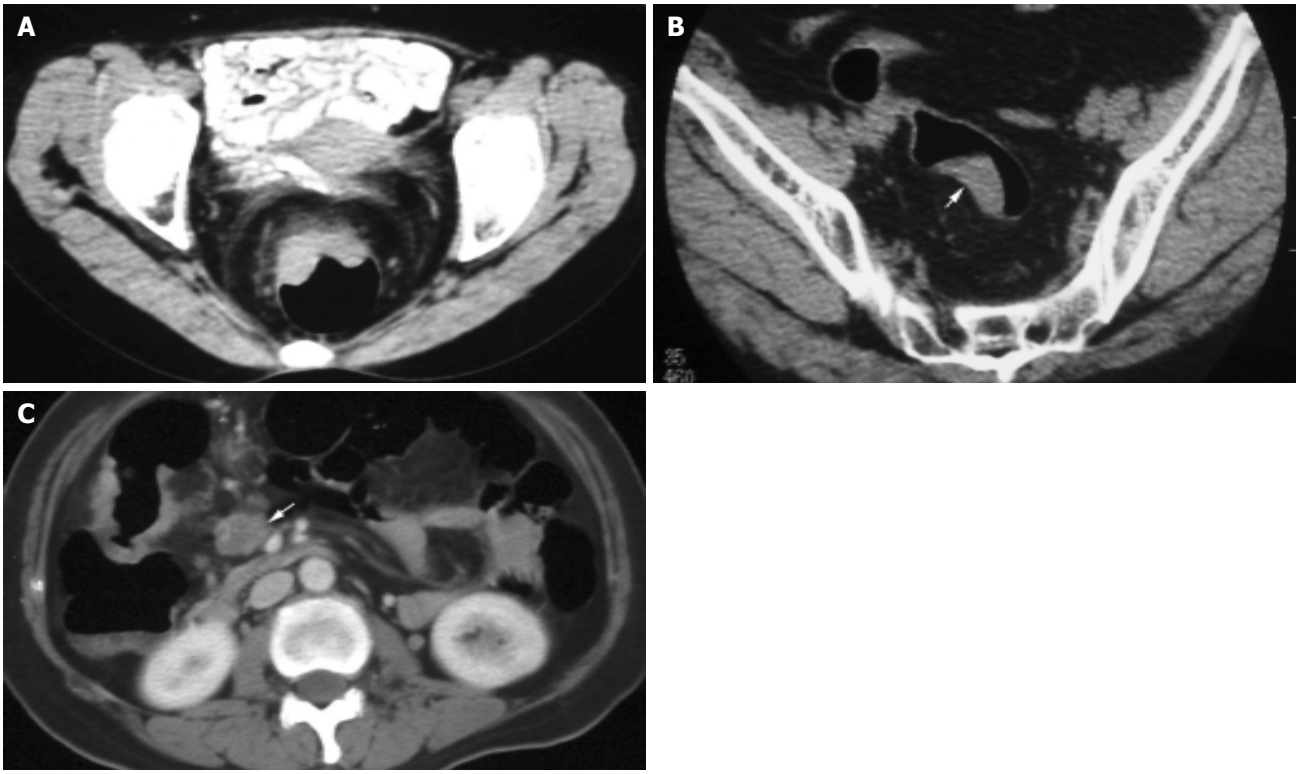

Figure 3 Incorrectly staged lesions. **A:** Dukes stage A carcinoma; **B:** Dukes stage B carcinoma (arrow); **C:** Dukes stage B carcinoma.

or barium incontinence may be poor candidates for the two examinations. Our study showed that CT pneumocolon had the potential utility as an adjunctive imaging technique for patients with colorectal carcinoma.

Imaging with spiral CT pneumocolon could clearly show the lumen and wall of the colon and colonic lesions. Normal colonic wall thickness should not exceed 3 mm in a well-distended segment, and the thickness greater than 6 mm is

Table 1 CT findings and pathologic staging

CT staging	Pathologic staging				
	A	B	C	D	Total
A	6	2	1		9
B	12	18	4		34
C		3	10	1	14
D				7	7
Total	18	23	15	8	64

considered abnormal[1]. In our study with spiral CT pneumocolon technique, the thickness of the normal colonic wall ranged 1-2 mm, and the thickness of the lesion was greater than 6 mm. We were unable to identify the mucosal lining nor the different anatomic layers of the colonic wall as reported by others who used water enema technique[6,7].

The sensitivity of CT detection depends mainly on the size of the lesion and on the quality of the CT examination. It varies from 68% if no special attempts are made to promote visualization of the colonic lumen to 95% when the colonic lumen is distended well. In this study, the overall detection rate was 100%, and masses with a diameter in 1 cm were identified. Our results corresponded favorably with previous reports[10,11]. This may be due to the adequate preparation of patients and CT pneumocolon technique. CT colonography generated from CT pneumocolon has emerged in recent years. This technique can detect lesions less than 5 mm in diameter, and its sensitivity is over 85% in detection of polyps 10 mm or greater in size, 70-80% of polyps 5-9 mm in size and 60% of polyps smaller than 5 mm[12,13]. It is a viable alternative for screening primary colorectal neoplasms and examining portions of the colon proximal to an obstructing lesion that cannot be traversed by colonoscopy or by barium[3,10,13].

In our experience, CT has a sensitivity of 95.2% and an accuracy of 76.6% in evaluating the local invasion. However, the specificity is only 40.9%. Harvey *et al*.[8], reported that its sensitivity is 100% and specificity is 33%. Zhou *et al*.[2], reported that its sensitivity is 92.9% and specificity is 50.0%. The reasons for the low specificity in local extension may be that CT is not possible to distinguish the single layers comprising the wall and there is no simple CT criterion to differentiate inflammation of the serosa from tumor invasion[2,8]. Matsuoka *et al*.[14], reported that using sagittal or coronal sections improves diagnostic accuracy from 79.4% to 90.4% in assessing the depth of tumor invasion. Endoscopic ultrasonography (EUS) is superior to CT in detecting the exact depth of parietal invasion, and its accuracy is 84.9%[15]. In our study, the accuracy of EUS was 87.5%, and its specificity was 100% in assessing the local extension.

Traditionally, CT detection of abnormal lymph nodes is based on imaging nodes greater than 1 cm in diameter or finding of clustered lymph nodes[5,8]. However, lymph node metastasis in colon cancer occurs frequently in lymph nodes measuring less than 5 mm. Herrera-Ornelas *et al*.[16], have reported a 65% incidence of lymph node metastasis. Whereas enlarged lymph nodes may be infiltrated by inflammatory or neoplastic cells. A relatively low sensitivity of CT in detecting nodal metastases is anticipated. Harvey *et al*.[8], reported that its sensitivity is 56% and specificity is 95%. Gazelle *et al*.[5], reported that its sensitivity is 60% and specificity is 79%. Hundt *et al*.[4], reported that its sensitivity is 84.3%, its specificity being 60% and accuracy being 81.0%. In this present study, its sensitivity, specificity, and accuracy in detecting lymph node involvement were 75.0%, 90.9%, and 85.9%, respectively. The disparity in these reports is probably due to the different criteria used. In our study, five patients with clustered lymph nodes (<1 cm) had no pathologic evidence of nodal involvement, suggesting that this criterion is unreliable. Further investigation is needed.

The data in this series showed that compared to the Dukes classification, CT correctly staged 64.1% of all patients, which is consistent with previous reports[2,8]. CT staging accuracy, however, showed significant variations in different Dukes categories. It correctly staged 6 (33.3%) of 18 patients with Dukes A lesion, 18 (78.3%) of 23 patients with Dukes B lesion, 10 (66.7%) of 15 patients with Dukes C tumor, and 7 (87.5%) of 8 patients with Dukes D tumor.

Colon cancer is potentially curable and decision on treatment is based on the extent of tumor. If extensive local spread of tumor is shown by CT or MRI, the patients can be treated with radiation therapy alone or undergo tumor resection after radiation therapy. The success of subsequent chemotherapy and irradiation can be determined in patients by follow-up CT or MRI, which can be compared to the base-line study before treatment. Recent studies showed that endorectal surface coil MR imaging is valuable in patients with rectal carcinoma to assess involvement of the levator ani[1]. If involvement of the levator ani is demonstrated, an abdominoperineal resection is needed.

In conclusion, spiral CT pneumocolon is a quick and noninvasive method for detecting colorectal carcinoma, and can provide valuable information preoperatively. In addition, it may represent a useful adjunct to colonoscopy or barium enema in patients with colorectal carcinoma.

REFERENCES

1 **Dobos N,** Rubesin SE. Radiologic imaging modalities in the diagnosis and management of colorectal cancer. *Hematol Oncol Clin North Am* 2002; **16**: 875-895

2 **Zhou C,** Li J, Zhao X. Spiral CT in the preoperative staging of colorectal carcinoma-radiologic-pathologic correlation. *Zhonghua Zhongliu Zazhi* 2002; **24**: 274-277

3 **Laghi A,** Iannaccone R, Trenna S, Mangiapane F, Sinibaldi G, Piacentini F, Sammartino P, Stipa V, Passariello R. Multislice spiral CT colonography in the evaluation of colorectal neoplasms. *Radiol Med* 2002; **104**: 394-403

4 **Hundt W,** Braunschweig R, Reiser M. Evaluation of spiral CT in staging of colon and rectum carcinoma. *Eur Radiol* 1999; **9**: 78-84

5 **Gazelle GS,** Gaa J, Saini S, Shellito P. Staging of colon carcinoma using water enema CT. *J Comput Assist Tomogr* 1995; **19**: 87-91

6 **Gossios KJ,** Tsianos EV, Kontogiannis DS, Demou LL, Tatsis CK, Papakostas VP, Merkouropoulos MM, Tsimoyiannis EC. Water as contrast medium for computed tomography study of colonic wall lesions. *Gastrointest Radiol* 1992; **17**: 125-128

7 **Angelelli G,** Macarini L, Lupo L, Caputi-Jambrenghi O, Pannarale O, Memeo V. Rectal carcinoma: CT staging with water as contrast medium. *Radiology* 1990; **177**: 511-514

8 **Harvey CJ,** Amin Z, Hare CM, Gillams AR, Novelli MR, Boulos PB, Lees WR. Helical CT pneumocolon to assess colonic tumors: radiologic-pathologic correlation. *Am J Roentgenol* 1998; **170**: 1439-1443

9 **Song JH,** Francis IR, Platt JF, Cohan RH, Mohsin J, Kielb SJ, Korobkin M, Montie JE. Bladder tumor detection at virtual cystoscopy. *Radiology* 2001; **218**: 95-100
10 **Britton I,** Dover S, Vallance R. Immediate CT pneumocolon for failed colonoscopy; comparison with routine pneumocolon. *Clin Radiol* 2001; **56**: 89-93
11 **Miao YM,** Amin Z, Healy J, Burn P, Murugan N, Westaby D, Allen-Mersh TG. A prospective single centre study comparing computed tomography pneumocolon against colonoscopy in the detection of colorectal neoplasms. *Gut* 2000; **47**: 832-837
12 **Yee J,** Kumar NN, Hung RK, Akerkar GA, Kumar PR, Wall SD. Comparison of supine and prone scanning separately and in combination at CT colonography. *Radiology* 2003; **226**: 653-661
13 **Harvey CJ,** Renfrew I, Taylor S, Gillams AR, Lees WR. Spiral CT pneumocolon: applications, status and limitations. *Eur Radiol* 2001; **11**: 1612-1625
14 **Matsuoka H,** Nakamura A, Masaki T, Sugiyama M, Takahara T, Hachiya J, Atomi Y. Preoperative staging by multidetector-row computed tomography in patients with rectal carcinoma. *Am J Surg* 2002; **184**: 131-135
15 **Shimizu S,** Tada M, Kawai K. Use of endoscopic ultrasonography for the diagnosis of colorectal tumors. *Endoscopy* 1990; **22**: 31-34
16 **Herrera-Ornelas L,** Justiniano J, Castillo N, Petrelli NJ, Stulc JP, Mittelman A. Metastases in small lymph nodes from colon cancer. *Arch Surg* 1987; **122**: 1253-1256

Science Editor Wang XL and Guo SY **Language Editor** Elsevier HK

PO Box 2345, Beijing 100023, China
www.wjgnet.com
wjg@wjgnet.com

ELSEVIER

World J Gastroenterol 2005;11(25):3871-3876
World Journal of Gastroenterology ISSN 1007-9327

Urinary nucleosides as biological markers for patients with colorectal cancer

Yu-Fang Zheng, Jun Yang, Xin-Jie Zhao, Bo Feng, Hong-Wei Kong, Ying-Jie Chen, Shen Lv, Min-Hua Zheng, Guo-Wang Xu

Yu-Fang Zheng, Jun Yang, Xin-Jie Zhao, Hong-Wei Kong, Shen Lv, Guo-Wang Xu, National Chromatographic R&A Center, Dalian Institute of Chemical Physics, the Chinese Academy of Sciences, Dalian 116023, Liaoning Province, China
Bo Feng, Min-Hua Zheng, Department of Surgical, the Ruijin Affiliated Hospital of Shanghai Second Medical University, Shanghai 200025, China
Ying-Jie Chen, Shen Lv, Center of Experiment, the Second Affiliated Hospital of Dalian Medical University, Dalian 116023, Liaoning Province, China
Supported by the High-tech R and D Plan, No. 2003AA223061 and the Sociality Commonweal Project of State Ministry of Science and Technology of China, the Knowledge Innovation Program of the Chinese Academy of Sciences, No. K2003A16 and Liaoning Province Foundation of Science and Technology
Correspondence to: Professor Dr. Guo-Wang Xu, National Chromatographic R and A Center, Dalian Institute of Chemical Physics, Chinese Academy of Sciences, Dalian 116023, Liaoning Province, China. dicp402@mail.dlptt.ln.cn
Telephone: +86-411-84379530 Fax: +86-411-84379559
Received: 2004-10-02 Accepted: 2004-12-03

Abstract

AIM: Fourteen urinary nucleosides, primary degradation products of tRNA, were evaluated to know the potential as biological markers for patients with colorectal cancer.

METHODS: The concentrations of 14 kinds of urinary nucleosides from 52 patients with colorectal cancer, 10 patients with intestinal villous adenoma and 60 healthy adults were determined by column switching high performance liquid chromatography method.

RESULTS: The mean levels of 12 kinds of urinary nucleosides (except uridine and guanosine) in the patients with colorectal cancer were significantly higher than those in patients with intestinal villous adenoma or the healthy adults. Using the levels of 14 kinds of urinary nucleosides as the data vectors for principal component analysis, 71% (37/52) patients with colorectal cancer were correctly classified from healthy adults, in which the identification rate was much higher than that of CEA method (29%). Only 10% (1/10) of patients with intestinal villous adenoma were indistinguishable from patients with colorectal cancer. The levels of m1G, Pseu and m1A were positively related with tumor size and Duke's stages of colorectal cancer. When monitoring the changes in urinary nucleoside concentrations of patients with colorectal cancer associated with surgery, it was found that the overall correlations with clinical assessment were 84% (27/32) and 91% (10/11) in response group and progressive group, respectively.

CONCLUSION: These findings indicate that urinary nucleosides determined by column switching high performance liquid chromatography method may be useful as biological markers for colorectal cancer.

Key words: Nucleosides; Biological markers; Colorectal cancer; High performance liquid chromatography

Zheng YF, Yang J, Zhao XJ, Feng B, Kong HW, Chen YJ, Lv S, Zheng MH, Xu GW. Urinary nucleosides as biological markers for patients with colorectal cancer. *World J Gastroenterol* 2005; 11(25): 3871-3876
http://www.wjgnet.com/1007-9327/11/3871.asp

INTRODUCTION

Modified nucleosides, derived predominantly from transfer ribonucleic acid (tRNA)[1-3], have been shown to be excreted in abnormal amounts in the urine of cancer patients[4-7]. Interest in these materials as potential biological markers was stimulated following evidence that tRNA methyltransferase from cancer tissue had both increased activity and capacity when compared to the enzyme derived from the corresponding normal tissue of origin[8]. Studies by Borek *et al*.[9], also showed that tRNA from neoplastic tissue had a much more rapid turnover rate than the tRNA from the corresponding normal tissue. Evidence indicates that methylation of tRNA occurs only after synthesis of the intact macromolecule. Because there are no specific enzyme systems to incorporate the modified nucleosides into the macromolecular nucleic acid, these nucleosides once released in the process of tRNA turnover cannot be reutilized, nor are they further degraded, but are excreted in urine[10]. Studies have also shown that urinary nucleosides excretion in human beings is little affected by diet, and when normalized to urinary creatinine the daily excretion rate is remarkably constant in a healthy individual[11].

Methodically in most of the studies urinary nucleosides are isolated by phenylboronate affinity gel chromatography and separated by reverse-phase high performance liquid chromatography (HPLC)[1,5,6,12,13]. But these methods still involve elaborate and manually performed sample-processing steps due to the complexity of the sample matrix. Among the various types of cancer, colorectal cancer is known to be one of the most prevalent and its early

detection is thus desirable. However, attempts were rarely made to measure the levels of urinary nucleosides from patients with colorectal cancer to date. In this study, we developed the automated column switching HPLC method to investigate the excretion pattern of urinary nucleosides associated with colorectal cancer and intestinal villous adenoma. Differences in 14 urinary nucleoside levels were quantified in 52 patients with colorectal cancer, 10 patients with intestinal villous adenoma and 60 healthy adults. The relationship of urinary excretion of these compounds from patients with colorectal cancer with the tumor size, Duke's stages and differentiation were studied. Changes in the levels of urinary nucleosides were examined preoperatively and postoperatively in patients with colorectal cancer. These data were collected to test the utility of urinary nucleosides as biological markers for colorectal cancer.

MATERIALS AND METHODS

Chemicals and equipment

The following 14 nucleoside standards including the internal standard 8-bromoguanosine hydrate (Br8G) were obtained from Sigma (St. Louis, MO, USA): pseudouridine (Pseu), cytidine (C), uridine (U), 1-methyladenosine (m1A), inosine (I), 5-methyluridine (m5U), guanosine (G), 1-methylinosine (m1I), 1-methylguanosine (m1G), N^4-acetylcytidine (ac4C), N^2-methylguanosine (m2G), adenosine (A), N^2, N^2-methylguanosine (m22G), N^6-methyladenosine (m6A). Methanol (MeOH) was HPLC-grade purchased from Tedia (Fairfield, OH, USA). Ammonium acetate (NH_4AC), ammonia ($NH_3{\cdot}H_2O$) and potassium dihydrogenphosphate (KH_2PO_4) were all analytical reagents obtained from China. Water was deionized and purified by a Milli-Q system (Millipore, Bedford, MA, USA).

The HPLC system (Figure 1) consisted of three Shimadzu LC-10ATVP pumps (Kyoto, Japan), an autoinjector model SIL 10ADVP, an SPD-10AVP UV-Vis detector and an SCL 10AVP interface. An electric six-port valve (Rheodyne, USA) was used for the automated column switching. Valve switching and data acquisition were done on Shimadzu Class-VP version 6.10 software. The column 1 (40 mm×4.0 mm ID) was packed with a laboratory prepared boronic acid-substituted silica material. It can tolerate pH values of the buffers from 2 to 12 as well as the usual organic solvents. The column 2 (250 mm×4.6 mm ID) was packed with 5 μm Hypersil ODS_2 (Elite, Dalian, China).

Urine samples

Sixty healthy adults (31 males, 29 females, from 21 to 71 years, median age 52 years), who have the normal physical indices including hepatic function, renal function, chest X-ray and colonoscopy during a regular physical examination period in our institute, have been chosen as control material. Fifty-two patients with colorectal cancer and 10 patients with intestinal villous adenoma were from Ruijin Affiliated Hospital of Shanghai Second Medical University, the First and Second Affiliated Hospitals of Dalian Medical University of China. No patient had received chemotherapy or radiation therapy before surgery. Diagnoses of colorectal cancer and intestinal villous adenoma were made on the basis of usual clinical and laboratory findings and were confirmed by histopathology. Table 1 shows the clinical pathological parameters of patients with colorectal cancer.

Spontaneous urine samples were collected from healthy adults, patients with colorectal cancer and intestinal villous adenoma. In 43 patients with colorectal cancer, urine samples were also obtained 2 wk after surgery. All persons had normal renal function and were free of bacterial infection at the time when the urine was collected. After collection the samples free of preservatives were frozen immediately and stored at -20 ℃. Prior to analysis, the samples were thawed at room temperature and adjusted to pH 8.0 with 50 mL/L $NH_3{\cdot}H_2O$ and vortex for 3 min at 5 000 r/min. Aliquots of 1 mL centrifuged urine containing 30 μL of Br8G (0.30 mmol/L) were transferred to autosampler vials and samples of 150 μL were injected to a column-switching HPLC system.

Table 1 Clinicopathological parameters of 52 patients with colorectal carcinoma

Clinicopathological parameters		Numbers(%)
Gender	Male	29 (55.8)
	Female	23 (44.2)
Age (yr)	Range	26-87
	Mean	56.4
	Median	60.0
Primary site	Rectum	15 (28.8)
	Sigmoid colon	6 (11.5)
	Colon	31 (59.6)
Duke's stage	Duke's A	7 (13.5)
	Duke's B	23 (44.2)
	Duke's C	15 (28.8)
	Duke's D	7 (13.5)
Tumor size	≥5 cm	23 (44.2)
	<5 cm	29 (55.8)
Histological grade	Well differentiated tumor	9 (17.3)
	Moderately differentiated tumor	32 (61.5)
	Poorly differentiated tumor	11 (21.2)
CEA	≥5 mg/L	15 (28.8)
	<5 mg/L	37 (71.2)

Column switching HPLC method

Column 1 (Figure 1) was equilibrated for 5 min with the mobile phase delivered by pump 1. After sample injection (150 μL urine), column 1 was washed for 7 min with the same buffer. During that time, nucleosides were selectively retarded on the column 1 and the sample matrix was discharged. At the same time, column 2 was conditioned with the mobile phase delivered by pump 2 (position 1; Figure 1). After this clean-up step, column 1 was series-connected in front of the column 2. The group-specifically bound nucleosides on the column 1 were then eluted and concentrated on top of the column 2 over a period of 3 min (position 2; Figure 1). Separation of nucleosides on the column 2 was carried out with a linear gradient elution program over 40 min, while the column 1 was regenerated for a new extraction cycle (position 1; Figure 1). The nucleosides were detected at 260 nm and quantified using the internal standard method. Table 2 shows the time events

used for the analytical procedure.

Peak identification was performed on the basis of retention times. Standard solutions were run daily before and after the samples to monitor reproducibility of retention times. The standard addition method was also used to confirm peak identification. The levels of the urinary nucleosides were calculated by the calibration curves, and then were transformed into nmoL/μmoL creatinine. Urinary creatinine levels were determined as described by Zheng *et al*.[7].

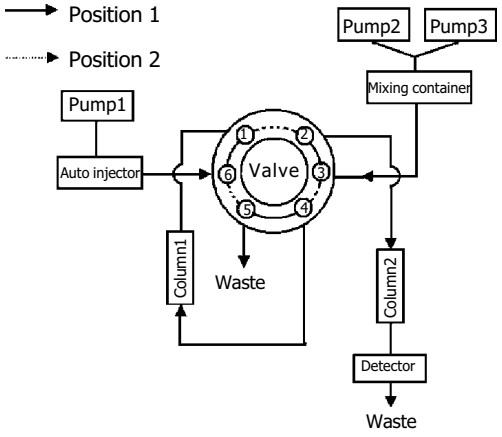

Figure 1 Schematic diagram of the column-switching HPLC system.

Data analysis

The mean excreted amounts of urinary nucleosides have been calculated using MS Excel software. Differences of urinary nucleoside concentrations of healthy adults, patients with intestinal villous adenoma and colorectal cancer were compared with SPSS 10.0 software. Spearman Correlation Analysis was used to examine the relationship of urinary nucleoside concentrations from patients of colorectal cancer with the tumor size, clinical stage and differentiation. Principal component analysis (PCA) software, a home-made pattern recognition software, was used to classify healthy controls, patients with intestinal villous adenoma and colorectal cancer. It was also used to monitor changes in the urinary excretion of nucleosides before and after surgery. Principal components plots were drawn on the basis of the first principal component analysis function (PC1) against the second principal component analysis function (PC2) of the nucleosides for each urine specimen. The oblique rotational method used in the software is the Promax method[6].

RESULTS

Analytical characteristics of the method

Figure 2A is a standard chromatogram showing the resolution of 14 nucleosides as well as the internal standard Br8G under the condition newly developed. The calibration curves for 14 nucleosides, linear responses in peak area ratios of nucleosides to the internal standard *vs* the nucleoside concentrations were obtained with the correlation coefficients varying from 0.995 to 0.9995. The intra- and inter-day precisions of the method were determined by five repetitive analyses of an aqueous solution of standard nucleosides on three nonconsecutive days. The relative standard deviation (RSD) of retention times was less than 1.70% (intraday) and 3.51% (interday), and that of peak areas was less than 3.84% (intraday) and 7.85% (interday). The limits of detection ranged from 0.05 to 0.56 μmol/L, which are better than the previous reports[13,15,16], thus being suitable for the quantitative analysis.

When applied to the urine specimens from 60 healthy adults, 10 patients with intestinal villous adenoma and 52 patients with colorectal cancer, a total of 14 nucleosides were positively identified. A typical chromatogram of urinary nucleosides from a normal person with peak identification is given in Figure 2B.

Comparison of urinary excretion of nucleosides in healthy adults, patients with intestinal villous adenoma and colorectal cancer

Fourteen nucleoside concentrations of healthy adults (group 1), patients with intestinal villous adenoma (group 2) and patients with colorectal cancer (group 3) are listed in Table 3. In the mean values of three groups, the most abundant nucleoside was Pseu, followed by m1A and m1I. Pseu level was elevated above the normal values plus two standard deviation (s) in the 58% (30/52) of patients with colorectal cancer, while 20% (2/10) of patients with intestinal villous adenoma was elevated. Clearly, the concentrations of 12 nucleosides (except U, G) were significantly elevated in patients with colorectal cancer ($P<0.05$). Only four kinds of nucleoside concentrations of patients with intestinal villous adenoma were higher in comparing with those of

Table 2 Time events for the switching of column and of mobile phase[1]

Time (min)	Pump	Event	Valve position
0.00–7.00	Pump 1 (eluent A)	Sample matrix are discharged by column 1	1
	Pump 2 (eluent B)	Conditioning of column 2	
7.00–10.00	Pump 2 (eluent B)	Analytes are transferred from column 1 to column 2	2
10.00–50.00	Pump 2 and Pump 3 (eluents B and C)	Analysis of nucleosides on column 2 by using a linear gradient elution program	1
	Pump 1 (eluent A)	Conditioning of column	1

[1]Eluent A: 0.25 mol/L NH_4AC (pH 8.5); eluent B: 25 mmol/L KH_2PO_4 (pH 4.5); eluent C: methanol:water (3:2, v/v). Flow rate: pump 1, 0.2 mL/min; pump 2, 1.2 mL/min. Detection wavelength: 260 nm.

healthy adults. Using 14 nucleoside concentrations as the data vectors for PCA technique, 71% (37/52) patients with colorectal cancer was distinguishable from healthy adults, while healthy adults are correctly classified at 96% (58/60) specificity. Serum CEA is the tumor marker being used in clinic to diagnose colorectal cancer (cut-off level: 5 mg/L). But the sensitivity of CEA method is 29% (15/52) based on the data provided by the hospitals. Based on the equation of classification of patients with colorectal cancer and healthy adults, 14 urinary nucleoside concentrations of patients with intestinal villous adenoma were calculated and the results was marked into Figure 3A, it was found that 10% (1/10) of patients with intestinal villous adenoma were in the area of patients with colorectal cancer.

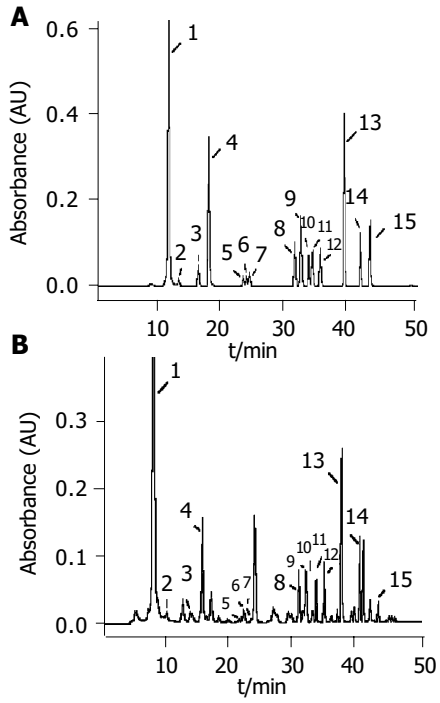

Figure 2 Typical chromatograms of (**A**) 14 standard nucleoside mixtures (**B**) urinary nucleosides of a normal urine obtained under the established analysis conditions. Column-switching HPLC conditions as Table 2. Peak identification: 1 Pseu; 2 C; 3 U; 4 m1A; 5 I; 6 m5U; 7 G; 8 m1I; 9 m1G; 10 ac4C; 11 m2G; 12 A; 13 m22G; 14 Br8G; 15 m6A.

Table 3 Comparison of levels of urinary nucleosides from healthy adults, patients with intestinal villous adenoma and colorectal cancer (mean±SD, nmoL/μmoL creatinine)

Nucleoside	Healthy adults	Patients with intestinal villous adenoma	Patients with colorectal cancer
Pseu	22.08±5.11	23.99±5.61	42.19±22.25[a]
C	0.15±0.12	0.40±0.21[c]	0.43±0.49[a]
U	0.30±0.15	0.31±0.12	0.31±0.23
m1A	2.04±0.53	2.30±0.62	2.74±0.80[a]
I	0.28±0.11	0.27±0.11	0.50±0.35[a]
m5U	0.04±0.06	0.12±0.06[c]	0.13±0.08[a]
G	0.09±0.03	0.08±0.02	0.10±0.04
m1I	1.25±0.28	1.97±0.50[c]	2.76±1.94[a]
m1G	0.82±0.24	1.21±0.26[c]	1.44±0.51[a]
ac4C	0.69±0.20	0.70±0.19	0.84±0.30[a]
m2G	0.55±0.14	0.52±0.28	0.63±0.26[a]
A	0.52±0.16	0.59±0.25	0.66±0.30[a]
m22G	1.25±0.23	1.43±0.27	1.81±0.55[a]
m6A	0.04±0.02	0.06±0.05	0.07±0.05[a]

[a]$P<0.05$ patients with colorectal cancer *vs* healthy adults. [c]$P<0.05$ patients with intestinal villous adenoma *vs* healthy adults.

Urinary excretion of nucleosides and clinical pathological characteristics of colorectal cancer

We examined the relationship of urinary nucleoside concentrations from patients of colorectal cancer with the tumor size, Duke's stages and differentiation. These results are listed in Table 4. The level of m1G, Pseu and m1A were positively correlated with the tumor size and Duke's stages of colorectal cancer, respectively ($P<0.05$). No significant correlation was noted in observed values with regard to tumor differentiation.

Preoperative and postoperative urinary excretion of nucleosides

The changes in six urinary modified nucleoside concentrations (Pseu, m1A, m1I, m1G, ac4C, m22G) before and after surgery in 43 patients with colorectal cancer were studied. The patients were classified into two groups: response group (32 persons) and progressive disease group (11 persons). Using the paired *t*-test, these urinary modified nucleoside concentrations of response group before surgery were

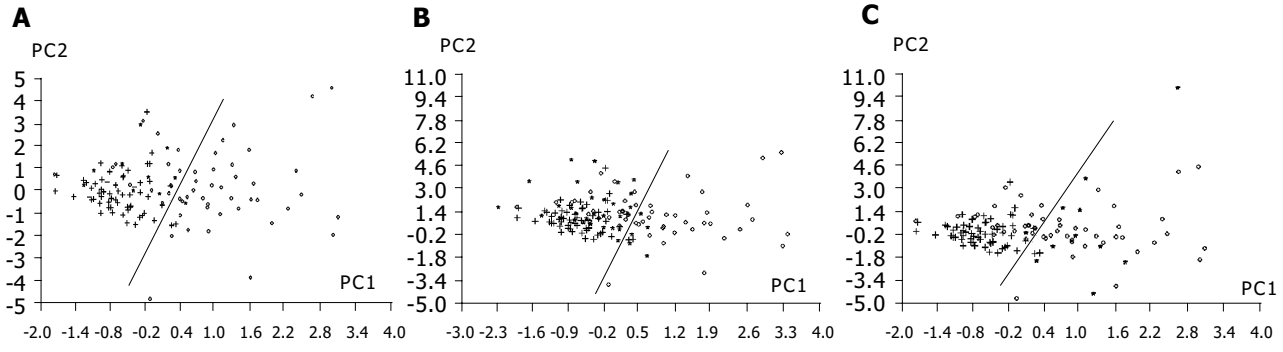

Figure 3 PCA based on 14 nucleoside concentrations from healthy controls (+) and patients with colorectal cancer (o). **A**: Positions of patients with intestinal villous adenoma (*) were marked into the figure based on classification equation from healthy controls and patients with colorectal cancer; **B**: Positions of 32 of responsive cases after surgery (*) were marked into the figure based on classification equation from healthy controls and patients with colorectal cancer; **C**: Positions of 11 of progressive cases after surgery (*) were marked into the figure based on classification equation from healthy controls and patients with colorectal cancer.

Table 4 Relationship of the levels of urinary nucleosides from patients of colorectal cancer with the tumor size, Duke's stage and differentiation

Nucleoside	Tumor size R	Duke's stage R	Differentiation R
Pseu	0.192	0.325 [a]	-0.051
C	0.199	0.103	0.109
U	0.159	0.190	0.142
m1A	0.188	0.303[a]	-0.014
I	0.241	0.198	-0.009
m5U	0.056	0.149	0.033
G	0.262	0.135	0.113
m1I	0.287	0.202	0.045
m1G	0.376[a]	0.256	0.041
ac4C	0.053	0.189	0.008
m2G	0.275	0.261	0.091
A	0.068	0.224	0.023
m22G	0.287	0.270	0.051
m6A	0.097	0.157	0.201

R: relationship coefficient; [a]$P<0.05$ nucleosides *vs* Duke's stage.

significantly higher than those of patients after surgery ($P<0.05$). However, the pre- and post-surgery difference in levels of these nucleosides for progressive disease group had no significant changes.

PCA technique based on 14 nucleoside concentrations as the data vectors was used to monitor changes in the urinary excretion of nucleosides for patients with colorectal cancer before and after surgery. When urinary nucleoside concentrations of patients with colorectal cancer after surgery were fed to the principal component regression and marked to the space produced by the first two principal components (PC1, PC2) of healthy adults and patients with colorectal cancer before surgery (the process was similar to the position prediction of the patients with intestinal villous adenoma), it can be seen that points of 84% (27/32) patients with effective treatment have come back to the normal person area (Figure 3B). In the mean time, points of 91% (10/11) patients with ineffective treatment have entered into the area of colorectal cancer (Figure 3C).

DISCUSSION

Urinary nucleosides as biological markers of malignancy have previously been reported for a wide variety of cancers[1-7,17,18]. However, only few reports existed regarding colorectal cancer. Our preliminary examination revealed that patients with colorectal cancer excreted in their urine significantly elevated amounts of nucleosides by HPLC method[13]. But the method analysis of urinary nucleosides involves manual sample extraction steps, resulting in artificial error and time-consumption. In the current study, we developed the automated column switching HPLC method to examine the relationship between urinary nucleosides and pathological characteristics of colorectal cancer and the potential value of these compounds in monitoring progress of the disease during surgery. The method is simple and rapid, requiring a total analysis time of 50 min per sample, with no time involved for sample processing. Its application to routine urine samples suggests utility for mass patient screening.

The present study also confirmed that significantly elevated levels of urinary nucleosides were detected in patients with colorectal cancer by the column-switching HPLC method developed. Our data revealed that the mean nucleoside concentrations from patients with intestinal villous adenoma were significantly lower than those from patients with colorectal cancer. Only 10% (1/10) of patients with intestinal villous adenoma were in the area of patients with colorectal cancer. This is in accordance with the previous studies showing that patients with noncancerous diseases and acute infections[19,20] do not excrete significantly elevated levels of urinary nucleosides. A current study on urinary nucleosides in colorectal cancer patients demonstrate that in the malignant disease not just one but several of the nucleosides is elevated. In such a multi-component alteration of the nucleoside levels, a pattern recognition method could reveal more information on difference among healthy adults, patients with intestinal villous adenoma and colorectal cancer than the evaluation of single components. The PCA method was applied for evaluation of the nucleoside levels in the three groups. The sensitivity of urinary nucleosides in patients with colorectal cancer was 71%, whereas the sensitivity of currently used tumor marker CEA is 29%. Urinary nucleosides may be a satisfactory biological marker for this disease.

It was also found that the level of m1G, Pseu and m1A were positively correlated with the tumor size and Duke's stages of colorectal cancer, respectively. These nucleosides may be useful as prognostic factors. Modified nucleosides have a much shorter half-life in the body than protein. A faster response to therapy and recurrence of disease is therefore feasible. Our results show that the changes in urinary nucleoside concentrations of patients with colorectal cancer almost paralleled with the change of disease status of patients after surgery (Figures 3B and C). The results are in agreement with the previous studies about urinary nucleosides being useful for monitoring progress of lymphoma and small cell carcinoma of the lung[21,22]. These facts indicated that urinary nucleosides may be of value for a rapid assessment of disease course in monitoring colorectal cancer.

These studies have indicated the potential utility of urinary nucleosides as biological marker for colorectal cancer, especially when the column switching HPLC method developed is combined with the PCA data processing method. Because the whole-body RNA turnover correlates quite well with the protein turnover[23], attention has to be paid to the alterations of urinary nucleosides under various catabolic conditions other than those occurring in malignancies, e.g. malnutrition, endocrine abnormalities, alcoholism and stress. More works are currently in progress to evaluate the usefulness of urinary nucleosides in differentiating cancer from other disease status.

ACKNOWLEDGMENTS

We are very grateful to Professor K.-S. Boos of Institute of Clinical Chemistry, University Hospital Grosshadern, Munich, Germany for the denotation of boronic acid-substituted silica column.

REFERENCES

1 **Xu G,** Di Stefano C, Liebich HM, Zhang Y, Lu P. Reversed-phase high-performance liquid chromatographic investigation of urinary normal and modified nucleosides of cancer patients. *J Chromatogr B* 1999; **732**: 307-313
2 **Liebich HM,** Xu G, Di Stefano C, Lehmann R. Capillary electrophoresis of urinary normal and modified nucleosides of cancer patients. *J Chromatogr A* 1998; **793**: 341-347
3 **Xu G,** Lu X, Zhang Y, Lu P, Di Stefano C, Lehmann R, Liebich HM. Two approaches to determining the urinary excretion patterns of nucleosides- HPLC and CE. *Se Pu* 1999; **17**: 97-101
4 **Zhao R,** Xu G, Yue B, Liebich HM, Zhang Y. Artificial neural network classification based on capillary electrophoresis of urinary nucleosides for the clinical diagnosis of tumors. *J Chromatogr A* 1998; **828**: 489-496
5 **Xu G,** Liebich HM, Lehmann R, Muller-Hagedorn S. Capillary electrophoresis of urinary normal and modified nucleosides of cancer patients. *Methods Mol Biol* 2001; **162**: 459-474
6 **Xu G,** Schmid HR, Lu X, Liebich HM, Lu P. Excretion pattern investigation of urinary normal and modified nucleosides of breast cancer patients by RP-HPLC and factor analysis method. *Biomed Chromatogr* 2000; **14**: 459-463
7 **Zheng YF,** Xu GW, Liu DY, Xiong JH, Zhang PD, Zhang C, Yang Q, Lv S. Study of urinary nucleosides as biological marker in cancer patients analyzed by micellar electrokinetic capillary chromatography. *Electrophoresis* 2002; **23**: 4104-4109
8 **Borek E,** Kerr SJ. A typical transfer RNA's and their origin in neoplastic cells. *Adv Cancer Res* 1972; **15**: 163-190
9 **Borek E,** Baliga BS, Gehrke CW, Kuo CW, Belman S, Troll W, Waalkes TP. High turnover rate of transfer RNA in tumor tissue. *Cancer Res* 1977; **37**: 3362-3366
10 **Mandel LR,** Srinivasan PR, Borek E. Origin of urinary methylated purines. *Nature* 1966; **209**: 586-588
11 **Sander G,** Topp H, Heller-Schoch G, Wieland J, Schoch G. Ribonucleic acid turnover in man: RNA catabolites in urine as measure for the metabolism of each of the three major species of RNA. *Clin Sci* 1986; **71**: 367-374
12 **Liebich HM,** Di Stefano C, Wixforth A, Schmid HR. Quantitation of urinary nucleosides by high-performance liquid chromatography. *J Chromatogr A* 1997; **763**: 193-197
13 **Zheng YF,** Chen YJ, Pang T, Shi XZ, Kong HW, Lu S, Yang Q, Xu GW. Investigation of urinary nucleosides excretion of intestinal cancer patients by reversed-phase high performance liquid chromatography. *Se Pu* 2002; **20**: 498-501
14 **Gehrke CW,** Kuo KC, Waalkes TP, Borek E. Patterns of urinary excretion of modified nucleosides. *Cancer Res* 197; **39**: 1150-1153
15 **Liebich HM,** Xu G, Di Stefanoc C, Lehmann R, Haring HU, Lu P, Zhang Y. Analysis of normal and modified nucleosides in Urine by Capillary Electrophoresis. *Chromatographia* 1997; **45**: 396-401
16 **Zheng YF,** Zhang Y, Liu DY, Guo XL, Mei SR, Xiong JH, Kong HW, Zhang C, Xu G. Analysis of Urinary Nucleosides by Micellar Electrokinetic Chromatography. *Chemical J Chinese Universities* 2001; **22**: 912-915
17 **Kim KR,** La S, Kim A, Kim JH, Liebich HM. Capillary electrophoretic profiling and pattern recognition analysis of urinary nucleosides from uterine myoma and cervical cancer patients. *J Chromatogr B* 2001; **754**: 97-106
18 **La S,** Cho JH, Kim JH, Kim KR. Capillary electrophoretic profiling and pattern recognition analysis of urinary nucleoside from throid cancer patients. *Anal Chim Acta* 2003; **486**: 171-182
19 **Borek E,** Sharma OK, Buschman FL, Cohn DL, Penley KA, Judson FN, Dobozin BS, Horsburgh CR Jr, Kirkpatrick CH. Altered excretion of modified nucleosides and beta-aminoisobutyric acid in subjects with acquired immunodeficiency syndrome or at risk for acquired immunodeficiency syndrome. *Cancer Res* 1986; **46**: 2557-2561
20 **Fischbein A,** Sharma OK, Selikoff IJ, Borek E. Urinary excretion of modified nucleosides in patients with malignant mesothelioma. *Cancer Res* 1983; **43**: 2971-2974
21 **Rasmuson T,** Bjork GR. Urinary excretion of pseudouridine and prognosis of patients with malignant lymphoma. *Acta Oncol* 1995; **34**: 61-67
22 **Waalkes TP,** Abeloff MD, Ettinger DS, Woo KB, Gehrke CW, Kuo KC, Borek E. Biological markers and small cell carcinoma of the lung: a clinical evaluation of urinary ribonucleosides. *Cancer* 1982; **50**: 2457-2464
23 **Sander G,** Hulsemann J, Topp H, Heller-Schoch G, Schoch G. Protein and RNA turnover in preterm infants and adults: a comparison based on urinary excretion of 3-methylhistidine and of modified one-way RNA catabolites. *Ann Nutr Metab* 1986; **30**: 137-142

Science Editor Guo SY **Language Editor** Elsevier HK

PO Box 2345, Beijing 100023, China
www.wjgnet.com
wjg@wjgnet.com

ELSEVIER

World J Gastroenterol 2005;11(25):3877-3881
World Journal of Gastroenterology ISSN 1007-9327

Effects of hepatocyte growth factor/scatter factor on the invasion of colorectal cancer cells *in vitro*

Hong-Wu Li, Ji-Xian Shan

Hong-Wu Li, Ji-Xian Shan, Department of Oncology, First Affiliated Hospital, China Medical University, Shenyang 110001, Liaoning Province, China
Correspondence to: Ji-Xian Shan, Department of Oncology, First Affiliated Hospital, China Medical University, Shenyang 110001, Liaoning Province, China. lhw-005@163.com
Telephone: +86-24-23256666-6227
Received: 2004-12-02 Accepted: 2005-01-05

Abstract

AIM: Hepatocyte growth factor (HGF) is a multifunctional growth factor which has pleiotrophic biological effects on epithelial cells, such as proliferation, motogenesis, invasiveness and morphogenesis. There are few reports about the role of HGF played in the colorectal cancer invasion. In the present study, we tried to investigate the possible mechanism of HGF involved in the invasion of colorectal cancer cells *in vitro*.

METHODS: Matrigel migration assay was used to analyze the migrational ability of Caco-2 and Colo320 *in vitro*. We detected the mRNA expressive levels of MMP-2, MMP-9 and their natural inhibitors TIMP-1, TIMP-2 in Caco-2 cells by reverse-transcription polymerase chain reaction (PCR) technique.

RESULTS: After 48 h incubation, there were notable differences when we compared the migrational numbers of Caco-2 cells in the group of HGF and PD98059 (the inhibitor of p42/p44MAPK) with the control (104.40±4.77 *vs* 126.80±5.40, $t = 7.17$, $P = 0.002<0.01$; 104.40±4.77 *vs* 82.80±4.15, $t = 7.96$, $P = 0.001<0.01$). The deviation between the HGF and PD98059 was significant ($P<0.01$). Compared with controls, MMP-2 and MMP-9 mRNA expres-sions were up-regulated by HGF (0.997±0.011 *vs* 1.207±0.003, $t = 35.002$, $P = 0.001<0.01$; 0.387±0.128 *vs* 0.971±0.147, $t = 106.036$, $P = 0.0000<0.01$, respectively); compared with controls, TIMP-1, TIMP-2 mRNA expressions were increased by PD98059 (1.344±0.007 *vs* 1.905±0.049, $t = 17.541$, $P = 0.003<0.01$; 1.286±0.020 *vs* 1.887±0.022, $t = 24.623$, $P = 0.002<0.01$, respectively).

CONCLUSION: HGF promoted Caco-2 migration mainly by p42/p44MAPK pathway; HGF/SF stimulated the expression of MMP-2, MMP-9 in Caco-2 and enabled tumoral cells to damage the ECM and reach the distant organ and develop metastasis; HGF played the function of promoted-invasion and promoted-metastasis, in which cellular selection was possible.

Key words: HGF; Colorectal cancer cells; Invasion; MMPs

Li HW, Shan JX. Effects of hepatocyte growth factor/scatter factor on the invasion of colorectal cancer cells *in vitro*. *World J Gastroenterol* 2005; 11(25): 3877-3881
http://www.wjgnet.com/1007-9327/11/3877.asp

INTRODUCTION

Hepatocyte growth factor/scatter factor is a polypeptide growth factor, which enhances strong cellular disintegration, tissue formation, inducing the migration, invasion and angiogenesis of epithelial cells[1]. The protein production of the c-met proto-oncogene encodes trans-membrane tyrosine kinase and is the receptor for hepatocyte growth factor, which regulates proliferation, differentiation, morphogenesis and motility in various cells after being activated by HGF. Thus, it relates with the genesis and progress in many types of human tumors. The mechanism for HGF-c-met in the invasion and metastasis of malignant tumor includes that they can promote cellular migration and increase the abilities of invasion, they also can trigger Ca^{++}-dependent signaling system, so activate the Ras, then activate extracellular-signal regulated kinase (Erk), thereby regulate the contraction and motion of cells and phosphorylate microfilament relating-protein, regulate cellular skeleton and reinforce the ability of cellular movement. HGF can coordinate other factors *in vivo* and therefore enlighten the abilities of migration and invasion in some malignant cells[2]. Yi found that HGF could increase the invasion of 13 lung cancer cells in which the receptor of c-met was expressed[3]. The motility of tumoral cells correlated closely with the metastasis in tumor.

Tumoral invasion occurs in three main steps: adhesion, degradation of basement membrane and movement, in which the degradation of basement membrane passes mainly through proteolytic kinases. Matrix metalloproteinases (MMPs) are part of these kinases, in which MMP-2 and MMP-9 correlated with the tumoral metastasis. The report showed that HGF could regulate the expression of MMPs.

Mitogen-activated protein kinases (MAPK) are the kinases between the receptors of cell membrane and the significant intracellular regulating-targets. Cells apply this system conducting extracellular stimulating-signal to the nucleus of cell so that the biological effects from the cells can be trasmitted. The pathway of intracellular signal conduction for HGF-c-met induced-biological effects is not clear.

Cellular migration is the premise of tumoral metastasis. The characters of tumoral infiltration and metastasis are the key factors affecting the survival and prognosis in patients. To

confirm the conclusion that HGF can promote migration *in vitro*, regulate the expression of MMPs and exist the MAPK pathway during these processes, we applied the HGF together with the inhibitors of p42/p44MAPK(PD98059) and p38MAPK(SB203580) dealt with the colorectal cancer cells: in Caco-2 and Colo320, we also observed mRNA expression of MMP-2, MMP-9 and tissue inhibitor of metalloproteinase-1 (TIMP-1) and tissue inhibitor of metalloproteinase-2(TIMP-2) in order to investigate the function of HGF in the invasion of colorectal cancer cells *in vitro*.

MATERIALS AND METHODS

Materials

Cells and cell culture The human colorectal cancer cell lines Caco-2 and Colo320 were purchased from China Academy of Science in Shanghai Institute of Life Science, Caco-2 were cultured in DMEM supplemented with 10% fetal bovine serum, 100 U/mL penicillin and 100 μg/mL streptomycin at 37 ℃ in a 50 mL/L CO_2 atmosphere. Medium were exchanged every other day, when the cells reached confluence, we digested them with 0.02% EDTA+trypsin and delivered them according to 1∶2 or 1:4∶. Colo320 were cultured in DMEM supplemented with 20% fetal bovine serum, others were identical with Caco-2.

Reagent and apparatus DMEM were purchased from Gibcobrl; FBS from TBD; HGF from JingMei Biol in ShenZhen and were compounded with free serum medium, the concentration was 20 ng/mL. PD98059 and SB203580 were from Promega, they were compounded with DMSO and made up to 10 and 20 mmol/L for storage and the applicable concentration was 40 μmmol/L combined with free serum, stored at 4 ℃. Matrigel from Gene Company in ShenYang was compounded with DMEM according to 1∶3, 0 ℃ fusion; 8 μmmol/L polycarbonate size membrane and TRIzol were from HuaMei Company, Boyden chamber were from the Department of Oncology in China Medical University. RT-PCR kit was from Takara, the primers of MMP-2, MMP-9, TIMP-1, TIMP-2, β-actin were synthesized by BoYa Bio Company in Shanghai. Amplified sections were 307, 215, 285, 265, and 690 bp respectively. Autoradiography were purchased from Olympus and PCR amplification instrument were from PE Company in the USA.

Methods

Matrigel migration assay This assay is similar to that described previously[5], Boyden chambers system whose upper and lower compartments were used to analyze the invasive ability of Caco-2 and Colo320. The chambers were washed, dried and irradiated under ultraviolet rays for 30 min, the experiments were divided into four groups DMEM, HGF, PD98059, and SB203580.

DMEM, 20 ng/mL HGF, 10% FBS (Caco-2) or 20% FBS (Colo320), 200 μL in the lower compartment with 50 μg Matrigel onto a polycarbonate membrane, and then 1 mL (about 3 ± 10^5 cell/mL) colorectal cancer cells were put in the upper compartment of the chamber, and the chambers were incubated at 37 ℃ in humidified air containing 50 mL/L CO_2 for 48 h, at the end of incubation, the cells on the upper side of polycarbonate membrane were wiped off with a cotton swab and the remaining cells that traversed the Matrigel and spread on the lower surface of the membrane were rinsed using distilled water twice, the membrane were fixed for 30 min with 5 mL methanol, dried and stained with hematoxylin for 10 min, rinsed with 1% HCl+10% alcohol and distilled water for 1-5 min, rinsed with 1% ammonia water and distilled water for 1-5 min, stained with eosin 1-10 min, at last rinsed and fixed with gradient alcohol and xylene, enclosed and counted five fields of vision using light microscope. Results were expressed as the number of colorectal cancer cells invaded per filter. Experiments were done in triplicate and results are shown as mean±SD.

Effect of PD98059 on HGF-induced migration 40 μmol/L PD98059 were added to the upper compartment with 1 mL cells for 30 min before 20 ng/mL HGF was added to the lower side of chamber which was incubated at 37 ℃ in a 50 mL/L CO_2 atmosphere for 48 h. After incubation, similar treatment as the above-mentioned, was carried out.

Effect of SB203580 on HGF-induced migration: 40 μmol/L SB203580 were added to the upper compartment with 1 mL cells for 30 min before 20 ng/mL HGF was added to the lower side of chamber which was incubated at 37 ℃ in a 50 mL/L CO_2 atmosphere for 48 h. After incubation, the treatment was identical with the above-mentioned.

Detection of MMP-2, MMP-9, TIMP-1, TIMP-2 mRNA by RT-PCR

Total RNA was extracted from subconfluent cell layers according to Single-step method of RNA isolation by acid guanidinium thiocyanate-phenol-chloroform extraction, 2 μL RNA was reverse-transcribed using AMV, 3 μL of the reaction were used for amplification. The primers used are as follows:

MMP-2-F: 5'-TCAACGGTCGGGAATACA-3'
MMP-2-R: 5'-CCCACAGTGGACATAGCG-3'
MMP-9-F: 5'-TCGAACTTTGACAGCGACAAGAA-3'
MMP-9-R: 5'-TCAGGGCGAGGACCATAGAGG-3'
TIMP-1-F: 5'-CTTCCACAGGTCCCACAACC-3'
TIMP-1-R: 5'-CAGCCCTGGCTCCCGAGGC-3'
TIMP-2-F: 5'-AAACGACATTTATGGCAACCCT-ATC-3'
TIMP-2-R: 5'-ACAGGAGCCGTCACTTCTCTTG-ATG-3'
β-actin-R: 5'-GATTGCCTCAGGACATTTCTG-3'
β-actin-F: 5'-GATTGCTCAGGACATTTCTG-3

PCR reaction conditions were as follows: Thirty-five cycles of MMP-2 PCR were performed, each consisting of denaturation for 3 min and 45 s at 94 ℃, annealing for 1 min at 55 ℃ and elongation for 1 and 7 min at 72 ℃. Thirty-five cycles of MMP-9 PCR were performed, each consisting of denaturation for 3 min and 45 s at 94 ℃, annealing for 1 min at 60.5 ℃ and elongation for 1 and 7 min at 72 ℃. Thirty cycles of TIMP-1 PCR were performed, each consisting of denaturation for 3 min and 30 s at 94 ℃, annealing for 1 min at 63 ℃ and elongation for 30 s and 7 min at 72 ℃. Thirty cycles of TIMP-2 PCR were performed, each consisting of denaturation for 3 min and 45 s at 94 ℃, annealing for 1 min at 65 ℃ and elongation for 30 s and 7 min at 72 ℃. Agarose gel electrophoresis consisting of 20 g/L ethidium bromide (EB) was used to analyze the production of PCR. Electrophoresis zones were reserved for 1 D kodak autoradiography system, β-actin was for controls; measure values were counted/β-actin.

Statistical analysis

SPSS12.0 software was used, all values were expressed as mean±SD, *t*-test was used to determine the significance of differences in multiple comparisons. Values of $P<0.05$ were considered to be statistically significant.

RESULTS

Migration of Caco-2

After 48 h incubation, there were notable differences when we compared the migrational numbers of Caco-2 cells in the group of HGF and PD98059 with the control ($P<0.01$). The deviation between the HGF and PD98059 was significant ($P<0.01$). The group of SB203580 had no implication. We did not find the phenomenon in the Colo320 cells. HGF increased the number of invading Matrigel cells, the more numbers, the more the invading ability. We found that PD98059 inhibited the migration of HGF-induced Caco-2. (Figure 1 and Table 1).

Table 1 Migrational numbers of Caco-2 in different factors

	The migrational numbers of Caco-2 (mean±SD)
Control	104.40±4.77
HGF/SF	126.80±5.40[b]
PD98059	82.80±4.15[d]
SB203580	108.4±14.38

[b]$P<0.01$, $t = 7.17$; [d]$P<0.01$, $t = 7.96$.

Expression of MMP-2, MMP-9, TIMP-1, TIMP-2 mRNA in Caco-2 cell conditions were identified with Matrigel migration assay .Examination of MMP-2, MMP-9, TIMP-1,TIMP-2 expression were by RT-PCR. DMEM was control, MMP-9 expressed all groups except control, MMP-2 was high expression in HGF group, TIMP-1 and TIMP-2 were high expression in the group of PD98059. HGF could stimulate the expression of MMP-2 and MMP-9, but the function was inhibited in the presence of PD98059 ($P<0.01$).There were different expressions of MMP-2, MMP-9 and TIMP-1, TIMP-2 in the group of PD98059, with no significance. Expression of MMP-2, MMP-9 and TIMP-1, TIMP-2 in the group of HGF were not divergent. (Figure 2 and Table 2).

Table 2 Expression of MMPs and its inhibitors in Caco-2 (mean±SD)

	MMP-2	MMP-9	TIMP-1	TIMP-2
Control	0.997±0.011	0.387±0.128	1.344±0.007	1.286±0.020
HGF	1.207±0.003	0.971±0.147	0.846±0.075	0.992±0.009
PD98059	0.824±0.037	0.350±0.007	1.905±0.049	1.887±0.022

DISCUSSION

In vitro, HGF/SF has the function of strongly promoting mitogen and stimulating the growth of normal and malignant cells[6]. HGF/SF could agitate directly cellular mobility and spreadable effects and colon formation gets diffused by it.

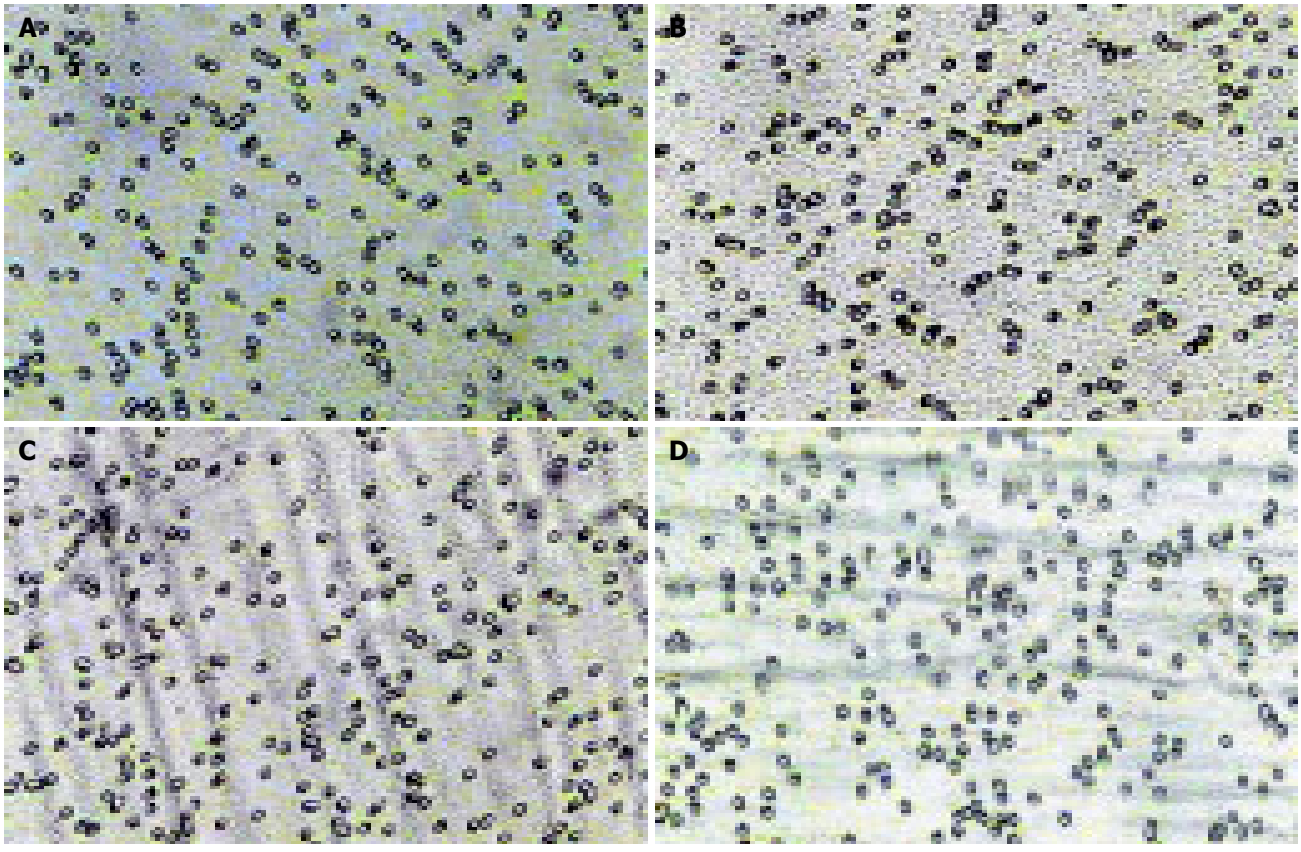

Figure 1 Migration of Caco-2 in different factors: control (**A**), Effect of HGF (**B**), PD98059 (**C**), and SB203580 (**D**).

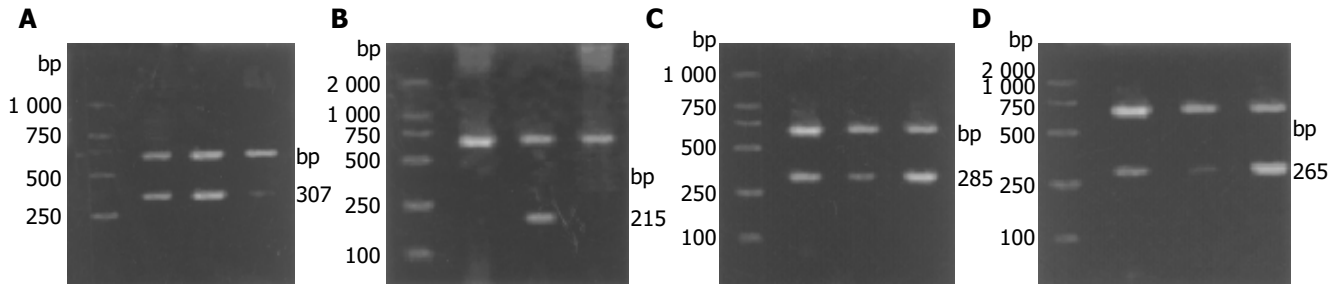

Figure 2 Expression of MMPs and TIMPs in Caco-2 cell: MMP-2 amplification section (**A**), MMP-9 amplification section (**B**), TIMP-1 amplification section (**C**), TIMP-2 amplification section (**D**).

The activity of HGF-promoted motogen and morphogen could promote adhesion, migration and infiltration of the cancer cells[7], as it enhanced Integrins-modulated adhesion so that lymphocyte invasion increased six-fold[8]. About the mechanism of HGF-promoted tumoral metastasis, Fujisaki[9] reported that the stimulation of CD44 could induce the expression of c-met; HGF/SF amplified CD44-induced adhesion of LFA-1 (lymphocyte function associated antigen-1), further amplified and agitated the Integrin-modulated adhesion, enabled the cancer cells to adhere blood vessel endothelium and pass through the vessel walls. The experiments of cotransfection for c-met and CD44 found that CD44, acted as the co-receptor of HGF, promoted the c-met tyrosine kinases phosphorylation and downstream signaling conduction protein kinases activation (activated MAPK), induced tumoral growth and metastasis[10].

Recently, the research of extracellular-signal transduction has made great progress in the interior and exterior parts of the country. Extracellular stimulation entered from the cellular surface and activated the signaling transduction pathway in the cytoplasm, transduced the signaling to the nucleus through many pathways and promoted or inhibited special expression of the target-gene[11], including the pathway of Ras-MAPK which played a main role in promoting cellular proliferation and regulating genetic transcription. The character of the cytokine receptor decided the manner of signaling transduction, many cytokines transmitted to the nucleus through mainly MAPK-cascades, induced the same genetic expression procedures, produced the same biological effects so that MAPK-cascades originated together or from the last pathway in which many membrane receptors transducted growth signaling to pass through the membrane[12]. MAPK was the important intercellular signaling system, cells applied it to transmit stimulating extracellular signal to the nucleus and modulated biological effects produced by cells[13]. It had decided four MAPK pathways in eukaryotic cell, including ERK, JNK, p38MAPK, and ERK5[14]. MAPK was a kind of serine/threonine protein kinase, activated by phosphorylation[15]. An extracellular stimulator could activate synchronously several members of MAPK families, Xia[16]found if they removed neurogenic growth factor from incubation systems, and then induced the apoptosis of PCI2, there existed activation of p38MAPK, JNK and inhibition of ERK, the deduced apoptosis and survival were decided by the balance between ERK-activated by growth factor and p38MAPK, and JNK-activated by stress.

In our study, we found that PD98059, the inhibitor of p42/p44MAPK, could restrain the numbers of HGF-induced colorectal cancer cells passed Matrigel, as such, we confirmed that p42/p44MAPK was one of the pathways of HGF-promoted Caco-2 invasion.

The main components of extracellular matrix (ECM) including collagen, glucoprotein, proteoglycan and glycosamine existed as the form of basement membrane and intercellular tissues. There was a kind of anti-adhesion protein in extracellular matrix called basement membrane protein, the sections of these molecules degradation had chemotaxis so that promoted the mobility of the cancer cells[13]. A lot of barriers were during the metastatic processes, it was of significance for the basement membrane beside tumoral cells and interstitial matrix to maintain tissue morphogenesis and biological specificity. Tumor cells might produce proteolytic ferment through autosecretion or stimulate host to cross basement membrane so that metastasis occurred. Therefore, the degradation of tumor to ECM was the prerequisite for tumoral invasion and metastasis[14]. Matrix metalloproteinases (MMPs) were this kind of peptidase which Zn^{2+}-dependently degraded ECM, at present, 20 members of MMPs families were determined. According to the different substrates, MMPs were divided as follows: interstitial collagenase, gelatinase, stromelysin, membrane-type MMPs[17]. In the 1980s, it was first reported that MMPs related with the potency of cancer metastasis[18]. The mechanism of tumor cells degraded ECM including the activation of MAPK, cells applied the pathway to promote the secretion of MT-MMPs and the rearrangement of microfilament skeleton formed by myoprotein and increased the ability of decomposing collage of ECM and migration, then, induced tumoral infiltration and metastasis. MMPs were the major kinases during the physiological and pathological processes in the rebuilding or degradation of ECM, they were the key to removing the barrier of cellular migration. Increasing activities of MMPs was one of the essential conditions in tumor invasion and metastasis, MMPs could affect cellular adhesion and migration directly. But the total degradation of ECM was controlled strictly by the balance between activated MMPs and TIMPs (inhibitors of MMPs)[19]. Our results showed that HGF/SF up-regulated the expression of MMP-2, MMP-9 and TIMPs in Caco-2 compared with the control groups, we confirmed *in vitro* that HGF increased the numbers of migrational Caco-2, the results suggested that increasing activities of MMPs in the presence of HGF enabled tumoral cells to damage the

ECM and easily developed metastasis.

In conclusion, HGF promoted Caco-2 migration mainly by p42/p44MAPK pathway; HGF/SF up-regulated the expression of MMP-2, MMP-9 in Caco-2 and enabled tumoral cells to damage the ECM; HGF played the function of promoted-invasion and promoted-metastasis in cellular selection; HGF could play the biological effects by MAPK, therefore, it had a major significance for we studied the regulation about MAPK in tumoral metastasis to understand the relationship between the MAPK pathway and colorectal cancer, furthermore, it would provide the evidence for MAPK to become the target of tumoral treatment.

REFERENCES

1 **Zeng Q,** Chen S, You Z, Yang F, Carey TE, Saims D, Wang CY. Hepatocyte growth factor inhits anoikis in head and neck squamous cell carcinoma cells by activation of ERK and Akt signaling independent of NF-KB. *J Biol Chem* 2002; **277**: 25203-25208

2 **Rosenthal EL,** Johnson TM, Allen ED, Apel IJ, Punturieri A, Weiss SJ. Role of the plasminogen activator matrix metalloproteinase systems in epidermal growth factor and scatter factor stimulated invasion of carcinoma cells. *Cancer Res* 1998; **58**: 5221-5230

3 **Yi S,** Chen JR, Viallet J, Schwall RH, Nakamura T, Tsao MS. Paracrine effects of hepatocyte growth factor/scatter factor on non-small-cell lung carcinoma cell lines. *Br J Cancer* 1998; **77**: 2162-2170

4 **Harvey P,** Clark IM, Jaurand MC, Warn RM, Edwards DR. Hepatocyte growth factor/scatter factor enhances the invasion of mesothelioma cell lines and the expression of matrix metalloproteinases. *Br J Cancer* 2000; **83**: 1147-1153

5 **Kundra V,** Anand-Apte B, Feig LA, Zetter BR. The chemotactic response to PDGF-BB: evidence of a role of ras. *J Cell Biol* 1995; **130**: 725-731

6 **Tamatani T,** Hattori K, Iyer A, Tamatani K, Oyasu R. Hepatocyte growth factor is an invasion/migration factor of rat urothelial carcinoma cells *in vitro*. *Carcinogenesis* 1999; **20**: 957- 962

7 **Li XN,** Ding YQ. HGF/SF-met signaling pathway and tumoral metastasis. *Medical Recapitulate* 2001; **7**: 643-644

8 **Weimar IS,** de Jong D, Muller EJ, Nakamura T, van Gorp JM, de Gast GC, Gerritsen WR. Hepatocyte growth factor/scatter factor promotes adhesion of lymphoma cells to extracellular matrix molecules via alpha4 beta 1 and alpha 5 beta 1 integrins. *Blood* 1997; **89**: 990-1000

9 **Fujisaki T,** Tanaka Y, Fujii K, Mine S, Saito K, Yamada S, Yamashita U, Irimura T, Eto S. CD44 stimulation induces integrin-mediated adhesion of colon cancer cell lines to endothelial cells by up-regulation of integrins and c-Met and activation of integrins and c-Met and activation of integrins. *Cancer Res* 1999; **59**: 4427-4434

10 **van der Voort R,** Taher TE, Wielenga VJ, Spaargaren M, Prevo R, Smit L, David G, Hartmann G, Gherardi E, Pals ST. Heparan sulfate-modified CD44promotes hepatocyte growth factor/scatter factor-induced signal transduction through the receptor tyrosine kinase c-Met. *J Biol Chem* 1999; **274**: 6499-6506

11 **Lenferink AE,** Busse D, Flanagan WM, Yakes FM, Arteaga CL. ErbB2/neu kinase modulates cellular p27(kip1) and cyclinD_1 through multiple signaling pathways. *Cancer Res* 2001; **61**: 6583-6591

12 **Donovan JC,** MilicA, Slingerland JM. Constitutive MEK/MAPK activation leads to p27(kip1) deregulation and antiestmgen resistance in human breast cancer cells. *J Biol Chem* 2001; **276**: 40888-40895

13 **Mao H,** Yuan AL, Zhao MF, Lai ZS. The effect of signal passway of mitogen activated protein kinase on hepatocellular carcinoma metastasis induced by VEGF. *Chin J Di* 2000; **20**: 14-16

14 **Feng S,** Song JD. Extracellular matrix degradational kinases in tumoral invasion and metastasis. *Zhongliu Fangzhi Yanjiu* 1999; **26**: 72-73

15 **Dinev D,** Jordan BW, Neufeld B, Lee JD, Lindemann D, Rapp UR, Ludwig S. Extracellular signal regulated kinase 5(ERK5) is required for the differentiation of muscle cells. *EMBO Rep* 2001; **2**: 829-834

16 **Testa JE,** Quigley JP. Principle and Practice of Cancer- Oncology (volume one). Translator: Xu CG, Zhang MH, Yang XJ. The Fifth Edition, Jinan: *Shandong Science and Technology Press* 2001: 146

17 **Yamamoto S,** Konishi I, Mandai M, Kuroda H, Komatsu T, Nanbu K, Sakahara H, Mori T. Expression of vascular endothelial growth factor (VEGF) in epithelial ovarian neoplasms: correlation with clinicopathology and patient survival, and analysis of serum VEGF levels. *Br J Cancer* 1997; **76**: 1221-1227

18 **Liotta LA,** Tryggvason K, Garbisa S, Hart I, Foltz CM, Shafie S. Metastatic potential correlates with enzymatic degradation of basement membrance collagen. *Nature* 1980; **284**: 67-68

19 **Kong LL,** Yang JW, Cui W. Progress of the relationship between matrix metalloproteinases and tumor. *J Jining Medical College* 2003; **26**: 64-66

Science Editor Guo SY **Language Editor** Elsevier HK

PO Box 2345, Beijing 100023, China
www.wjgnet.com
wjg@wjgnet.com

ELSEVIER

World J Gastroenterol 2005;11(25):3882-3886
World Journal of Gastroenterology ISSN 1007-9327

Natural history of major complications in hepatitis C virus-related cirrhosis evaluated by per-rectal portal scintigraphy

Etsushi Kawamura, Daiki Habu, Takehiro Hayashi, Ai Oe, Jin Kotani, Hirotaka Ishizu, Kenji Torii, Joji Kawabe, Wakaba Fukushima, Takashi Tanaka, Shuhei Nishiguchi, Susumu Shiomi

Etsushi Kawamura, Takehiro Hayashi, Ai Oe, Jin Kotani, Hirotaka Ishizu, Kenji Torii, Joji Kawabe, Susumu Shiomi, Department of Nuclear Medicine, Graduate School of Medicine, Osaka City University, 1-4-3, Asahimachi, Abenoku, Osaka 545-8585, Japan
Daiki Habu, Shuhei Nishiguchi, Department of Hepatology, Graduate School of Medicine, Osaka City University, 1-4-3, Asahimachi, Abenoku, Osaka 545-8585, Japan
Wakaba Fukushima, Takashi Tanaka, Department of Public Health, Graduate School of Medicine, Osaka City University, 1-4-3, Asahimachi, Abenoku, Osaka 545-8585, Japan
Supported by the Study Group of Portal Malcirculation supported by Ministry of Health, Labour and Welfare
Correspondence to: Dr. Etsushi Kawamura, Department of Nuclear Medicine, Graduate School of Medicine, Osaka City University, 1-4-3, Asahimachi, Abenoku, Osaka 545-8585, Japan. etsushi-k@med.osaka-cu.ac.jp
Telephone: +81-6-66453885 Fax: +81-6-66460686
Received: 2004-12-07 Accepted: 2004-12-20

Abstract

AIM: To examine the correlation between the porto-systemic hypertension evaluated by portal shunt index (PSI) and life-threatening complications, including hepatocellular carcinoma (HCC), liver failure (Child-Pugh stage progression), and esophagogastric varices.

METHODS: Two hundred and twelve consecutive subjects with HCV-related cirrhosis (LC-C) underwent per-rectal portal scintigraphy. They were allocated into three groups according to their PSI: group I, PSI≤10%; group II, 10%<PSI<30%; and group III, 30%≤PSI. Of these, selected 122 Child-Pugh stage A (Child A) subjects were included in analysis (a mean follow-up period of 5.9±5.4 years, range 6 mo-21 years).

RESULTS: No significant correlation between PSI and cumulative probability of HCC incidence was observed. Cumulative probability of Child A to B progression was tended to be higher in group III than in group I, and significantly higher in group III than in group II (62% *vs* 34%, 62% *vs* 37%; $P = 0.060$, <0.01; respectively). Cumulative probability of varices tended to be higher in group III than in group I (31% *vs* 12%, $P = 0.090$). On multivariate analyses, significant correlation between PSI and Child A to B progression was observed, and no significant correlation between PSI and HCC incidence or varices progression was observed.

CONCLUSION: Patients with LC-C of Child A will progress to Child B rapidly after their PSI reaches 30% or higher. PSI can be used to predict occult progressive porto-systemic shunting and liver failure non-invasively. It indicates that PSI may play an important role in follow-up of the porto-systemic hypertension gradient for outpatients with LC unlike hepatic venous catheterization.

Key words: Portal shunt index; Porto-systemic shunting; Per-rectal portal scintigraphy; Natural history; Liver cirrhosis; HCV; Hepatocellular carcinoma; Liver failure; Varix

Kawamura E, Habu D, Hayashi T, Oe A, Kotani J, Ishizu H, Torii K, Kawabe J, Fukushima W, Tanaka T, Nishiguchi S, Shiomi S. Natural history of major complications in hepatitis C virus-related cirrhosis evaluated by per-rectal portal scintigraphy. *World J Gastroenterol* 2005; 11(25): 3882-3886
http://www.wjgnet.com/1007-9327/11/3882.asp

INTRODUCTION

Hepatitis C virus (HCV) is the most common cause of chronic liver disease in several countries, including Japan, and chronic hepatitis due to HCV (CH-C), which exhibits a variable natural course, is becoming a subject of worldwide interest. CH-C progresses to cirrhosis of the liver (LC), and may be complicated by hepatocellular carcinoma (HCC), hepatic decompensation, and esophagogastric varices[1,2], although its clinical course has not been fully defined. Despite treatment such as injection of interferon plus oral ribavirin[3], many patients with CH-C progress to cirrhosis[4], and develop portal hypertension as CH-C advances to the early phase of LC[5].

Portal hypertension evaluated by "invasive" hepatic venous pressure gradient (HVPG) is associated with progression of liver failure and death[6-8]. Using the method described in this study, the extent of porto-systemic shunting (PSS) can be evaluated with the portal shunt index (PSI) using relatively "non-invasive" per-rectal portal scintigraphy with ^{99m}Tc pertechnetate, because PSI correlates strongly with portal pressure[9,10]. This study monitored three life-threatening complications of LC, including the incidence of HCC, Child-Pugh stage progression, and progression of esophagogastric varices, and examined the correlation between PSI and these three complications.

MATERIALS AND METHODS

Patients

A retrospective cohort study was performed on 212 subjects with HCV-related cirrhosis (LC-C), who were admitted to

our hospital during the 24 years between March 1979 and June 2002, and who were evaluated with PSI obtained by per-rectal portal scintigraphy with ^{99m}Tc pertechnetate. These subjects were diagnosed by examination of liver specimens obtained by laparoscopy, or needle biopsy performed under ultrasonic guidance. Exclusion criteria for this study were as follows: other causes of cirrhosis such as HBV, autoimmune disease, any alcohol consumption; past treatment with interferon, endoscopic sclerotherapy or open surgery for varices; and trans-arterial embolization or open surgery for HCC. Within a week of hospitalization, all subjects underwent abdominal ultrasonography for detection of ascites, Child-Pugh staging as an index of liver failure and endoscopy for detection of esophagogastric varices[11]. Three Child-Pugh stages were considered: stage A (score 5-6), stage B (7-9), and stage C (10-15). The 212 subjects with cirrhosis were distributed as follows: Child-Pugh stage A (Child A), 122; Child B, 73; and Child C, 17. At entry, we used other possible predictors of LC prognosis, including sex, age, serum albumin, total bilirubin (T-bil), prothrombin time (PT), and platelets[12].

Longitudinal study

We selected 122 Child A subjects for a longitudinal study; these subjects gave their informed consent to participate, and agreed to return after discharge to our outpatient clinic for monitoring. The procedures were approved by the Ethics Committee of Graduate School of Medicine, Osaka City University. A total of 122 subjects were monitored for a mean period of 5.9±5.4 years (range 6 mo to 21 years). Monitoring was maintained for each evaluation until confirmation of HCC, or Child A to B progression, or varices progression, or the end of the outcome observation period (June 2002). Subjects were excluded from the study if they were followed by another hospital, or their monitoring periods were less than 6 mo.

After excluding dropouts, we were able to monitor the following subjects for at least 6 mo: for HCC incidence, 108 subjects; for Child A to B progression, 107; and for varices progression, 109. A PSI value of 10% or higher is considered to be abnormal[9], and a PSI of 30% or higher has an especially poor prognosis for chronic liver diseases[5]. We defined three groups according to their PSI: group I, PSI$\leqslant$10%; group II, 10%<PSI<30%; and group III, 30% $\leqslant$PSI. The subjects were further divided as follows: for HCC incidence, 108 subjects-group I, 33; group II, 41; and group III, 34; for Child A to B progression, 107 subjects-group I, 32; group II, 41; and group III, 34; for varices progression, 109 subjects-group I, 33; group II, 41; and group III, 35. These subjects underwent the following examinations: laboratory studies and physical assessment of the extent of hepatic encephalopathy for Child's staging, with a mean interval of 4.1±0.8 mo; abdominal ultrasonography or dynamic CT for assessment of the extent of ascites or the existence of HCC, with a mean interval of 2.1±0.6 mo; and endoscopy for varices, with a mean interval of 8.1±2.1 mo. HCC was confirmed by histology obtained by needle biopsy performed under ultrasonic guidance, or confirmed by selective angiography. The extent of hepatic encephalopathy was defined from detection of tremor and/or disorientation by physicians. The extent of ascites was confirmed by abdominal ultrasonography and/or physical assessment. We defined progression (or incidence) of each complication as the first confirmation of HCC, or Child B or a new variceal factor[13]. Figure 1 shows flow of participants through monitoring.

Measurement of the portal shunt index

The subjects fasted after the evening meal on the day before examination. In the morning, the rectum was emptied by administration of a laxative. First, 370 MBq of ^{99m}Tc pertechnetate (2 mL solution) was given per rectum through a polyethylene tube (Nélaton's catheter, French 16) into the upper rectum, followed by 15 mL of air. Time–activity curves for the heart and liver areas were obtained every 4 s using a large-field scintillation camera (Vertex-Plus, ADAC Laboratories, Silicon Valley, USA). It was equipped with a low-energy, multipurpose, parallel-hole collimator and was interfaced with a digital computer. The camera was positioned over the patient's abdomen so that the field of view included the heart, liver, and spleen. At the end of the 5-min examination, a 5-min summed color image was recorded. To measure the extent of PSS by PSI, we calculated the number of counts for the heart as a percentage of the counts for the heart and liver integrated for 24 s immediately after the appearance of the liver time-activity curve[9].

Statistical analysis

Results were analyzed by SAS 8.12 statistical software (SAS

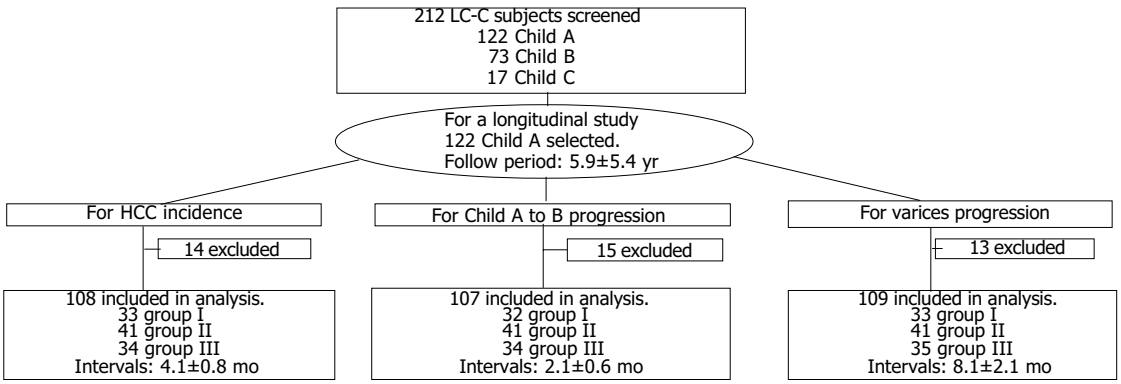

Figure 1 Flow of monitoring, group I, PSI $\leqslant$ 10%; group II, 10%<PSI<30%; group III, 30% $\leqslant$ PSI. LC-C, HCV-related cirrhosis; Child A, Child-Pugh stage A; PSI, portal shunt index.

Institute Inc., Cary, NC)[14,15]. Data were expressed as mean±SD. Comparisons between PSI groups were made by the Kruskal-Wallis test, the Mantel-Haenszel test, or ANOVA. The cumulative progression rates were calculated and plotted by the Kaplan-Meier method, and were compared by the log-rank test. Any significant variable was considered suitable for the multivariate analysis using Cox's regression model. $P<0.05$ was taken as statistically significant.

RESULTS

Patient characteristics at entry

Table 1 presents patient data at entry classified by PSI. The differences between the PSI groups were significant for the following parameters: age, albumin, T-bil, platelets ($P<0.01$, <0.01, <0.05, and <0.01, respectively).

Cumulative progression

No significant correlation between PSI and cumulative probability of HCC incidence was observed (Figure 2A). Cumulative probability of Child A to B progression was tended to be higher in group III than in group I, and significantly higher in group III than in group II (62% *vs* 34%, 62% *vs* 37%; $P = 0.060$, <0.01; respectively) (Figure 2B). Cumulative probability of esophagogastric varices tended to be higher in group III than in group I (31% *vs* 12%, $P = 0.090$) (Figure 2C).

Morbidity

Table 2 presents the proportions of Child A to B progression and relative risks as uni- and multivariates of possible predictors, which were classified at the entry of the study. The total proportion of each predictor, except PSI, was divided into two between better (upper line) and worse (lower line) at a cut-off value according to Child staging, or reports by other authors: for instance, albumin, at 3.5 g/dL[11,12,16].

Group III had the highest rate of Child A to B progression (21 of 34, 61.8%), followed by <3.5 albumin (50.0%), and <100 PT (48.8%) (Table 2). A significant relationship was found between group (I+II) and group III (crude RR = 2.44, 95%CI = 1.33-4.48, $P<0.01$), and between group II and group III (2.95, 1.40-6.24, $P<0.01$), with a trend of significance ($P<0.05$). No significant increase of other predictors was revealed. PSI and the common useful predictors such as albumin and platelets were included in multivariate analysis; only group III remained significant (adjusted RR = 2.98, 95%CI = 1.29-6.87, $P<0.05$).

The group with <10 platelets had the highest incidence of HCC and the highest progression of varices (30.3%, 47.1%, respectively). On multivariate analyses, no significant associations were found between PSI and incidence of HCC or progression of esophagogastric varices.

DISCUSSION

Even if physical symptoms and serum biochemical tests indicate the early phase of LC-C, the patient may already have occult advanced hepatic damage. PSI is a possible predictor of occult progressive stages of LC-C for outcome patients. While PSI obtained by per-rectal portal scintigraphy has its own weaknesses (it emphasizes PSS via the inferior mesenteric vein, rather than via the superior mesenteric vein, and

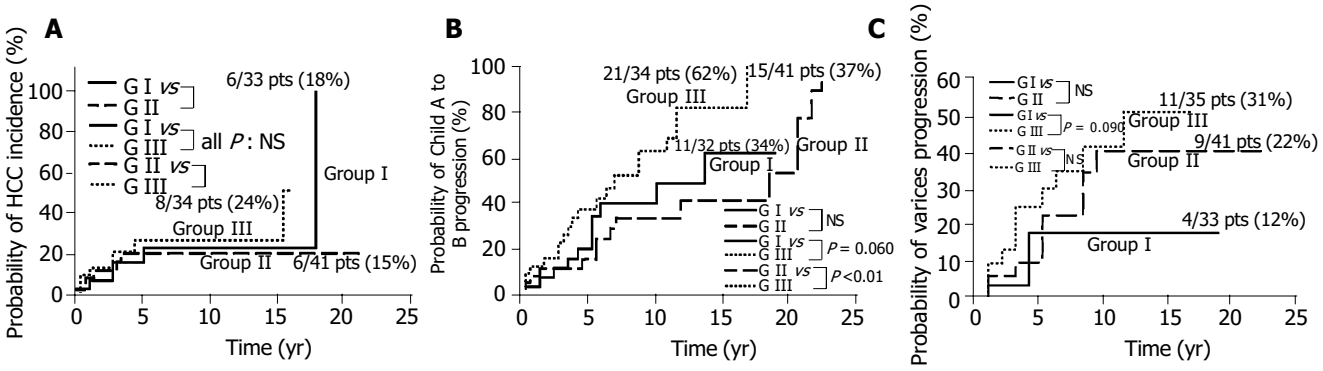

Figure 2 The probability of each life-threatening complication. **A:** The cumulative incidence rate of HCC (n = 108). **B:** The cumulative progression rate of Child A to B (n = 107). **C:** The cumulative progression rate of esophagogastric varices (n = 109). The continuous line shows group I (PSI ≤ 10%); the large dotted line shows group II (10%<PSI<30%); and the small dotted line shows group III (30% ≤ PSI). Child A, Child-Pugh stage A; PSI, portal shunt index; pts, patients; GI, group I; GII, group II; GIII, group III; NS, not significant.

Table 1 Characteristics by portal shunt index at entry

	Group I PSI≤10%	Group II 10%<PSI<30%	Group III 30%≤PSI	P	
Sex (Male / Female), n	25 / 13	31 / 15	30 / 8	NS	2
Age, yr	48.4±11.7	54.3±13.0	54.9±9.9	<0.01	1
Albumin, g / dL	4.0±0.5	4.0±0.3	3.6±0.4	<0.01	3
Total bilirubin, mg / dL	0.8±0.3	0.9±0.4	1.1±0.4	<0.05	1
Prothrombin time, %	95.4±17.2	94.5±15.5	92.5±20.2	NS	1
Platelets, / mm^3	16.4±5.7	14.7±6.9	10.6±5.0	<0.01	1

ANOVA: analysis of variance, PSI: portal shunt index, NS: not significant. Data are expressed as mean±SD. [1]Kruskal-Wallis test, [2]Mantel-Haenszel test, [3]ANOVA.

Table 2 Relative risks of possible predictors for Child-Pugh stage A to B progression

	Classification of predictor at entry	Proportion of Child-Pugh stage A to B progression, *n* / *N* (%)	[1]Relative risks	
			Crude RR (95%CI)	[2]Adjusted RR (95%CI)
Sex	Female	16 / 34 (47.1)	1.00	
	Male	31 / 73 (42.5)	1.47 (0.76-2.84)	
Age (per 1 yr)			0.99 (0.96-1.01)	
Albumin, g / dL	3.5+	25 / 63 (39.7)	1.00	1.00
	<3.5	22 / 44 (50.0)	1.49 (0.83-2.67)	0.98 (0.49-1.95)
Total bilirubin, mg / dL	<1.0	32 / 69 (46.4)	1.00	
	1.0+	15 / 38 (39.5)	1.27 (0.68-2.39)	
Prothrombin time, %	100+	27 / 66 (40.9)	1.00	
	<100	20 / 41 (48.8)	1.06 (0.59-1.91)	
Platelets, / mm^3	10+	32 / 73 (43.8)	1.00	1.00
	<10	13 / 32 (40.6)	1.60 (0.81-3.16)	1.40 (0.68-2.86)
Portal shunt index	Group I	11 / 32 (34.4)	1.51 (0.65-3.51)	1.67 (0.70-3.99)
	Group II	15 / 41 (36.6)	1.00	1.00
	Group III	21 / 34 (61.8)	2.95 (1.40-6.24)[b]	2.98 (1.29-6.87)[a]
			(*P* trend <0.05)	(*P* trend: NS)
	Group (I+II)	26 / 73 (35.6)	1.00	1.00
	Group III	21 / 34 (61.8)	2.44 (1.33-4.48)[d]	2.36 (1.17-4.78)[c]

[a]*P*<0.05 *vs* Group II PSI, [b]*P*<0.01 *vs* Group II PSI, [c]*P*<0.05 *vs* Group (I+II) PSI, [d]*P*<0.01 *vs* Group (I+II) PSI, NS: not significant. [1]RR and their 95% CI were determined by a Cox's regression model. [2]This model includes albumin, platelets, PSI. Group I, PSI≤10%; Group II, 10%<PSI<30%; Group III, 30%≤PSI; Group (I+II), PSI<30%. CI: Confidence interval, RR: Relative risk, PSI: Portal shunt index, *n*; progression proportion, *N*; total proportion.

expresses the extent of PSS indirectly), it should be useful for the observation of LC-C because it is a simple and non-invasive technique unlike hepatic venous catheterization[9].

In this study, we used ^{99m}Tc pertechnetate for per-rectal portal scintigraphy because of its short half-life and low cost[17]. Our study had three major findings.

First, there was no correlation between the porto-systemic hypertension and HCC incidence. This finding suggests that HCC occurs independently of the decrease in hepatic blood flow due to the development of PSS.

Second, patients with LC-C of Child A will progress to Child B rapidly after their PSI reaches 30% or higher. Shiomi *et al*.[5], have reported that changes in the portal hemodynamics of chronic liver disease subjects were not gradual. The development of PSS causes hepatic functional reserve to deteriorate rapidly. We propose that per-rectal portal scintigraphy is useful to predict occult progressive portal hypertension and liver failure in the early phase of LC-C, on the basis of the strong relationship between PSI and the Child-Pugh staging.

Third, the natural advance of PSS has relevance to esophagogastric varices progression in patients with the early phase of LC-C. Other authors have reported that the porto-systemic pressure gradient is a strong predictor for varices progression[18,19]. But in this study, PSI showed no statistical advantage over platelets, albumin, or T-bil for detecting the progression of varices. The reason why PSI was worse than these laboratory data is because esophagogastric varices mainly reflect the flow of superior mesenteric vein.

Progressive viral hepatitis has been acknowledged as a major indication for liver transplantation[20,21]. Kiuchi *et al*.[22], have emphasized the need to evaluate the recipients preoperatively. One of the important recipient factors is the presence of collateral circulation[23]. Bruix *et al*.[24], have reported that LC patients with increased portal pressure are at high risk of hepatic decompensation after resection of HCC. We propose that preoperative per-rectal portal scintigraphy would be useful for early detection of occult portal hypertension, to assess graft size requirement to prevent graft failure after liver transplantation, or to avoid liver failure after hepatectomy.

In summary, physicians can monitor the porto-systemic hypertension gradient in LC patient during the outcome observation period by using "non-invasive" per-rectal portal scintigraphy; on the other hand, measurement of HVPG needs hospitalization. In the early phase of LC-C, PSI can be used to predict occult progressive PSS and liver failure. Therefore, even for patients diagnosed as being in the early phase of LC-C on the basis of other indicators, those with an initial PSI ⩾30% should be observed by keeping early liver transplantation, or liver failure after hepatectomy in mind; HCC should be watched for, regardless of PSI.

REFERENCES

1 **Sorbi D,** Gostout CJ, Peura D, Johnson D, Lanza F, Foutch PG, Schleck CD, Zinsmeister AR. An assessment of the management of acute bleeding varices: a multicenter prospective member-based study. *Am J Gastroenterol* 2003; **98**: 2424-2434

2 **Davis GL,** Albright JE, Cook SF, Rosenberg DM. Projecting future complications of chronic hepatitis C in the United States. *Liver Transpl* 2003; **9**: 331-338

3 **Fattovich G,** Zagni I, Minola E, Felder M, Rovere P, Carlotto A, Suppressa S, Miracolo A, Paternoster C, Rizzo C, Rossini A, Benedetti P, Capanni M, Ferrara C, Costa P, Bertin T, Pantalena M, Lomonaco L, Scattolini C, Mazzella G, Giusti M, Boccia S, Milani S, Marin R, Lisa Ribero M, Tagger A. A randomized trial of consensus interferon in combination with ribavirin as initial treatment for chronic hepatitis C. *J Hepatol* 2003; **39**: 843-849

4 **Iino S.** Natural history of hepatitis B and C virus infections. *Oncology* 2002; **62**: 18-23

5 **Shiomi S,** Sasaki N, Habu D, Takeda T, Nishiguchi S, Kuroki T, Tanaka T, Ochi H. Natural course of portal hemodynamics in patients with chronic liver diseases, evaluated by per-rectal portal scintigraphy with Tc-99m pertechnetate. *J Gastroenterol* 1998; **33**: 517-522

6 **Debernardi-Venon W,** Bandi JC, Garcia-Pagan JC, Moitinho

E, Andreu V, Real M, Escorsell A, Montanya X, Bosch J. CO (2) wedged hepatic venography in the evaluation of portal hypertension. *Gut* 2000; **46**: 856-860

7 **Abraldes JG,** Tarantino I, Turnes J, Garcia-Pagan JC, Rodes J, Bosch J. Hemodynamic response to pharmacological treatment of portal hypertension and long-term prognosis of cirrhosis. *Hepatology* 2003; **37**: 902-908

8 **Patch D,** Nikolopoulou V, McCormick A, Dick R, Armonis A, Wannamethee G, Burroughs A. Factors related to early mortality after transjugular intrahepatic portosystemic shunt for failed endoscopic therapy in acute variceal bleeding. *J Hepatol* 1998; **28**: 454-460

9 **Shiomi S,** Kuroki T, Kurai O, Kobayashi K, Ikeoka N, Monna T, Ochi H. Portal circulation by technetium-99m pertechnetate per-rectal portal scintigraphy. *J Nucl Med* 1988; **29**: 460-465

10 **Boldys H,** Hartleb M, Rudzki K, Nowak A, Nowak S. Effect of propranolol on portosystemic collateral circulation estimated by per-rectal portal scintigraphy with technetium-99m pertechnetate. *J Hepatol* 1995; **22**: 173-178

11 **Pugh RN,** Murray-Lyon IM, Dawson JL, Pietroni MC, Williams R. Transection of the oesophagus for bleeding oesophageal varices. *Br J Surg* 1973; **60**: 646-649

12 **Kusaka K,** Harihara Y, Torzilli G, Kubota K, Takayama T, Makuuchi M. Objective evaluation of liver consistency to estimate hepatic fibrosis and functional reserve for hepatectomy. *J Am Coll Surg* 2000; **191**: 47-53

13 **Idezuki Y.** General rules for recording endoscopic findings of esophagogastric varices. Japanese Society for Portal Hypertension. *World J Surg* 1995; **19**: 420-422

14 **Schlichting P,** Christensen E, Andersen PK, Fauerholdt L, Juhl E, Poulsen H, Tygstrup N. Prognostic factors in cirrhosis identified by Cox's regression model. *Hepatology* 1983; **3**: 889-895

15 **Holford TR.** Life tables with concomitant information. *Biometrics* 1976; **32**: 587-597

16 **Meijer K,** Haagsma EB, Kok T, Schirm J, Smid WM, van der Meer J. Natural history of hepatitis C in HIV-negative patients with congenital coagulation disorders. *J Hepatol* 1999; **31**: 400-406

17 **Urbain D,** Jeghers O, Ham HR. Per-rectal portal scintigraphy: comparison between technetium-99m, thallium-201, and iodine-123-HIPDM. *J Nucl Med* 1988; **29**: 2020-2021

18 **Vorobioff J,** Groszmann RJ, Picabea E, Gamen M, Villavicencio R, Bordato J, Morel I, Audano M, Tanno H, Lerner E, Passamonti M. Prognostic value of hepatic venous pressure gradient measurements in alcoholic cirrhosis: a 10-year prospective study. *Gastroenterology* 1996; **111**: 701-709

19 **Groszmann RJ,** Bosch J, Grace ND, Conn HO, Garcia-Tsao G, Navasa M, Alberts J, Rodes J, Fischer R, Bermann M. Hemodynamic events in a prospective randomized trial of propranolol versus placebo in the prevention of a first variceal hemorrhage. *Gastroenterology* 1990; **99**: 1401-1407

20 **Villeneuve JP,** Durantel D, Durantel S, Westland C, Xiong S, Brosgart CL, Gibbs CS, Parvaz P, Werle B, Trepo C, Zoulim F. Selection of a hepatitis B virus strain resistant to adefovir in a liver transplantation patient. *J Hepatol* 2003; **39**: 1085-1089

21 **Rosen HR,** Gretch D, Kaufman E, Quan S. Humoral immune response to hepatitis C after liver transplantation: assessment of a new recombinant immunoblot assay. *Am J Gastroenterol* 2000; **95**: 2035-2039

22 **Kiuchi T,** Tanaka K, Ito T, Oike F, Ogura Y, Fujimoto Y, Ogawa K. Small-for-size graft in living donor liver transplantation: how far should we go? *Liver Transpl* 2003; **9**: S29-35

23 **Fevery J.** Liver transplantation: problems and perspectives. *Hepatogastroenterology* 1998; **45**: 1039-1044

24 **Bruix J,** Castells A, Bosch J, Feu F, Fuster J, Garcia-Pagan JC, Visa J, Bru C, Rodes J. Surgical resection of hepatocellular carcinoma in cirrhotic patients: prognostic value of preoperative portal pressure. *Gastroenterology* 1996; **111**: 1018-1022

Science Editor Guo SY **Language Editor** Elsevier HK

PO Box 2345, Beijing 100023, China
www.wjgnet.com
wjg@wjgnet.com

ELSEVIER

World J Gastroenterol 2005;11(25):3887-3892
World Journal of Gastroenterology ISSN 1007-9327

C-terminal domain of hepatitis C virus core protein is essential for secretion

Soo-Ho Choi, Kyu-Jin Park, So-Yeon Kim, Dong-Hwa Choi, Jung-Min Park, Soon B. Hwang

Soo-Ho Choi, Kyu-Jin Park, So-Yeon Kim, Dong-Hwa Choi, Jung-Min Park, Soon B. Hwang, Ilsong Institute of Life Science, Hallym University, Chuncheon 200-702, South Korea
Supported by a grant from the Korean Ministry of Science and Technology (Korean Systems Biology Research Grant, M1-0309-06-0002) and partly by the research grant from Hallym University, Korea
Co-first-authors: Kyu-Jin Park
Correspondence to: Soon B. Hwang, Ilsong Institute of Life Science, Hallym University, 1 Ockcheon-dong, Chuncheon 200-702, South Korea. sbhwang@hallym.ac.kr
Telephone: +82-31-380-1732 Fax: +82-31-384-5395
Received: 2004-12-12 Accepted: 2005-01-05

Abstract

AIM: We have previously demonstrated that hepatitis C virus (HCV) core protein is efficiently released into the culture medium in insect cells. The objective of this study is to characterize the HCV core secretion in insect cells.

METHODS: We constructed recombinant baculoviruses expressing various-length of mutant core proteins, expressed these proteins in insect cells, and examined core protein secretion in insect cells.

RESULTS: Only wild type core was efficiently released into the culture medium, although the protein expression level of wild type core was lower than those of other mutant core proteins. We found that the shorter form of the core construct expressed the higher level of protein. However, if more than 18 amino acids of the core were truncated at the C-terminus, core proteins were no longer secreted into the culture medium. Membrane flotation data show that the secreted core proteins are associated with the cellular membrane protein, indicating that HCV core is secreted as a membrane complex.

CONCLUSION: The C-terminal 18 amino acids of HCV core were crucial for core secretion into the culture media. Since HCV replication occurs on lipid raft membrane structure, these results suggest that HCV may utilize a unique core release mechanism to escape immune surveillance, thereby potentially representing the feature of HCV morphogenesis.

Key words: Hepatitis C virus; Core secretion; Morphogenesis; Virus assembly

Choi SH, Park KJ, Kim SY, Choi DH, Park JM, Hwang SB. C-terminal domain of hepatitis C virus core protein is essential for secretion. *World J Gastroenterol* 2005; 11(25): 3887-3892
http://www.wjgnet.com/1007-9327/11/3887.asp

INTRODUCTION

Hepatitis C virus (HCV) is the major etiologic agent of transfusion-associated hepatitis[1-3] and is associated with a chronic infection that leads to liver cirrhosis and hepatocellular carcinoma[4,5]. HCV is an enveloped virus and its virion size has been estimated at a diameter of 30-60 nm[6]. The virion contains a single-stranded, positive-sense RNA genome of approximately 9 600 nucleotides[7-10]. HCV belongs to the *Flaviviridae* family[11,12] and its genomic sequence is related to the flaviviruses and the pestiviruses[9,13]. The viral genome encodes a polyprotein precursor of 3 010-3 030 amino acids from one long open reading frame and is further processed into multiple viral proteins[14-16]. The structural proteins are processed by a host signal peptidase into a core protein, envelope proteins E1 and E2, and p7[13,16,17]. The viral nonstructural proteins are cleaved by viral proteinase into serine protease, helicase, RNA polymerase, and functionally undefined proteins. Biochemical properties of many structural and nonstructural proteins have been extensively characterized. However, studies on virion morphogenesis and viral replication have been hampered by the inability to propagate the viruses in a cell culture system.

The mechanism of HCV virion assembly is not yet known because the expression of the HCV structural gene in mammalian cells generates no detectable virion particles. However, it has been reported that either virus-like particles (VLPs) were produced in insect cells infected with recombinant baculoviruses expressing HCV structural proteins[18] or nucleocapsid-like particles were self-assembled from recombinant proteins purified in *E. coli*[19]. Furthermore, previous study showed that HCV core proteins were secreted in insect cells[20] and in mammalian cell culture[21]. In the present study, we have further characterized the HCV core secretion using recombinant baculovirus expression system in insect cells. We found that C-terminal 18 amino acids of the core were necessary for the secretion of core protein into the culture media. Furthermore, HCV core is efficiently released into the culture medium as a membrane-associated protein, which may represent a unique mechanism of HCV core assembly.

MATERIALS AND METHODS

Construction of recombinant baculovirus shuttle vector

HCV cDNA sequence corresponding to the core protein of the Korean isolate (genotype 1b)[22] was subcloned into the baculovirus shuttle vector, pVL941, as described previously[23]. Briefly, cDNAs corresponding to the both wild type and mutant forms of HCV core protein were amplified by polymerase chain reaction (PCR) using *Taq*

DNA polymerase (Boehringer Mannheim). Each primer contains a *Bam*HI or a *Bgl*II site and a protein initiation codon (ATG) at the front, and a stop codon (TGA) plus a *Bam*HI or a *Bgl*II endonuclease site at the end. The amplified PCR product was gel-purified and digested with either *Bam*HI or *Bgl*II and inserted into the *Bam*HI site of the pVL941 vector behind polyhedrin promoter.

Production of recombinant baculoviruses

Spodoptera frugiperda (Sf9) insect cells were co-transfected with wild type baculovirus (*Autographa californica* nuclear polyhedrosis virus, AcNPV) DNA and each recombinant transfer vector DNA as described previously[23]. The supernatant was harvested at 4 d after transfection and used for plaque assays. Each virus isolated from a plaque was used to infect Sf9 cells to obtain high titer of recombinant viruses. Protein expression was examined either by SDS-PAGE and Coomassie blue staining or by Western blot analysis.

Purification of secreted core protein

Sf9 cells were infected with recombinant baculoviruses at a multiplicity of infection (m.o.i.) of 3 and incubated at 27 ℃. The culture supernatant was collected at 3 d after infection and cell debris were removed by centrifugation at 3 500 r/min for 15 min. Supernatant was further subjected to centrifugation at 12 000 *g* for 30 min to eliminate the baculoviruses. The supernatant was pelleted through 300 g/L sucrose cushion for 90 min at 27 000 *g* using a SW 28 rotor. For velocity centrifugation, the pellet was resuspended in PBS and layered onto 200-600 g/L sucrose gradient and centrifuged at 38 000 *g* for 12 h at 4 ℃ using a SW 41 rotor. Twelve fractions were collected from the top, diluted in PBS, and subjected to centrifugation at 48 000 *g* for 90 min using a SW 55 Ti rotor. The peak fractions were pooled and pelleted as described above. The pellet was dissolved in sample buffer and analyzed by Western blot using HCV patient sera.

Western blot analysis

Recombinant baculovirus-infected Sf9 cells were harvested at 3 d after infection and washed twice in PBS. Either cell lysates or secreted proteins were separated by electrophoresis in 10-15% polyacrylamide gel containing 0.5% SDS and transferred to a nitrocellulose membrane for 1 h. The membrane was incubated with either HCV patient serum or rabbit anti-HCV core antibody and proteins were visualized as previously described[23].

Membrane flotation analysis

Sf9 insect cells were infected with recombinant baculoviruses expressing full-length of HCV core protein. At 60 h after infection, the culture supernatant was collected and cell debris was removed by centrifugation at 3 500 r/min for 20 min. Culture supernatant was further subjected to centrifugation at 12 000 *g* for 30 min to eliminate the baculoviruses. The supernatant was pelleted through 300 g/L sucrose cushion for 90 min at 27 000 *g* using a SW 28 rotor. The secreted HCV core proteins were subjected to equilibrium density centrifugation and 1 mL of each fraction was analyzed by immunoblotting using rabbit anti-HCV core antibody as previously described[23].

RESULTS

Expression of HCV core protein in insect cells

In order to understand the mechanism of HCV core secretion in culture media, we generated recombinant baculoviruses encoding full-length of HCV core protein and used them to infect insect cells with low m.o.i. (10^3). Cell lysates were prepared at 3 d after infection and analyzed for protein expression by immunoblotting with HCV patient sera. As shown in Figure 1A, recombinant baculovirus-infected cells expressed the corresponding HCV core protein (lane 3). Both wild type baculovirus (AcNPV)-infected and recombinant baculovirus expressing small hepatitis delta antigen (SHDAg)-infected cells[24] were compared as controls. To examine whether HCV core proteins are released into the culture medium, Sf9 cells were infected with either wild type or recombinant baculoviruses and cell culture supernatants were harvested at d 3 postinfection. The supernatants were pelleted through a 300 g/L sucrose cushion and examined for core secretion using HCV patient serum. The result showed that the supernatant collected from the core-expressing cells contained the core protein reacting with HCV patient serum (Figure 1B, lane 3). Although SHDAg protein was highly expressed in insect cells[24], this protein was not released into the culture medium (data not shown). We further looked for SHDAg release in the culture supernatant harvested from SHDAg-expressing cells at d 4 postinfection. Although cytolysis started to occur at d 4 postinfection in insect cells[25], we were unable to detect SHDAg in supernatant collected from SHDAg-expressing cells (data not shown).

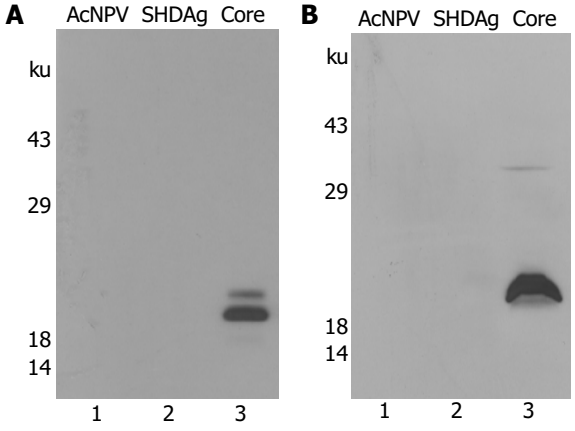

Figure 1 Core proteins are secreted into the culture medium in insect cells. **A**: Expression of HCV core protein in insect cells. cDNA corresponding to the HCV core was subcloned into the *Bam*HI site of the transfer vector pVL941 behind polyhedrin promoter. Recombinant baculoviruses expressing HCV core protein were produced as described in Materials and methods. Sf9 cells were infected with either wild type (AcNPV) or recombinant baculoviruses expressing SHDAg, or recombinant baculoviruses expressing HCV core protein and were harvested at d 3 postinfection. Cell lysates were separated by SDS-containing polyacrylamide gel electrophoresis, transferred to a nitrocellulose membrane. Proteins were detected by Western blotting using HCV patient sera. Lane 1, Sf9 cells infected with wild type baculoviruses; lane 2, Sf9 cells infected with recombinant baculovirus expressing SHDAg; lane 3, Sf9 cells infected with recombinant baculovirus expressing HCV core; **B**: The culture medium from (*A*) was centrifuged at 3 500 r/min for 15 min to remove cell debris. Supernatant was further centrifuged at 12 000 *g* for 30 min to remove baculoviruses. The resultant supernatant was then pelleted through a 300 g/L sucrose cushion for 90 min at 27 000 *g*. The pellet was dissolved in sample buffer and analyzed by Western blotting using HCV patient sera.

Characterization of secreted core proteins

To characterize the secreted core proteins, culture supernatant harvested from recombinant baculovirus-infected cells was pelleted through the 300 g/L sucrose cushion. The pellet was then further subjected to sucrose velocity gradient centrifugation. As shown in Figure 2, secreted core proteins were located in specific fractions. When the peak fractions were examined by electron microscopy, most of the released core proteins were heterogeneous in size as reported[19] with amorphous structure (Choi *et al*.[20], and data not shown). We observed that some of the core proteins were easily aggregated during preparation for electron microscopy. As we previously reported, these secreted proteins have a buoyant density of 1.25 g/mL in CsCl gradient separation[20].

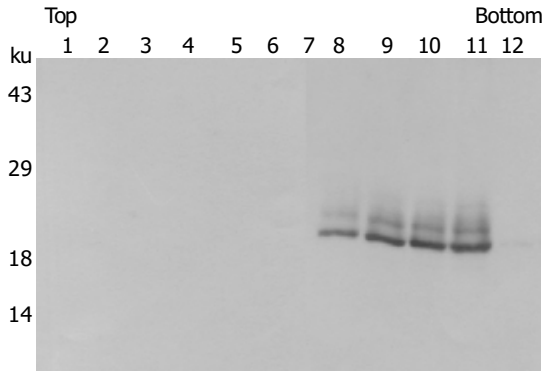

Figure 2 Isolation of core proteins from cell culture supernatant. Sf9 cells were infected with recombinant baculoviruses expressing HCV core protein. The culture supernatant was collected at d 3 postinfection. Following removal of cell debris and recombinant baculoviruses, the released core proteins were partially purified through a sucrose cushion and were subjected to velocity gradient centrifugation. Twelve fractions were collected and proteins were detected by Western blot analysis using HCV patient sera.

Kinetics of core secretion

The HCV core secretion in recombinant baculovirus-infected cells was examined over a 4-d period following infection. Sf9 cells were infected with recombinant baculovirus expressing full-length HCV core and kinetics of protein expression in cells and core secretion in culture media were examined. Cell lysates and secreted core protein were prepared from d 1 to d 4 after infection as described above. Two species of HCV core proteins, M_r 19 000 and M_r 21 000, were expressed in cells as early as d 1 (Figures 3A and C). Two days after virus infection, intracellular core levels reached plateau and gradually decreased thereafter. In contrast, secreted core proteins were detected 2 d after the infection, efficiently released into the culture medium and reached plateau on the 3rd d, and maintained the similar level for an additional day (Figures 3B and D). Trypan blue staining result indicated that most of the recombinant baculovirus-infected cells were viable for 4 d (data not shown).

C-terminal 18 amino acids of core protein are essential for core secretion

To examine which domain of the HCV core is required for core secretion in insect cells, we constructed a series of C-terminal-deleted mutants (Figure 4A) and generated

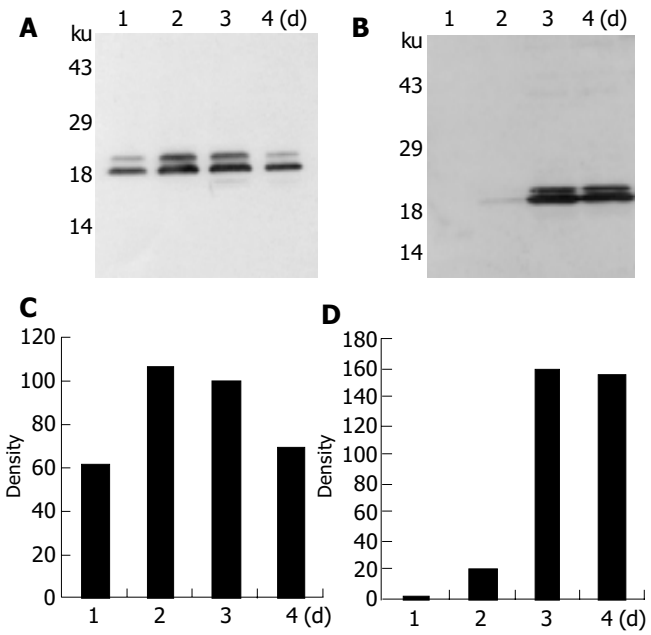

Figure 3 Kinetics of core protein secretion in culture medium of the recombinant baculovirus-infected insect cells. Sf9 insect cells were infected with recombinant baculoviruses expressing full-length core protein (**A**). Cell lysates were prepared from d 1 to d 4 postinfection, and separated by SDS-PAGE on a 15% gel and Western blotted with an HCV patient serum (**B**); Culture supernatants were harvested from d 1 to d 4 postinfection and secreted core proteins were detected by Western blot analysis. Kinetics of intracellular core protein (**C**) and extracellular core protein (**D**) productions were quantified using a densitometric scanner (Molecular Dynamics).

recombinant baculoviruses by co-transfecting insect cells with each mutant DNA and wild type baculovirus DNA. Using low titer (10^3 PFU/mL) of these recombinant baculoviruses, Sf9 insect cells were infected and protein expressions were determined using cell lysates. As shown in Figure 4B, all mutant viruses expressed the expected molecular mass of proteins. This was further confirmed by Western blot analysis (Figure 4C). It is noteworthy that the shorter form of the core construct expressed the higher level of protein. We proceeded to purify the secreted core from each culture supernatant in the same way as described above. Figure 4D showed that full-length core (C191) was efficiently released into the culture medium, although the protein expression level of C191 was lower than those of other mutant core proteins. However, if C-terminal 18 amino acids of the core were deleted, core proteins were no longer secreted into the culture medium, indicating that C-terminal 18 amino acids of HCV core were crucial for core secretion into the culture media. We next examined whether the C-terminal domain of HCV core could be replaced with the comparable domains of other related hepatitis viruses. For this purpose, we replaced C-terminal 18 aa of HCV core with either C-terminal 18 aa of hepatitis B virus surface antigen (HBsAg) or C-terminal 19 aa of large delta antigen of hepatitis delta virus[24]. Although these chimera proteins were highly expressed in insect cells, none of these proteins were released into the culture medium (data not shown), suggesting that authentic core sequence is necessary for secretion.

Membrane association of the secreted core protein

Recently, we showed that HCV core and NS5A protein are

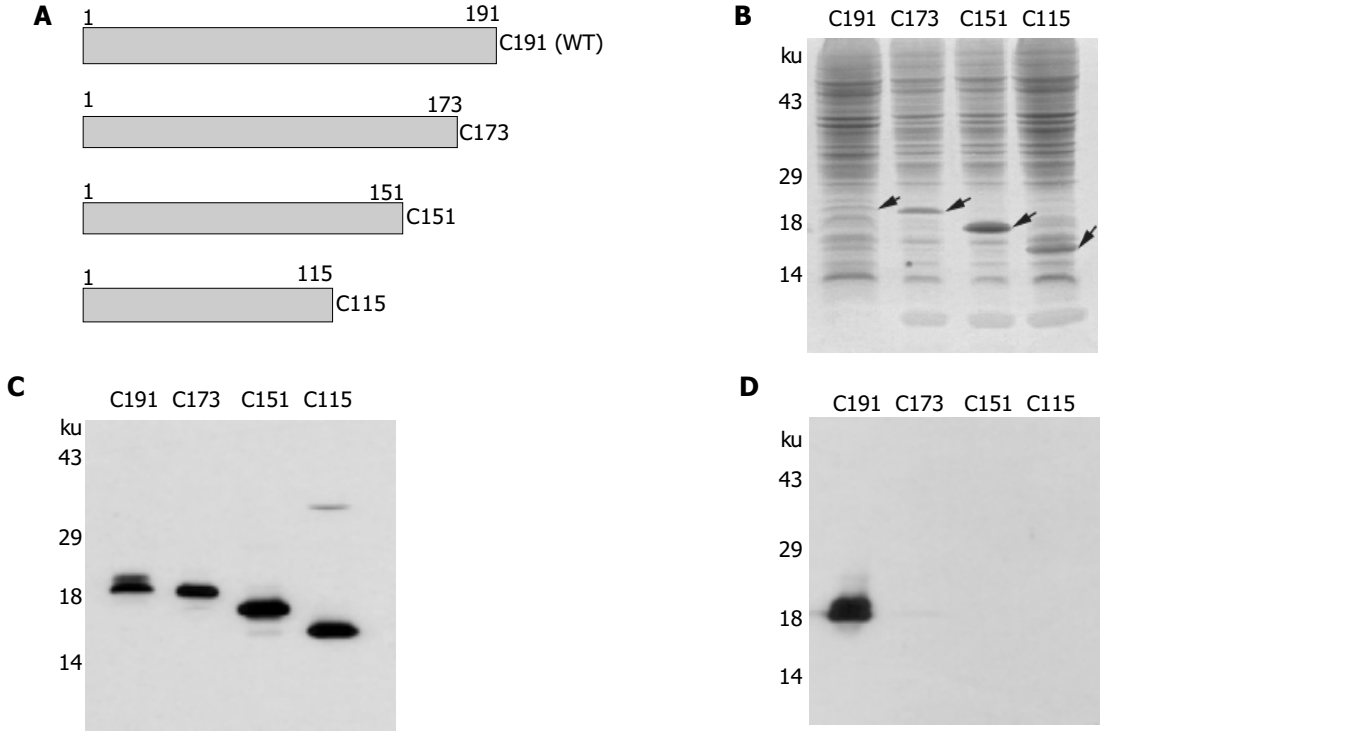

Figure 4 Effects of mutant core proteins on core secretion. (**A**) Schematic diagram illustrating the recombinant baculoviruses expressing truncated forms of core protein. Mutant core constructs were generated by PCR and the subsequent recombinant baculoviruses were made as described in Materials and methods. Protein expression of each mutant was confirmed by SDS-PAGE and Coomassie Brilliant Blue staining (**B**) and Western blot analysis by using HCV patient serum (**C**). (**D**) Determination of extracellular core release among wild type and mutant core proteins. Insect cells were infected with recombinant baculoviruses expressing wild type and various mutant forms of core proteins and harvested at d 3 postinfection. Culture supernatants were partially purified and determined for core secretion by Western blot analysis as described in the legend to Figure 1B.

associated with cellular membrane[26] and HCV replication occurs on lipid raft membrane structure[27]. To investigate whether extracellular form of core proteins were secreted as a membrane complex, we separated the released core proteins into membrane and cytosol fractions using the membrane flotation method as previously described[23]. The presence of the core protein in each fraction was determined by immunoblotting using a rabbit anti-core antibody. As shown in Figure 5, the secreted HCV core protein was found in both membranous and cytosolic fractions. This result indicates that the secreted core proteins are associated with some membranous materials.

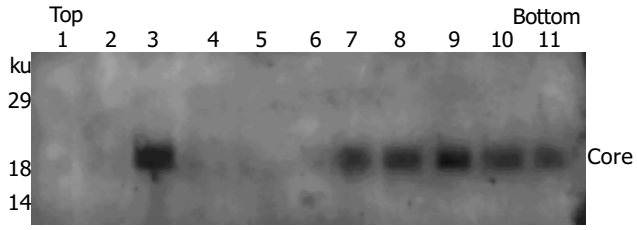

Figure 5 Membrane flotation analysis of secreted core proteins. Sf9 insect cells were infected with recombinant baculoviruses expressing full-length HCV core protein. Culture supernatant was collected at 60 h postinfection and secreted core proteins were partially purified as described in Materials and methods. The sample was then subjected to fractionation by equilibrium sucrose gradient centrifugation. Eleven fractions collected from the top were analyzed by Western blotting using rabbit anti-HCV core antibody.

DISCUSSION

It has been previously reported that HCV core without envelope proteins could form a capsid in an acellular assay[19,28] and secreted core protein has also been detected in mammalian cells[21]. Recently, we have demonstrated that HCV core protein is efficiently released into the culture medium in insect cells[20]. To further understand the mechanisms of core assembly and HCV morphogenesis, we studied the HCV core secretion in insect cells using mutant forms of core protein. We constructed recombinant baculoviruses expressing various-length of HCV core proteins and were used to infect Sf9 insect cells. Culture supernatants harvested from recombinant baculovirus-infected cells were examined to see which domain of core protein is required for core secretion. As we previously reported[20], full-length HCV core protein was efficiently released in cell culture media. However, C-terminal-truncated mutant core proteins were not able to be released into culture media although protein expression levels were higher than that of wild type core protein. This result suggests that C-terminal 18 amino acids are essential for core protein secretion in insect cells. We further showed that secreted core proteins are amorphous in structure and are released into the medium as a membrane complex. This result is consistent with the finding that both core and NS5A are associated with intracellular membranes[27], which may play a role in the pathogenesis of HCV. Previously, it has been demonstrated that VLPs produced from recombinant baculoviruses expressing a part of the 5' UTR and structural proteins were retained in intracellular membrane vesicles

and were not released into the culture medium[18]. In fact, transmembrane domains of E1 and E2 function as retention signals in the endoplasmic reticulum (ER) compartment. It has been reported that E1 and E2 of HCV formed a complex and were retained to the ER[29,30]. Moreover, core protein co-localized with the E2 protein[31]. This may be the reason why core protein alone, if envelope proteins were not present, was efficiently released into the culture media.

Previously, many capsid proteins of non-enveloped viruses were reported to assemble into VLPs, including B19 parvovirus[32], Norwalk virus[33], papillomavirus[34], rotavirus[35,36], and rabbit hemorrhagic disease virus[37]. Similarly, HCV core protein without envelope proteins may be assembled into particle-like structure. HCV is an enveloped virus. How HCV core alone, in the absence of envelope proteins, could be assembled into particles is an intriguing question. Nevertheless, there are similar bodies of evidence that gag protein precursor of HIV-1[38], HIV-2[39], or simian immunodeficiency virus[40] self-assembled into VLPs in recombinant baculovirus-infected insect cells. Budding of rabies virus particles also occurred in the absence of glycoprotein[41]. Therefore, HCV seems to employ a similar assembly mechanism to those of retroviruses and rhabdoviruses. One study showed that VLPs were not produced from the Huh-7 cells carrying the full-length HCV genome[42]. To date, it is uncertain how virions are assembled in HCV-infected patients.

It is not clear how HCV core protein itself can be efficiently secreted into insect culture media. In this study, core protein was released out of the cells as early as 2 d after infection. This result suggests that HCV core has the intrinsic capacity to be secreted in culture media. Kunkel *et al*.[19], reported that N-terminal 124 aa residues of the core (genotype 1a) were sufficient for self-assembly into nucleocapsid-like particles. In contrast, our data suggest that full-length of core should be necessary for core assembly. The discrepancy between the two systems may be due to the different genotypes or different expression systems. However, it is consistent that C-terminal hydrophobic sequence (E1 peptidase signal) inhibits high level of protein expression in both prokaryotic and eukaryotic cell culture systems. In mammalian cells, the C-terminally truncated core 173 is translocated into the nucleus, whereas intact core is destined to the ER[43,44]. This is why core 173 could not be released into the medium although its intracellular expression level was high. In this study we showed that only the full-length core was efficiently released into the culture medium, although the protein expression level of the full-length core was lower than those of other mutant core proteins. Furthermore, the comparable domains of other hepatitis viruses were unable to replace the function of C-terminal region of HCV core. It is hence conceivable that the C-terminal domain of HCV core, in addition to being a signal sequence for E1 protein, has intrinsic function in secretion. It is also possible that C-terminal domain of HCV core may interact with cellular proteins specifically.

We have compared the viability of cells infected with recombinant baculovirus expressing HCV core and those infected with wild type or recombinant baculoviruses expressing HCV 5A or 5B. All of these cells showed the similar level of viability after virus infection, indicating that HCV core was not toxic to the insect cells (data not shown). We also used low titer of virus (m.o.i. of 3) to infect cells in order to prevent cells from baculovirus-induced cytolysis[25]. Since most of the cells were alive at the time of harvest, the release of core protein in culture media is not due to cytolysis. It may represent a unique mechanism of the HCV core secretion. Indeed, it has been shown that HCV core protein was also secreted from mammalian cell lines in culture[21]. Recently, Maillard *et al*.[45], reported that nonenveloped HCV nucleocapsids were overproduced in the plasma of HCV patients and released into the bloodstream. They also found that nucleocapsid-like particles but not VLPs were produced in insect cells infected with recombinant baculovirus expressing entire structural proteins. Our study together with these reports strongly suggests that the production of nonenveloped HCV capsids may represent the feature of HCV morphogenesis. HCV may utilize a unique core release mechanism to escape immune surveillance and hence may play a role in HCV pathogenesis.

REFERENCES

1 **Alter HJ,** Purcell RH, Shih JW, Melpolder JC, Houghton M, Choo QL, Kuo G. Detection of antibody to hepatitis C virus in prospectively followed transfusion recipients with acute and chronic non-A, non-B hepatitis. *N Engl J Med* 1989; **321**: 1494-1500

2 **Kuo G,** Choo QL, Alter HJ, Gitnick GL, Redeker AG, Purcell RH, Miyamura T, Dienstag JL, Alter MJ, Tegtmeier CE, Bonino F, Colombo M, Lee WS, Kuo C, Berger K, Shuster RJ, Overby LR, Bradley DW, Houghton M. An assay for circulating antibodies to a major etiologic virus of human non-A, non-B hepatitis. *Science* 1989; **244**: 362-364

3 **Kato N,** Hijikata M, Ootsuyama Y, Nakagawa M, Ohkoshi S, Sugimura T, Shimotohno K. Molecular cloning of the human hepatitis C virus genome from Japanese patients with non-A, non-B hepatitis. *Proc Natl Acad Sci USA* 1990; **87**: 9524-9528

4 **Saito I,** Miyamura T, Ohbayashi A, Harada H, Katayama T, Kikuchi S, Watanabe Y, Koi S, Orji M, Ohta Y, Choo QL, Houghton M, Kuo G. Hepatitis C virus infection is associated with the development of hepatocellular carcinoma. *Proc Natl Acad Sci USA* 1990; **87**: 6547-6549

5 **Shimotohno K.** Hepatocellular carcinoma in Japan and its linkage to infection with hepatitis C virus. *Semin Virol* 1993; **4**: 305-312

6 **He LE,** Alling D, Popkin D, Shapiro M, Alter HJ, Purcell RH. Determining the size of non-A, non-B hepatitis virus by filtration. *J Infect Dis* 1987; **156**: 636-640

7 **Choo QL,** Kuo G, Weiner AJ, Overby LR, Bradley DW, Houghton M. Isolation of a cDNA clone derived from a blood-borne non-A, non-B hepatitis genome. *Science* 1989; **244**: 359-362

8 **Inchauspe G,** Zebedee S, Lee DH, Sugitani M, Nasoff M, Prince AM. Genomic structure of the human protype strain H of hepatitis C virus: Comparision with American and Japanese isolates. *Proc Natl Acad Sci USA* 1991; **88**: 10292-10296

9 **Miller RH,** Purcell RH. Hepatitis C virus shares amino acids sequence similarity with pestiviruses and flaviviruses as well as members of two plant virus super groups. *Proc Natl Acad Sci USA* 1990; **87**: 2057-2061

10 **Takamizawa A,** Mori C, Fuke I, Manabe S, Murakami S, Fujita J, Onishi E, Andoh T, Yoshida I, Okayama H. Structure and organization of the hepatitis C virus genome isolated from human carriers. *J Virol* 1991; **65**: 1105-1113

11 **Francki RB,** Fauquet CM, Knudson DL, Brown F. Classification and nomenclature of viruses. Fifth report of the International Committee on Taxonomy of Viruses. *Arch Virol* 1991; **2** (Suppl): 223

12 **Rice CM.** *Flaviviridae*: The viruses and their replication. In: Fields BN, Knipe DM, Howley PM, eds. Fields virology, 3rd ed. Lippincott-Raven, philadelphia, PA 1996: 931-959
13 **Hijikata M,** Kato N, Ootsuyama Y, Nakagawa M, Shimotohno K. Gene mapping of the putative structural region of the hepatitis C virus genome by in vitro processing analysis. *Proc Natl Acad Sci USA* 1991; **88**: 5547-5551
14 **Grakoui A,** Wychowski C, Lin C, Feinstone SM, Rice CM. Expression and identification of hepatitis C virus polyprotein cleavage products. *J Virol* 1993; **67**: 1385-1395
15 **Matsuura Y,** Miyamura T. The molecular biology of hepatitis C virus. *Semin Virol* 1993; **4**: 297-304
16 **Lin C,** Lindenbach BD, Pragai B, McCourt DW, Rice CM. Processing of the hepatitis C E2-NS2 region: identification of p7 and two distinct E2-specific products with different C termini. *J Virol* 1994; **68**: 5063-5073
17 **Mizushima H,** Hijikata M, Asabe SI, Hirota M, Kimura K, Shimotohno K. Two hepatitis C virus glycoprotein E2 products with different C termini. *J Virol* 1994; **68**: 6215-6222
18 **Baumert TF,** Ito S, Wong DT, Liang TJ. Hepatitis C virus structural proteins assemble into viruslike particles in insect cells. *J Virol* 1998; **72**: 3827-3836
19 **Kunkel M,** Lorinczi M, Rijnbrand R, Lemon SM, Watowich S. Self-assembly of nucleocapsid-like particles from recombinant hepatitis C virus core protein. *J Virol* 2001; **75**: 2119-2129
20 **Choi SH.** Kim SY, Park KJ, Kim YJ, Hwang SB. Hepatitis C virus core protein is efficiently released into the culture medium in insect cells. *J Biochem Mol Biol* 2004; **37**: 735-740
21 **Sabile A,** Perlemuter G, Bono F, Kohara K, Demaugre F, Kohara M, Matsuura Y, Miyamura T, Brechot C, Barba G. Hepatitis C virus core protein binds to apolipoprotein AII and its secretion is modulated by fibrates. *Hepatology* 1999; **30**: 1064-1076
22 **Cho YG,** Yoon JW, Jang KL, Kim CM, Sung YC. Full genome cloning and nucleotide sequence analysis of hepatitis C virus from sera of chronic hepatitis patients in Korea. *Mol Cells* 1993; **3**: 195-202
23 **Hwang SB,** Park KJ, Kim YS, Sung YC, Lai MMC. Hepatitis C virus NS5B protein is a membrane-associated phosphoprotein with a predominantly perinuclear localization. *Virology* 1997; **227**: 439-446
24 **Hwang SB,** Lai MMC. Hepatitis delta antigen expressed by recombinant baculoviruses: comparison of biochemical properties and post-translational modifications between the large and small forms. *Virology* 1992; **190**: 413-422
25 **Hwang SB,** Park KJ, Kim YS. Overexpression of hepatitis delta antigen protects insect cells from baculovirus-induced cytolysis. *Biochem Biophys Res Commun* 1998; **244**: 652-658
26 **Shi ST,** Polyak SJ, Tu H, Taylor DR, Gretch DR, Lai MMC. Hepatitis C virus NS5A colocalizes with the core protein on lipid droplets and interacts with apolipoproteins. *Virology* 2002; **292**: 198-210
27 **Shi ST,** Lee KJ, Aizaki H, Hwang SB, Lai MMC. Hepatitis C virus RNA replication occurs on a detergent-resistant membrane that cofractionates with caveolin-2. *J Virol* 2003; **77**: 4160-4168
28 **Klein KC,** Polyak SJ, Lingappa JR. Unique features of hepatitis C virus capsid formation revealed by de novo cell-free assembly. *J Virol* 2004; **78**: 9257-9269
29 **Cocquerel L,** Meunier JC, Pillez A, Wychoeski C, Dubuisson J. A retension signal necessary and sufficient for endoplasmic reticulum localization maps to the transmembrane domain of hepatitis C virus glycoprotein E2. *J Virol* 1998; **72**: 2183-2191
30 **Deleersnyder V,** Pillez A, Wychowski C, Blight K, Xu J, Hahn YS, Rice CM, Dubuisson J. Formation of native hepatitis C virus glycoprotein complexes. *J Virol* 1997; **71**: 697-704
31 **Santolini E,** Migliaccio G, La Monica N. Biosynthesis and biochemical properties of the hepatitis C virus core protein. *J Virol* 1994; **68**: 3631-3641
32 **Kajigaya S,** Fujii H, Field A, Anderson S, Rosenfeld S, Anderson LJ, Shimada T, Young NS. Self-assembled B19 parvovirus capsids, produced in a baculovirus system, are antigenically and immunogenically similar to native virions. *Proc Natl Acad Sci USA* 1991; **88**: 4646-4650
33 **Jiang X,** Wang M, Graham DY, Estes MK. Expression, self-assembly, and antigenicity of the norwalk virus capsid protein. *J Virol* 1992; **66**: 6527-6532
34 **Kirnbauer R,** Booy F, Cheng N, Lowy DR, Schiller JT. Papillomavirus L1 major capsid protein self-assembles into virus-like particles that are highly immunogenic. *Proc Natl Acad Sci USA* 1992; **89**: 12180-12184
35 **Crawford SE,** Labbe M, Cohen J, Burroughs MH, Zhou YJ, Estes MK. Characterization of virus-like particles produced by the expression of rotavirus capsid protein in insect cells. *J Virol* 1994; **68**: 5945-5952
36 **Zeng C,** QY, Wentz MJ, Cohen J, Estes MK, Ramig RF. Characterization and replicase activity of double-layered and single-layered rotavirus-like particles expressed from baculovirus recombinants. *J Virol* 1996; **70**: 2736-2742
37 **Sibilia M,** Boniotti MB, Angoscini P, Capucci L, Rossi C. Two independent pathways of expression lead to self-assembly of the rabbit hemorrhagic disease virus capsid protein. *J Virol* 1995; **69**: 5812-5815
38 **Gheysen D,** Jacobs E, de Foresta F, Thiriart C, Francotte M, Thines D, De Wilde M. Assembly and release of HIV-1 precursor pr55gag virus-like particles from recombinant baculovirus-infected insect cells. *Cell* 1989; **59**: 103-112
39 **Luo L,** Li Y, Kang CY. Expression of gag precursor protein and secretion of virus-like gag particles of HIV-2 from recombinant baculovirus-infected insect cells. *Virology* 1990; **179**: 874-880
40 **Delchambre M,** Gheysen D, Thines D, Thiriart C, Jacobs E, Verdin E, Horth M, Burny A, Bex F. The GAG precursor of simian immunodeficiency virus assembles into virus-like particles. *EMBO J* 1989; **8**: 2653-2660
41 **Mebatsion T,** Konig M, Conzelmann KK. Budding of rabies virus particles in the absence of the spike glycoprotein. *Cell* 1996; **84**: 941-951
42 **Pietschmann T,** Lohmann V, Kaul A, Krieger N, Rinck G, Rutter G, Strand D, Bartenschlager R. Persistent and transient replication of full-length hepatitis C virus genomes in cell culture. *J Virol* 2002; **76**: 4008-4021
43 **Liu Q,** Tackney C, Bhat RA, Prince AM, Zhang P. Regulated processing of hepatitis C virus core protein is linked to subcellular localization. *J Virol* 1997; **71**: 657-662
44 **Lo SY,** Masiarz F, Hwang SB, Lai MMC, Ou JH. Differential subcellular localization of hepatitis C virus core gene products. *Virology* 1995; **213**: 455-461
45 **Maillard P,** Krawczynski K, Nitkiewicz J, Bronnert C, Sidorkiewicz M, Gounon P, Dubuisson J, Faure G, Crainic R, Budkowska A. Nonenveloped nucleocapsids of hepatitis C virus in the serum of infected patients. *J Virol* 2001; **75**: 8240-8250

Science Editor Guo SY **Language Editor** Elsevier HK

PO Box 2345, Beijing 100023, China
www.wjgnet.com
wjg@wjgnet.com

ELSEVIER

World J Gastroenterol 2005;11(25):3893-3898
World Journal of Gastroenterology ISSN 1007-9327

Transactivating effect of complete S protein of hepatitis B virus and cloning of genes transactivated by complete S protein using suppression subtractive hybridization technique

Gui-Qin Bai, Yan Liu, Jun Cheng, Shu-Lin Zhang, Ya-Fei Yue, Yan-Ping Huang, Li-Ying Zhang

Gui-Qin Bai, Shu-Lin Zhang, Ya-Fei Yue, Yan-Ping Huang, The First Hospital of Xi'an Jiaotong University, Xi'an 710004, Shaanxi Province, China
Yan Liu, Jun Cheng, Li-Ying Zhang, Gene Therapy Research Center, Institute of Infectious Diseases, 302 Hospital of PLA, 100 Xisihuanzhong Road, Beijing 100039, China
Supported by the National Natural Science Foundation of China, No. C03011402, No. C30070690; the Science and Technique Foundation of PLA during the 9th Five-year Plan period, No. 98D063; the Launching Foundation for Students Studying Abroad of PLA, No. 98H038; the Youth Science and Technique Foundation of PLA during the 10th Five-year plan period, No. 01Q138; and the Science and Technique Foundation of PLA during the 10th Five-year Plan period, No. 01MB135
Correspondence to: Dr. Gui-Qin Bai, Department of Obstetrics and Gynecology of First Hospital , Xi'an Jiaotong University, Jiankang Road 1, Xi'an 710061, Shaanxi Province, China
Telephone: +86-29-85213194 Fax: +86-29-85252812
Received: 2004-11-08 Accepted: 2004-12-26

Abstract

AIM: To investigate the transactivating effect of complete S protein of hepatitis B virus (HBV) and to construct a subtractive cDNA library of genes transactivated by complete S protein of HBV by suppression subtractive hybridization (SSH) technique and to clone genes associated with its transactivation activity, and to pave the way for elucidating the pathogenesis of hepatitis B virus infection.

METHODS: pcDNA3.1(-)-complete S containing full-length HBV S gene was constructed by insertion of HBV complete S gene into *BamH I/Kpn I* sites. HepG2 cells were cotransfected with pcDNA3.1(-)-complete S and pSV-lacZ. After 48 h, cells were collected and detected for the expression of β-galactosidase (β-gal). Suppression subtractive hybridization and bioinformatics techniques were used. The mRNA of HepG2 cells transfected with pcDNA3.1(-)-complete S and pcDNA3.1(-) empty vector was isolated, and detected for the expression of complete S protein by reverse transcription polymerase chain reaction (RT-PCR) method, and cDNA was synthesized. After digestion with restriction enzyme *RsaI*, cDNA fragments were obtained. Tester cDNA was then divided into two groups and ligated to the specific adaptors 1 and 2, respectively. After tester cDNA had been hybridized with driver cDNA twice and underwent nested PCR twice, amplified cDNA fragments were subcloned into pGEM-Teasy vectors to set up the subtractive library. Amplification of the library was carried out within *E. coli* strain DH5α. The cDNA was sequenced and analyzed in GenBank with BLAST search after polymerase chain reaction (PCR) amplification.

RESULTS: The complete S mRNA could be detected by RT-PCR in HepG2 cells transfected with the pcDNA3.1(-)-complete S. The activity of β-gal in HepG2 cells transfected with the pcDNA3.1(-)-complete S was 6.9 times higher than that of control plasmid. The subtractive library of genes transactivated by HBV complete S protein was constructed successfully. The amplified library contains 86 positive clones. Colony PCR showed that 86 clones contained DNA inserts of 200-1 000 bp, respectively. Sequence analysis was performed in 35 clones randomly, and the full length sequences were obtained with bioinformatics method and searched for homologous DNA sequence from GenBank, altogether 33 coding sequences were obtained. These cDNA sequences might be target genes transactivated by complete S protein of HBV. Moreover, two unknown genes were discovered, full length coding sequences were obtained by bioinformatics techniques, one of them was named complete S transactivated protein 1 (CSTP1) and registered in GenBank (AY553877).

CONCLUSION: The complete S gene of HBV has a transactivating effect on SV40 early promoter. A subtractive cDNA library of genes transactivated by HBV complete S protein using SSH technique has been constructed successfully. The obtained sequences may be target genes transactivated by HBV complete S protein among which some genes coding proteins are involved in cell cycle regulation, metabolism, immunity, signal transduction, cell apoptosis and formation mechanism of hepatic carcinoma.

Key words: Complete S protein; Transactivated genes; Hepatitis virus B

Bai GQ, Liu Y, Cheng J, Zhang SL, Yue YF, Huang YP, Zhang LY. Transactivating effect of complete S protein of hepatitis B virus and cloning of genes transactivated by complete S protein using suppression subtractive hybridization technique. *World J Gastroenterol* 2005; 11(25): 3893-3898
http://www.wjgnet.com/1007-9327/11/3893.asp

INTRODUCTION

Hepatitis B virus (HBV) genome is defined as four open

read frames (ORFs), which are named as the regions of S, C, P, X, respectively. The region of S is divided into the sub-regions of pre-S1, pre-S2 and S according to different initial code ATG in frame. Dong *et al*.[1], have shown that there is ORF before pre-S1 region in the genome of HBV from serum of patients with long and accurate polymerase chain reaction (LA-PCR). This region is 135 bp, which is named temporarily as pre-pre-S and its promoter activities are confirmed in 277 bp upstream nucleotide sequences before pre-S1 gene[2]. Pre-pre-S, pre-S1, pre-S2 and S genes are translated in frame according to the same ORF. It is well-known that HBV causes acute and chronic infections of the liver, especially chronic infections may result in remarkable consequences[3]. HBV is considered to be a major etiological factor in the development of human hepatocellular carcinoma (HCC)[4-9]. Although the precise role of HBV in the etiology of HCC is not well understood, data have shown that some HBV proteins can exert a significant transactivating activity on both viral and cellular promoter[10]. This mechanism may have a close relation with the formation of HCC.

Suppression subtractive hybridization (SSH) is a widely used new technique in the cloning of genes transactivated by viral proteins[11]. Complete S of HBV includes pre-pre-S, pre-S1, pre-S2 and S regions, complete S protein functions as a transcriptional transactivator. In the present study, we have successfully constructed the subtractive library of genes transactivated by HBV complete S protein.

MATERIALS AND METHODS

Construction and identification of expression vector

The complete S gene was prepared by PCR amplification using plasmid G376 A7 (GenBank number: AF384371) as template[1,12,13], sense (5'-GGA TCC ATG CAG TTA ATC ATT ACT TCC-3') and antisense (5'-GGT ACC AAT GTA TAC CCA AAG ACA AAA G-3') primers (Shanghai BioAsia Biotech Co., Ltd, China). As these primers contain *BamHI* and *KpnI* (Takara) recognition sites on their respective 5'-ends, the amplified 1 338 bp PCR fragment was subcloned into the *BamHI* and *KpnI* sites of pcDNA3.1(-) vector (Invitrogen Co., USA). The expression vector, pcDNA3.1 (-)-complete S which could directly express complete S fusion protein was obtained, then identified by PCR and digested by *BamHI*/*KpnI*.

Expression of pcDNA3.1 (–)-complete S in HepG2 cells

HepG2 cells were transiently transfected with pcDNA3.1 (-)-complete S. At the same time, empty vectors were also transfected into cells as controls. HepG2 cells were plated at a density of 1.5×10^6 in a 35 mm plate in Dulbecco's modified Eagle's medium (DMEM) supplemented with 100 mL/L heat-inactivated fetal bovine serum (FBS). After 24 h of growth to 40-50% confluence, the cells were transfected with plasmids using FuGENE6 transfection reagent following the manufacturer's protocol (Roche C, USA).

mRNA and cDNA isolation

The mRNA from HepG2 cells transfected with pcDNA3.1 (-)-complete S and pcDNA3.1(-) empty vector was isolated using micro mRNA purification kit (Amersham Biosciences, Co., USA). cDNAs were reverse-transcribed from total RNA. Identification was done by PCR with complete S sequence-specific primers.

Cotransfection with reporter vector pSV-lacZ

HepG2 cells were transfected with various concentrations of plasmid pSV-lacZ (0.1-1.8 μg) (Promega Co., USA). Expression of β-gal was detected by a β-gal assay kit (Promega, Co., USA). In pSV-LacZ the LacZ gene was under the control of the SV40 early promoter element. The optimal concentration of pSV-lacZ plasmid DNA was selected, HepG2 cells was cotransfected with pSV-lacZ and pcDNA3.1 (-)-complete S (2.0 μg). At the same time, cotransfected HepG2 cells transfected with empty pcDNA3.1(-) (2.0 μg) and pSV-lacZ were used as controls. After 48 h, cells were collected and detected for the expression of β-gal.

Generation of subtractive cDNA library

Gene expression comparisons by suppression subtractive hybridization according to the manufacturer's instructions of PCR-select™ cDNA subtraction kit (Clontech Co., USA). In brief, 2 μg of mRNA from the tester and the driver was subjected to cDNA synthesis. Tester and driver cDNAs were digested with *RsaI*. The tester cDNA was subdivided into two portions, and each was ligated with a different cDNA adapter. In the first hybridization reaction, an excess of driver cDNA was added to each sample of tester. The samples were heat denatured and allowed to anneal. Because of the second-order kinetics of hybridization, the concentration of high- and low-abundance sequences was equalized among the single-stranded tester molecules. At the same time single-stranded tester molecules were significantly enriched for differentially expressed sequences. During the second hybridization, two primary hybridization samples were mixed without denaturization. Only the remaining equalized and subtracted single-stranded tester cDNAs could re-associate forming double-stranded tester molecules with different ends. After filling in the ends with DNA polymerase, the entire population of molecules was subjected to nested PCR with two adapter-specific primer pairs.

PCR analysis of subtraction efficiency

PCR was performed on un-subtracted and subtracted secondary PCR products with the G3PDH 5'- and 3'-primers, respectively. From each reaction, 5 μL sample was removed, and the rest of the reaction was put back into the thermal cycler for five more cycles. The above step was repeated thrice, and then 5 μL sample (i.e., the aliquots were removed from each reaction after 18, 23, 28, and 33 cycles) was examined on 2.0% agarose gel.

Cloning subtractive library into pGEM-teasy vector

The amplified products containing a subtractive cDNA library (6 μL) were cloned into a pGEM-teasy vector (Promega Co., USA). Subsequently, Plasmid DNA was transformed into *E. coli* strain DH5α. Bacteria were taken up in 800 μL of LB medium and incubated for 45 min at 37 ℃. Bacteria were plated onto agar plates containing

ampicillin (100 μg/mL), 5-bromo-4-chloro-3-indolyl-β-D-galactoside (X-Gal; 20 μg/cm^2), and isopropyl-β-D-thiogalactoside (IPTG; 12.1 μg/cm^2) and incubated overnight at 37 ℃. Positive (white) colonies were picked out and identified by PCR. Primers were T7/SP6 primer of pGEM-teasy vector. After the positive colonies were sequenced (Shanghai BioAsia Biotechnology Co., Ltd, China), nucleic acid sequence homology searches were performed using the BLAST (basic local alignment search tool) server at the National Center for Biotechnology Information.

RESULTS

Identification of expression vector

Restriction enzyme analysis of pcDNA3.1(-)-complete S plasmid cleaved with *BamHI* and *KpnI* yielded two bands: 5 396 bp empty pcDNA3.1(-) and 1 338 bp HBV complete S, and only one 6 734 bp band (5 396 bp+1 338 bp), it was cleaved with *Kpnl*. The plasmid by PCR amplification with complete S-specific primers got a clear band with the expected size (1 338 bp). The sequence of the PCR product was correct (Figure 1).

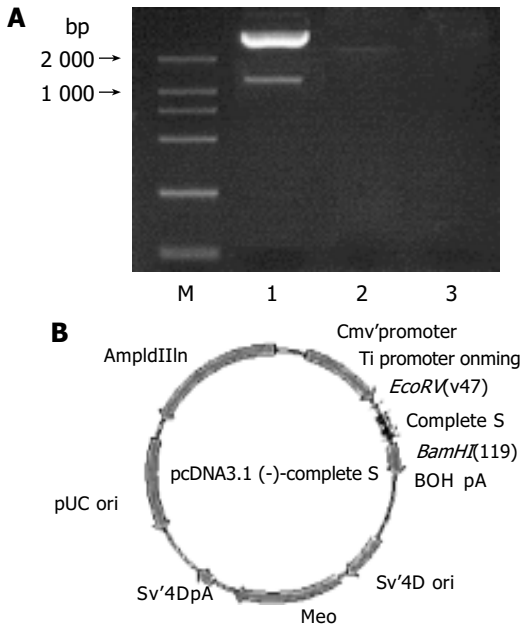

Figure 1 Electrophoresis of PCR products of pcDNA3-complete S and cleaved restriction enzyme (**A**). Structure of expression vector pcDNA3.1(-)-complete S plasmid(**B**).

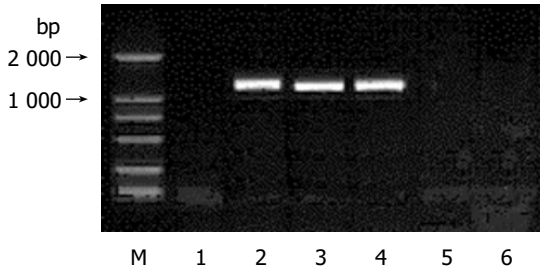

Figure 2 Electrophoresis of RT-PCR products in 0.9% agarose gel. Lane 1: negative control; lanes 2-4: mRNA isolated from pcDNA3.1(-)-complete S; lane 5: blank control; M: DNA marker (2 000 bp).

Identification of HBV complete S transient expression

Reverse-transcription by three different Oligo dT, identification of cDNA by PCR yielded a common 1.338 bp band (Figure 2).

The stable expression of pcDNA3.1(-)-complete S in HepG2 cells was also confirmed by Western blotting hybridization at a high level.

Result of cotransfection of pSV-lacZ and pcDNA3.1(-)-complete S

The best concentration was at 1.0 μg of pSV-lacZ. When cotransfected with pcDNA3.1(-)-complete S and pSV-lacZ, the *A* data about the expression of β-gal were 0.228. In contrast, the expression of β-gal cotransfected with empty pcDNA3.1(-) and pSV-lacZ was 0.033. Expression of β-gal was 6.9-fold higher when cotransfected with pcDNA3.1(-)-complete S and pSV-lacZ than when cotransfected with empty pcDNA3.1(-) and pSV-lacZ. The significant increase of expression of β-gal was attributed to the transactivating effect of HBV complete S protein on early promoter of SV40, thus increasing the expression of downstream gene lacZ (Figure 3).

Result of PCR analysis of subtraction efficiency

The G3PDH (a housekeeping gene) primers were used to confirm the reduced relative abundance of G3PDH following the PCR selection procedure. The result displayed that the G3PDH abundance of subtracted secondary PCR products significantly decreased compared to the un-subtracted one, indicating that the subtractive library had a high subtraction efficiency (Figure 4).

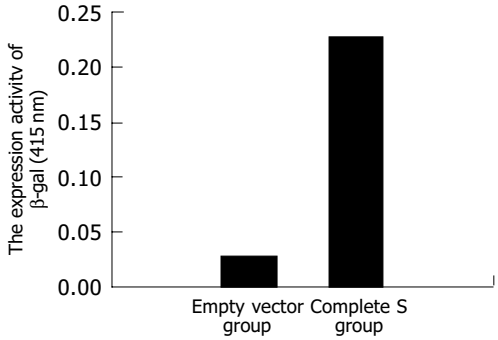

Figure 3 Result of β-galactosidase enzyme analysis.

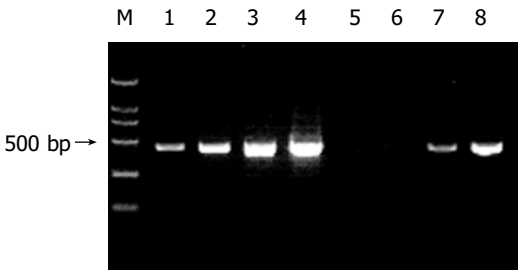

Figure 4 Reduction of G3PDH abundance by PCR-selection subtraction. Lanes 1 and 5: 18 cycles; lanes 2 and 6: 23 cycles; lanes 3 and 7: 28 cycles; lanes 4 and 8: 33 cycles. Lane M: marker (2 000 bp).

Analysis of subtractive library

Using suppression subtractive hybridization technique, we obtained a total of 86 positive clones. These clones were prescreened by PCR amplification to ensure that only clones with different inserts were subjected to sequencing analysis (Figure 5). Eighty-six clones contained 200-1 000 bp inserts. A total of 35 clones from cDNA library were randomly selected and sequenced, and 33 coding sequences were obtained. The data are presented in Table 1. The smear difference in subtractive library was displayed after electrophoresis of PCR products on 2% agarose gel (Figure 6).

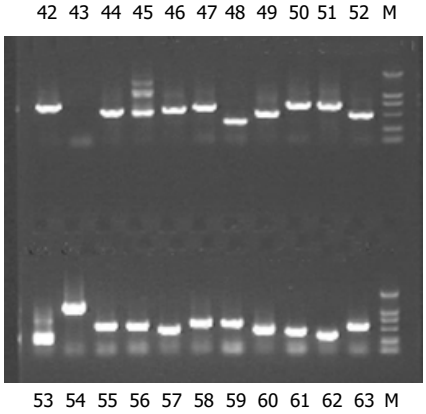

Figure 5 Electrophoresis of PCR products of part clones (42-63) on 0.9% agarose gel; M: marker (2 000 bp).

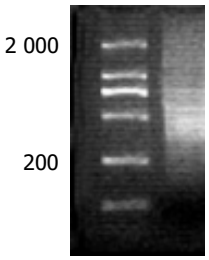

Figure 6 Smears of HBV complete S after PCR.

Table 1 Comparison between positive clones and GenBank homology sequences

High similarity between proteins and known genes	Number of similar clones
Homo sapiens amino acid transporter system A2 (ATA2)	2
Homo sapiens heat shock 90 ku protein 1, (HSPCA)	4
Homo sapiens fibrinogen	1
Homo sapiens CDK4	5
Homo sapiens ribosomal protein	1
Homo sapiens translational initiation factor	1
Homo sapiens synaptophysin-like protein	1
Human mRNA for cytosolic malate dehydrogenase	1
Homo sapiens cytochrome c oxidase subunit I	2
Homo sapiens adenylate kinase 2 (AK2)	1
Homo sapiens NADH dehydrogenase	1
Human complement component C3 mRNA	1
Homo sapiens insulin-like growth factor binding protein 1	1
Homo sapiens SMT3 suppressor of mif two 3 homolog 2	1
Homo sapiens succinate dehydrogenase complex	1
Homo sapiens apolipoprotein H (beta-2-glycoprotein I) (APOH)	1
Homo sapiens BRCA2 and Cip1/p21 interacting protein splice variant	1
Homo sapiens Sec23 homolog A	1
Homo sapiens glutamate dehydrogenase 1	1
Homo sapiens proteasome (prosome, macropain) subunit	2
Homo sapiens eukaryotic translation elongation factor 1	1
Homo sapiens polymerase (RNA) I polypeptide D	2

DISCUSSION

The open reading frame of HBV complete S gene consists of four coding regions: pre-pre-S, pre-S1, pre-S2 and S, each starting with an ATG codon in frame. Through in frame translational initiation at each of the four ATG codons, complete S (pre-pre-S +pre-S1+pre-S2+S), large (LHBs; pre-S1+pre-S2+S), middle (MHBs; pre-S2+S) and small (SHBs; S) envelope glycoproteins can be synthesized[14-18]. The transactivator function of the surface protein requires the cytoplasmic orientation of the pre-S2 domain (the minimal functional unit) that occurs in the case of MHBs^t and in a fraction of Labs[19,20]. Some studies indicate the biological significance of the pre-S2 transactivators[21]. But we firstly discussed the transactivator function of HBV complete S protein in the present study.

We cotransfected HepG2 cells with pcDNA3.1(-)-complete S and pSV-lacZ and demonstrated that the HBV complete S protein was successfully expressed in transfected HepG2 cells. Expression of β-gal was 6.9-fold higher when cotransfected with pcDNA3.1(-)-complete S and pSV-lacZ than when cotransfected with empty pcDNA3.1(-) and pSV-lacZ. HBV complete S had significant transactivating effect on early promoter of SV40 virus, thus increasing the expression of downstream gene lacZ. This result indicates that the HBV complete S protein expressed in HepG2 cells retains its biological activity in terms of transcriptional activation.

To get insight into the transactivation mechanism of HBV complete S protein, SSH was used for identification of transactivating target genes of complete S protein, and subtractive library was set up successfully. Sequence analysis was performed for 35 clones, and 33 coding sequences were obtained. These genes can be divided into four groups:

(1) The genes involved in cell structure and cell cycle that possess the important ability to control cell growth, differentiation and adherence, such as ribosomal protein, mitochondrion, eukaryotic translation elongation factor.

(2) The genes related to cell energy or substance metabolism (i.e., NADH dehydrogenase 2, cytochrome C oxidase II, *etc.*).

(3) The genes involved in the mechanism underlying the development of hepatocellular carcinoma. Cyclin-dependent kinase 4 (CDK4) is a key regulator of cell cycle. It has been shown that a variety of cell cycle-related proteins play an important role in the process of hepatocarcinogenesis. CDK4 is related to the regulation of the cyclin G1 phase, and significantly elevates in HCC compared to surrounding cirrhotic tissues by Western blot and *in vitro* kinase assays. The enhanced cyclin D1-related kinase activity in HCC was accompanied with the up-regulation of CDK4 activity. In addition, the protein levels and kinase activities of CDK4 are higher in poorly differentiated and advanced HCC. In

conclusion, the increases of cyclin D1 and CDK4 play an important role in the development of HCC. CDK4 activation may be closely related to the histopathologic grade and progression of HCC[22-24]. But CDK4 does not increase in children with hepatic carcinoma[25]. Amino acid transporter system A2 (ATA2) is responsible for Na+-independent amino acid transporter system. When amino acid is starved, the expression of ATA2 increases, suggesting that this expression is directly related to the activity of amino acid transporter[26]. Its mRNA increases in the biopsy of hepatocirrhosis and hepatic carcinoma[27], especially in chorion after hepatectomy, suggesting that ATA2 is closely associated with hepatic regeneration[26,28]. ATA2 is cloned in hepatic carcinoma HepG2, and increases in patients of hepatic carcinoma[29].

(4) The genes controlling hepatic cell infection and apoptosis, such as adenylate kinase 2(AK2) protein. AK2 gene located at the right arm of the second chromosome may play a role in maintaining the levels of ADP/ATP by releasing two-molecule ADP from ATP to AMP[30]. The release of two mitochondrial proteins, cytochrome C and apoptosis-inducing factor (AIF), into the soluble cytoplasm of cells undergoing apoptosis has been well established. Since only AK2 intermembrane proteins release from mitochondria during the early phase of the apoptotic process, AK2 is very important in cell apoptosis. AK2 and cytochrome C are translocated in cytoplasm gelatum in apoptosis model[31]. Therefore AK2 plays a role in inducing cell apoptosis. Apolipoprotein H (APOH), is named as beta-2-glycoprotein I and anticoagulative serum protein. The polyomorphous APOH gene is closely related to fat metabolism, coagulation and hypertension[32]. It is the pre-S of HBsAg that results in HBsAg combination with APOH. Resecting phosphatide and oxygenated phosphatide could disturb this mutual action, suggesting that this action is involved in the ectoblastic phosphatide[33]. Furthermore, it is restrained from rebuilding HBsAg, anti-HBsAg and APOH. APOH may be the vector of HBV and plays a role in HBV infection. APOH chiefly combines with complete Dane HBV particle with telescope, and the activity of APOH-HBsAg is the highest in patients with active duplication[33]. This combination facilitates virus particle entrancing hepatic cells, and plays an important role in the beginning of HBV infection[34].

We testified the transactivator ability of HBV complete S protein, and constructed the subtractive cDNA library of genes transactivated by complete S protein. These genes are closely correlated with carbohydrate metabolism, immunoregulation, occurrence and development of tumor. How these genes affect occurrence and development of chronic hepatitis B, hepatic fibrosis and hepatocarcinoma needs to be further studied.

REFERENCES

1 **Dong J,** Cheng J. Study on definition of pre-per-s region in hepatitis B virus genome. *Shijie Huaren Xiaohua Zazhi* 2003; **8**: 1091-1096

2 **Yang Q,** Dong J, Cheng J, Liu Y, Hong Y, Wang JJ, Zhuang SL. Definition of pre-pre-s promoter sequence from hepatttis B virus genome and identification of its transcription activtty. *Jiefangjun Yixue Zazhi* 2003; **9**: 761-762

3 **Beasley RP.** Hepatitis B virus. The major etiology of hepatocellular carcinoma. *Cancer* 1988; **61**: 1942-1956

4 **Dong J,** Cheng J, Wang Q, Wang G, Shi S, Liu Y, Xia X, Li L, Zhang G, Si C. Quasispecies and variations of hepatitis B virus: core promoter region as an example. *Zhonghua Shiyan He Linchuang Bingduxue Zazhi* 2002; **16**: 264-266

5 **Dong J,** Cheng J, Wang Q, Shi S, Wang G, Si C. Cloning and analysis of the genomic DNA sequence of augmenter of liver regeneration from rat. *Chin Med Sci J* 2002; **17**: 63-67

6 **Deng H,** Dong J, Cheng J, Huangfu KJ, Shi SS, Hong Y, Ren XM, Li L. Quasispecies groups in the core promoter region of hepatitis B virus. *Hepatobiliary Pancreat Dis Int* 2002; **1**: 392-396

7 **Parkin DM,** Pisani P, Ferlay J. Estimates of the worldwide incidence of 25 major cancers in 1990. *Int J Cancer* 1999; **80**: 827-841

8 **Dong J,** Cheng J, Wang Q, Huangfu J, Shi S, Zhang G, Hong Y, Li L, Si C. The study on heterogeneity of hepatitis B virus DNA. *Zhonghua Yixue Zazhi* 2002; **82**: 81-85

9 **Xia X,** Cheng J, Yang J, Zhong Y, Wang G, Fang H, Liu Y, Li K, Dong J. Construction and expression of humanized anti-HBsAg scFv targeting interferon-alpha in *Escherichia coli*. *Zhonghua Ganzangbing Zazhi* 2002; **10**: 28-30

10 **Seeger C,** Mason WS. Hepatitis B virus biology. *Microbiol Mol Biol Rev* 2000; **64**: 51-68

11 **Kuang WW,** Thompson DA, Hoch RV, Weigel RJ. Differential screening and suppression subtractive hybridization identified genes differentially expressed in an estrogen receptor-positive breast carcinoma cell line. *Nucleic Acid Res* 1998; **26**: 1116-1123

12 **Liu Y,** Cheng J, Shao DZ, Wang L, Zhong YW, Dong J, Li K, Li L. Synergetic transactivating effect of HCV core and HBV X proteins on SV40 early promoter/enhancer. *Zhonghua Shiyan He Linchuang Bingduxue Zazhi* 2003; **17**: 70-72

13 **Huangfu J,** Dong J, Deng H, Cheng J, Shi S, Hong Y, Ren X, Li L. A preliminary study on the heterogeneity of preS2 region in hepatitis B virus. *Zhonghua Neike Zazhi* 2002; **41**: 233-236

14 **Borchani-Chabchoub I,** Mokdad-Gargouri R, Gargouri A. Glucose dependent [correction of dependant] negative translational control of the heterologous expression of the pre-S2 HBV antigen in yeast. *Gene* 2003; **311**: 165-170

15 **Soussan P,** Pol S, Garreau F, Brechot C, Kremsdorf D. Vaccination of chronic hepatitis B virus carriers with pre-S2/S envelope protein is not associated with the emergence of envelope escape mutants. *J Gen Virol* 2001; **82**: 367-371

16 **Park JH,** Lee MK, Kim HS, Kim KL, Cho EW. Targeted destruction of the polymerized human serum albumin binding site within the preS2 region of the HBV surface antigen while retaining full immunogenicity for this epitope. *J Viral Hepat* 2003; **10**: 70-79

17 **Borchani-Chabchoub I,** Gargouri A, Mokdad-Gargouri R. Genotyping of Tunisian hepatitis B virus isolates based on the sequencing of pre-S2 and S regions. *Microbes Infect* 2000; **2**: 607-612

18 **Tai PC,** Suk FM, Gerlich WH, Neurath AR, Shih C. Hypermodification and immune escape of an internally deleted middle-envelope (M) protein of frequent and predominant hepatitis B virus variants. *Virology* 2002; **292**: 44-58

19 **Hildt E,** Urban S, Hofschneider PH. Characterization of essential domains for the functionality of the MHBst transcriptional activator and identification of a minimal MHBst activator. *Oncogene* 1995; **11**: 2055-2066

20 **Bruss V,** Lu X, Thomssen R, Gerlich WH. Post-translational alterations in transmembrane topology of the hepatitis B virus large envelope protein. *EMBO J* 1994; **13**: 2273-2279

21 **Hildt E,** Munz B, Saher G, Reifenberg K, Hofschneider PH. The Pre-S2 activator MHBs (t) of hepatitis B virus activates c-raf-1/Erk2 signaling in transgenic mice. *EMBO J* 2002; **21**: 525-535

22 **Kita Y,** Masaki T, Funakoshi F, Yoshida S, Tanaka M, Kurokohchi K, Uchida N, Watanabe S, Matsumoto K,

Kuriyama S. Expression of G1 phase-related cell cyclemolecules in naturally developing hepatocellular carcinoma of Long-Evans Cinnamon rats. *Int J Oncol* 2004; **24**: 1205-1211

23 **Edamoto Y,** Hara A, Biernat W, Terracciano L, Cathomas G, Riehle HM, Matsuda M, Fujii H, Scoazec JY, Ohgaki H. Alterations of RB1, p53 and Wnt pathways in hepatocellular carcinomas associated with hepatitis C, hepatitis B and alcoholic liver cirrhosis. *J Cancer* 2003; **106**: 334-341

24 **Masaki T,** Shiratori Y, Rengifo W, Igarashi K, Yamagata M, Kurokohchi K, Uchida N, Miyauchi Y, Yoshiji H, Watanabe S, Omata M, Kuriyama S. Cyclins and cyclin-dependent kinases: comparative study of hepatocellular carcinoma versus cirrhosis. *Hepatology* 2003; **37**: 534-543

25 **Kim H,** Lee MJ, Kim MR, Chung IP, Kim YM, Lee JY, Jang JJ. Expression of cyclin D1, cyclin E, cdk4 and loss of heterozygosity of 8p, 13q, 17p in hepatocellular carcinoma: comparison study of childhood and adult hepatocellular carcinoma. *Liver* 2000; **20**: 173-178

26 **Freeman TL,** Mailliard ME. Posttranscriptional regulation of ATA2 transport during liver regeneration. *Biochem Biophys Res Commun* 2000; **278**: 729-732

27 **Bode BP,** Fuchs BC, Hurley BP, Conroy JL, Suetterlin JE, Tanabe KK, Rhoads DB, Abcouwer SF, Souba WW. Molecular and functional analysis of glutamine uptake in human hepatoma and liver-derived cells. *Am J Physiol Gastrointest Liver Physiol* 2002; **283**: G1062-1673

28 **Freeman TL,** Thiele GM, Tuma DJ, Machu TK, Mailliard ME. ATA2-mediated amino acid uptake following partial hepatectomy is regulated by redistribution to the plasma membrane. *Arch Biochem Biophys* 2002; **400**: 215-222

29 **Hatanaka T,** Huang W, Wang H, Sugawara M, Prasad PD, Leibach FH, Ganapathy V. Primary structure, functional characteristics and tissue expression pattern of human ATA2, a subtype of amino acid transport system A. *Biochim Biophys Acta* 2000; **1467**: 1-6

30 **Villa H,** Perez-Pertejo Y, Garcia-Estrada C, Reguera RM, Requena JM, Tekwani BL, Balana-Fouce R, Ordonez D. Molecular and functional characterization of adenylate kinase 2 gene from Leishmania donovani. *Eur J Biochem* 2003; **270**: 4339-4347

31 **Kohler C,** Gahm A, Noma T, Nakazawa A, Orrenius S, Zhivotovsky B. Release of adenylate kinase 2 from the mitochondrial intermembrane space during apoptosis. *FEBS Lett* 1999; **447**: 10-12

32 **Xia J,** Yang QD, Yang QM, Xu HW, Liu YH, Zhang L, Zhou YH, Wu ZG, Cao GF. Apolipoprotein H gene polymorphisms and risk of primary cerebral hemorrhage in a chinese population. *Cerebrovasc Dis* 2004; **17**: 197-203

33 **Stefas I,** Rucheton M, D'Angeac AD, Morel-Baccard C, Seigneurin JM, Zarski JP, Martin M, Cerutti M, Bossy JP, Misse D, Graafland H, Veas F. Hepatitis B virus Dane particles bind to human plasma apolipoprotein H. *Hepatology* 2001; **33**: 207-217

34 **Gao P,** Guo Y, Qu L, Shi T, Zhang H, Dong C, Yang H. Relation between Beta-2-glycoprotein I and hepatitis B virus surface antigen *Zhonghua Ganzangbing Zazhi* 2002; **10**: 31-33

Science Editor Wang XL and Guo SY **Language Editor** Elsevier HK

PO Box 2345, Beijing 100023, China
www.wjgnet.com
wjg@wjgnet.com

ELSEVIER

World J Gastroenterol 2005;11(25):3899-3904
World Journal of Gastroenterology ISSN 1007-9327

Screening of hepatocyte proteins binding to complete S protein of hepatitis B virus by yeast-two hybrid system

Gui-Qin Bai, Jun Cheng, Shu-Lin Zhang, Yan-Ping Huang, Lin Wang, Yan Liu, Shu-Mei Lin

Gui-Qin Bai, Shu-Lin Zhang, Yan-Ping Huang, Shu-Mei Lin, First Hospital of Xi'an Jiaotong University, Xi'an 710004, Shaanxi Province, China
Jun Cheng, Lin Wang, Yan Liu, Institute of Infectious Diseases, Ditan Hospital, Anwai Street, Beijing 100011, China
Supported by the National Natural Science Foundation of China, No. C03011402, No. C30070690; the Science and Technique Foundation of PLA during the 9th Five-year plan period, No. 98D063; the Launching Foundation for Students Studying Abroad of PLA, No. 98H038; the Youth Science and Technique Foundation of PLA during the 10th Five-year plan period, No. 01Q138; and the Science & Technique Foundation of PLA during the 10th Five-year plan period, No. 01MB135
Correspondence to: Dr. Gui-Qin Bai, Department of Obstetrics and Gynecology of First Hospital, Xi'an Jiaotong University, Jiankang Road 1, Xi'an 710061, Shaanxi Province, China
Telephone: +86-29-85213194 Fax: +86-29-85252812
Received: 2004-11-08 Accepted: 2004-12-26

Abstract

AIM: To investigate the biological function of complete S protein and to look for proteins interacting with complete S protein in hepatocytes.

METHODS: We constructed bait plasmid expressing complete S protein of HBV by cloning the gene of complete S protein into pGBKT7, then the recombinant plasmid DNA was transformed into yeast AH109 (a type). The transformed yeast AH109 was mated with yeast Y187 (α type) containing liver cDNA library plasmid in 2×YPDA medium. Diploid yeast was plated on synthetic dropout nutrient medium (SD/-Trp-Leu-His-Ade) containing X-α-gal for selection and screening. After extracting and sequencing of plasmids from positive (blue) colonies, we underwent sequence analysis by bioinformatics.

RESULTS: Nineteen colonies were selected and sequenced. Among them, five colonies were *Homo sapiens* solute carrier family 25, member 23 (SLC25A23), one was *Homo sapiens* calreticulin, one was human serum albumin (ALB) gene, one was *Homo sapiens* metallothionein 2A, two were *Homo sapiens* betaine-homocysteine methyltransferase, three were *Homo sapiens* Na^+ and H^+ coupled amino acid transport system N, one was *Homo sapiens* CD81 antigen (target of anti-proliferative antibody 1) (CD81), three were *Homo sapiens* diazepam binding inhibitor, two colonies were new genes with unknown function.

CONCLUSION: The yeast-two hybrid system is an effective method for identifying hepatocyte proteins interacting with complete S protein of HBV. The complete S protein may bind to different proteins i.e., its multiple functions *in vivo*.

Key words: Complete S protein; Yeast-two hybrid system; Hepatitis B virus

Bai GQ, Cheng J, Zhang SL, Huang YP, Wang L, Liu Y, Lin SM. Screening of hepatocyte proteins binding to complete S protein of hepatitis B virus by yeast-two hybrid system. *World J Gastroenterol* 2005; 11(25): 3899-3904
http://www.wjgnet.com/1007-9327/11/3899.asp

INTRODUCTION

Hepatitis B virus (HBV) causes acute and chronic infections of the liver. Acute infections may produce serious diseases, and approximately 0.5% of the diseases will develop into fatal, fulminant hepatitis. Chronic infections may also have remarkable consequences[1]. Thus HBV is considered to be a major etiological factor in the development of human hepatocellular carcinoma (HCC), one of the most frequent fatal malignancies worldwide, and worldwide deaths of HCC exceed one million per year[2-7]. Epidemiological studies have demonstrated an approximately 10-fold increase in the relative risk of HCC among HBV carriers compared to non-carrier.

The precise role of HBV in the etiology of HCC is not well understood. Only occasionally, genes controlling cell growth and differentiation are disturbed by integration of HBV DNA sequences. An alternative mechanism of chronic infections and hepatocarcinogenesis may be the key steps to mutual interaction between viral proteins and hepatocellular proteins, this action may mediate virus to enter into the liver cells and affect the activities and function of these proteins. Moreover, the protein from hepatocytes infected with HBV inversely disturbs virus replication and reduces immunity of the host, resulting in chronic liver diseases and HCC. Elucidating this interaction between these proteins may help to bring some new clues for discovering the pathogenesis of viral hepatitis.

The first full length nucleotide sequence of HBV was published in 1979. Its length is 3 182 nt, and the serum type is ayw. The four open read frames (ORF) defined in HBV genome at that time, are named as the regions of S, C, P and X. The region of S is divided into the sub-regions of pre-S1, pre-S2 and S according to different initial code ATG in frame. Dong *et al*.[8], have shown that there is an

open read frame (ORF) before pre-S1 region in the genome of HBV, amplified from serum of patients infected with HBV by long and accurate polymerase chain reaction (LA-PCR). This region is 135 bp, and named temporarily as pre-pre-S and its promoter activities have been confirmed in 277 bp upstream nucleotide sequences before pre-S1 gene[9]. Pre-pre-S, pre-S1, pre-S2 and S genes are translated in frame according to the same ORF, complete S of HBV, including pre-pre-S, pre-S1, pre-S2 and S regions.

The function of the complete S protein in the life cycle of HBV remains unknown. To investigate the biological importance of the complete S protein, we screened and identified the proteins interacting with HBV complete S protein by yeast-two hybrid system to elucidate the biological functions of complete S protein of HBV genome.

MATERIALS AND METHODS

Bacterials, yeast strains and plasmids

All yeast strains and plasmids for yeast-two hybrid experiments were obtained from Clontech Co. (Palo Alto, CA, USA) as components of the MATCHMAKER two hybrid system 3. Yeast strain AH109 (MATa, *trp1-901*, *leu2-3,112*, *ura3-52*, *his3-200*, *gal4*△, *gal80*△, *LYS2*: $GAL1_{UAS}$-$GAL1_{TATA}$-*HIS3*, $GAL2_{UAS}$-$GAL2_{TATA}$-*ADE2*, *URA3*: $MEL1_{UAS}$-MEL_{1TATA}-*LacZ*) containing pGBKT7-53, coding for DNA-BD/mouse p53 fusing protein was used for cloning of bait plasmid. Yeast strain Y187 (MATa *ura3-52, his3-200, Ade2-101, trp1-901, leu2-3, 112, gal4*△*, gal80*△*, met-, URA3:* $GAL1_{UAS}$-$GAL1_{TATA}$-*lacZ MEL1*) containing pTD1-1, coding for AD/SV40 large T antigen fusing protein was used for cloning of library plasmids. Pre-transformed human cDNA liver cell library Y187 and bacterial strain DH5a were used for cloning of shuttle plasmids. Yeast-*Escherichia coli* shuttle plasmids, pGBKT7 DNA-BD cloning plasmid, pGADT7 AD cloning plasmid, pGBKT7-53 control plasmid, pGADT7, pGBKT7-Lam control plasmid, pCL1 plasmid were all from Clontech Co. (K1612-1). pGEM T vector was from Promega Co., USA.

Chemical agents and culture media

Taq DNA polymerase was purchased from MBI Co., T4 DNA ligase, *Eco*RI and *BamH*I restriction endonuclease were from Takara Co., Japan. Anti-c-myc monoclonal antibody secreted by 1-9E10.2 hybridoma (ATCC) was prepared in our laboratory. Goat anti-mouse IgG conjugated with horseradish peroxidase was from Zhongshan Co., China. Lithium acetate, semi-sulfate adenine, acrylamide and N, N'-bis-acrylamide were from Sigma Co., and TEMED was from Boehringer Mannheim Co. Tryptone and yeast extracts were from OXOID Co. X-α-gal and culture media: YPDA, SD/-Trp SD/-Leu, SD/-Trp/-Leu, SD/-Trp/-Leu/-His, SD/-Trp/-Leu/-His/-Ade were from Clontech C., protein-G agarose was from Roche C., and pGEM-T vector was from Promega Co.

RT-PCR kit and TNT® coupled reticulocyte lysate systems were from Promega Co. [^{35}S]-methionine (1 000 Ci/mmol, 10 mCi/mL) was from Isotope Company of China. Amplification fluorographic reagent (#NAMP100) was from Amersham Life Sciences Co. Others reagents were from Sigma Co., USA.

Construction of "bait" plasmid and expression of HBV complete S protein

HBV-complete S sequences were generated by PCR amplification using the plasmid G376 A7 (GenBank number: AF384371[8,10-13]) as template. The sequences of the primers containing the *Eco*RI and *BamH*I restriction enzyme sites were: sense primer (*Eco*RI): 5'-GAA TTC ATG CAG TTA ATC ATT ACT TCC-3'; antisense primer (*BamH*I): 5'-GGA TCC TCA AAT GTA TAC CCA AAG AC-3'. The PCR conditions were at 94 ℃ for 60 s, at 55 ℃ for 60 s, at 72 ℃ for 90 s. Ten nanograms of PCR product was cloned with pGEM-T vector. The primary structure of insert was confirmed by direct sequencing. The fragment of encoding complete S was released from the pGEM-T- complete S by digestion with *Eco*RI and *BamH*I, and ligated to pGBKT7. Vector pGBKT7 expressing proteins were fused with amino acids 1-147 of the GAL4 DNA binding domain (DNA-BD), pGADT7 expressing proteins were fused with amino acids 768-881 of the GAL4 activation domain (AD). Plasmid pGBKT7-complete S (Figure 1) containing full-length HBV complete S gene could express DNA binding domain, c-myc and complete S fusion protein. The plasmid was transformed into yeast strain AH109 by lithium acetate method[14]. Western blotting was performed to confirm the expression of the fusion protein using anti-c-myc monoclonal antibody. Transformed AH109 (bait) was cultured on quadruple dropout media to exclude the auto-activation activity.

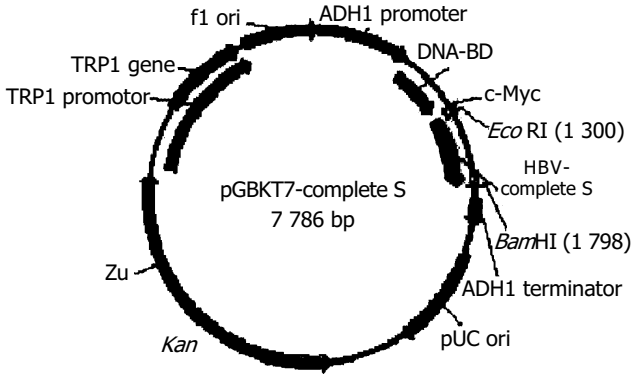

Figure 1 Structure of "bait" plasmid pGBKT7-complete S.

Yeast-two hybrid library screening using yeast mating

One large (2-3 mm), fresh (<2 mo old) colony of AH109 [bait] was inoculated into 50 mL of SD/-Trp and incubated at 30 ℃ overnight (16-24 h) and shaken at 250-270 r/min. Then the cells were spanned down by centrifuging the entire 50 mL culture at 1 000 r/min for 5 min. After the supernatant was decanted, the cell pellet was resuspended in the residual liquid by vortexing. A human liver cDNA library cloned into pACT2 and yeast reporter strain Y187 (Clontech Co., USA) were co-cultured. The entire AH109 [bait] culture and the 1 mL human liver cDNA library (1×10^6 cfu/mL) were combined and cultured in a 2-L sterile flask and 45 mL of 2X YPDA/Kan was added and swirled gently. After 20 h of mating, the cells were spanned down and resuspended, and then spread on 50 large (150 mm) plates containing 100 mL of SD/-Ade/-His/-

Leu/-Trp (QDO). After 6-15 d of growth, the yeast colonies were transferred onto the plates containing X-α-gal to check for expression of the MEL1 reporter gene (blue colonies).

Plasmid isolation from yeast and transformation of E. coli with yeast plasmid

Approximately 1×10^6 colonies were screened and positive clones were identified. Yeast plasmid was isolated from positive yeast colonies with lyticase method (Clontech Co., USA), and transformed into super-competence *E.coli* DH5α using chemical method. Transformants were plated on ampicillin SOB selection media and grown under selection. Subsequently, pACT2-cDNA constructs were re-isolated, analyzed by restriction digestion and sequencing.

Bioinformatic analysis

After the positive colonies were sequenced, the sequences were blasted with GenBank to analyze the function of the genes (http://www.ncbi.nlm.nih.gov.blast).

Cell culture and new gene cloning

Hepatoblastoma cell line HepG2 was propagated in DMEM supplemented with 10% FBS, 200 μmol/L L-glutamine, penicillin, and streptomycin. HepG2 cells were plated at a density of 1×10^6/well in 35-mm dishes. Total cellular RNA was isolated using TRIzol (Invitrogen Co., USA) according to the manufacturer's instructions. cDNAs were reverse-transcribed from total RNA.

On the basis of liver cDNA library of genes of proteins interacting with HBV-complete S protein, the coding sequence of a new gene without known function, HBV CSBP1, was obtained by bioinformatics methods. The standard PCR cloning technique was used to amplify HBV CSBP1 gene. Total cell RNA was isolated from HepG2 cells. RNA was used for RT-PCR amplification. The PCR conditions were: 94 ℃ for 60 s, 58 ℃ for 60 s, and 72 ℃ for 60 s, for 35 cycles. The PCR product was cloned with pGEM-T vector (Promega Co., USA). The primary structure of insert was confirmed by direct sequencing. The gene fragment was cloned into yeast plasmids pGBKT7 and pGADT7.

Confirmation of the true interaction in yeast

To confirm the true protein-protein interaction and exclude false positives, the plasmids of positive colonies were transformed into yeast strain Y187, and then mating experiments were carried out by mating with yeast strain AH109 containing pGBKT7-complete S or pGBKT7-Lam. After mating, the diploids yeast was plated on SD/-Ade-His-Leu-Trp (QDO) covered with X-α-gal to test the specificity of interactions.

In vitro translation

Twenty-five microliter mixture of TNT®reticulocytes, 2 μL TNT® reaction buffer, 1 μL T7 TNT® RNA polymerase, 1 μL amino acids mixture (minus methionine, 1 mol/L), 1 μL [^{35}S]-methionine 2 μL, RNasin RNase inhibitor (40 u/mL), 2 μL DNA template (pGBKT7-complete S or pGADT7-library gene) (0.5 μg/mL), 16 μL ddH_2O, were incubated at 30 ℃ for 90 min.

Coimmunoprecipitation

The following reactants were combined in a 1.5 mL microcentrifugation tube on ice: 5 μL *in vitro*-translated bait protein, 5 μL *in vitro*-translated library protein. The only control added was 10 μL pGBKT7-complete S plasmid. The mixtures were incubated at 30 ℃ for 1 h. Then, the following reagents were added into the reaction tubes: 470 μL coimmunoprecipitation buffer (20 mol/L Tris-HCl (pH 7.5), 150 mol/L NaCl, 1 mol/L DTT, 5 μg/mL aprotinin, 0.5 mol/L PMSF, 0.1 % Tween 20, 10 μL protein-G agarose beads, 10 μL anti-c-myc monoclonal antibody. Incubation was done at 4 ℃ for 2 h with continuous shaking. The tubes were centrifuged at 14 000 *g* for 1-2 min. The supernatants were removed. Half a milliliter of TBST was added into the tubes. Rinse steps were repeated thrice. Fifteen microliters of SDS-loading buffer was added. The samples were heated at 80 ℃ for 5 min. The tubes were placed on ice and then briefly centrifuged, and 10 μL was loaded onto a SDS-PAGE mini-gel to begin the electrophoretic separation. After electrophoresis, the gel was transferred onto a tray containing gel fixation solution, and placed on a rotary shaker for 10 min at room temperature. The gel was rinsed with H_2O, then amplification fluorographic reagent was added and shaken for 20 min at room temperature, then dried at 80 ℃ under constant vacuum. The gel was exposed to an X-ray film overnight at room temperature. The film was developed by standard techniques.

RESULTS

Identification of recombinant plasmid

The full length sequences of HBV complete S were generated by PCR amplification of the plasmid G376 A7 (GenBank number: AF384371)[1,10-13], and a 942-bp fragment of HBV CSBP1 was amplified by RT-PCR after total RNA was prepared from HepG2 cells, sequenced and analyzed by comparing Vector NTI 6 and BLAST database homology search (http://www.ncbi.nlm.nih.gov/blast). After being cut by *Eco*RI/*BamH*I, the fragments were in-frame ligated, respectively into pGBKT7 and pGADT7 at the *Eco*RI/*BamH*I sites. Restriction enzyme analysis of pGBKT7-complete S, pGBKT7-CSBP1 and pGADT7-CSBP1 plasmids with *Eco*RI/*BamH*I yielded respectively two bands: 7 300 bp empty pGBKT7 and 1 338 bp HBV complete S, 7 300 bp empty pGBKT7 and 942 bp of HBV CSBP1, 7 900 bp empty pGADT7 and 942 bp HBV CSBP1. The products of plasmid were amplified by PCR. Analysis of the PCR amplified products by agarose gel electrophoresis showed the clear bands with the expected size (1 338 bp of complete S, 942 bp of CSBP1). Sequences of the PCR products were correct (Figures 2A-D).

Expression of "bait" fusion protein

Yeast strain AH109 transformed with pGBKT7-complete S and pGBKT7-CSBP1 could stably express the fusion protein at high level (Figure 3) and could only grow on SD/-Trp medium but not on QDO medium. Thus, the transformed yeast could be used for yeast hybrid analysis.

Screening of liver cell cDNA library

We isolated plasmids from the blue colonies containing only pGBKT7-complete S and one library plasmid other than other plasmids. Because plasmid pACT2-cDNA contains

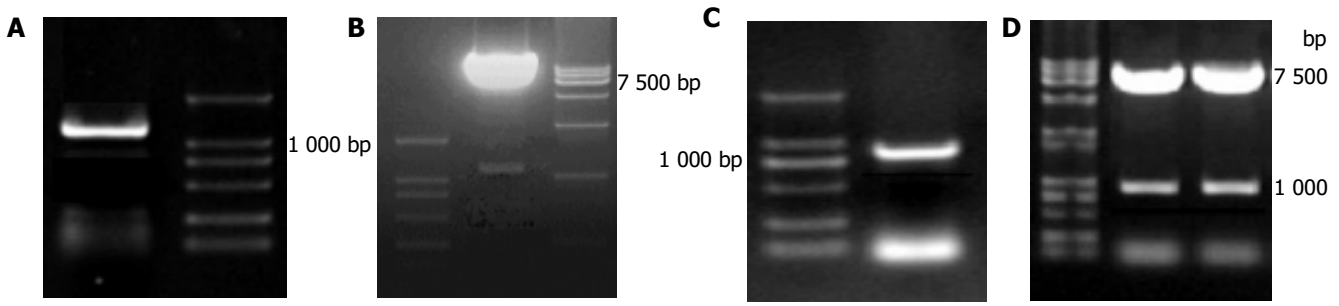

Figure 2 One thousand three hundred and thirty eight basepair fragment-complete S amplified by RT-PCR (**A**), pGBKT7-complete S cut by *Eco*RI/*BamH*I (**B**), a 945 bp fragment-CSBP1 amplified by RT-PCR (**C**), pGBKT7-CSBP1 and pGADT7-CSBP1 cut by *Eco*RI/*BamH*I (**D**).

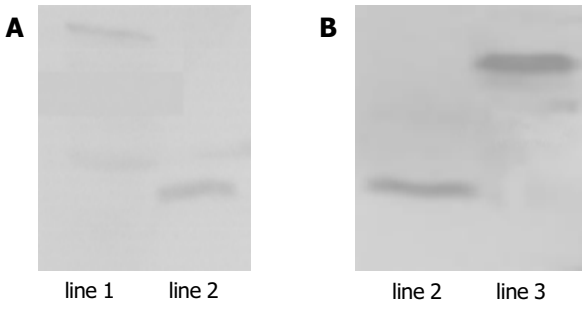

Figure 3 Expression of HBV complete S and HBV CSBP1 protein in yeast confirmed by Western blotting. Lane 1: HBV complete S protein; lane 2: positive control; lane 3: HBV CSBP1 protein.

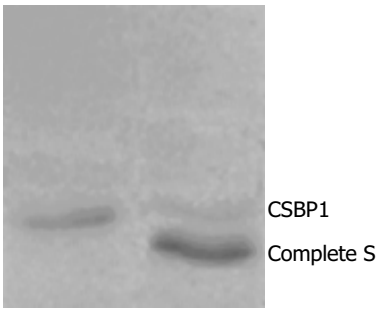

Figure 5 Interaction between HBV complete S protein and CSBP1 protein identified by coimmunoprecipitation. Lane 1: HBV complete S protein; lane 2: interaction with two proteins.

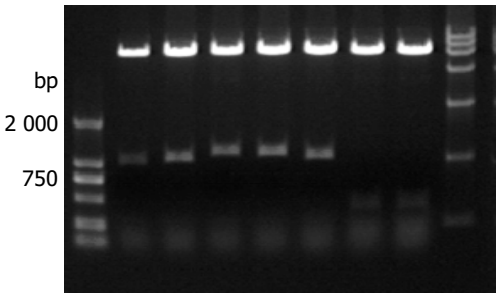

Figure 4 Identification of different colonies with *Bgl*II digestion.

two restriction endonuclease sites of *Bgl*II on both sides of multiple cloning sites, the gene fragments of the liver cell cDNA library (pACT2-cDNA) screened were released by *Bgl*II digestion (Figure 4). The gene fragments of different lengths in Figure 5 proved that these screened clones were positive colonies growing on SD/-Trp/-Leu/-His/-Ade culture medium after mating.

Analysis of cDNA sequencing and homology

We obtained a total of 19 positive colonies growing on the selective SD/-trp-leu-his-ade/X-α-gal medium. These colonies were prescreened by *Bgl*II digestion to make sure that only colonies with different inserts were subjected to sequencing. Nineteen colonies from cDNA library were sequenced. Using the BLAST program at the National Center for Biotechnology Information, 17 sequences had a high similarity to known genes. The data are presented in Table 1.

Table 1 Comparison between positive clones and similar sequences in GenBank

High similarity to known genes	Number of similar (%)	Homology (%)
Homo sapiens calreticulin	1	99
Homo sapiens solute carrier family 25, member 23 (SLC25A23)	5	99
Human serum albumin (ALB) gene	1	100
Homo sapiens metallothionein 2A	1	98
Homo sapiens betaine-homocysteine methyltransferase, mRNA	2	98
Homo sapiens diazepam binding inhibitor	3	96
Homo sapiens Na+ and H+ coupled amino acid transport system N	3	100
Homo sapiens CD81 antigen (CD81)	1	100

In vitro coimmunoprecipitation

HBV complete S protein containing 447 aa, was smaller than CSBP1 containing 280 aa (Figure 5).

DISCUSSION

The open reading frame of HBV complete S gene consists of four coding regions: pre-pre-S, pre-S1, pre-S2 and S, each starting with an ATG codon in frame. Through in frame translational initiation at each of the four ATG codons, complete S (pre-pre-S+pre-S1+pre-S2+S), large (LHBs; pre-S1+pre-S2+S), middle (MHBs; pre-S2+S) and small (SHBs; S) envelope glycoproteins can be synthesized[12,13,15-17]. Interactions between viral and hepatocellular proteins play an important role in the pathogenesis of the virus and may mediate virus

to enter into hepatocytes. Their network interactions can change normal biological functions of proteins, influence self-replication of virus, and result in diseases. Yeast-two hybrid system 3 is an effective gene analysis method to analyze the interactions between protein and protein, protein and DNA, protein and RNA in eukaryotic cells and a new genetics technique for studying interactions of proteins in physiologic conditions *in vivo*.

Yeast-two hybrid system 3 is based on the system originally designed by Fields and Song by taking advantage of the properties of the GAL4 protein of the yeast *Saccharomyces cerevisiae*. GAL4-yeast-two hybrid assay uses two expression vectors, one uses GAL4-DNA-binding domain (DBD) and the other uses GAL4-actibationg domain (AD). The GAL4-DBD fused to protein 'X' and a GAL4-AD fused to protein 'Y' to form the bait and the target of the interaction trap, respectively. A selection of host cells with different reporter genes and different growth selection markers provides a means to detect and confirm protein-protein interactions and has significantly fewer false positives[18-21].

In this study, the "bait" plasmid pGBKT7-complete S was transformed into yeast strain AH109. HBV complete S gene was expressed in yeast cells. After the "bait" plasmid pGBKT7-complete S yeast strain AH109s mated with liver cDNA library yeast strain Y187, the diploid yeast cells were plated on QDO media containing X-α-gal, 19 true positives were obtained. By sequencing analysis of isolated library plasmids, we got the sequences of the 17 genes with known functions and two genes with unknown functions, one of them was named as complete S-binding protein 1 (CSBP1). In order to further confirm the interaction between the expressed protein and HBV complete S protein, we performed the experiment of coimmunoprecipitation of both proteins. A strong interaction between HBV complete S protein and CSBP1 protein *in vitro* was observed.

We screened *Homo sapiens* metallothionein 2A (MT) interacting with complete S protein from liver cDNA library. Metallothionein is a low-molecular weight protein with pleiotropic functions and a family member of metal binding proteins. MT is localized in nuclei and/or cytoplasm of tumor cells[22]. It may be involved in the regulation of carcinogenesis and apoptosis in addition to various physiological processes. Metallothionein is a small stress response protein that can be induced by exposure to heavy metal cations, oxidative stressors, and acute phase cytokines that mediate inflammation[23]. In humans, there are four groups of MT proteins. MT-2A is highly expressed in epithelial cells of breast cancer, and differentially up-regulated in invasive breast cancer cells[24]. Jin *et al*.[25], reported that 26-100% of invasive ductal breast cancers express the MT protein, and are associated with cell proliferation and higher histological grade in invasive ductal breast cancer tissues. Rao *et al*.[26], thought that the mechanism may be completed through interaction between protein kinase C (PKC) signal transduction and MT 2A. Therefore this protein plays an important role in maintaining transition metal ion homoeostasis, redox balance in cells and fundamental cellular processes such as proliferation, apoptosis, and regulation of carcinogenesis[27,28]. MT 2A is also involved in human prostate homeostasis and carcinogenesis[29]. MT-2A is expressed in retinal pigment epithelial (RPE) cells, photoreceptor cells, inner nuclear layer cells and ganglion cells, and can protect cells against oxidative stress and apoptosis[30].

Another important protein interacting with complete S protein from liver cDNA library is *Homo sapiens* calreticulin. Yoon *et al*.[31], have analyzed nuclear matrix proteins in 11 hepatocellular carcinomas and compared them with corresponding non-neoplastic liver tissue by two-dimensional gel electrophoresis. Calreticulin is also found in the nuclear matrices of various carcinoma cell lines. The formation and/or expansion of calreticulin-nuclear matrix may be related to the activated cell growth. Le Naour *et al*.[32], showed that autoantibodies of calreticulin are detectable in patients with HCC (27%), suggesting that a distinct repertoire of autoantibodies is associated with HCC. Therefore it may play a role in early diagnosis of HCC.

HBV complete S protein also interacts with *Homo sapiens* CD81 antigen (CD81). The protein encoded by this gene is a member of the transmembrane four superfamily, also known as the tetraspanin family[33]. Most of these members are cell-surface proteins characterized by the presence of four hydrophobic domains. CD81, a signal transducing molecule, significantly increases in peripheral blood and more dramatic in the liver of HCV-infected individuals[34]. Recently, CD81 has been identified as a hepatitis C virus (HCV) receptor of B lymphocytes, the large extracellular loop of CD81 is a determinant combination position for viral entry[35-39]. These data suggest a functional role for CD81 as a coreceptor for HCV glycoprotein-dependent viral cell entry, providing a mechanism by which B cells are infected with and activated by the virus. It has recently been shown that peripheral B-cell CD81 overexpression is associated with HCV viral load and development of HCV-related autoimmunity. The human CD81 (hCD81) molecule has been identified as a putative receptor in B lymphocytes for hepatitis C virus with murine fibroblast cell line NIH/3T3 model. CD81 chimeras could internalize recombinant E2 protein and E2-enveloped viral particles from serum of HCV-infected patients into Huh7 liver cells. The latter result in persistent positive-strand viral RNA and accumulation of replication, therefore CD81 represents one of the pathways by which HCV can infect hepatocytes. Although CD81 can bind to HCV E2 protein, its role as a receptor for HBV remains controversial. These questions need further study. Whether CD81 could be used as the receptor or co-receptor for hepatocytes, should be studied intensively. CD81 proteins mediate signal transduction events that play a role in the regulation of cell development, activation, growth and motility. This protein appears to promote muscle cell fusion and support myotube maintenance. Also it may be involved in signal transduction. This gene is localized in the tumor-suppressor gene region, thus it is a candidate gene for malignancies.

These interacting proteins screened by yeast-two hybrid are closely correlated with carbohydrate metabolism, immunoregulation, occurrence and development of tumor, and may provide a new study clue for revealing biological functions of HBV complete S protein, pathogenesis of HBV and causes of malignancy conversion. How the interactions between HBV complete S protein and the above-mentioned interacting proteins affect the occurrence and development

of chronic hepatitis B, hepatic fibrosis and hepatocarcinoma, needs to be further studied.

REFERENCES

1 **Beasley RP.** Hepatitis B virus. The major etiology of hepatocellular carcinoma. *Cancer* 1988; **61**: 1942-1956
2 **Xia X,** Cheng J, Yang J, Zhong Y, Wang G, Fang H, Liu Y, Li K, Dong J. Construction and expression of humanized anti-HBsAg scFv targeting interferon-alpha in *Escherichia coli*. *Zhonghua Ganzangbing Zazhi* 2002; **10**: 28-30
3 **Dong J,** Cheng J, Wang Q, Huang FJ, Shi S, Zhang G, Hong Y, Li L, Si C. The study on heterogeneity of hepatitis B virus DNA. *Zhonghua Yiyue Zazhi* 2002; **82**: 81-85
4 **Dong J,** Cheng J, Wang Q, Wang G, Shi S, Liu Y, Xia X, Li L, Zhang G, Si C. Quasispecies and variations of hepatitis B virus: core promotor region as an example. *Zhonghua Shiyan He Linchuang Bingduxue Zazhi* 2002; **16**: 264-266
5 **Dong J,** Cheng J, Wang Q, Shi S, Wang G, Si C. Cloning and analysis of the genomic DNA sequence of augmenter of liver regeneration from rat. *Chin Med Sci J* 2002; **17**: 63-67
6 **Deng H,** Dong J, Cheng J, Huangfu KJ, Shi SS, Hong Y, Ren XM, Li L. Quasispecies groups in the core promoter region of hepatitis B virus. *Hepatobiliary Pancreat Dis Int* 2002; **1**: 392-396
7 **Parkin DM,** Pisani P, Ferlay J. Estimates of the worldwide incidence of 25 major cancers in 1990. *Int J Cancer* 1999; **80**: 827-841
8 **Dong J,** Cheng J. Study on definition of pre-pre-S region in hepatitis B virus genome. *Shijie Huaren Xiaohua Zazhi* 2003; **8**: 1091-1096
9 **Yang Q,** Dong J, Cheng J, Liu Y, Hong Y, Wang JJ, Zhuang SL. Definition of pre-pre-S promoter sequence from hepatttis B virus genome and identtfication of its transcription activity. *Jiefangjun Yixue Zazhi* 2003; **9**: 761-762
10 **Liu Y,** Cheng J, Shao DZ, Wang L, Zhong YW, Dong J, Li K, Li L. Synergetic transactivating effect of HCV core and HBV X proteins on SV40 early promoter/enhancer. *Zhonghua Shiyan He Linchuang Bingduxue Zazhi* 2003; **17**: 70-72
11 **Huangfu J,** Dong J, Deng H, Cheng J, Shi S, Hong Y, Ren X, Li L. A preliminary study on the heterogeneity of preS2 region in hepatitis B virus. *Zhonghua Neike Zazhi* 2002; **41**: 233-236
12 **Borchani-Chabchoub I,** Mokdad-Gargouri R, Gargouri A. Glucose dependent [correction of dependant] negative translational control of the heterologous expression of the pre-S2 HBV antigen in yeast. *Gene* 2003; **311**: 165-170
13 **Soussan P,** Pol S, Garreau F, Brechot C, Kremsdorf D. Vaccination of chronic hepatitis B virus carriers with pre-S2/S envelope protein is not associated with the emergence of envelope escape mutants. *J Gen Virol* 2001; **82**: 367-371
14 **Matsumoto M,** Hsieh TY, Zhu N, VanArsdale T, Hwang SB, Jeng KS, Gorbalenya AE, Lo SY, Ou JH, Ware CF, Lai MM. Hepatitis C virus core protein interacts with the cytoplasmic tail of lymphotoxin-beta receptor. *J Virol* 1997; **71**: 1301-1309
15 **Park JH,** Lee MK, Kim HS, Kim KL, Cho EW. Targeted destruction of the polymerized human serum albumin binding site within the preS2 region of the HBV surface antigen while retaining full immunogenicity for this epitope. *J Viral Hepat* 2003; **10**: 70-79
16 **Borchani-Chabchoub I,** Gargouri A, Mokdad-Gargouri R. Genotyping of Tunisian hepatitis B virus isolates based on the sequencing of preS2 and S regions. *Microbes Infect* 2000; **2**: 607-612
17 **Tai PC,** Suk FM, Gerlich WH, Neurath AR, Shih C. Hypermodification and immune escape of an internally deleted middle-envelope (M) protein of frequent and predominant hepatitis B virus variants. *Virology* 2002; **292**: 44-58
18 **Fields S,** Song O. A novel genetic system to detect protein-protein interactions. *Nature* 1989; **340**: 245-246
19 **Osman A.** Yeast two-hybrid assay for studying protein-protein interactions. *Methods Mol Biol* 2004; **270**: 403-422
20 **Gietz RD,** Woods RA. Screening for protein-protein interactions in the yeast two-hybrid system. *Methods MolBiol* 2002; **185**: 471-486
21 **Zhen Z.** Progress in proteomics. *Shengwu Gongcheng Xuebao* 2001; **17**: 491-493
22 **Yamamura Y,** Ohta Y, Iguchi T, Matsuzawa A. Metallothionein expression and apoptosis in pregnancy-dependent and -independent mouse mammary tumors. *Anticancer Res* 2001; **21**: 1145-1149
23 **Canpolat E,** Lynes MA. *In vivo* manipulation of endogenous metallothionein with a monoclonal antibody enhances a T-dependent humoral immune response. *Toxicol Sci* 2001; **62**: 61-70
24 **Jin R,** Bay BH, Chow VT, Tan PH, Dheen T. Significance of metallothionein expression in breast myoepithelial cells. *Cell Tissue Res* 2001; **303**: 221-226
25 **Jin R,** Chow VT, Tan PH, Dheen ST, Duan W, Bay BH. Metallothionein 2A expression is associated with cell proliferation in breast cancer. *Carcinogenesis* 2002; **23**: 81-86
26 **Rao PS,** Jaggi M, Smith DJ, Hemstreet GP, Balaji KC. Metallothionein 2A interacts with the kinase domain of PKCmu in prostate cancer. *Biochem Biophys Res Commun* 2003; **310**: 1032-1038
27 **Jin R,** Huang J, Tan PH, Bay BH. Clinicopathological significance of metallothioneins in breast cancer. *Pathol Oncol Res* 2004; **10**: 74-79
28 **Tai SK,** Tan OJ, Chow VT, Jin R, Jones JL, Tan PH, Jayasurya A, Bay BH. Differential expression of metallothionein 1 and 2 isoforms in breast cancer lines with different invasive potential: identification of a novel nonsilent metallothionein-1H mutant variant. *Am J Pathol* 2003; **163**: 2009-2019
29 **Hasumi M,** Suzuki K, Matsui H, Koike H, Ito K, Yamanaka H. Regulation of metallothionein and zinc transporter expression in human prostate cancer cells and tissues. *Cancer Lett* 2003; **200**: 187-195
30 **Lu H,** Hunt DM, Ganti R, Davis A, Dutt K, Alam J, Hunt RC. Metallothionein protects retinal pigment epithelial cells against apoptosis and oxidative stress. *Exp Eye Res* 2002; **74**: 83-92
31 **Yoon GS,** Lee H, Jung Y, Yu E, Moon HB, Song K, Lee I. Nuclear matrix of calreticulin in hepatocellular carcinoma. *Cancer Res* 2000; **60**: 1117-1120
32 **Le Naour F,** Brichory F, Misek DE, Bréchot C, Hanash SM, Beretta L. A distinct repertoire of autoantibodies in hepatocellular carcinoma identified by proteomic analysis. *Mol Cell Proteomics* 2004; **1**: 197-203
33 **Levy S,** Todd SC, Maecker HT. CD81 (TAPA-1): a molecule involved in signal transduction and cell adhesion in the immune system. *Annu Rev Immunol* 1998; **16**: 89-109
34 **Curry MP,** Golden-Mason L, Doherty DG, Deignan T, Norris S, Duffy M, Nolan N, Hall W, Hegarty JE, O'Farrelly C. Expansion of innate CD5pos B cells expressing high levels of CD81 in hepatitis C virus infected liver. *J Hepatol* 2003; **38**: 642-650
35 **Van Compernolle SE,** Wiznycia AV, Rush JR, Dhanasekaran M, Baures PW, Todd SC. Small molecule inhibition of hepatitis C virus E2 binding to CD81. *Virology* 2003; **314**: 371-380
36 **Cao J,** Zhao P, Miao XH, Zhao LJ, Xue LJ, Qi Zt Z. Phage display selection on whole cells yields a small peptide specific for HCV receptor human CD81. *Cell Res* 2003; **13**: 473-479
37 **Cao J,** Zhao P, Zhao LJ, Wu SM, Zhu SY, Qi ZT. Identification and expression of human CD81 gene on murine NIH/3T3 cell membrane. *J Microbiol Methods* 2003; **54**: 81-85
38 **Zhang J,** Randall G, Higginbottom A, Monk P, Rice CM, McKeating JA. CD81 is required for hepatitis C virus glycoprotein-mediated viral infection. *J Virol* 2004; **78**: 1448-1455
39 **Bartosch B,** Vitelli A, Granier C, Goujon C, Dubuisson J, Pascale S, Scarselli E, Cortese R, Nicosia A, Cosset FL. Cell entry of hepatitis C virus requires a set of co-receptors that include the CD81 tetraspanin and the SR-B1 scavenger receptor. *J Biol Chem* 2003; **278**: 41624-41630

Science Editor Wang XL and Guo SY **Language Editor** Elsevier HK

PO Box 2345, Beijing 100023, China
www.wjgnet.com
wjg@wjgnet.com

ELSEVIER

World J Gastroenterol 2005;11(25):3905-3908
World Journal of Gastroenterology ISSN 1007-9327

• *BRIEF REPORTS* •

Prevalence of HFE mutations and relation to serum iron status in patients with chronic hepatitis C and patients with nonalcoholic fatty liver disease in Taiwan

Tsung-Jung Lin, Chih-Lin Lin, Chaur-Shine Wang, Shu-O Liu, Li-Ying Liao

Tsung-Jung Lin, Chih-Lin Lin, Chaur-Shine Wang, Shu-O Liu, Li-Ying Liao, Division of Gastroenterology, Department of Internal Medicine, Taipei Municipal Jen-Ai Hospital, Taipei, Taiwan, China
Correspondence to: Dr. Li-Ying Liao, Division of Gastroenterology, Department of Internal Medicine, Taipei Municipal Jen-Ai Hospital, 5F, No. 52, Lane 240, Guangfu S. Road, Da-an District Taipei City 106, Taiwan, China. ronlin@aptg.net
Telephone: +886-2-27093600 Fax: +886-2-27047859
Received: 2004-08-14 Accepted: 2004-10-05

Abstract

AIM: To assess the prevalence of the two mutations, C282Y and H63D of HFE gene, in healthy subjects, patients with chronic hepatitis C (CHC), and patients with nonalcoholic fatty liver disease (NAFLD) in Taiwan and to explore the contribution of the HFE mutation on serum iron stores in CHC and NAFLD groups.

METHODS: We examined C282Y and H63D mutations of HFE gene in 125 healthy subjects, 29 patients with CHC, and 33 patients with NAFLD. The serum iron markers, including ferritin, iron, and total iron binding capacity (TIBC), were assessed in all patients.

RESULTS: All of the healthy subjects and patients were free from C282Y mutation. The prevalence of H63D heterozygosity was 4/125 (3.20%) in healthy subjects, 2/29 (6.90%) in CHC group, and 1/33 (3.03%) in NAFLD group. The healthy subjects showed no significant difference in the prevalence of H63D mutation as compared with the CHC or NAFLD group. Increased serum iron store was found in 34.48% of CHC patients and 36.36% of NAFLD patients. In three patients of H63D heterozygosity, only one CHC patient had increased serum iron store. There was no significant difference in the prevalence of HFE mutations between patients with increased serum iron store and those without in CHC or NAFLD group.

CONCLUSION: The HFE mutations may not contribute to iron accumulation in the CHC or NAFLD group even when serum iron overload is observed in more than one-third of these patients in Taiwan.

Key words: Hereditary hemochromatosis; HFE gene; Serum iron; Chronic hepatitis C; Nonalcoholic fatty liver disease

Lin TJ, Lin CL, Wang CS, Liu SO, Liao LY. Prevalence of HFE mutations and relation to serum iron status in patients with chronic hepatitis C and patients with nonalcoholic fatty liver disease in Taiwan. *World J Gastroenterol* 2005; 11(25): 3905-3908
http://www.wjgnet.com/1007-9327/11/3905.asp

INTRODUCTION

Hereditary hemochromatosis is one of the most common inherited diseases among Caucasians. It occurs with a frequency of 1:200 to 1:400 and a carrier rate approaching 1:10[1,2]. Hereditary hemochromatosis is an autosomal recessive condition in which excessive iron is absorbed by the intestine. Iron accumulation in many organs causes the clinical manifestations including heart failure, diabetes, and liver cirrhosis. Early diagnosis has been difficult because the tests based on measurement of serum transferrin saturation and serum ferritin concentration not only gave many false positive results but do not always identify patients in the early stage of iron accumulation[3]. The excessive iron can be removed by venesection[4]. Although venesection is a simple, effective and safe therapy, much of the organ damage is irreversible when hereditary hemochromatosis is diagnosed. Because the major clinical presentations are often non-specific, appropriate screening tests are important.

The gene responsible for hereditary hemochromatosis was identified and designated as HFE in 1996[5]. The two recognized recessively-inherited missense mutations of the HFE gene result in amino acid substitutions at position 282 (cysteine to tyrosine, C282Y) and at position 63 (histidine to aspartic acid, H63D). A total of 64-100% patients of Western population with hereditary hemochromatosis were C282Y homozygotes[6-10]. In individuals of the northern European descent, the frequency of C282Y homozygote was about 0.5%[1]. The allele frequencies for C282Y mutation and H63D mutation were 5-10% and 6-30%, respectively[1,2,11]. In Taiwan, a very low frequency of C282Y mutation in the general population (0.33% of carrier rate) was reported[12]. The C282 heterozygote may have higher serum and hepatic iron levels than controls, but levels are only mildly elevated[13]. The clinical significance of the H63D mutation still remains undetermined. It seems to be associated with hereditary hemochromatosis only when inherited together with the C282Y mutation (compound C282Y/H63D heterozygote).

Mild to moderate hepatic iron overload is common in patients with chronic hepatitis C (CHC)[14-16] and in patients with nonalcoholic fatty liver disease (NAFLD)[17,18]. Iron-induced oxidative stress may play an important role in the

exacerbation of liver cell injury[19,20]. The HFE mutation may also be associated with elevated markers of iron store in the two disorders. This study was performed to assess the prevalence of the two mutations, C282Y and H63D of HFE gene, in healthy subjects, patients with CHC, and patients with NAFLD in Taiwan. We also checked the serum iron markers and explored the contribution of the HFE mutation on serum iron stores in patients with CHC and patients with NAFLD.

MATERIALS AND METHODS

Healthy subjects and patients

C282Y and H63D mutations of HFE gene were analyzed in 125 healthy subjects, 29 patients with CHC, and 33 patients with NAFLD. Local healthy subjects with normal liver function test, no history of liver disease, other severe chronic disease, heavy drinking (ethanol consumption >20 g/d), anemia or iron overload were collected from the health checkup at our hospital in 2003. The patients with CHC or NAFLD were collected at our out-patient department from 2002 to 2003. CHC was diagnosed by biochemical liver damage for more than 6 mo and positivity of serum antibody to hepatitis C virus (HCV). Patients with secondary causes of iron overload were excluded, including heavy drinking, ribavirin therapy, and multiple transfusions. Co-infection with HBV was also excluded. The diagnosis of NAFLD was made on the basis of the presence of elevated serum AST or ALT and fatty change of liver by sonography. No subject consumed alcohol more than 20 g/d. They were negative for hepatitis B surface antigen and HCV antibody. Their serum levels of ceruloplasmin were within normal range. Serological tests for autoimmune hepatitis (anti-nuclear antibody, anti-smooth muscle antibody) and for primary biliary cirrhosis (anti-mitochondrial antibody) were negative.

Serological evaluation

The serum aspartate aminotransferase (AST) and alanine aminotransferase (ALT) were determined using an Olympus 5000 analyzer. The upper limit of normal for ALT is 34 U/L. HCV antibody was tested by a commercially available ELISA (AxSYM, Abbott Diagnostic Corporation, USA). Total iron status of each patient was evaluated using biochemical tests. Serum iron (normal range, 60-160 μg/dL) was measured by the colorimetry and ferritin (normal range: 18-274 ng/mL in men and 6-283 ng/mL in women) was measured by a commercially available ELISA (AxSYM, Abbott Diagnostic Corporation). Transferrin saturation was calculated as (the serum iron divided by the total iron binding capacity (TIBC)) ×100%. The increased serum iron store was defined by transferrin saturation >50% and/or ferritin >upper normal limit.

Mutational analysis of HFE gene

We used the method of polymerase chain reaction-restriction fragment length polymorphism (PCR-RFLP) to analyze the HFE mutations. Genomic DNA was isolated from whole peripheral blood using the High Pure Viral Nuclear Kit (Roche Diagnosis Corporation, USA). The DNA fragments of HFE gene were amplified by PCR using the following primers[5]: 5'-TGGCAAGGGTAAACAGATCC and 5'-CTCAGGCACTCCTCTCAACC for C282Y; and 5'-ACATGGTTAAGGCCTGTTGC and 5'-GCCACATCT-GGCTTGAAATT for H63D. Restriction fragment length analysis was then performed by digesting the PCR products with *Rsa*I for C282Y and *Bcl*I for H63D[21].

Statistical analysis

Data are summarized as mean±SD. Categorical variables were compared with the χ^2 test or Fisher's exact test as required. Comparison between groups was performed using the unpaired *t*-test as appropriate.

RESULTS

The demographic and laboratory data of subjects are summarized in Table 1. CHC patients were older than healthy subjects (60.83±8.55 years *vs* 44.62±11.19 years, $P<0.01$) and NAFLD patients were not (49.48±14.58 years *vs* 44.62±11.19 years, $P = 0.082$). There was no significant difference in the male to female ratio between healthy subjects (44/81) and CHC (12/17) or NAFLD (16/17) group.

All of the healthy subjects and patients were free from C282Y mutation. Four healthy subjects (one man and three women) were heterozygotes of H63D, two CHC patients (one man and one woman) and one NAFLD patient (woman) were heterozygotes of H63D. The prevalence of H63D mutation was 4/125 (3.20%) in healthy subjects, 2/29 (6.90%) in CHC group, and 1/33 (3.03%) in NAFLD

Table 1 Demographic and laboratory data of healthy subjects, CHC and NAFLD (mean±SD)

	Reference range	Healthy subjects	Chronic hepatitis C	*P*	NAFLD	*P*
Age (yr)		44.62±11.19	60.83±8.55	<0.01	49.48±14.58	0.082
Sex (male:female)		44:81	12:17	0.533	16:17	0.162
AST (IU / L)	10-34		97.17± 52.62		74.68±42.09	
ALT (IU / L)	7-33		114.28±61.87		108.52±65.07	
Iron (μg / dL)	60-160		146.39±48.19		108.73±31.06	
TIBC (μg / dL)	250-410		377.93±41.10		361.57±42.73	
Transferrin saturation (%)	20-50		39.01±13.20		30.53±9.80	
Ferritin (ng / mL)	Male: 18-294		225.95±178.24		331.20±283.82	
	Female: 6-283					
Increased serum iron store (%)			10 / 29 (34.48)		12 / 33 (36.36)	

CHC, chronic hepatitis C; NAFLD, nonalcoholic fatty liver disease. *P* value: comparing data obtained from healthy subjects with chronic hepatitis C or NAFLD. The increased serum iron store was defined by transferrin saturation >50% and / or ferritin >upper normal limit.

group. The healthy subjects showed no significant difference in the prevalence of H63D mutation as compared with the CHC or NAFLD group (Table 2).

Table 2 Statistical analysis of H63D mutation between healthy subjects and CHC, and healthy subjects and NAFLD

	Male	Female	Total
Healthy subjects:CHC	1/44:1/12	3/81:1/17	4/125:2/29
P	0.386	0.539	0.315
Healthy subjects:NAFLD	1/44:0/16	3/81:1/17	4/125:1/33
P	0.999	0.539	0.999

CHC, chronic hepatitis C; NAFLD, nonalcoholic fatty liver disease.

Ten CHC patients (4 men and 6 women) and 12 NAFLD patients (8 men and 4 women) had increased serum iron stores. The percentage was 34.48% and 36.36% in CHC and NAFLD patients, respectively. There was no gender-related difference in the frequency of increased serum iron stores in either the CHC or NAFLD group (Table 3). In the three patients of H63D heterozygosity, only one CHC patient had increased serum iron store. There was no significant difference in the prevalence of HFE mutations between patients with increased serum iron store and those without in the CHC or NAFLD group (Table 4).

Table 3 Statistical analysis of increased serum iron stores between male and female patients with CHC or NAFLD

	CHC	NAFLD
Male:female	4/12:6/17	8/16:4/17
P	0.913	0.114

CHC, chronic hepatitis C; NAFLD, nonalcoholic fatty liver disease.

Table 4 Statistical analysis of HFE mutation between patients with increased serum iron store and those without in CHC or NAFLD group

Increased serum iron store	CHC	NAFLD
With:without	1/10:1/19	0/12:1/21
P	0.999	0.999

CHC, chronic hepatitis C; NAFLD, nonalcoholic fatty liver disease.

DISCUSSION

A population study of global prevalence in HFE mutation showed that there were nine H63D heterozygotes in one Asian population of 242 cases and no other HFE genotypes were found[1]. The H63D allele frequency was 1.9% (9/484). Similar results were reported in a Japanese population[22]. All of the 151 healthy volunteers were free from C282Y mutation and only 8 subjects were H63D heterozygotes. The prevalence of chromosomes with H63D was 2.6% (8/302). We firstly found no C282Y mutation and an incidence of 1.6% (4/250) for H63D allele in 125 healthy subjects in Taiwan. The results were similar to that in other Asian area. No mutations of C282Y were found probably because of the limited number of subjects studied. The very low frequency of HFE mutation in the Asians, especially C282Y, reflects the ethnic differences in the prevalence of hereditary hemochromatosis from Caucasians.

Similar prevalence of HFE mutations was found between controls and patients with CHC[22-25]. Our findings were in lines with these studies. However, the equal distribution of HFE mutations does not allow the conclusion that HFE mutations play no or only a minor role in patients with CHC. It should depend on the contribution of HFE mutations on the iron stores. Either the prevalence of C282Y mutation[18,26] or combined C282Y and H63D mutations[27] was increased in nonalcoholic steatohepatitis (NASH) population. Because there was no pathological diagnosis of steatohepatitis in our patients, the patient group in our study is called NAFLD, instead of NASH. Our study showed no significant difference in the frequency of HFE mutations between healthy subjects and NAFLD patients. In another study of NAFLD, the prevalence of the two HFE mutations also was not significantly increased in NAFLD patients and matched those of the general population. These findings gave us a hint that HFE mutation may play a role in the progression of NAFLD.

Elevations in serum iron, ferritin, and transferrin saturation are common in patients with CHC or NASH, as are mild increases in hepatic iron concentration. In CHC, 40-46% of patients had elevated serum iron, ferritin, or transferrin saturation level[14,15], and 10-36% of patients had increased hepatic iron concentration[15,16]. In NASH, 58% of patients had elevated serum iron indices and in some cases increased hepatic iron stores[18]. In our study, we found that 34.48% and 36.36% of patients had increased serum iron stores in CHC and NAFLD group, respectively. Normal or only mildly increased amounts of iron in the liver can be damaging because iron increases oxidative stress[19,20]. It appears that iron overload may play a role in pathogenesis of some chronic liver diseases, especially when iron is combined with other hepatotoxic factors such as virus, free fatty acid, and alcohol[17]. In addition to the effect of production of oxidative stress, the iron may enhance the rates of viral replication and mutation as well as cause impairment of the host immunity[20]. However, the iron can be released from damaged hepatocytes in inflammatory conditions, and it has not been clear whether the iron accumulation is the cause or result of liver injury.

Our data demonstrated no significant difference in the prevalence of HFE mutations between the subgroup of HCV or NAFLD patients with increased serum iron store and the subgroup without. The findings suggested that HFE mutations played no or only a minor role in contribution to serum iron overload in patients with CHC or NAFLD in Taiwan. In addition to the reason of low prevalence of HFE mutations in Taiwan, the fact that only H63D heterozygote was found in our study may explain the results. The H63D heterozygosity usually does not lead to iron overload. Only in conjunction with the heterozygous C282Y mutation (compound C282Y/H63D heterozygote) has the H63D mutation been associated with an increased risk of iron overload[5].

There were many reports suggesting that the C282Y mutation plays a role in the hepatic iron accumulation and favors the progression of CHC[23-25]. However, the relationship

between HFE mutations, iron stores, and NASH still remains as a controversial area. Previous studies have found conflicting results. George *et al*.[18], found that the C282Y mutation was responsible for most of the mild iron overload in NASH and had a significant association with hepatic damage in these patients. Bonkovsky *et al*.[27], also found that C282Y heterozygotes were more likely to have advanced fibrosis. These authors did not adjust for potential confounders such as age, body mass index, and diabetes. After adjustment for these confounders, Chitturi *et al*.[26], reported in NASH and Bugianesi *et al*., reported in NAFLD patients that iron burden and HFE mutations did not contribute significantly to hepatic fibrosis. Therefore, we believe that continued exploration of the link between hepatic iron, HFE mutation, and NAFLD patients is warranted.

In conclusion, HFE mutations are infrequent in Taiwan. The prevalence of HFE mutations associated with hereditary hemochromatosis is not increased in the patients with CHC or NAFLD. The HFE mutations may not contribute to iron accumulation in the CHC or NAFLD group even when serum iron overload is observed in more than one-third of these patients in Taiwan.

REFERENCES

1 **Merryweather-Clarke AT,** Pointon JJ, Shearman JD, Robson KJ. Global prevalence of putative haemochromatosis mutations. *J Med Genet* 1997; **34**: 275-278

2 **Edwards CQ,** Griffen LM, Goldgar D, Drummond C, Skolnick MH, Kushner JP. Prevalence of hemochromatosis among 11,065 presumably healthy blood donars. *N Engl J Med* 1988; **318**: 1355-1362

3 **Powell LW,** Halliday JW, Cowlishaw JL. Relationship between serum ferritin and total body iron stores in idiopathic haemochromatosis. *Gut* 1978; **19**: 538

4 **Niederau C,** Fischer R, Purschel A, Stremmel W, Haussinger D, Strohmeyer G. Long-term survival in patients with hereditary hemochromatosis. *Gastroenterology* 1996; **110**: 1107-1119

5 **Feder JN,** Ginirke A, Thomas W, Tsuchihashi Z, Ruddy DA, Basava A, Dormishian F, Domingo R Jr, Ellis MC, Fullan A, Hinton LM, Jones NL, Kimmel BE, Kronmal GS, Lauer P, Lee VK, Loeb DB, Mapa FA, McClelland E, Meyer NC, Mintier GA, Moeller N, Moore T, Morikang E, Prass CE, Quintana L, Starnes SM, Schatzman RC, Brunke KJ, Drayna DT, Risch NJ, Bacon BR, Wolff RK. A novel MHC class-like gene is mutated in patients with hereditary haematochromatosis. *Nat Genet* 1996; **13**: 399-408

6 **Jazwinska EC,** Cullen LM, Busfield F, Pyper WR, Webb SI, Powell LW, Morris CP, Walsh TP. Haematochromatosis and HLA-H. *Nat Genet* 1996; **14**: 249

7 **Jouanolle AM,** Gandon G, Jezequel P, Blayau M, Campion ML, Yaouanq J, Mosser J, Fergelot P, Chauvel B, Bouric P, Carn G, Andrieux N, Gicquel I, Le Gall JY, David V. Haematochromatosis and HLA-H. *Nat Genet* 1996; **14**: 251

8 **Consortium UH.** A simple genetic test identifies 90% of UK patients with hemochromatosis. *Gut* 1997; **41**: 841-844

9 **Datz C,** Lalloz MR, Vogel W, Graziadei I, Hackl F, Vautier G, Layton DM, Maier-Dobersberger TH, Ferenci P, Penner E, Sandhofer F, Bomford A, Paulweber B. Predominance of the HLA-H Cys282Tyr mutation in Austrian patients with genetic hemochromatosis. *J Hepatol* 1997; **27**: 773-779

10 **Piperno A,** Sampietro M, Pietrangelo A, Arosio C, Lupica L, Montosi G, Vergani A, Fraquelli M, Girelli D, Pasquero P, Roetto A, Gasparini P, Fargion S, Conte D, Camaschella C. Heterogeneity of hemochromatosis in Italy. *Gastroenterology* 1998; **114**: 996-1002

11 **Olynyk JK,** Cullen DJ, Aquilia S, Rossi E, Summerville L, Powell LW. A population-based study of the clinical expression of the hemochromatosis gene. *N Engl J Med* 1999; **341**: 718-724

12 **Chang JG,** Liu TC, Lin SF. Rapid diagnosis of the HLA-H gene Cys 282 Tyr mutation in haemochromatosis by polymerase chain reaction-A very rare mutation in the Chinese population. *Blood* 1997; **89**: 3492

13 **Bulaj ZJ,** Griffen LM, Jorde LB, Edwards CQ, Kushner JP. Clinical and biochemical abnormalities in people heterozygous for hemochromatosis. *N Engl J Med* 1996; **335**: 1799-1805

14 **Di Bisceglie AM,** Axiotis CA, Hoofnagle JH, Bacon BR. Measurements of iron status in patients with chronic hepatitis. *Gastroenterology* 1992; **102**: 2108-2113

15 **Riggio O,** Montagnese F, Fiore P, Folino S, Giambartolomei S, Gandin C, Merli M, Quinti I, Violante N, Caroli S, Senofonte O, Capocaccia L. Iron overload in patients with chronic viral hepatitis: how common is it? *Am J Gastroenterol* 1997; **92**: 1298-1301

16 **Piperno A,** D'Alba R, Fargion S, Roffi L, Sampietro M, Parma S, Arosio V, Fare M, Fiorelli G. Liver iron concentration in chronic viral hepatitis: a study of 98 patients. *Eur J Gastroenterol Hepatol* 1995; **7**: 1203-1208

17 **Bonkovsky HL,** Banner BE, Lambrecht RW, Rubin RB. Iron in liver diseases other than hemochromatosis. *Semin Liver Dis* 1996; **16**: 65-82

18 **George DK,** Goldwurm S, MacDonald GA, Cowley LL, Walker NI, Ward PJ, Jazwinska EC, Powell LW. Increased hepatic iron concentration in nonalcoholic steatohepatitis is associated with increased fibrosis. *Gastroenterology* 1998; **114**: 311-318

19 **Bacon BR,** Britton RS. The pathology of hepatic iron overload: a free radical-mediated process? *Hepatology* 1990; **11**: 127-137

20 **Bonkovsky HL,** Banner BF, Rothman AL. Iron and chronic viral hepatitis. *Hepatology* 1997; **25**: 759-768

21 **Caroline L.** A cheaper and more rapid polymerase chain reaction-restriction fragment length polymorphism method for the detection of the HLA-H gene mutations occurring in hereditary hemochromatosis. *Blood* 1007; **90**: 4235

22 **Shiono Y,** Ikeda R, Hayashi H, Wakusawa S, Sanae F, Takikawa T, Imaizumi Y, Yano M, Yoshioka K, Kawanaka M, Yamada G. C282Y and H63D mutations in the HFE gene have no effect on iron overload disorders in Japan. *Internal Medicine* 2001; **40**: 852-856

23 **Smith BC,** Grove J, Guzail MA, Day CP, Daly AK, Burt AD, Bassendine MF. Heterozygosity for hereditary hemochromatosis is associated with more fibrosis in chronic hepatitis C. *Hepatology* 1998; **27**: 1695-1699

24 **Kazemi-Shirazi L,** Datz C, Maier-Dobersberger T, Kaserer K, Hackl F, Polli C, Steindl PE, Penner E, Ferenci P. The relation of iron status and hemochromatosis gene mutations in patients with chronic hepatitis C. *Gastroenterology* 1999; **116**: 127-134

25 **Erhardt A,** Maschner-Olberg A, Mellenthin C, Kappert G, Adams O, Donner A, Willers R, Niederau C, Haussinger D. HFE mutations and chronic hepatitis C: H63D and C282Y heterozygosity are independent risk factors for liver fibrosis and cirrhosis. *J Hepatol* 2003; **3**: 335-342

26 **Chitturi S,** Weltman M, Farrell GC, McDonald D, Liddle C, Samarasinghe D, Lin R, Abeygunasekera S, George J. HFE mutations, hepatic iron, and fibrosis: ethnic-specific association of NASH with C282Y but not with fibrotic severity. *Hepatology* 2002; **36**: 142-149

27 **Bonkovsky HL,** Jawaid Q, Tortorelli K, LeClair P, Cobb J, Lambrecht RW, Banner BF. Non-alcoholic steatohepatitis and iron: increased prevalence of mutations of the HFE gene in the non-alcoholic steatohepatitis. *J Hepatol* 1999; **31**: 421-429

Science Editor Guo SY **Language Editor** Elsevier HK

PO Box 2345, Beijing 100023, China
www.wjgnet.com
wjg@wjgnet.com

ELSEVIER

World J Gastroenterol 2005;11(25):3909-3914
World Journal of Gastroenterology ISSN 1007-9327

• *BRIEF REPORTS* •

Polymerase chain reaction: A sensitive method for detecting *Helicobacter pylori* infection in bleeding peptic ulcers

Ching-Chu Lo, Kwok-Hung Lai, Nan-Jing Peng, Gin-Ho Lo, Hui-Hwa Tseng, Chiun-Ku Lin, Chang-Bih Shie, Chao-Ming Wu, Yu-Shan Chen, Wen-Keui Huang, Angela Chen, Ping-I Hsu

Ching-Chu Lo, Kwok-Hung Lai, Gin-Ho Lo, Chiun-Ku Lin, Chang-Bih Shie, Chao-Ming Wu, Yu-Shan Chen, Ping-I Hsu, Division of Gastroenterology, Department of Internal Medicine, Kaohsiung Veternans General Hospital, National Yang-Ming University, Taiwan, China
Nan-Jing Peng, Department of Nuclear Medicine, Kaohsiung Veternans General Hospital, National Yang-Ming University, Taiwan, China
Hui-Hwa Tseng, Department of Pathology, Kaohsiung Veternans General Hospital, National Yang-Ming University, Taiwan, China
Wen-Keui Huang, Division of Infectious Diseases, Department of Internal Medicine, Kaohsiung Veternans General Hospital, National Yang-Ming University, Taiwan, China
Angela Chen, Institute of Biomedical Sciences, National Sun Yat-Sen University, Kaohsiung, Taiwan, China
Supported by the Research Foundation of Kaohsiung Veterans General Hospital, No. VGHKS-91-35 and No. VTY88-G3-2, VGH-NYMU Joint Research Program, Taiwan, China
Correspondence to: Ping-I Hsu, Division of Gastroenterology, Department of Internal Medicine, Kaohsiung Veterans General Hospital, 386, Ta-Chung 1st Road, Kaohsiung, 813, Taiwan, China. williamhsup@yahoo.com.tw
Telephone: +886-7-3422121-2075 Fax: +886-7-3468237
Received: 2004-02-23 Accepted: 2004-04-14

Abstract

AIM: To assess the sensitivity and specificity of polymerase chain reaction (PCR) in detecting *Helicobacter pylori* (*H pylori*) infection in patients with bleeding peptic ulcers, and to compare its diagnostic efficacy with other invasive and non-invasive tests.

METHODS: From April to September 2002, *H pylori* status in 60 patients who consecutively presented with gastroduodenal ulcer bleeding was examined by rapid urease tests (RUT), histology, culture, PCR, serology and urea breath tests (UBT).

RESULTS: The sensitivity of PCR was significantly higher than that of RUT, histology and culture (91% *vs* 66%, 43% and 37%, respectively; $P = 0.01$, <0.001, <0.001, respectively), but similar to that of serology (94%) and UBT (94%). Additionally, PCR exhibited a greater specificity than serology (100% *vs* 65%, $P<0.01$). However, the specificity of PCR did not differ from that of other tests. Further analysis revealed significant differences in the sensitivities of RUT, culture, histology and PCR between the patients with and those without blood in the stomach ($P<0.01$, $P = 0.09$, $P<0.05$, and $P<0.05$, respectively).

CONCLUSION: PCR is the most accurate method among the biopsy-based tests to detect *H pylori* infection in patients with bleeding peptic ulcers. Blood may reduce the sensitivities of all biopsy-based tests.

Key words: Polymerase chain reaction; *Helicobacter pylori*; Bleeding peptic ulcers

Lo CC, Lai KH, Peng NJ, Lo GH, Tseng HH, Lin CK, Shie CB, Wu CM, Chen YS, Huang WK, Chen A, Hsu PI. Polymerase chain reaction: A sensitive method for detecting *Helicobacter pylori* infection in bleeding peptic ulcers. *World J Gastroenterol* 2005; 11(25): 3909-3914
http://www.wjgnet.com/1007-9327/11/3909.asp

INTRODUCTION

Bleeding is a common and serious complication of peptic ulcer diseases. It is estimated that peptic ulcer bleeding accounts for approximately 150 000 hospitalizations per year in the USA[1,2]. The prevalence of *Helicobacter pylori* (*H pylori*) in bleeding peptic ulcers has not been definitely determined, but it is estimated to be 70%[3-5]. The accurate diagnosis of *H pylori* infection is crucial in the short-term and long-term management of patients with bleeding peptic ulcers[6]. If a patient with a bleeding ulcer requires surgical intervention, knowledge of his or her *H pylori* status may guide the selection of procedures for the patient (i.e., a simple closure *vs* full-blown ulcer surgery)[6]. Patients whose bleeding episodes cease in the short term, one-third of those who do not receive maintenance therapy, surgery or anti-*H pylori* therapy will experience recurrent bleeding within the next 1-2 years[7]. However, numerous studies have demonstrated that eradicating *H pylori* can drastically reduce the incidence of rebleeding in patients with bleeding peptic ulcers, preventing the need for long-term antisecretory therapy or surgical intervention[8-10]. Therefore, the *H pylori* status in a patient with bleeding peptic ulcers must be documented.

Currently, *H pylori* infection can be diagnosed by invasive assays, i.e., those requiring esophagogastroduodenoscopy (EGD), or by non-invasive assays in which EGD is not necessary. Invasive diagnostic tests include culture, histology, rapid urease test (RUT) and polymerase chain reaction (PCR). Non-invasive tests comprise serology, stool antigen test and urea breath test (UBT). The choice of a diagnostic test should depend on the clinical circumstances, sensitivity

and specificity of the tests, and the cost effectiveness of the testing strategy. Because of its simplicity, accuracy and rapid determination of *H pylori* status, RUT is generally considered to be the initial endoscopic test of choice for uncomplicated peptic ulcers[11]. However, many studies have demonstrated that RUT lacks sensitivity in *H pylori* diagnosis when peptic ulcer diseases are presented with bleeding[5,12]. Moreover, a recent study by Colin *et al*.[13], indicated that all direct tests on *H pylori* including RUT, culture and histology reduced the sensitivity in the setting of ulcer bleeding. The sensitivities of aforementioned three tests were 31%, 25% and 26%, respectively.

PCR can diagnose *H pylori* infection under non-bleeding conditions much more accurately than histology or culture[14,15]. The level of sensitivity of this test is extremely high and has a threshold of 10 to 100 *H pylori* strains per specimen[14-16]. An accurate diagnosis of *H pylori* at the time of bleeding episode is essential, but few studies have addressed the application of PCR to bleeding ulcers. We performed this prospective study to evaluate the sensitivity, specificity and accuracy of PCR assay for detecting *H pylori* infection in patients with bleeding peptic ulcers and to compare its diagnostic efficacy with that of other invasive and non-invasive tests.

MATERIALS AND METHODS

Patients

From April to September 2002, 60 consecutive patients with hematemesis, melena, or both due to gastroduodenal ulcer bleeding, who underwent an EGD, were enrolled in this study. Exclusion criteria included: age <15 or >80 years; history of coagulopathy or other disorders contraindicated for EGD or biopsy sampling; previous history of anti-*H pylori* therapy. Data regarding age, sex, medical history, drug history, presenting symptoms, gastroduodenal lesions and presence or absence of blood in the stomach were recorded. Written informed consent was obtained from each subject. This study was approved by the Human Medical Research Committee of the Kaohsiung Veterans General Hospital, Kaohsiung, Taiwan.

Endoscopy and biopsy sampling

During endoscopy, gastric biopsy specimens were taken from the lesser curvature of the antrum and corpus for RUT (one antrum biopsy specimen), histology (one antrum and one corpus biopsy specimen), culture (one antrum biopsy specimen) and PCR (one antrum biopsy specimen). Endoscopes were cleaned by a mechanical wash and then washed in an Olympus washing machine. They were then air-dried and cleaned with 70% ethanol.

RUT

RUT was performed according to our previous study[17,18]. A biopsy specimen from antrum was immediately placed in 1 mL of a 10% solution of urea in deionized water (pH 6.8) to which two drops of 1% phenol red solution was added and incubated at 37 ℃ for up to 24 h. If the yellowish color around the area of inserted specimen changed to bright pink within the 24-h limit, the urease test was considered positive. In our laboratory, the sensitivity and specificity of RUT were 96% and 91%, respectively[17].

Histological examination

Biopsy specimens were fixed in 10% buffered formalin, embedded in paraffin, and sectioned. One 4-μm-thick section was cut and stained with hematoxylin-eosin to observe the presence of curved rod shaped bacteria on the mucosal surface[19,20]. The specimens were interpreted by a histopathologist (H-H Tseng) blinded to the patient status and the results of other laboratory tests.

Culture

The specimen for culture was transferred with brain heart infusion on ice for microbiological examination and inoculated onto the CDC anaerobic blood agar (Becton Dickinson Microbiology System, Cockeysville, MD) according to our previous studies[21,22]. The agar was incubated at 35 ℃ for two days in a micro-aerophilic gas mixture containing 5% O_2, 100 mL/L CO_2, and 85% N_2. Culture-positive patients were those with bacterial colonies grown in culture within 7 d. The organisms were identified as *H pylori* by Gram staining, colony morphology and positive oxidase, catalase and urease reaction.

PCR amplification

DNA extraction was performed using a commercially available kit (QIAamp Tissue kit, QIAGEN Inc., Valencia, CA) according to the manufacturer's instructions[23]. The primers used were derived from the internal 411-bp fragment of the *urease A* gene as described by Clayton *et al*.[24]: HPU1 (5'GCCAATGGTAAATTAGTT3') and HPU2 (5'CTCCT-TAATTGTTTTTAC3'). Reactions were performed in a 25 μL volume in a thermal cycler 480 (Perkin Elmer Applied Biosystems, Foster City, CA). A reaction mixture contained 2.5 μL of extracted DNA, 0.5 μmol/L of each primer, 2.5 mmol/L of $MgCl_2$, 2.5 μL of 10× PCR buffer, 1 U of Ampli*Taq* DNA polymerase (Perkin-Elmer Corp., Foster City, CA) and 100 μmol/L of each of dATP, dCTP, dGTP and dTTP. The amplification cycle consisted of an initial denaturation at 94 ℃ for 1 min, primer annealing at 45 ℃ for 1 min, and extension for 5 min at 72 ℃ to ensure a full extension of the products. Samples were amplified in 35 consecutive cycles. The final cycle included a 7-min extension step to ensure a full extension of the PCR products. PCR products were analyzed on a 2% agarose electrophoresis gel stained with ethidium bromide.

UBT

UBT was performed according to our previous studies[21,25] within 1 d of EGD. The patients were fasted for at least 6 h. Fresh milk (1 000 mL) was taken to delay gastric emptying. The test consisted of a baseline breath sample and a second breath sample collected 15 min after oral administration of 100 mg of ^{13}C-labeled urea (INER-Hp C-tester, Taiwan) dissolved in 50 mL sterile water. Values were expressed as an excess $\delta^{13}CO_2$‰ excretion. The $\delta^{13}CO_2$ was the ratio of ^{13}C to ^{12}C in the sample compared to the Pee Dee Belemnite (PDB) standard. The equation was given as: $\delta^{13}CO_2 = (R_{samp}-R_{std})/R_{std}\times 1\,000$. R_{samp} and R_{std}

represented the ratio of ^{13}C to ^{12}C in samples and standard, respectively. If the value of $\delta^{13}CO_2$ was more than 4.8‰, this was considered as a positive result.

Serology

Blood samples for serological evaluation were obtained before EGD. A serological assay for IgG antibodies against *H pylori* was performed by an indirect solid-phase immunochromatographic assay using the ASSURE™ *H pylori* rapid test kit (Genelabs Diagnostics, Cavendish Singapore Science Park, Singapore). The sensitivity and specificity of the assay were 96% and 92%, respectively according to the manufacturer's instructions.

Gold standard definition

A patient was classified as being *H pylori*-positive on the basis of either a positive culture or a negative culture, at least three positive results of RUT, histology, UBT and serological tests.

Statistical analysis

Statistical tests were performed using the SPSS system. Sensitivity, specificity, accuracy, predictive values of positive and negative results were calculated in accordance with standard methods. χ^2 test and 95%CI were used to compare the sensitivity, specificity and accuracy of different diagnostic methods. Two-sample *t*-tests were used to compare the excess $\delta^{13}CO_2$ values of UBT between the true-positive and false-negative groups of various invasive tests. $P<0.05$ was considered statistically significant.

RESULTS

Of the 60 patients initially enrolled in this study, five did not complete all the tests and were excluded from the statistical analysis. Table 1 presents the demographic data of the remaining 55 patients (37 males, 18 females; mean age: 62.2±14.5 years) who finished all of the invasive and non-invasive assays. EGD of these subjects showed a gastric ulcer in 19 patients (35%), a duodenal ulcer in 13 (24%) and both gastric and duodenal ulcers in 23 (42%). According to the gold standard definition, 35 (63.6%) were *H pylori*-positive and 20 (36.4%) were *H pylori*-negative.

Comparison of various tests for detecting H pylori infection in bleeding peptic ulcers

Table 2 presents the sensitivity, specificity and accuracy of various tests in diagnosing *H pylori* infection. The sensitivities of RUT, histology and culture were low (66%, 43% and 37%, respectively) although these assays exhibited a high specificity (95-100%). Their overall accuracies were 76%, 62% and 60%, respectively. Among the four biopsy-based methods, only PCR exhibited the satisfactory sensitivity (91%), specificity (100%), and accuracy (94%). Its sensitivity and accuracy were significantly higher than those of RUT, histology and culture (sensitivity: $P<0.05$, $P<0.001$ and $P<0.001$, respectively; accuracy: $P<0.05$, $P<0.001$, $P<0.001$, respectively).

Of the non-invasive assays, the serological test had a high sensitivity (95%) but its specificity (65%) was lower than that of PCR ($P<0.05$). The sensitivity (94%), specificity (85%) and accuracy (91%) of UBT were similar to those of PCR. Among all of the tests investigated herein, PCR and UBT were the most accurate methods for diagnosing *H pylori* infection in patients with bleeding peptic ulcers.

Relationship between intragastric blood and sensitivity of various tests in diagnosis of H pylori infection

The patients were divided into two groups according to the presence or absence of blood in the stomach, to investigate the relationships between intragastric blood and sensitivities

Table 1 Baseline characteristics of patients with bleeding peptic ulcers (*n*, %)

	Number of patients (*n* = 55)
Age (mean±SD)	62.2 (14.5)
Sex	
Male	37 (67)
Female	18 (33)
Smoking	13 (24)
Alcohol consumption	4 (7)
Coffee consumption	5 (9)
Ingestion of tea	18 (33)
Ingestion of NSAID[1]	26 (47)
Sites of ulcer	
Stomach	19 (35)
Duodenum	13 (24)
Stomach and duodenum	23 (42)
Ulcer lesions	
Bleeding visible vessel	2 (4)
Non-bleeding visible vessel	3 (6)
Adherent clot	15 (27)
Red or black spot	21 (38)
Clean base	14 (26)

[1]NSAID: non-steroidal anti-inflammatory drugs.

Table 2 Sensitivity, specificity, and accuracy of various tests for diagnosis of *H pylori* infection in bleeding peptic ulcers (*n* = 55) [%(95%CI)]

	Sensitivity	Specificity	Accuracy	PPV	NPV
RUT	66 (49–82)[b]	95 (84–100)	76 (64–88)[b]	96 (87–100)	61 (43–79)[a]
Histology	43 (26–60)[d]	95 (84–100)	62 (48–75)[d]	100	48 (31–64)[b]
Culture	37 (20–54)[d]	100	60 (46–73)[d]	100	48 (32–63)[b]
PCR	91 (82–100)	100	95 (88–100)	100	87 (72–100)
Serology	94 (86–100)	65 (42–88)[b]	84 (73–93)	83 (70–95)[a]	87 (67–100)
UBT	94 (86–100)	85 (68–100)	91 (83–98)	92 (82–100)	90 (74–100)

[a]$P<0.05$ *vs* PCR; [b]$P<0.01$ *vs* PCR; [d]$P<0.001$ *vs* PCR.

of biopsy-based tests for *H pylori* infection. The sensitivities of RUT, histology, culture, PCR, serology and UBT were 29%, 21%, 21%, 79%, 93% and 100% in the patients with intragastric blood, respectively, and 90%, 57%, 48%, 100%, 95% and 91% in the patients without intragastric blood, respectively. There were statistically significant differences in the sensitivities of RUT, histology and PCR between the patients with and without blood in the stomach (Figure 1; $P<0.01$, $P<0.05$ and $P<0.05$, respectively). Additionally, there was a trend towards decreased sensitivity of culture in the patients with blood in the stomach ($P = 0.09$).

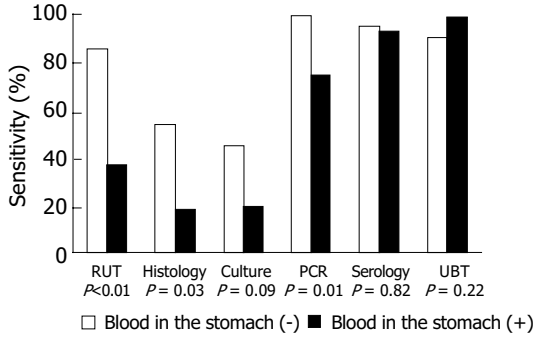

Figure 1 Sensitivities of various tests for detecting *H pylori* infection between the bleeding ulcer patients with and without blood in the stomach.

Comparison of bacterial loads between true-positive and false-negative groups of biopsy-based tests

Since the quantitative data obtained by UBT could reflect the intragastric bacterial load of *H pylori*, we further compared the excess $\delta^{13}CO_2$ values of UBT between the true-positive and false-negative groups in biopsy-based tests. The excess $\delta^{13}CO_2$ values of RUT, histology, culture and PCR were 26.7±18.1, 31.5±21.4, 33.7±21.8 and 26.3±19.4 in the group with true-positive results respectively, and 20.5±16.3, 19.5±16.3, 19.3±15.9 and 7.2±2.6 in the group with false-negative results respectively. The excess $\delta^{13}CO_2$ values in the false-negative group were significantly lower than that in the true-positive group of culture test (Figure 2; $P = 0.03$). In addition, there was also a trend toward decreased $\delta^{13}CO_2$ values in the false-negative group of histological examination and PCR assay (both $P = 0.07$).

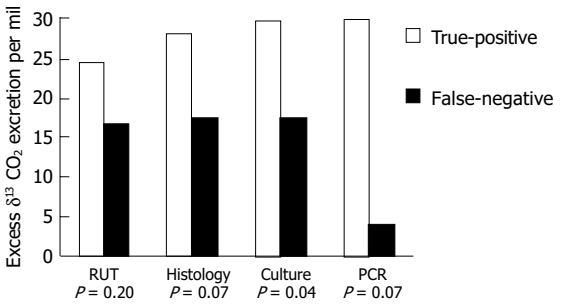

Figure 2 Comparison of the excess $\delta^{13}CO_2$ values of UBT between the true-positive and false-negative groups in the biopsy-based methods.

DISCUSSION

The *H pylori* status in a patient presenting with a bleeding ulcer must be documented to determine the method of further management. However, many studies have disclosed that biopsy-based tests including RUT, histology and culture have low sensitivities in detecting *H pylori* in bleeding peptic ulcers[5,12,13]. Additionally, two recent reports[26,27] also revealed a lack of accuracy in *H pylori* stool antigen (HpSA) tests in patients with ulcer bleeding. In this study, we also demonstrated that the sensitivities of RUT, histology and culture in bleeding peptic ulcer were only 66%, 43% and 37%, respectively. However, PCR could reach a diagnostic sensitivity of 91%, much higher than that of RUT, histology and culture. Additionally, the test had 100% specificity in diagnosing *H pylori* infection under bleeding conditions. This, therefore, is the most accurate biopsy-based method for determining *H pylori* status in bleeding peptic ulcers.

UBT is one of the non-invasive methods for diagnosing *H pylori* infection. Both its sensitivity and specificity are greater than 90% in patients with bleeding peptic ulcers. Its accuracy is comparable to that of PCR. Although the serological test has a high sensitivity in patients with bleeding peptic ulcers, it may not be a good choice for diagnosing *H pylori* infection in patients with a complicated ulcer because antibody tests lack a good specificity (only 65%). The presence of anti-*H pylori* IgG antibody implies prior exposure to the organisms, but does not imply the presence of a current infection. If a patient presenting with ulcer bleeding has a false-positive antibody test and is treated by eradication therapy, the physician may mistakenly believe that the cause of bleeding has been removed and will then not provide further preventive therapy to the patient. In such a case, the patient would have a high risk of recurrent bleeding[6]. Therefore, establishing the *H pylori* status with certainty at the time of bleeding episode is quite important.

Following this work, we recommend that an endoscopist may initially perform a RUT to detect *H pylori* infection in a patient with bleeding peptic ulcer because of its simplicity, low cost, moderate sensitivity and excellent specificity. If the RUT is negative, either PCR or UBT can be used for the definite diagnosis of *H pylori* status. The choice of the final diagnostic modality may depend on the availability of tests in the hospital. Nonetheless, the aim of PCR is to detect specific DNA sequences rather than the whole viable bacterium. No special requirements pertain to the treatment, transport, or storage of the biopsy specimens for PCR[28,29]. Several laboratories have reported the successful detection of *H pylori* by PCR from a biopsy specimen placed and transported by mail in the RUT[16,30,31]. This capability is particularly useful for a gastroenterologist who does not have access to laboratory facilities and requires a confirmation of the RUT[16].

In this study, the sensitivities of RUT, histology, culture and PCR were found to be 29%, 21%, 21% and 79% in patients with intragastric blood, and 90%, 57%, 48% and 100% in patients without intragastric blood. These data imply that blood may reduce the diagnostic yield of all endoscopic biopsy tests in patients with bleeding peptic ulcers. Additionally, we also demonstrated that the bacterial load in the false-negative group of culture was significantly lower

than that in the true-positive group. Furthermore, there was also a trend toward decreased bacterial load in the false-negative group of histological examination and PCR assay. The decreased bacterial density therefore, may be the major cause for decreased sensitivities of all biopsy-based assays. There are several possible reasons for the aforementioned findings. The decreased bacterial load in bleeding ulcer patients may be related to a direct suppression effect of intraluminal blood on *H pylori*, the administration of antisecretory drugs, or the removal of some *H pylori* from the gastric epithelium or mucus by gastric lavage before EGD[32]. Recently, Leung *et al*.[33], reported that a false-negative result of RUT in bleeding ulcer might be caused by the buffered effects of blood. An *in vitro* study[34] also showed that sheep's blood inhibited the growth of *H pylori* in broth media. The exact reason concerning the association between bleeding ulcer and intragastric bacterial density merits further investigations.

In conclusion, PCR is the most accurate biopsy-based method for determining *H pylori* status in patients with bleeding peptic ulcers. RUT, histology and culture have a poor sensitivity under bleeding conditions. A decline in the intragastric bacterial density during bleeding ulcer may be a major cause of the reduced sensitivity of biopsy-based assays.

ACKNOWLEDGMENTS

The authors express their deep appreciation to Dr. Wei-Lun Tsai, Dr. Wen-Chi Chen, Dr. Lung-Chih Cheng, Dr. Hsien-Chung Yu, Dr. Chung-Jen Wu, Miss Min-Rong Huang and Miss Pei-Min Tsai for their assistance in the clinical follow up of the patients.

REFERENCES

1 **Kurata JH,** Corboy ED. Current peptic ulcer time trends: An epidemiological profile. *J Clin Gastroenterol* 1988; **10**: 259-268
2 **Vaira D,** Menegatti M, Miglioli M. What is the role of *Helicobacter pylori* in complicated ulcer disease? *Gastroenterology* 1997; **113**: S78-84
3 **Hosking SW,** Yung MY, Chung SC, Li AKC. Differing prevalence of *Helicobacter pylori* in bleeding and non-bleeding ulcers. *Gastroenterology* 1992; **102**: A85
4 **Jensen DM,** You S, Pelayo E, Jensen ME. The prevalence of *Helicobacter pylori* and NSAID use in patients with severe UGI hemorrhage and their potential role in recurrence of ulcer bleeding. *Gastroenterology* 1992; **102**: A85
5 **Lee JM,** Breslin NP, Fallon C, O'Morain CA. Rapid urease test lack sensitivity in *Helicobacter pylori* diagnosis when peptic ulcer disease presents with bleeding. *Am J Gastroenterol* 2000; **95**: 1166-1170
6 **Laine L,** Cohen H. *Helicobacter pylori*: drowning in a pool of blood? *Gastrointest Endosc* 1999; **49**: 398-402
7 **Laine L.** *Helicobacter pylori* and complicated ulcer diseases. *Am J Med* 1996; **100**: S52-59
8 **Rokkas T,** Karameris A, Mavrogeorgis A, Rallis E, Giannikos N. Eradication of *Helicobacter pylori* reduces the possibility of rebleeding in peptic ulcer disease. *Gastrointest Endosc* 1995; **41**: 1-4
9 **Graham DY,** Hepps KS, Ramirez FC, Lew GM, Saeed ZA. Treatment of *Helicobacter pylori* reduces the rate of rebleeding in peptic ulcer disease. *Scand J Gastroenterol* 1993; **28**: 939-942
10 **Labenz J,** Borsch G. Role of *Helicobacter pylori* eradication in the prevention of peptic ulcer bleeding relapse. *Digestion* 1994; **55**: 19-23
11 **Cutler AF,** Havstad S, Ma CK, Blaser MJ, Perez-Perez GI, Schubert TT. Accuracy of invasive and noninvasive testes to diagnose *Helicobacter pylori* infection. *Gastroenterology* 1995; **109**: 136-141
12 **Tu TC,** Lee CL, Wu CH, Chen TK, Chan CC, Huang SH, Lee MS. Comparison of invasive and noninvasive tests for detecting *Helicobacter pylori* infection in bleeding peptic ulcers. *Gastrointest Endosc* 1999; **49**: 302-306
13 **Colin R,** Czernichow P, Baty V, Touze I, Brazier F, Bretagne JF, Berkelmans I, Barthelemy P, Hemet J. Low sensitivity of invasive tests for the detection of *Helicobacter pylori* infection in patients with bleeding ulcer. *Gastroenterol Clin Biol* 2000; **24**: 31-35
14 **Fabre R,** Sobhani I, Laurent-Puig P, Hedef N, Yazigi N, Vissuzaine C, Rodde I, Potet F, Mignon M, Etienne JP. Polymerase chain reaction assay for the detection of *Helicobacter pylori* in gastric biopsy specimens: Comparison with culture, rapid urease test, and histopathological tests. *Gut* 1994; **35**: 905-908
15 **Lin SY,** Jeng YS, Wang CK, Ko FT, Lin KY, Wang CS, Lie JD, Chen PH, Chang JG. Polymerase chain reaction diagnosis of *Helicobacter pylori* in gastroduodenal diseases: comparison with culture and histopathological examinations. *J Gastroenterol Hepatol* 1996; **11**: 286-289
16 **Ho GY,** Windsor HM. Accurate diagnosis of *Helicobacter pylori*: polymerase chain reaction tests. *Gastroenterol Clin North Am* 2000; **29**: 903-915
17 **Hsu PI,** Lai KH, Tseng HH, Lin YC, Yen MY, Lin CK, Lo GH, Huang RL, Huang JS, Cheng JS, Huang WK, Ger LP, Chen W, Hsu PN. Correlation of serum immunoglobulin G *Helicobacter pylori* antibody titers with histological and endoscopic findings in patients with dyspepsia. *J Clin Gastroenterol* 1997; **25**: 587-591
18 **Hsu PI,** Lai KH, Chien EJ, Lin CK, Lo GH, Jou HS, Cheng JS, Chan HH, Hsu JH, Ger LP, Hsu PN, Tseng HH. Impact of bacterial eradication on the cell proliferation and p53 protein accumulation in *Helicobacter pylori*-associated gastritis. *Anticancer Res* 2000; **20**: 1221-1228
19 **Dixon MF,** Genta RM, Yardley JH, Correa P. Classification and grading of gastritis. The Updated Sydney System. *Am J Surg Pathol* 1996; **20**: 1161-1181
20 **Hsu PI,** Lai KH, Lo GH, Tseng HH, Lo CC, Chen HC, Tsai WL, Jou HS, Peng NJ, Chien CH, Chen JL, Hsu PN. Risk factors for ulcer development in patients with non-ulcer dyspepsia: Prospective two year follow up study of 209 patients. *Gut* 2002; **51**: 15-20
21 **Peng NJ,** Hsu PI, Lee SC, Tseng HH, Huang WK, Tsay DG, Ger LP, Lo GH, Lin CK, Tsai CC, Lai KH. A 15-minute [13C]-urea breath test for the diagnosis of *Helicobacter pylori* infection in patients with non-ulcer dyspepsia. *J Gastroenterol Hepatol* 2000; **15**: 284-289
22 **Peng NJ,** Lai KH, Liu RS, Lee SC, Tsay DG, Lo CC, Tseng HH, Huang WK, Lo GH, Hsu PI. Clinical significance of oral urease in diagnosis of *Helicobacter pylori* infection by [13C] urea breath test. *Dig Dis Sci* 2001; **46**: 1772-1778
23 **Hsu PI,** Hwang IR, Cittelly D, Lai KH, El-Zimaity HM, Gutierrez O, Kim JG, Osato MS, Graham DY, Yamaoka Y. Clinical presentation in relation to diversity within the *Helicobacter pylori cag* pathogenicity island. *Am J Gastroenterol* 2002; **97**: 2231-2238
24 **Clayton CL,** Kleanthous H, Coates PJ, Morgan DD, Tabaqchali S. Sensitive detection of *Helicobacter pylori* by using polymerase chain reaction. *J Clin Microbiol* 1992; **30**: 192-200
25 **Peng NJ,** Lai KH, Liu RS, Lee SC, Tsay DG, Lo CC, Tseng HH, Huang WK, Lo GH, Hsu PI. Endoscopic 13C-urea breath test for the diagnosis of *Helicobacter pylori* infection. *Dig Liver Dis* 2003; **35**: 73-77
26 **van Leerdam ME,** van der Ende A, ten Kate FJ, Rauws EA, Tytgat GN. Lack of accuracy of the noninvasive *Helicobacter pylori* stool antigen test in patients with gastroduodenal ulcer bleeding. *Am J Gastroenterol* 2003; **98**: 798-801

27 **Peitz U,** Leodolter A, Kahl S, Agha-Amiri K, Wex T, Wolle K, Gunther T, Steinbrink B, Malfertheiner P. Antigen stool test for assessment of *Helicobacter pylori* infection in patients with upper gastrointestinal bleeding. *Aliment Pharmacol Ther* 2003; **17**: 1075-1084

28 **Ho SA,** Hoyle JA, Lewis FA, Secker AD, Cross D, Mapstone NP, Dixon MF, Wyatt JI, Tompkins DS, Taylor GR. Direct polymerase chain reaction test for detection of *Helicobacter pylori* in humans and animals. *J Clin Microbiol* 1991; **29**: 2543-2549

29 **van Zwet AA,** Thijs JC, Kooistra-Smid AM, Schirm J, Snijder JA. Sensitivity of culture compared with that of polymerase chain reaction for detection of *Helicobacter pylori* from antral biopsy samples. *J Clin Microbiol* 1993; **31**: 1918-1920

30 **Hua J,** Roux D, de Mascarel A, Megraud F. PCR for *Helicobacter pylori* on biopsy samples in CLO test sent by mail [abstract]. *Gastroenterology* 1994; **106**: A97

31 **Lin TT,** Yeh CT, Yang E, Chen PC. Detection of *Helicobacter pylori* by polymerase chain reaction assay using gastric biopsy specimens taken for CLO test. *J Gastroenterol* 1996; **31**: 329-332

32 **Hsu PI,** Lai KH, Tseng HH, Lin CK, Lo GH, Cheng JS, Chan HH, Chen GC, Jou HS, Peng NJ, Ger LP, Chen W, Hsu PN. Risk factors for presentation with bleeding in patients with *Helicobacter pylori*-related peptic ulcer diseases. *J Clin Gastroenterol* 2000; **30**: 386-391

33 **Leung WK,** Sung JJ, Siu KL, Chan FK, Ling TK, Cheng AF. False-negative biopsy urease test in bleeding ulcers caused by the buffering effects of blood. *Am J Gastroenterol* 1998; **93**: 1914-1918

34 **Coudron PE,** Stratton CW. Factors affecting growth and susceptibility testing of *Helicobacter pylori* in liquid media. *J Clin Microbiol* 1995; **33**: 1028-1030

Science Editor Wang XL and Li WZ **Language Editor** Elsevier HK

PO Box 2345, Beijing 100023, China
www.wjgnet.com
wjg@wjgnet.com

ELSEVIER

World J Gastroenterol 2005;11(25):3915-3919
World Journal of Gastroenterology ISSN 1007-9327

• *BRIEF REPORTS* •

Role of cytokines in promoting immune escape of FasL-expressing human colon cancer cells

Tong Xu, Bao-Cun Sun, Qiang Li, Xi-Shan Hao

Tong Xu, Qiang Li, Xi-Shan Hao, Department of Abdominal Surgery, Cancer Hospital Affiliated to Tianjin Medical University, Tianjin 300060, China
Bao-Cun Sun, Institute of Oncology, Tianjin Medical University, Tianjin 300060, China
Supported by the Science and Technology Commission Foundation of Tianjin, No. 003119711
Correspondence to: Dr. Tong Xu, Department of Abdominal Surgery, Cancer Hospital Affiliated to Tianjin Medical University, Tianjin 300060, China. tong_xu@126.com
Telephone: +86-22-23537796 Fax: +86-22-23359984
Received: 2004-08-18 Accepted: 2004-11-19

Abstract

AIM: To investigate the potential role of cytokines in promoting Fas ligand (FasL)-expressing colon cancer cells.

METHODS: Immunohistochemical SABC method was used to observe the expression of Fas receptor and ligand in SW620 colon cancer cell line and Jurkat T cells in order to provide the morphological evidence for the functions of Fas receptor and ligand. To examine the cytotoxicity of effector cells, CytoTox96® non-radioactive cytotoxicity assay was adopted to measure the lactate dehydrogenase-releasing value after SW620 cells were co-cultured with Jurkat T lymphocytes.

RESULTS: The FasL of colon cancer SW620 cells was positive. The positive substances were distributed in the cell membrane and cytoplasm. The Fas receptor of colon cancer SW620 cells was negative. The Fas receptor and ligand of Jurkat T lymphocytes turned out to be positive. The positive substances were distributed in the cell membrane. After phytohemagglutinin (PHA)-stimulated Jurkat T lymphocytes were co-cultured with phorbol 12-myristate 13-acetate (PMA)-plus-ionomycin-stimulated (for 48 h) SW620 cells or tumor necrosis factor-alpha (TNF-α)-stimulated (for 48 h) SW620 cells or unstimulated SW620 cells for 4 h, the cytotoxicity of SW620 cells to PHA-stimulated Jurkat cells at effector-to-target ratios of 10:1, 5:1, 2.5:1, and 1.25:1 was 74.6%, 40.8%, 32.4%, and 10.9% ($F = 8.19$, $P<0.05$); or 54.9%, 35.3%, 22.0%, and 10.3% ($F = 11.12$, $P<0.05$); or 14.9%, 10.5%, 6.9%, and 5.8% ($F = 3.45$, $P<0.05$). After PHA-stimulated Jurkat T lymphocytes were co-cultured with unstimulated SW620 cells for 8 h, the cytotoxicity of SW620 cells to PHA-stimulated Jurkat cells at effector-to-target ratios of 5:1, 2.5:1, and 1.25:1 from the experiment was 83.9%, 74.1%, and 28.5% ($F = 137.04$, $P<0.05$) respectively. Non-radioactive cytotoxicity assay showed that the apoptotic rate of Jurkat cells remarkably increased with the increase of planting concentration of SW620 cells and co-culture time after the SW620 cells were co-cultured with the Jurkat T lymphocytes. The cytotoxicity was significantly enhanced by PMA+ionomycin or TNF-α.

CONCLUSION: The FasL expressed in human colon cancer cells may be regulated by endogenous factors in the microenvironment of the host and facilitate the escape of tumor cells from the host immune system.

Key words: Cytokines; Fas/Fas ligand; Colon cancer; Apoptosis; Immune escape

Xu T, Sun BC, Li Q, Hao XS. Role of cytokines in promoting immune escape of FasL-expressing human colon cancer cells. *World J Gastroenterol* 2005; 11(25): 3915-3919
http://www.wjgnet.com/1007-9327/11/3915.asp

INTRODUCTION

The Fas/Fas ligand (FasL) system plays an important role in the transduction of apoptotic signal into cells. In recent years, numerous studies have demonstrated that Fas is expressed on the surface of cells, whereas FasL expression is restricted to a small number of cell types, such as lymphocytes, cells of the immune-privileged organs and many types of malignant tumor cells[1]. Evidence has pointed to an abnormal increase in apoptosis among activated Fas-positive lymphocytes, mainly in the periphery of the FasL-expressing tumors[2]. On the other hand, the occurrence of tumor is due to the fact that the converted cells cannot undergo a normal process of apoptosis. Resistance to apoptosis through the Fas receptor pathway coupled with expression of the FasL might enable many cancers to deliver a pre-emptive strike or counterattack against the immune system[2-4]. This study aimed to observe the interaction *in vitro* between T cells expressing Fas and tumor cells expressing FasL, and to investigate the potential role of FasL-expressing colon cancer cells *in vitro* and the effect of endogenous cytokines on tumor cells counterattacking T lymphocytes.

MATERIALS AND METHODS

Reagents, antibodies, and apparatus

Ionomycin, PMA, and phytohemagglutinin (PHA) were purchased from Sigma Chemical Co., USA. Tumor necrosis factor-alpha (TNF-α) and CytoTox96® non-radioactive

cytotoxicity assay kits were purchased from Promega Co., USA. RPMI1640 and DMEM were obtained from Gibco Co. Fetal bovine serum (FBS) was purchased from Hyclone Co. Monoclonal mouse anti-human CD95/FAS and monoclonal mouse anti-human FasL were purchased from Zhongshan Co., Beijing, China. SABC detection kit was purchased from Bosden Co., Wuhan, China. A-5082 Sunrise automated ELISA reader was purchased from Tecan, Austria.

Cell lines and cell culture

The human colon cancer cell line SW620 from American Tissue Culture Collection (ATCC) was kindly donated by Dr. Joe O'Connell, Cork University Hospital, Ireland. The acute T cell leukemia cell line Jurkat (ATCC) was provided by Institute of Hematology, Chinese Academy of Medical Sciences. The human glioma cell line TJ905 was kindly donated by Dr. Zhang WZ, Tianjin Huanhu Hospital, China. SW620 and TJ905 cells were cultured in DMEM supplemented with 100 mL/L FBS. Jurkat T lymphocytes were cultured in RPMI1640 medium (with 100 mL/L FBS) and stimulated with 4 mg PHA/L[3]. All cell lines were incubated at 37 ℃ in a humidified 50 mL/L CO_2 atmosphere.

Immunocytochemical procedures for detection of FasL and Fas protein

Jurkat, TJ905, and SW620 cells were cultured on glass chamber slides respectively. After fixation in 4% paraformaldehyde for 60 min respectively, slides were washed twice for 5 min in a wash buffer containing 50 mmol/L Tris-Cl, pH 7.6, 50 mmol/L NaCl, and 0.001% saponin. Endogenous peroxidase was quenched with 3% hydrogen peroxide in methanol for 5 min. Slides were washed as before except that the wash buffer contained 1% normal goat serum, and then blocked for 1 h in wash buffer containing 5% normal goat serum[5]. Slides were washed and incubated overnight at a dilution of 1:200 with monoclonal mouse anti-human primary antibodies at 4 ℃ in a high-humidity chamber. Antibody binding was localized using biotinylated secondary antibody, avidin-conjugated horseradish peroxidase, and diaminobenzidine substrate. Slides were counterstained with hematoxylin, washed for 1 h with PBS, air-dried and covered with mounting medium. Negative control slides were processed with PBS in place of primary antibodies.

Fas-mediated cytotoxicity assay

To examine the cytotoxicity of effector cells, CytoTox96® non-radioactive cytotoxicity assay[6] was adopted to measure lactate dehydrogenase (LDH)-releasing value after SW620 or TJ905 cells (control) were co-cultured with Jurkat T lymphocytes. Jurkat cells were incubated with PHA (4 mg/L)[3] in RPMI1640 (50 mL/L FBS) for 24 h and counted with a hemocytometer before cytotoxicity assay. SW620 or TJ905 cells (control) were seeded on 96-well U-bottom tissue culture plates (Falcon) at a density of 2×10^9/L, 1×10^9/L, 5×10^8/L, and 2.5×10^8/L respectively, and kept under controlled conditions or stimulated with 10 μg/L PMA+500 μg/L ionomycin or with 20 μg/L TNF-α for 48 h. For a further 24 h of culture PHA-stimulated Jurkat cells (2×10^4 in 100 μL) were added, keeping effector-to-target cell ratios at 10:1, 5:1, 2.5:1, and 1.25:1. PHA-stimulated Jurkat cells were co-cultured with effector cells in 100 μL RPMI1640 medium (50 mL/L FBS) each well. Tissue culture plate was centrifuged at 250 r/min for 5 min at 4 ℃ to ensure cell-cell contact[6]. In each experiment triplicate wells were analyzed. At the same time, the values of effector cell spontaneous LDH release, target cell spontaneous LDH release, target cell maximum LDH release, volume correction control, and culture medium background were measured. Then the following formula was applied in the calculation of percent cytotoxicity:cytotoxicity (%) = (experimental LDH release-effector cell spontaneous LDH release-target cell spontaneous LDH release)/(target cell maximum LDH release-target cell spontaneous LDH release)×100.

Statistical analysis

Results were compared by analysis of variance (ANOVA) using SPSS10.0 software. $P<0.05$ was considered statistically significant.

RESULTS

Immunocytochemical detection of FasL and Fas protein in SW620, Jurkat and TJ905 cells

FasL expression in colon cancer SW620 cells was strongly positive. The positive substances were distributed in the cell membrane and cytoplasm (Figure 1A), while Fas expression in SW620 cells was negative (Figure 1B). Fas and FasL expression in Jurkat T lymphocytes turned out to be positive. The positive substances were distributed in the cell membrane and cytoplasm, while the nuclei of the cells were negative (Figures 1C and D). Fas expression in TJ905 cells was positive. The positive substances were distributed in the cell membrane and cytoplasm (Figure 1E). FasL expression in TJ905 cells was weakly positive (Figure 1F).

Results of cytotoxicity assay

After the SW620 cells were co-cultured with the PHA-stimulated Jurkat T lymphocytes for 4 h, the cytotoxicity (Figure 2) of SW620 cells to PHA-stimulated Jurkat cells at different effector-to-target ratios had significant differences ($F = 3.45$, $P<0.05$). After stimulation with 10 μg/L PMA+500 μg/L ionomycin for 48 h, the SW620 cells were co-cultured with the PHA-stimulated Jurkat T lymphocytes for 4 h. The cytotoxicity (Figure 2) of SW620 cells to PHA-stimulated Jurkat cells at different effector-to-target ratios had significant differences ($F = 8.19$, $P<0.05$). After stimulation with 20 μg/L TNF-α for 48 h, the SW620 cells were co-cultured with the PHA-stimulated Jurkat T lymphocytes for 4 h. The cytotoxicity (Figure 2) of SW620 cells to PHA-stimulated Jurkat cells at different effector-to-target ratios had significant differences ($F = 11.12$, $P<0.05$). After the SW620 cells were co-cultured with the PHA-stimulated Jurkat T lymphocytes for 8 h, the cytotoxicity of SW620 cells to PHA-stimulated Jurkat cells at effector-to-target ratios of 5:1, 2.5:1, and 1.25:1 was 83.9%, 74.1%, and 28.5% respectively and had significant differences ($F = 137.04$, $P<0.05$). The cytotoxicity of Jurkat cells after co-culture with SW620 (different effector-to-target ratios) for 8 h was much higher than that after being co-cultured with SW620 (different effector-to-target ratios) for 4 h ($P<0.05$, Table 1).

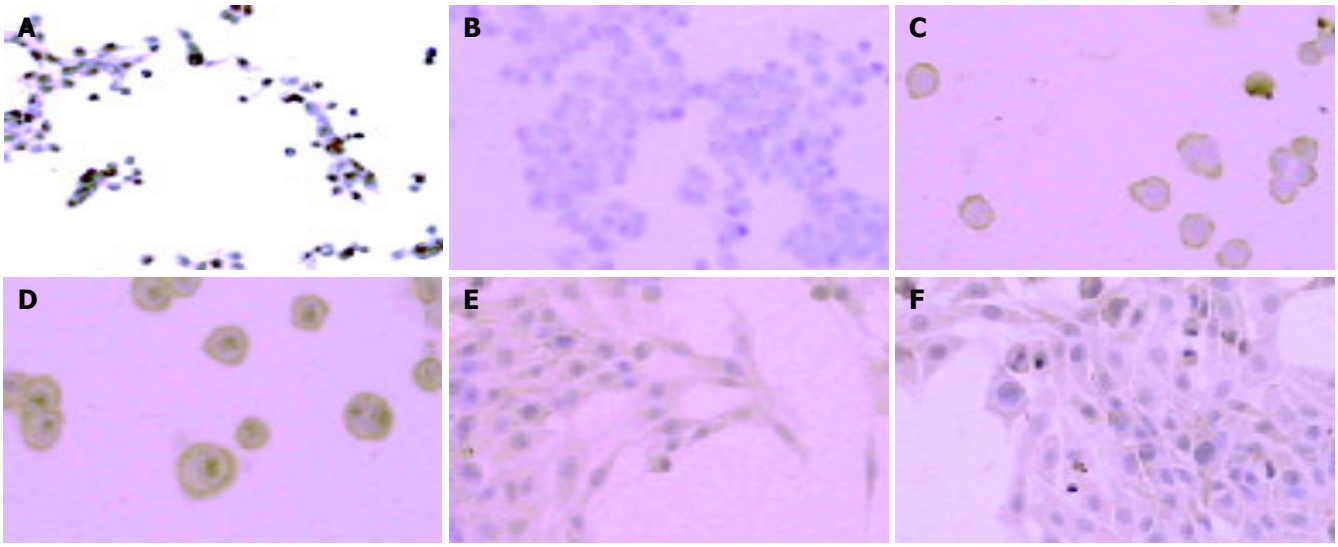

Figure 1 Expression of FasL and Fas in SW620 cells (**A** and **B**), Jurkat cells (**C** and **D**), and TJ905 cells (**E** and **F**).

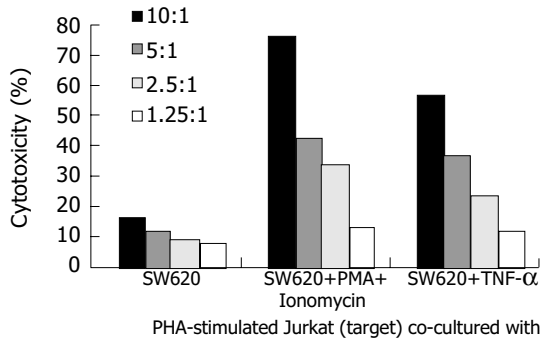

Figure 2 Comparison of cytotoxicity assay among three groups.

After PMA-plus-ionomycin-stimulated (for 48 h) SW620 cells or unstimulated SW620 cells were co-cultured with PHA-stimulated Jurkat T lymphocytes for 4 h, the cytotoxicity of PMA-plus-ionomycin-stimulated SW620 cells was much higher than that of control. The cytotoxicity had significant differences between the two groups ($P<0.05$, Table 1). After TNF-α-stimulated (for 48 h) SW620 cells or unstimulated SW620 cells were co-cultured with PHA-stimulated Jurkat T lymphocytes for 4 h, the cytotoxicity of TNF-α-stimulated SW620 cells was much higher than that of control. The cytotoxicity had significant differences between the two groups ($P<0.05$, Table 1).

After the TJ905 cells were co-cultured with the PHA-stimulated Jurkat T lymphocytes for 4 h, the cytotoxicity of TJ905 cells to PHA-stimulated Jurkat cells at different effector-to-target ratios had no differences ($F = 0.25$, $P>0.05$). TJ905 cells were not cytotoxic to Jurkat cells. After the TJ905 cells were co-cultured with the PHA-stimulated Jurkat T lymphocytes for 8 h, the cytotoxicity of TJ905 cells to PHA-stimulated Jurkat cells at different effector-to-target ratios had no differences ($F = 2.92$, $P>0.05$). TJ905 cells were not cytotoxic to Jurkat cells. After the TJ905 cells were stimulated with 10 μg/L PMA+500 μg/L ionomycin for 48 h, the TJ905 cells were co-cultured with the PHA-stimulated Jurkat T lymphocytes for 4 h. The cytotoxicity of TJ905 cells to PHA-stimulated Jurkat cells at different effector-to-target ratios had no differences ($F = 0.04$, $P>0.05$), TJ905 cells were not cytotoxic to Jurkat cells. After the TJ905 cells were stimulated with 20 μg/L TNF-α for 48 h, the TJ905 cells were co-cultured with the PHA-stimulated Jurkat T lymphocytes for 4 h. The cytotoxicity of TJ905 cells to PHA-stimulated Jurkat cells at different effector-to-target ratios had no differences ($F = 0.97$, $P>0.05$), TJ905 cells were not cytotoxic to Jurkat cells. Cytotoxicity assay showed that no cytotoxicity to human glioma TJ905 cells was observed in the PHA-stimulated Jurkat T lymphocytes.

DISCUSSION

Fas is constitutively expressed in lymphocytes of normal subjects. After lymphocytes are triggered by inflammatory cytokines or tumor antigen, Fas expression is significantly augmented. Since the expansion of tumor-specific CD4 and CD8 cells is the current goal of many promising immunotherapeutic strategies, it is important to understand the factors that may influence the fate of such specific cells. Moreover, uncloned CD4 cell line originally isolated from human tumor tissue[7]

Table 1 Comparison of cytotoxicity assay after co-culturing PHA-stimulated Jurkat T lymphocytes with SW620 cells

Sources of deviations	*F* (8 h)	*P*	*F* (PMA-plus-ionomycin)	*P*	*F* (TNF-α)	*P*
Sample	475.99	<0.05	27.71	<0.05	57.87	<0.05
Column	77.62	<0.05	10.29	<0.05	129.92	<0.05
Intercept	51.09	<0.05	5.14	<0.05	15.75	<0.05

Two-way ANOVA.

as well as tumor-specific human cytotoxic T lymphocytes (CTLs) clones[8] are also reported to express Fas *in vitro* and to be sensitive to its ligation. Recent evidence shows that tumor-infiltrating lymphocytes (TILs) exhibit significantly increased expression of Fas relative to peripheral blood lymphocytes[9]. There is evidence that the lack of co-stimulatory signals such as B7.1, a feature of many tumors, promotes T-cell sensitivity to FasL in the tumor microenvironment[10]. Since TILs are difficult to be isolated and expanded *in vitro*, we chose Jurkat T lymphocytes instead of TILs in our study.

Fas is expressed in each colonocyte of normal colon mucosa, and downregulated or lost in the majority of colon cancers. Immunohistology revealed that the majority of colon cancers express Fas at abnormally low levels or entirely lack Fas[11]. Our results are compatible with these findings. Further more data have confirmed that colon cancer cell line is constitutively or at least relatively resistant to Fas-mediated apoptosis[12,13]. Resistance to Fas-mediated apoptosis is a common feature of cancers, irrespective of cell surface expression of Fas[14]. Thus, the downmodulation or abrogation of Fas on tumor cells and/or acquirement of relative resistance to Fas ligation might be a selection advantage, and constitute a mechanism of immune evasion to Fas-mediated killing by T cells[15,16].

The FasL-expressing SW620 cell line is derived from a lymph node metastasis of primary colon cancer. The present study further confirmed that the expressed FasL was demonstrated to be functional, since co-culture experiments using FasL-expressing SW620 cells resulted in the apoptosis of Jurkat T leukemia cells that are sensitive to Fas-mediated apoptosis, which consequently may facilitate metastatic development. Our findings and other data suggest that tumor cells can evade immune attack by downregulating the Fas and inducing apoptosis in activated T lymphocytes through the expression of FasL. Furthermore, the constitutive expression of FasL in hepatic metastatic tumors suggests that FasL may also be important in their colonization in the liver through induction of apoptosis in the surrounding Fas-expressing hepatocytes[17]. FasL expression in human colon cancers is associated with apoptotic depletion of TILs *in vivo*[2]. In addition, upregulation of FasL expression probably induces killing of Fas-bearing tumor cells by promoting the selection of malignant tumor variants, because its Fas pathway has become insensitive to FasL binding. In the tumor microenvironment, IFN and other potentially relevant cytokines may be provided endogenously by immune system interaction, such as $CD4^+$ T cells, following interaction with MHC class II^+ antigen-presenting cells. Ag-specific $CD8^+$ CTLs may then lyse cytokine-modified tumor cells through Fas-dependent and/or Fas-independent pathways, depending upon the intrinsic susceptibility of the tumor population to one or more immune effector mechanisms. Zeytun *et al*.[18], reported a mutual killing model in which $FasL^+$, Fas^+ tumor cells, LSA and EL-4, kill Fas^+ tumor-specific CTLs and are also killed by tumor-specific $FasL^+$ CTLs. They concluded that the survival of the tumor or the host might depend on the cells which can accomplish FasL-based killing more efficiently. It is clear that the highly sophisticated and flexible adaptive immune response of higher vertebrates requires subtle regulation, particularly of receptors that can deliver such a devastating outcome as cell death. Ding *et al*.[19], reported that PMA+ionomycin and endogenous cytokines such as interleukin-18 (IL-18), TNF-α and IFN-γ upregulate the expression of FasL protein in human colon cancer cell lines DLD-1 and SW620. We further showed that the cytotoxicity was significantly enhanced by PMA+ionomycin and TNF-α. Since IFN-γ, TNF-α, and other potentially relevant cytokines are mainly secreted by activated T cells and macrophages, the upregulation of FasL in cancer cells in response to some cytokines may thus counterselect activated TILs and favor a microenvironment of T-cell anergy and the immune escape of cancer cells. Our data suggest that the FasL expressed in human colon cancer cells may be regulated by endogenous factors in the microenvironment of the host and facilitate the escape of tumor cells from the host immune system. Pages *et al*.[20], observed that synthesis of IL-18 decreases or is abolished in colon adenocarcinomas compared to that in normal mucosa, thus resulting in decreasing IFN-γ production and impairing FasL-dependent cytotoxicity of immune cells. This feature is correlated with the existence of distant metastasis and an unfavorable outcome. Xu *et al*.[21], reported that IFN-γ upregulates the expression of Fas and FasL in HT29 cells, a human colon adenocarcinoma cell line, and subsequently induces apoptosis of these cells in an autocrine and paracrine manner. However, it is important to note that many mechanisms of Fas-resistance can also occur, such as Fas-associated phosphatase-1, overexpression of bcl-2 and secretion of soluble Fas from tumor cells in a variety of human tumor cell lines that express Fas[22,23]. TNF-α and IFN-γ are potent immunostimulatory cytokines with tumoricidal effects in a variety of cancers. But at the same time these cytokines might facilitate escape of tumor cells from the host immune system.

Taken together, we also considered a new mechanism of immune evasion, namely, the active destruction of T lymphocytes by tumor cells expressing CD95 ligand. It may provide insights into the processes of both tumor immunity and tumor escape for at least a potential subset or fraction of malignancies. Disarming the Fas counterattack is a conceptually appealing and exciting potential goal for tumor immunotherapy. Ongoing studies are aimed at further understanding the basis of Fas resistance and counterattack, thus determining how to restore tumor cell sensitivity to Fas or block expression or function of FasL in tumor cells.

ACKNOWLEDGMENTS

The authors thank Dr. Joe O'Connell (Cork University Hospital, Ireland) for generously providing the SW620 cell line. The authors also thank Dr. WZ Zhang for excellent technical assistance.

REFERENCES

1 **Lamhamedi-Cherradi SE,** Chen Y. Fas (CD95, Apo-1) ligand gene transfer. *J Clin Immunol* 2001; **21**: 24-29

2 **Houston A,** Bennett MW, O'Sullivan GC, Shanahan F, O'Connell J. Fas ligand mediates immune privilege and not inflammation in human colon cancer, irrespective of TGF-beta expression. *Br J Cancer* 2003; **89**: 1345-1351

3 **Muschen M,** Moers C, Warskulat U, Even J, Niederacher D, Beckmann MW. CD95 ligand expression as a mechanism of

immune escape in breast cancer. *Immunology* 2000; **99**: 69-77
4 **Xu T,** Hao XS, Sun BC. Progress in the research of the relationship between Fas/FasL and tumor. *Zhongguo Zhongliu Linchuang Zazhi* 2003; **30**: 444-448
5 **O'Connell J,** O'Sullivan GC, Collins JK, Shanahan F. The Fas counterattack: Fas-mediated T cell killing by colon cancer cells expressing Fas ligand. *J Exp Med* 1996; **184**: 1075-1082
6 **Fischer U,** Ototake M, Nakanishi T. *In vitro* cell-mediated cytotoxicity against allogeneic erythrocytes in ginbuna crucian carp and goldfish using a non-radioactive assay. *Dev Comp Immunol* 1998; **22**: 195-206
7 **Saff RR,** Spanjaard ES, Hohlbaum AM, Marshak-Rothstein A. Activation-induced cell death limits effector function of CD4 tumor-specific T cells. *J Immunol* 2004; **172**: 6598-6606
8 **Zaks TZ,** Chappell DB, Rosenberg SA, Restifo NP. Fas-mediated suicide of tumor-reactive T cells following activation by specific tumor: selective rescue by caspase inhibition. *J Immunol* 1999; **162**: 3273-3279
9 **Cardi G,** Heaney JA, Schned AR, Ernstoff MS. Expression of Fas (APO-1/CD95) in tumor-infiltrating and peripheral blood lymphocytes in patients with renal cell carcinoma. *Cancer Res* 1998; **58**: 2078-2080
10 **Daniel PT,** Kroidl A, Cayeux S, Bargou R, Blankenstein T, Dorken B. Costimulatory signals through B7.1/CD28 prevent T cell apoptosis during target cell lysis. *J Immunol* 1997; **159**: 3808-3815
11 **Zhu Q,** Deng C. The role of Fas/Fas ligand in tumorgenesis, immune escape, and counterattack in colonic cancer. *Zhonghua Neike Zazhi* 2002; **41**: 378-380
12 **Owen-Schaub LB,** Radinsky R, Kruzel E, Berry K, Yonehara S. Anti-Fas on nonhematopoietic tumors: levels of Fas/APO-1 and bcl-2 are not predictive of biological responsiveness. *Cancer Res* 1994; **54**: 1580-1586
13 **French LE,** Tschopp J. Defective death receptor signaling as a cause of tumor immune escape. *Semin Cancer Biol* 2002; **12**: 51-55
14 **Houston A,** O'Connell J. The Fas signalling pathway and its role in the pathogenesis of cancer. *Curr Opin Pharmacol* 2004; **4**: 321-326
15 **Kim R,** Emi M, Tanabe K, Uchida Y, Toge T. The role of Fas ligand and transforming growth factor beta in tumor progression: molecular mechanisms of immune privilege via Fas-mediated apoptosis and potential targets for cancer therapy. *Cancer* 2004; **100**: 2281-2291
16 **Bennett MW,** O'Connell J, Houston A, Kelly J, O'Sullivan GC, Collins JK, Shanahan F. Fas ligand upregulation is an early event in colonic carcinogenesis. *J Clin Pathol* 2001; **54**: 598-604
17 **Shiraki K,** Tsuji N, Shioda T, Isselbacher KJ, Takahashi H. Expression of Fas ligand in liver metastases of human colonic adenocarcinomas. *Proc Natl Acad Sci USA* 1997; **94**: 6420-6425
18 **Zeytun A,** Hassuneh M, Nagarkatti M, Nagarkatti PS. Fas-Fas ligand-based interactions between tumor cells and tumor-specific cytotoxic T lymphocytes: a lethal two-way street. *Blood* 1997; **90**: 1952-1959
19 **Ding EX,** Zhang W, Wang Q, Chen XY, Fu ZR. Cytokines upregulate Fas ligand protein expression in human colon cancer cells. *Aizheng* 2000; **19**: 966-968
20 **Pages F,** Berger A, Henglein B, Piqueras B, Danel C, Zinzindohoue F, Thiounn N, Cugnenc PH, Fridman WH. Modulation of interleukin-18 expression in human colon carcinoma: consequences for tumor immune surveillance. *Int J Cancer* 1999; **84**: 326-330
21 **Xu X,** Fu XY, Plate J, Chong AS. IFN-gamma induces cell growth inhibition by Fas-mediated apoptosis: requirement of STAT1 protein for up-regulation of Fas and FasL expression. *Cancer Res* 1998; **58**: 2832-2837
22 **Yanagisawa J,** Takahashi M, Kanki H, Yano-Yanagisawa H, Tazunoki T, Sawa E, Nishitoba T, Kamishohara M, Kobayashi E, Kataoka S, Sato T. The molecular interaction of Fas and FAP-1. A tripeptide blocker of human Fas interaction with FAP-1 promotes Fas-induced apoptosis. *J Biol Chem* 1997; **272**: 8539-8545
23 **Ivanov VN,** Lopez Bergami P, Maulit G, Sato TA, Sassoon D, Ronai Z. FAP-1 association with Fas (Apo-1) inhibits Fas expression on the cell surface. *Mol Cell Biol* 2003; **23**: 3623-3635

Science Editor Wang XL and Guo SY **Language Editor** Elsevier HK

PO Box 2345, Beijing 100023, China
www.wjgnet.com
wjg@wjgnet.com

ELSEVIER

World J Gastroenterol 2005;11(25):3920-3924
World Journal of Gastroenterology ISSN 1007-9327

• *BRIEF REPORTS* •

Isoflurane preserves energy balance in isolated hepatocytes during *in vitro* anoxia/reoxygenation

Quan Li, Wei-Feng Yu, Mai-Tao Zhou, Xin Lu, Li-Qun Yang, Ming Zhu, Jian-Gang Song, Jun-Hua Lu

Quan Li, Wei-Feng Yu, Mai-Tao Zhou, Xin Lu, Li-Qun Yang, Ming Zhu, Jian-Gang Song, Department of Anesthesiology, Eastern Hepatobiliary Surgery Hospital, the Second Military Medical University, Shanghai 200438, China
Jun-Hua Lu, Department of Clinical Surgery, Eastern Hepatobiliary Surgery Hospital, the Second Military Medical University, Shanghai 200438, China
Supported by the National Natural Science Foundation of China, No. 39900140
Correspondence to: Dr. Wei-Feng Yu, Department of Anesthesiology, Eastern Hepatobiliary Surgery Hospital, the Second Military Medical University, Shanghai 200438, China. quanligene@sohu.com
Telephone: +86-21-55051447 Fax: +86-21-25070783
Received: 2004-09-23 Accepted: 2004-11-24

Abstract

AIM: To investigate the protective effect of isoflurane on energy balance in isolated hepatocytes during *in vitro* anoxia/reoxygenation, and to compare isoflurane with halothane.

METHODS: Hepatocytes freshly isolated from fed rats were suspended in Krebs-Henseleit buffer, and incubated in sealed flasks under O_2/CO_2 or N_2/CO_2 (95%/5%, V/V) for 30 or 60 min, followed by 5 or 10 min of reoxygenation, with an added volatile anesthetic or not. ATP, ADP, and adenosine monophosphate in hepatocytes were determined by high performance liquid chromatography, and energy charge was calculated.

RESULTS: During 30 min of anoxia, the energy charge and total adenine nucleotide steadily increased with the isoflurane dose from 0 to 2 minimum alveolar anesthetic concentration (MAC), then decreased from 2 to 3 MAC. In short incubations (30-35 min) at 1 MAC isoflurane, energy charge modestly decreased during anoxia, which was partially prevented by isoflurane and completely reversed by reoxygenation, and total adenine nucleotide did not decrease. In long incubations (60-70 min), both energy charge and total adenine nucleotide greatly decreased during anoxia, with partial and no reversal by reoxygenation, respectively. Isoflurane partly prevented decreases in both energy charge and total adenine nucleotide during anoxia and reoxygenation. In addition, 1 MAC isoflurane obviously increased ATP/ADP, which could not be changed by 1 MAC halothane.

CONCLUSION: Isoflurane partially protects isolated hepatocytes against decreases in both energy charge and total adenine nucleotide during short (reversible) or long (irreversible) anoxia.

Key words: Isoflurane; Hepatocytes; Anoxia; Energy balance

Li Q, Yu WF, Zhou MT, Lu X, Yang LQ, Zhu M, Song JG, Lu JH. Isoflurane preserves energy balance in isolated hepatocytes during *in vitro* anoxia/reoxygenation. *World J Gastroenterol* 2005; 11(25): 3920-3924
http://www.wjgnet.com/1007-9327/11/3920.asp

INTRODUCTION

Hepatic anoxia, alone or as a component of ischemia, is an ever-present concern during abdominal surgery, because associated inhibition of energy supply threatens liver cell function and viability[1,2]. Evidence is mounting that the inability of the liver to maintain or regain energy balance during and after surgery is one of the strongest predictors of liver damage and adverse outcome[3,4]. Also, release from injured tissue of metabolites, such as adenosine, with cardiovascular effects may further compromise the anesthetic management of seriously ill or injured patients. Thus, surgeons and anesthesiologists need to be aware of, and to use, whatever measures are available to preserve energy balance in tissues.

The sum of ATP splitting by many concurrent energy-requiring reactions is called "ATP demand." ATP supply occurs mainly via mitochondrial oxidative phosphorylation, which is absolutely dependent on O_2. Under normal conditions, ATP supply easily keeps pace with ATP demand, and adenine nucleotide (high-energy phosphate) exists mainly in the form of ATP, along with relatively small amounts of ADP and adenosine monophosphate (AMP). However, when ATP supply is inhibited by lack of oxygen, ATP demand predominates, ADP and AMP then accumulate at the expense of ATP, and eventually adenosine and other non-nucleotide metabolites appear. Thus, shifts in the balance between ATP supply and demand can be assessed by measuring changes in the absolute and relative levels of ATP and its metabolites. A more complete and accurate expression is energy charge. Energy charge = (ATP+1/2ADP)/(ATP+ADP+AMP).

MATERIALS AND METHODS

Hepatocytes were isolated from adult male Sprague-Dawley rats (250-300 g) having free access to food and water[5]. Livers were perfused *in situ* by using Ca^{2+}-free Krebs-Henseleit buffer (pH 7.4) supplemented with 20 mmol/L

4-(2-hydroxyethyl)-1-piperazineethanesulfonic acid, maintained at 37 ℃ and equilibrated with O_2/CO_2 (95/5). Perfusion was continued for 10 min with buffer alone, then for another 12-14 min with added collagenase (Type I, Sigma Chemical Co., St. Louis, MO). The softened liver was transferred to a plastic weighing dish containing 25 mL Krebs+2% dissolved bovine serum albumin, teased apart with a spatula and chopped finely with sharp scissors. After further dilution to 100 mL with Krebs+2% dissolved bovine serum albumin, the cell slurry was washed into a 500-mL Erlenmeyer flask, gently swirled under a flowing O_2/CO_2 (95%/5% V/V) atmosphere at 37 ℃ for 15 min, then filtered through nylon mesh. Each 12 mL of crude cell suspension was mixed with 28 mL Percoll (Pharmacia, Sweden, obtained from Sigma) and centrifuged at 10 000 *g* for 10 min. The layer of intact, purified hepatocytes at the bottom of the gradient was rinsed free of Percoll by suspension in Krebs and centrifugation for 2 min at 50 r/min. The final pellet contained a total of 2-4×10^8 cells that were 90-95% viable by dye exclusion. Cells were stored for 2 h on ice before use without loss of viability.

In 25-mL round-bottomed flasks, 12.5 million cells were suspended in a total volume of 2.5 mL Krebs+2% dissolved bovine serum albumin (pH 7.4). Flasks were sealed with rubber caps through which 14-gauge needles were inserted for in- and out-flow of gas mixture. After 10 min preincubation under O_2/CO_2, regassing and experimental incubations were carried out as follows: O_2/CO_2 for 35 or 70 min (= oxygenated), N_2/CO_2 for 30 or 60 min (= anoxic), or N_2/CO_2 for 30 or 60 min followed by O_2/CO_2 for 5 or 10 min, respectively (= reoxygenated). All incubations were performed by swirling the flasks in a water bath at 37 ℃. When needed, anesthetics were added at the desired concentrations to the gas mixture used for gassing the flasks by means of a copper kettle vaporizer. Gas chromatography measurements established that anesthetic concentrations in liquid phase reached a constant value within 5-10 min. (The absolute concentrations in the liquid phase varied with anesthetic dose and cell concentration.) Incubations were terminated by injecting 0.5 mL 2 mol/L perchloric acid forcefully into the suspension to arrest enzyme-catalyzed reactions. After removal of precipitated membranes and protein by centrifugation, the clear supernatant containing extracted adenine nucleotides and other metabolites was neutralized with 2 mol/L potassium hydroxide and cooled on ice to precipitate excess potassium perchlorate. The supernatant was decanted and stored at-20 ℃ before metabolite measurements.

ATP, ADP, and AMP were analyzed by high performance liquid chromatography (LDC Analytical, Riviera Beach, FL, USA) using a CM4000 pump interfaced with a SM5000 detector. The separation was accomplished on a C18 reversed phase column. Elution with a binary gradient was carried out at a flow rate of 1.0 mL/min. Mobile phase A consisted of 30 mmol/L potassium phosphate as buffer (pH 6.0) and 8 mmol/L tetrabutylammonium hydrogen sulfate as ion-pairing reagent. Mobile phase B was identical except that it contained 500 mL/L methanol. Recovery of ATP, ADP, and AMP routinely exceeded 90-95%, as estimated from the concentration of caffeine added as an internal standard.

Statistical analysis

Data were presented as mean±SD. One- or two-way analysis of variance with replications and Scheffe's or paired *t*-tests were used for statistical analysis. $P<0.05$ was considered statistically significant.

RESULTS

Figure 1A shows the effect of isoflurane dose on adenine nucleotide levels in isolated hepatocytes after exposure to anoxia for 30 min. ATP levels increased and AMP levels decreased from their respective control values as isoflurane increased from 0 to 2 minimum alveolar anesthetic concentration (MAC, 0-3% concentration), with a slight reversal from 2 to 3 MAC (3-5% concentration). Total adenine nucleotide increased to a lesser degree with isoflurane dose and was significantly higher than baseline only at 2 MAC. Values of ADP did not change significantly from baseline at any dose of isoflurane. Values of energy charge (not shown) paralleled to those of ATP.

Figure 1B shows data obtained from incubations performed for 30-35 min. In cells incubated under O_2 for 35 min, amounts of ATP were maximal and balanced by relatively small amounts of ADP and AMP. Isoflurane slightly decreased ATP while increasing ADP and AMP. Although changes in individual nucleotide concentrations were not statistically significant, they combined to produce a significant decrease in energy charge.

In cells anoxic for 30 min (under N_2 rather than O_2), ATP substantially decreased and ADP and AMP increased compared to oxygenated cells. The associated decrease in energy charge confirmed that anoxia shifted energy balance toward a much lower degree of phosphorylation in the adenine nucleotide pool. When isoflurane was present during anoxia, ATP remained significantly higher and AMP lower than in anoxic cells without isoflurane. These two effects of isoflurane combined to maintain a proportionately higher value of energy charge.

Cells exposed to 30 min of anoxia followed by 5 min of reoxygenation showed values of all three adenine nucleotides and energy charge that were not significantly different from those of cells exposed to O_2 continuously for 30 min. Furthermore, no difference in any of these variables was seen for +isoflurane compared to -isoflurane.

Figure 1C shows results obtained from a second set of cell preparations subjected to incubations for 60-70 min. In cells incubated under O_2 alone for 70 min, absolute and relative amounts of ATP, ADP, and AMP were not significantly different from those incubated for 30 min. The changes produced by inclusion of isoflurane along with O_2 decreased ATP, increased ADP and AMP, and a statis-tically significant decrease in energy charge were only slightly (and not significantly) larger than in cells incubated for 35 min.

In cells that were anoxic (exposed to N_2) for 60 min, values of ATP, ADP, AMP, total adenine nucleotide, and energy charge were all significantly lower than in cells exposed anoxia for 30 min. The effects of including isoflurane during anoxia were also generally more pronounced in cells exposed to anoxia for 60 min: compared to values in the absence of isoflurane, ATP was more than double and energy charge almost double, ADP and total

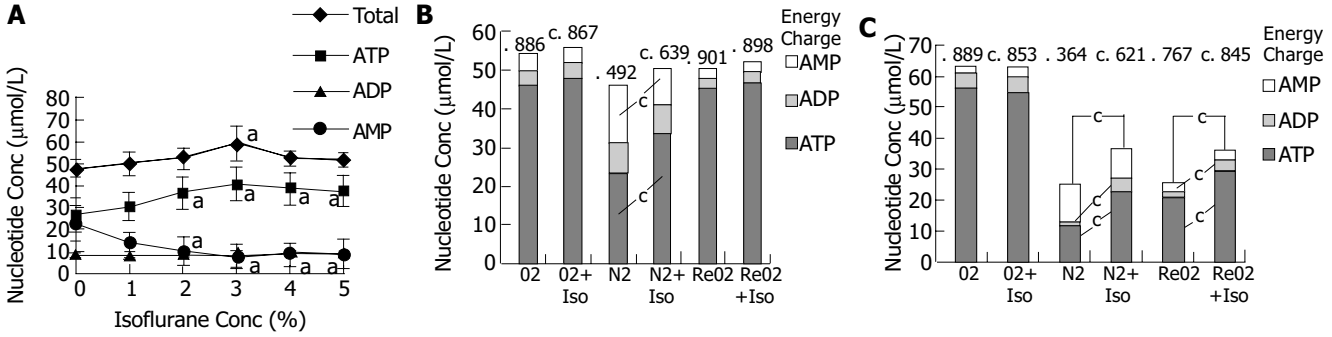

Figure 1 Dependence of ATP, ADP, AMP and total adenine nucleotide and energy charge in isolated hepatocytes on isoflurane during 30 min exposure to anoxia (**A**), anesthetic and oxygenation status during 30-35 min incubation (**B**) and during 60-70 min incubation (**C**). Iso, isoflurane; O_2, oxygenated; N_2, anoxic; ReO_2, reoxygenated after anoxia. Values shown are means for n = 8 experiments. [a]P<0.05 *vs* initial values at 0% isoflurane; [c]P<0.05 *vs* control groups (isoflurane absent).

adenine nucleotide were significantly higher while AMP was not significantly lower.

Reoxygenated cells incubated for longer periods (N_2 for 60 min, O_2 for 10 min) differed greatly from cells subjected to shorter incubations (N_2 30 min, O_2 5 min), whereas values of ADP and AMP were not much different from those of oxygenated cells. Energy charge, ATP and total adenine nucleotide were drastically decreased. Another difference between longer and shorter incubations of reoxygenated cells was that in the longer ones, isoflurane-related differences in energy status persisted into the reoxygenation period; increases in ATP, ADP, and total adenine nucleotide during anoxia were maintained during reoxygenation.

Table 1 shows the data from a separate experiment carried out solely to compare isoflurane and halothane at approximately 1 MAC for their ability to alter energy status in isolated hepatocytes during 30-min exposure to anoxia. ATP/ADP was again higher with 1 MAC isoflurane present than in paired control incubation (isoflurane absent) using cells from the same preparation. With 1 MAC halothane, no difference at all in ATP/ADP during anoxia was seen, each incubated in the presence and absence of that agent.

Table 1 Different effects of isoflurane and halothane on energy status in hepatic cells during 30 min exposure to anoxia (mean±SE)

ATP/ADP	Isoflurane		Halothane	
	O_2	N_2	O_2	N_2
Non-anesthetics Group	5.3±0.6	0.7±0.1	7.4±1.1	1.1±0.3
Anesthetics Group	4.8±0.5	1.2±0.1[a]	7.3±1.5	1.2±0.2

[a]P<0.05 *vs* non-anesthetics group, n = 8.

DISCUSSION

Intact isolated hepatocytes embody a physiologic balance of the reactions involved in ATP supply and demand in a form that permits uniform control and ready measurement of biochemical variables. We have studied these cells extensively under simulated intra-operative conditions to predict energetic responses at the tissue and organ level.

The data in Figure 1B show that the energy-protective effect of isoflurane in anoxic hepatocytes varied in a systematic way with isoflurane dose. There was a graded dose-response relationship from 0 to 2 MAC, with a slight reversal of protection at 3 MAC. It seems that, at least in isolated cells, the energy-protective effect of isoflurane is optimal in the dose range used for clinical anesthesia. The basis for the response "ceiling" at 2 MAC awaits an understanding of the biochemical basis of the protective effect. An important question still to be addressed in this line of investigation is the extent to which the protective effect is associated with the anesthetic state. Is this effect limited to isoflurane or to other halogenated or volatile agents? Does ED50 for the protective effect correlate with MAC?

In the shorter incubation (30-35 min) that examined varying oxygenation status, 1 MAC isoflurane tended to decrease ATP and increase ADP and AMP in cells exposed to oxygen, presumably because isoflurane inhibits mitochondrial recycling of ADP to ATP via oxidative phosphorylation[6,7]. An opposite and larger effect of isoflurane on energy status was found in anoxic cells: superimposed on the great decrease in ATP and energy charge produced by anoxia, the effect of isoflurane was to enhance energy balance rather than to further impair it. In reoxygenated cells, there were neither protective nor detrimental effects of isoflurane on energy balance; and isoflurane produced no effect at all on any of the measured variables of energy status. The similarity between reoxygenated and continuously oxygenated cells indicates that exposure to 30-min anoxia with or without isoflurane has no irreversible effect on the energy status of hepatocytes.

The longer incubation (60-70 min) produced physiologically significant and/or irreversible effects of anoxia on cellular energy status. As in the 35-min incubation, data from cells oxygenated for 70 min showed that non-anoxic injury might have occurred during that period of incubation. The similarities in ATP, ADP, AMP, and total adenine nucleotide values suggest that the longer period of incubation is well tolerated, because damaged cells rapidly lose adenine nucleotides. The effects of anoxia on adenine nucleotide content and energy balance were considerably greater after 60-min exposure to anoxia than after 30-min exposure to anoxia. In anoxic cells after 60-min exposure to anoxia, there was a great decrease in total adenine nucleotide compared to oxygenated cells (*vs*

none at 30 min), the decrease in energy charge was also greater after 60-min exposure to anoxia than after 30-min exposure to anoxia. In reoxygenated cells, none of the effects of 60-min exposure to anoxia were reversed, in contrast to all of the effects of 30-min exposure to anoxia. The importance of total adenine nucleotide in limiting the levels of ATP, ADP, and AMP during brief recovery from anoxia was shown clearly by the almost identically lowered values of total adenine nucleotide in corresponding anoxic and reoxygenated cells after 70-min exposure to anoxia. Also, in contrast to the shorter incubation, in the longer incubation the protective effect of isoflurane was observed during anoxia-increased energy charge and total adenine nucleotide was persistent through the reoxygenation period.

As mentioned earlier, the measured values of ATP, ADP, and AMP concentrations and the calculated values of total adenine nucleotide and energy charge in isolated hepatocytes are sensitive indicators of changes in the dynamic balance of ATP supply and demand. The anesthetic effects reported here may well be due to the direct action of the drug on one or more of the intracellular reactions involved in producing or consuming ATP[8-10]. The results of other studies suggested that the protective effect of isoflurane may be due to "decreased metabolism" and, more precisely, due to inhibition of ATP demand[11-13]. The conclusion holds also for the findings of the present study. Previous studies showed that isoflurane causes a dose-related decrease in O_2 consumption in isolated hepatocytes[14]. However, it would be erroneous to conclude that this decrease in O_2 consumption reflects primary inhibition of ATP demand (with secondary inhibition of mitochondrial oxidative phosphorylation via respiratory control), because volatile anesthetics are also able to inhibit oxidative phosphorylation directly[15,16]. In fact, inhibition of ATP demand in intact cells can be ascertained only by direct measurement of ATP consumption.

Two possible mechanisms may be mentioned by which decreased AMP formation can maintain ATP levels. An anoxia-induced increase in AMP promotes its degradation to adenosine and other non-nucleotide metabolites[17]. The latter step seems to be a physiologic "point of no return", because ATP is not easily resynthesized from its non-nucleotide metabolites when oxygen and ATP supply are restored[17]. Thus, a decrease in AMP formation would decrease the rate of ensuing AMP degradation and loss of total adenine nucleotide. Also, a decrease in AMP formation from ADP via inhibition of adenylate kinase can preserve the availability of ADP for conversion back to ATP via glycolysis.

The present study demonstrates that 1 MAC isoflurane actually helps to preserve liver cell energy balance during anoxia (whereas 1 MAC halothane has no such effect). The demonstration of this protective effect might be crucially dependent on the specific experimental conditions used in this study. Relatively short periods of anoxic exposure may prevent enzymes that catalyze ATP-consuming reactions from being degraded to the extent that inhibition of their activity by isoflurane could not be detected. Also, the use of anoxia (0% O_2) rather than hypoxia may eliminate vestiges of mitochondrial ATP formation, anesthetic inhibition of which may decrease ATP/ADP and thus opposing or even canceling ATP/ADP increases resulting from anesthetic inhibition of ATP consumption[18,19].

For optimal anesthetic and surgical care, we need to know as much as possible about the effects and actions of the drugs we use, especially with regard to a process as essential as energy balance. The work described here has documented certain effects of isoflurane on ATP supply and demand at the cellular level and laid the groundwork for explaining them in terms of actions on specific biochemical reactions that produce and consume ATP. In addition to further elucidate such basic mechanisms, we also need to examine the consequence of these cellular effects in physiologic and clinical terms, by using more intact systems and measures of outcome.

REFERENCES

1 **Vagts DA,** Iber T, Puccini M, Szabo B, Haberstroh J, Villinger F, Geiger K, Noldge-Schomburg GF. The effects of thoracic epidural anesthesia on hepatic perfusion and oxygenation in healthy pigs during general anesthesia and surgical stress. *Anesth Analg* 2003; **97**: 1824-1832

2 **Ishida H,** Kadota Y, Sameshima T, Nishiyama A, Oda T, Kanmura Y. Comparison between sevoflurane and isoflurane anesthesia in pig hepatic ischemia-reperfusion injury. *J Anesth* 2002; **16**: 44-50

3 **Net M,** Valero R, Almenara R, Deulofeu R, Lopez-Boado MA, Capdevila L, Barros P, Bombi JA, Agusti M, Adalia R, Ruiz A, Arce Y, Manyalich M, Garcia-Valdecasas JC. Hepatic preconditioning after prolonged warm ischemia by means of S-adenosyl-L-methionine administration in pig liver transplantation from non-heart-beating donors. *Transplantation* 2003; **75**: 1970-1977

4 **Diskin MG,** Mackey DR, Roche JF, Sreenan JM. Effects of nutrition and metabolic status on circulating hormones and ovarian follicle development in cattle. *Anim Reprod Sci* 2003; **78**: 345-370

5 **Liu XL,** Li LJ, Chen Z. Isolation and primary culture of rat hepatocytes. *Hepatobiliary Pancreat Dis Int* 2002; **1**: 77-79

6 **Da-Silva WS,** Gomez-Puyou A, Gomez-Puyou MT, Moreno-Sanchez R, De Felice FG, De Meis L, Oliveira MF, Galina A. Mitochondrial bound hexokinase activity as a preventive antioxidant defense: Steady-state ADP formation as a regulatory mechanism of membrane potential and reactive oxygen species generation in mitochondria. *J Biol Chem* 2004; **279**: 39846-39855

7 **Ason B,** Handayani R, Williams CR, Bertram JG, Hingorani MM, O'Donnell M, Goodman MF, Bloom LB. Mechanism of loading the Escherichia coli DNA polymerase III beta sliding clamp on DNA. Bona fide primer/templates preferentially trigger the gamma complex to hydrolyze ATP and load the clamp. *J Biol Chem* 2003; **278**: 10033-10040

8 **Leal NA,** Olteanu H, Banerjee R, Bobik TA. Human ATP: Cob(I)alamin adenosyltransferase and its interaction with methionine synthase reductase. *J Biol Chem* 2004; **10**: 694-698

9 **Halestrap AP.** Mitochondrial permeability: dual role for the ADP/ATP translocator? *Nature* 2004; **430**: 1

10 **Kokoszka JE,** Waymire KG, Levy SE, Sligh JE, Cai J, Jones DP, MacGregor GR, Wallace DC. The ADP/ATP translocator is not essential for the mitochondrial permeability transition pore. *Nature* 2004; **427**: 461-465

11 **Korzeniewski B.** Influence of substrate activation (hydrolysis of ATP by first steps of glycolysis and beta-oxidation) on the effect of enzyme deficiencies, inhibitors, substrate shortage and energy demand on oxidative phosphorylation. *Biophys Chem* 2003; **104**: 107-119

12 **Koebmann BJ,** Westerhoff HV, Snoep JL, Solem C, Pedersen MB, Nilsson D, Michelsen O, Jensen PR. The extent to which ATP demand controls the glycolytic flux depends strongly on

the organism and conditions for growth. *Mol Biol Rep* 2002; **29**: 41-45

13 **Korzeniewski B.** Parallel activation in the ATP supply-demand system lessens the impact of inborn enzyme deficiencies, inhibitors, poisons or substrate shortage on oxidative phosphorylation *in vivo*. *Biophys Chem* 2002; **96**: 21-31

14 **Pathak BL,** Becker GL, Reilly PJ, Hanson KA, Landers DF. Isoflurane partially preserves energy balance in isolated hepatocytes during *in vitro* anoxia. *Anesth Analg* 1991; **72**: 571-577

15 **Kayser EB,** Morgan PG, Sedensky MM. Mitochondrial complex I function affects halothane sensitivity in Caenorhabditis elegans. *Anesthesiology* 2004; **101**: 365-372

16 **Liu ZH,** He Y, Jin WQ, Chen XJ, Shen QX, Chi ZQ. Effect of chronic treatment of ohmefentanyl stereoisomers on cyclic AMP formation in Sf9 insect cells expressing human mu-opioid receptors. *Life Sc* 2004; **74**: 3001-3008

17 **Vincent MF,** Van den Berghe G, Hers HG. The pathway of adenine nucleotide catabolism and its control in isolated rat hepatocytes subjected to anoxia. *Biochem J* 1982; **202**: 117-123

18 **Becker GL,** Hensel P, Holland AD, Miletich DJ, Albrecht RF. Eenergy deficits in hepatocytes isolated from phenobarbital treated or fasted rats and briefly exposed to halothane and hypoxia *in vitro*. *Anesthesiology* 1986; **65**: 379-384

19 **Kenniston JA,** Baker TA, Fernandez JM, Sauer RT. Linkage between ATP consumption and mechanical unfolding during the protein processing reactions of an AAA+ degradation machine. *Cell* 2003; **114**: 511-520

Science Editor Wang XL and Guo SY **Language Editor** Elsevier HK

PO Box 2345, Beijing 100023, China
www.wjgnet.com
wjg@wjgnet.com

ELSEVIER

World J Gastroenterol 2005;11(25):3925-3930
World Journal of Gastroenterology ISSN 1007-9327

• *BRIEF REPORTS* •

Clinical evidence of growth hormone for patients undergoing abdominal surgery: Meta-analysis of randomized controlled trials

Yong Zhou, Xiao-Ting Wu, Gang Yang, Wen Zhuang, Mao-Ling Wei

Yong Zhou, Xiao-Ting Wu, Gang Yang, Wen Zhuang, Department of General Surgery, West China Hospital, Sichuan University, Chengdu 610041, Sichuan Province, China
Mao-Ling Wei, Chinese Evidence-Based Medicine/Cochrane Center, Chengdu 610041, Sichuan Province, China
Supported by the China Medical Board of New York No. 98-680
Correspondence to: Professor Xiao-Ting Wu, Department of General Surgery, West China Hospital, Sichuan University, 37 Guo Xue Road, Chengdu 610041, Sichuan Province, China. nutritioner@163.com
Telephone: +86-28-85422480 Fax: +86-28-85422411
Received: 2004-05-27 Accepted: 2004-06-17

Abstract

AIM: To assess the effectiveness and safety of perioperative growth hormone (GH) in patients undergoing abdominal surgery.

METHODS: We searched the following electronic databases: MEDLINE, EMBASE, the Cochrane Controlled Trials Register, Chinese Bio-medicine Database. The search was undertaken in February 2003. No language restrictions were applied. Randomized controlled trials (RCT) comparing GH with placebo in patients undergoing abdominal surgery were extracted and evaluated. Methodological quality was evaluated using the Jadad scale.

RESULTS: Eighteen trials involving 646 patients were included. The combined results showed that GH had a positive effect on improving postoperative nitrogen balance (standardized mean difference [SMD] = 3.37, 95%CI [2.46, 4.27], $P<0.00001$), and decreasing the length of hospital stay (weighted mean difference [WMD] = -2.07, 95%CI [-3.03, -1.11], $P = 0.00002$), and reducing the duration of postoperative fatigue syndrome (SMD = -1.83, 95%CI [-2.37, -1.30], $P<0.00001$), but it could increase blood glucose levels (WMD = 0.91, 95%CI [0.56, 1.25], $P<0.00001$).

CONCLUSION: GH for patients undergoing abdominal surgery is effective and safe, if blood glucose can be controlled well. Further trials are required with a sufficient size to account for clinical heterogeneity and to measure other important outcomes such as infection, morbidity, mortality, fluid retention, immunomodulatory effects, and tumor recurrence.

Key words: Perioperative growth hormone; Abdominal surgery

Zhou Y, Wu XT, Yang G, Zhuang W, Wei ML. Clinical evidence of growth hormone for patients undergoing abdominal surgery: Meta-analysis of randomized controlled trials. *World J Gastroenterol* 2005; 11(25): 3925-3930
http://www.wjgnet.com/1007-9327/11/3925.asp

INTRODUCTION

Catabolism and negative nitrogen balance is a part of the metabolic reaction to major abdominal surgical trauma. It is a concern to surgeons because the catabolic response is correlated with the overall surgical morbidity rate, causing prolonged convalescence. Growth hormone (GH) has been shown to have anabolic effects and to reduce or even prevent nitrogen catabolism in patients undergoing abdominal surgery. The effect of GH has recently been studied by many researchers. In 1974 Wilmore *et al*.[1], suggested that adequate nutritional intake was necessary for GH to have nitrogen-saving effects. In 1986 the study by Phillips[2] demonstrated that GH stimulated hepatic production of somatomedin (insulin-like growth factor-I, IGF-I) whose action could promote diverse anabolic processes, such as synthesis of RNA, DNA, proteins or proteoglycans. However, the effects of GH on nonmetabolic clinical outcome remain unclear.

Meta-analysis has been gradually used in medicine to improve the statistical efficiency, to evaluate the disadvantages of formulated researches and hypothesis, and to reach reliable conclusions from the mixed assortment of potentially relevant studies to determine the most promising directions for future researches. We performed a meta-analysis of available studies to assess the effectiveness and safety, in order to improve our understanding of the clinical effects of perioperative GH treatment of patients undergoing abdominal surgery; clinical outcomes including nitrogen balance, length of hospital stay, blood glucose, and postoperative fatigue syndrome were measured. Other important outcomes, such as infection, morbidity, mortality, fluid retention, immunomodulatory effects and tumor recurrence, were also measured.

MATERIALS AND METHODS

Identification of trials

Our aim was to identify all relevant randomized controlled trials (RCT) that compared GH with placebo in patients undergoing abdominal surgery. A RCT was defined as a

trial in which patients were assigned prospectively to one of two interventions by random allocation. We used a multimethod to identify relevant studies for the present review. A computerized literature search of MEDLINE from 1966 to October 2002 was conducted using the following search terms: operation OR surgery OR postoperative OR perioperative AND GH AND RCT (publication type) or controlled clinical trials or clinical trials, randomized. In addition, we searched Embase (1980-2002), Cochrane Controlled Trials Register (Issue 1, 2003), and Chinese Biomedicine Database (1979-2002), reviewed our personal files, and contacted experts in the field. Bibliographies of all selected articles and review articles that included information on GH were reviewed for other relevant articles. This search strategy was done iteratively, until no new potential, randomized, controlled trial citations were found on review of the reference lists of retrieved articles.

Study selection and data extraction

The following selection criteria were used to identify published studies for inclusion in this analysis: study design - randomized clinical trial, population - hospitalized adult patients undergoing abdominal surgery, intervention - GH *vs* placebo initiated at the same time and with the same nutrition support, and outcome variables - at least one of the following primary outcome variables: nitrogen balance, length of hospital stay, blood glucose, postoperative fatigue syndrome, incidence of infection, morbidity, mortality, fluid retention, immunomodulatory effects, and tumor recurrence. Study selection and data abstraction were conducted independently by the two investigators.

Data analysis

The incidences of infection, tumor recurrence, fluid retention, morbidity, and mortality were treated as binary variables. Nitrogen balance, length of hospital stay, blood glucose, postoperative fatigue syndrome, and immunomodulatory effects were treated as continuous variables. Data analysis was performed using the random effect model with meta-analysis software (RevMan 4.2; Cochrane Collaboration, Oxford, UK). The continuous data outcomes were presented with 95% confidence intervals (CIs). When authors reported standard deviations, we used them directly. When standard deviations were not available, we computed them from the observed mean differences (either differences in changes or absolute readings) and the test statistics. When the test statistics were not available, given a *P* value, we computed the corresponding test statistics from tables for the normal distribution. We tested heterogeneity between trials with χ^2 tests, with $P<0.05$ indicating significant heterogeneity[3]. Methodological quality was evaluated using the Jadad scale[4].

RESULTS

From 460 articles screened, 38 were identified as RCT comparing GH with placebo and included for data extraction. Twenty studies were excluded, and the remaining 18 trials were included in the present meta-analysis[5-22]. Only one study[19] was in Chinese. Articles were excluded for the following reasons, namely the outcomes of interest were not recorded[23-37] and some articles repeated[38-42]. A total of 646 patients were enrolled in the included studies. The characteristics of studies included in meta-analysis comparing GH with placebo are presented in Table 1. Not all of the studies reported the outcome of interest, postoperative nitrogen balance was reported in 11 studies[5-15], length of hospital stay in 3 studies[17-19], postoperative fatigue syndrome in 3 studies[20-22], blood glucose in 6 studies[12-17].

The combined results showed that GH had a positive effect on improving the postoperative nitrogen balance (standardized mean difference [SMD] = 3.37, 95%CI [2.46, 4.27], $P<0.00001$) (Table 2A), and decreasing the length of hospital stay (weighted mean difference [WMD]=-2.07, 95%CI [-3.03, -1.11], $P = 0.00002$) (Table 2B), and reducing the duration of postoperative fatigue syndrome (SMD = -1.83, 95%CI [-2.37, -1.30], $P<0.00001$) (Table 2C), but it could increase blood glucose levels (WMD = 0.91, 95%CI [0.56, 1.25], $P<0.00001$) (Table 2D).

Table 1 Characteristics of studies included in meta-analysis comparing GH with placebo

Study	Year	Jadad score	Reference	Operation	GH
Lehner	1992	3	6	Major abdominal surgery	0.3 IU / kg / d for 5 d
López	1993	1	7	Major surgery of the digestive tract	0.2 IU / kg / d for 6 d
Wong	1995	2	8	Major abdominal surgery	0.2 IU / kg / d for 7 d
Tacke	1994	1	9	Major gastrointestinal surgery	0.3 IU / kg / d for 5 d
Saito	1992	3	10	Major abdominal operation	0.4 IU / kg / d for 6 d
Kolstad	2001	5	11	Laparoscopic cholecystectomy	13 IU / m^2 / d for 3 d
Jensen	1998	5	12	Ileoanal anastomosis with a J pouch	12 IU / d for 6 d
Ponting	1988	2	13	Major gastrointestinal surgery	0.1 mg / kg / d for 7 d
Hammarqvist	1992	1	14	Elective cholecystectomy	0.3 IU / kg / d for 3 d
Jiang	1989	4	15	Gastrectomy or colectomy	0.15 IU / kg / d for 7 d
Mjaaland	1991	3	16	Gastrointestinal surgery	24 IU / d for 5 d
Barle	2001	1	17	Laparoscopic cholecystectomy	12 IU / d for 5 d
Vara-Thorbeck 1	1993	3	18	Cholecystectomy	8 IU / d for 7 d
Barry 2	1998	4	19	Abdominal aortic aneurysm repair	0.3 IU / kg / d for 6 d
Liu	2001	5	20	Abdominal surgery	0.3 IU / kg / d for 5 d
Barry 1	1999	3	21	Abdominal aortic aneurysm repair	0.3 IU / kg / d for 6 d
Kissmeyer-Nielsen	1999	5	22	Ileoanal J-pouch surgery	12 IU / d for 6 d
Vara-Thorbeck 2	1996	3	23	Cholecystectomy	8 IU / d for 7 d

Table 2 Random effect model of standardized mean difference (95%CI) in improving postoperative nitrogen balance (A) and in reducing the duration of postoperative fatigue syndrome (C) and weighted mean difference (95%CI) in decreasing the length of hospital stay (B) and in increasing blood glucose levels (D) with GH as compared with placebo

A

Study	Treatment *n*	Treatment Mean (SD)	Control *n*	Control Mean (SD)	Weight %	SMD (random) 95%CI
Ponting	6	1.80 (0.40)	5	-0.90 (0.70)	6.23	4.46 [1.85, 7.07]
Jiang	9	-7.10 (3.12)	9	-32.60 (4.20)	6.27	6.56 [3.97, 9.16]
Mjaaland	9	4.10 (1.10)	10	-3.10 (1.80)	8.36	4.55 [2.69, 6.41]
Hammarqvist	8	-2.32 (1.66)	9	-7.09 (0.71)	8.91	3.63 [1.94, 5.32]
Lehner	19	-4.30 (9.60)	21	-14.80 (3.30)	11.94	1.46 [0.76, 2.17]
Saito	18	-18.00 (3.30)	18	-185.00 (58.00)	10.60	3.98 [2.80, 5.15]
López	9	-7.30 (2.80)	9	-20.70 (4.10)	9.09	3.64 [2.00, 5.27]
Tacke	9	-10.00 (2.61)	10	-20.47 (3.86)	9.85	3.00 [1.60, 4.40]
Wong	8	3.00 (0.90)	7	-1.30 (0.75)	7.15	4.85 [2.59, 7.11]
Jenson	9	-47.00 (20.00)	10	-73.00 (20.00)	11.12	1.24 [0.24, 2.25]
Kolstad	11	-3.90 (0.40)	10	-5.70 (0.90)	10.49	2.53 [1.32, 3.73]
Total (95%CI)	115		118		100.00	3.37 [2.46, 4.27]

Test for heterogeneity: x^2 = 44.48, df = 10 (*P*<0.00001), I^2 = 77.5%. Test for overall effect: *Z* = 7.27 (*P*<0.00001).

B

Study	Treatment *n*	Treatment Mean (SD)	Control *n*	Control Mean (SD)	Weight %	WMD (fixed) 95%CI
Barry 2	8	13.00 (2.00)	10	17.00 (3.00)	17.05	-4.00 [-6.32, -1.68]
Liu	10	9.70 (1.80)	10	10.50 (1.30)	48.41	-0.80 [-2.18, 0.58]
Vara-Thorbeck 1	87	9.60 (3.60)	93	12.50 (7.10)	34.54	-2.90 [-4.53, -1.27]
Total (95%CI)	105		113		100.00	-2.07 [-3.03, -1.11]

Test for heterogeneity: x^2 = 6.93, df = 2 (*P*= 0.03), I^2 = 71.1%. Test for overall effect: *Z* = 4.24 (*P*<0.0001).

C

Study	Treatment *n*	Treatment Mean (SD)	Control *n*	Control Mean (SD)	Weight %	SMD (fixed) 95%CI
Barry 1	7	1.60 (1.20)	10	4.90 (2.20)	21.23	-1.68 [-2.84, -0.52]
Kissmeyer-Nielsen	9	1.37 (0.55)	10	2.73 (2.00)	31.57	-0.86 [-1.82, 0.09]
Vara-Thorbeck 2	22	1.52 (0.43)	26	3.14 (0.75)	47.20	-2.55 [-3.33, -1.77]
Total (95%CI)	38		46		100.00	-1.83 [-2.37, -1.30]

Test for heterogeneity: x^2 = 7.32, df = 2 (*P* = 0.03), I^2 = 72.7%. Test for overall effect: *Z* = 6.72 (*P*<0.00001).

D

Study	Treatment *n*	Treatment Mean (SD)	Control *n*	Control Mean (SD)	Weight %	WMD (random) 95%CI
Barle	10	6.40 (1.00)	10	5.40 (0.50)	11.98	1.00 [0.31, 1.69]
Hammarqvist	8	5.60 (0.30)	9	4.80 (0.20)	20.69	0.80 [0.55, 1.05]
Jiang	9	6.17 (0.51)	9	6.06 (0.50)	16.26	0.11 [-0.36, 0.58]
Mjaaland	9	5.75 (0.43)	10	4.90 (0.30)	18.94	0.85 [0.51, 1.19]
Ponting	6	9.40 (0.70)	5	7.20 (0.50)	11.68	2.20 [1.49, 2.91]
Vara-Thorbeck 1	87	6.56 (1.02)	93	5.66 (0.71)	20.46	0.90 [0.64, 1.16]
Total (95%CI)	129		136		100.00	0.91 [0.56, 1.25]

Test for heterogeneity: x^2 = 23.97, df = 5 (*P* = 0.0002), I^2 = 79.1%. Test for overall effect: *Z* = 5.13 (*P*<0.00001).

DISCUSSION

The results must be interpreted with the difference in patients, dose or length of treatment, and unexplained heterogeneity. Clinical heterogeneity in the form of age, etiology and operation of patients points to the possibility of bias.

This meta-analysis did not show that GH had a positive effect on improving postoperative nitrogen balance. Eleven studies involving 233 patients were included. Although there was a heterogeneity (test for heterogeneity χ^2 = 44.48, df = 10, *P*<0.00001), the result was sure. Because all the 11 studies showed that GH had a positive effect on improving postoperative nitrogen balance with a statistical significance (minimum of SMD = 1.24, 95%CI [0.24, 2.25]). However, it seems that different doses had different effects, subgroup was not used. What attention should be paid to is that some studies only reported the cumulated nitrogen balance or the daily nitrogen balance. Further research should be done to assess the possible best dose.

To date, only three studies involving 218 patients, have examined whether treatment with GH could influence the length of hospital stay. The combined results showed that administration of GH could decrease the length of hospital stay. The results must be interpreted with caution due to the small size. Two of three trials[17,18] showed statistically and clinically significant differences in the length of hospital stay. So, further trials are required with a sufficient size to

account for clinical heterogeneity and length of hospital stay.

This meta-analysis showed that administration of GH could reduce the duration of postoperative fatigue syndrome after 1 mo. Three studies involving 84 patients were included. The evidence was not strong due to the small size and unexplained heterogeneity. It is also important to recognize that two[20,21] of the RCTs included in this review were not designed specifically to reduce postoperative fatigue and provided few or no theoretical rationales as to why the intervention under study might be expected to attenuate it. Attempts to assess fatigue objectively by measuring, for example, physical activity, time taken to return to normal routine, or involuntary or voluntary muscle force were problematic because they could be confounded by numerous factors including pain and anxiety. Much effort has therefore been devoted to developing short and easy-to-use questionnaires that could provide some quantification of a patient's subjective feeling of fatigue. Future research should ensure that an adequate measure of subjective fatigue is employed, possibly in tandem with important objective measures, such as time taken to return to work.

This meta-analysis did not show that GH might increase blood glucose levels. Six studies involving 265 patients were included. Of the six, only the study of Jiang *et al*.[14], did not reach a statistical significance (SMD = 0.11, 95%CI [-0.36, 0.58]). Low-dose GH and hypocaloric nutrition may be the reason. Confirmation of the diabetogenic properties of GH was made after it was administered in excess to experimental animals and men. Transgenic animals, which over-expressed GH, developed insulin resistance, marked hyperinsulinemia, hyperglycemia, and hypertriglyceridemia in association with a number of molecular abnormalities[43,44]. Patients with acromegaly developed insulin resistance and hyperinsulinemia, while up to 40% became diabetic[45,46]. There is evidence that insulin resistance caused by GH plays an important role in the rise of blood glucose. In addition, GH could stimulate lipolysis with the release of glycerol and non-esterified fatty acids (NEFA). This provides a further mechanism for the diabetogenic properties of GH through the effect of NEFA to increase hepatic glucose output and decrease peripheral glucose oxidation according to the glucose-fatty acid cycle[47,48]. In fact, in the study of Berman *et al*.[23], the GH group had significantly elevated urine glucose levels throughout the study period, consistent with the demonstrated hyperglycemia and only moderately elevated insulin levels. Treatment with GH did result in hyperglycemia, and two patients were removed from the study. Hyperglycemia associated with GH administration could be treated easily by insulin, especially in long-term GH administration.

Only one RCT[36] conducted an analysis of a multicenter study with 104 patients undergoing major gastrointestinal surgery to assess the risk of long-term tumor recurrence after short-term (5 d) postoperative GH treatment. The study was a follow-up of a previous randomized study investigating the effect of three different doses of GH (0.075, 0.15, and 0.30 IU/kg/d) on the postoperative cumulative nitrogen balance in patients undergoing major surgery. Tumors recurred in 20 (35%) patients who were evaluated for and treated with GH (n = 57). This accounted for 4 of 17 (23%) patients given 0.075 IU/kg/d of GH, 9 of 20 (45%) given 0.15 IU/kg/d of GH, and 7 of 20 (35%) given 0.30 IU/kg/d. By comparison, tumors recurred in 8 of 18 (44%) of patients given placebo. The result of this study demonstrated that short-term treatment with GH for 5 d after major gastrointestinal surgery for adenocarcinoma did not increase the risk of tumor recurrence. But the group size was too small to further stratify the patients according to tumor type and tumor stage, so that no information was gained about the influence of GH dose in certain tumor stages.

Fluid retention is one of known side effects of GH administration. The sodium and fluid retaining impact of GH was demonstrated in humans almost 50 years ago by Ikkos *et al*.[49]. Underlying mechanisms of GH-induced fluid retention are as follows. GH could increase glomerular filtration rate mediated by insulin-like growth factor (IGF-I)[50-52], stimulate the renin-angiotensin-aldosterone system (RAAS)[53-57], reduce atrial natriuretic factors[58-61], and prostaglandins could play a role in GH-induced fluid retention[62]. In the study of Berman *et al*.[23], two GH patients were removed from the study for fluid retention. These patients were in the immediate postoperative period. However, whether the fluid retention was a result of surgery or GH administration could not be determined.

GH should not be given in acute inflammatory disease states. Findings by Takala *et al*.[63], pointed to the immunomodulatory effects of GH. These authors described higher hospital mortality in a Finish and an European study on critically ill non-cancer patients. It was proposed that the higher mortality was due to the application of GH at a later stage during the inflammatory disease process, leading to uncontrolled systemic inflammation. However, infection was not measured in these trials except one[17]. Only one RCT[18] reported the morbidity and mortality, so we could not draw a conclusion due to the small size. But there are still four studies[64-67] awaiting assessment in other languages or we cannot find the full text.

In conclusion, perioperative GH treatment of patients undergoing abdominal surgery can improve the postoperative nitrogen balance, and decrease the length of hospital stay, and reduce the duration of postoperative fatigue syndrome. But it might increase blood glucose levels. However, the evidence is not strong due to the difference in patients, dose or length of treatment, and unexplained heterogeneity. In order to examine the effectiveness and safety of perioperative GH treatment of patients undergoing abdominal surgery, further trials are required with a sufficient size to account for the clinical heterogeneity and to measure other important outcomes such as infection, morbidity, mortality, fluid retention, immunomodulatory effects, and tumor recurrence.

ACKNOWLEDGEMENTS

We are sincerely grateful to the principal investigators of all the trials who provided additional unpublished information. We also thank Susanne Ebrahim and Karla Bergerhoff for diligent working in Cochrane Metabolic and Endocrine Disorders Group and Ming Liu, He-Ming Huang, Bin Lv, Eewen, Jian-Kun Hu, Hua Jiang and Shu-Ai Xiao for providing additional references.

REFERENCES

1 **Wilmore DW,** Moylan JA Jr, Bristow BF, Mason AD Jr, Pruitt BA Jr. Anabolic effects of human growth hormone and high caloric feedings following thermal injury. *Surg Gynecol Obstet* 1974; **138**: 875-884

2 **Phillips LS.** Nutrition, somatomedins, and the brain. *Metabolism* 1986; **35**: 78-87

3 **Oxman AD,** Cook DJ, Guyatt GH. Users' guides to the medical literature. VI. How to use an overview. Evidence-Based Medicine Working Group. *JAMA* 1994; **272**: 1367-1371

4 **Jadad AR,** Moore RA, Carroll D, Jenkinson C, Reynolds DJ, Gavaghan DJ, McQuay HJ. Assessing the quality of reports of randomized clinical trials: is blinding necessary? *Control Clin Trials* 1996; **17**: 1-12

5 **Lehner JH,** Jauch KW, Berger G. A multicentre study of the dose response effect of human recombinant growth hormone (rhGH) on cumulative nitrogen balance (CNB) in patients after major abdominal surgery [abstract]. *Clin Nutr* 1992; **11** (Suppl): 75-76

6 **López J,** Fernández C, Carriedo D. Metabolic effects of recombinant growth hormone following major surgery of the digestive tract [abstract]. *Medicina Intensiva* 1993; **17**(Suppl): 82

7 **Wong WK,** Soo KC, Nambiar R, Tan YS, Yo SL, Tan IK. The effect of recombinant growth hormone on nitrogen balance in malnourished patients after major abdominal surgery. *Aust N Z J Surg* 1995; **65**: 109-113

8 **Tacke J,** Bolder U, Lohlein D. Improved cumulated nitrogen balance after administration of recombinant human growth hormone in patients undergoing gastrointestinal surgery. *Infusionsther Transfusionsmed* 1994; **21**: 24-29

9 **Saito H,** Taniwaka K, Muto T. Effects of growth hormone dose after major abdominal operation: a randomized, prospective, multicenter trial [abstract]. *Clin Nutr* 1992; **11**(Suppl): 9

10 **Kolstad O,** Jenssen TG, Ingebretsen OC, Vinnars E, Revhaug A. Combination of recombinant human growth hormone and glutamine-enriched total parenteral nutrition to surgical patients: effects on circulating amino acids. *Clin Nutr* 2001; **20**: 503-510

11 **Jensen MB,** Kissmeyer-Nielsen P, Laurberg S. Perioperative growth hormone treatment increases nitrogen and fluid balance and results in short-term and long-term conservation of lean tissue mass. *Am J Clin Nutr* 1998; **68**: 840-846

12 **Ponting GA,** Halliday D, Teale JD, Sim AJ. Postoperative positive nitrogen balance with intravenous hyponutrition and growth hormone. *Lancet* 1988; **1**: 438-440

13 **Hammarqvist F,** Stromberg C, von der Decken A, Vinnars E, Wernerman J. Biosynthetic human growth hormone preserves both muscle protein synthesis and the decrease in muscle-free glutamine, and improves whole-body nitrogen economy after operation. *Ann Surg* 1992; **216**: 184-191

14 **Jiang ZM,** He GZ, Zhang SY, Wang XR, Yang NF, Zhu Y, Wilmore DW. Low-dose growth hormone and hypocaloric nutrition attenuate the protein-catabolic response after major operation. *Ann Surg* 1989; **210**: 513-525

15 **Mjaaland M,** Unneberg K, Hotvedt R, Revhaug A. Nitrogen retention caused by growth hormone in patients undergoing gastrointestinal surgery with epidural analgesia and parenteral nutrition. *Eur J Surg* 1991; **157**: 21-27

16 **Barle H,** Rahlen L, Essen P, McNurlan MA, Garlick PJ, Holgersson J, Wernerman J. Stimulation of human albumin synthesis and gene expression by growth hormone treatment. *Clin Nutr* 2001; **20**: 59-67

17 **Vara-Thorbeck R,** Guerrero JA, Rosell J, Ruiz-Requena E, Capitan JM. Exogenous growth hormone: effects on the catabolic response to surgically produced acute stress and on postoperative immune function. *World J Surg* 1993; **17**: 530-538

18 **Barry MC,** Mealy K, Sheehan SJ, Burke PE, Cunningham AJ, Leahy A, Bouchier Hayes D. The effects of recombinant human growth hormone on cardiopulmonary function in elective abdominal aortic aneurysm repair. *Eur J Vasc Endovasc Surg* 1998; **16**: 311-319

19 **Liu W.** The impact of pretreatment with recombinant human growth hormone on intestinal barrier function and cell immune function. *Zhongguo Linchuang Yingyang Zazhi* 2001; **4**: 77-80

20 **Barry MC,** Mealy K, O'Neill S, Hughes A, McGee H, Sheehan SJ, Burke PE, Bouchier-Hayes D. Nutritional, respiratory, and psychological effects of recombinant human growth hormone in patients undergoing abdominal aortic aneurysm repair. *JPEN* 1999; **23**: 128-135

21 **Kissmeyer-Nielsen P,** Jensen MB, Laurberg S. Perioperative growth hormone treatment and functional outcome after major abdominal surgery: a randomized, double-blind, controlled study. *Ann Surg* 1999; **229**: 298-302

22 **Vara-Thorbeck R,** Guerrero JA, Ruiz-Requena E, Garcia-Carriazo M. Can the use of growth hormone reduce the postoperative fatigue syndrome? *World J Surg* 1996; **20**: 81-87

23 **Berman RS,** Harrison LE, Pearlstone DB, Burt M, Brennan MF. Growth hormone, alone and in combination with insulin, increases whole body and skeletal muscle protein kinetics in cancer patients after surgery. *Ann Surg* 1999; **229**: 1-10

24 **Carli F,** Webster JD, Halliday D. A nitrogen-free hypocaloric diet and recombinant human growth hormone stimulate postoperative protein synthesis: fasted and fed leucine kinetics in the surgical patient. *Metabolism* 1997; **46**: 796-800

25 **Carli F,** Webster JD, Halliday D. Growth hormone modulates amino acid oxidation in the surgical patient: leucine kinetics during the fasted and fed state using moderate nitrogenous and caloric diet and recombinant human growth hormone. *Metabolism* 1997; **46**: 23-28

26 **Hammarqvist F,** Sandgren A, Andersson K, Essen P, McNurlan MA, Garlick PJ, Wernerman J. Growth hormone together with glutamine-containing total parenteral nutrition maintains muscle glutamine levels and results in a less negative nitrogen balance after surgical trauma. *Surgery* 2001; **129**: 576-586

27 **Inoue Y,** Copeland EM, Souba WW. Growth hormone enhances amino acid uptake by the human small intestine. *Ann Surg* 1994; **219**: 715-724

28 **Kissmeyer P,** Moller J, Bach Jensen M, Laurberg S. Effect of growth hormone on the atabolic response to elective J-pouch surgery [abstract]. *Int J Colorectal Dis* 1997; **12**: 189

29 **Mjaaland M.** Growth hormone after gastrointestinal surgery: effect on skeletal muscle metabolism [abstract]. *Clin Nutr* 1990; **9**(Suppl): 13

30 **Mjaaland M.** The effect of growth hormone on postoperative nitrogen balance [abstract]. *Ann Chir Gynaecol* 1989; **78**: 14

31 **Mjaaland M,** Unneberg K, Larsson J, Nilsson L, Revhaug A. Growth hormone after abdominal surgery attenuated forearm glutamine, alanine, 3-methylhistidine, and total amino acid efflux in patients receiving total parenteral nutrition. *Ann Surg* 1993; **217**: 413-422

32 **Mjaaland M,** Unneberg K, Bjoro T, Revhaug A. Growth hormone treatment after abdominal surgery decreased carbohydrate oxidation and increased fat oxidation in patients with total parenteral nutrition. *Metabolism* 1993; **42**: 185-190

33 **Moller J,** Jensen MB, Frandsen E, Moller N, Kissmeyer P, Laurberg S. Growth hormone treatment improves body fluid distribution in patients undergoing elective abdominal surgery. *Clin Endocrinol* 1998; **49**: 597-602

34 **Plank LD,** Hill GL. Use of bioimpedance spectroscopy to assess effects of perioperative treatment with growth hormone on fluid changes in patients undergoing major surgery. *Ann N Y Acad Sci* 2000; **904**: 190-192

35 **Saito H,** Taniwaka K, Fukushima R, Sawada T, Muto T, Morioka Y. Growth hormone treatment stimulates immune responsiveness after abdominal surgery [abstract]. *Clin Nutr* 1990; **9**(Suppl): 16

36 **Tacke J,** Bolder U, Herrmann A, Berger G, Jauch KW. Long-term risk of gastrointestinal tumor recurrence after postoperative treatment with recombinant human growth hormone. *JPEN* 2000; **24**: 140-144

37 **Vara-Thorbeck R,** Guerrero JA, Ruiz-Requena ME, Capitan J, Rodriguez M, Rosell J, Mekinassi K, Maldonado M, Martin

R. Effects of growth hormone in patients receiving total parenteral nutrition following major gastrointestinal surgery. *Hepatogastroenterology* 1992; **39**: 270-272

38 **Barle H,** Essen P, Nyberg B, Olivecrona H, Tally M, McNurlan MA, Wernerman J, Garlick PJ. Depression of liver protein synthesis during surgery is prevented by growth hormone. *Am J Physiol* 1999; **276**(4 Pt 1): E620-627

39 **He G,** Jiang Z, Yang N, Shu H, Wilmore DW. Effect of recombinant growth hormone on amino acids metabolism in blood and urine after major operation. *Zhongguo Yixue Kexueyuan Xuebao* 1997; **19**: 192-196

40 **Jiang Z,** He G, Wang X, Yang N, Wilmore DW. The effect of nutrition support and recombinant growth hormone on body composition and muscle function in postoperative patients. *Zhongguo Yixue Kexueyuan Xuebao* 1994; **16**: 443-447

41 **Mealy K,** Barry M, O'Mahony L, Sheehan S, Burke P, McCormack C, Whitehead AS, Bouchier-Hayes D. Effects of human recombinant growth hormone (rhGH) on inflammatory responses in patients undergoing abdominal aortic aneurysm repair. *Intensive Care Med* 1998; **24**: 128-131

42 **Vara-Thorbeck R,** Ruiz-Requena E, Guerrero-Fernandez JA. Effects of human growth hormone on the catabolic state after surgical trauma. *Horm Res* 1996; **45**: 55-60

43 **Valera A,** Rodriguez-Gil JE, Yun JS, McGrane MM, Hanson RW, Bosch F. Glucose metabolism in transgenic mice containing a chimeric P-enolpyruvate carboxykinase/bovine growth hormone gene. *FASEB J* 1993; **7**: 791-800

44 **Ikeda A,** Chang KT, Matsumoto Y, Furuhata Y, Nishihara M, Sasaki F, Takahashi M. Obesity and insulin resistance in human growth hormone transgenic rats. *Endocrinology* 1998; **139**: 3057-3063

45 **Ezzat S,** Forster MJ, Berchtold P, Redelmeier DA, Boerlin V, Harris AG. Acromegaly. Clinical and biochemical features in 500 patients. *Medicine* 1994; **73**: 233-240

46 **Colao A,** Baldelli R, Marzullo P, Ferretti E, Ferone D, Gargiulo P, Petretta M, Tamburrano G, Lombardi G, Liuzzi A. Systemic hypertension and impaired glucose tolerance are independently correlated to the severity of the acromegalic cardiomyopathy. *J Clin Endocrinol Metab* 2000; **85**: 193-199

47 **Gerich JE,** Lorenzi M, Bier DM, Tsalikian E, Schneider V, Karam JH, Forsham PH. Effects of physiologic levels of glucagon and growth hormone on human carbohydrate and lipid metabolism. Studies involving administration of exogenous hormone during suppression of endogenous hormone secretion with somatostatin. *J Clin Invest* 1976; **57**: 875-884

48 **Ferrannini E,** Barrett EJ, Bevilacqua S, DeFronzo RA. Effect of fatty acids on glucose production and utilization in man. *J Clin Invest* 1983; **72**: 1737-1747

49 **Ikkos D,** Luft R, Sjogren B. Body water and sodium in patients with acromegaly. *J Clin Invest* 1954; **33**: 989-994

50 **Guler HP,** Schmid C, Zapf J, Froesch ER. Effects of recombinant insulin-like growth factor I on insulin secretion and renal function in normal human subjects. *Proc Natl Acad Sci USA* 1989; **86**: 2868-2872

51 **Hirschberg R,** Kopple JD. Evidence that insulin-like growth factor I increases renal plasma flow and glomerular filtration rate in fasted rats. *J Clin Invest* 1989; **83**: 326-330

52 **Hirschberg R,** Brunori G, Kopple JD, Guler HP. Effects of insulin-like growth factor I on renal function in normal men. *Kidney Int* 1993; **43**: 387-397

53 **Venning EH,** Lucis OJ. Effect of growth hormone on the biosynthesis of aldosterone in the rat. *Endocrinology* 1962; **70**: 486-491

54 **Ho KY,** Weissberger AJ. The antinatriuretic action of biosynthetic human growth hormone in man involves activation of the renin-angiotensin system. *Metabolism* 1990; **39**: 133-137

55 **Cuneo RC,** Salomon F, Wilmshurst P, Byrne C, Wiles CM, Hesp R, Sonksen PH. Cardiovascular effects of growth hormone treatment in growth-hormone-deficient adults: stimulation of the renin-aldosterone system. *Clin Sci* 1991; **81**: 587-592

56 **Herlitz H,** Jonsson O, Bengtsson BA. Effect of recombinant human growth hormone on cellular sodium metabolism. *Clin Sci* 1994; **86**: 233-237

57 **Ross EJ,** Vant Hoff W, Crabbe J, Thorn GW. Aldosterone excretion in hypopituitarism and after hypophysectomy in man. *Am J Med* 1960; **28**: 229-238

58 **Donath MY,** Zierhut W, Gosteli-Peter MA, Hauri C, Froesch ER, Zapf J. Effects of IGF-I on cardiac growth and expression of mRNAs coding for cardiac proteins after induction of heart hypertrophy in the rat. *Eur J Endocrinol* 1998; **139**: 109-117

59 **Donath MY,** Gosteli-Peter MA, Hauri C, Froesch ER, Zapf J. Insulin-like growth factor-I stimulates myofibrillar genes and modulates atrial natriuretic factor mRNA in rat heart. *Eur J Endocrinol* 1997; **137**: 309-315

60 **Tanaka N,** Ryoke T, Hongo M, Mao L, Rockman HA, Clark RG, Ross J Jr. Effects of growth hormone and IGF-I on cardiac hypertrophy and gene expression in mice. *Am J Physiol* 1998; **275**: H393-399

61 **Harder BA,** Schaub MC, Eppenberger HM, Eppenberger-Eberhardt M. Influence of fibroblast growth factor (bFGF) and insulin-like growth factor (IGF-I) on cytoskeletal and contractile structures and on atrial natriuretic factor (ANF) expression in adult rat ventricular cardiomyocytes in culture. *J Mol Cell Cardiol* 1996; **28**: 19-31

62 **Tonshoff B,** Nowack R, Kurilenko S, Blum WF, Seyberth HW, Mehls O, Ritz E. Growth hormone-induced glomerular hyperfiltration is dependent on vasodilating prostanoids. *Am J Kidney Dis* 1993; **21**: 145-151

63 **Takala J,** Ruokonen E, Webster NR, Nielsen MS, Zandstra DF, Vundelinckx G, Hinds CJ. Increased mortality associated with growth hormone treatment in critically ill adults. *N Engl J Med* 1999; **341**: 785-792

64 **Gottardis M,** Gruber E, Benzer A, Murr C, Schmoigl C, Hackl JM, Balogh D. Effects of short-term application of recombinant human growth hormone on urea production rate in patients in the early postoperative phase. *Infusionsther Transfusionsmed* 1993; **20**: 142-147

65 **Guerrero JA,** Capitan JM, Rosell J, Ruiz ME, Garcia E, Garcia-Carriazo M, Maldonado MJ, Vara Thorbeck R. Effect of growth hormone and parenteral nutrition on the catabolic phase following major digestive surgery. *Rev Esp Enferm Dig* 1992; **81**: 379-382

66 **Martin R,** Cano MD, Guerrero JA, Segovia E, Vara Thorbeck R. Growth hormone and its effects on cholesterol and lipoprotein metabolism following surgical intervention (hGH and cholesterol metabolism during surgery). *Nutr Hosp* 1998; **13**: 181-185

67 **Wennstrom I,** Wernerman J, Hammarqvist F. Postoperative effects of growth hormone and insulin-like growth factor-I on the nitrogen balance and muscle amino acid pattern [abstract]. *Clin Nutr* 1999; **18**(Suppl): 14

Science Editor Wang XL and Li WZ **Language Editor** Elsevier HK

PO Box 2345, Beijing 100023, China
www.wjgnet.com
wjg@wjgnet.com

ELSEVIER

World J Gastroenterol 2005;11(25):3931-3934
World Journal of Gastroenterology ISSN 1007-9327

• *BRIEF REPORTS* •

Autofluorescence excitation-emission matrices for diagnosis of colonic cancer

Bu-Hong Li, Shu-Sen Xie

Bu-Hong Li, Shu-Sen Xie, Biomedical Optics Laboratory, Institute of Laser and Optoelectronics Technology, Fujian Normal University, Fuzhou 350007, Fujian Province, China
Supported by the Natural Science Foundation of Fujian Province, No. A0310018 and No. 2002F008, and the Scientific Research Program of Fujian Province, No. JA03041
Correspondence to: Dr. Bu-Hong Li, Biomedical Optics Laboratory, Institute of Laser and Optoelectronics Technology, Fujian Normal University, Fuzhou 350007, Fujian Province, China. bhli@fjnu.edu.cn
Telephone: +86-591-83165373 Fax: +86-591-83465373
Received: 2004-09-22 Accepted: 2004-12-21

Abstract

AIM: To investigate the autofluorescence spectroscopic differences in normal and adenomatous colonic tissues and to determine the optimal excitation wavelengths for subsequent study and clinical application.

METHODS: Normal and adenomatous colonic tissues were obtained from patients during surgery. A FL/FS920 combined TCSPC spectrofluorimeter and a lifetime spectrometer system were used for fluorescence measurement. Fluorescence excitation wavelengths varying from 260 to 540 nm were used to induce the autofluorescence spectra, and the corresponding emission spectra were recorded from a range starting 20 nm above the excitation wavelength and extending to 800 nm. Emission spectra were assembled into a three-dimensional fluorescence spectroscopy and an excitation-emission matrix (EEM) to exploit endogenous fluorophores and diagnostic information. Then emission spectra of normal and adenomatous colonic tissues at certain excitation wavelengths were compared to determine the optimal excitation wavelengths for diagnosis of colonic cancer.

RESULTS: When compared to normal tissues, low NAD (P)H and FAD, but high amino acids and endogenous phorphyrins of protoporphyrin IX characterized the high-grade malignant colonic tissues. The optimal excitation wavelengths for diagnosis of colonic cancer were about 340, 380, 460, and 540 nm.

CONCLUSION: Significant differences in autofluorescence peaks and its intensities can be observed in normal and adenomatous colonic tissues. Autofluorescence EEMs are able to identify colonic tissues.

Key words: Autofluorescence spectroscopy; Excitation-emission matrix; Optical diagnosis; Colonic cancer

Li BH, Xie SS. Autofluorescence excitation-emission matrices for diagnosis of colonic cancer. *World J Gastroenterol* 2005; 11(25): 3931-3934
http://www.wjgnet.com/1007-9327/11/3931.asp

INTRODUCTION

Colonic cancer is an important public health concern in industrialized countries and around the world. Diagnosis and localization of early carcinoma play an important role in the prevention and curative treatment of colonic cancer. However, physical biopsies do not fully solve this problem because they are sampled at random locations, which is highly dependent on the skill and experience of the investigator. As a result, a significant number of lesions, especially the carcinoma *in situ* lesions, are not sampled and subsequently diagnosed[1,2]. Laser-induced autofluorescence depends on endogenous fluorophores in the biological tissue, which undergoes a change related to malignant transformations. Therefore, it is possible for us to develop more sensitive techniques for the detection of early colonic tissue. During the past two decades, autofluorescence spectroscopy has been investigated as an effective and noninvasive method for detecting and imaging the abnormal tissues from the surrounding normal tissues.

Measurement of three-dimensional fluorescence spectroscopy or fluorescence excitation-emission matrices (EEMs) for tissue samples *in vitro* is a crucial step to exploit the endogenous fluorophores and determine which excitation wavelengths contain the most diagnostic information for clinical diagnostic analysis[3-6]. However, an important limitation of most studies on the autofluorescence diagnosis of colonic cancer is that the selection of excitation wavelengths is based on the availability of a special light source, and few studies have been done to understand the real reasons responsible for the spectral differences[6-9]. In this study, we conducted the measurement of autofluorescence EEMs in order to investigate the spectroscopic differences in normal and adenomatous colonic tissues, and to further determine the optimal excitation wavelengths. It is hoped that information from this investigation may be useful for subsequent studies and clinical diagnosis.

MATERIALS AND METHODS

Adenomatous colonic tissues (n = 5) were obtained from four patients during surgery for malignant tumors of the colon, and normal tissue sample (n = 4, matched controls) was also collected from the same patient. Each tissue sample was cut into two specimens. One specimen was sent to the

pathologist for standard histopathological evaluation, the other unstained and unfixed specimen was placed on a non-fluorescence quartz substrate for laser-induced autofluorescence within 2 h after surgical resection.

Autofluorescence EEM was performed using a FL/FS920 combined TCSPC spectrofluorimeter and a lifetime spectrometer system (Edinburgh Instruments Ltd, UK). The wavelength-selected excitation light onto the sample with a 60° incident angle and fluorescence emission was collected at 45° with respect to the normal quartz substrate in order to minimize the detection of the backscattered excitation light. The slit sizes of excitation and emission monochromator were 1.5 and 0.5 mm, respectively. The wavelength dependence of the excitation power and the detector response was corrected and calibrated for all emission spectra. Fluorescence EEMs were recorded by measuring the fluorescence emission spectra over a range of excitation wavelengths. The excitation wavelengths varied from 260 to 540 nm in 20-nm increments. At each excitation wavelength, the fluorescence emission spectra were recorded from a range starting 20 nm above the excitation wavelength and extending to 800 nm at 5-nm intervals. These wavelength ranges enabled characterization of all endogenous fluorophores, tryptophan, collagen, and elastin, NAD(P)H, FAD and endogenous phorphyrins, present in tissues in the UV-Vis spectrum[10,11]. This resulted in a total measurement time about 25 min for each EEM. After each measurement, a repeat fluorescence spectrum was measured at 260 nm excitation and compared to that measured at the beginning of the experiment to confirm that the measurement protocol used did not induce photobleaching. Fluorescence data from each single measurement were then combined to construct EEM containing fluorescence intensity as a function of both excitation and emission wavelengths.

RESULTS

No significant differences were observed in the autofluorescence spectra of normal and cancerous tissues. However, remarkable differences in fluorescence peaks and intensities were detected between normal and adenomatous tissue from the same patient. The representative three-dimensional autofluorescence spectra for the normal colonic tissue and adenomatous colonic tissue are shown in Figures 1A and B, respectively. The relative fluorescence intensity was recorded as a function of both excitation and emission wavelengths. Although the fluorescence intensities were indicated in arbitrary units, the same experimental set-ups were maintained throughout our measurements for comparison.

The corresponding autofluorescence EEMs for normal and adenomatous colonic tissue are displayed in Figures 2A and B, respectively. The colorized scale represents different fluorescence intensities. The plots are shown on a log contour scale, where each contour connects points of equal fluorescence intensity.

In the case of autofluorescence EEM for normal colonic tissue in Figure 2A, the primary fluorescence peaks occurred at the excitation-emission wavelength pairs of 280-330, 350-480, 350/460-605, and 460-520 nm. According to the previous studies, these fluorescence peaks were attributed to the amino acids tryptophan and tyrosine, reduced nicotinamide adenine dinucleotide (NADH) or reduced nicotinamide adenine dinucleotide phosphate (NADPH), ceroid and flavin adenine dinucleotide (FAD), respectively[10,12]. Adenomatous tissues exhibited emission peaks at 635 and 710 nm (Figure 2B) that were not observed in the emission spectra of normal colonic tissues. These remarkable peaks were the contribution of naturally occurring high endogenous phorphyrins of protoporphyrin IX in cancerous tissues[13-15]. Furthermore, the emission intensity from tryptophan and

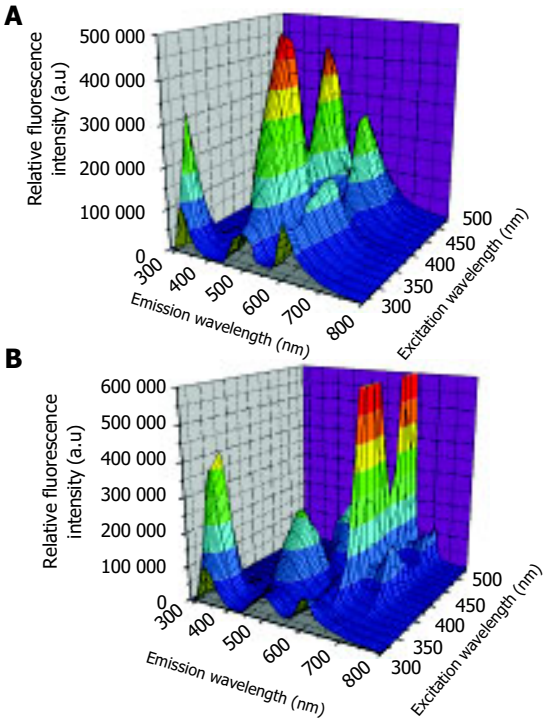

Figure 1 Three-dimensional autofluorescence spectra for normal colonic tissue (**A**) and adenomatous colonic tissue (**B**).

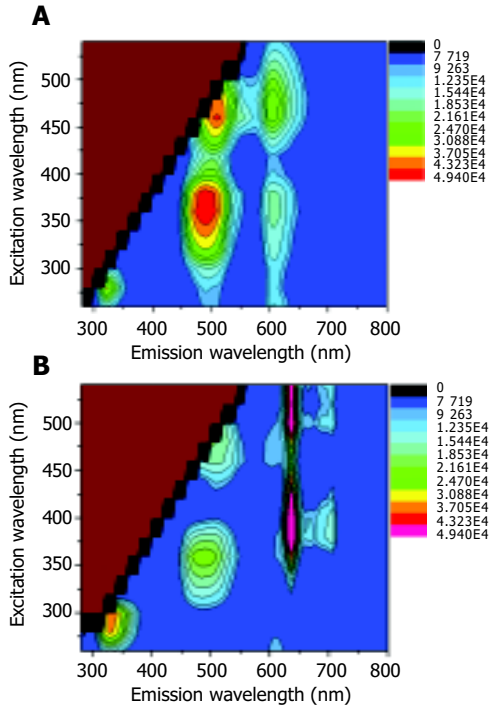

Figure 2 Autofluorescence EEMs for normal colonic tissue (**A**) and adenomatous colonic tissue (**B**).

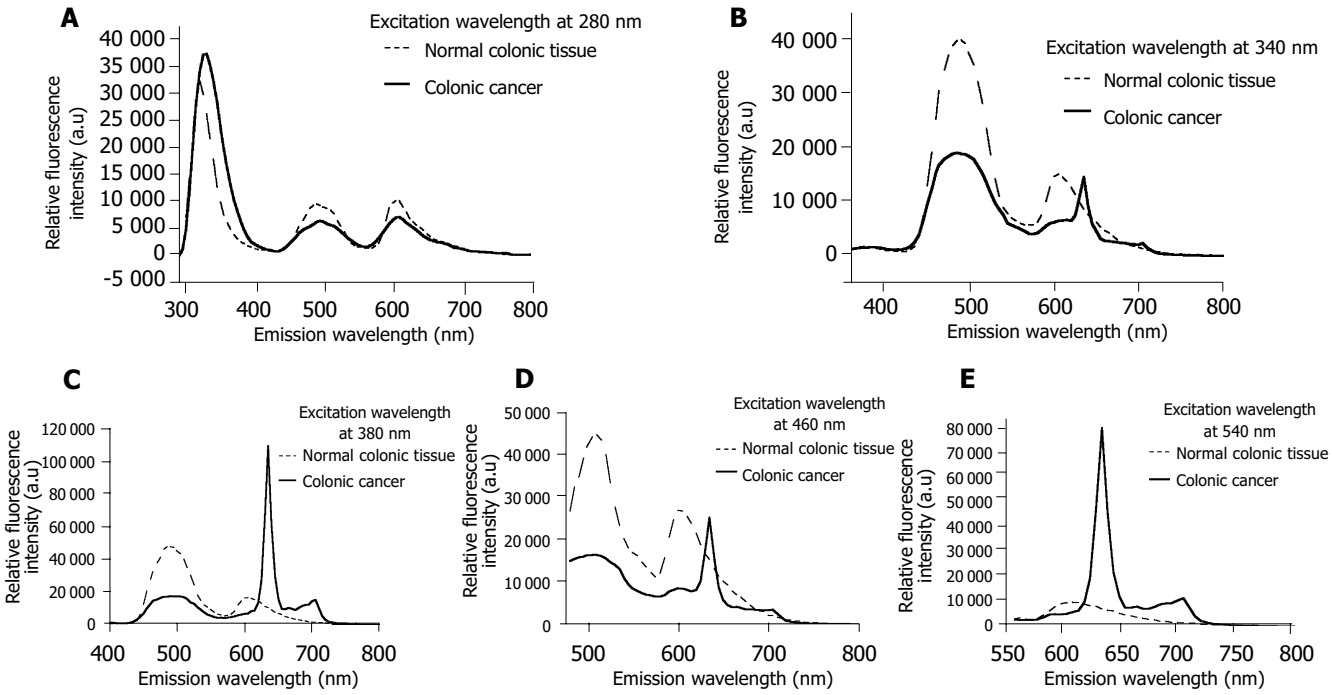

Figure 3 Fluorescence spectra of normal and cancerous tissues at excitation wavelengths of 280 (**A**), 340 (**B**), 380 (**C**), 460 (**D**), and 540 nm (**E**).

tyrosine was more intense in cancerous tissue than in normal tissue EEM. However, the endogenous fluorescence near 500 nm reduced in tumor tissues relative to normal colonic tissues. The differences might lie in the decrease of the oxidized forms of flavins and the relative amount of NAD(P)H in malignant tissues. As a result, low NAD(P)H and FAD but high amino acids and protoporphyrin IX accumulated in the human colonic malignancy. An evaluation of the average fluorescence spectrum at 260 nm excitation collected at the end of each EEM indicated that its peak fluorescence intensity was within 8% of that acquired at the beginning of each EEM. This means that minimal photobleaching occurred during the process of the 25-min EEM measurement.

In order to further determine the optimized excitation wavelengths for the diagnosis of colonic cancer, autofluorescence emission spectra at certain excitation wavelengths of 280, 340, 380, 460, and 540 nm for normal and adenomatous colonic tissues were compared in Figure 3, respectively. The greatest spectroscopic differences could be achieved for diagnosis of colonic cancer when the excitation wavelengths were 340, 380, 460, and 540 nm. In particular, the emission from endogenous phorphyrins of protoporphyrin IX demonstrably characterized the autofluorescence spectroscopy of cancerous tissues when the excitation wavelength was higher than 380 nm.

DISCUSSION

In this study, autofluorescence EEMs were measured using a standard spectrofluorimeter to determine the location of the endogenous fluorescent peaks and their relative intensity in normal and adenomatous colonic tissues. We observed significant differences in the autofluorescence spectra of normal tissues and adenomatous colonic tissues, and these differences could be attributed to the differences in fluorophores expression. The endogenous fluorophores that are speculated to cancerous transformations are the amino acids tryptophan and tyrosine, the structural proteins collagen and elastin, the coenzymes NAD(P)H and FAD, and phorphyrins[12].

Our results indicate that the fluorescence intensity of the amino acids tryptophan and tyrosine is dominant in both normal and cancerous colonic tissues at 280 nm excitation, which demonstrates the fact that amino acids are the basic structural units of protein and play an important role in biological tissues. These results also agree well with those of Pradhan *et al*.[16], who suggested that there is an increase in tryptophan as cells progress from normal to cancerous state. Secondly, we observed that the intensity in the blue region of the autofluorescence spectra significantly reduced in adenomatous colonic tissues compared to normal tissues, which is in substantial agreement with the early work showing that the concentration of NADH and NADPH in adenomatous tissues is lower than that in normal tissues[6,7]. Moreover, Anidjar *et al*.[17], have demonstrated a decrease of FDA in cancerous tissues, which is proved in our research. However, Georgakoudi *et al*.[18] and Drezek *et al*.[19], suggested that low collagen and high NAD(P)H fluorescence characterize the high-grade dysplastic lesions when compared to nondysplastic cervix tissues. It is possible that the differences in NAD(P)H fluorescence may be due to different colonic and cervix tissues and the comparable measurements should be carried out for further confirmation. In addition, it should be noted that the emission specific peaks from collagen and elastin were not shown in our tissue EEMs except for one case, suggesting that the increments of excitation wavelength should be limited to 10 nm in order to exploit the emission fluorescence from structural proteins collagen and elastin. Bottiroli *et al*.[7], have observed

a red fluorescence in some parts of tissue section from a cancerous colon. The red fluorescence has been reported by Moesta *et al*.[13], and also demonstrated in this investigation, which can be definitely attributed to high endogenous phorphyrins of protoporphyrin IX accumulating naturally in colonic cancer.

In summary, the presence or absence of fluorescence peaks in both normal and adenomatous colonic tissues can be explained by the different endogenous fluorophores to generate autofluorescence signals, and the ability of laser-induced autofluorescence EEMs to distinguish normal from cancerous colonic tissues. The present investigation offers evidence that low NAD(P)H and FAD but high amino acids and protoporphyrin IX characterize the high-grade malignant colonic tissues. Based on our results, the optimal excitation wavelengths for diagnosis of colonic cancer are 340, 380, 460, and 540 nm.

ACKNOWLEDGMENTS

We thank Professor Ming-Ren Li at the Department of Oncology of the First Affiliated Hospital of Fujian Medical University for providing the colonic tissue samples and the results of standard histopathological diagnosis.

REFERENCES

1 **Yova D,** Atlamazoglou V, Kavantzas N, Loukas S. Development of a fluorescence-based imaging system for colon cancer diagnosis using two novel rhodamine derivatives. *Lasers Med Sci* 2000; **15**: 140–147
2 **Prosst RL,** Gahlen J. Fluorescence diagnosis of colotrctal neoplasms: a review of clinical applications. *Int J Colorectal Dis* 2002; **17**: 1-10
3 **Heintzelman DL,** Utzinger U, Fuchs H, Zuluaga A, Gossage K, Gillenwater AM, Jacob R, Kemp B, Richards-Kortum RR. Optimal excitation wavelengths for *in vivo* detection of oral neoplasia using fluorescence spectroscopy. *Photochem Photobiol* 2000; **72**: 103-113
4 **Palmer GM,** Marshek CL, Vrotsos KM, Ramanujam N. Optimal methods for fluorescence and diffuse reflectance measurements of tissue biopsy samples. *Lasers Surg Med* 2002; **30**: 191-200
5 **Chang SK,** Follen M, Malpica A, Utzinger U, Staerkel G, Cox D, Atkinson EN, MacAulay C, Richards-Kortum R. Optimal excitation wavelengths for discrimination of cervical neoplasia. *IEEE Trans Biomed Eng* 2002; **49**: 1102-1111
6 **Richards-Kortum R,** Rava RP, Petras RE, Fitzmaurice M, Sivak M, Feld MS. Spectroscopic diagnosis of colonic dysplasia. *Photochem Photobiol* 1991; **53**: 777-786
7 **Bottiroli G,** Croce AC, Locatelli D, Marchesini R, Pignoli E, Tomatis S, Cuzzoni C, Di Palma S, Dalfante M, Spinelli P. Natural fluorescence of normal and neoplastic human colon: a comprehensive ''*ex vivo*'' study. *Lasers Surg Med* 1995; **16**: 48–60
8 **Banerjee B,** Miedema B, Chandrasekhar HR. Emission spectra of colonic tissue and endogenous fluorophores. *Am J Med Sci* 1998; **316**: 220-226
9 **Sheng JQ,** Li SR, Chen ZM, Gao G. Value of LIAF spectra for detection of colorectal carcinoma during colonoscopy. *Zhongguo Jiguang Yixue Zazhi* 2001; **10**: 145-147
10 **Richards-Kortum R,** Sevick-Muraca E. Quantitative optical spectroscopy for tissue diagnosis. *Annu Rev Phys Chem* 1996; **47**: 555-606
11 **Palmer GM,** Keely PJ, Breslin TM, Ramanujam N. Autofluorescence spectroscopy of normal and malignant human breast cell lines. *Photochem Photobiol* 2003; **78**: 462-469
12 **Ramanujam N.** Fluorescence spectroscopy *in vivo*, in Meyers RA ed. Encyclopedia of Analytical Chemistry. *Chichester, John Wiley Sons Ltd* 2000: 20-56
13 **Moesta KT,** Ebert B, Handke T, Nolte D, Nowak C, Haensch WE, Pandey RK, Dougherty TJ, Rinneberg H, Schlag PM. Protoporphyrin IX occurs naturally in colorectal cancers and their metastases. *Cancer Res* 2001; **61**: 991-999
14 **DaCosta RS,** Andersson H, Wilson BC. Molecular fluorescence excitation-emission matrices relevant to tissue spectroscopy. *Photochem Photobiol* 2003; **78**: 384-392
15 **Huang Z,** Zheng W, Xie S, Chen R, Zeng H, McLean DI, Lui H. Laser-induced autofluorescence microscopy of normal and tumor human colonic tissue. *Int J Oncol* 2004; **24**: 59-63
16 **Pradhan A,** Pal P, Durocher G, Villeneuve L, Balassy A, Babai F, Gaboury L, Blanchard L. Steady state and time-resolved fluorescence properties of metastatic and non-metastatic malignant cells from different species. *J Photochem Photobiol B* 1995; **31**: 101-112
17 **Anidjar M,** Cussenot O, Blais J, Bourdon O, Avrillier S, Ettori D, Villette JM, Fiet J, Teillac P, Le Duc A. Argon laser induced autofluorescence may distinguish between normal and tumor human urothelial cells: a microspectrofluorimetric study. *J Urol* 1996; **155**: 1771-1774
18 **Georgakoudi I,** Jacobson BC, Muller MG, Sheets EE, Badizadegan K, Carr-Locke DL, Crum CP, Boone CW, Dasari RR, Van Dam J, Feld MS. NAD(P)H and collagen as *in vivo* quantitative fluorescent biomarkers of epithelial precancerous changes. *Cancer Res* 2002; **62**: 682-687
19 **Drezek R,** Sokolov K, Utzinger U, Boiko I, Malpica A, Follen M, Richards-Kortum R. Understanding the contributions of NADH and collagen to cervical tissue fluorescence spectra: modeling, measurements, and implications. *J Biomed Opt* 2001; **6**: 385-396

Science Editor Guo SY **Language Editor** Elsevier HK

PO Box 2345, Beijing 100023, China
www.wjgnet.com
wjg@wjgnet.com

ELSEVIER

World J Gastroenterol 2005;11(25):3935-3938
World Journal of Gastroenterology ISSN 1007-9327

• *BRIEF REPORTS* •

Application of dietary fiber in clinical enteral nutrition: A meta-analysis of randomized controlled trials

Gang Yang, Xiao-Ting Wu, Yong Zhou, Ying-Li Wang

Gang Yang, Xiao-Ting Wu, Yong Zhou, Ying-Li Wang, Department of General Surgery, West China Hospital, Sichuan University, Chengdu 610041, Sichuan Province, China
Correspondence to: Professor Xiao-Ting Wu, Department of General Surgery, West China Hospital, Sichuan University, 37 Guo Xue Road, Chengdu 610041, Sichuan Province, China. yanggang2000@hotmail.com
Telephone: +86-28-88036679 Fax: +86-28-85422411
Received: 2004-05-29 Accepted: 2004-06-24

Abstract

AIM: To evaluate the effects of dietary fiber (DF) as a part of enteral nutrition (EN) formula on diarrhea, infection, and length of hospital stay.

METHODS: Following electronic databases were searched for randomized controlled trials about DF: Chinese Biomedicine Database (CBM), MEDLINE, EMBASE and Cochrane Controlled Trials Register. RevMan 4.1 was used for statistical analysis.

RESULTS: Seven randomized controlled trials with 400 pat-ients were included. The supplement of DF in EN was compared with standard enteral formula in five trials. Combined analysis did not show a significant reduction in occurrence of diarrhea, but there were valuable results for non-critically ill patients. Combined analysis of two trials observing the infection also did not show any valid evidence that DF could decrease the infection rate, though the length of hospital stay was reduced significantly.

CONCLUSION: Based on the current eligible randomized controlled trials, there is no evidence that the value of DF in the diarrhea can be proved. Though length of hospital stay was shortened by the use of DF, there is no available evidence in preventing infection by DF. Further studies are needed for evaluating the value of DF in EN.

Key words: Dietary fiber; Enteral nutrition; Meta-analysis

Yang G, Wu XT, Zhou Y, Wang YL. Application of dietary fiber in clinical enteral nutrition: A meta-analysis of randomized controlled trials. *World J Gastroenterol* 2005; 11(25): 3935-3938
http://www.wjgnet.com/1007-9327/11/3935.asp

INTRODUCTION

Dietary fiber (DF) is a category of carbohydrates that cannot be ingested by endogenic digestive enzymes in human body[1]. Nevertheless, DF can be fermented into methane, hydrogen, CO_2, and short-chain fatty acid (SCFA) by bowel microflorae. SCFA, a primary important energy substance for colonal mucosal epithelium, is essential to maintain the metabolism and regeneration of epithelia, protect the structure and function, promote absorption of water and sodium, and regulate the function of bowel[2-6]. Recent studies also suggest that SCFA can protect the intestinal barrier and prevent bacterial translocation[7-9]. So DF has been widely recommended as an essential component of enteral nutrition (EN) in the last 20 years[10-13]. It is believed that DF may play an important role in controlling diarrhea associated with EN, improving restoration of bowel function, reducing infection and improving prognosis of critically ill patients[14-18]. But the conclusions of existing trials are controversial. The practical value of DF in clinical EN lacks evidence. This review is to evaluate the value of DF in clinical EN with the method of meta-analysis and to seek the best evidence for clinical EN.

MATERIALS AND METHODS

Data extraction and outcomes

We searched the following electronic databases for eligible trials: PubMed (from January 1980 to January 2003), EMBASE (from January 1989 to December 2002), Cochrane Controlled Trials Register and Chinese Biomedicine Database (from 1980 to 2002). The searching words were dietary fiber and enteral nutrition. Languages were restricted to English and Chinese.

The criteria were open or blind randomized studies. Patients were randomly allocated into receiving EN emented with DF or EN without DF, regardless of the type of DF.

Assessment of methodological quality

The assessment of methodological quality was undertaken by two of the authors independently, differences in assessment were solved by consensus. From each study, data were extracted on the type of patients, the method of administration of EN. Outcomes were the occurrence of diarrhea, infection of any type and length of hospital stay.

Jadad score and allocation concealment were adopted to evaluate the methodological quality of each trial: 0 for non-randomized controlled trials, 1-2 scores for poor-quality trials and 3-5 scores for high-quality trials. The concealment of allocation also was divided into three grades: A for adequate concealment, B for unclear concealment, C for inadequate concealment.

Analysis

RevMan 4.1 software supplied by Cochrane Collaboration

was used. The effect size of categorical variables was odds ratio (OR). For numerical variables, if the unit was identical, weighed mean difference (WMD) was used, and standardized mean difference was used when the unit was different. The homogeneity of adopted trials was tested before meta-analysis. If the heterogeneity had no statistical significant difference, a fixed effect model was used during meta-analysis. In contrast, we used a random effect model and subgroup analysis. Sensitivity analysis was also proceeded after the non-blinded, inadequate concealed trials were excluded.

RESULTS

Characteristics of trials and patients

Eight hundred and eleven papers were obtained by searching the databases, 587 in English, 224 in Chinese. Seventeen trials, all in English, were identified for further evaluation after the title and abstract were read. Seven measured up to the criteria and were included[19-25]. There were no repetitive studies and meta-analysis. Seven of the 17 included trials, three were conducted in Germany[19,20,24], one in USA[22], one in Australia[25], one in Belgium[21] and Singapore[23]. Two included critically ill patients[22,25], three included postoperative patients[19,20,23], one included sepsis[21] and the other included a variety of diseases[24]. The earliest study was published in 1990[25], all were published in the past 14 years.

Methodological quality of trials

Of the seven trials, three were of a high quality (one had five scores according to Jadad, one had four scores, one had three scores), the other four were of a poor quality. Computerized random number was used in two trials, sealed envelopes in two, no randomization method in three. Four trials were double-blinded. The baselines of included subjects were compared in all studies, and no statistically significant differences existed. Table 1 gives the details of the seven trials.

Outcomes

Effect of DF on diarrhea in EN The occurrence of diarrhea in 276 patients receiving EN supplemented with or without DF was observed in five trials. There was no heterogeneity ($P = 0.087$) and fixed effect model was used. The combined OR was 0.61, 96% confidence interval was from 0.36 to 1.05 ($P = 0.07$) (Table 2). Subgroup analysis of two trials on uncritically ill patients showed that the combined OR was 0.33 (from 0.13 to 0.87, $P = 0.03$).

Effect of DF on infection The risk of infection was reported in two trials. The types of infection included pneumonia, sepsis, abdominal infection, urinary infection and incision infection. Two trials had homogeneity. Combined OR was 0.44 when the fixed effect model was used (0.20-1.00, $P = 0.05$).

Effect of DF on length of hospital stay Three trials reported the length of hospital stay of 124 postoperative patients. Among the three trials, one was excluded because it did not supply the standard deviation. Two adopted trials had homo-geneity, combined WMD was -2.85 (from -3.76 to -1.93, $P<0.00001$).

Sensitivity analysis

Three high-quality trials on diarrhea of 160 cases in EN were included. There was no heterogeneity among them ($P = 0.069$). Combined OR was 0.83 (0.43-1.60, $P = 0.6$). The result was identical with the previous analysis (Table 3). Sensitivity analysis was abandoned for the quality of trials about infection and length of hospital stay was poor.

DISCUSSION

Diarrhea is the most frequent complication in EN. Infusion speed, temperature, osmolality, bacterial contamination, hypoalbuminemia and antibiotics may play a part in diarrhea[26]. Laboratory studies suggested that DF and SCFA, fermentation products of DF, were able to improve the rhythm of bowel peristalsis, promote absorption of water and sodium, and

Table 1 Characteristics of RCTs about EN supplemented with DF

	Number of patients (intervention / control)	Methodological quality	Patients	Diarrhea	Infection	Days of hospital stay (mean±SD)
Schultz 2000	44(22 / 22)	C: A J: 5	Critically ill	6 / 7	NR	NR
Dobb 1990	91(45 / 46)	C: B J: 4	Critically ill	16 / 13	NR	NR
Spapen 2001	25(13 / 12)	C: A J: 3	Sepsis	6 / 11	NR	NR
Rayes 2002	64(32 / 32)	C: B J: 2	Liver transplantation	NR	11 / 15	36±2.7 / 39±0.5
Rayes 2002(2)	60(30 / 30)	C: B J: 2	Abdominal surgery	NR	3 / 9	15±7.4 / 16±5.5
Homann 1994	100(50 / 50)	C: B J: 2	Inpatients	6 / 15	NR	NR
Khalil 1998	16(8 / 8)	C: B J: 2	Postoperative	1 / 2	NR	NR

C = concealment of allocation; J = Jadad score; NR = not reported.

Table 2 Effect of EN with DF on diarrhea

Study	Favors DF-supplement n / N	Favors DF-free n / N	Weight %	OR (95%CI fixed)
Dobb 1990	16 / 45	13 / 46	24.0	1.40 [0.58,3.40]
Homann 1994	6 / 50	15 / 50	38.3	0.32 [0.11,0.91]
Khalil 1998	1 / 8	2 / 8	5.1	0.43 [0.03,5.99]
Schultz 2000	6 / 22	7 / 22	14.8	0.80 [0.22,2.94]
Spapen 2001	6 / 13	11 / 12	17.9	0.08 [0.01,0.79]
Total(95%CI)	35 / 138	48 / 138	100.0	0.61 [0.36,1.05]

Test for heterogeneity chi-square = 8.13, df = 4, $P = 0.087$; Test for overall effect $z = -1.79$, $P = 0.07$.

Table 3 Sensitivity-analysis of effects of EN with DF on diarrhea

Study	Favors DF-supplement n / N	Favors DF-free n / N	Weight %	OR (95%CI fixed)
Dobb 1990	16 / 45	13 / 46	24.0	1.40 [0.58,3.40]
Schultz 2000	6 / 22	7 / 22	14.8	0.80 [0.22,2.94]
Spapen 2001	6 / 13	11 / 12	17.9	0.08 [0.01,0.79]
Total(95%CI)	28 / 80	31 / 80	100.0	0.83 [0.43,1.60]

Test for heterogeneity $\chi^2 = 5.34$, df = 2, $P = 0.069$, Test for overall effect z = -0.56, $P = 0.6$.

regulate the inhibitor feedback mechanism[27-31]. Accordingly, DF may have potentials beneficial to controlling diarrhea in EN[32-35]. But the existing clinical trials did not show identical results, so strict evaluation is essential. The occurrence of diarrhea in trials adopted in this review was 30.01%, combined OR was 0.61, 95% confidence interval was from 0.36 to 1.05 ($Z = -1.79$, $P = 0.07$). The difference was not statistically significant. Subgroup analysis revealed that DF was beneficial to diarrhea in non-critically ill patients but uncertain in critically ill patients. Critically ill patients were apt to complicate severe hypoalbuminemia and superinfection, which could lead to refractory diarrhea[34,35]. In the review, diarrhea occurred in 34.78% of critically ill patients, far higher than that in the non-critical patients (20.69%).

Diarrhea diagnosis is lack of objective criteria. Three trials in the review adopted Hatt and Dobb diarrhea score, which records defecation by volume and consistency. Diarrhea was defined as the scores more than 12. This score was convenient to compare different trials.

High attention has been paid to intestinal bacterial translocation leading to a considerable amount of infections. A series of animal experiments suggested that DF could effectively reduce the intestinal bacterial translocation in stress status[36]. The mechanism remains unclear. DF is able to maintain the structure and function of epithelia, regulate immunological reactions, promote secretion of IgA and mucus, all these may play a role in diarrhea[37-39]. Administration of DF can reduce the infection theoretically. However, analysis of the seven trials failed to show the anticipated results (combined OR 0.44, $P = 0.05$). The review suggests that DF could significantly shorten the length of hospital stay of patients who had undergone liver transplantation or abdominal surgery.

There is little evidence from these trials that DF is beneficial to diarrhea and infection of critically ill patients. It is necessary to design more large size and high-quality randomized controlled trials. The effect of DF on a variety of patients should also be further studied.

REFERENCES

1 **Englyst HN,** Quigley ME, Hudson GJ. Definition and measurement of dietary fibre. *Eur J Clin Nutr* 1995; **49**(Suppl 3): S48-62

2 **Cummings JH,** Macfarlane GT. Role of intestinal bacteria in nutrient metabolism. *JPEN J Parenter Enteral Nutr* 1997; **21:** 357-365

3 **Spaeth G,** Gottwald T, Hirner A. Fibre is an essential ingredient of enteral diets to limit bacterial translocation in rats. *Eur J Surg* 1995; **161**: 513-518

4 **Kanauchi O,** Suga T, Tochihara M, Hibi T, Naganuma M, Homma T, Asakura H, Nakano H, Takahama K, Fujiyama Y, Andoh A, Shimoyama T, Hida N, Haruma K, Koga H, Mitsuyama K, Sata M, Fukuda M, Kojima A, Bamba T. Treatment of ulcerative colitis by feeding with germinated barley foodstuff: first report of a multicenter open control trial. *J Gastroenterol* 2002; **37**(Suppl 14): 67-72

5 **Wisker E,** Daniel M, Rave G, Feldheim W. Fermentation of non-starch polysaccharides in mixed diets and single fibre sources: comparative studies in human subjects and *in vitro*. *Br J Nutr* 1998; **80:** 253-261

6 **Demetriades H,** Botsios D, Kazantzidou D, Sakkas L, Tsalis K, Manos K, Dadoukis I. Effect of early postoperative enteral feeding on the healing of colonic anastomoses in rats. Comparison of three different enteral diets. *Eur Surg Res* 1999; **31:** 57-63

7 **Kripke SA,** Fox AD, Berman JM, Settle RG, Rombeau JL. Stimulation of intestinal mucosal growth with intracolonic infusion of short-chain fatty acids. *J Parenter Enteral Nutr* 1989; **13:** 109-116

8 **Bowling TE,** Raimundo AH, Grimble GK, Silk DB. Reversal by short-chain fatty acids of colonic fluid secretion induced by enteral feeding. *Lancet* 1993; **342:** 1266-1268

9 **Gomez Candela C,** de Cos Blanco AI, Iglesias Rosado C. Fiber and enteral nutrition. *Nutr Hosp* 2002; **17**(Suppl 2): 30-40

10 **Nakao M,** Ogura Y, Satake S, Ito I, Iguchi A, Takagi K, Nabeshima T. Usefulness of soluble dietary fiber for the treatment of diarrhea during enteral nutrition in elderly patients. *Nutrition* 2002; **18:** 35-39

11 **Wright J.** Total parenteral nutrition and enteral nutrition in diabetes. *Curr Opin Clin Nutr Metab Care* 2000; **3:** 5-10

12 **Coulston AM.** Clinical experience with modified enteral formulas for patients with diabetes. *Clin Nutr* 1998; **17**(Suppl 2): 46-56

13 **Sobotka L,** Bratova M, Slemrova M, Manak J, Vizd'a J, Zadak Z. Inulin as the soluble fiber in liquid enteral nutrition. *Nutrition* 1997; **13:** 21-25

14 **Hebden JM,** Blackshaw E, D'Amato M, Perkins AC, Spiller RC. Abnormalities of GI transit in bloated irritable bowel syndrome: effect of bran on transit and symptoms. *Am J Gastroenterol* 2002; **97:** 2315-2320

15 **Olah A,** Belagyi T, Issekutz A, Gamal ME, Bengmark S. Randomized clinical trial of specific lactobacillus and fibre supplement to early enteral nutrition in patients with acute pancreatitis. *Br J Surg* 2002; **89:** 1103-1107

16 **Parisi GC,** Zilli M, Miani MP, Carrara M, Bottona E, Verdianelli G, Battaglia G, Desideri S, Faedo A, Marzolino C, Tonon A, Ermani M, Leandro G. High-fiber diet supplementation in patients with irritable bowel syndrome (IBS): a multicenter, randomized, open trial comparison between wheat bran diet and partially hydrolyzed guar gum (PHGG). *Dig Dis Sci* 2002; **47:** 1697-1704

17 **Tonstad S,** Smerud K, Hoie L. A comparison of the effects of 2 doses of soy protein or casein on serum lipids, serum lipoproteins, and plasma total homocysteine in hypercholesterolemic subjects. *Am J Clin Nutr* 2002; **76:** 78-84

18 **Jenkins DJ,** Kendall CW, Vuksan V, Augustin LS, Li YM, Lee B, Mehling CC, Parker T, Faulkner D, Seyler H, Vidgen E, Fulgoni V. The effect of wheat bran particle size on laxation and colonic fermentation. *Am Coll Nutr* 1999; **18:** 339-345

19 **Rayes N,** Seehofer D, Hansen S, Boucsein K, Muller AR, Serke S, Bengmark S, Neuhaus P. Early enteral supply of lactobacillus and fiber versus selective bowel decontamination: a controlled trial in liver transplant recipients. *Transplantation* 2002; **74:** 123-127

20 **Rayes N,** Hansen S, Seehofer D, Muller AR, Serke S, Bengmark S, Neuhaus P. Early enteral supply of fiber and Lactobacilli versus conventional nutrition: a controlled trial in patients with major abdominal surgery. *Nutrition* 2002; **18:** 609-615

21 **Spapen H,** Diltoer M, Van Malderen C, Opdenacker G, Suys E, Huyghens L. Soluble fiber reduces the incidence of diarrhea in septic patients receiving total enteral nutrition: a prospective, double-blind, randomized, and controlled trial. *Clin Nutr* 2001; **20:** 301-305

22 **Schultz AA,** Ashby-Hughes B, Taylor R, Gillis DE, Wilkins

M. Effects of pectin on diarrhea in critically ill tube-fed patients receiving antibiotics. *Am J Crit Care* 2000; **9:** 403-411

23 **Khalil L,** Ho KH, Png D, Ong CL. The effect of enteral fibre-containing feeds on stool parameters in the post-surgical period. *Singapore Med J* 1998; **39:** 156-159

24 **Homann HH,** Kemen M, Fuessenich C, Senkal M, Zumtobel V. Reduction in diarrhea incidence by soluble fiber in patients receiving total or supplemental enteral nutrition. *J Parenter Enteral Nutr* 1994; **18:** 486-490

25 **Dobb GJ,** Towler SC. Diarrhoea during enteral feeding in the critically ill: a comparison of feeds with and without fibre. *Intensive Care Med* 1990; **16:** 252-255

26 **Burks AW,** Vanderhoof JA, Mehra S, Ostrom KM, Baggs G. Randomized clinical trial of soy formula with and without added fiber in antibiotic-induced diarrhea. *J Pediatr* 2001; **139:** 578-582

27 **Lin HC,** Zhao XT, Chu AW, Lin YP, Wang L. Fiber-supplemented enteral formula slows intestinal transit by intensifying inhibitory feedback from the distal gut. *Am J Clin Nutr* 1997; **65:** 1840-1844

28 **Bliss DZ,** Jung HJ, Savik K, Lowry A, LeMoine M, Jensen L, Werner C, Schaffer K. Supplementation with dietary fiber improves fecal incontinence. *Nurs Res* 2001; **50:** 203-213

29 **Bouin M,** Savoye G, Herve S, Hellot MF, Denis P, Ducrotte P. Does the supplementation of the formula with fibre increase the risk of gastro-oesophageal reflux during enteral nutrition? A human study. *Clin Nutr* 2001; **20:** 307-312

30 **Silk DB,** Walters ER, Duncan HD, Green CJ. The effect of a polymeric enteral formula supplemented with a mixture of six fibres on normal human bowel function and colonic motility. *Clin Nutr* 2001; **20:** 49-58

31 **Murray SM,** Patil AR, Fahey GC Jr, Merchen NR, Wolf BW, Lai CS, Garleb KA. Apparent digestibility and glycaemic responses to an experimental induced viscosity dietary fibre incorporated into an enteral formula fed to dogs cannulated in the ileum. *Food Chem Toxicol* 1999; **37:** 47-56

32 **Reese JL,** Means ME, Hanrahan K, Clearman B, Colwill M, Dawson C. Diarrhea associated with nasogastric feedings. *Oncol Nurs Forum* 1996; **23:** 59-66

33 **Kapadia SA,** Raimundo AH, Grimble GK, Aimer P, Silk DB. Influence of three different fiber-supplemented enteral diets on bowel function and short-chain fatty acid production. *J Parenter Enteral Nutr* 1995; **19:** 63-68

34 **Bass DJ,** Forman LP, Abrams SE, Hsueh AM. The effect of dietary fiber in tube-fed elderly patients. *J Gerontol Nurs* 1996; **22:** 37-44

35 **Lien KA,** McBurney MI, Beyde BI, Thomson AB, Sauer WC. Ileal recovery of nutrients and mucin in humans fed total enteral formulas supplemented with soy fiber. *Am J Clin Nutr* 1996; **63:** 584-595

36 **Nakamura T,** Hasebe M, Yamakawa M, Higo T, Suzuki H, Kobayashi K. Effect of dietary fiber on bowel mucosal integrity and bacterial translocation in burned rats. *J Nutr Sci Vitaminol* 1997; **43:** 445-454

37 **Caparros T,** Lopez J, Grau T. Early enteral nutrition in critically ill patients with a high-protein diet enriched with arginine, fiber, and antioxidants compared with a standard high-protein diet. The effect on nosocomial infections and outcome. *J Parenter Enteral Nutr* 2001; **25:** 299-308

38 **Tariq N,** Jenkins DJ, Vidgen E, Fleshner N, Kendall CW, Story JA, Singer W, D'Costa M, Struthers N. Effect of soluble and insoluble fiber diets on serum prostate specific antigen in men. *J Urol* 2000; **163:** 114-118

39 **Frankel W,** Zhang W, Singh A, Bain A, Satchithanandam S, Klurfeld D, Rombeau J. Fiber: effect on bacterial translocation and intestinal mucin content. *World J Surg* 1995; **19:** 144-148

Science Editor Wang XL and Li WZ **Language Editor** Elsevier HK

PO Box 2345, Beijing 100023, China
www.wjgnet.com
wjg@wjgnet.com

ELSEVIER

World J Gastroenterol 2005;11(25):3939-3943
World Journal of Gastroenterology ISSN 1007-9327

• *BRIEF REPORTS* •

Personal experience with the procurement of 32 liver allografts

Guang-Wen Zhou, Cheng-Hong Peng, Hong-Wei Li

Guang-Wen Zhou, Cheng-Hong Peng, Hong-Wei Li, Department of Surgery, Ruijin Hospital, Shanghai Second Medical University, Shanghai 200025, China
Correspondence to: Guang-Wen Zhou, Department of Surgery, Ruijin Hospital, Shanghai Second Medical University, Shanghai 200025, China. gw_vrai@yahoo.com.cn
Telephone: +86-21-64370045-666705
Received: 2004-07-23 Accepted: 2004-09-19

Key words: Liver transplantation; Liver procurement; Donor; Arterial anomalies

Zhou GW, Peng CH, Li HW. Personal experience with the procurement of 32 liver allografts. *World J Gastroenterol* 2005; 11(25): 3939-3943
http://www.wjgnet.com/1007-9327/11/3939.asp

Abstract

AIM: To introduce the American Pittsburgh's method of rapid liver procurement under the condition of brain death and factors influencing the quality of donor liver.

METHODS: To analyze 32 cases of allograft liver procurement retrospectively and observe the clinical outcome of orthotopic liver transplantation.

RESULTS: Average age of donors was 38.24±12.78 years, with a male:female ratio of 23:9. The causes of brain death included 21 cases of trauma (65.63%) and nine cases of cerebrovascular accident (28.13%). Fourteen grafts (43.75%) had hepatic arterial anomalies, seven cases only right hepatic arterial anomalies (21.88%), five cases only left hepatic arterial anomalies (15.63%) and two cases of both right and left hepatic arterial anomalies (6.25%) among them. Eight cases (57.14%) of hepatic arterial anomalies required arterial reconstruction prior to transplantation. Of the 32 grafts evaluated for early function, 27 (84.38%) functioned well, whereas three (9.38%) functioned poorly and two (6.25%) failed to function at all. Only one recipient died after transplantation and thirty-one recipients recovered. Four recipients needed retransplantation. The variables associated with less than optimal function of the graft consisted of donor age (35.6±12.9 years *vs* 54.1±4.3 years, $P<0.05$), duration of donor's stay in the intensive care unit (ICU) (3.5±2.4 d *vs* 7.4±2.1 d, $P<0.005$), abnormal graft appearance (19.0% *vs* 100%, $P<0.05$), and such recipient problems as vascular thromboses during or immediately following transplantation (89.3% *vs* 50.0%, $P<0.005$).

CONCLUSION: During liver procurement, complete heparization, perfusion *in situ* with localized low temperature and standard technique procedures are the basis ensuring the quality of the graft. The hepatic arterial anomalies should be taken care of to avoid injury. The donor age, duration of donor's staying in ICU, abnormal graft appearance and recipient problem are important factors influencing the quality of the liver graft.

INTRODUCTION

Enormous progress including surgical techniques has been achieved since the first orthotopic liver transplantation (OLTx) was performed in humans in 1963 and OLTx has established its role as a therapeutic option for patients with end-stage liver disease. Primary graft nonfunction (PGN) remains a dreadful complication of OLTx, one that is associated with a high mortality and morbidity, and therefore liver allograft with good function is the most important point for ensuring the success of liver transplantation. A single donor surgeon's experience procuring the livers from 32 donors in Pittsburgh Transplant Center is analyzed in order to identify the role of a number of variables pertinent to the clinical outcome of OLTx.

MATERIALS AND METHODS

Donor data

The author performed 32 allograft hepatectomies at the University of Pittsburgh Transplant Center. All donors were brain dead and the age of the donors varied from 12 to 63 years with the average of 38.24±12.78 years. Among them, there were 23 male donors and 9 female donors. Table 1 lists the causes of death of the donors.

Table 1 Causes of brain death among 32 liver donors

Cause	*n* (%)
Trauma	21 (65.63)
Motor vehicle accident	16
Gunshot wound	1
Fall	2
Other	2
Cerebrovascular accident	9 (28.13)
Cerebral infarct	6
Subarachnoid hemorrhage	3
Others	2 (6.24)
Total	32 (100)

Donor selection criteria

In general, donors were selected who were less than 65 years

of age, had no history of liver disease such as hepatitis or alcoholism, and a total serum bilirubin less than 34 μmol/L, normal or near-normal alanine aminotransferase (ALT), aspartate aminotransferase (AST), alkaline phosphatase (AKP), γ-glutathione transferase (γ-GT) and prothrombin time (PT), and adequate arterial blood gas. Elevations of ALT, AST, AKP and γ-GT, with a tendency to decline, were not regarded as a contraindication for donation of the liver.

Donor maintenance

Donors were fluid-resuscitated once they had been pronounced brain dead in order to maintain a central venous pressure of 8-10 cm H_2O and urine output over 1 mL/(kg • h) as a guide. For donors receiving vasopressin for diabetes insipidus, the vasopressin was discontinued as soon as possible to avoid liver ischemia secondary to a decreased splanchnic blood flow. Urine output was replaced vigorously with intravenous fluids, usually one-half or quarter normal saline solution with potassium chloride. Electrolytes were checked frequently, especially to correct hypokalemia. Normothermia was maintained with a thermoblanket. Blood was transfused to maintain the hematocrit above 30% in order to maintain adequate oxygen delivery to the tissues.

Operative technique

The technique of allograft hepatectomy involved both rapid perfusion and modified rapid perfusion[1-3]. Rapid perfusion technique is as follows. Briefly, both the terminal aorta and the inferior mesenteric vein were dissected to insert aortic and portal perfusion cannulae. The supraceliac abdominal aorta was encircled and crossclamped. Following cardiectomy, dissection of liver hilum was performed in a bloodless field[4,5]. Following identification of whether or not an aberrant right hepatic artery (HA) originating from superior mesenteric artery (SMA) in the retropancreatic portion, the right side of the SMA was dissected toward the aorta. A Carrel patch of aorta was excised, with care not to injure the origin of the renal arteries. This has been our preferred method of hepatectomy in unstable donors, or in cases of extreme urgency when the recipient is in fulminant liver failure due to fulminant hepatitis or graft nonfunction following OLTx. Modified rapid perfusion technique differs from the rapid perfusion technique in that dissection of the liver hilum occurs prior to crossclamping of the aorta and cannulation of the distal splenic vein with a larger caliber catheter for a quicker portal perfusion. This preliminary dissection allows more selective and rapid cooling of the liver than does the rapid perfusion technique. These additional preparatory steps required 30-45 min. This technique has been our choice for stable donors and for donors whose livers are of a questionable quality. During the preparatory dissection, changes in the color or consistency of the allograft were observed in response to diuresis, or better oxygenation.

Technique of vascular reconstruction for arterial anomalies

Arterial reconstruction of the liver graft is required prior to transplantation and is very pivotal if a common arterial channel is absent due to an anomaly. The most common arterial anomaly requiring reconstruction was the aberrant right HA arising from the SMA, for which an end-to-end anastomosis was performed between the distal donor splenic artery and the proximal aberrant right HA. This was achieved with a Carrel patch of the SMA, obviating a small caliber anastomosis[6]. Care was taken to avoid an inadvertent anastomosis with rotation. The continuous suture technique with 8-0 monofilament polypropylene (Prolene) was used for the reconstruction. Just before the sutures were tied, the reconstructed HA was allowed to distend by pulsatile infusion of cold solution. With the application of "growth factor" principle to the *ex vivo* condition, this method facilitated migration of Prolene sutures into the anastomosis and allowed secure anastomosis without leakage or stricture.

Classification of early graft function

Early graft function was divided into four grades as good, fair, poor and PGN. Good meant AST<1 500 IU/L, ALT <1 000 IU/L and fresh frozen plasma (FFP) was not necessary. Fair meant AST 1 500-3 500 IU/L, ALT 1 000-2 500 IU/L and FFP was not required. Poor meant AST> 3 500 IU/L, ALT>2 500 IU/L and FFP was required. PGN was defined as the inability of graft to sustain the metabolic homeostasis of the recipient during the first postoperative week, presenting with the clinical manifestations of grade III or IV coma, coagulopathy with prothrombin time over 20 s, high ALT and AST values, renal failure, and progressive or persistent hyperbilirubinemia, resulting in retransplantation of the graft or death of the recipient.

Statistical analysis

Student's *t* and χ^2 tests were used for the statistical evaluation of the data.

RESULTS

Vascular anomalies

Table 2 lists the incidence of hepatic arterial anomalies and various methods of arterial reconstruction. Hepatic arterial anomalies were present in 14 grafts (43.75%): the aberrant right HA in seven (21.88%), the aberrant left HA in five (15.63%), and both aberrant right and left hepatic arteries in two grafts (6.25%). Of these, eight grafts (57.14%) required vascular reconstruction at the back table in order to construct a common arterial channel, and one of the anastomoses constructed at the back table required the revision due to rotation.

Table 2 Vascular reconstruction for hepatic arterial anomalies

Anomaly	*n* (%)	Method of reconstruction (*n*)
Aberrant RHA	7 (21.88)	
From SMA	6	Donor SpA to aberrant RHA (4)
From aorta	1	Donor SpA to aberrant RHA (1)
Aberrant LHA	5 (15.63)	
From CA	3	
From aorta	2	Donor SpA to PHA (1)
Aberrant RHA and LHA	2 (6.25)	
RHA from SMA	1	Donor SpA to RHA (1)
LHA from CA	1	CA to distal SMA (1)
Total	14 (43.75)	

RHA: right hepatic artery; SMA: superior mesenteric artery; SpA: splenic artery; LHA: left hepatic artery; CA: celiac axis, PHA: proper hepatic artery.

Injury of hepatic artery

A total of four complications (6.25%) occurred during or after allograft hepatectomy due to aberrant HA: inadvertent transection of the aberrant right HA, once originating directly from the aorta and once from the left side of the SMA. The transected aberrant right hepatic arteries were reconstructed using end-to-end anastomosis with the donor splenic artery with interrupted 8-0 Prolene sutures. Overall, none of the complications affected the outcome of the liver or other organ recipients.

Early graft function

Table 3 lists the early graft function of the 32 allografts after OLTx. Graft function was good or fair in 25 out of 28 (89.3%) of the grafts without recipient problems, whereas as many as two out of four (50%) of the grafts with recipient problems during or immediately following OLTx exhibited poor or nonfunction ($P<0.005$; $\chi^2 = 12.96$). This was due to HA thrombosis and multi-organ failure and meanwhile HA thrombosis was caused not by HA anomaly during allograft procurement but by HA reconstruction. Table 4 shows the correlation between the donor or graft variables and the early graft function of the 28 grafts that survived the operation and did not develop the aforementioned recipient complications during or immediately following OLTx. A statistically significant difference was noticed in the duration of patient's stay in ICU, requirement of cardiopulmonary resuscitation and the presence of abnormal graft appearance ($P<0.05$).The donors of grafts with fair or poor function stayed in ICU longer than those with good function ($P<0.005$), and the grafts with abnormal appearance were associated with a higher incidence of fair or poor graft function in recipients ($P<0.05$; $\chi^2 = 6.21$). The donors of graft with poor or nonfunction were significantly older than those with good or fair function and there was no significant difference between good and fair groups. On the other hand, no definitive correlation with early graft function was observed in sex, results of liver function tests, infusion of high-dose vasopressors and cold ischemia time.

Table 3 Early graft function after orthotopic liver transplantation

Early graft function	Number of recipient problems		Total (%)
	No (%)	Yes[1] (%)	
Good	21 (75)	1 (25)	22 (68.75)
Fair	4 (14.29)	1 (25)	5 (14.29)
Poor	2 (7.14)	1 (25)	3 (9.38)
PGN	1 (3.57)	1 (25)	2 (6.25)
Total	28 (100)	4 (100)	32 (100)

[1]Including hepatic artery thrombosis in one patient, intraoperative incidence from severe hemorrhage in two patients, and multi-organ failure in one patient.

Table 4 Correlation between donor or graft variables and early graft function

Variable	Good (n = 21)	Fair (n = 4)	Poor (n = 2)	PGN (n = 1)
Age (yr)	35.6±12.9	43.5±13.8	54.1±4.3	63
Sex (M:F)	15:6	2:2	2:0	1:0
AST(IU/L)	76.4±23.6	63.3±37.1	89.2±42.1	151
ALT(IU/L)	43.2±26.1	69.8±34.9	68.1±31.2	78.1
T. Bil (μmol/L)	12.5±3.4	14.5±7.4	11.8±7.9	20.5
PT(s)	15.2±1.4	14.8±1.2	14.2±1.6	15.5
CPR	4 (19.0%)	2 (50%)		
ICU stay (d)	3.5±2.4	6.2±3.3	7.4±2.1	12
High dose vasopressors	8 (38.1%)	2 (50%)	1 (50%)	0
Abnormal graft appearance	4 (19.0%)	1 (25%)	2 (100%)	1 (100%)
CIT (min)	379±128	421±183	389±214	402±103

CIT: cold ischemia time; T. Bil: total bilirubin; CPR: cardiopulmonary resuscitation.

Recipient survival

Of the 32 patients who received liver allografts, 27 patients recovered and remained alive and well after first liver transplantation, four patients needed retransplantation and all were discharged. One patient died of multi-organ failure in one month after transplantation due to primary graft nonfunction.

DISCUSSION

Early graft function is very closely associated with donor age, duration of patient's stay in ICU and the presence of abnormal graft appearance. The effect of increased donor age on the outcome of OLTx remains controversial[7,8]. Previously the upper limit of donor age was 50 years. As gradual accumulation of experience of clinical OLTx, now some transplant centers elevate the upper limit of donor age to 65 years. But we suggest that the donor age should be limited to below 60 years, or allograft dysfunction or non-function would easily appear and increase mortality[9]. When the appearance of the liver has changes in color, blunt edge and anomalous nodulae, it is necessary for frozen pathological examination before transplantation. Steatosis is the most important cause of PGN. The comparatively simple differentiating method is that white four-by being put into the container will turn into pale yellowish after several minutes and this will suggest that the degree of fat infiltrating liver tissue will be over 30%, however, pathological examination to evaluate the degree of fatty infiltration is the most reliable method. As to the hemodynamic stability of the donor, hypotension or the requirement of high-dose dopamine has been associated with nonfunction or delayed function, respectively. Although no obvious harmful effects of cardiopulmonary resuscitation on the early function of the liver allograft were demonstrated in this study, suboptimal perfusion of the liver and warm ischemic injury were strongly suggested. As to the abnormal appearance of the graft, little is known about the correlation between gross appearance and quality of the graft. Livers from donors with diabetes insipidus, who have been on vasopressin for a prolonged period of time, are often firm and suggest the presence of ischemic injury and liver allograft will be harder to touch. Since the use of vasopressin has been associated with a marked reduction in the blood flow to the

liver, donors scheduled for liver procurement should stop vasopressin as soon as possible in order to minimize ischemic damage. Overhydration can distend the liver by an increase in central venous pressure and give a false impression as to the consistency of the liver. If the liver is distended from overhydration, the administration of intravenous diuretics can be used immediately.

As far as now, there have been two methods for procurement of liver allografts including aortic perfusion only (APO)[10] and aortic and portal perfusion (APP). Due to shortage of donors, most American transplantation centers adopt multi-organ procurement, which means APO is the sole choice. The experience of Pittsburgh is that APO has no harm to allograft liver and its advantage is simple surgical procedure compared with APP[11], meanwhile, superior mesenteric vein need not be exposed and therefore it reduces the separation and division of tissue. If RHA originates from superior mesenteric artery, the unexposition of superior mesenteric vein might avoid injuring aberrant right hepatic artery and ischemic injury of splenic organ due to arterial spasm by surgical procedure[12-14].

The aberrant hepatic artery is very common; the aberrant rate was as high as 43.75% in our group. The right hepatic artery originating from SMA is the most common[15]. In order to avoid injuring hepatic artery, it is very important to decide by touch whether or not there are pulses behind hepatoduodenal ligament before the abdominal aorta is clamped in the process of procurement of allograft liver. Even if there is no pulse, it could not exclude aberrant right hepatic artery. So routinary division of the right side of SMA can often protect aberrant right hepatic artery before dissection of hepatoduodenal ligament. Once there exist the injuries of aberrant hepatic arteries, several aspects should be noticed in the process of the reconstruction of hepatic arteries as follows: (1) the inner membrane of hepatic artery should not be dragged; (2) it is achieved with Carrel patch of the SMA to obviate a small caliber anastomosis; (3) whether the continuous suture will be used depends on operator's mastering of the technique of vascular anastomosis; (4) just before the sutures were tied, the reconstructed HA was allowed to distend by pulsatile infusion of cold solution while the distal HA was occluded digitally and such method can identify whether the reconstructed anastomosis has leakage and stricture, or thrombosis of HA will occur which could cause biliary tract complication[16-19].

Although division of third hepatic hilum caused severe bleeding for two recipients in our group, this would not affect the early function of allograft liver. Hepatic artery thrombosis and multi-organ failure in earlier stage after transplantation caused poor and non-function for another two patients. Pittsburgh Transplant Center adopts the anastomosis between hepatic artery at the level of gastroduodenal artery in recipient and hepatic artery in donor, hepatic artery thrombosis in earlier stage after transplantation is associated with the technique of anastomosis. The simple differentiating method is to observe the pulse of hepatic artery after anastomosis, Doppler for hepatic artery the first day after liver transplantation is the optimal for finding thrombosis as soon as possible. Multi-organ failure often accompanies the instability of systemic hemodynamics and the liver is much easier to be affected by ischemic-reperfusion injury, while the injury of the liver also worsens the multi-organ failure and this pernicious recycle can cause patients to die.

For the assessment of allograft viability in clinical OLTx, there is, to date, no practical and simple technique available that is discriminately predictive of allograft function before the actual transplant procedure. Primary graft non-function remains a major cause of mortality, and although the shortage of donor organs remains a major limiting factor in clinical liver transplantation[20], still we should have a careful attitude toward the choice of liver allograft and take into serious account several predictive factors. If so, better therapeutic effect will be achieved.

REFERENCES

1 **Starzl TE,** Miller C, Bronznick B, Makowka L. An improved technique for multiple organ harvesting. *Surg Gynecol Obstet* 1987; **165**: 343-348

2 **Boggi U,** Vistoli F, Del Chiaro M, Signori S, Pietrabissa A, Costa A, Bartolo TV, Catalano G, Marchetti P, Del Prato S, Rizzo G, Jovine E, Pinna AD, Filipponi F, Mosca F. A simplified technique for the en bloc procurement of abdominal organs that is suitable for pancreas and small-bowel transplantation. *Surgery* 2004; **135**: 629-641

3 **Nunez A,** Goodpastor SE, Goss JA, Washburn WK, Halff GA. Enlargement of the cadaveric-liver donor pool using *in-situ* split-liver transplantation despite complex hepatic arterial anatomy. *Transplantation* 2003; **76**: 1134-1136

4 **Fukumori T,** Kato T, Levi D, Olson L, Nishida S, Ganz S, Nakamura N, Madariaga J, Ohkohchi N, Satomi S, Miller J, Tzakis A. Use of older controlled non-heart-beating donors for liver transplantation. *Transplantation* 2003; **75**: 1171-1174

5 **Pinna AD,** Dodson FS, Smith CV, Furukawa H, Sugitani A, Fung JJ, Corry RJ. Rapid en bloc technique for liver and pancreas procurement. *Transplant Proc* 1997; **29**: 647-648

6 **Jeon H,** Ortiz JA, Manzarbeitia CY, Alvarez SC, Sutherland DE, Reich DJ. Combined liver and pancreas procurement from a controlled non-heart-beating donor with aberrant hepatic arterial anatomy. *Transplantation* 2002; **74**: 1636-1639

7 **Marino IR,** Doria C, Doyle HR, Gayowski TJ. Matching donors and recipients. *Liver Transpl Surg* 1998; **4**(5 Suppl 1): S115-119

8 **Lopez-Navidad A,** Caballero F. For a rational approach to the critical points of the cadaveric donation process. *Transplant Proc* 2001; **33**: 795-805

9 **Oh CK,** Sanfey HA, Pelletier SJ, Sawyer RG, McCullough CS, Pruett TL. Implication of advanced donor age on the outcome of liver transplantation. *Clin Transplant* 2000; **14** (4 Pt 2): 386-390

10 **Chui AK,** Thompson JF, Lam D, Koutalistras N, Wang L, Verran DJ, Sheil AG. Cadaveric liver procurement using aortic perfusion only. *Aust NZ J Surg* 1998; **68**: 275-277

11 **de Ville de Goyet J,** Hausleithner V, Malaise J, Reding R, Lerut J, Jamart J, Barker A, Otte JB. Liver procurement without in situ portal perfusion. A safe procedure for more flexible multiple organ harvesting. *Transplantation* 1994; **57**: 1328-1332

12 **Wei WI,** Lam LK, Ng RW, Liu CL, Lo CM, Fan ST, Wong J. Microvascular reconstruction of the hepatic artery in live donor liver transplantation: experience across a decade. *Arch Surg* 2004; **139**: 304-307

13 **Soliman T,** Bodingbauer M, Langer F, Berlakovich GA, Wamser P, Rockenschaub S, Muehlbacher F, Steininger R. The role of complex hepatic artery reconstruction in orthotopic

liver transplantation. *Liver Transpl* 2003; **9**: 970-975
14 **Turrion VS,** Alvira LG, Jimenez M, Lucena JL, Ardaiz J. Incidence and results of arterial complications in liver transplantation: experience in a series of 400 transplants. *Transplant Proc* 2002; **34**: 292-293
15 **Hesse UJ,** Troisi R, Maene L, de Hemptinne B, Pattyn P, Lameire N. Arterial reconstruction in hepatic and pancreatic allograft transplantation following multi-organ procurement. *Transplant Proc* 2000; **32**: 109-110
16 **Zhou GW,** Cai WY, Li HW, Zhu Y, Dodson F, Fung JJ. Transjugular intrahepatic portosystemic shunt for liver transplantation. *Hepatobiliary Pancreat Dis Int* 2002; **1**: 179-182
17 **Thuluvath PJ,** Atassi T, Lee J. An endoscopic approach to biliary complications following orthotopic liver transplantation. *Liver Int* 2003; **23**: 156-162
18 **Rerknimitr R,** Sherman S, Fogel EL, Kalayci C, Lumeng L, Chalasani N, Kwo P, Lehman GA. Biliary tract complications after orthotopic liver transplantation with choledochochooledochostomy anastomosis: endoscopic findings and results of therapy. *Gastrointest Endosc* 2002; **55**: 224-231
19 **Nemec P,** Ondrasek J, Studenik P, Hokl J, Cerny J. Biliary complications in liver transplantation. *Ann Transplant* 2001; **6**: 24-28
20 **First MR.** The organ shortage and allocation issues. *Transplant Proc* 2001; **33**: 806-810

Science Editor Zhu LH **Language Editor** Elsevier HK

PO Box 2345, Beijing 100023, China
www.wjgnet.com
wjg@wjgnet.com

ELSEVIER

World J Gastroenterol 2005;11(25):3944-3947
World Journal of Gastroenterology ISSN 1007-9327

• *BRIEF REPORTS* •

5-Fluorouracil concentration in blood, liver and tumor tissues and apoptosis of tumor cells after preoperative oral 5′-deoxy-5-fluorouridine in patients with hepatocellular carcinoma

Jin-Fang Zheng, Hai-Dong Wang

Jin-Fang Zheng, Hai-Dong Wang, Department of Hepatobiliary Surgery, Hainan Provincial People's Hospital, Haikou 570311, Hainan Province, China
Correspondence to: Dr. Jin-Fang Zheng, Department of Hepatobiliary Surgery, Hainan Provincial People's Hospital, Haikou 570311, Hainan Province, China. zhengjf2000@hotmail.com
Telephone: +86-898-66771028 Fax: +86-898-68661664
Received: 2004-08-31 Accepted: 2004-12-21

Zheng JF, Wang HD. 5-Fluorouracil concentration in blood, liver and tumor tissues and apoptosis of tumor cells after preoperative oral 5′-deoxy-5-fluorouridine in patients with hepatocellular carcinoma. *World J Gastroenterol* 2005; 11 (25): 3944-3947
http://www.wjgnet.com/1007-9327/11/3944.asp

Abstract

AIM: To study the levels of 5-fluorouracail (5-FU) in plasma, liver and tumor in patients with hepatocellular carcinoma after oral administration of 5′-deoxy-5-fluorouridine (5′-DFUR).

METHODS: Thirty-nine patients with hepatocellular carcinoma were treated with oral 5′-DFUR for more than 4 d before operation. The contents of 5-FU in plasma, liver and tumor were measured by high performance liquid chromatography (HPLC) and apoptosis of tumor cells was evaluated by *in-situ* TUNEL after resection of tumor.

RESULTS: The concentrations of 5-FU were 1.1 μg/mL, 5.6, 5.9, and 10.5 μg/g in plasma, the liver tissue, the center of tumor and the periphery of tumor, respectively. 5-FU concentration was significantly higher in the periphery of tumor than that in the liver tissue and the center of tumor (10.5±1.6 μg/g *vs* 5.6±0.8 μg/g, $t = 21.38$, $P<0.05$; 10.5±1.6 μg/g *vs* 5.9±0.9 μg/g, $t = 20.07$, $P<0.05$). 5-FU level was significantly lower in plasma than that in the liver and the tumor (1.1±0.3 μg/mL *vs* 5.6±0.8 μg/g, $t = 19.63$, $P<0.05$; 1.1±0.3 μg/mL *vs* 10.5±1.6 μg/g, $t = 41.01$, $P<0.05$). Apoptosis of tumor cells was significantly increased after oral 5′-DFUR compared to the control group without 5′-DFUR treatment.

CONCLUSION: There is a higher concentration of 5-FU distributed in the tumor compared with liver tissue and apoptosis of tumor cells is increased following oral 5′-DFUR compared with the control group. The results indicate that 5′-DFUR is hopeful as neo-adjuvant chemotherapy to prevent recurrence after resection of hepatocellular carcinoma.

Key words: Hepatocellular carcinoma; 5′-Deoxy-5-fluorouridine; 5-Fluorouracail; Apoptosis

INTRODUCTION

Hepatocellular carcinoma (HCC) remains one of the most common neoplasms in the world[1,2]. 5'-Deoxy-5-fluorouridine (5'-DFUR) is an oral fluoropyrimidine derivative and it is converted to 5-fluorouracil (5-FU) by Pyrimidine nucleoside phosphorylase (PyNPase) which is expressed with higher level in tumor tissues compared with normal tissues[3,4]. Oral 5-FU derivatives have shown comparable antitumor activity and long-term oral administration of low-dose has been considered as postoperative adjuvant chemotherapy after curative resection of the cancer to reduce recurrence and improve survival rate[5-9]. The selective antitumor activity of 5'DFUR is correlated with PyNPase activity in tumor[10]. Although the activity of 5-FU in tumor is well recognized, resistance to this agent is frequently observed and remains its major limitation. It was reported that doxifluridine still showed antitumor activity to tumor cells which were resistant to 5-FU[11].

The purpose of the present study was to investigate the impact of preoperative oral 5'-DFUR on distribution of 5-FU in plasma, liver and tumor and apoptosis of tumor cells in patients with hepatocellular carcinoma.

MATERIALS AND METHODS

Chemicals and reagents

5'-DFUR capsule (Furtulon) was produced by Shanghai Roche Pharmaceuticals Co. (Shanghai, China), and standard 5-FU was provided by Sigma Chemicals Co. (USA). Methyl-tert butyl ether, acetonitrile, methanol (HPLC grade) and potassium hydrogen phosphate (AR grade) were purchased from Peking Chemical Plant (Beijing, China).

Chromatographic conditions

HPLC system consisted of LC-10AT HPLC pump and SPD-10A Detector (SHIMADZU Co. Japan). The analytical column was Kromasil C_{18} (5 μm 200 mm×4.6 mm ID). The mobile phase consisted of acetonitrile, methanol, and 0.25 mol/L potassium hydrogen phosphate (1:4:5). The

flow rate was 1.0 mL/min and the wavelength was at 265 nm.

Collection of samples

Thirty-nine patients of 27 male and 12 female with hepatocellular carcinoma were included in this study. Their average age was 49.1 years and the diamters of tumors were from 5 to 7 cm. 5'-DFUR was administered orally and preoperatively (1 200 daily for more than 4 d before operation and 400 mg on the day of operation). The mean total dosage was 6.4 g. Blood sample and specimens of the normal liver tissue and the tumor tissue were collected 3-5 h after final administration. The liver and tumor tissues were cleaned by distilled water and blotted by filter paper. One gram tissue was weighed accurately and 4 mL distilled water was added to the container to crush the tissue. The blood samples and the crushed tissues were centrifuged, and 1 mL plasma or aqueous layer sample was then stored under -20 ℃.

Extraction and determination of samples

Each 0.5 mL plasma or aqueous layer sample was added and mixed with 0.1 mL of potassium hydrogen phosphate (0.5 mol/L), followed by the addition of 5 mL methyl-tert butyl ether to each tube. The tube was then capped and shaken for 10 min on a shaker. The aqueous layer and the organic layer were separated by centrifugation at 3 000 r/min for 10 min. The aqueous layer was transferred to a clean test tube and evaporated to dryness under gentle stream of nitrogen at 50 ℃. The residue was dissolved with 0.1 mL of mobile phase and vortexed. Then the sample was transferred into a micro-spin filter tube and was centrifuged at 3 000 r/min for 10 min. The filtrate was collected and the injection volume was 20 μL and the content of 5-FU was measured by high performance liquid chromatography (HPLC)[12-14].

In vivo detection of apoptosis

TUNEL staining was used to detect DNA degradation *in situ* in the relatively late stage of apoptosis. Apoptotic cells were labeled by the TUNEL reaction using an in situ Cell Apoptosis Detection Kit. *In situ* Cell Apoptosis Detection Kits were purchased from Roche Diagnostics GmbH Co. in Germany. The detailed manipulation was conducted according to instructions for users. The procedure was performed following the instructions of the manufacturer and in reference of the previous observations[15,16].

The positive cells were identified and analyzed based on morphological characteristics of apoptotic cells as previously described. Under the fluorescence microscopy, apoptotic cells manifested as brownish staining in the nuclei. Non-necrotic zone was selected in the tissue section and images were randomly selected. The positive cells were determined in at least five areas at ×400 magnification and divided into three categories as follows: (+) only sporadic positive cells were detected; (++) a cluster of apoptotic cells were observed; (+++) positive cells in a large scale or multi-cluster apoptotic cells were seen in representative tissue sections of each individual case. Twenty patients of HCC without oral 5'-DFUR treatment were included as the control group.

Statistical analysis

The data were expressed as mean±SD. Student's *t*-test was performed for statistical analysis. *P* value less than 0.05 was considered statistically significant.

RESULTS

Concentration of 5-FU in plasma, liver and tumor following oral administration of 5'-DFUR

The concentrations of 5-FU were 1.1 μg/mL, 5.6, 5.9, and 10.5 μg/g in plasma, the liver tissue, the center of tumor and the periphery of tumor, respectively. The 5-FU content was significantly higher in the periphery of tumor than that in the liver tissue and the center of tumor ($P<0.05$). Moreover, the 5-FU concentration was significantly lower in plasma than liver and tumor ($P<0.05$). However, the 5-FU level in the center of tumor was similar to that in the liver tissue (Table 1).

Table 1 5-FU concentrations in blood, liver and tumor after oral 5'-DFUR

Tissue	Level of 5-FU
Plasma (μg / mL)	1.1±0.3[a]
Liver tissue (μg / g)	5.6±0.8
Central tissue of tumor (μg / g)	5.9±0.9
Periphery tissue of tumor (μg / g)	10.5±1.6[a]

[a]$P<0.05$ *vs* 5-FU concentration in liver tissue.

Apoptosis of the tumor cell demonstrated by TUNEL

Under the fluorescence microscope, apoptotic cells manifested as brownish staining in the nuclei. The degree of apoptosis was shown + in tissue sections of the control group in which sporadic positive cells were detected, and ++ in cases with oral 5'-DFUR in which clusters of apoptotic cells were seen (Figures 1A and B).

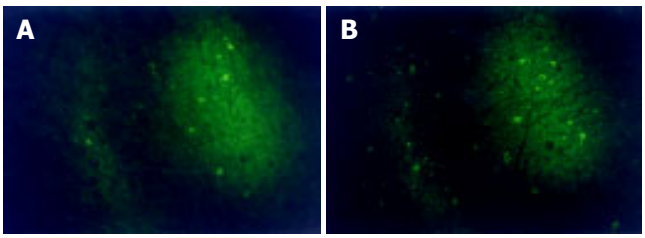

Figure 1 Apoptotic cancer cells detected by TUNEL method after oral administration of 5'-DFUR ×400. **A**: Sporadic apoptotic cells were detected; **B**: clusters of apoptotic cells were detected.

DISCUSSION

It is well known that hepatocellular carcinoma is one of the malignant tumors with poor chemosensitivity to anticancer agents[17,18]. 5-FU is still the first choice for the chemotherapy of hepatocellular carcinoma[19,20], because of its strong killing effects on the cancer cells. 5-FU can damage proliferating cells, reduce the tumor mass in size and prevent tumor

cells from spreading and metastasis. However, its usage is limited due to the rapid development of acquired resistance. The effects of 5-FU are not so satisfactory because 5-FU has a lower concentration in tumor tissue and relatively higher concentrations in blood after intravenous administration of 5-FU. Moreover, its side effects are serious and many patients are unable to tolerate.

5'-DFUR is a prodrug of 5-FU and it is converted to 5-FU by Pyrimidine nucleoside phosphorylase (PyNPase). PyNPase exists in all kinds of tumor tissues and its expression and activity in tumor tissue are higher than that in normal tissue[3,4]. Nagata *et al*.[21-24] reported that transfection of PyNPase gene into tumor cell can increase the sensitivity to 5'-DFUR, and thereby decreases the toxicity of the agent. In our study, it had been found that 5-FU level in tumor was 10 times higher than in plasma and 5-FU level was significantly higher in the periphery of tumor than in the liver tissue. The results suggested that more 5-FU was converted and accumulated within tumor tissue. This difference may be related to the higher PyNPase expression and activity in hepatocellular carcinoma. It had also been found that the 5-FU level was significantly higher in the periphery of tumor than the center of tumor. There was more 5-FU accumulated and converted in the periphery of tumor following oral 5'-DFUR administration. Oxygen, nutrition and growth factors were not equally distributed within the tumor tissue. Oxygen and nutrient of the central tumor tissue are supplied mainly by hepatic artery, and proliferation of the tumor in this region is slower and even partial necrosis appears. However, the periphery of tumor has effluent blood flow supplied by hepatic artery and portal vein, so the tumor cells can grow more rapidly. These results may indicate that large liver tumor is not sensitive to 5'-DFUR.

Oral 5'-DFUR is very convenient and its side effect is slight[25]. The drug arrives in the liver firstly after being absorbed by the intestine. So most of 5'-DFUR can be converted to 5-FU in the liver or the liver tumor and accumulated in these tissues with higher concentration than that administered by iv approach. In this study, the 5-FU level in peripheral vein was only one-tenth of that in tumor tissue. 5-FU can be maintained at a certain level within the tumor tissue but not accumulated in the peripheral vein after regular oral administration of 5'-DFUR.

The expression and activity of PyNPase is higher in the tumor with vascular permeation and lymph node metastasis[4,26,27]. Akao *et al*.[28], reported that PyNPase activity was significantly higher in metastatic lymph node. Tazawa *et al*.[29], found that 5'-DFUR could inhibit hepatic metastasis of tumor, which would be effective for the prophylactic treatment of metastatic disease. These indicate that PyNPase activity appears to be a new useful parameter for identifying both a poor prognosis and a highly malignant potential of tumor and 5'-DFUR is preferably sensitive in cancer patients with lymph node metastasis and vascular infiltration. 5-DFUR is still effective to the tumor which is resistant to 5-FU therapy[11]. Monden *et al*.[30], found that vessel density and stage of tumor were correlated with expression of PyNPase which showed prognosis. 5-DFUR not only is effective on primary tumor and metastatic lesion but also suitable to postoperative prevention of tumor. Apoptosis of the tumor was enhanced after oral administration of 5'-DFUR. In this study, it was found that there were more apoptosis cells in the tumor after oral administration of 5'-DFUR.

In summary, our results showed that there was a higher concentration of 5-FU accumulated in the tumor tissue compared with liver tissue and apoptosis of the tumor cells was increased after oral administration of 5'-DFUR. 5'-DFUR is a hopeful agent for neo-adjuvant chemotherapy to prevent recurrence after resection of hepatocellular carcinoma.

REFERENCES

1 **Yu MC,** Yuan JM, Govindarajan S, Ross RK. Epidemiology of hepatocellular carcinoma. *Can J Gastroenterol* 2000; **14**: 703-709

2 **El-Serag HB.** Hepatocellular carcinoma: an epidemiologic view. *J Clin Gastroenterol* 2002; **35**(5 Suppl 2): S72-78

3 **Kobayashi N,** Kubota T, Watanabe M, Otani Y, Teramoto T, Kitajima M. Pyrimidine nucleoside phosphorylase and dihydropyrimidine dehydrogenase indicate chemosensitivity of human colon cancer specimens to doxifluridine and 5-fluorouracil, respectively. *J Infect Chemother* 1999; **5**: 144-148

4 **Hiroyasu S,** Shiraishi M, Samura H, Tokashiki H, Shimoji H, Isa T, Muto Y. Clinical relevance of the concentrations of both pyrimidine nucleoside phosphorylase (PyNPase) and dihydropyrimidine dehydrogenase (DPD) in colorectal cancer. *Jpn J Clin Oncol* 2001; **31**: 65-68

5 **Ito K,** Okushiba S, Morikawa T, Kondo S, Katoh H. Appropriate duration of postoperative oral adjuvant chemotherapy with HCFU for colorectal cancer. *Gan To Kagaku Ryoho* 2004; **31**: 55-59

6 **Min JS,** Kim NK, Park JK, Yun SH, Noh JK. A prospective randomized trial comparing intravenous 5-fluorouracil and oral doxifluridine as postoperative adjuvant treatment for advanced rectal cancer. *Ann Surg Oncol* 2000; **7**: 674-679

7 **Andre T,** Boni C, Mounedji-Boudiaf L, Navarro M, Tabernero J, Hickish T, Topham C, Zaninelli M, Clingan P, Bridgewater J, Tabah-Fisch I, de Gramont A. Oxaliplatin, fluorouracil, and leucovorin as adjuvant treatment for colon cancer. *N Engl J Med* 2004; **350**: 2343-2351

8 **Takiguchi N,** Fujimoto S, Koda K, Oda K, Okui K, Nakajima N, Miyazaki M. Postoperative adjuvant chemotherapy is effective in gastric cancer with serosal invasion: significance in patients chosen for multivariate analysis. *Oncol Rep* 2002; **9**: 801-806

9 **Zhou J,** Tang ZY, Fan J, Wu ZQ, Ji Y, Xiao YS, Shi YH, Li XM, Sun QM, Liu YK, Ye SL. Capecitabine inhibits postoperative recurrence and metastasis after liver cancer resection in nude mice with relation to the expression of platelet-derived endothelial cell growth factor. *Clin Cancer Res* 2003; **9**(16 Pt 1): 6030-6037

10 **Hata Y,** Takahashi H, Sasaki F, Ogita M, Uchino J, Yoshimoto M, Akasaka Y, Nakanishi Y, Sawada Y. Intratumoral pyrimidine nucleoside phosphorylase (PyNPase) activity predicts a selective effect of adjuvant 5'-deoxy-5-fluorouridine (5'DFUR) on breast cancer. *Breast Cancer* 2000; **7**: 37-41

11 **Bajetta E,** Di Bartolomeo M, Somma L, Del Vecchio M, Artale S, Zunino F, Bignami P, Magnani E, Buzzoni R. Doxifluridine in colorectal cancer patients resistant to 5-fluorouracil (5-FU) containing regimens. *Eur J Cancer* 1997; **33**: 687-690

12 **Zufia L,** Aldaz A, Castellanos C, Giraldez J. Determination of 5-fluorouracil and its prodrug tegafur in plasma and tissue by high-performance liquid chromatography in a single injection: validation for application in clinical pharmacokinetic studies. *Ther Drug Monit* 2003; **25**: 221-228

13 **Nassim MA,** Shirazi FH, Cripps CM, Veerasinghan S, Molepo

MJ, Obrocea M, Redmond D, Bates S, Fry D, Stewart DJ, Goel R. An HPLC method for the measurement of 5-fluorouracil in human plasma with a low detection limit and a high extraction yield. *Int J Mol Med* 2002; **10**: 513-516

14 **Ozawa S,** Hamada M, Murayama N, Nakajima Y, Kaniwa N, Matsumoto Y, Fukuoka M, Sawada J, Ohno Y. Cytosolic and microsomal activation of doxifluridine and tegafur to produce 5-fluorouracil in human liver. *Cancer Chemother Pharmacol* 2002; **50**: 454-458

15 **Xu Y,** Kajimoto S, Nakajo S, Nakaya K. Beta-hydroxyisovalerylshikonin and cisplatin act synergistically to inhibit growth and to induce apoptosis of human lung cancer DMS114 cells via a tyrosine kinase-dependent pathway. *Oncology* 2004; **66**: 67-75

16 **Barnett KT,** Fokum FD, Malafa MP. Vitamin E succinate inhibits colon cancer liver metastases. *J Surg Res* 2002; **106**: 292-298

17 **Huesker M,** Folmer Y, Schneider M, Fulda C, Blum HE, Hafkemeyer P. Reversal of drug resistance of hepatocellular carcinoma cells by adenoviral delivery of anti-MDR1 ribozymes. *Hepatology* 2002; **36**(4 Pt 1): 874-884

18 **Warmann S,** Gohring G, Teichmann B, Geerlings H, Pietsch T, Fuchs J. P-glycoprotein modulation improves *in vitro* chemosensitivity in malignant pediatric liver tumors. *Anticancer Res* 2003; **23**: 4607-4611

19 **Tono T,** Hasuike Y, Ohzato H, Takatsuka Y, Kikkawa N. Limited but definite efficacy of prophylactic hepatic arterial infusion chemotherapy after curative resection of colorectal liver metastases: A randomized study. *Cancer* 2000; **88**: 1549-1556

20 **Guo WJ,** Yu EX. Evaluation of combined therapy with chemoembolization and irradiation for large hepatocellular carcinoma. *Br J Radiol* 2000; **73**: 1091-1097

21 **Nagata T,** Nakamori M, Iwahashi M, Yamaue H. Overexpression of pyrimidine nucleoside phosphorylase enhances the sensitivity to 5'-deoxy-5-fluorouridine in tumour cells *in vitro* and *in vivo*. *Eur J Cancer* 2002; **38**: 712-717

22 **Evrard A,** Cuq P, Ciccolini J, Vian L, Cano JP. Increased cytotoxicity and bystander effect of 5-fluorouracil and 5-deoxy-5-fluorouridine in human colorectal cancer cells transfected with thymidine phosphorylase. *Br J Cancer* 1999; **80**: 1726-1733

23 **Kanyama H,** Tomita N, Yamano T, Miyoshi Y, Ohue M, Fujiwara Y, Sekimoto M, Sakita I, Tamaki Y, Monden M. Enhancement of the anti-tumor effect of 5'-deoxy-5-fluorouridine by transfection of thymidine phosphorylase gene into human colon cancer cells. *Jpn J Cancer Res* 1999; **90**: 454-459

24 **Evrard A,** Cuq P, Robert B, Vian L, Pelegrin A, Cano JP. Enhancement of 5-fluorouracil cytotoxicity by human thymidine-phosphorylase expression in cancer cells: *in vitro* and *in vivo* study. *Int J Cancer* 1999; **80**: 465-470

25 **Min JS,** Kim NK, Park JK, Yun SH, Noh JK. A prospective randomized trial comparing intravenous 5-fluorouracil and oral doxifluridine as postoperative adjuvant treatment for advanced rectal cancer. *Ann Surg Oncol* 2000; **7**: 674-679

26 **Yamagata M,** Mori M, Mimori K, Mafune KI, Tanaka Y, Ueo H, Akiyoshi T. Expression of pyrimidine nucleoside phosphorylase mRNA plays an important role in the prognosis of patients with oesophageal cancer. *Br J Cancer* 1999; **79**: 565-569

27 **Mimori K,** Ueo H, Shirasaka C, Shiraishi T, Yamagata M, Haraguchi M, Mori M. Up-regulated pyrimidine nucleoside phosphorylase in breast carcinoma correlates with lymph node metastasis. *Ann Oncol* 1999; **10**: 111-113

28 **Akao S,** Inoue K. PyNPase and DPD expression potentially predict response to 5'-DFUR treatment for node-positive breast cancer patients. *Gan To Kagaku Ryoho* 2003; **30**: 1361-1364

29 **Tazawa K,** Sakamoto T, Kuroki Y, Yamashita I, Okamoto M, Katuyama S, Fujimaki M. Inhibitory effects of fluorinated pyrimidines, 5'-DFUR, UFT and T-506, in a model of hepatic metastasis of mouse colon 26 adenocarcinoma-assessment of inhibitory activity and adverse reactions at the maximum tolerated dose. *Clin Exp Metastasis* 1997; **15**: 266-271

30 **Monden T,** Haba A, Amano M, Kanoh T, Tsujie M, Ikeda K, Izawa H, Ohnishi T, Sekimoro M, Tomita N, Okamura J, Monden M. PyNPase expression and cancer progression in the colorectum. *Nippon Geka Gakkai Zasshi* 1998; **99**: 446-451

Science Editor Guo SY **Language Editor** Elsevier HK

PO Box 2345, Beijing 100023, China
www.wjgnet.com
wjg@wjgnet.com

ELSEVIER

World J Gastroenterol 2005;11(25):3948-3952
World Journal of Gastroenterology ISSN 1007-9327

• *BRIEF REPORTS* •

Prognostic value of KIT mutation in gastrointestinal stromal tumors

Xiao-Hong Liu, Chen-Guang Bai, Qiang Xie, Fei Feng, Zhi-Yun Xu, Da-Lie Ma

Xiao-Hong Liu, Zhi-Yun Xu, Institute of thoracic cardiac surgery, Changhai Hospital, Second Military Medical University, Shanghai 200433, China
Chen-Guang Bai, Qiang Xie, Fei Feng, Da-Lie Ma, Department of Pathology, Changhai Hospital, Second Military Medical University, Shanghai 200433, China
Co-first-authors: Qiang Xie
Co-correspondents: Zhi-Yun Xu
Correspondence to: Da-Lie Ma, Chief of Department of Pathology, Changhai Hospital, Second Military Medical University, Changhai Road, Shanghai 200433, China. madalie@yahoo.com.cn
Telephone: +21-25070660 Fax: +21-25072135
Received: 2004-07-12 Accepted: 2004-09-19

Abstract

AIM: To examine the prevalence and prognostic significance of C-kit gene mutation and analysis the correlation of C-kit gene mutation and the clinicalpathologic parameters of GISTs.

METHODS: Eighty-two GISTs were studied for the mutation of C-kit gene by PCR-SSCP, DNA sequence. Statistical comparison were used to analysis the correlation of C-kit gene mutation and clinicalpathology, clinical behavior, recurrence.

RESULTS: (1) Mutation-positive and mutation-negative GISTs were 34 and 48,respectively; (2) Among these patients with C-kit mutation remained a significantly poor prognosis associated with 59% 3-year survival compared to those whose tumors did not; (3) Tumor size, PCNA index, mitotic cell number, presence of necrosis, microscopic invasion to adjacent tissues, recurrence and distant metastasis among mutation-positive and mutation-negative GISTs were significantly different.

CONCLUSION: C-kit mutation is a undoubtedly pivotal event in GIST and may be associated with poor prognosis. Evaluation of C-kit gene mutation may have both prognosis and therapeutic significances.

Key words: Gastrointestinal stromal tumor; Gene mutation; C-kit oncogene; Prognostic factor

Liu XH, Bai CG, Xie Q, Feng F, Xu ZY, Ma DL. Prognostic value of KIT mutation in gastrointestinal stromal tumors. *World J Gastroenterol* 2005; 11(25): 3948-3952
http://www.wjgnet.com/1007-9327/11/3948.asp

INTRODUCTION

Gastrointestinal stromal tumor (GIST) is designation for a major subset of mesenchymal tumors of the gastrointestinal tract. Their biological behavior is a persistent source of controversy. Concerning prognosis ,various studies[1-3] have endeavored in the establishment of clinicopathologic correlations, such as tumor size, location, mitotic cell count, proliferative activity, presence of necrosis, presence of hemorrhage, microscopic invasion to adjacent tissues, recurrence, distant metastasis, age, sex, cell type. Yet the criteria claimed to predict the biological behavior of GIST remains vague and do not even enable a confident discrimination between benign and malignant lesions. Discrimination of malignant GISTs based on an objectively defined factor would be of practical importance. In this study, we intend to contribute to this issue by examining the prevalence and prognostic significance of the above-mentioned parameters, C-kit expression and C-kit gene mutation, and analysis the correlation of C-kit gene mutation and the above-mentioned clinical parameters.

MATERIALS AND METHODS

Patients

During the period 1997-2001, 82 patients with primary mesenchymal tumors of the gastrointestinal tract underwent surgery at Changhai Hospital and were diagnosed as GISTs. Of these, 56 men and 26 women, the mean age of the GIST patients at the time of diagnosis was 53 years. The locations of the tumors were as follows: 3 in the esophagus, 42 in the stomach, 35 in the intestine, and 2 in the mesentery. According to the standard of Lewin's[4], 82 cases were divided into 2 groups, 20 benign and 62 malignant GISTs. At the time of diagnosis, 16 were found microscopic invasion to mucous myometrium or placenta percreta, distant metastasis was found in 16 patients, 9 to the liver, 2 to bone, 1 to lung and 4 extensive metastasis; the remaining patients were free of distant metastasis. Thus ,curative surgery was performed for 73 patients, and the patients with distant metastasis or peritoneal dissemination underwent only local resection. The mean follow-up period was 4.1 years, during the follow-up period, 18 patients suffered from recurrences, and 10 patients received reoperation for recurrences.

Immuohistochemistry

Paraffin sections (3 mm thick) of formalin-fixed tissues were used for conventional H&E staining and for immunohistochemistry. Rabbit polyclonal antibody against

human KIT and mouse monoclonal antibody against human PCNA were purchased from DAKO. Immunohistochemistry was performed using EnVision kit by two-step technique. PCNA index indicating the percentage of positive tumor nuclei was obtained by visual quantitative assessment of 100 tumor cells. Random fields were selected, excluding areas with excessive or scant immunostaining. Nuclear staining without cytoplasmic staining was considered a positive result. Negative result was set as "-", PCNA index <10% +, PCNA index 10%-30%++, >30% +++.

PCR-SSCP

DNA was extracted from formalin-fixed, paraffin-embedded tissues using standard methods with proteinase K digested and phenol/chloroform purified. Exon11 of the C-kit gene was amplified by PCR using the following oligonucleotide primer pairs: sense primer 5'-aactcagcctgtttctgg-3'-antisense primer: 5'-gatctatttttccctttctc-3'. PCR products were subjected to 8% non-denaturation polyacrylamide gel electrophoresis (aer:bis = 49:1) with 5% glycerin and silver nitrate staining.

DNA sequencing

PCR products that showed abnormal gel shift by PCR-SSCP were selected for sequencing after cloned into PMD18-T vector. The sequencing procedures were performed by Songon Co., Shanghai.

Statistical analysis

Eighty-two GISTs were divided into mutation-positive and mutation-negative subtypes according to C-kit gene detection. χ^2 test was used to analyze the correlation of C-kit mutation and clinicopathological and prognostic factors. Two-sided $P<0.05$ were considered to represent statistical significance. The relative importance of various prognostic factors for the postoperative was analyzed with Cox's proportional hazard model. Logistic regression analysis with the forward stepwise method was used to compare the difference of survival curves between the C-kit mutation-positive and mutation-negative subtypes. The possible prognostic factors included age, sex, location of tumors, tumor size, cell type, microscopic invasion to neighboring structures, mitotic cell number, PCNA index, distant metastasis at the time of diagnosis, peritoneal dissemination at the time of surgery, recurrences during the follow-up period, presence of necrosis, presence of hemorrhage, presence of C-kit mutation and expression.

RESULTS

Immunohistochemistry

Immunohistochemical analyses revealed strong and diffuse C-kit expression in 80 of 82 cases. PCNA staining intensity varied from very weak to intensely strong and from finely granular to uniformly dark red-brown (Table 1).

Evaluation of mutations in exon11 of C-kit gene

Two alleles were observed for the normal PCR segments, fast and slow fragments were designated as A and B alleles, respectively. Comparing to normal cases, 34 (41.5%) malignant GISTs showed abnormal gel shifts while no mutant bands were observed in benign GISTs. Abnormal gel shifts included multiple shift bands, monomorphic fragment or band shifting. Sequencing of abnormal bands revealed point mutation, deletion mutation and insertion deletion. Mutation-positive and mutation-negative GISTs were 34 and 48, respectively.

Survival analysis

Three-year survival rate was 77%(63/82) of 82 cases. Among these patients with C-kit mutation remained a significantly poor prognosis associated with 59% 3-year survival compared to those whose tumors did not. ($\chi^2 = 11.6464$, $P<0.05$, Figure 1).

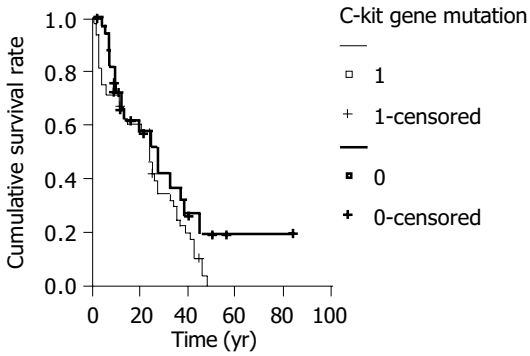

Figure 1 C-kit gene mutation and cumulative survival rate.

The relationship of C-kit mutation and clinicopathological marker

We examined whether the presence of C-kit mutation could be associated with clinicopathological features of GISTs (Table 1).Statistical analysis indicated that significant differences were detected with tumor size ($\chi^2 = 16.7950$, $P<0.05$), PCNA index ($\chi^2 = 17.0990$, $P<0.05$), mitotic cell number ($\chi^2 = 11.2327$, $P<0.05$), presence of necrosis ($\chi^2 = 4.4036$, $P<0.05$), microscopic invasion to adjacent tissues ($\chi^2 = 22.3912$, $P<0.05$) between two terms. The age, sex, location of tumor, cell type, the presence of hemorrhage, and C-kit expression were independently related to the presence of C-kit mutation.

The correlation between C-kit mutation and prognostic factors

We also examined whether the presence of C-kit mutation was associated with the clinical outcome (Table 2). The mutation-positive GISTs showed more frequent recurrences ($\chi^2 = 16.333$, $P<0.05$), distant metastasis ($\chi^2 = 12.9649$, $P<0.05$) and higher mortality ($\chi^2 = 11.6464$, $P<0.05$) than the mutation-negative GISTs. Of the patients with mutation-positive GIST ,developed distant metastasis.

DISCUSSION

GISTs are the most common mesenchymal tumors of the human gastrointestinal tract which are enigmatic in terms of their line of differentiation or cell of origin and clinical behavior[5]. Recently, many studies have shown that tumor size, location, mitotic cell count, cell type, proliferative

Table 1 Relationship of C-kit mutation and clinicopathological marker

Clinicalpathological	Total	C-kit		C-kit		χ^2	*P*
		Case	Percent	Case	Percent		
Total	82	34		48			
Age (yr)							
<40	12	5	15	7	15%	0.0002	0.9877
≥40	70	29	85	41	85%		
Sex							
Man	56	24	71	32	67%	0.1413	0.7069
Woman	26	10	29	16	33%		
Tumor size							
1-5.4	46	10	29	36	75%	16.7950	<0.0001
≥5.5	36	24	71	12	25%		
Location of tumors							
Esophagus	3	0	0	3	6%		
Stomach	42	14	41	28	58%	7.5243	0.0569
Intestine	35	18	53	17	36%		
Mesentery	2	2	6	0	0%		
Cell type							
Spindle	73	29	85	44	92%	0.8272	0.3631
Epithelioid	9	5	15	4	8%		
PCNA index							
0	19	7	21	12	25%		
+	49	15	44	34	71%	17.0990	0.0007
++	13	12	35	1	2%		
+++	1	0	0	1	2%		
Mitotic							
<5	67	22	65	45	94%	11.2327	0.00008
≥5/50	15	12	35	3	6%		
Hemorrhage							
Yes	25	12	35	13	27%	0.6331	0.4262
No	57	22	65	35	73%		
Necrosis							
Yes	37	20	59	17	35	4.4036	0.0359
No	45	14	41	31	65		
Microscopic							
Yes	16	15	44	1	2	22.3912	<0.0001
No	66	19	56	47	98		
C-kit expression							
Positive	80	33	97	47	98	0	1
Negative	2	1	3	1	2		

Table 2 Correlation between C-kit mutation and prognostic factors

Prognostic	Total	C-kit mutation-positive subtype		C-kit mutation-negative subtype		χ^2	*P*
		Case	Percent	Case	Percent		
Total	82	34	48				
Recurrence							
Yes	18	13	38	5	10	16.333	0.0001
No	64	21	62	43	90		
Metastasis	16	13	38	3	6	12.9649	0.0003
Live	10	9	26	1	2		
Abdominal cavity	3	2	6	1	2		
Distant	3	2	6	1	2		
Prognosis							
Survival	63	20	59	43	90	11.6464	0.0006
Death	19	14	41	5	10		

activity, presence of necrosis, presence of hemorrhage, microscopic invasion to adjacent tissues, recurrence, distant metastasis, as favorable factors of GIST. But histologic distinction of benign from malignant tumors is often difficult, and prediction of clinical outcome on the basis of histologic characteristics alone is not always reliable, many histologically malignant neoplasms were clinically benign. Moreover, some tumors had conflicting features of both benignancy and malignancy, and their malignant potential has been labeled uncertain or indeterminate. In recent years, C-kit protein expression and activated gene mutation have been found in GIST[6-9], aggressive mastocytosis[10], mast cell leukemia[11], ANLL with/without mast cell involvement [10], myeloproliferative disorders[10], colon carcinoma[12] and germ cell tumors[13]. Dections of gene mutation have shown a good correlation with biologic behavior in such tumors and providing valuable adjunctive prognostic information. In this study, we examined whether the presence of mutation of C-kit gene is important as a prognostic factor of GIST and found it to indicate a significantly poorer prognosis.

First, we examined whether the presence of C-kit mutation could be associated with clinicopathological features of GISTs. Statistical analysis indicated that significant differences were detected with tumor size, PCNA index, mitotic cell number, presence of necrosis, microscopic invasion to adjacent tissues between mutation-positive and mutation-negative GISTs. While the age, sex, location of tumor, cell type, the presence of hemorrhage, and C-kit expression were independently related to the presence of C-kit mutation. This states that the mutation-positive GISTs were larger in size and showed more frequent invasion of adjacent tissues, the mutation-positive GISTs showed higher mitotic counts and PCNA index and more necrosis within the tumors histologically. Taken together, the mutation-positive GISTs had more malignant histological features than the mutation-negative GISTs. We also examined whether the presence of C-kit mutation was associated with the clinical outcome. The mutation-positive GISTs showed more frequent recurrences, distant metastasis and, higher mortality than the mutation-negative GISTs. There are at least possible two explanations for this : GIST may be classified into two subtypes, C-kit mutation-positive and mutation-negative GISTs mutation-positive GISTs showed more malignant features,; mutation-negative GISTs may acquire more malignant phenotype due to the addition of C-kit mutation.

Recently, gain-of-function mutations of the juxtramemebrane domain of C-kit , including deletions or point mutations in exon11 were described in GIST[14-18]. These mutations were shown to lead to spontaneous, lilgand-independent tyrosine kinase activation. The stable transfection of murine lymphoid cells with the mutant C-kit complementary DNA was shown to induce malignant transformation, suggesting pathogenetic significance of such mutations. We have expanded these observations and found that the C-kit mutation in the exon11 predominantly occur in those GISTs that are histologically and clinically malignant while benign GISTs were not detected. This suggest that C-kit mutation in the exon11 may be an important pathogenetic mechanism of tumor malignant behavior. Moreover ,we found C-kit mutations only in 60% of the malignant GISTs. This may suggest that additional pathogenetic mechanisms exist in other cases, or that mutations occur in alternative sites. Another study also showed correlation between the mutations and disease progression.

There is no effective therapy for unresectable or metastatic gastrointestinal stromal tumor, which is invariably fatal. STI571, a phenylaminopyrimidine derivative, is a small molecule that selectively inhibits the enzymatic activity of C-kit gene. Joensuu *et al*.[19], found that inhibition by STI571 of the constitutively active mutant C-kit tyrosine kinase of gastrointestinal stromal tumors was an effective therapy for these tumors. There are two explanations for this: STI571 may be active in solid tumors that rely on the expression of C-kit, ABL, or platelet-derived growth factor receptor while GIST uniformly express C-kit; a tumor-specific C-kit mutation appears to be the chief cause of this neoplasm. Considering these findings, we conclude that C-kit mutation is a undoubtedly pivotal event in GIST and may be associated with poor prognosis. Evaluation of C-kit gene mutation may have both prognosis and therapeutic significances as the new tyrosine kinase inhibitor (STI571) treatments are available.

REFERENCES

1 **Wong NA,** Young R, Malcomson RD, Nayar AG, Jamieson LA, Save VE, Carey FA, Brewster DH, Han C, Al-Nafussi A. Prognostic indicators for gastrointestinal stromal tumours: a clinicopathological and immunohistochemical study of 108 resected cases of the stomach. *Histopathology* 2003; **43**: 118-126

2 **Nagasako Y,** Misawa K, Kohashi S, Hasegawa K, Okawa Y, Sano H, Takada A, Sato H. Evaluation of malignancy using Ki-67 labeling index for gastric stromal tumor. *Gastric Cancer* 2003; **6**: 168-172

3 **Kim MK,** Lee JK, Park ET, Lee SH, Seol SY, Chung JM, Kang MS, Yoon HK. Gastrointestinal stromal tumors: clinical, pathologic features and effectiveness of new diagnostic criteria. *Korean J Gastroenterol* 2004; **43**: 341-348

4 **Lewin KJ,** Riddle R, Weinstein W. Gastrointestinal Pathology and Its Clinical Implications. 2thnd. *New York: Igaku-Shoin Medical Pub* 1992: 284-341

5 **Ballarini C,** Intra M, Ceretti AP, Prestipino F, Bianchi FM, Sparacio F, Berti E, Perrone S, Silva F. Gastrointestinal stromal tumors: a "benign" tumor with hepatic metastasis after 11 years. *Tumori* 1998; **84**: 78-81

6 **Goldblum JR.** Gastrointestinal stromal tumors. A review of characteristics morphologic, immunohistochemical, and molecular genetic features. *Am J Clin Pathol* 2002; **117**(Suppl): S49-61

7 **Corless CL,** Fletcher JA, Heinrich MC. Biology of gastrointestinal stromal tumors. *J Clin Oncol* 2004; **22**: 3813-3825

8 **Ma DL,** Liu XH, Bai CG, Xie Q, Feng F. Effect of C-kit gene mutation on prognosis of gastrointestinal stromal tumor. *Zhonghua Waike Zazhi* 2004; **42**: 140-144

9 **Theou N,** Tabone S, Saffroy R, Le Cesne A, Julie C, Cortez A, Lavergne-Slove A, Debuire B, Lemoine A, Emile JF. High expression of both mutant and wild-type alleles of C-kit in gastrointestinal stromal tumors. *Biochim Biophys Acta* 2004; **1688**: 250-256

10 **Pardanani A,** Reeder TL, Kimlinger TK, Baek JY, Li CY, Butterfield JH, Tefferi A. Flt-3 and C-kit mutation studies in a spectrum of chronic myeloid disorders including systemic mast cell disease. *Leuk Res* 2003; **27**: 739-742

11 **Noack F,** Escribano L, Sotlar K, Nunez R, Schuetze K, Valent P, Horny HP. Evolution of urticaria pigmentosa into indolent

systemic mastocytosis: abnormal immunophenotype of mast cells without evidence of C-kit mutation ASP-816-VAL. *Leuk Lymphoma* 2003; **44**: 313-319

12 **Sammarco I,** Capurso G, Coppola L, Bonifazi AP, Cassetta S, Delle Fave G, Carrara A, Grassi GB, Rossi P, Sette C, Geremia R. Expression of the proto-oncogene C-kit in normal and tumor tissues from colorectal carcinoma patients. *Int J Colorectal Dis* 2004; **19**: 545-553

13 **Looijenga LH,** de Leeuw H, van Oorschot M, van Gurp RJ, Stoop H, Gillis AJ, de Gouveia Brazao CA, Weber RF, Kirkels WJ, van Dijk T, von Lindern M, Valk P, Lajos G, Olah E, Nesland JM, Fossa SD, Oosterhuis JW. Stem cell factor receptor (C-kit) codon 816 mutations predict development of bilateral testicular germ-cell tumors. *Cancer Res* 2003; **63**: 7674-7678

14 **Beghini A,** Tibiletti MG, Roversi G, Chiaravalli AM, Serio G, Capella C, Larizza L. Germline mutation in the juxtamembrane domain of the kit gene in a family with gastrointestinal stromal tumors and urticaria pigmentosa. *Cancer* 2001; **92**: 657-662

15 **Lee JR,** Joshi V, Griffin JW Jr, Lasota J, Miettinen M. Gastrointestinal autonomic nerve tumor: immunohistochemical and molecular identity with gastrointestinal stromal tumor. *Am J Surg Pathol* 2001; **25**: 979-987

16 **Fukuda R,** Hamamoto N, Uchida Y, Furuta K, Katsube T, Kazumori H, Ishihara S, Amano K, Adachi K, Watanabe M, Kinoshita Y. Gastrointestinal stromal tumor with a novel mutation of KIT proto-oncogene. *Intern Med* 2001; **40**: 301-303

17 **Hirota S,** Nishida T, Isozaki K, Taniguchi M, Nakamura J, Okazaki T, Kitamura Y. Gain-of-function mutation at the extracellular domain of KIT in gastrointestinal stromal tumours. *J Pathol* 2001; **193**: 505-510

18 **Taniguchi M,** Nishida T, Hirota S, Isozaki K, Ito T, Nomura T, Matsuda H, Kitamura Y. Effect of C-kit mutation on prognosis of gastrointestinal stromal tumors. *Cancer Res* 1999; **59**: 4297-4300

19 **Joensuu H,** Roberts PJ, Sarlomo-Rikala M, Andersson LC, Tervahartiala P, Tuveson D, Silberman SL, Capdeville R, Dimitrijevic S, Druker B, Demetri GD. Effect of the tyrosine kinase inhibitor STI571 in a patient with a metastatic gastrointestinal stromal tumor. *N Engl J Med* 2001; **344**: 1052-1056

Science Editor Guo SY **Language Editor** Elsevier HK

PO Box 2345, Beijing 100023, China
www.wjgnet.com
wjg@wjgnet.com

ELSEVIER

World J Gastroenterol 2005;11(25):3953-3957
World Journal of Gastroenterology ISSN 1007-9327

• *BRIEF REPORTS* •

Somatostatin receptor subtype 2-mediated scintigraphy and localization using ^{99m}Tc-HYNIC-Tyr^3-octreotide in human hepatocellular carcinoma-bearing nude mice

Yong Li, Jian-Ming Si, Jun Zhang, Jin Du, Fan Wang, Bing Jia

Yong Li, Jian-Ming Si, Jun Zhang, Gastrointestinal Laboratory of Clinical Medical Institute of Sir Run Run Shaw Hospital, Zhejiang University, Hangzhou 310016, Zhejiang Province, China
Jin Du, Fan Wang, Bing Jia, the Medicine Isotope Research Center of Beijing University, Beijing 100083, China
Correspondence to: Jian-Ming Si, MD, Gastrointestinal Laboratory of Clinical Medical Institute of Sir Run Run Shaw Hospital, Zhejiang University, Hangzhou 310016, Zhejiang Province, China. sijm@163.net
Telephone: +86-571-87217002
Received: 2004-04-09 Accepted: 2004-05-24

Abstract

AIM: To investigate the uptake of ^{99m}Tc-HYNIC-Tyr^3-octreotide (^{99m}Tc-HYNIC-TOC) in human hepatocellular carcinoma (HCC), which can provide the localizable diagnosis in hepatic carcinoma.

METHODS: The expression of somatostatin receptor 2 (SSTR2) messenger RNA (mRNA) in human HCC cell line $HepG_2$ was examined by reverse transcriptase-polymerase chain reaction (RT-PCR). Uptake of ^{99m}Tc-HYNIC-TOC was evaluated in the human HCC implanted into BALB/c nude mice. ANMIS2000 nuclear medicine analysis system was used to calculate the ratio of ^{99m}Tc uptake between tumor tissue and vital organs.

RESULTS: We demonstrated the expression of SSTR2 mRNA in human HCC cell line $HepG_2$ by RT-PCR. The size of the RT-PCR products was 364 bp detected by sequence analysis of the human SSTR2 mRNA. Scintigraphy proved that ^{99m}Tc-HYNIC-TOC was uptaken in the tumor tissue, liver and kidney of the tumor-bearing mice.

CONCLUSION: Based on expression of the SSTR2 mRNA in human HCC, ^{99m}Tc-HYNIC-TOC can markedly bind with and be uptaken by human HCC tissues as compared with normal liver tissue. The significant retention of radionuclide in kidney and bladder is probably related to non-specific peptide uptake in the tubulus cells of kidney and possibly due to excretion by kidney. Our results show that localizable diagnosis and targeting radiotherapy with radionuclide-labeled somatostatin analog for HCC are of great value to be further studied.

Key words: Hepatocellular carcinoma; ^{99m}Tc-HYNIC-Tyr^3-octreotide; Somatostatin receptor 2

Li Y, Si JM, Zhang J, Du J, Wang F, Jia B. Somatostatin receptor subtype 2-mediated scintigraphy and localization using ^{99m}Tc-HYNIC-Tyr^3-octreotide in human hepatocellular carcinoma-bearing nude mice. *World J Gastroenterol* 2005; 11(25): 3953-3957
http://www.wjgnet.com/1007-9327/11/3953.asp

INTRODUCTION

The role of somatostatin (SS) analogs in the tumor diagnostic and therapeutic applications has attracted the concern of the people. It has been widely reported about the growth suppressing effects of SS and its analogs on many tumors[1-4]. To date, it is known that their suppressing effect on tumor cell proliferation is mediated by the somatostatin receptors (SSTRs) presented in the tumor constitution[5]. Like most neuroendocrine tumors, adenocarcinomas originating in the breast, colon, or pancreatic tumor, as well as meningiomas, express SSTRs, and the majority of these tumors express the somatostatin receptor subtype 2 (SSTR2)[6,7]. However, all five receptor subtypes (SSTR1-5) bind native SS with a high affinity, while octreotide, an SS analog, binds with a very high affinity only to subtype 2 (SSTR2) and shows a moderately high affinity for SSTR5[8]. Overexpression of the SSTR2 in some tumors has made it possible to use SS-receptor scintigraphy with indium111 or technetium 99m-labeled octreotide for the visualization of SS receptor-positive cancers[9,10]. In addition to tumor scintigraphy, a new application of these radiolabeled peptides is peptide receptor radionuclide therapy[11,12].

It has been known that hepatocellular carcinoma (HCC) is a leading cause of cancer-related death. At present, surgical resection of malignant liver lesions offers the best outcome and the only hope of cure. The 5-year survival rate for selected patients undergoing surgical resection of primary HCC was 30%, with a median survival of 30 mo. However, approximately 90% of patients presenting with primary HCC have inoperable disease[13]. These patients must rely largely on various forms of chemotherapy and radiotherapy[14,15]. These treatments have at times shown promising response rates, symptom palliation and have occasionally down-staged hepatic tumors to allow surgical resection, but these treatment modalities have not improved 5-year survival rates, which remain in the order of 1%[16]. The persisting poor survival among the vast majority of patients presenting with liver cancer has led to renewed interest in developing targeted radiotherapy with radiolabeled SS analogs as a

possible treatment option for patients with non-resectable liver cancer. However, it has not been known that HCC can uptake radiolabeled SS analogs. The aim of this study was to scintigraphically identify the localization of HCC in order to reveal a possible role of radiolabeled SS analogs in the treatment of HCC, and determine the target cell of receptor subtype selective radiolabeled SS analogs for targeting radiotherapy of HCC.

MATERIALS AND METHODS

Materials

All reagents and solvents were obtained from commercial sources and were used without further purification except HYNIC-[Tyr^3]-octreotide (HYNIC-TOC). We applied hydrazinonicotinic acid (HYNIC) as the ligand for ^{99m}Tc. Labeling with ^{99m}Tc was performed using a co-ligand required to stabilize ^{99m}Tc bound to the hydrazino residue of the peptide conjugate. HYNIC-TOC was synthesized at the Medicine Isotope Research Center of Peking University. Na^{99m}TcO4 was obtained from commercial ^{99}Mo/^{99m}Tc generator. The methods of HYNIC-TOC synthesis and ^{99m}Tc labeling were employed as previously described[17,18]. Reaction solutions were tested for radiochemical purity by the C18-SepPak column of high-performance liquid chromatography immediately and up to 24 h after preparation. ^{99m}Tc of radioactive purity > 95% was bound to HYNIC-TOC.

RT-PCR and sequencing of products

The human HCC cell line HepG2 was assessed for the presence of somatostatin receptor subtypes (SSTR1-5) messenger RNA (mRNA) to confirm the presence of the target receptor subtype for ^{99m}Tc-HYNIC-Tyr^3-octreotide (^{99m}Tc-HYNIC-TOC), especially SSTR2. The following primer pairs (Boya Co., Shanghai, China) were applied: for human SSTR1, sense (1 543-1 652) 5'-TCATCCTCGGCT-ATGCCAAC-3' and antisense (1 789-1 898) 5'-GCAGGTG-CCATTACGGAAGA-3'; for SSTR2, sense (359-378) 5'-CTGTGGATGGCATCAATCAG-3' and antisense (723-741) 5'-TCGGATTCCAGAGGACTTCA-3'; for SSTR3, sense (1 193-1 212) 5'-GCCTCTGCTACCTGCTCATC-3' and antisense (1 618-1 637) 5'-CCATCCTCCTCCTCC-TCATC-3'; for SSTR4, sense (480-499) 5'-CAGCGTGGC-CAAGCTCATCA-3' and antisense (962-981) 5'-GATCGG-CGGAAGTTGTCGGA-3'; for SSTR5, sense (205-224) 5'-GCCAAGATGAAGACCGTCAC-3' and antisense (668-887) 5'-AGCAGGTAGCACAGGCAGAT-3'; for β-actin, sense 5'-ACGTTATGGATGATGTATCGC-3' and antisense 5'-CTTAATGTCACGCACGATTTCC-3'. RNA extraction and reverse transcription were performed according to the manufacturer's instructions. cDNA was amplified in a reaction mixture (total volume 20 μL) comprising cDNA (transcribed from 12 μg of total RNA), 2 μL of 10× PCR buffer, 0.4 μL of 10 mmol/L dNTP, and 1.5 μL of 25 mmol/L $MgCl_2$, 10 pmol/L of each of sense and antisense primers, and 2.5 U of Taq DNA polymerase. Following an initial denaturing step at 94 ℃ for 5 min, the amplification program of 30 cycles, each cycle consisting of denaturation at 94 ℃ for 30 s, annealing at 60 ℃ for 20 s, and extension at 72 ℃ for 30 s, was carried out by a Gene Amplification PCR system 2 400 (PE Corp., USA). The amplification was terminated with the final extension step at 72 ℃ for 10 min. The amplified products, subsequently, were electrophoresed and photographed on 15 g/L agarose gel stained with ethidium bromide. The final products were verified by sequencing in Boya Co. (Shanghai, China). β-actin specific primers were used to amplify the cDNA fragment as an internal standard.

Tumor cell inoculation and tumor growth assessment

The human HCC cell line HepG2 was from Clinical Medical Institute of Sir Run Run Shaw Hospital. The cells were grown in RPMI1640 (Gibco Co., USA) supplemented with 100 mL/L fetal bovine serum (Hangzhou Sijiqing Co., China) at 37 ℃ in a humidified atmosphere containing 50 mL/L CO_2 and 950 mL/L O_2. Subculturing was executed every 2-3 d and the cells grew well along the walls of culture tube. Then, the cells (2×10^6 cells/mouse) at logarithmic growth period were subcutaneously inoculated into right flank of BALB/c nude mice, aged 6-8 wk, weighing 18-20 g (purchased from Animal Center of Academy of Science, Shanghai, China). The total tumor load per mouse was approximately 1 cm^3 at about 28 d post-injection. We took out the whole tumors, then, immediately put into saline containing 100 U/mL penicillin and streptomycin. Tumor pieces with a size 1-2 mm^3 were made from the margins of the whole mass after winkling the connective tissue around the mass. The mice were randomly divided into three groups in accordance with subcutaneous re-transplantation of tumor into right flanks (subcutaneous group) or *in situ* liver (intra-liver group), or without re-transplantation (control group). Each group consisted of three mice. The experiments were started at 21 d post re-implantation, when the size of tumor per mice was approximately 1 cm^3.

In vivo imaging with ^{99m}Tc-HYNIC-TOC

Each mouse of tumor-bearing groups (subcutaneous group and intra-liver group) and control mice group received 100 μCi of ^{99m}Tc-HYNIC-TOC injected into the caudal vein under soluble pentobarbitone anesthesia. The mice were imaged at 2 and 4.5 h, respectively, after injection of ^{99m}Tc-HYNIC-TOC with mini-radioisotope gamma camera equipped with a pinhole collimator (Bingsong Corp., China). During imaging, the mice were maintained with a fixed band and positioned on dorsal recumbency with the legs extending from the body. The imaging analyses of ^{99m}Tc uptake in tumor tissue and vital organs were conducted using ANMIS 2000 nuclear medicine analysis system (Bingsong Corp.). Animals of the intra-liver group were killed after the second imaging session (4.5 h after injection of ^{99m}Tc-HYNIC-TOC) for examination of intra-liver tumor growth.

RESULTS

Expression and PCR products sequencing of SSTR2 mRNA in HCC cell line HepG2

PCR products of SSTRs were obtained for HepG2 cells. The size of the products corresponded to the predicted length of the synthesized cDNA fragment based on the position of the PCR primer. SSTR1-5 mRNAs were variably expressed in HepG2 cells. Expressions of SSTR1, SSTR2, and SSTR4 mRNA were found in HepG2 cells, respectively

(Figure 1), but those of SSTR3 and SSTR5 mRNAs were not observed. We identified that the product of SSTR2 mRNA was the specific fragment that we needed after performing sequencing and comparison with SSTRs mRNA rank of the GenBank[19], it turned out to be a perfect coincidence with the fragment rank (Figure 2). The result showed that the amplification we executed was specific.

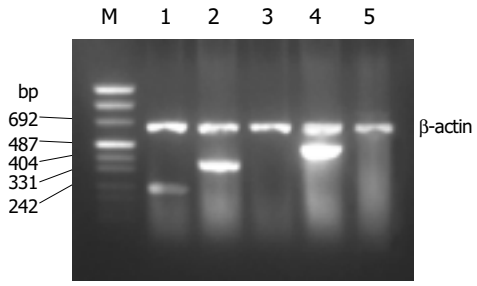

Figure 1 RT-PCR analysis for SSTR1-5 mRNA expression in HepG2. Lane m: marker; lane 1: SSTR1 (246 bp); lane 2: SSTR2 (384 bp); lane 3: SSTR3; lane 4: SSTR4 (502 bp); lane 5: SSTR5.

In vivo imaging with ^{99m}Tc-HYNIC-TOC

The gamma camera imagings of a representative mouse from the subcutaneous, intra-liver and control groups at 2 and 4.5 h after being injected with ^{99m}Tc- HYNIC-TOC are shown in Figure 3. These imagings showed visual accumulation of ^{99m}Tc-HYNIC-TOC detected in the tumor xenografts of mice (including subcutaneous group and intra-liver group). The retention of radioactivity in the kidney and excretion through the bladder were observed. The high-level uptake of radioactivity in the liver of tumor-bearing mice was also observed and compared with the control group. This tumor uptake was important to validate the dosing regimen that was used in therapy studies of liver cancer.

DISCUSSION

Radiolabeled SS analogs have brought new prospects to nuclear oncology for diagnosis and therapy of tumor. Due to their low molecular weight and high affinity to SSTRs, good tissue penetration properties, and being internalized

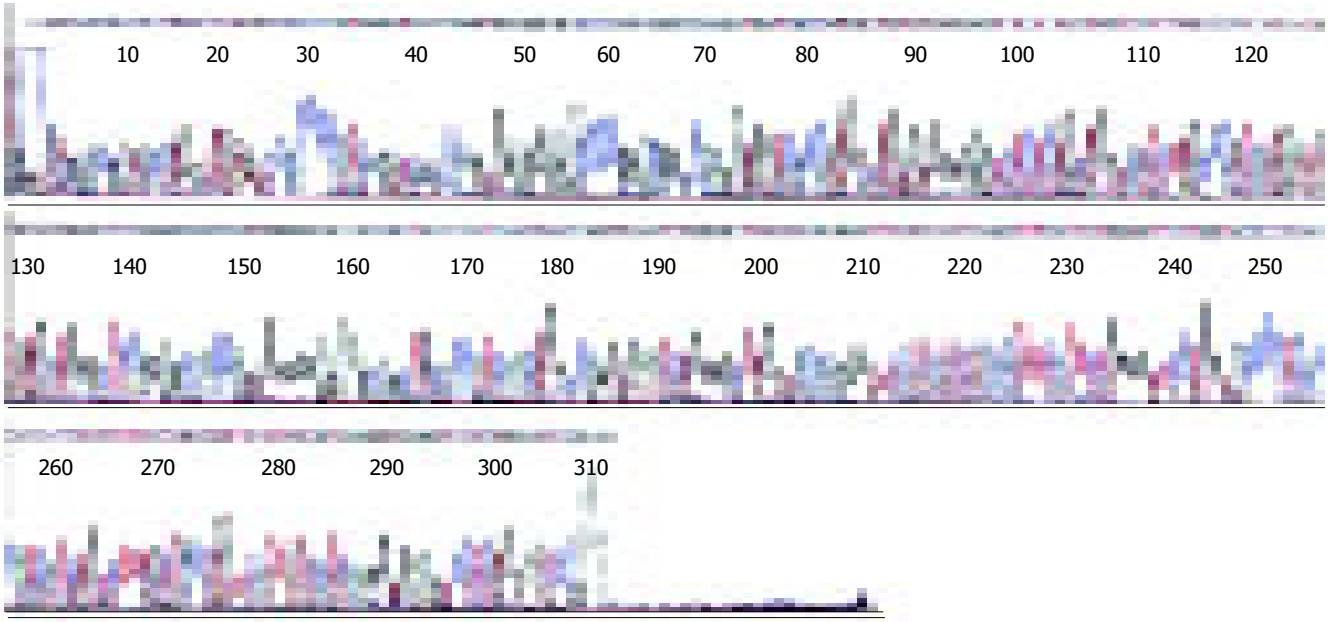

Figure 2 Sequencing of SSTR2 mRNA PCR products. The products were specifically amplified after the sequencing fragment was compared with human SSTR2 of GenBank, and was a perfect coincidence with the fragment rank of human SSTR2 mRNA.

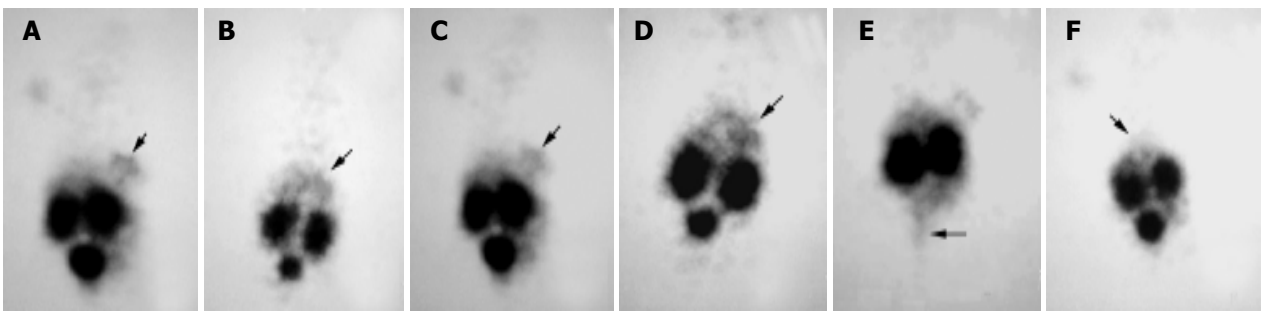

Figure 3 Scintigrams of mice at different times after injection of ^{99m}Tc-HYNIC-TOC. **A** and **C**: subcutaneous group at 2 and 3 h, respectively; **B** and **D**: intra-liver group at 2 and 4 h, respectively; **E**: subcutaneous group at 4.5 h, when the bladder was emptied; **F**: control group at 2 h. The marked decrease in the liver (arrows) uptake was apparent in the control group mouse.

into the tumor cells after receptor binding[20-22], they provide promising strategies for diagnosis and internal radionuclide therapy for various cancer types. Before radiolabeled, octreotide was employed in HCC, it has been studied with ^{125}I-[Tyr^3]-octreotide for tumor diagnosis[11]. However, some studies demonstrated that the SSTRs density in HCC was considerably lower than the receptor density found[23,24], thus it has rarely been studied in the liver cancer. As radiotherapy of SS receptor-positive tumors with compounds such as ^{90}Y-labeled ones was applied, it is necessary to develop a new strategy for the treatment of liver cancer.

In this study, we evaluated the expression of SS receptor in human HCC cell line HepG2. The results showed that SSTR1, SSTR2 and SSTR4 were frequently expressed in human HCC, which was similar to previous reports[25,26]. As the normal human liver does not express SSTR2 (predominant receptor subtype was SSTR1[27]), the presence of SSTRs in HCC may be regarded as an overexpression of the receptors in this tumor. Like previous therapeutic experiments[28], unlabeled octreotide was shown to bind with a high affinity to SSTR2, suggesting that the predominant receptor subtype was SSTR2. As to radiolabeled octreotide targeting therapy for HCC, the expression of SSTR2 in HCC is of high significance.

In scintigraphy experiment with ^{99m}Tc-HYNIC-TOC, the significant uptake of radionuclide by tumor xenografts in nude mice was found in both subcutaneous group and intra-liver group. And it was demonstrated that the hepatocarcinoma tissues had a fairly steady rate in uptaking ^{99m}Tc-HYNIC-TOC by the fact that there was still obvious radionuclide gathering at the tumor tissues at 4 h after administration. The results showed that the intensity of the signal was not as strong as for neuroendocrine tumor metastases. As a therapeutic tool, there are certainly potential clinical implications linked with the SS receptor expression in HCC.

The expression of some SS receptor subtypes was found in the liver and kidney as well[24,29]. However, the physiological uptake of ^{99m}Tc-HYNIC-TOC in these organs was probably mainly due to some loss of technetium out of chelation (liver) and non-specific peptide uptake in the tubulus cells (kidney). Thus, in our receptor scintigram, the retention of radionuclide prominently in both kidney and bladder as well as the less uptake in liver, which was similar to previous reports[30,31], was shown after injection of ^{99m}Tc-HYNIC-TOC. Because of the absence of SSTR2, the retention of technetium in the bladder, which was possibly due to the kidney excretion, almost vanished when bladder emptied (Figure 3E). Meanwhile, based on recent studies[32-34], most of the radiolabeled octreotide, like our results, would accumulate in the kidney after glomerular filtration, followed by re-absorption into renal cells. It is necessary to take into consideration the induction of the kidney damage while performing targeting radiotherapy with radiolabeled octreotide.

In conclusion, HCC cell line HepG2 expresses SSTR2 mRNA. ^{99m}Tc-HYNIC-TOC, relying on the receptor mediation, can markedly bind with and be uptaken by human HCC tissues as compared to the normal liver tissue, which is probably mainly due to some loss of technetium out of chelation. The significant retention of radionuclide in kidney and bladder is probably related to non-specific peptide uptake in the tubulus cells of kidney and possibly due to the excretion by kidney. This phenomenon has clued to potential radiation nephrotoxicity of the agents, which needs to be solved before a widespread application of targeting radiotherapy.

REFERENCES

1 **Lamberts SW,** de Herder WW, Hofland LJ. Somatostatin analogs in the diagnosis and treatment of cancer. *Trends Endocrinol Metab* 2002; **13**: 451-456

2 **Froidevaux S,** Eberle AN. Somatostatin anlogs and radiopeptides in cancer therapy. *Bioploymers* 2002; **66**: 161-183

3 **Celinski SA,** Fisher WE, Amaya F, Wu YQ, Yao Q, Youker KA, Li M. Somatostatin receptor gene transfer inhibits established panceatic cancer xenografts. *J Surg Res* 2003; **115**: 41-47

4 **Kumar M,** Liu ZR, Thapa L, Wang DY, Tian R, Qin RY. Mechanisms of inhibition of growth of human pancreatic carcinoma implanted in nude mice by soamtostatin receptor subtype 2. *Pancreas* 2004; **29**: 141-151

5 **Pollak MN,** Schally AV. Mechanisms of antineoplastic action of somatostatin analogs. *Proc Soc Exp Biol Med* 1998; **217**: 143-152

6 **Reubi JC,** Kvols L, Krenning E, Lamberts SW. Distribution of somatostatin receptors in normal and tumor tissue. *Metabolism* 1990; **39**(9 Suppl 2): 78-81

7 **Lamberts SW,** Krenning EP, Reubi JC. The role of somatostatin and its analogs in the diagnosis and treatment of tumors. *Endocr Rev* 1991; **12**: 450-482

8 **Lamberts SW,** Van der Lely AJ, de Herder WW, Hofland LJ. Octreotide. *N Engl J Med* 1996; **334**: 246-254

9 **Weiner RE,** Thakur ML. Radiolabeled peptide in the diagnosis and therapy of oncological diseases. *Appl Radiat Isot* 2002; **57**: 749-763

10 **Decristoforo C,** Mather SJ. Technetium-99m somatostatin analogues: effect of labelling methods and peptide sequence. *Eur J Nucl Med* 1999; **26**: 869–876

11 **Towu E,** Boxer G, Begent R, Zweit J, Spitz L, Hobbs K, Winslet M. *In-vitro* uptake of radioactive lipiodol I-131 and I-125 by hepatoblastoma: implications for targeted radiotherapy. *Pediatr Surg Int 2001*; **17**: 609-613

12 **Heppeler A,** Froidevaux S, Eberle AN, Maecke HR. Receptor targeting for tumor localisation and therapy with radiopeptides. *Curr Med Chem* 2000; **7**: 971-979

13 **Hussain SA,** Ferry DR, El-Gazzaz G, Mirza DF, James ND, McMaster P, Kerr DJ. Hepatocellular carcinoma. *Ann Oncol* 2001; **12**: 161-172

14 **Rougier P,** Mitry E, Clavero-Fabri MC. Chemotherapy and medical treatment of hepatocellular carcinoma (HCC). *Hepatogastroenterology* 1998; **45**(Suppl 3): 1264–1266

15 **Perez CA,** Brady LW. Principles and Practice of Radiation Oncology: Pancreatic and Hepatobiliary Cancer. *Lippincott Company* 1987: P810

16 **Liu CL,** Fan ST. Nonresectional therapies for hepatocellular carcinoma. *Am J Sur* 1997; **173**: 358-365

17 **Decristoforo C,** Mather SJ, Cholewinski W, Donnemiller E, Riccabona G, Moncayo R. ^{99m}Tc-EDDA / HYNIC-TOC: a new ^{99m}Tc-labelled radiopharmaceutical for imaging somatostatin receptor-positive tumours: first clinical results and intra-patient comparison with ^{111}In-labelled octreotide derivatives. *Eur J Nucl Med* 2000; **27**: 1318–1325

18 **von Guggenberg E,** Sarg B, Lindner H, Alafort LM, Mather SJ, Moncayo R, Decristoforo C. Preparation via coligand exchange and characterization of [^{99m}Tc-EDDA-HYNICD-Phe1, Tyr3] Octreotide (^{99m}Tc–EDDA / HYNIC–TOC). *J Label Compd Radiopharm* 2003; **46**: 307–318

19 http://www.ncbi.nlm.nih.gov/blast
20 **Krenning EP,** de Jong M, Kooij PP, Breeman WA, Bakker WH, de Herder WW, van Eijk CH, Kwekkeboom DJ, Jamar F, Pauwels S, Valkema R. Radiolabelled somatostatin analogue (s) for peptide receptor scintigraphy and radionuclide therapy. *Ann Oncol* 1999; **10**(Suppl 2): S23-29
21 **Weckbecker G,** Raule F, Stolz B, Bruns C. Somatostatin analogs for diagnosis and treatment of cancer. *Pharmacol Ther* 1993; **60**: 245-264
22 **Paganelli G,** Zoboli S, Cremonesi M, Bodei L, Ferrari M, Grana C, Bartolomei M, Orsi F, De Cicco C, Macke HR, Chinol M, de Braud F. Receptor-mediated radiotherapy with ^{90}Y-DOTA-D-Phe1-Tyr3-octreotide. *Eur J Nucl Med* 2001; **28**: 426-434
23 **Reubi JC,** Zimmermann A, Jonas S, Waser B, Neuhaus P, Laderach U, Wiedenmann B. Regulatory peptide receptors in human hepatocellular carcinomas. *Gut* 1999; **45**: 766–774
24 **Deng-Guo YAN,** Qing-Jia OU. Somatostatin receptor subtype SSTR2 and SSTR3 mRNA expression in primary hepatic Carcinoma. *Aizheng* 2001; **20**: 152-155
25 **Hofland LJ,** Lamberts SW. Somatostatin receptor subtype expression in human tumors. *Ann Oncol* 2001; **12**(Suppl 2): S31-36
26 **Rohrer L,** Raulf F, Bruns C, Buettner R, Hofstaedter F, Schule R. Cloning and characterization of a fourth human somatostatin receptor. *Proc Natl Acad Sci USA* 1993; **90**: 4196–4200
27 **Kouroumalis E,** Skordilis P, Termos K, Vasilaki A, Moschandrea J, Manousos ON. Treatment of hepatocellular carcinoma with octreotide: a randomized controlled study. *Gut* 1998; **42**: 442-447
28 **Holfland LJ,** Lamberts SW. Somatostatin receptors and disease: Role of receptor subtypes. *Bailliéres Clin Endocrinol Metab* 1996; **10**: 163-176
29 **Patel YC.** Somatostatin and its receptor family. *Front Neuroendocrinol* 1999; **20**: 157-198
30 **Reubi JC,** Horisberger U, Studer UE, Waser B, Laissue JA, Human kidney as target for somatostatin: high affinity receptors in tubules and vasa recta. *J Clin Endocrinol Metab* 1993; **77**: 1323–1328
31 **Bass LA,** Lanahan MV, Duncan JR, Erion JL, Srinivasan A, Schmidt MA, Anderson CJ. Identification of the soluble *in vivo* metabolites of ndium-111-diethylenetriaminepentaacetic acid-DPhe^{1}- octreotide. *Bioconjug Chem* 1998; **9**: 192–200
32 **Duncan JR,** Stephenson MT, Wu HP, Anderson CJ. Indium-111-diethylenetriaminepentaacetic acid-octreotide is delivered *in vivo* to pancreatic, tumor cells, renal, and hepatocyte lysosomes. *Cancer Res* 1997; **57**: 659–671
33 **Akizawa H,** Arano Y, Uezono T, Ono M, Fujioka Y, Uehara T, Yokoyama A, Akaji K, Kiso Y, Koizumi M, Saji H. Renal metabolism of ^{111}In-DTPA-D-Phe^{1}-octreotide *in vivo*. *Bioconjug Chem* 1998; **9**: 662–670
34 **Akizawa H,** Arano Y, Mifune M, Iwado A, Saito Y, Mukai T, Uehara T, Ono M, Fujioka Y, Ogawa K, Kiso Y, Saji H. Effect of molecular charges on renal uptake of ^{111}In-DTPA- conjugated Peptides. *Nucl Med Biol* 2001; **28**: 761–768

Science Editor Kumar M and Zhu LH **Language Editor** Elsevier HK

PO Box 2345, Beijing 100023, China
www.wjgnet.com
wjg@wjgnet.com

ELSEVIER

World J Gastroenterol 2005;11(25):3958-3961
World Journal of Gastroenterology ISSN 1007-9327

• *BRIEF REPORTS* •

Effects of He-Ne laser irradiation on chronic atrophic gastritis in rats

Xue-Hui Shao, Yue-Ping Yang, Jie Dai, Jing-Fang Wu, Ai-Hua Bo

Xue-Hui Shao, Yue-Ping Yang, Department of Medical Physics, Hebei North University, Zhangjiakou 075000, Hebei Province, China
Jie Dai, Ai-Hua Bo, Department of Pathology, Hebei North University, Zhangjiakou 075000, Hebei Province, China
Jing-Fang Wu, Department of Histology and Embryology, Hebei North University, Zhangjiakou 075000, Hebei Province, China
Supported by the Natural Science Foundation of Hebei Province, No. 301427
Co-correspondents: Jie Dai
Correspondence to: Xue-Hui Shao, Department of Medical Physics, Hebei North University, 14 Changqing Road, Zhangjiakou 075000, Hebei Province, China. sxhwby@sina.com
Telephone: +86-313-8041657
Received: 2004-08-26 Accepted: 2005-03-16

Abstract

AIM: To study the effects of He-Ne laser irradiation on experimental chronic atrophic gastritis (CAG) in rats.

METHODS: Sixty-three male adult Wistar rats were randomly divided into five groups including normal control group, model control group and three different dosages He-Ne laser groups. The chronic atrophic gastritis (CAG) model in rats was made by pouring medicine which was a kind of mixed liquor including 2% sodium salicylate and 30% alcohol down the throat for 8 wk to stimulate rat gastric mucosa, combining with irregular fasting and compulsive sporting as pathogenic factors; 3.36, 4.80, and 6.24 J/cm^2 doses of He-Ne laser were used, respectively for three different treatment groups, once a day for 20 d. The pH value of diluted gastric acid was determined by acidimeter, the histopathological changes such as the inflammatory degrees in gastric mucosa, the morphology and structure of parietal cells were observed, and the thickness of mucosa was measured by micrometer under optical microscope.

RESULTS: In model control group, the secretion of gastric acid was little, pathologic morphological changes in gastric mucosa such as thinner mucous, atrophic glands, notable inflammatory infiltration were found. After 3.36 J/cm^2 dose of He-Ne laser treatment for 20 d, the secretion of gastric acid was increased (P<0.05), the thickness of gastric mucosa was significantly thicker than that in model control group (P<0.01), the gastric mucosal inflammation cells were decreased (P<0.05). Morphology, structure and volume of the parietal cells all recuperated or were closed to normal.

CONCLUSION: 3.36 J/cm^2 dose of He-Ne laser has a significant effect on CAG in rats.

Key words: Chronic atrophic gastritis; Laser; He-Ne; Rat

Shao XH, Yang YP, Dai J, Wu JF, Bo AH. Effects of He-Ne laser irradiation on chronic atrophic gastritis in rats. *World J Gastroenterol* 2005; 11(25): 3958-3961
http://www.wjgnet.com/1007-9327/11/3958.asp

INTRODUCTION

Chronic atrophic gastritis (CAG) is one of the most common digestive diseases worldwide[1-4]. The patient's gastric mucosa atrophies, gastric sinus secret cells reduce, function is weakened, gastric acid secretion reduces, especially pathological changeable epithelium often contains intestine epithelium metaplasia and atypical hyperplasia, which are often seen as precancerous lesions of gastric carcinoma[5-7]. To the author's knowledge, clinics still have no perfect and effective treatment projects[8]. So we successfully established an animal model with CAG in rats[9], used different radiation intensity of He-Ne laser to irradiate at the gastric projective area of rat with CAG, to study the therapeutic effects by examining changes of gastric acid and observing changes of pathologic histology in gastric mucosa.

MATERIALS AND METHODS

Animals

A total of 52 male adult Wistar rats weighing 180-230 g were purchased from Experimental Animal Center, Capital Medical University. They were housed in an air-conditioned room with 12 h dark/light cycle, and randomly divided into five groups: eight in normal control group, 11 in model control group, 11 in 3.36 J/cm^2 dose He-Ne laser group (small dose He-Ne laser group), 11 in 4.80 J/cm^2 dose He-Ne laser group (inside dose He-Ne laser group), 11 in 6.24 J/cm^2 dose He-Ne laser group (big dose He-Ne laser group). CAG model in rats were made by mixing 2% sodium salicylate and 30% alcohol and poured down their throats for 8 wk to stimulate their gastric mucosa, combined with irregular fasting and compulsive sporting.

He-Ne laser therapy

He-Ne laser therapy was carried out using the HJ-3DB He-Ne laser machine (wavelength 632.8 nm) which was made by Nanjing laser instrument factory, the He-Ne laser was amplified by convex lens, vertically radiated at the gastric projective area. The anterioposterior diameter of laser was 1 cm, its power density was 8 mW/cm^2. The following formed the course of treatment once a day for 20 d.

Small dose He-Ne laser treatment: irradiated 7 min each time, 3.36 J/cm^2 of dosage;

Inside dose He-Ne laser treatment: irradiated 10 min each time, 4.80 J/cm^2 of dosage;

Big dose He-Ne laser irradiation: irradiated 13 min each time, 6.24 J/cm^2 of dosage.

Process

The rats in each group were killed at the desired time-point. The animals were deprived of food but were offered enough water before being killed at 24 h. The rats were anesthetized with ether, the belly was opened immediately, cadre was ligature, the whole stomach was taken off, and the surface blood stains were washed by normal saline water, sucked dry with filter paper, then the gastric cavity was opened along greater curvature of stomach, flushed with distilled water, and the dilution gastric liquid (provided to measure the gastric acid pH value) was collected, then front and back gastric sinus and parts of stomach organized roughly into 3 mm×10 mm were taken in parallel with lesser curvature of stomach, fixed in neutral formalin, embedded in paraffin wax, 6 μm sections, stained with hematoxylin-eosin (HE) for pathological examination.

Determination of gastric acid

The rat's gastric acid (pH value) was determined five times for each example by acidimeter (PHS-3C) from Shanghai Instrument Factory, and took the average value as the pH value of this animal.

Pathology examinations

Take three sliced pieces for each example, and select three different visual fields for each slice such as the body of stomach, gastric sinus and the area of the body of stomach marked with gastric sinus. The whole gastric mucosa was observed under light microscope, which included the following aspects: (1) the immunity degree of the gastric mucosal ingluvitis cellular was divided into two grades such as negative (-) (no ingluvitis cells or some ingluvitis that jot spread at the gastric mucus) and positive (+) (more ingluvitis cell at the gastric mucosa or series of ingluvitis cells aggregated inside the mucus), counted the positive rate respectively by each visual field; (2) measured the thickness of the gastric mucosa with microscope, regarded μm as the unit, adopted the average of the mucosa thickness to show the reflection hyperplasia circumstance; (3) observed the parietal cell including the appearance, construction and arrangement.

Statistical analysis

Software SPSS 10.0 was used in the statistical analysis, parameters were expressed as mean±SD, and compared using One-way ANOVA analysis of variance, followed by χ^2 tests and differences were considered significant at $P<0.05$.

RESULTS

Gastric acid

The determination results of gastric acid showed that the secret function of gastric mucosa in model control rats was more decreased than that in both normal control group and small dose He-Ne laser group ($P<0.05$, Table 1).

Table 1 Detection of gastric results of pH value in Wistar rats

Group	*n*	pH value (mean±SD)
Normal control	6	3.72±1.02[a]
Model control	7	5.86±1.45
Small dose He-Ne laser	7	4.43±1.18[a]
Inside dose He-Ne laser	6	4.66±1.00
Big dose He-Ne laser	7	4.57±1.48

[a]$P<0.05$ *vs* control group.

Pathological findings

The pathological histologies were observed under microscope. In normal control group, the gastric mucosa was thick, the epithelium was complete, only fell ingluvitis were spread, there was no obvious ingluvitis cellular immunity (Table 2). The parietal cells in normal control group were as follows: large volume, pyramid form, cell edge tactful, full, numerous, were arranged neatly and above 2/3 at a fundic gland (Figure 1A). In model control group, the gastric mucosa was thinner than that in normal control group ($P<0.01$), there were large quantities of immunity ingluvitis ($P<0.01$), most of the cells were lymphocytes and plasma cells. The parietal cells in model control group were as follows: volume sterigma, cell edge anomaly polygon, afterbirth syrup was wrinkled and arranged foul-up, intercellular space was enlarged, the ratio in syrup and nucleosidase increased the breadth of the gland antrum, and large quantity of cells were put through empty transformation (Figure 1B). In He-Ne laser groups, the gastric mucosa was thicker than that in model group ($P<0.01$), ingluvitis cells were less than that in model control group, particularly the small dose He-Ne laser group ($P<0.05$). The parietal cells in small dosage He-Ne laser

Table 2 Changes of gastric mucosa thickness and the observations of ingluvitis cellular immunity degree

Group	*n*	The thickness of gastric mucosa (μm) (mean±SD)	Ingluvitis cellular immunity degree			Ingluvitis edema	
			-	+	Positive rate (%)	Yes	No
Normal control	8	525.17±57.52[b]	7	1	13[b]		√
Model control	11	387.21±51.60	1	10	91		√
Small dose He–Ne laser	11	499.06±57.25[b]	6	5	45[a]		√
Inside dose He–Ne laser	11	456.77±47.56[b]	1	10	91	√	
Big dose He–Ne laser	11	475.62±53.75[b]	2	9	82	√	

[a]$P<0.05$, [b]$P<0.01$ *vs* model control group.

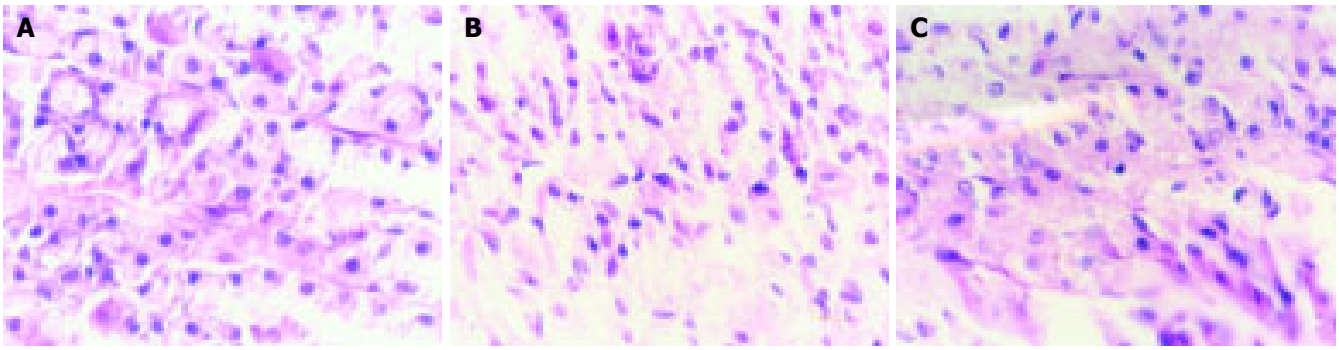

Figure 1 Pathology changes of parietal cells. **A:** parietal cells of gastric mucosa in normal control group (HE ×400); **B:** parietal cells of gastric mucosa in model control group (HE ×400); **C:** parietal cells of gastric mucosa in small dose He-Ne laser group (HE ×400).

group were as follows: cell appearance, volume and construction were all near to normal, and arranged neatly (Figure 1C). Besides, there was no obvious ingluvitis edema in normal control group, model control group and small dosage He-Ne laser group, but it was obvious in inside and large dose He-Ne laser groups, and the cells were transformed in the two groups.

DISCUSSION

The cause of disease and pathogenesis of chronic atrophic arthritis (CAG) are not yet completely clean, generally speaking, it is a synthesis factor with more effects and actions such as immunity, gall back streaming, pyloric infection, food, wine, smoke, and drugs[2,8,9]. Research expressed that sodium salicylate could hurt gastric mucosa and enzyme could inhibit gastric cell growth[10], alcohol could incite gastric mucosa. In our experiment, we poured a mixture of 2% sodium salicylate and 30% alcohol down the rat's throat for 8 wk, which could affect the natural cover and organize variety in gastric mucus, combined with fatigue from overwork, hunger and dissatisfaction in order to make the pathological changes of CAG appear on the gastric mucosa appear[9]. Since the parietal cells reduced and degenerated, there was disorder both in gastric acid secretion and digestion enzyme weakness, the performance was a series of weak symptoms of the function of digestion and absorption such as the reduction of gastric acid secretion, diminishing of the gland and atrophy, and metaplasis of the intestinal epithelium[9].

He-Ne laser, its characteristics such as 632.8 nm of wavelength, good directivity , high intensity, good monochromaticity, is a low-level laser[11-14]. The low-level laser has some biology effects such as cell vitality[15-18], phagocytosis[19-21], immune responses[22-25], but as far as its usage for the treatment of digestive disease, there were only few reports[26-28]. On one hand, there was no difference between treating gastric ulcer through bark and by endoscope[29]. On the other hand, external irradiation is easy, and patients can bear some pain with ease. We treated rats with CAG by external irradiation with He-Ne laser as amplified by a convex mirror, radiated at the gastric projective area. The results implied that the gastric acid secretion of the rats in CAG treated by He-Ne laser irradiation was increased, the best effect was on the animals treated by small dosage He-Ne laser. Some changes in gastric mucus such as thickness of gastric mucosa, alleviated ingluvitis, and parietal cell hyperplasia were found in this experiment. We think the mechanism of He-Ne laser treated CAG in rats as follows: (1) partial microcirculation was ameliorated; (2) body immunity was enhanced; (3) the organized growth of gastric mucosa was promoted; (4) inflammation was eliminated. Moreover, in our experiment we found that three different dosages of He-Ne laser preceding the incitement to the rat in CAG, resulted in different effects. The best effect was the small dosage of He-Ne laser, the inside dose and the large dose were not as well as the small dose of He-Ne laser, which showed the dependence on dosage[20,30,31]. Perhaps it is because the biology effect of He-Ne laser closely related to the action time, power density that organized He-Ne laser. Under the same power density (8 mW/cm^2), different action time (small dose for 7 min, inside dose for 10 min, large dose for 13 min), produced different effects. These results showed that small dose He-Ne laser was a positive action, but large dose was an inhibitory action to incite lombricine organization[32]. Besides, some damaged cells, individual swelling, afterbirth syrup degeneration and ingluvitis edema in the inside dose He-Ne laser group and the big dose He-Ne laser group were found in gastric mucus of rats under microscope. This may indicate the light dynamic damage of He-Ne laser. So we draw a further conclusion that big doses of He-Ne laser were deformative. In a word, the experiment showed that 3.36 J/cm^2 dose of He-Ne laser is a valid dose of external irradiation to incite life, it could promote the secretion of gastric acid and recover the function of gastric mucus to the CAG in rats.

In summary, 3.36 J/cm^2/d dose of He-Ne laser irradiation is a well-tolerated, safe, and effective treatment in rats with CAG. The technique is easy, inexpensive, and of short duration[25]. It is necessary to translate the outcome of this study into clinically relevant interventions by further studies which would develop a new way for the treatment of CAG.

REFERENCES

1 **He WB,** Gao GL, Hou S, Song G. Relationship between mucosal vascular lesion and gastric carcinoma in chronic atrophic gastritis of mice. *Shijie Huaren Xiaohua Zazhi* 1999; **7**: 130-132
2 **He RZ.** Pathology (fourth edition). *Renmin Weisheng Chubanshe* 2003: 128-129
3 **Asaka M,** Sugiyama T, Nobuta A, Kato M, Takeda H, Graham DY. Atrophic gastritis and intestinal metaplasia in

Japan: results of a large multicenter study. *Helicobacter* 2001; **6**: 294-299
4 **Wang RJ,** Du Q, Shao TY, Zhong TJ, Wu YL, Wang JH. Pathologic studies of Chinese drug Weiyanxiao on experimental chronic atrophic gastritis in rats. *Shijie Huaren Xiaohua Zazhi* 2000; **4**: 382-285
5 **Chen SY,** Wang JY, Ji Y, Zhang XD, Zhu CW. Effects of *Helicobacter pylori* and protein kinase C on gene mutation in gastric cancer and precancerous lesions. *Shijie Huaren Xiaohua Zazhi* 2001; **9**: 302-307
6 **Wang XB,** Wang X, Zhang NZ. Inhibition of somatostatin analog Octreotide on human gastric cancer ce ll MKN45 growth *in vitro*. *Shijie Huaren Xiaohua Zazhi* 2002; **10**: 40-42
7 **Yao XX,** Yin L, Zhang JY, Bai WY, Li YM, Sun ZC. hTERT expression and cellular immunity in gastric cancer and precancerosis. *Shijie Huaren Xiaohua Zazhi* 2001; **9**: 508-512
8 **El-Zimaity HM,** Ota H, Graham DY, Akamatsu T, Katsuyama T. Patterns of gastric atrophy in intestinal type gastric carcinoma. *Cancer* 2002; **94**: 1428-1436
9 **Shao XH,** Wang JG, Dai J. Establishment of chronic atrophic gastritis in a rat model. *Zhangjiakou Yixueyuan Xuebao* 2002; **2**: 11-13
10 Nanjing pharmaceutical college. Medicament Chemistry. Beingjing, *Renmin Weisheng Chubanshe* 1978: 172
11 **Hu XM.** Medical physics (fifth edition). Beijing: *Renmin Weisheng Chubanshe* 2001: 351-352
12 **Qin RJ.** Medical physics (third edition). Guilin: *GuangXi Shifan Daxue Chubanshe* 2002: 131-132
13 **Stadler I,** Lanzafame RJ, Oskoui P, Zhang RY, Coleman J, Whittaker M. Alteration of skin temperature during low-level laser irradiation at 830 nm in a mouse model. *Photomed Laser Surg* 2004; **22**: 227-231
14 **Rochkind S,** Ouaknine GE. New trend in neuoscience: low-power laser effect on peripheral and central nervous system (basic science preclinical and clinical studies). *Neurol Res* 1992; **14**: 2-11
15 **Pogrel MH,** Chen JW, Zhang K. Effects of low-energy gallium-alrminum-arsenide laser irradiation on cultured fibroblasts and keratinocytes. *Lasers Surg Med* 1997; **20**: 426-432
16 **Ben-Dov N,** Shefer G, Irintchev A, Oron U, Halevy O, Irinitchev A. Low energy laser irradiation affects satellite cell proliferation and differentiation *in vitro*. *Biochim Biophys Acta* 1999; **14**: 372-380
17 **Grossman N,** Schneid N, Reuveni H, Halevy S, Lubart R. 780 nm low power diode laser irradiation stimulates proliferation of keratinocyte cultures: involovement of reactive oxygen species. *Lasers Surg Med* 1998; **22**: 212-218
18 **Rochkind S,** Ouaknine GE. New trend in neuoscience: low-power laser effect on peripheral and central nervous system. *Neurol Res* 1992; **14**: 2-11
19 **Pessoa ES,** Melhado RM, Theodoro LH, Garcia VG. A histologic assessment of the influence of low-intensity laser therapy on wound healing in steroid-treated animals. *Photomed Laser Surg* 2004; **22**: 199-204
20 **Brosseau L,** Welch V, Wells G, DeBie R, Gam A, Harman K, Morin M, Shea B, Tugwell P. Low level laser therapy (Classes I, II and III) for treating osteoarthritis. *Cochrane Database Syst Rev* 2004; **3**: CD002046
21 **Kans JS,** Hutschenreiter T, Haina D, Waidelich W. Effect of low-power density laser radiation on healing of open skin wounds in rats. *Arch Surg* 1981; **116**: 293-296
22 **Hrnjak M,** Kulijic-Kapulica N, Budisin A, Giser A. Stimulatory effect of low-power density He-Ne laser radiation on human fibroblasts *in vitro*. *Vojnosanit Pregl* 1995; **52**: 539-546
23 **Monteforte P,** Baratto L, Molfetta L, Rovetta G. Low-power laser in osteoarthritis of the cervical spine. *Int J Tissue React* 2003; **25**: 131-136
24 **Ohta A,** Abergel RP, Uitto J. Laser modulation of human immune system, inhibition lymphocyte proliferation by a gallium-arsenide laser energy. *Lasers Surg Med* 1987; **7**: 199-201
25 **Karu T.** Photobiology of low-power laser effects. *Health Phys* 1989; **56**: 691-704
26 **Fukutomi H,** Kawakita 1, Nakahara A. Endoscopic diagnosis and treatment of gastric cancer by laser beam. Laser Tokyo 81, Session 20. *Laser Endoscopy* 1981; **20**: 26
27 **Overholt BF,** Danjehpour M, Haydek JM. Photodynamic therapy for Barrett's esophagus: follow-up in 100 patients. *Gastrointest Endosc* 1999; **49**: 1-7
28 **Etienne J,** Dorme N, Bourg-Heckly G, Raimbert P, Flijou JF. Photodynamic therapy with green light and m-tetrahydroxyphenyl chlorin for intramucosal adenocarcinoma and high-grade dysplasia in Barrett's esophagus. *Gastrointest Endosc* 2004; **59**: 880-889
29 **Wang KR.** The comparison of laser therapy on gastric ulcer through bark and by endoscopes. *Guowai Yixue* 1997; **4**: 188
30 **Pinheiro AL,** do Nascliento SC, de Vieira AL, Rolim AB, da Silva PS, Brugnera A Jr. Does LLLT stimulate laryngeal carcinoma cells? An *in vitro* study. *Braz Dent J* 2002; **13**: 109-112
31 **De Scheerder IK,** Wang K, Zhou XR, Verbeken E, Keelan MH Jr, Horn JB, Sahota H, Kipshidze N. Intravascular low power red laser light as an adjunc coronary stent implantation evaluated in a porcine C model. *J Invasive Cardiol* 1998; **10**: 263-268
32 **Huang BX,** Wang HB, Liu HQ, Qu ZN, Liu XF, Cheng ZH, Gao L. Study on the Effects of He-Ne Laser Irradiation on the Activity of Humoral Immune Factors IL-2 in Mice. *Zhongguo Jiguang Zazhi* 2004; **2**: 249-252

Science Editor Guo SY **Language Editor** Elsevier HK

PO Box 2345, Beijing 100023, China
www.wjgnet.com
wjg@wjgnet.com

ELSEVIER

World J Gastroenterol 2005;11(25):3962-3965
World Journal of Gastroenterology ISSN 1007-9327

• *BRIEF REPORTS* •

Expression of interferon-alpha/beta receptor protein in liver of patients with hepatitis C virus-related chronic liver disease

Xiang-Wei Meng, Bao-Rong Chi, Li-Gang Chen, Ling-Ling Zhang, Yan Zhuang, Hai-Yan Huang, Xun Sun

Xiang-Wei Meng, Bao-Rong Chi, Li-Gang Chen, Ling-Ling Zhang, Yan Zhuang, Hai-Yan Huang, Xun Sun, Department of Gastroenterology, the First Affiliated Hospital, Jilin University, Changchun 130021, Jilin Province, China
Correspondence to: Dr. Xiang-Wei Meng, Department of Gastroenterology, the First Affiliated Hospital, Jilin University, Changchun 130021, Jilin Province, China. xiangweimeng2003@yahoo.com.cn
Telephone: +86-431-5612437 Fax: +86-431-5612437
Received: 2004-07-09 Accepted: 2004-09-19

Abstract

AIM: To study the expression of interferon-alpha/beta (IFN-α/β) receptor protein in liver of patients with hepatitis C virus (HCV)-related chronic liver disease and its clinical significance.

METHODS: A total of 181 patients with HCV-related chronic liver disease included 56 with HCV-related liver cirrhosis (LC) and 125 with chronic hepatitis C (CHC). CHC patients were treated with five megaunits of interferon-α1b six times weekly for the first 2 weeks and then every other day for 22 wk. The patients were divided into interferon (IFN) treatment-responsive and non-responsive groups, but 36 patients lost follow-up shortly after receiving the treatment. The expression of IFN-α/β receptor (IFN-α/βR) protein in liver of all patients was determined with immunofluorescence.

RESULTS: In liver of patients with HCV-related chronic liver disease, the expression of IFN-α/βR protein in liver cell membrane was stronger than that in cytoplasm and more obvious in the surroundings of portal vein than in the surroundings of central vein. Moreover, it was poorly distributed in hepatic lobules. The weak positive, positive and strong positive expression of IFN-α/βR were 40% (50/125), 28% (35/125), 32% (40/125), respectively in CHC group, and 91.1% (51/56), 5.35% (3/56), and 3.56% (2/56), respectively in LC group. The positive and strong positive rates were higher in CHC group than in LC group ($P<0.01$). In IFN treatment responsive group, 27.8% (10/36) showed weak positive expression; 72.2% (26/36) showed positive or strong positive expression. In the non-responsive group, 71.7% (38/53) showed weak positive expression; 28.3% (15/53) showed positive or strong positive expression. The expression of IFN-α/βR protein in liver was more obvious in IFN treatment responsive group than in non-responsive group.

CONCLUSION: Expression of IFN-α/βR protein in liver of patients with HCV-related chronic liver disease is likely involved in the response to IFN treatment.

Key words: IFN-α/β receptor; Chronic hepatitis C; HCV-related liver cirrhosis

Meng XW, Chi BR, Chen LG, Zhang LL, Zhuang Y, Huang HY, Sun X. Expression of interferon-alpha/beta receptor protein in liver of patients with hepatitis C virus-related chronic liver disease. *World J Gastroenterol* 2005; 11(25): 3962-3965
http://www.wjgnet.com/1007-9327/11/3962.asp

INTRODUCTION

Interferon (IFN) is effective in the treatment of chronic hepatitis C. It results in viral eradication and normalization of liver function in about 35-40% of the patients[1-4]. The anti-virus mechanism of IFN is to transmit the signal to nuclei and to activate 2'-5' adenylic acid synthase and protein kinase after IFN molecule combines with IFN receptor, which then blocks the translations of virus protein and RNA. IFN receptor (IFN-R) is the initial protein for the chain reaction of IFN[5]. Human interferon receptors are divided into type I IFN-R which can combine with IFN-α/β, and type II IFN-R which has specific sensitivity to IFN-γ. Furthermore, it has been proved that type II IFN-R is also sensitive to IFN-α/β to some extent[6], meanwhile IFN-β and subtypes of IFN-α have high sensitivity to IFN-R[7].

In this study, we determined the expression of IFN-R protein in liver of patients with HCV-related chronic liver disease and its clinical significance.

MATERIALS AND METHODS

Patients

A total of 181 patients were enrolled in this study, including 125 patients with chronic hepatitis C and 56 patients with HCV-related liver cirrhosis. All the patients were seropositive for HCV-RNA and underwent liver biopsy. None of the patient was infected with other hepatitis viruses. All the patients with chronic hepatitis C received IFN treatment. However, only 89 patients were evaluated for treatment response since 36 patients lost follow-up shortly after receiving the treatment. According to the response to IFN treatment, we studied the expression of IFN-α/βR protein in liver of 89 patients with chronic hepatitis C at least six months after IFN treatment.

IFN treatment

IFN treatment was standardized as follows. Five megaunits of IFN-α1b was administrated to 89 patients with chronic hepatitis C by intramuscular injection six times weekly for the first 2 weeks and then every other day for 22 wk. The total dosage of IFN was 470 MU[8]. The study followed the ethical guidelines of the Declaration of Helsinki and was approved by the institutional ethics committee. Informed consent was obtained from all patients before IFN treatment.

Appraisal of IFN treatment

According to the response to IFN, 89 patients with chronic hepatitis C who were seropositive for HCV-RNA and received IFN treatment were divided into responder group (36) and non-responder group (53). Responders were defined as patients who were seronegative for HCV-RNA with their serum alanine aminotransferase (ALT) decreased to the normal range for at least 6 mo after IFN treatment. The other patients were non-responders.

Histopathological evaluation

Liver biopsy specimens were defined by Knodell's pathologic classification. The degree of liver fibrosis was determined according to the criteria for staging fibrosis (F_0 to F_4), including F_0 (no fibrosis), F_1(portal area fibrosis), F_2 (bridging fibrosis), F_3(bridging fibrosis with lobule deformation), F_4 (cirrhosis). Inflammation activities were scored as follows: 1-3 points (mild hepatitis), 4-8 points (moderate hepatitis), 9-12 points (severe hepatitis).

Determination of IFN-α/βR in liver

Making specimens with immunofluorescence technique

IFN-α/βR in the liver was immunostained with an indirect immunofluorescence technique. The liver biopsy specimens were sampled during laparoscopy, fixed with fixatives, and frozen to make histological sections. The sections were incubated with non-marked antibody for 45 min at 37 ℃, washed thrice in 0.15 mol/L pH7.6 phosphate buffered saline (PBS) for 3 min and once in 0.01 mol/L pH 7.6 PBS for 1 min, then incubated with anti-idiotype antibody (AId) for 30-45 min at 37 ℃ and washed with PBS. The sections were dehydrated at room temperature and mounted in glycerol. We cloned the gene coding for the outside-membrane of IFN-α/βR in Daudi's cells and immunized white rabbits with protein produced by the gene-transfected *E.coli* to get the first antibody (Amersham, Buckinghamshire, UK). The AId (Amersham, Buckinghamshire, UK) was an anti-rabbit-IgG class antibody labeled with fluorochrome. Negative control was serum of rabbits.

Criteria of fluoroimmunoassay

Intensity of fluorescence was standardized as follows (Figure 1): weak positive (+), positive (++) and strong positive (+++). If a minority of hepatocytes in the portal area were stained, it was defined as weak positive (+). The strong positive (+++) means almost all hepatocytes in the hepatic lobule were stained, and hepatocytes between the two grades were defined as positive (++).

Statistical analysis

Statistical significance of difference was determined by χ^2-test.

RESULTS

Expression of IFN-α/βR protein in liver

IFN-α/βR protein was expressed in all the samples of HCV-related chronic liver disease, however the degree of expression varied. Expression of IFN-α/βR protein in cell membrane was stronger than that in cytoplasm (Figure 2A).The expression of protein in the surroundings of the portal vein was stronger than that in the surroundings of the central vein. The protein was poorly distributed in hepatic lobules (Figure 2B). Almost all the IFN-α/βR proteins expressing cells were hepatic parenchymal cells. However, IFN-α/βR proteins were also expressed in part of interlobular cholangioepithelia (Figure 2C).

Expression of IFN-α/βR protein in patients with chronic hepatitis C and HCV-related liver cirrhosis

Among the 125 patients with chronic hepatitis C, 40% (50/125) showed weak positive (+), 28% (35/125) showed positive (++), 32% (40/125) showed strong positive (+++) expression of IFN-α/βR protein. Among the 56 patients with HCV-related liver cirrhosis, 91.1% (51/56) showed weak positive (+), 5.35% (3/56) showed positive (++), 3.56% (2/56) showed strong positive (+++) expression of IFN-α/βR protein. The total frequency of positive and strong positive expression in chronic hepatitis C patients was much higher than that in patients with HCV-related liver cirrhosis (P<0.01 Table 1).

Table 1 Expression of IFN-α/βR protein in liver of patients with HCV-related chronic liver disease

Group	*n*	Fluorescence intensity in cases, *n* (%)	
		+	++,+++
CHC	125	50 (40)[b]	75 (60)[b]
LC	56	51 (91.1)	5 (8.9)

[b]P<0.01 *vs* LC.

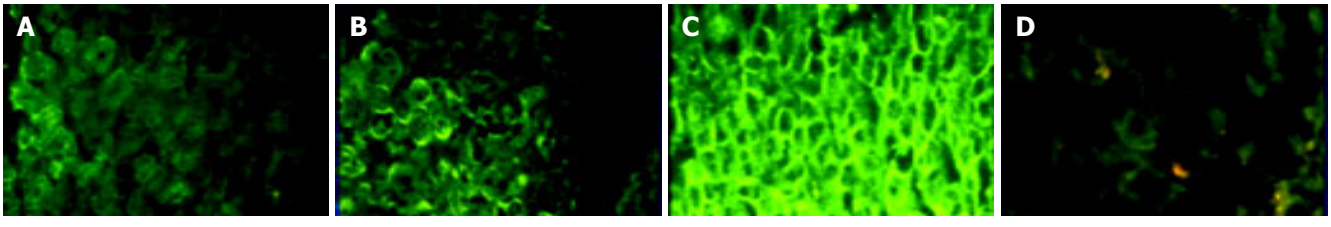

Figure 1 Weak positive (**A**), positive (**B**), strong positive (**C**) and negative (**D**) expression of IFN-α/βR (×200).

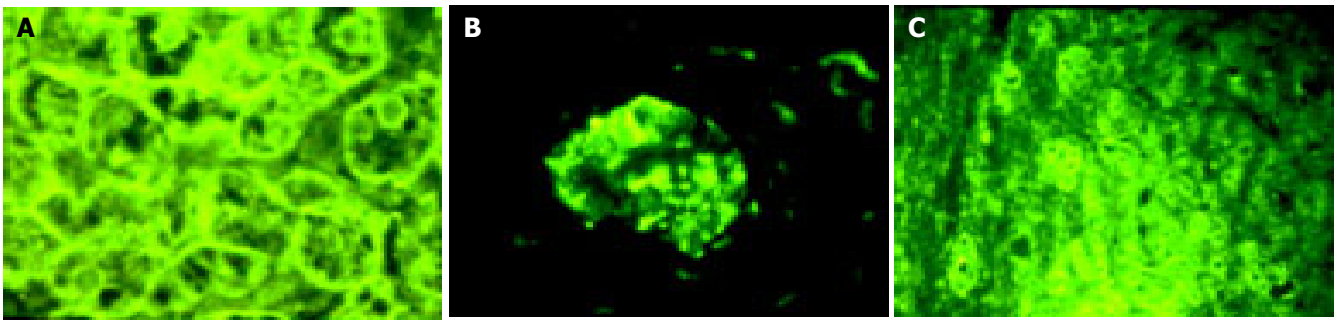

Figure 2 Expression of IFN-α/βR protein in cell membrane and cytoplasm (**A**), hepatic lobules (**B**), and hepatic parenchymal cells and part of interlobular cholangioepithelia (**C**).

Expression of IFNα/βR protein in liver of patients with chronic hepatitis C after IFN treatment

Six months after IFN treatment, the responders and non-responders were 36 and 53 respectively, and 27.8% (10/36) of the responders showed weak positive (+), and 72.2% (26/36) showed positive (++) or strong positive (+++) expression of the IFNα/βR protein; 71.7% (38/53) of non-responders showed weak positive (+), and 28.3% (15/53) showed positive (++) or strong positive (+++) expression of the IFN-α/βR protein. After the treatment, the total frequency of positive (++) and strong positive (+++) expression of the IFN-α/βR protein in responder group was much higher ($P<0.05$) than that in non-responder group (Table 2).

Table 2 Effect of IFN and expression of IFN-α/βR protein

IFN treatment effect	*n*	Fluorescence intensity in cases, *n* (%)	
		+	++, +++
Responders	36	10 (27.8)[a]	26 (72.2)[a]
Non-responders	53	38 (71.7)	15 (28.3)

[a]$P<0.05$ *vs* non-responders.

DISCUSSION

Isimura[9] has proved that IFN R protein exists in liver by ELISA and reported that the expression degree of IFN-αR protein in cytoplasm is different. By immunohistochemical method and competitive polymerase chain reaction assay, Fujiwara *et al*.[9], found that determination of the expression of IFN-α/βR protein is more useful than that of its mRNA. In this study, we found that expression of IFN-α/βR protein in cell membrane was stronger than that in cytoplasm by immunofluorescence assay. IFN-α/βR protein is a membrane receptor just like other cytoplasm receptors. Moreover, this study also found that the expression of IFN-α/βR protein in the surroundings of the portal vein was stronger than that in the central vein, and the protein was poorly distributed in hepatic lobules. This may be attributed to the following aspects. The blood stream in surrounding of the portal vein is more affluent, providing a good nutritional condition for virus infection which then induces the expression of IFN-α/βR. The expression intensity of IFN-α/βR protein varies in different chronic hepatic diseases. It is weaker in patients with HCV-related liver cirrhosis than in patients with chronic C hepatitis. The reason may be that the bloodstream in patients with cirrhosis is not well-distributed and the blood supply becomes deficient due to various kinds of fibrosclerosis in hepatic lobules, and liver function and liver cell membrane are damaged because of hepatic cellular inflammation. Because of these factors, liver could not provide a good condition for the expression of IFN-α/βR protein in patients with cirrhosis. Defective expression of IFN-α/βR protein can reduce the intake of IFN, resulting in increased reproduction of virus and activity of hepatitis.

This study demonstrated that expression of IFN-α/βR protein had a close correlation with hepatic fibrosis. The majority of responders with chronic hepatitis C had a very strong expression of IFN-α/βR protein prior to the treatment, which coincides with other researches[10-12]. The reasons are as follows. The infection of hepatitis virus C can induce expression of protein effectively[13], since some patients with HCV-related chronic liver disease become very sensitive to IFN treatment. Expression of IFN-α/βR protein in liver in responsive cases is much stronger than that in non-responsive cases. That is to say, non-responsive reaction to the treatment may be caused by the defective expression of protein in patients with chronic hepatitis C. Although expression of IFN-α/βR protein in the responder group is stronger than that in non-responder group, the expression also exists in some non-responsive cases. On the contrary, expression of IFN-α/βR protein in some responsive cases is as weak as that in non-responsive cases. These inconsistencies are attributed to the following aspects. IFN-α/βR protein cannot represent all IFN R proteins involved in the anti-virus mechanism in chronic hepatitis C. The protein we studied is IFN-α/βR protein which could respond to IFN-α and IFN-β[7]. The protein plays a key role, in the anti-virus mechanism against HCV-related chronic disease. The combining activity of R proteins maybe changed in the responsive cases when IFN-α/βR protein is expressed. Among the responsive and non-responsive cases, some patients with severe chronic hepatitis C and cirrhosis were not sensitive to IFN treatment, and defective expression of IFN-α/βR protein in these patients was a major cause. It coincides with other studies[14,15]. In conclusion, expression of IFN-α/βR protein in liver of patients with HCV-related chronic disease is likely involved in response to IFN treatment, the expression of IFN-α/βR protein may be useful in

predicting IFN therapeutic effect, and defective expression of IFN-α/βR protein in liver may result in resistance to IFN treatment in patients with HCV-related chronic liver disease.

REFERENCES

1 **Hagiwara H,** Hayashi N, Mita E, Takehara T, Kasahara A, Fusamoto H, Kamada T. Quantitiative analysis of hepatitis C virus RNA in serum during interferon alpha therapy. *Gastroenterology* 1993; **104**: 877-883

2 **Kanai K,** Kato M, Okamoto H. HCV genotypes in chronic hepatits C and response to interferon. *Lancet* 1992; **339**: 1543

3 **Tsubota A,** Chayama K, Ikeda K, Yasuji A, Koida I, Saitoh S, Hashimoto M, Iwasaki S, Kobayashi M, Hiromitsu K. Factors predictive of response to interferon -alpha therapy in hepatitis C virus infection. *Hepatology* 1994; **19**: 1088-1094

4 **Poynard T,** Leroy V, Cohard M, Thevenot T, Mathurin P, Opolon P, Zarski JP. Meta-analysis of interferon randomized trials in the treatment of viral hepatitis C: Effects of dose and duration. *Hepatology* 1996; **24**: 778-789

5 **Muller U,** Steinhoff U, Reis LF, Hemmi S, Pavlovic J, Zinkernagel RM, Aguet M. Functional roles of type I and type II interferons in antiviral defense. *Science* 1994; **264**: 1918-1921

6 **Novick D,** Cohen B, Rubinstein M. The human interferon-α/βreceptor Characterization and molecular cloning. *Cell* 1994; **77**: 391-400

7 **Colamonici OR,** Domanski P. Identification of a novel subunit of the Type I interferon receptor localized to human chromosome. *J Biol Chem* 1993; **268**: 10895-10899

8 Isimura. The significance of interferon in liver as an impact factor for hepatitis C therapy. *Hepatology* 1997; **38**: 292-299

9 **Fujiwara D,** Hino K, Yamaguchi Y, Ren F, Satoh Y, Korenaga M, Okuda M, Okita K. Hepatic expression of type I interferon receptor for predicting response to interferon therapy in chronic hepatitis C patients: a comparison of immunohistochemical method *vs* competitive polymerase chain reaction assay. *Hepatol Res* 2003; **25**: 377-384

10 **Morita K,** Tanaka K, Saito S, Kitamura T, Kondo M, Sakaguchi T, Morimoto M, Sekihara H. Expression of interferon receptor genes (IFNAR1 and IFNAR2 mRNA) in the liver may predict outcome after interferon therapy in patients with chronic genotype 2a or 2b hepatitis C virus infection. *Clin Gastroenterol* 1998; **26**: 135-140

11 **Mizukoshi E,** Kaneko S, Yanagi M, Ohno H, Kaji K, Terasaki S, Shimoda A, Matsushita E, Kobayashi K. Expression of interferon alpha/beta receptor in the liver of chronic hepatitis C patients. *J Med Virol* 1998; **56**: 217-223

12 **Fujiwara D,** Hino K, Yamaguchi Y, Kubo Y, Yamashita S, Uchida K, Konishi T, Nakamura H, Korenaga M, Okuda M, Okita K. Type I interferon receptor and response to interferon therapy in chronic hepatitis C patients: a prospective study. *J Viral Hepat* 2004; **11**: 136-140

13 **Yamaguchi Y,** Hino K, Fujiwara D, Ren F, Katoh Y, Satoh Y, Okita K. Expression of type I interferon receptor in liver and peripheral blood mononuclear cells in chronic hepatitis C patients. *Dig Dis Sci* 2002; **47**: 1611-1617

14 **Affabris E,** Romeo G, Belardelli F, Jemma C, Mechti N, Gresser I, Rossi GB. 2-5A synthetase activity does not increase in interferon-resistant Friend leukemia cell variants treated with alpha/beta interferon despite the presence of high-affinity interferon receptor sites. *Virology* 1983; **125**: 508-512

15 **Roffi L,** Colloredo G, Antonelli G, Beliati G, Panizzuti F, Piperno A, Pozzi M, Ravizza D, Angeli G, Diaazani F, Mancia G. Breakthrough during recombinant interferon alpha therapy in patients with chronic hepatitis C virus infection: prevalence, etiology, and management. *Hepatology* 1995; **21**: 645-649

Science Editor Wang XL and Guo SY **Language Editor** Elsevier HK

PO Box 2345, Beijing 100023, China
www.wjgnet.com
wjg@wjgnet.com

ELSEVIER

World J Gastroenterol 2005;11(25):3966-3969
World Journal of Gastroenterology ISSN 1007-9327

• *BRIEF REPORTS* •

Surgical treatment of hepatocellular carcinoma with bile duct tumor thrombi

Bao-Gang Peng, Li-Jian Liang, Shao-Qiang Li, Fan Zhou, Yun-Peng Hua, Shi-Min Luo

Bao-Gang Peng, Li-Jian Liang, Shao-Qiang Li, Fan Zhou, Yun-Peng Hua, Shi-Min Luo, Department of Hepatobiliary Surgery, the First Affiliated Hospital of Sun Yat-Sen University, Guangzhou 510080, Guangdong Province, China
Correspondence to: Dr. Bao-Gang Peng, Department of Hepatobiliary Surgery, the First Affiliated Hospital of Sun Yat-Sen University, Guangzhou 510080, Guangdong Province, China. pengbaogang@163.net
Telephone: +86-20-87755766-8214 Fax: +86-20-87755766-8663
Received: 2004-06-28 Accepted: 2004-07-22

Abstract

AIM: To study the surgical treatment effect and outcome of hepatocellular carcinoma (HCC) with bile duct tumor thrombi (BDTT).

METHODS: Fifty-three consecutive HCC patients with BDTT admitted in our department from July 1984 to December 2002 were reviewed retrospectively. The clinical data, diagnostic methods, surgical procedures and outcome of these patients were collected and analyzed.

RESULTS: One patient rejected surgical treatment, 6 cases underwent percutaneous transhepatic cholangial drainage (PTCD) for unresectable primary disease, and the other 46 cases underwent surgical operation. The postoperative mortality was 17.6%, and the morbidity was 32.6%. Serum total bilirubin levels of these patients with obstructive jaundice decreased gradually after surgery. The survival time of six cases who underwent PTCD ranged from 2 to 7 mo (median survival of 3.7 mo). The survival time of the patients who received surgery was as follows: 2 mo for one patient who underwent laparotomy, 5-46 mo (median survival of 23.5 mo, which was the longest survival in comparison with patients who underwent other procedures, $P = 0.0024$) for 17 cases who underwent hepatectomy, 5-17 mo (median survival of 10.0 mo) for 5 cases who underwent HACE, 3-9 mo (median survival of 6.1 mo) for 11 cases who underwent simple thrombectomy and biliary drainage, and 3-8 mo (median survival of 4.3 mo) for four cases who underwent simple biliary drainage.

CONCLUSION: Jaundice caused by BDTT in HCC patients is not a contraindication for surgery. Only curative resection can result in long-term survival. Early diagnosis and surgical treatment are the key points to prolong the survival of patients.

Key words: Hepatocellular carcinoma; Bile duct tumor thrombi

Peng BG, Liang LJ, Li SQ, Zhou F, Hua YP, Luo SM. Surgical treatment of hepatocellular carcinoma with bile duct tumor thrombi. *World J Gastroenterol* 2005; 11(25): 3966-3969
http://www.wjgnet.com/1007-9327/11/3966.asp

INTRODUCTION

Jaundice is present in 19-40% of patients with hepatocellular carcinoma (HCC) at the time of diagnosis and usually occurs in advanced stages of diseases. The etiology of jaundice is mainly due to diffuse tumor infiltration of liver parenchyma, progressive liver failure (advanced underlying cirrhosis) and hepatic hilar invasion[1]. Obstructive jaundice caused by bile duct tumor thrombi (BDTT) arising from HCC is uncommon[2,3]. Only 1-12% of HCC patients manifest obstructive jaundice as the initial manifestation[4]. We have noticed this kind of obstructive jaundice caused by HCC with BDTT since 1980, and our initial report of HCC with BDTT was published in 1996[5]. However, BDTT caused by HCC thrombus is often misdiagnosed as hilar cholangiocarcinoma, and has a particular mode of growth and clinical features. Herein, we report a total of 53 HCC patients with BDTT to make a better understanding of the nature of this disease.

MATERIALS AND METHODS

Patients

From July 1984 to December 2002, 53 consecutive HCC patients (47 males, 6 females, age range 20-69 years, mean age 48.2±10.2 years) with BDTT were treated in our department. The common clinical manifestations included: jaundice, abdominal pain, poor appetite, abdominal distension, skin itch, clay-colored stools, *etc*. Eight cases had previous treatment in other hospitals before admission. Among them, four cases had recurrent HCC after hepatectomy, three received transcatheter arterial chemoembolization (TACE), and one underwent ^{32}P glass microspheres (^{32}P-GMS) internal radiotherapy thrice through hepatic artery cannulation and subcutaneous implantation of a drug pump.

Laboratory examination

The average level of serum total bilirubin was 311.9±186.9 μmol/L (range 20.3-776.6 μmol/L), ALT was 119±82 IU/L (range 16-428 IU/L), ALP was 423±241 IU/L (range 116-1 038 IU/L), γ-GT was 410±346 IU/L (range 98-1 637 IU/L), ALB was 37±6 g/L (range 24-46 g/L). The hepatitis B surface antigen was positive in 35 cases (35/53, 66.0%). The hepatitis C antibody assay was positive in one case. The concentration of a-fetoprotein (AFP) was higher than

400 μg/L in 29 cases (29/53, 54.7%). Cirrhosis was found in 28 cases (28/53, 52.8%), ascites in 10 cases (10/53, 18.9%).

Imaging findings

Primary tumors and total BDTT in the common hepatic duct or the common bile duct (CBD) were detected by image investigations including ultrasonography (US), computed tomography (CT), endoscopic retrograde cholangiopancreatography and magnetic resonance cholangiopancreatography (MRCP). Three patients were misdiagnosed as cholangiocarcinoma, among them two cases underwent laparotomy and T-tube drainage in other hospitals, one case was found to have lung metastasis at the initial diagnosis.

Location and size of HCC and BDTT

No obvious primary liver tumor was found in seven cases, among them three cases were misdiagnosed as hilar cholangiocarcinoma (Figure 1). The diameter of the primary tumors ranged from 0.9 to 12 cm (mean value 5.0±2.6 cm) in the remaining 46 cases. Of these, the diameter of the major tumor was larger than 10 cm in 6 cases, between 5 and 10 cm in 15 cases, less than 5 cm in 25 cases. Seventeen cases had multiple nodules, 29 had a single nodule. The tumors were involved in the right lobe (n = 19), the left lobe (n = 13), and the caudate lobe of liver (n = 3), the whole liver (n = 11). The tumor thrombi of CBD occurred in all cases. Thrombi coexisted in intrahepatic bile duct (n = 38), the right hepatic duct (n = 5), the left hepatic duct (n = 4), and the left and right hepatic ducts (n = 6). In addition, the tumor thrombi presented in the right branch (n = 1), and the left branch of portal vein (n = 1), the right branch of portal vein and the right hepatic vein (n = 1).

Statistical analysis

A database was established by SPSS 10.0 software. Data were expressed as mean±SD. Kaplan-Meier method and log-rank test were used for survival statistics. P<0.05 was considered statistically significant.

RESULTS

Treatments

One patient refused surgery for other reasons. Fifty-two cases received treatments. Among them, six cases received non-surgical procedures including percutaneous transhepatic cholangio-drainage (PTCD, n = 4), biliary stent placement (n = 2). Forty-six cases underwent surgical operations including hepatectomy with thrombectomy and biliary drainage (n = 21), hepatic artery chemoembolization (HACE) for unresectable primary diseases and biliary drainage (n = 5), simple thrombectomy with biliary drainage (n = 14), and simple biliary drainage (n = 4). Among the 21 cases who underwent hepatectomy for their primary liver tumors, 2 cases underwent right hemihepatectomy, 2 left hemihepatectomy, 11 partial right lobectomy, 4 partial left lobectomy, 1 left hemihepatectomy with caudate lobectomy, 1 left hemihepatectomy with caudate lobectomy and segmentectomy. Simultaneously, one case underwent thrombectomy for the right branch thrombi of portal vein and the right hepatic vein thrombi via the transaction surfaces. Of the 14 cases who underwent simple thrombectomy and biliary drainage, one underwent proper hepatic artery ligation (HAL), and the other right HAL at the same time.

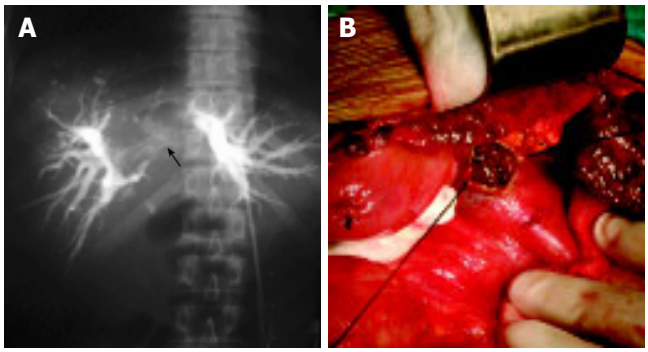

Figure 1 Location and size of HCC. **A:** Hilar obstruction indicating hilar cholangiocarcinoma (white arrow) shown by PTC. **B:** CBD tumor thrombi seen during intra-operation.

Pathology

All the 53 cases were pathologically diagnosed as HCC by professional surgical pathologists. The BDTT consisted of tumor cells arranged like a nest of primary tumors, coexisting with red blood cells (RBC), leukocytes and necrotic tumor tissues.

Postoperative mortality and morbidity

Among the 46 patients who underwent operations, 8 died of hepatic failure postoperatively, the hospitalization mortality was 17.4% (8/46). One died 3 d after laparotomy, one died 26 d after simple thrombectomy with biliary drainage and right HAL, two died 7 and 45 d after simple thrombectomy with biliary drainage respectively, four died 7, 12, 15 and 38 d after hepatectomy with thrombectomy and biliary drainage respectively. Fifteen patients developed postoperative complications including liver function failure (n = 8), upper gastrointestinal hemorrhage (n = 4), pleural effusion (n = 4), serious coagulopathy (n = 1), intra-abdominal hemorrhage (n = 1), pleural hemorrhage (n = 1), biliary leakage (n = 1), subphrenic infection (n = 1), and lower limb venous thrombosis (n = 1). The postoperative morbidity was 32.6%. Of the six cases who received PTCD, one suffered from acute cholangitis, no death occurred.

Effect of treatment

The serum total bilirubin levels of these patients with obstructive jaundice decreased gradually. A total of 45 patients were followed up. One patient refused treatment and died 1 mo later. The survival time of six cases who underwent PTCD ranged from 2 to 7 mo (median survival of 3.7 mo). The survival time of the patients who received surgery was 2 mo for one patient who underwent laparotomy, 5-46 mo (median survival of 23.5 mo) for 17 cases who underwent hepatectomy, which was the longest survival compared to the patients who underwent other procedures (log-rank test, P = 0.0024), 5-17 mo (median survival of 10.0 mo) for 5 cases who underwent HACE, 3-9 mo (median survival of 6.1 mo) for 11 cases who underwent simple thrombectomy and biliary drainage, and 3-8 mo (median survival of 4.3 mo) for 4 cases who underwent simple biliary drainage.

DISCUSSION

BDTT derived from HCC is uncommon. However, bile duct invasion was commonly detected at necropsy in HCC patients with obstructive jaundice. In 1975, Lin *et al*.[6], clinically classified such cases as "icteric type hepatoma", which manifested as obstructive jaundice even at the early stage of tumors, and pointed out that its differential diagnosis was very difficult. In 1982, Kojiro *et al*.[7], first described the clinical and pathological features of HCC invading the bile duct, and clarified that it was not equal to the portal vein thrombi (PVT), indicating the possibility of extensive dissemination in terms of severity of the disease. They considered that it was not necessarily a criterion of advanced disease. Actually, the rapid growth of the BDTT was rare and there was no report of BDTT extending to the duodenum. But BDTT could enlarge through blending with blood clotting and bile mucus, subsequently resulting in full obstruction of the biliary tract and obstructive jaundice.

The typical clinical features of BDTT were repeated episodes of cholangitis and fluctuating jaundice, which could be relieved by conservative treatment. For these manifestations, BDTT was often misdiagnosed as cholangiocarcinoma. Actually, in our series, three cases were misdiagnosed as hilar cholangiocarcinoma. In addition, it is essentially important to differ obstructive jaundice from hepatic jaundice caused by liver dysfunction due to extensive metastasis within the liver and underlying hepatitis and cirrhosis, because the later has no chance of surgery, but the former can gain a good outcome through operation and/or multi-modality treatment. We concluded that the following clues could help us differentiate BDTT from other types of jaundice. Patients had underlying hepatitis or liver cirrhosis, elevating serum AFP, and characteristic features of primary liver tumors presented in US and CT.

As to the imaging investigations, US is the most convenient and effective method to detect BDTT and intrahepatic primary tumors. Endoscopic sonography (EUS) can show a tumor thrombus with central echogenicity and a "nodule-in-nodule" pattern, which provides more accurate evidence for the diagnosis. Lee *et al*.[8], reported a patient with a small HCC in caudate lobe and presence of obstructive jaundice. Preoperative EUS showed that it was tumor thrombi in CBD. In addition, intraoperative US could detect smaller or more deeply seated intrahepatic tumors. CT, MRI and MRCP could provide more information for us to know the extension of tumors and location of thrombi, and help us adopt proper treatment, in particular surgical procedure selection for patients. Intraoperative choledochoscopy and cholangiography can show the location of tumor thrombi and differentiate obstructions due to intraluminal mass, infiltrating ductal lesions or extrinsic mass compression. Jan and Chen[9] reported 28 patients with obstructive jaundice as a result of floating tumor debris from ruptured tumors in CBD. Of these, 18 cases underwent choledochoscopy, and the tumor ruptured into right intrahepatic bile duct (n = 9), left intrahepatic bile duct (n = 7), and the confluence of the left and right hepatic ducts (n = 2). Hepatectomies were performed for four patients under the guide of choledochoscopy.

The size of primary tumors did not correlate with biliary metastasis[10], and the primary liver tumors with obstructive jaundice might be small and resectable. In our series, primary liver tumors were not detectable in seven cases. Twenty-five cases had tumors with a diameter of less than 5 cm, suggesting that obstructive jaundice is not a criterion of late-stage HCC and a contraindication for surgery necessarily[11].

The managements of BDTT include hepatectomy, thrombectomy, biliary drainage, TACE, internal biliary stenting, radiotherapy, percutaneous transhepatic ethanol injection (PTEI), *etc*. Surgical resection has been the ideal treatment and the only way for patients to achieve a long-term survival[12-14]. Most patients might have satisfactory palliation and opportunity for cure after surgery[15]. The selection of surgical procedures was based on the nature and location of the main tumor and thrombi, severity of cirrhosis, associated biliary neoplastic strictures, the overall status of patients, and the experience of surgeons. If the condition of patients was good and the primary liver tumor was resectable, the primary tumor should be resected after thrombectomy. Even if it was only a palliative resection, it could increase the survival time. If no liver tumor was detected, biliary decompression and drainage should be performed through choledochotomy and thrombectomy. To the unresectable diseases, HAL and HACE might be beneficial to some selected cases[16-19]. Shiomi *et al*.[12], reviewed 132 patients with HCC who underwent hepatectomy between 1980 and 1999. Of these, 17 with BDTT underwent right hemihepatectomy, 1 caudate lobectomy, 11 right or left hemihepatectomy and 5 segmentectomy. Their 3- and 5-year survival rates were 47% and 28% respectively, and the median survival time was 2.3 years, similar to those achieved in 115 patients without BDTT. Fukuda *et al*.[20], reported that after the patients with HCC and extrahepatic bile duct thrombi underwent tumor resection and HACE, the longest survival time of some patients reached 215 mo. In our 46 cases undergoing surgery, the postoperative mortality was 17.4%, and the morbidity was 32.6%. The survival time of the patients who underwent hepatectomy, thrombectomy and biliary drainage ranged from 5 to 46 mo with a median time of 23.5 mo. We concluded that the poor prognosis of these patients was due to the late diagnosis and obstructive jaundice that resulted in irreversible liver failure. In our study, one patient died 3 d after laparotomy, indicating that early diagnosis and surgical treatment are critically important to improve the prognosis of HCC patients.

BDTT is different from PVT. Complete removal of the later is sometimes difficult because portal vein provides the main blood supply for thrombi. However, it is easy to remove BDTT because most of thrombi do not adhere to the wall of bile duct tightly. Narita *et al*.[21], reported one case of small HCC in the left lobe with bile duct thrombi, and they found that the thrombi just adhered to the mucosa of bile duct, rather than invaded submucosa. Primary tumor resection and thrombectomy may achieve satisfactory palliation and cure. However, active hemorrhage occurred during operation in some cases, this may be due to the continuity of BDTT with the main intrahepatic tumor or BDTT invading the bile duct wall. But bleeding could be easily controlled after primary tumor was removed. For patients with multiple and unresectable tumors or biliary hemorrhage, thrombectomy and T-tube drainage with HAL could control bleeding and

relieve jaundice, and subsequently improve liver function. The survival time of these patients may be prolonged.

PTCD and biliary stent placement could alleviate jaundice[22,23]. TACE and PTEI could control the growth of tumors, improve the quality of life and survival rate after jaundice was relieved[24-26]. Endoscopic biliary drainage (EBD) for unresectable HCC with obstructive jaundice remains controversial because of no benefit to survival. Matsueda *et al*.[27], suggested that EBD was one of the effective treatments for patients with unresectable malignant biliary stenosis, and obstructive jaundice due to bile duct thrombi. However, EBD was often difficult in HCC patients with obstructive jaundice because of proximal biliary obstruction at the hilum, and multiple tumors diffusing in the whole liver. The decision to perform EBD should be based on the nature and location of thrombi, the condition of liver function, and the presence of PVT. In addition, endoscopic sphincterotomy could benefit the discharge of necrotic thrombi and further improvement of overall status, after endoscopic nasobiliary drainage resolved the obstruction[28,29].

There is a considerable controversy over the role of transplantation in patients with HCC. Liver transplantation for HCC patients with BDTT is rare. Peng *et al*.[30,31], have reported one patient who underwent piggyback orthotopic liver transplantation and survived for 27 mo. This suggests that selected HCC patients with BDTT may benefit from liver transplantation, but it needs to be studied further.

REFERENCES

1 **Becker FF.** Hepatoma-nature's model tumor. *Am J Pathol* 1974; **74**: 179-210
2 **Chen MF.** Icteric type hepatocellular carcinoma: clinical features, diagnosis and treatment. *Chang Gung Med J* 2002; **25**: 496-501
3 **Huang GT,** Sheu JC, Lee HS, Lai MY, Wang TH, Chen DS. Icteric type hepatocellular carcinoma: revisited 20 years later. *J Gastroenterol* 1998; **33**: 53-56
4 **Kew MC,** Paterson AC. Unusual clinical presentations of hepatocellular carcinoma. *Trop Gastroenterol* 1985; **6**: 10-22
5 **Peng BG,** Huang JF, Liang LJ, Lu MD. The surgical treatment of hepatocellular carcinoma involving the bile duct: 20 cases reported. *Chin J Practical Surg* 1996; **16**: 484-485
6 **Lin TY,** Chen KM, Chen YR, Lin WS, Wang TH, Sung JL. Icteric type hepatoma. *Med Chir Dig* 1975; **4**: 267-270
7 **Kojiro M,** Kawabata K, Kawano Y, Shirai F, Takemoto N, Nakashima T. Hepatocellular carcinoma presenting as intrabile duct tumor growth: a clinicopathologic study of 24 cases. *Cancer* 1982; **49**: 2144-2147
8 **Lee YC,** Wang HP, Huang SP, Chang YT, Wu CT, Yang CS, Wu MS, Lin JT. Obstructive jaundice caused by hepatocellular carcinoma: detection by endoscopic sonography. *J Clin Ultrasound* 2001; **29**: 363-366
9 **Jan YY,** Chen MF. Obstructive jaundice secondary to hepatocellular carcinoma rupture into the common bile duct: choledochoscopic findings. *Hepatogastroenterology* 1999; **46**: 157-161
10 **Tseng JH,** Hung CF, Ng KK, Wan YL, Yeh TS, Chiu CT. Icteric-type hepatoma: magnetic resonance imaging and magnetic resonance cholangiographic features. *Abdom Imaging* 2001; **26**: 171-177
11 **Hu J,** Pi Z, Yu MY, Li Y, Xiong S. Obstructive jaundice caused by tumor emboli from hepatocellular carcinoma. *Am Surg* 1999; **65**: 406-410
12 **Shiomi M,** Kamiya J, Nagino M, Uesaka K, Sano T, Hayakawa N, Kanai M, Yamamoto H, Nimura Y. Hepatocellular carcinoma with biliary tumor thrombi: aggressive operative approach after appropriate preoperative management. *Surgery* 2001; **129**: 692-698
13 **Nishio H,** Miyata K, Hanai M, Kato M, Yoneyama F, Kobayashi Y. Resection of an icteric type hepatoma with tumor thrombi filling the right posterior bile duct. *Hepatogastroenterology* 2002; **49**: 1682-1685
14 **Shimada M,** Takenaka K, Hasegawa H, Shirabe K, Gion T, Kano T, Sugimachi K. Hepatic resection for icteric type hepatocellular carcinoma. *Hepatogastroenterology* 1997; **44**: 1432-1437
15 **Murakami Y,** Yokoyama T, Kanehiro T, Uemura K, Sasaki M, Morifuji M, Sueda T. Successful diagnosis and resection of icteric type hepatocellular carcinoma. *Hepatogastroenterology* 2003; **50**: 1634-1636
16 **Jan YY,** Chen MF, Chen TJ. Long term survival after obstruction of the common bile duct by ductal hepatocellular carcinoma. *Eur J Surg* 1995; **161**: 771-774
17 **Tantawi B,** Cherqui D, Tran van Nhieu J, Kracht M, Fagniez PL. Surgery for biliary obstruction by tumour thrombus in primary liver cancer. *Br J Surg* 1996; **83**: 1522-1525
18 **Lau W,** Leung K, Leung TW, Liew CT, Chan MS, Yu SC, Li AK. A logical approach to hepatocellular carcinoma presenting with jaundice. *Ann Surg* 1997; **225**: 281-285
19 **Wang HJ,** Kim JH, Kim JH, Kim WH, Kim MW. Hepatocellular carcinoma with tumor thrombi in the bile duct. *Hepatogastroenterology* 1999; **46**: 2495-2499
20 **Fukuda S,** Okuda K, Imamura M, Imamura I, Eriguchi N, Aoyagi S. Surgical resection combined with chemotherapy for advanced hepatocellular carcinoma with tumor thrombus: report of 19 cases. *Surgery* 2002; **131**: 300-310
21 **Narita R,** Oto T, Mimura Y, Ono M, Abe S, Tabaru A, Yoshikawa I, Tanimoto A, Otsuki M. Biliary obstruction caused by intrabiliary transplantation from hepatocellular carcinoma. *J Gastroenterol* 2002; **37**: 55-58
22 **Lee JW,** Han JK, Kim TK, Choi BI, Park SH, Ko YH, Yoon CJ, Yeon KM. Obstructive jaundice in hepatocellular carcinoma: response after percutaneous transhepatic biliary drainage and prognostic factors. *Cardiovasc Intervent Radiol* 2002; **25**: 176-179
23 **Okazaki M,** Mizuta A, Hamada N, Kawamura N, Nakao K, Kikuchi T, Osada T. Hepatocellular carcinoma with obstructive jaundice successfully treated with a self-expandable metallic stent. *J Gastroenterol* 1998; **33**: 886-890
24 **Hu P,** Zhou DY, Gong B, Wang SZ, Yang GS, Wu MC. Endoscopic management of 1 215 malignant bile duct obstructions. *Chin J Surg* 2001; **39**: 195-198
25 **Tada K,** Kubota K, Sano K, Noie T, Kosuge T, Takayama T, Makuuchi M. Surgery of icteric-type hepatoma after biliary drainage and transcatheter arterial embolization. *Hepatogastroenterology* 1999; **46**: 843-848
26 **Huang JF,** Wang LY, Lin ZY, Chen SC, Hsieh MY, Chuang WL, Yu MY, Lu SN, Wang JH, Yeung KW, Chang WY. Incidence and clinical outcome of icteric type hepatocellular carcinoma. *J Gastroenterol Hepatol* 2002; **17**: 190-195
27 **Matsueda K,** Yamamoto H, Umeoka F, Ueki T, Matsumura T, Tezen T, Doi I. Effectiveness of endoscopic biliary drainage for unresectable hepatocellular carcinoma associated with obstructive jaundice. *J Gastroenterol* 2001; **36**: 173-180
28 **Naranjo Rodriguez A**, Puente Gutierrez J, Hervas Molina A, de Dios Vega JF, Monrobel Lancho A, Gonzalez Galilea A, Mino Fugarolas G. Endoscopic drainage with polyethylene endoprosthesis of malignant obstructive jaundice *Gastroenterol Hepatol* 1999; **22**: 391-397
29 **Spahr L,** Frossard JL, Felley C, Brundler MA, Majno PE, Hadengue A. Biliary migration of hepatocellular carcinoma fragment after transcatheter arterial chemoembolization therapy. *Eur J Gastroenterol Hepatol* 2000; **12**: 243-244
30 **Peng SY,** Wang JW, Liu YB, Cai XJ, Deng GL, Xu B, Li HJ. Surgical intervention for obstructive jaundice due to biliary tumor thrombus in hepatocellular carcinoma. *World J Surg* 2004; **28**: 43-46
31 **Peng SY,** Wang JW, Liu YB, Cai XJ, Xu B, Deng GL, Li HJ. Hepatocellular carcinoma with bile duct thrombi: analysis of surgical treatment. *Hepatogastroenterology* 2004; **51**: 801-804

Science Editor Wang XL and Li WZ **Language Editor** Elsevier HK

PO Box 2345, Beijing 100023, China
www.wjgnet.com
wjg@wjgnet.com

ELSEVIER

World J Gastroenterol 2005;11(25):3970
World Journal of Gastroenterology ISSN 1007-9327

Acknowledgements to Reviewers of *World Journal of Gastroenterology*

Many reviewers have contributed their expertise and time to the peer review, a critical process to ensure the quality of *World Journal of Gastroenterology*. The editors and authors of the articles submitted to the journal are grateful to the following reviewers for evaluating the articles (including those were published and those were rejected in this issue) during the last editing period of time.

Satoshi Kondo, Professor and Chairman
Department of Surgical Oncology, Hokkaido University Graduate School of Medicine, N15 W7, Kita-ku, Sapporo 060-8638, Japan

Shoji Kubo, M.D.
Hepato-Billiary-Pancreatic Surgery, Osaka City University Graduate School of Medicine, 1-4-3 Asahimachi, Abeno-ku, Osaka 545-8585, Japan

Nicholas F LaRusso, M.D.
Department of Internal Medicine, Distinguished Investigator of the Mayo Foundation Mayo Medical School, 200 First Street, SW, Rochester MN 55905, United States

Frederick H Leibach, Professor
Department of Biochemistry and Molecular Biology, Medical College of Georgia, 1120 15th Street, Augusta 30912-2100, United States

Jie-Shou Li, M.D.
Academician of Chinese Academy of Engineering, Department of General Surgery, General Hospital of Nanjing Command Area, 305 East Zhongshan Road, Nanjing 210002, Jiangsu Province, China

Richard W McCallum, M.D.
Professor of Medicine, Director The Center for Gastrointestinal Nerve and Muscle Function & the Division of GI Motility, MS 1058, 901 Rainbow Boulevard, Kansas City, KS 66160, United States

Timothy H Moran, Professer
Department of Psychiatry, Johns Hopkins University School of Medicine, Ross 618, 720 Rutland Ave, Baltimore, Maryland 21205, United States

Hiroshi Nakagawa, Assistant Professor
Gastroenterology Division, University of Pennsylvania, 415 Curie Blvd. 638B CRB, Philadelphia 19104, United States

Josep M. Pique, M.D.
Department of Gastroenterology, Hospital Clínic of Barcelona, Villarroel, 170, Barcelona 08036, Spain

Gabriele Bianchi Porro, Professor
Gastroenterology Unit, "L. Sacco" University Hospital, Via G.B. Grassi 74, Milano 20157, Italy

Piero Portincasa, Professor
Internal Medicine - DIMIMP, University of Bari Medical School, Hospital Policlinico Piazza G. Cesare 11, Bari 70124, Italy

Lun-Xiu Qin, Professor
Liver Cancer Institute and Zhongshan Hospital, Fudan University, 180 Feng Lin Road, Shanghai 200032, China

Vasiliy Ivanovich Reshetnyak, Professor
Institute of General Reanimatology, 25-2, Petrovka Str., Moscow 107031, Russian Federation

Jose Sahel, Professor
Hepato-gastroenterology, Hospital sainti Marevenite, I270 Boolevard AE Sainti Margrenise, Marseille 13009, France

Peng Shang, Professor
Department of Cell Biology, Faculty of Life Sciences, 127 Western Youyi Road, Northwestern Polytechnological University, Xi'an, 710072, Shaanxi Province, China

Ian David Wallace, M.D.
Gastroenterologist, President, New Zealand Society of Gastroenterology, School of Medicine Auckland University; Department Gastroenterology North Shore Hospital; Shakespeare Specialist Group, 181 Shakespeare Rd Milford, Auckland, New Zealand

Benjamin Wong, M.D.
Department of Medicine, University of Hong Kong, Pokfulam Road, Pokfulam, Hong Kong, China

George Y Wu, Professor
Department of Medicine, Division of Gastroenterology-Hepatology University of Connecticut Health Center, 263 Farmington Ave, Farmington, CT 06030, United States

Yuan Yuan, Professor
Cancer Institute of China Medical University, 155 North Nanjing Street, Heping District, Shenyang 110001, Liaoning Province, China

Man-Fung Yuen, Associate Professor
Department of Medicine, The University of Hong Kong, Queen Mary Hospital, Hong Kong, China

Jian-Zhong Zhang, Professor
Department of Pathology and Laboratory Medicine, Beijing 306 Hospital, 9 North Anxiang Road, PO Box 9720, Beijing 100101, China